Adaptive Phased Management

Postclosure Safety Assessment of a Used Fuel Repository in Sedimentary Rock

Pre-Project Report

NWMO TR-2013-07

December 2013

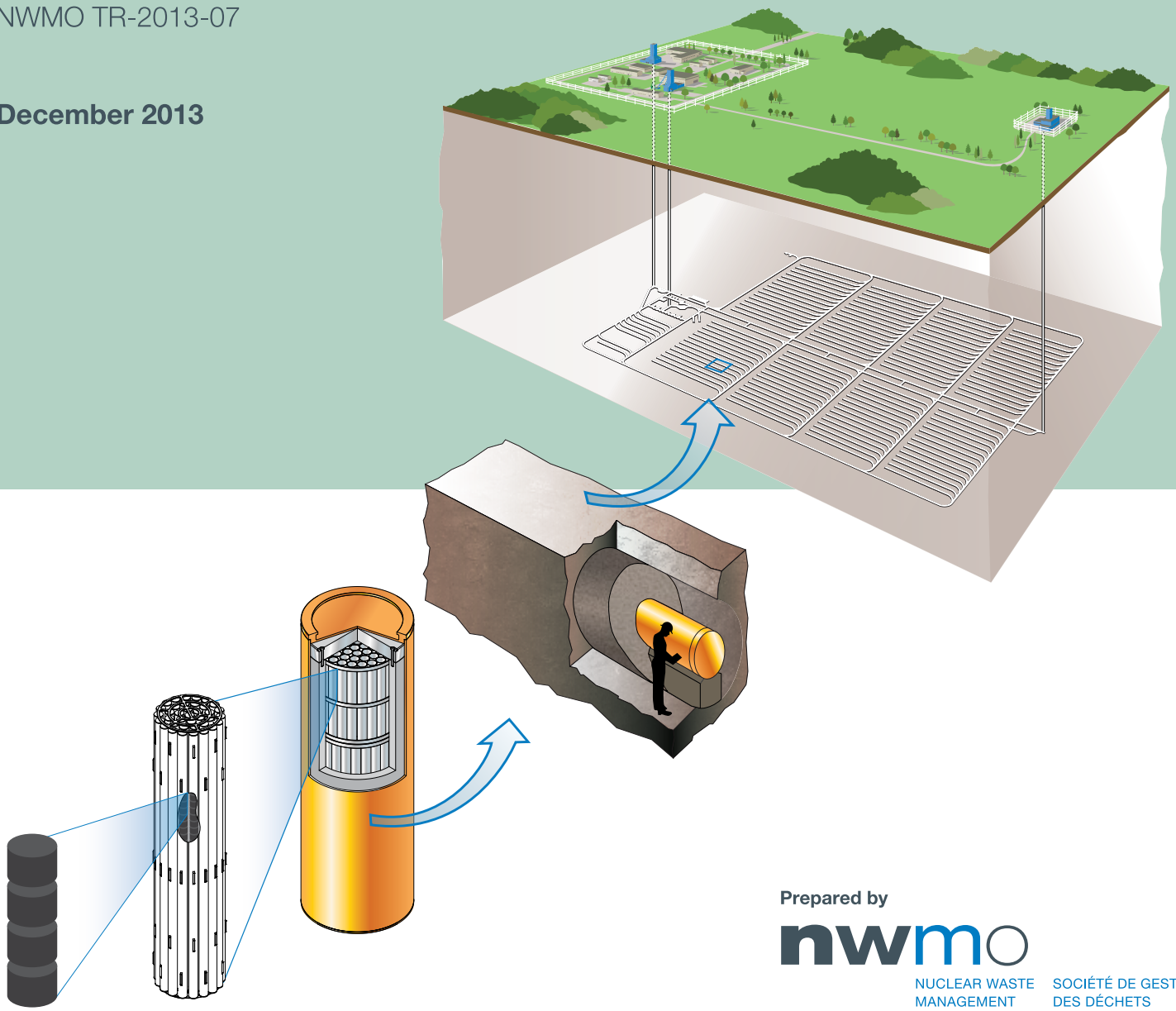

Prepared by

nwmo
NUCLEAR WASTE MANAGEMENT ORGANIZATION
SOCIÉTÉ DE GESTION DES DÉCHETS NUCLÉAIRES

Nuclear Waste Management Organization
22 St. Clair Avenue East, 6th Floor
Toronto, Ontario
M4T 2S3
Canada

Tel: 416-934-9814
Web: www.nwmo.ca

Adaptive Phased Management

Postclosure Safety Assessment of a Used Fuel Repository in Sedimentary Rock

Pre-Project Report

NWMO TR-2013-07

December 2013

Prepared by:
Nuclear Waste Management Organization

Nuclear Waste Management Organization
22 St. Clair Avenue East, 6th Floor
Toronto, Ontario
M4T 2S3
Canada

Tel: 416-934-9814
Web: www.nwmo.ca

EXECUTIVE SUMMARY

For decades Canadians have been using electricity generated by nuclear power reactors in Ontario, Quebec and New Brunswick. When used nuclear fuel is removed from a reactor, it is considered a waste product, is radioactive and requires careful management. Although its radioactivity decreases with time, chemical toxicity persists and the used fuel will remain a potential health risk for many hundreds of thousands of years. Canada's used nuclear fuel is now safely stored on an interim basis at licensed facilities located where it is produced.

The Nuclear Waste Management Organization (NWMO) is responsible for the implementation of Adaptive Phased Management (APM), the federally-approved plan for safe long-term management of Canada's used nuclear fuel. Under the APM plan, used nuclear fuel will ultimately be placed within a deep geological repository in a suitable rock formation.

The repository and its surroundings comprise a system that is designed to protect people and the environment through multiple barriers. These barriers include the ceramic used fuel, long-lived corrosion resistant containers, engineered sealing materials and the surrounding geosphere.

Safety is a priority for the implementation of the APM program. To support the focus on safety, the NWMO conducts a wide range of complementary activities, including research, design development, technology demonstration and safety assessment, which are necessary to assess the performance of the multi-barrier repository concept at timeframes relevant to illustrating long-term safety.

A site selection process is currently underway to identify a safe site for a deep geological repository in an informed and willing host community. The process of site selection will take several years. As potentially suitable sites are identified with interested communities, detailed field studies and geoscientific site characterization activities will be conducted to assess whether the APM multi-barrier repository concept could be safely implemented to meet rigorous regulatory requirements.

At this very early stage in the process, before specific sites have been identified for detailed examination, it is useful to conduct generic studies to illustrate the long-term performance and safety of the multi-barrier repository system within various geological settings.

This report provides an illustrative case study of the current multi-barrier design and postclosure safety of a deep geological repository in a hypothetical sedimentary setting. The purpose of this case study is to present and illustrate a postclosure safety assessment methodology that demonstrates how Canadian Nuclear Safety Commission (CNSC) expectations are met, as documented in CNSC Guide G-320 on Assessing the Long Term Safety of Radioactive Waste Management. For a licence application for an actual candidate site, a full safety case would be prepared that would include the results of site-specific geoscience investigations, an associated deep geological repository design and a more comprehensive safety assessment than described in this document.

Geosphere

A hypothetical geosphere was derived, in part, from experience gained in the Canadian Nuclear Fuel Waste Management Program. It was developed for the purpose of this illustrative case study while the NWMO proceeds with the APM siting process and selection of a preferred site in an informed and willing host community. While the hypothetical site represents one example of a possible sedimentary rock setting in southern Ontario, other characteristics are considered in the safety assessment to illustrate an approach to assessing both long-term safety and the functionality of various barrier systems.

The long-term safety and performance of a used fuel repository will rely in part on the geological setting that surrounds the repository. The geosphere will provide a geomechanically, hydrogeologically and geochemically stable environment. Geomechanical stability enables safe excavation and placement of the containers and engineered barrier system, and also, together with hydrogeological and geochemical stability, isolates the containers from a wide range of future human and natural events. A stable geochemical environment supports the container durability and minimizes contaminant mobility. The ability of the geosphere to support these attributes will be dependent on site-specific conditions.

For the purposes of this illustrative assessment, the hypothetical geosphere is divided into three groundwater systems, which are assumed to have the following characteristics:

1. The shallow groundwater system, located between 0 and 215 m below ground surface, is predominately driven by local and sub-regional scale topographic changes. The average travel time for groundwater to recharge, and then subsequently discharge, in the shallow groundwater zone is typically less than 1000 years. The groundwater in the shallow groundwater zone is fresh and oxygen-rich with a low total dissolved solids concentration.
2. The intermediate groundwater system between 215 and 250 m below ground surface is a transition zone from fresh and oxygen-rich to more mineralized and chemically reducing with depth. At the hypothetical site, the shift from oxidizing to reducing conditions occurs within this system. In the intermediate groundwater system, larger domains of low permeability rock tend to decrease mass transport rates.
3. In contrast with the shallow and intermediate groundwater systems, the groundwater in the deep system below 250 m has a higher total dissolved solids concentration and fluid density, and is chemically reducing. The increased fluid density will influence both energy gradients within the groundwater regime and vertical upward movement of groundwater between the shallow/intermediate and deep groundwater zones.

Design Concept

The current conceptual design for sedimentary rock consists of a repository constructed at a depth of approximately 500 m below surface. This depth was arbitrarily selected for illustrative purposes only; at an actual site the repository depth would be selected based on site-specific attributes to enhance passive long-term safety and the presentation of a repository safety case. The host rock at 500 m at this hypothetical site is assumed to be a massive limestone formation overlain by a thick shale sequence that is suitable for construction and operation of a used fuel repository. The repository contains a network of horizontal tunnel placement rooms for the base case inventory of 4.6 million used fuel bundles encapsulated in about 12,800 long-lived used

fuel containers. The container design consists of a copper outer vessel, or shell, that encloses a steel inner vessel. The outer copper shell provides effective resistance to container corrosion under deep geological conditions, while the inner steel vessel provides strength for the container to withstand expected hydraulic and mechanical loads, including earthquakes and glaciation. The report also describes observations on sedimentary rock considerations in other countries. A notable difference in this case study is with the copper-shell container design as opposed to the steel-only design primarily being considered in other countries. The design will be further refined and optimized for a licence application.

The used fuel container is supported by a highly compacted bentonite pedestal in its assigned position in the placement room. Bentonite pellets, placed by pneumatic methods, are used to fill all the remaining voids in the container placement room. Bentonite is a durable natural material that is expected to maintain its properties over the long term. Bentonite is a type of clay that swells on contact with water, resulting in its natural self-sealing property.

Postclosure Safety Assessment

The primary safety objective for the deep geological repository is the long-term containment and isolation of the used nuclear fuel. The safety of the repository would be based on a combination of the geology, engineered design, careful operations, and quality assurance processes including review and monitoring. Safety assessment provides a quantitative evaluation of the overall performance of the repository system and its impact on human health and on the environment. In this respect, it is able to identify features or processes that contribute to an understanding and confidence in long-term repository safety.

This illustrative case study focuses on long-term or postclosure safety. This is the period after the repository has been filled with used fuel containers, and has been sealed off and closed. Consistent with CNSC Guide G-320, the study identifies scenarios, models and methods for evaluating safety, with which to assess dose consequences and the influence of uncertainties. The results are compared against interim acceptance criteria for protecting persons and the environment.

The assessment does not try to predict the future, but instead examines the consequences for a range of scenarios, from likely to unlikely to “what if”. The likely scenarios are considered under the heading of “Normal Evolution Scenario.”

Normal Evolution Scenario

The normal evolution scenario presented in this report is based on a reasoned extrapolation of the reference case site and repository characteristics over time, consistent with the expectations of CNSC Guide G-320. The report describes why the used fuel copper containers are expected to remain intact over the timeframe of interest. For the purpose of the reference case normal evolution scenario, a small number of containers are assumed to be placed in the repository with undetected defects in the copper shell. Conservatively, these containers are assumed to be positioned within a placement room associated with the shortest travel time through the geosphere to the surface biosphere. The anticipated effects of glaciations on the assessment are also described.

The postclosure safety assessment adopts scientifically informed, physically realistic assumptions for processes and data that are understood and can be justified on the basis of the results of research. Where there are high levels of uncertainty associated with processes and data, conservative assumptions are adopted and documented to allow the impacts of uncertainties to be bounded. Data from site investigations will further support the assumptions and be incorporated into future safety assessments.

For the reference case safety assessment, the primary contributor to the public dose over the long term from an assumed small number of defective used fuel containers is the instant release fraction of Iodine-129, a long-lived radionuclide in used fuel that is non-sorbing in the geosphere. The calculated maximum dose for the reference case is about 150,000 times lower than the interim dose acceptance criterion of 0.3 mSv per year for the normal evolution scenario and occurs at the modelling cut-off time of 10 million years after closure. This long timeframe is due, in part, to the combined performance of the repository barrier systems and the time required for Iodine-129 to reach the biosphere. The barrier systems include the long-lived containers, the integrity of the engineered sealing systems and the near-field rock surrounding the repository.

The radiological impact on non-human biota is discussed in the report and the assessment concludes that the effects are negligible for the normal evolution scenario.

The report also concludes that contaminant concentrations are below their associated interim acceptance criteria in the assessment for protecting persons and the environment from hazardous substances, such as copper and other elements released from the used fuel and the containers.

Sensitivity Analyses and Bounding Assessments

Recognizing that there are uncertainties associated with the future evolution of a repository, the NWMO has varied a number of important parameters and assumptions, completed bounding assessments and has developed a number of hypothetical “what-if” scenarios to explore the influence of parameter and scenario uncertainty in assessing long-term safety. This approach is consistent with CNSC Guide G-320 on the use of different assessment strategies.

Key parameters that could potentially affect long-term safety are varied in sensitivity cases to understand the impact of uncertainties in these parameters:

- An increase in fuel dissolution rate by a factor of 10;
- An increase of contaminant instant release fractions to 10%;
- An increase in rock mass and excavation damage zone hydraulic conductivities by a factor of 10;
- An increase in rock diffusivity by a factor of 10;
- A 158 m overpressure in the Shadow Lake Formation which is located at a depth of approximately 675 m at the hypothetical site;
- An increase in container degradation by increasing the assumed undetected container defect area by a factor of 10; and
- A decrease in geosphere sorption with a coincident increase in radionuclide solubility limits.

Some parameters are also pushed beyond the reasonable range of variations in bounding assessments. In these cases, parameters are completely ignored by setting their values to zero or by removing physical limits for the following:

- An increase in radionuclide solubility in groundwater by ignoring solubility limits;
- A decrease in radionuclide sorption in the geosphere by ignoring sorption; and
- A decrease in radionuclide sorption in the near field by ignoring sorption.

The results from the sensitivity analysis and the bounding assessments conducted as part of this illustrative case study are shown in Figure E1.

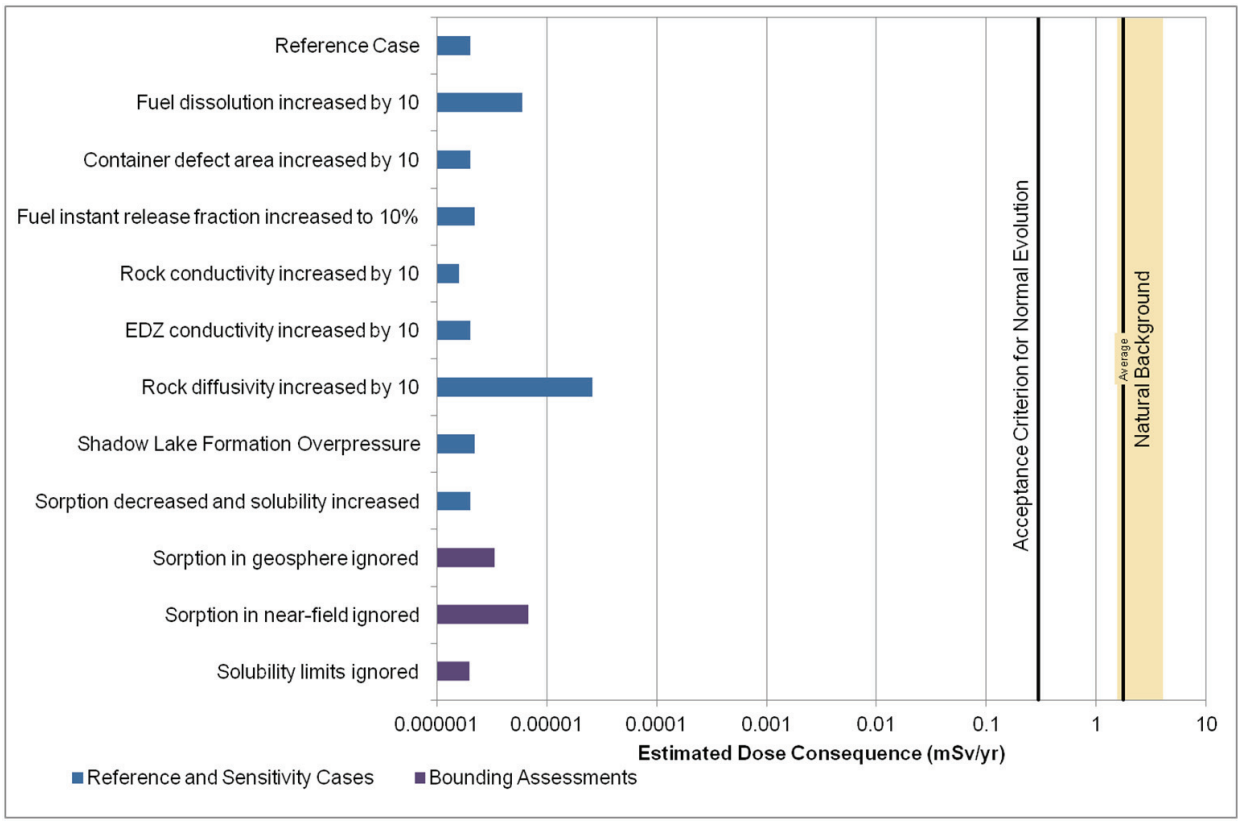

Figure E1: Results from Sensitivity Analysis and Bounding Assessments

The sensitivity analyses show that the impact on dose is small when key parameters are varied. As shown in Figure E1, the parameter with the most significant impact on dose is the rock diffusivity. The dose consequence when the rock diffusivity is increased by a factor of 10 is assessed to be 13 times greater than the reference case value.

The bounding assessments show a small impact on dose when sorption is ignored. When sorption is ignored in the near field, the dose consequence is assessed to be 3.4 times greater than in the reference case. When sorption is ignored in the geosphere, maximum dose is

increased to 1.6 times the reference case value and occurs at same time (modelling cut-off time of 10 million years). No impact on dose was observed when radionuclide solubility limits are ignored (see Figure E1).

Recognizing the importance of processes such as used fuel dissolution and sorption as shown in this case study, NWMO maintains active research programs in these areas to continue to improve our understanding of these processes. Nevertheless, even if highly conservative assumptions are adopted where there is uncertainty, the maximum dose rate to a member of the public is still estimated to be orders of magnitude lower than the interim dose acceptance criterion of 0.3 mSv per year.

All the previous results were obtained through deterministic analyses. A further understanding of uncertainties can be obtained through probabilistic modelling. In the present illustrative case study, a probabilistic analysis was conducted on the contaminant release and transport parameters. A total of 120,000 simulations were examined to identify a 95th percentile peak dose rate. The peak dose consequence in this case is assessed to be 37 times greater than for the reference case. This remains 4,000 times below the interim dose acceptance criterion of 0.3 mSv per year.

Disruptive Scenarios

A number of disruptive or “what-if” scenarios are identified by examining possible failure mechanisms. These scenarios are assessed to evaluate the potential impact of major barrier failures on safety, in accordance with CNSC Guide G-320. The disruptive event scenarios considered in this illustrative case study include:

- All containers fail at 60,000 years;
- All containers fail at 10,000 years; and
- Failure of shaft seal.

The container failure scenarios (i.e., all containers fail at 60,000 years and a variation where all containers fail at 10,000 years) indicate a notable increase in the dose results. However, the maximum dose rates remain well below the interim dose acceptance criterion of 1 mSv per year for disruptive scenarios.

The results also reveal that there is low sensitivity of the peak dose rate to the assumed failure time of all used fuel containers in the reference case geosphere. This occurs primarily as the assumed container failure time is longer than the short-lived fission product decay time, meaning that fuel dissolution rates are greatly reduced due to the decay of the gamma and beta radiation fields. Furthermore, the failure times are much smaller than the contaminant transit times to the surface. The remaining actinides and most of the long-lived fission products are delayed principally by diffusion within the natural barrier of the enclosing rock mass so that the peak dose rate, which is dominated by the long-lived and non-sorbing Iodine-129, does not materially change.

The impact of gas generated in the repository is considered for the case where all the containers fail at 10,000 years. The largest potential for gas generation (from the corrosion of steel within the copper container) is examined for this scenario and the model shows that gas could travel upward to the permeable Guelph Formation where it will disperse and dilute

laterally underground. However, to provide a bounding estimate, the gas-borne dose consequences are assessed using a set of extremely conservative assumptions to bound the potential dose consequences. A peak dose rate of 0.17 mSv per year is obtained when all the Carbon-14 is assumed to discharge into a house above the repository. This remains a factor of six below the 1 mSv per year interim dose acceptance criterion. For a more realistic case of failure of copper containers over longer times, the dose rates would be substantially lower. For example, if the copper fails on time scales associated with the next glaciation or later, the corresponding dose rates would be well below 0.001 mSv per year due to decay of Carbon-14.

The seal failure scenario has shown negligible effect on the predicted dose consequence in this study due to the distance between the containers with undetected defects and the shaft seal.

And finally, a stylized analysis was completed for inadvertent human intrusion. This scenario is a special case, as recognized in CNSC Guide G-320, since it circumvents all engineered and natural repository barriers. The results show that the potential dose to the drill crew, and to a site resident, from early intrusion, that exceeds the dose limit. However, the likelihood of this event occurring is very small due to placing the used fuel containers deep underground in a location with institutional controls in place for a period of time, no economically viable mineral resources, and no potable groundwater resources. Normal deep drilling practices (e.g., control of drilling fluids, use of gamma logging, etc.) will also tend to reduce consequences relative to those estimated here. Although the likelihood of human intrusion cannot be readily defined, it will be very low. The annual risk of health effects from human intrusion is estimated to be less than 1 in 100,000 per year.

Conclusion

This report provides an illustrative postclosure safety assessment of a deep geological repository in a hypothetical sedimentary rock setting. The objective is to provide a partial postclosure safety assessment that shows a structured and systematic approach that is consistent with expectations described in CNSC Guide G-320. The illustrative assessment includes a description of the repository system, systematically identifies scenarios, models and methods for evaluating safety, uses different assessment strategies, addresses uncertainty, and compares the results of the assessment with interim acceptance criteria. It indicates where additional analyses would be undertaken as part of a full safety case for an actual repository site.

The postclosure safety assessment shows, for the normal evolution scenario and associated sensitivity cases, that radiological and non-radiological interim acceptance criteria could be met during the repository's postclosure period.

THIS PAGE HAS BEEN LEFT BLANK INTENTIONALLY

TABLE OF CONTENTS

Page

EXECUTIVE SUMMARY ..... **i**

1. INTRODUCTION **1**

1.1 Purpose and Scope **1**

1.2 Background and Project Overview **2**

1.3 APM Project Phases **5**

1.3.1 Siting and Preparing for Construction 5

1.3.2 Site Preparation and Construction 7

1.3.3 Operation 7

1.3.4 Extended Monitoring 7

1.3.5 Decommissioning 7

1.4 Repository Timeframes **8**

1.4.1 Preclosure Period 8

1.4.2 Postclosure Period 8

1.5 Relevant Legislation **11**

1.5.1 CNSC Regulatory Requirements 11

1.5.2 Transportation of Used Nuclear Fuel 13

1.5.3 Canadian Codes and Standards 14

1.5.4 Safeguards 14

1.5.5 Traditional Knowledge 15

1.5.6 International Guidance 15

1.6 Safety Case **16**

1.6.1 Safety Case Context 18

1.6.2 Safety Strategy 18

1.6.3 Deep Geological Repository System 18

1.6.3.1 Geology 19

1.6.3.2 Waste Characteristics 21

1.6.3.3 Design 21

1.6.3.4 Institutional Controls 21

1.6.3.5 Long-Term Evolution of Repository 22

1.6.4 Safety Assessment 22
1.6.5 Management of Uncertainties 22
1.6.6 Iterative Approach 23
1.6.7 Integration of Safety Arguments 25
1.6.8 Stakeholder and Regulatory Involvement 25
1.6.9 Management System 26
1.7 Development of National Deep Geological Repositories 27
1.8 Report Structure and Content 28
1.9 References for Chapter 1 30
2. DESCRIPTION OF A HYPOTHETICAL SITE 33
2.1 Introduction 33
2.1.1 Site Attributes 33
2.1.2 Modelling Strategy 33
2.2 Conceptual Model for Hypothetical Site 34
2.2.1 Descriptive Geological Model 34
2.2.1.1 Geologic Description 34
2.2.1.2 Surface Features 37
2.2.2 Descriptive Hydrogeologic Model 39
2.2.2.1 Groundwater Systems 39
2.2.2.2 Hydraulic Parameters 39
2.2.2.3 Paleohydrogeology Boundary Conditions 43
2.2.2.4 Abnormal Pressure Distributions 46
2.2.2.5 Unsaturated Groundwater Flow 46
2.2.3 Descriptive Geochemical Model 46
2.2.3.1 Microbial Conditions in Sedimentary Environments 51
2.2.3.2 Sorption 52
2.2.3.3 Gas Characterization 52
2.3 Regional Scale Hydrogeologic Modelling 53
2.3.1 Computational Models 53
2.3.2 System Performance Measures 54
2.3.3 Regional Scale Conceptual Model 54
2.3.3.1 Model Domain and Spatial Discretization 54
2.3.3.2 Model Parameters 57

2.3.3.3 Flow Boundary Conditions 61
2.3.3.4 Initial Conditions and Solution of Density-Dependent Flow 61
2.3.3.5 Model Uncertainties and Sensitivities 64
2.3.4 Regional Scale Analyses 65
2.3.4.1 Reference Case Simulation 65
2.3.4.2 Temperate Transient Sensitivity Cases 70
2.3.4.3 Paleohydrogeologic Sensitivity Cases 74
2.3.4.4 Groundwater System Behaviour 90
2.3.5 Additional Temperate Transient Sensitivity Analyses 97
2.4 Summary and Conclusions 103
2.5 References for Chapter 2 104
3. USED FUEL CHARACTERISTICS 109
3.1 Used Fuel Description 109
3.1.1 Used Fuel Type and Amount 109
3.1.2 Geometry 110
3.1.3 Burnup and Linear Power 111
3.1.4 Effect of Irradiation 112
3.2 Radionuclide and Chemical Element Inventory 116
3.3 References for Chapter 3 124
4. REPOSITORY FACILITY – CONCEPTUAL DESIGN 127
4.1 General Description 127
4.2 Surface Facilities 129
4.3 Used Fuel Container 132
4.4 Used Fuel Packaging Plant 133
4.4.1 Transport Cask Receiving and Unloading 134
4.4.2 Module Handling Cells 134
4.4.3 Empty Used Fuel Container Receiving 135
4.4.4 Used Fuel Container Transport within the Plant 135
4.4.5 Fuel Handling Operations 137
4.4.6 Used Fuel Container Processing 137
4.4.6.1 Inerting Station 137
4.4.6.2 Welding Station 139
4.4.6.3 Machining and NDT Stations 140

4.4.6.4 Handling of Defective Containers 141
4.4.7 Filled Used Fuel Container Storage Cell 142
4.4.8 Used Fuel Container Dispatch Hall 142
4.5 Seals and Sealing Materials 149
4.5.1 General Description 149
4.5.2 Placement Room Backfill Materials 150
4.5.3 Placement Room Configuration 150
4.5.4 Access Tunnels Backfill 151
4.5.5 Concrete 152
4.5.6 Grout 152
4.5.7 Asphalt 153
4.6 Sealing Materials Production Plants 153
4.7 Shafts and Hoists 154
4.8 Underground Facility Design 155
4.8.1 Ventilation System 157
4.9 Repository Construction 159
4.10 Repository Operation 159
4.10.1 Container Placement 160
4.10.2 Backfilling Operation 160
4.11 Extended Monitoring 167
4.12 Decommissioning 168
4.12.1 Sealing of Underground Horizontal Openings 168
4.12.2 Sealing of Shafts 168
4.12.3 Decommissioning of Monitoring Wells and Sealing of Geological Boreholes 169
4.13 References for Chapter 4 170
5. LONG-TERM EVOLUTION OF THE MULTIPLE BARRIER SYSTEM 173
5.1 Long-Term Evolution of Used Fuel 175
5.1.1 Radioactive Decay 176
5.1.2 Changes in Temperature 177
5.1.3 Changes in the UO_2 178
5.1.3.1 Radionuclide Diffusion 179
5.1.3.2 Changes in the Oxidation State of Fuel 179
5.1.3.3 Build-Up of He Gas 179

5.1.3.4 Alpha Radiation Damage 180
5.1.4 Changes in the Zircaloy Cladding 180
5.1.4.1 Zircaloy Creep and Rupture 181
5.1.4.2 Uniform Corrosion (Oxidation) of Cladding 181
5.1.4.3 Hydrogen Absorption and Zircaloy Embrittlement 181
5.1.4.4 Delayed Hydride Cracking 182
5.1.4.5 Stress Corrosion Cracking 182
5.1.4.6 Pellet Swelling and Cladding “Unzipping” 182
5.1.5 Other Processes 182
5.1.5.1 Criticality 183
5.1.5.2 Hydraulic Processes 183
5.1.5.3 Mechanical Stresses 183
5.1.5.4 Biological Processes 183
5.1.6 Confidence 183
5.2 Long-Term Evolution of the Repository Environment 184
5.2.1 Repository-Induced Disturbances 184
5.2.2 Excavation Damaged Zone 185
5.2.3 Repository Saturation 185
5.2.4 Temperature 186
5.2.5 Near-Field Chemistry 187
5.2.6 Steel Corrosion and Gas Generation 188
5.2.7 Confidence 193
5.3 Long-Term Evolution of a Used Fuel Container 194
5.3.1 Evolution of Intact Containers 194
5.3.1.1 Irradiation of Container Materials 195
5.3.1.2 Changes in Container Temperature 196
5.3.1.3 Changes to Mechanical Integrity 198
5.3.1.3.1 Early Conditions 198
5.3.1.3.2 Effects of Hydrostatic and Buffer Swelling Pressures 198
5.3.1.3.3 Effects of Glacial Loading 199
5.3.1.3.4 Effect of Seismic Stresses 199
5.3.1.3.5 Effect of Creep 200
5.3.1.4 Effect of Chemical Processes Inside the Container 201

5.3.1.5 Effect of Chemical Processes Outside the Container 202
5.3.1.5.1 Uniform Corrosion 203
5.3.1.5.2 Localized Corrosion 208
5.3.1.5.3 Stress Corrosion Cracking 208
5.3.1.5.4 Microbiologically Influenced Corrosion 210
5.3.1.6 Summary 210
5.3.2 Evolution of a "Breached Used Fuel Container" 211
5.3.2.1 Repository Conditions Prior to Saturation for a "Breached Container" 212
5.3.2.2 Description of Post-Saturation Processes for a "Breached Container" 213
5.3.2.3 Anaerobic Corrosion of the Steel Vessel 214
5.3.2.4 Galvanic Corrosion 214
5.3.2.5 Deformation of the Copper Shell 215
5.3.2.6 Deformation of the Steel Vessel 216
5.3.2.7 Corrosion and Deformation of the Zircaloy Cladding 217
5.3.2.8 Dissolution of the Used Fuel Matrix 217
5.3.2.9 Radionuclide Release from the Fuel Pellets 219
5.3.2.10 Fate of Released Radionuclides 220
5.3.3 Confidence 221
5.4 Long-Term Evolution of Buffer, Backfill and Seals 223
5.4.1 Changes during Saturation 224
5.4.2 Temperature Changes 226
5.4.3 Chemical Changes 228
5.4.4 Changes due to Biological Processes 228
5.4.5 Radiation 230
5.4.6 Sorption 231
5.4.7 Vertical Movement of Containers 231
5.4.8 Buffer Erosion and Colloid Formation 231
5.4.9 Confidence 231
5.5 Long-Term Evolution of the Geosphere 233
5.5.1 Geological Disturbances 233
5.5.1.1 Seismicity and Seismic Hazard Assessment 233
5.5.1.2 Fault Rupture and Reactivation 234

5.5.1.3 Volcanism 234
5.5.2 Climate Change (Glaciation) 234
5.5.2.1 Glacial Erosion 235
5.5.2.2 Glacial Loading 236
5.5.2.3 Permafrost Formation (Changes in Groundwater Recharge) 237
5.5.3 Confidence 241
5.6 Summary 242
5.7 References for Chapter 5 242
6. SCENARIO IDENTIFICATION AND DESCRIPTION 251
6.1 The Normal Evolution Scenario 252
6.1.1 External FEPs 253
6.1.2 Internal FEPs 262
6.1.3 Description of the Normal Evolution of the Repository System 262
6.1.3.1 Events Occurring for Intact Containers 263
6.1.3.2 Events Occurring for Defective Containers 266
6.2 Disruptive Event Scenarios 268
6.2.1 Identification of Disruptive Scenarios 268
6.2.2 Description of Disruptive Event Scenarios 290
6.2.2.1 Inadvertent Human Intrusion Scenario 290
6.2.2.2 Shaft Seal Failure Scenario 290
6.2.2.3 Abandoned Repository Scenario 291
6.2.2.4 Poorly Sealed Borehole Scenario 291
6.2.2.5 Undetected Fault Scenario 291
6.2.2.6 Severe Erosion Scenario 291
6.2.2.7 All Containers Fail Scenario 292
6.2.2.8 Container Failure 292
6.3 References for Chapter 6 292
7. POSTCLOSURE SAFETY ASSESSMENT – CONTAMINANT TRANSPORT 295
7.1 Interim Acceptance Criteria 296
7.1.1 Interim Acceptance Criteria for the Radiological Protection of Persons 296
7.1.2 Interim Acceptance Criteria for the Protection of Persons from Hazardous Substances 298
7.1.3 Interim Acceptance Criteria for the Radiological Protection of the Environment 300

7.1.4 Interim Acceptance Criteria for the Protection of the Environment from Hazardous Substances 301

7.2 Scope 301

7.2.1 Analysis Cases for the Normal Evolution Scenario 302

7.2.2 Analysis Cases for Disruptive Scenarios 309

7.2.3 Analyses for Miscellaneous Modelling Parameters 310

7.2.4 Analysis Exclusions 314

7.3 Conceptual Model 315

7.3.1 Used Fuel Containers 317

7.3.2 Engineered Barrier System 320

7.3.3 Geosphere 321

7.3.4 Biosphere 323

7.4 Computer Codes 326

7.5 Analysis Methods and Key Assumptions 332

7.5.1 Overall Approach 332

7.5.2 Radionuclide and Chemical Hazard Screening Model 335

7.5.3 Detailed Flow and Transport Models 337

7.5.3.1 Site-Scale Model 343

7.5.3.2 Repository-Scale Model 357

7.5.3.3 Radionuclide Source Term 365

7.5.4 System Model 365

7.5.4.1 Radionuclide Source Term 366

7.5.4.2 Repository Model 367

7.5.4.3 Geosphere Model 369

7.5.4.4 Biosphere Model 374

7.6 Results of Radionuclide and Chemical Hazard Screening Analysis 379

7.7 Results of Detailed 3D Groundwater Flow and Transport Analysis 381

7.7.1 Site-Scale Model 381

7.7.1.1 Flow Results 382

7.7.1.1.1 Reference Case – No Well 382

7.7.1.1.2 Reference Case 386

7.7.1.2 Radionuclide Transport Results 390

7.7.1.2.1 Location of the Well and Defective Containers 390

7.7.1.2.2 Reference Case 390

7.7.1.2.3 Sensitivity to a Factor of 10 Increase in Geosphere Hydraulic Conductivity 394
7.7.1.2.4 Sensitivity to 100 m of Surface Erosion 398
7.7.1.2.5 Sensitivity to Spatial Resolution and Time Step Size 398
7.7.1.2.6 Other Sensitivity Cases 402
7.7.1.2.7 Effect of Barriers on Radionuclide Transport 403
7.7.2 Repository-Scale Model 405
7.7.2.1 Flow Results 406
7.7.2.1.1 Reference Case 406
7.7.2.2 Radionuclide Transport Results 408
7.7.2.2.1 Reference Case 409
7.8 Results of System Modelling 416
7.8.1 Transport Model Verification 417
7.8.2 Deterministic Analysis 421
7.8.2.1 Reference Case 421
7.8.2.2 Sensitivity to a Degraded Physical Barrier 424
7.8.2.3 Sensitivity to a Degraded Chemical Barrier 430
7.8.3 Probabilistic Analysis 436
7.9 Disruptive Scenarios 442
7.9.1 Inadvertent Human Intrusion 442
7.9.1.1 Description 443
7.9.1.2 Model and Assumptions 445
7.9.1.3 Results 448
7.9.2 All Containers Fail 453
7.9.2.1 Model and Assumptions 454
7.9.2.2 Results 454
7.9.3 Shaft Seal Failure 457
7.9.3.1 Model and Assumptions 458
7.9.3.2 Results 458
7.10 The Anticipated Effects of Glaciation on the Normal Evolution Scenario 458
7.10.1 Regional Glaciation Modelling Summary 459
7.10.2 Applicability to the Dose Assessment 460
7.11 Other Considerations 461
7.11.1 Complementary Indicators for the Radiological Assessment 462

7.11.1.1 Reference Indicator Values 462
7.11.1.2 Results for Complementary Indicators 466
7.11.2 Radiological Protection of the Environment 468
7.11.3 Protection of Persons and the Environment from Hazardous Substances 471
7.11.3.1 Contaminants from the Used Fuel Bundles 472
7.11.3.2 Copper Container Chemical Hazard Assessment 476
7.11.3.3 Complementary Indicators 479
7.12 Summary and Conclusions 481
7.12.1 Scope Overview 481
7.12.2 Results for the Normal Evolution Scenario 483
7.12.3 Results for the Disruptive Scenarios 486
7.12.4 Conclusion 487
7.13 References for Chapter 7 488
8. POSTCLOSURE SAFETY ASSESSMENT – GAS GENERATION AND TRANSPORT 495
8.1 Interim Acceptance Criteria 495
8.2 Scope 496
8.3 Conceptual Model 496
8.3.1 Gas Generation 496
8.3.2 Gas Migration and Transport 497
8.4 Computer Code 501
8.5 Analysis Methods and Key Assumptions 504
8.5.1 Overall Approach 504
8.5.2 Detailed Transport Models 505
8.5.2.1 Room-Scale Model 505
8.5.2.2 Repository-Scale Model 510
8.6 Results of Gas Generation and Transport Modelling 513
8.6.1 Room-Scale Model 513
8.6.2 Repository-Scale Model 520
8.7 Dose Consequences 523
8.8 Summary and Conclusions 525
8.9 References for Chapter 8 526
9. TREATMENT OF UNCERTAINTIES 529
9.1 Approach 529

9.2 Key Uncertainties 532
9.3 References for Chapter 9 533
10. NATURAL ANALOGUES 535
10.1 Analogues for Used Nuclear Fuel 535
10.1.1 Natural Uranium Deposits 535
10.1.2 Natural Fissioned Uranium 537
10.1.3 Fractured Uranium Deposits 539
10.2 Analogues for Barriers 539
10.2.1 Metals 539
10.2.1.1 Copper 539
10.2.1.2 Iron 540
10.2.2 Clays 541
10.2.3 Concrete 545
10.2.4 Asphalt 546
10.3 Analogue for Geosphere 546
10.4 Natural Analogue Summary 547
10.5 References for Chapter 10 547
11. QUALITY ASSURANCE 551
11.1 Introduction 551
11.2 Used Fuel Repository Conceptual Design and Postclosure Safety 551
11.2.1 APM Safety Case Project Quality Plan 551
11.2.2 Examples of Peer Review and Quality Assurance 552
11.2.3 Future Safety Case Quality Assurance 553
11.3 References for Chapter 11 553
12. SUMMARY AND CONCLUSIONS 555
12.1 Purpose of the Pre-Project Report 555
12.2 Repository System 556
12.2.1 Geologic Description of the Hypothetical Site 556
12.2.2 Used Fuel 557
12.2.3 Design Concept 557
12.3 Safety Assessment 558
12.3.1 Assessment Strategies 560
12.3.2 Modelling Tools and Computer Codes 561

12.3.2.1 Key Assumptions and Conservatisms in Modelling 562
12.3.3 Normal Evolution Scenario 563
12.3.3.1 Results from Sensitivity Analyses and Bounding Assessments 566
12.3.3.2 Results from the Probabilistic Analysis 567
12.3.3.3 Results from Complementary Indicators 570
12.3.4 Disruptive Events Scenarios 570
12.4 Future Work 573
12.5 Conclusion 573
12.6 References for Chapter 12 573
13. SPECIAL TERMS 575
13.1 Units 575
13.2 Abbreviations and Acronyms 576
APPENDIX A A-1

LIST OF TABLES

Page

Table 1-1: CNSC Regulatory Documents Applicable to the APM Project 12
Table 1-2: International Guidance Applicable to the APM Project 15
Table 1-3: Status of National Plans for High-Level Waste 27
Table 1-4: Pre-Project Report Content Mapped to CNSC Guide G-320 29
Table 2-1: Formation Thicknesses at the Hypothetical Site 35
Table 2-2: Regional Hydrogeologic Parameters 40
Table 2-3: Average TDS Values for Sedimentary Formation Groundwaters and Porewaters 49
Table 2-4: Reference SR-270-PW Composition 50
Table 2-5: Sub-divisions of Geologic Formations 55
Table 2-6: Loading Efficiency (ζ) and Specific Storage (S_s) for Scenario (fr-base-paleo-biot05) with a Biot Coefficient of 0.5 59
Table 2-7: Groundwater Transport Parameters 60
Table 2-8: Table of Regional Scale Simulations for this Study 71
Table 2-9: Computed MLE Values at the Repository Footprint for Alternate Temperate Scenarios 99
Table 3-1: Used Fuel Parameters 110
Table 3-2: Radionuclides Included in the Radiological Assessment 117
Table 3-3: List of Potentially Significant Chemically Hazardous Elements and Associated Radionuclide Decay Chains Included in the Hazardous Substance Assessment 118
Table 3-4: Inventories of Radionuclides of Interest in UO_2 Fuel for 220 MWh/kgU Burnup and 30 Years Decay Time 120
Table 3-5: Inventories of Radionuclides of Interest in Zircaloy for 220 MWh/kgU Burnup and 30 Years Decay Time 121
Table 3-6: ORIGEN-S: Pickering Fuel Inventory Comparison 122
Table 3-7: Inventories of Chemical Elements of Interest in UO_2 Fuel for 220 MWh/kgU Burnup and 30 Years Decay Time 123
Table 3-8: Inventories of Chemical Elements of Interest in Zircaloy for 220 MWh/kgU Burnup and 30 Years Decay Time 124
Table 4-1: APM Facility Number and Description 131
Table 4-2: Reference Copper Vessel Parameters 133
Table 4-3: Reference Steel Vessel Parameters 133

Table 4-4: Composition and As-Placed Properties of Clay-Based Sealing System Components 152
Table 4-5: Composition and Properties of a Cement Grout for Repository Use 153
Table 4-6: Sealing Materials Attributes 154
Table 4-7: Proposed Sealing System for Shafts 169
Table 5-1: General Parameters 174
Table 5-2: Processes with a Potential Influence on the Evolution of Used Fuel Bundles 175
Table 5-3: Processes with a Potential Influence on the Near-Field Geosphere 184
Table 5-4: Processes with a Potential Influence on the Evolution of Containers 195
Table 5-5: Typical Instant-Release Fractions for Selected Radionuclides 220
Table 5-6: Processes with a Potential Influence on the Evolution of Buffer/Backfill/Seals 223
Table 5-7: Processes with a Potential Influence on the Geosphere 233
Table 6-1: FEP List Showing FEPs Down to Level 2 252
Table 6-2: Status of External FEPs for the Normal Evolution of the Repository System 254
Table 6-3: External FEPs Potentially Compromising Arguments Relating to the Long-Term Safety 269
Table 6-4: Internal FEPs Potentially Compromising Arguments Relating to Long-Term Safety 279
Table 6-5: Potential Failure Mechanisms and Associated Scenarios 285
Table 6-6: Additional Scenarios Considered in Other Safety Assessments 289
Table 7-1: Interim Acceptance Criteria for the Protection of Persons and the Environment from Non-Radiological Impacts 299
Table 7-2: Interim Acceptance Criteria for the Radiological Protection of the Environment 301
Table 7-3: Sensitivity Cases for the Normal Evolution Scenario 304
Table 7-4: Analysis Cases for Disruptive Scenarios 311
Table 7-5: Modelling Parameter Cases 313
Table 7-6: RSM, Version RSM110 329
Table 7-7: SYVAC3-CC4, Version SCC4.09.1 330
Table 7-8: FRAC3DVS-OPG, Version 1.3 331
Table 7-9: HIMv2.0 332
Table 7-10: Screening Model Geosphere Zone Properties 336
Table 7-11: Cases Considered for the Radionuclide and Chemically Hazardous Element Screening Assessment 337
Table 7-12: Groundwater Composition for the Cobourg Formation (Repository Level) 338

Table 7-13: Element Solubilities 339
Table 7-14: Data for Effective Diffusion Coefficients, Reference Case Values 340
Table 7-15: Data for Sorption Coefficients (K_d), Reference Case Values 341
Table 7-16: Data for Material Porosity 342
Table 7-17: Geosphere Hydraulic Conductivity and Layering 345
Table 7-18: Engineered Barrier Hydraulic Conductivity 347
Table 7-19: Source and Well Locations, Release from All Containers 352
Table 7-20: Source and Well Locations, Release from Three Containers 354
Table 7-21: Fuel Instant-release Fractions for Selected Elements 366
Table 7-22: Container Distribution by Repository Sector 370
Table 7-23: I-129 Transport from the Repository to Surface 374
Table 7-24: Soil Properties 376
Table 7-25: Climate and Atmosphere Parameters 377
Table 7-26: Human Lifestyle Data 378
Table 7-27: Summary of Screened in Radionuclides and Chemically Hazardous Elements for Each Case Considered 379
Table 7-28: List of Potentially Significant Radionuclides 380
Table 7-29: List of Potentially Significant Chemically Hazardous Elements 380
Table 7-30: Site-Scale Transport Sensitivity Cases 402
Table 7-31: Comparison of Maximum Transport Rates to the Geosphere 419
Table 7-32: Comparison of Maximum Transport Rates to the Surface 421
Table 7-33: Radionuclide Dose Pathways for the Reference Case 424
Table 7-34: Result Summary for Defective Physical Barrier Sensitivity Cases 430
Table 7-35: Result Summary for Defective Chemical Barrier Sensitivity Cases 436
Table 7-36: Statistical Information Concerning the Distribution of the Peak Dose Rate 439
Table 7-37: Average and Median Maximum Dose Rates for Individual Radionuclides 439
Table 7-38: Human Intrusion Pathways Considered in Recent Safety Assessments 444
Table 7-39: Common Parameters for Human Intrusion Scenario 447
Table 7-40: Exposure Specific Parameters for Human Intrusion Scenario 448
Table 7-41: Background Concentration of Radionuclides in Surface Waters 463
Table 7-42: Background Concentration of Radionuclides in Surface Soils and Rocks 465
Table 7-43: Reference Values for Indicators 466
Table 7-44: Comparison of Reference Case Concentrations with Interim Acceptance Criteria for the Radiological Protection of the Environment 469

Table 7-45: Comparison of High Geosphere Diffusivity Sensitivity Case Concentrations with Interim Acceptance Criteria for the Radiological Protection of the Environment....470

Table 7-46: Comparison of All Containers Fail at 10,000 years Disruptive Scenario Concentrations with Interim Acceptance Criteria for the Radiological Protection of the Environment....471

Table 7-47: SYVAC3-CC4 - Concentration Quotients for the Reference Case....473

Table 7-48: SYVAC3-CC4 - Concentration Quotients for the High Geosphere Diffusivity Sensitivity Case....474

Table 7-49: SYVAC3-CC4 - Concentration Quotients for the All Containers Fail Case....475

Table 7-50: SYVAC3-CC4 - Concentration Maximum Impurity Levels in Copper and Estimated Impurity Element Concentration Quotients for Well Water....478

Table 7-51: Erosion Fluxes out of the Geosphere....480

Table 7-52: Result Summary....485

Table 8-1: Two-Phase Flow Properties....499

Table 8-2: T2GGM, V3.1....503

Table 8-3: Comparison of Volatile, Long-lived Radionuclides....524

Table 12-1: Summary and Key Findings from Sensitivity Analyses, Bounding Assessments and Probabilistic Analysis....568

Table 12-2: Summary of Key Findings from Disruptive Events....571

LIST OF FIGURES

Page

Figure 1-1: Illustration of Deep Geological Repository Concept....4

Figure 1-2: Illustrative APM Implementation Schedule for Planning Purposes....6

Figure 1-3: Perspective of Past Events and Expected Future Events in Earth's History Including Repository Events....10

Figure 1-4: Components of the Safety Case....17

Figure 1-5: Iterative Process for Developing the Safety Case....24

Figure 1-6: Site Evaluation Process....26

Figure 2-1: Regional Scale Topography....38

Figure 2-2: nn9930 GSM Model Outputs for the Grid Block Containing the Repository Footprint for this Study....44

Figure 2-3: nn9921 GSM Model Outputs for the Grid Block Containing the Repository Footprint for this Study 45

Figure 2-4: Block Cut View of FRAC3DVS-OPG Zone Identifiers for Regional Scale Domain 56

Figure 2-5: Block Cut View Showing Spatial Extent of the Bedrock Units 57

Figure 2-6: Precambrian Horizontal and Vertical Matrix Permeabilities as a Function of Depth 60

Figure 2-7: Plot of TDS versus Depth for Groundwater from the Canadian Shield 63

Figure 2-8: Block Cut View of Initial Total Dissolved Solids Concentration Distribution 63

Figure 2-9: Block Cut View of Steady-State Density-Independent Freshwater Heads 66

Figure 2-10: Block Cut View of Freshwater Heads at Pseudo Equilibrium Time of One Million Years with Temporally Varying TDS Distribution 66

Figure 2-11: Block Cut View of Total Dissolved Solids Concentration at Pseudo Equilibrium Time of One Million Years with Temporally Varying TDS Distribution 67

Figure 2-12: Base Case Total Dissolved Solids Concentration at Pseudo Equilibrium Time of One Million Years at East-West Cross-Section through the Hypothetical Repository Footprint 67

Figure 2-13: Block Cut View of Reference Case Porewater Velocity Magnitude at Pseudo Equilibrium Time of One Million Years 68

Figure 2-14: Block Cut View of Reference Case Ratio of Vertical Velocity to Velocity Magnitude at Pseudo Equilibrium Time of One Million Years 69

Figure 2-15: Block Cut View of Base Case Mean Life Expectancy at Pseudo Equilibrium Time of One Million Years 72

Figure 2-16: Reference Case Mean Life Expectancy at Pseudo Equilibrium Time of One Million Years at East-West Cross-Section through the Hypothetical Repository Footprint 72

Figure 2-17: Ratio of Velocity Magnitudes of Steady-State Groundwater Flow to Density-Dependent Flow Reference Case 73

Figure 2-18: Ratio of MLEs of Steady-State Groundwater Flow to Density-Dependent Flow Reference Case 73

Figure 2-19: The Total Dissolved Solids Concentrations at Pseudo Equilibrium Time of One Million Years for an Increased Rock Mass Hydraulic Conductivity 75

Figure 2-20: Difference in Freshwater Heads between a Simulation Using an Increased Rock Mass Hydraulic Conductivity and Reference Case 76

Figure 2-21: Ratio of Pore Velocity Magnitudes of Sensitivity Case using an Increased Rock Mass Hydraulic Conductivity to Reference Case 76

Figure 2-22: MLE Ratio of Increased Rock Mass Hydraulic Conductivities Simulation to Reference Case Simulation 77

Figure 2-23: Block View Showing the Depth of Penetration of a Tracer after 120,000 Years for a Reference Case Paleohydrogeologic Scenario 77

Figure 2-24: Vertical Profile Plots of Tracer Concentrations for the Paleohydrogeologic Simulations at the Location of the Hypothetical Repository Footprint at 120,000 Years 78

Figure 2-25: Block View Showing the Depth of Penetration of a Tracer after 120,000 Years for the nn9921 Paleoclimate Boundary Conditions (fr-base-paleo-cold) 80

Figure 2-26: Block View Showing the Depth of Penetration of a Tracer after 120,000 Years for the nn9930 Paleoclimate Boundary Conditions and a Loading Efficiency of 1 (fr-base-paleo-le1) 81

Figure 2-27: Block View Showing the Depth of Penetration of a Tracer after 120,000 Years for the nn9930 Paleoclimate Boundary Conditions and a Loading Efficiency of 0 (fr-base-paleo-le0) 81

Figure 2-28: Block View Showing the Depth of Penetration of a Tracer after 120,000 Years for the nn9930 Paleoclimate Boundary Conditions, a Loading Efficiency of 1, and a 0% of Ice-Sheet Thickness Equivalent Freshwater Head for the Surface Hydraulic Boundary Condition (fr-base-paleo-0-le1) 82

Figure 2-29: Péclet Number of Molecular Diffusion versus Time at the Hypothetical Repository Footprint for the Reference Paleohydrogeological Scenario (fr-base-paleo) 84

Figure 2-30: Péclet Number of Molecular Diffusion versus Time at the Hypothetical Repository Footprint for the Paleohydrogeological Scenario with Increased Rock Mass Hydraulic Conductivity (fr-base-paleo-sens) 85

Figure 2-31: Péclet Number of Molecular Diffusion versus Time at the Hypothetical Repository Footprint for nn9930 Paleoclimate Boundary Conditions and a Loading Efficiency of 0 (fr-base-paleo-le0) 86

Figure 2-32: Péclet Number of Molecular Diffusion versus Time at the Hypothetical Repository Footprint for nn9930 Paleoclimate Boundary Conditions, a Loading Efficiency of 1, and a 0% of Ice-Sheet Thickness Equivalent Freshwater Head for the Surface Hydraulic Boundary Condition (fr-base-paleo-0-le1) 87

Figure 2-33: Environmental Head versus Time for the Reference Paleohydrogeological Scenario (fr-base-paleo) 88

Figure 2-34: Environmental Head versus Time for nn9930 Paleoclimate Boundary Conditions and a Loading Efficiency of 0 (fr-base-paleo-le0) 89

Figure 2-35: Environmental Head versus Time for nn9930 Paleoclimate Boundary Conditions, a Loading Efficiency of 1, and a 0% of Ice-Sheet Thickness Equivalent Freshwater Head for the Surface Hydraulic Boundary Condition (fr-base-paleo-0-le1) 90

Figure 2-36: Vertical Profile Plots of TDS Concentrations for the Paleohydrogeologic Simulations at 120,000 Years at the Location of Hypothetical Repository Footprint 92

Figure 2-37: Environmental Head versus Time for the Paleohydrogeological Scenario without Salinity (fr-base-paleo-nobrine) 95

Figure 2-38: Vertical Profile Plots of Freshwater Heads for the Paleohydrogeologic Simulations at 120,000 Years at the Location of Hypothetical Repository Footprint 96

Figure 2-39: Vertical Profile Plots of Mean Life Expectancies at One Million Years for the Reference Case and Additional Sensitivity Scenarios 100

Figure 2-40: Vertical Profile Plots of Total Dissolved Solids Concentrations at One Million Years for the Reference Case and Additional Sensitivity Scenarios 101

Figure 2-41: Total Dissolved Solids Concentrations at One Million Years for a Three Order of Magnitude Enhancement in Hydraulic Conductivities 102

Figure 2-42: Porewater Velocity Magnitude for a Three Order of Magnitude Enhancement in Hydraulic Conductivities 102

Figure 3-1: Typical CANDU Fuel Bundle 111

Figure 3-2: Typical Microstructure of Unirradiated and Irradiated UO_2 Fuel 113

Figure 3-3: Grain Growth in Irradiated UO_2 Fuel 114

Figure 3-4: Segregation of Metallic Fission Products from UO_2 Fuel 114

Figure 3-5: Illustrative Distribution of Some Fission Products and Actinides within a Used-Fuel Element 116

Figure 4-1: Illustration of an APM Facility in Sedimentary Rock 128

Figure 4-2: APM Surface Facilities Layout 130

Figure 4-3: Copper Used-fuel Container and Fuel Basket 132

Figure 4-4: Shielded Frame and Air-cushion Transporter 136

Figure 4-5: Inerting Station 138

Figure 4-6: Welding Station 138

Figure 4-7: Friction Stir Welding of a Copper Lid 139

Figure 4-8: Machining Station 140

Figure 4-9: Non-destructive Testing Station 140

Figure 4-10: Used Fuel Packaging Plant – Container Transfer Level 143

Figure 4-11: Used Fuel Packaging Plant – Operation Level 145

Figure 4-12: Used Fuel Packaging Plant – Cross-Section 147

Figure 4-13: Container and Pedestal Configuration 150

Figure 4-14: Underground Repository Layout 156

Figure 4-15: Longitudinal Section of Placement Room 158

Figure 4-16: Legend for Container Placement Equipment 161

Figure 4-17: Container Placement – Sequence of Operations 162
Figure 5-1: Radioactivity of Used CANDU Fuel (220 MWh/kgU burnup) 176
Figure 5-2: Amounts of Key Long-Lived Radionuclides in Used Fuel (220 MWh/kg U burnup) 177
Figure 5-3: Heat Output of a Used Fuel Container with 360 Used Fuel Bundles 178
Figure 5-4: Equivalent Volume of Gas at Standard Temperature and Pressure Produced in a CANDU Fuel Element (220 MWh/kgU burnup) 180
Figure 5-5: Illustrative Example of the Range of Temperature Variation over Time in a Placement Room 187
Figure 5-6: Illustrative Container Temperature Profiles at Three Generalized Locations within a Repository 197
Figure 5-7: Schematic Representation of the Loading History in a Repository 199
Figure 5-8: Reaction Scheme for the Uniform Corrosion of Copper in Compacted Bentonite Saturated with O_2-Containing Chloride Solution 207
Figure 5-9: Early Evolution of Conditions in a Container with a Small Defect in the Copper Shell 213
Figure 5-10: Radiation Dose Rate in Water at the Fuel Surface (220 MWh/kgU burnup) 218
Figure 5-11: Hydraulic Conductivity and Swelling Pressure under Saline Water Conditions: Variation with Effective Montmorillonite Dry Density 225
Figure 5-12: Thermal Conductivity of 50:50 wt% Bentonite-Sand Buffer (BSB) and of 100 wt% MX-80 Bentonite 227
Figure 5-13: Effect of Water Activity on Aerobic Culturability in Compacted Bentonite 230
Figure 5-14: Simulated Evolution of Ice Sheet Load 237
Figure 5-15: Vertical Profile Plots of Tracer Concentrations for the Paleohydrogeologic Simulations at the Location of the Hypothetical Repository Footprint at 120,000 Years 239
Figure 5-16: Péclet Number of Molecular Diffusion versus Time at the Hypothetical Repository Footprint for the Reference Paleohydrogeological Scenario (fr-base-paleo) 240
Figure 6-1: Total Thermal Power of the Repository (Average 220 MWh/kgU Burnup) 264
Figure 7-1: General Conceptual Model for Defective Containers 316
Figure 7-2: Conceptual Model for the Waste Form and Container 317
Figure 7-3: Radiation Dose Rate in Water at the Fuel Surface (220 MWh/kgU Burnup) 319
Figure 7-4: Conceptual Model for the Geosphere 322
Figure 7-5: Conceptual Model for the Constant Biosphere 324
Figure 7-6: Environmental Transfer Model Showing Critical Group Exposure Pathways 326
Figure 7-7: Main Computer Codes 327

Figure 7-8: FRAC3DVS-OPG Site-Scale and Repository-Scale Model Domains 334
Figure 7-9: Site-Scale Model - Coordinate System and Domain Boundary 343
Figure 7-10: Site-Scale Model Element Volume 344
Figure 7-11: Site-Scale Model - Vertical Hydraulic Conductivity Profile 348
Figure 7-12: Site-Scale Model - Property Assignment on Vertical Cross-Section through Entire Model Domain 349
Figure 7-13: Site-Scale Model - Property Assignment on Vertical Cross-Section through Placement Room Seal 349
Figure 7-14: Site-Scale Model - Property Assignment on Vertical Cross-Section through Base of Vent Shaft 350
Figure 7-15: Site-Scale Model - Property Assignment on Plan View through Placement Rooms 350
Figure 7-16: Site-Scale Model - Property Assignment in 3D View 351
Figure 7-17: Site-Scale Model - Selecting Well Location 352
Figure 7-18: Site-Scale Model - Radionuclide Transport, Release from All Containers 353
Figure 7-19: Site-Scale Model - Radionuclide Transport to Different Well Locations, Release from Three Containers 354
Figure 7-20: Site Scale Model – Well Location on Cross-Section 355
Figure 7-21: Site-Scale Model - Reference Case Head Boundaries, Sides and Bottom. 356
Figure 7-22: Repository-Scale Model - 3D Visualization of Domain Elements 358
Figure 7-23: Repository-Scale Model - 3D View of Repository Room and Tunnel Seals 359
Figure 7-24: Repository-Scale Model - Section View of Repository and Geology 360
Figure 7-25: Repository-Scale Model - Plan View of Rooms and Tunnel 360
Figure 7-26: Repository-Scale Model - Vertical Slice along Placement Drift (Y = 0 m) 361
Figure 7-27: Repository-Scale Model - Vertical Slice through Placement Drift Room Seal (X = -13.0 m) 361
Figure 7-28: Repository-Scale Model - 3D View Showing Engineered Barrier System 362
Figure 7-29: Repository-Scale Model - 3D View Showing Defective Container Source Nodes 363
Figure 7-30: Repository-Scale Model - 3D View of Reference Case Head Boundary Conditions 364
Figure 7-31: Radionuclide Release Rate per Container 365
Figure 7-32: Fuel Dissolution Rate 367
Figure 7-33: SYVAC3-CC4 Repository Model 368
Figure 7-34: SYVAC3-CC4 Transport Network Showing Connectivity 372

Figure 7-35: Site-Scale Model - Comparison of Hydraulic Heads with Regional Model at Guelph Formation Elevation (87 mASL) 383
Figure 7-36: Site-Scale Model - Comparison of Velocities in the Guelph Formation with Regional Model 384
Figure 7-37: Site-Scale Model - Comparison of Velocities at a Vertical Cross-Section along Access Tunnel 1 385
Figure 7-38: Site-Scale Model - Mean Life Expectancy 386
Figure 7-39: Site-Scale Model - Reference Case Hydraulic Head Distribution 387
Figure 7-40: Site-Scale Model - Reference Case Advective Velocity Distribution 388
Figure 7-41: Site-Scale Model - Mean Life Expectancy at Repository Centre 389
Figure 7-42: Site-Scale Model - Mean Life Expectancy at Water Supply Well 389
Figure 7-43: Site-Scale Model - Reference Case I-129 Concentration at 500,000 Years 391
Figure 7-44: Site-Scale Model - Reference Case I-129 Concentration at One Million Years 392
Figure 7-45: Site-Scale Model - Reference Case Cs-135 Concentration at One Million Years 393
Figure 7-46: Site-Scale Model - Reference Case Radionuclide Transport to Well 394
Figure 7-47: Site-Scale Model - Geosphere Hydraulic Conductivity Increased by a Factor of 10: I-129 Concentration at 500,000 Years 395
Figure 7-48: Site-Scale Model - Geosphere Hydraulic Conductivity Increased by a Factor of 10: I-129 Concentration at One Million Years 396
Figure 7-49: Site-Scale Model - Hydraulic Conductivity Increase by a Factor of 10: Radionuclide Transport to Well 397
Figure 7-50: Site-Scale Model - Spatial Convergence Sensitivity Comparison of Head Contours 399
Figure 7-51: Site-Scale Model - Spatial Convergence Sensitivity I-129 Plume 400
Figure 7-52: Site-Scale Model - Spatial Convergence Sensitivity, I-129 Transport 401
Figure 7-53: Site-Scale Model - Time Step Convergence Sensitivity: I-129 Transport to the Well 402
Figure 7-54: Site-Scale Model - I-129 Transport in Sensitivity Cases 403
Figure 7-55: FRAC3DVS-OPG - I-129 Transport through Barriers and Selected Geosphere Formations 404
Figure 7-56: FRAC3DVS-OPG - Cs-135 Transport through Barriers and Selected Geosphere Formations 404
Figure 7-57: FRAC3DVS-OPG - U-238 Transport through Barriers and Selected Geosphere formations 405
Figure 7-58: Repository-Scale Model - Head at Tunnel Elevation 406

Figure 7-59: Repository-Scale Model - Advective Velocities at Tunnel Elevation 407
Figure 7-60: Repository-Scale Model - 3D View of Advective Velocity Magnitudes 408
Figure 7-61: Repository-Scale Model - Control Surface for Calculation of Radionuclide Releases from Repository 409
Figure 7-62: Repository-Scale Model - I-129 Concentrations at 25,000 Years 410
Figure 7-63: Repository-Scale Model - I-129 Concentrations at 100,000 Years 411
Figure 7-64: Repository-Scale Model - I-129 Concentrations at One Million Years 412
Figure 7-65: Repository-Scale Model - U-238 Concentration at One Million Years 413
Figure 7-66: Repository-Scale Model - Cs-135 Concentrations at 100,000 Years 414
Figure 7-67: Repository-Scale Model - Cs-135 Concentrations at One Million Years 415
Figure 7-68: Repository-Scale Model - Transport Rates out of the Placement Room for I-129, Cs-135, U-234 and U-238 416
Figure 7-69: Comparison of SYVAC3-CC4 and FRAC3DVS-OPG Transport of I-129 and Cs-135 to the Geosphere 417
Figure 7-70: Comparison of SYVAC3-CC4 and FRAC3DVS-OPG Transport of U-234 and U-238 to the Geosphere 418
Figure 7-71: Comparison of SYVAC3-CC4 and FRAC3DVS-OPG Transport of I-129 and Cs-135 420
Figure 7-72: SYVAC3-CC4 - Reference Case Total Dose Rate 422
Figure 7-73: SYVAC3-CC4 - Reference Case Individual Radionuclide Dose Rates 423
Figure 7-74: SYVAC3-CC4 - Sensitivity to a Factor of 10 Increase in Fuel Dissolution Rate 425
Figure 7-75: SYVAC3-CC4 - Sensitivity to a Factor of 10 Increase in Container Defect Area 426
Figure 7-76: SYVAC3-CC4 - Sensitivity to All Instant Release Fractions Set to 10 Percent 427
Figure 7-77: SYVAC3-CC4 - Sensitivity to a Factor of 10 Increase in Geosphere Diffusivity 428
Figure 7-78: SYVAC3-CC4 - Result Summary for Defective Physical Barrier Sensitivity Cases 429
Figure 7-79: SYVAC3-CC4 - Sensitivity to No Sorption in the Geosphere 431
Figure 7-80: SYVAC3-CC4 - Sensitivity to No Solubility Limits 432
Figure 7-81: SYVAC3-CC4 - Sensitivity to No Sorption in the EBS 433
Figure 7-82: SYVAC3-CC4 - Sensitivity to Low Sorption in the Geosphere with Coincident High Solubility Limits 434
Figure 7-83: SYVAC3-CC4 - Summary for Defective Chemical Barrier Sensitivity Cases 435
Figure 7-84: SYVAC3-CC4 - Distribution of Container Failures for 120,000 Simulations 437

Figure 7-85: SYVAC3-CC4 - Distribution of the Maximum Dose Rate for Simulations with at Least One Defective Container 438
Figure 7-86: SYVAC3-CC4 - Average Dose Rate With 95% Confidence Bounds 440
Figure 7-87: SYVAC3-CC4 - Dose Rate Percentile Bands 441
Figure 7-88: General Sequence of Events for Inadvertent Human Intrusion 443
Figure 7-89: Inadvertent Human Intrusion - General Conceptual Model 446
Figure 7-90: Inadvertent Human Intrusion - Exposure as a Function of Intrusion Time without Leaching 449
Figure 7-91: Inadvertent Human Intrusion - Exposure Pathway Doses for Drill Crew 450
Figure 7-92: Inadvertent Human Intrusion - Exposure Pathway Dose Rates for Resident 450
Figure 7-93: Dose Rate to Resident as a Function of Arrival Times Assuming Intrusion Occurs 300 Years after Closure 451
Figure 7-94: Effect of Rn-222 and Short-Lived Daughters in Groundshine Pathway on Resident Exposure 452
Figure 7-95: All Containers Fail at 60,000 Years - Dose Rate 455
Figure 7-96: All Containers Fail at 60,000 Years – Contributing Radionuclides 456
Figure 7-97: Sensitivity - All Containers Fail at 10,000 Years - Dose Rate 457
Figure 7-98: SYVAC3-CC4 – Reference Case Results for Complementary Indicators 467
Figure 7-99: SYVAC3-CC4 – Radiotoxicity Transport Complementary Indicator 468
Figure 7-100: FRAC3DVS-OPG - Copper Transport to the Surface both With and Without Sorption 476
Figure 8-1: Capillary Pressure Curves for Placement Room Bentonite (Homogenized Bentonite), Repository Inner EDZ, and the Cobourg Formation 500
Figure 8-2: Relative Gas Permeability Curves for Placement Room Bentonite (Homogenized Bentonite), Repository Inner EDZ, and the Cobourg Formation 500
Figure 8-3: Relative Liquid Permeability Curves for Placement Room Bentonite (Homogenized Bentonite), Repository Inner EDZ, and the Cobourg Formation 501
Figure 8-4: Main Computer Code 502
Figure 8-5: Room-Scale Model – Illustration 506
Figure 8-6: Room-Scale Model – Drift End of Room 506
Figure 8-7: Room-Scale Model – Cross-Sections showing Container and Seal 507
Figure 8-8: Room-Scale Model – Plan Section Cutting Middle of Placement Room 508
Figure 8-9: Room-Scale Model – Plan View Showing GGM Nodes 510
Figure 8-10: Repository-Scale Model – Plan View through the Main Drift 510

Figure 8-11: Repository-Scale Model – Drift and Shaft Discretization 511
Figure 8-12: Repository-Scale Model – Plan View of Main Shaft Discretization 512
Figure 8-13: Repository-Scale Model – Gas Injection Locations 513
Figure 8-14: Room Scale Model – Steel Consumption and Corrosion Processes 514
Figure 8-15: Room Scale Model – Conditions Prior to Container Failure 515
Figure 8-16: Room Scale Model – Nodal and Average Pressures Prior to Container Failure 516
Figure 8-17: Room Scale Model – Conditions after Container Failure 517
Figure 8-18: Room Scale Model – Nodal and Average Pressures after Container Failure 518
Figure 8-19: Room Scale Model – Gas Distribution 519
Figure 8-20: Room Scale Model – Gas Flow Rates 520
Figure 8-21: Repository-Scale Model – Distribution of Free-Phase Gas 521
Figure 8-22: Repository-Scale Model – Gas flow Out of the Top of the Model 522
Figure 8-23: Repository-Scale Model – Dissolved Gas Flow Out of the Top of the Model 522
Figure 8-24: Repository-Scale Model – Pore Pressure 523
Figure 8-25: Rate at Which C-14 Enters the Guelph Formation 525
Figure 10-1: Cigar Lake Ore Deposit 536
Figure 10-2: Naturally Occurring Fission Reactor 538
Figure 10-3: Copper Analogues 540
Figure 10-4: Bentonite Clay 542
Figure 10-5: 1.5 Ma Sequoia-like Tree Stumps at Dunarobba, Italy 543
Figure 10-6: Swelling Pressures of Various Bentonites across a Range of Equivalent Montmorillonite Dry Densities (EMDD) 544
Figure 12-1: Illustration of Radionuclide Transport in the Repository System 565
Figure A-1: The Swiss Repository Concept in Opalinus Clay A-2
Figure A-2: The French Repository Concept for Vitrified HLW in Callovo-Oxfordian Clay A-3
Figure A-3: The French Repository Concept for Spent Fuel in Callovo-Oxfordian Clay A-4
Figure A-4: Cross Section View of the Belgian Supercontainer Concept for HLW A-5

THIS PAGE HAS BEEN LEFT BLANK INTENTIONALLY

1. INTRODUCTION

1.1 Purpose and Scope

The purpose of this report is to present a case study that illustrates the Nuclear Waste Management Organization's (NWMO) approach to conducting a safety assessment of a repository for used CANada Deuterium-Uranium reactor (CANDU) fuel within a hypothetical sedimentary setting in southern Ontario. This study complements a similar study completed for a used fuel deep geological repository in crystalline rock (NWMO 2012). These studies are intended to show how the safety assessment approach can be applied to both geological settings and how the approach is consistent with Canadian Nuclear Safety Commission (CNSC) Guide G-320 on Assessing the Long Term Safety of Radioactive Waste Management (CNSC 2006).

As part of this case study, a reference Adaptive Phased Management (APM) facility is described and assessed. The APM facility is a self-contained complex with a combination of surface and underground engineered structures designed to provide multiple isolation barriers and passive systems to provide long-term containment and isolation. It consists of the surface facilities and the Deep Geological Repository (DGR). The approach, methods and tools for conducting a postclosure safety assessment, which contribute to the repository safety case, are fully described. The results of the safety assessment for a hypothetical site are presented to illustrate the multi-barrier deep geological repository concept and provide evidence of how Canadian regulatory requirements can and will be met.

An actual licence application to prepare the site and to construct a used fuel repository will be supported by a site-specific safety case. A safety case is defined as the integration of arguments and evidence that describe, quantify and substantiate the safety, and the level of confidence in the safety, of the deep geological repository and associated facilities. It includes the collection of scientific and technical arguments and evidence in support of the safety of the APM facility covering the site characterization and geosynthesis, the design, construction and operation of the facility, the assessment of risk during operation and postclosure, and quality assurance of all safety-related work associated with the facility.

This definition is consistent with the CNSC Guide G-320 as well as international guidance. The International Atomic Energy Agency (IAEA) also provides guidance in SSG-23 – Safety Case and Safety Assessment for the Disposal of Radioactive Waste (IAEA 2012), where it notes that the primary objective of a safety case is to allow for informed decisions to be made that are commensurate with the lifecycle phase of the project.

The level of detail in the current study is consistent with the pre-project stage of the APM facility and is not a full safety case. It considers a hypothetical site for a deep geological repository in sedimentary rock, and therefore does not include a geosynthesis. It identifies and analyzes key scenarios, but does not assess all possible scenarios associated with the safety case for an actual site. The current study builds upon previous safety studies that were completed by Atomic Energy of Canada Limited (AECL) and Ontario Power Generation.

Site-specific information will be used in a licence application for a selected site for the APM facility. However, at this pre-project stage and in place of site-specific information, data

representing a sedimentary setting are used to illustrate how the postclosure safety assessment can be carried out consistent with Canadian regulatory requirements.

A preclosure safety assessment is not included in the present report. However preclosure safety, including transportation safety, and conventional safety, will be assessed as part of a licence application for a future-selected site. A special project arrangement has been agreed to by NWMO and the CNSC that includes a CNSC review of the design concepts for the APM (CNSC and NWMO 2008). NWMO's request for a regulatory review of this pre-project report is consistent with CNSC Guide G-320 which states that:

> "*It is up to the applicant to determine an appropriate methodology for achieving the long term safety of radioactive waste based on their specific circumstances; however, applicants are encouraged to consult with CNSC staff throughout the pre-licensing period on the acceptability of their chosen methodology*."

This review is similar to other CNSC pre-project reviews conducted for new nuclear power plants.

1.2 Background and Project Overview

For decades Canadians have been using electricity generated by nuclear power reactors in Ontario, Quebec and New Brunswick. When used nuclear fuel is removed from a reactor, it is considered a waste product, is radioactive and requires careful management. Although its radioactivity decreases with time, chemical toxicity persists and the used fuel will remain a potential health risk for many hundreds of thousands of years. Canada's used nuclear fuel is now safely stored on an interim basis at licensed facilities located where it is produced.

Investigations into the long-term management of used nuclear fuel have a long history in Canada. The deep geological repository concept was identified at the start of the Canadian nuclear program. In 1977, a task force commissioned by Energy, Mines and Resources Canada recommended burial in geological formations with a preference for crystalline rock of the Canadian Shield, but noted that other rock types such as sedimentary rock and salt should also be studied (Hare et al. 1977). Also in 1978, the Porter Commission for Electricity Planning in Ontario recommended that an independent committee be established. The committee would be tasked with reporting progress on waste disposal research and demonstration, to support additional power plant capacity in Ontario. Subsequently, the governments of Canada and Ontario initiated the Canadian Nuclear Fuel Waste Management Program in 1980.

Based on this Canadian program and parallel international work, the concept for a deep geological repository was developed by AECL. The work included an underground research laboratory in Manitoba, in which approaches and materials were tested. The AECL concept was then submitted for review by a federal independent environmental assessment panel. For this review, AECL completed two case studies illustrating the deep geological repository concept in crystalline Canadian Shield settings. AECL submitted its Environmental Impact Statement to the federal review panel in 1994. In 1998, the panel made a number of recommendations and identified the following key conclusions (CEAA 1998):

- *"From a technical perspective, safety of the AECL concept has been on balance adequately demonstrated for a conceptual stage of development, but from a social perspective, it has not.*
- *As it stands, the AECL concept for deep geological disposal has not been demonstrated to have broad public support. The concept in its current form does not have the required level of acceptability to be adopted as Canada's approach for managing nuclear fuel wastes."*

After 1995, research on the deep geological repository concept continued under Ontario Power Generation funding. As part of this, Ontario Power Generation completed a case study identified as the "Third Case Study" in 2004, which considered a third hypothetical Canadian Shield site and used current design concepts, data and assessment methodologies (Gierszewski et al. 2004).

The NWMO was created by Canada's nuclear energy generators as a requirement of the *Nuclear Fuel Waste Act* in 2002, which largely incorporated the recommendations from the earlier federal review panel. It required the NWMO to study possible approaches, recommend an approach, and then implement the approved plan for the long-term management of Canada's used nuclear fuel.

In 2005, based on extensive discussions across Canada, the NWMO recommended the APM approach, which consists of both a technical method and a management system. Its key attributes include:

- Ultimate centralized containment and isolation of used nuclear fuel in an appropriate geological formation;
- Phased and adaptive decision-making; and
- Citizen engagement throughout all phases of implementation.

Following the 2007 decision by the Government of Canada to support the recommended approach, the NWMO collaboratively developed with Canadians an approach for the implementation of APM. The NWMO is implementing this approach that is consistent with Canadian federal government policy and with international best practice in its development of a deep geological repository.

A siting process was developed and initiated in May 2010 to find a suitable site for a used fuel deep geological repository in a willing host community. As of December 2013, there are 17 communities engaged in exploring potential interest in hosting this national infrastructure project. These communities are located in both crystalline and sedimentary rock settings.

The NWMO is developing a deep geological repository concept for both crystalline and sedimentary rock settings, associated surface facilities and a used fuel transportation system. The repository system is a multiple-barrier concept designed to safely contain and isolate used nuclear fuel over the long term.

The current conceptual design in sedimentary rock consists of a repository constructed for a reference inventory of 4.6 million used CANDU fuel bundles at a depth of approximately 500 metres. It contains a network of placement rooms for used fuel containers (see Figure 1-1).

The actual depth of the repository will depend on geologic characteristics at the selected site, along with other design features and safety considerations.

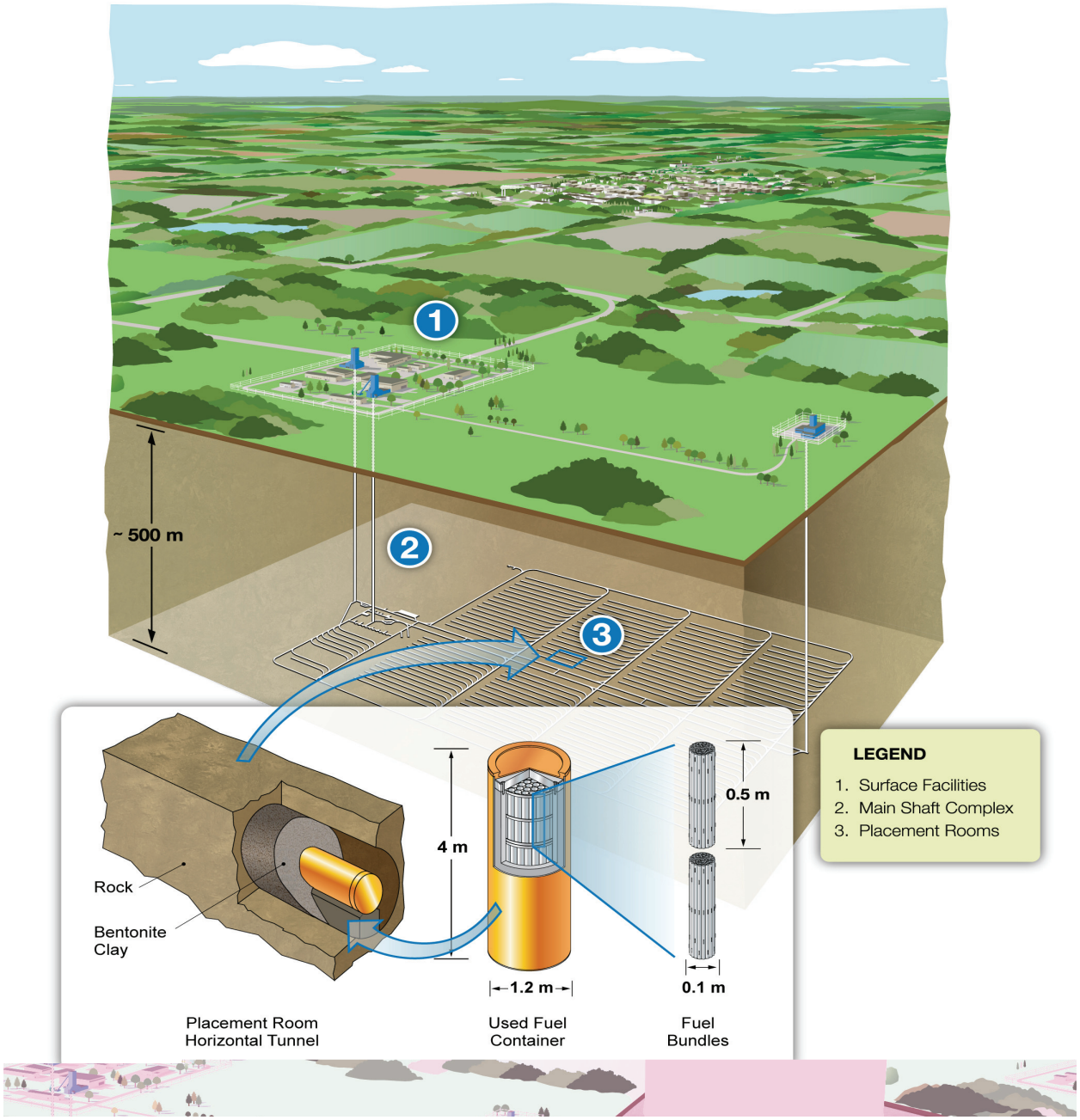

Note: This figure is not to scale.

Figure 1-1: Illustration of Deep Geological Repository Concept

Used fuel will be loaded into licensed transport casks at the interim storage facilities at the reactor sites and transported to the deep geological repository facility where it will be repackaged in corrosion-resistant containers for placement underground. In the reference concept for sedimentary rock, the used fuel containers will be transferred underground via a shaft, placed horizontally on high density bentonite pedestals along the axis of the placement room and surrounded by clay material, with the remaining void spaces backfilled and sealed.

A similar case study was completed in 2012 for used fuel deep geological repository in crystalline rock (NWMO 2012).

1.3 APM Project Phases

The APM project is divided into phases that are linked to the major licensing activities for a nuclear facility in Canada. NWMO is committed to a step-wise decision-making process and will only proceed to the next step after careful consideration and with societal support. Assumed progress through the phases of APM is based on a number of assumptions and decisions, which may differ in terms of scope of work and timing of activities.

This section briefly describes the phases of APM, along with the milestones and the assumed timeline associated with each, providing context for the broader implementation plan. The timeline illustrating these phases is provided in Figure 1-2. The legal framework that governs these licensing activities is further described in Section 1.5.

1.3.1 Siting and Preparing for Construction

The Site Selection Process was launched by the NWMO in 2010 after a dialogue with interested Canadians. It has been designed to identify an informed and willing host community for the APM facility and to ensure that the site selected to host the facility will safely contain and isolate used nuclear fuel. The Site Selection Process is a nine-step process based on social and technical considerations. Site screening criteria have been established to ensure that documented safety criteria are defined at an early step in the siting process. These criteria will be used in the site evaluations, which include studies to confirm site suitability that could support a future licence application. Section 1.6.3 of this report highlights the evaluation factors used in the process. The timeframe associated with completing surface and subsurface investigations at a candidate site is about 5 years.

An application for a licence to prepare the site and to construct the facility will be submitted for a selected site. Licences are issued under the *Nuclear Safety and Control Act*. Licences can only be issued once an environmental assessment has been completed and a series of steps in the CNSC's licensing process have been completed. This phase of the project is expected to last five years or more and will begin by submitting a project description to the CNSC. Subsequently, a Preliminary Safety Report, an Environmental Impact Statement (EIS) and other supporting documents, will demonstrate compliance with the regulatory requirements as set out in the *Nuclear Safety and Control Act* and its associated regulations, as well as in the EIS Guidelines for the environmental assessment (EA).

Figure 1-2: Illustrative APM Implementation Schedule for Planning Purposes

1.3.2 Site Preparation and Construction

On receipt of the licence to prepare the site and construct the facility, the site will be prepared for construction by clearing, site grading, installing fencing, installing temporary construction services, and establishing a surface water management system. The first phase of construction will be to excavate the shafts and an underground demonstration facility. This phase is expected to last about five years, the time needed to sink the shafts, construct the demonstration facility, complete the detailed design and update the safety case. It is described in more detail in Chapter 4.

After the final design is completed, the construction of the full-scale underground repository and associated surface facilities can begin. The purpose of this construction phase is to excavate and erect all of the facilities necessary for the operation of the repository. This phase is expected to last about five years.

Therefore, the total site preparation and construction phase could be about 10 years.

1.3.3 Operation

The operation of the repository will only begin once a licence to operate the facility has been issued. Operation will consist of receiving used nuclear fuel transported to the site, re-packaging the used fuel into long-lived containers, placing the used fuel containers in the repository, and continued underground development. All activities will be executed in compliance with the supporting documents used to obtain the operating licence.

For a reference used fuel inventory of 4.6 million used CANDU fuel bundles, these operational activities are expected to last about 40 years. The actual duration of repository operation will depend on the total inventory of used fuel to be managed at the site and the timing of its production, transportation considerations and other operational factors.

1.3.4 Extended Monitoring

Following placement of used fuel in the repository, a period of monitoring is assumed to continue for an extended period of time. The duration of extended monitoring will be decided in collaboration with a future society. For planning purposes, the period of extended monitoring is assumed to be up to 70 years.

Towards the end of the extended monitoring period (i.e., during the last five years), a detailed decommissioning plan will be prepared, the detailed design of the shaft sealing system will be finalized, and an application to decommission the facility will be submitted to the CNSC.

1.3.5 Decommissioning

Decommissioning will only begin once a licence to decommission has been issued. It is expected that an Environmental Assessment to cover decommissioning activities will also be needed prior to the issuance of a decommissioning licence. The decommissioning of the facility will include sealing of access tunnels and shafts, and removal of surface facilities. In the case of a deep geological repository, decommissioning does not include the removal of the used fuel placed in the repository. The site will be restored to a defined end-state that will depend largely

on future plans for the site (e.g., industrial, forestry, park, or wilderness). For planning purposes, the period of decommissioning is assumed to be 30 years.

A formal licence to abandon the facility could be obtained once the decommissioning and monitoring results have confirmed that it is acceptable to release the facility from CNSC regulatory control. An application for this licence will include a decommissioning end-state report and other supporting licensing documents. It is anticipated that appropriate institutional controls will be put in place at that time.

1.4 Repository Timeframes

In this safety assessment the potential impact of a repository is assessed in accordance with the CNSC Policy P-290 (CNSC 2004), which requires that, "the assessment of future impacts of radioactive waste on the health and safety of persons and the environment encompasses the period of time when the maximum impact is predicted to occur." In discussing the long-term evolution of a repository system, it is helpful to consider a sequence of timeframes during which certain events or processes dominate in the postclosure period.

1.4.1 Preclosure Period

The preclosure period is intended to cover the activities described in Sections 1.3.1 to 1.3.5 and is assumed to last up to about 160 years (see Figure 1-2).

During this time, the reference inventory of 4.6 million used nuclear fuel bundles will be transported to the APM facility, encapsulated in approximately 12,800 long-lived used fuel containers, transferred to the underground repository and surrounded by clay-based sealing materials. The total radioactivity in the repository will increase as more used fuel is placed in the repository, and then start to decrease due to radioactive decay.

1.4.2 Postclosure Period

The postclosure period starts at the end of decommissioning, after the shafts have been sealed and the surface facilities have been dismantled.

In the postclosure period, the site is assumed to remain under institutional controls for a period of time. Based on CNSC Guide G-320 (CNSC 2006), and IAEA Safety Series No. 111-F (IAEA 1995), institutional controls can be defined as, "the control of residual risks at a site (by a designated Institution or Authority) after it has been decommissioned." These controls can include both active measures (requiring activities on the site such as monitoring and maintenance) and passive measures (that do not require activities on the site, such as land use restrictions, as well as measures taken to support societal memory). Such measures should prevent inappropriate land use, including drilling, deep excavation, or disruption of the shaft seals.

Institutional controls and societal memory can continue indefinitely to preserve knowledge of the repository. However, it is assumed for safety assessment purposes that these institutional controls or societal memory are only effective for about 300 years. This is consistent with international practice for excluding inadvertent human intrusion during this period when assessing the risks associated with this scenario.

The postclosure period is described in four timeframes. Each of the timeframes is also described in this section. To provide context for these timeframes, Figure 1-3 highlights timescales for relevant past events and expected future events in the Earth's history.

1 - 1,000 years

At the beginning of this time, the facility is decommissioned. Distinct physical and chemical differences exist between the various components of the repository, and between the repository and the geosphere. The containers reach their peak temperature. Slow migration of groundwater into the repository occurs. Especially during the first 500 years, radioactivity and heat in the used fuel decrease significantly due to the decay of most of the fission products.

1,000 - 60,000 years

This time period represents conditions with no glaciation coverage of the site. During this period, the initial sharp physical and chemical gradients around the repository slowly diminish. Slow saturation of the repository by groundwater occurs, which is accompanied by swelling of bentonite sealing materials. The surrounding sedimentary rock reaches its peak temperature and largely cools back down to approximately ambient temperatures. Surface conditions are likely to change reflecting human activities and natural evolution, possibly in response to climate change. Although the overall climate is likely to remain temperate, climate changes could include global warming in the near term, and the advent of cooler climate in the long term.

60,000 - 1,000,000 years

Over this timescale, the main perturbations in the system cease to be repository-driven. Instead, there are regional-scale changes in the geosphere that in turn may be transmitted to the repository. In particular, during this timeframe, climate change initiated by broad changes in solar insolation patterns may occur leading to initiation of a new glaciation cycle. Based on past history, several cycles of glaciation are likely to occur over the next million years.

1,000,000 years and beyond

Beyond this timescale, the repository will be a relatively passive feature of the geosphere, in quasi-equilibrium with the surrounding rock. The dominant processes will be regional perturbations to the geosphere that in turn affect the repository. Over this longer time period, the changes will include slow-acting tectonic forces, and cumulative erosion or deposition processes.

In the safety analysis presented in this report, the discussion of the evolution of a repository focuses on the interval covered by the first three postclosure timeframes, i.e., up to one million years. It will be during this period that the differences between the natural environment and an engineered repository for used fuel are noticeable. Long before major changes will be apparent at times beyond one million years, the total amount of radioactivity in the waste will have diminished to the point that it is similar to that of a naturally occurring uranium ore body.[1] As part of the safety case prepared for an actual candidate site, geoscientific arguments and evidence supporting the long-term stability and resilience to change of a sedimentary rock environment would also be presented.

[1] With about 90,000 Mg of uranium, it will be smaller than large ore bodies like Cigar Lake and MacArthur River in Saskatchewan.

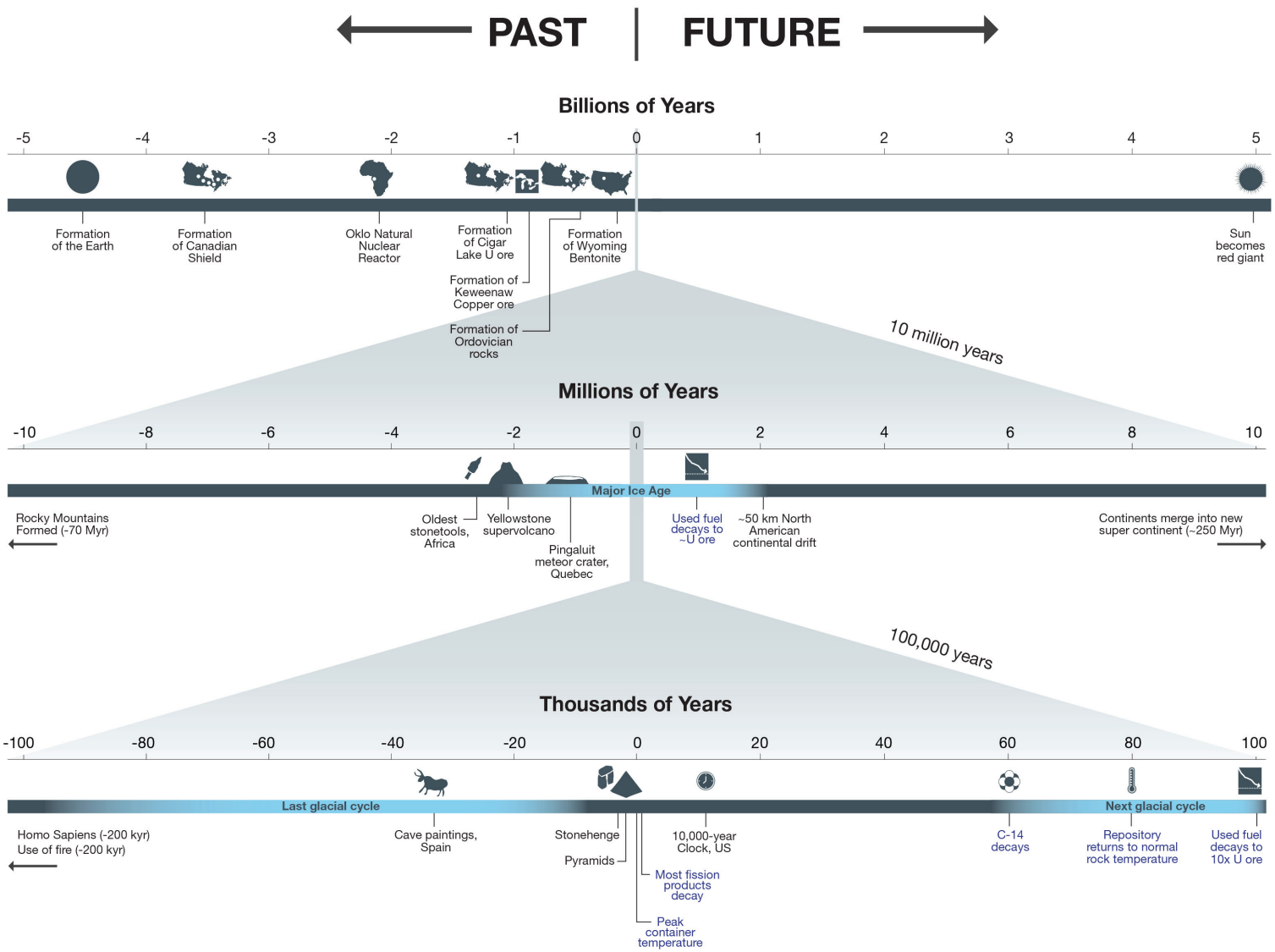

Figure 1-3: Perspective of Past Events and Expected Future Events in Earth's History Including Repository Events

1.5 Relevant Legislation

This section presents the regulatory requirements under the *Nuclear Safety and Control Act* and its associated regulations, as well as the international guidance on safety of a deep geological repository.

The intention is for the deep geological repository to meet or exceed all regulatory requirements and to be consistent with international practices during site preparation, construction, operation, and beyond.

1.5.1 CNSC Regulatory Requirements

In accordance with paragraph 2(g) of *Nuclear Safety and Control Act* and paragraph 1(e) of the Class I Nuclear Facilities Regulations, the repository is a Class 1B nuclear facility.

Paragraph 26(e) of the Act states that, "subject to the Regulations, no person shall, except in accordance with a licence…prepare a site for, construct, operate, modify, decommission or abandon a nuclear facility". The following licences are required over the life of the repository:

- Site Preparation Licence;
- Construction Licence;
- Operating Licence;
- Decommissioning Licence; and
- Abandonment Licence.

The detailed requirements to obtain a licence are described in Section 3 of the General Nuclear Safety and Control Regulations and in Sections 3, 4 and 5 of the Class I Nuclear Facilities Regulations. Other applicable regulations include the Nuclear Security Regulations, Radiation Protection Regulations, Packaging and Transport of Nuclear Substances Regulations, which apply to all nuclear facilities, and the Uranium Mines and Mills Regulations – due to similarities of some aspects of the APM facility (i.e., deep geological repository) to a mining project.

In addition to the regulations, a number of CNSC regulatory documents in the following categories are also applicable:

- Regulatory policies – describe general principles applied by the CNSC in their review;
- Regulatory documents and standards – establish regulatory standards; and
- Regulatory guides – set out regulatory expectations.

In Canada, the primary regulatory requirements and expectations for the assessment of long-term safety of radioactive waste management are given in the CNSC Policy P-290 (CNSC 2004) and CNSC Guide G-320 (CNSC 2006) and these are the focus of this pre-project report. These and other regulatory documents that will apply to the APM project in support of a future licence application are listed in Table 1-1.

Table 1-1: CNSC Regulatory Documents Applicable to the APM Project

Document Number	Title
Pre-project Report	
P-290	Managing Radioactive Waste (CNSC 2004)
G-320	Assessing the Long Term Safety of Radioactive Waste Management (CNSC 2006)
Licence Application	
P-119	Policy on Human Factors
P-211	Compliance
P-223	Protection of the Environment
P-299	Regulatory Fundamentals
P-325	Nuclear Emergency Management
R-72	Geological Considerations in Siting a Repository for Underground Disposal of High-Level Radioactive Waste
G-129 Rev.1	Keeping Radiation Exposures and Doses "As Low as Reasonably Achievable (ALARA)"
G-205	Entry to Protected and Inner Areas
G-206	Financial Guarantees for the Decommissioning of Licensed Activities
G-208	Transportation Security Plans for Category I, II or III Nuclear Material
G-219	Decommissioning Planning for Licensed Activities
G-221	A Guide to Ventilation Requirements for Uranium Mines and Mills
G-225	Emergency Planning at Class I Nuclear Facilities and Uranium Mines and Mills
G-274	Security Programs for Category I or II Nuclear Material or Certain Nuclear Facilities
G-276	Human Factors Engineering Program Plans
G-278	Human Factors Verification and Validation Plans
GD-314	Radiation Protection Programs for the Transport of Nuclear Substances
RD/GD-99.3	Public Information and Disclosure
RD-327/GD-327	Nuclear Criticality Safety
RD-336/GD-336	Accounting and Reporting of Nuclear Material
RD-353	Testing the Implementation of Emergency Measures
RD-363	Nuclear Security Officer Medical, Physical, and Psychological Fitness
RD-364	Joint Canada-United States Guide for Approval of Type B(U) and Fissile Material Transportation Packages
REGDOC- 2.9.1	Environmental Protection Policies, Programs and Procedures

Note: Current versions of the CNSC regulatory documents can be found on the CNSC website (www.cnsc-ccsn.gc.ca).

CNSC Policy P-290 (CNSC 2004) identifies the need for long-term management of radioactive waste and hazardous waste arising from licensed activities. The principles espoused by CNSC Policy P-290 that relate to long-term management are the following:

- The management of radioactive waste is commensurate with its radiological, chemical, and biological hazard to the health and safety of persons and the environment, and to national security;
- The assessment of future impacts of radioactive waste on the health and safety of persons and the environment encompasses the period of time when the maximum impact is predicted to occur; and
- The predicted impact on the health and safety of persons and the environment from the management of radioactive waste is no greater than the impact that is permissible in Canada at the time of the regulatory decision.

Key objectives for long-term management are *containment* and *isolation* of the waste, in accordance with the CNSC Guide G-320 (CNSC 2006). The guide states that:

> *"containment can be achieved through a robust design based on multiple barriers providing defence-in-depth. Isolation is achieved through proper site selection and, when necessary, institutional controls to limit access and land use".*

CNSC Guide G-320 identifies expectations for *"developing a long term safety case that includes a safety assessment complemented by various additional arguments based on:*

1. *Appropriate selection and application of assessment strategies;*
2. *Demonstration of system robustness;*
3. *The use of complementary indicators of safety; and*
4. *Any other evidence that is available to provide confidence in the long term safety of radioactive waste management."*

Guidance is also provided for defining acceptance criteria and performing long-term assessments that includes considerations for: selection of methodology, assessment context, system description, assessment timeframes, assessment scenarios, assessment models, and the interpretation of results.

A mapping that shows how the content of this report is consistent with aspects of CNSC Guide G-320 is shown in Table 1-4 and described in more detail in Chapter 12.

1.5.2 Transportation of Used Nuclear Fuel

The safe and secure transportation of used nuclear fuel is regulated through a comprehensive multi-agency framework of regulations, oversight, and inspections. The process builds on the roles of federal, provincial, and local agencies.

The regulatory oversight of safe transportation of used nuclear fuel in Canada is jointly shared by the CNSC and Transport Canada. Transport Canada's *Transportation of Dangerous Goods Regulations,* and the *Transportation of Dangerous Goods Act,* and CNSC's *Packaging and Transport of Nuclear Substances Regulations,* associated with *Nuclear Safety and Control Act,* and the *Nuclear Security Regulations* apply to all persons who handle, offer for transport, transport or receive nuclear substances.

Transport Canada and CNSC regulations follow the IAEA regulations (TS-R-1) for the safe transport of radioactive materials and cover certification of the package used to transport the used fuel, the licence to transport, the security planning, training requirements for the shipper, receiver and the transporter, emergency response planning, and communications. These are in addition to the normal commercial vehicle and rail operating regulations and are similar to those used internationally. Packages designed for the transport of used nuclear fuel require certification by the CNSC before they can be used in Canada.

The provinces are responsible for developing, maintaining, and operating the highway infrastructure and for inspecting the commercial vehicles and their drivers. Local governments provide law enforcement and emergency response to incidents. The interaction and cooperation between these agencies facilitates comprehensive regulation and oversight of all transportation of used nuclear fuel.

1.5.3 Canadian Codes and Standards

A number of Canadian codes and standards apply to a deep geological repository project. Compliance with these will be demonstrated in the future in support of a licence application. For example, requirements exist in the following areas and include the following:

- Civil structures will comply with the National Building Code of Canada and the National Fire Code of Canada;
- Electrical installations and components will be in accordance with the Canadian Electrical Code and associated Canadian Standards Association (CSA) standards;
- The management system will comply with the CSA N286 series of standards as well as International Organization for Standardization (ISO) 9001;
- The environmental management and monitoring programs will comply with the CSA N288 series of standards as well as ISO 14001; and
- The occupational health and safety management programs will comply with the CSA Z1000 standard.

Some regulatory requirements from the provincial jurisdiction will also be applicable. For example, the health and safety program will comply with provincial Occupational Health and Safety Requirements. Although there is presently no specific site and therefore no specific province identified, for purposes of this study some provincial regulations or criteria may be adopted to provide more specific context. For example, while Canadian Drinking Water Quality guidelines are generally used to assess water quality, in some cases in this study the criteria have been based on more complete provincial standards, such as the Ontario water quality objectives (MoEE 1994) and the soil, groundwater and sediment standards (MoE 2011).

1.5.4 Safeguards

Canada's international safeguards obligations are the result of treaty commitments (IAEA 1970, IAEA 1972, and IAEA 2000). The specific legal requirements to implement these commitments come in the form of licence conditions that are included in a CNSC licence. Compliance with these requirements will be demonstrated in support of a future licence application.

1.5.5 Traditional Knowledge

NWMO respects the status and rights of First Nations and understands that interweaving of Aboriginal Traditional Knowledge in the implementation of APM helps to build relationships with Aboriginal peoples and benefits the long-term management of used nuclear fuel. Early in the project this includes recognizing the importance of water, the relationships between various aspects of the environment as well as the health, trade and spiritual needs of people. The NWMO's Site Selection Process will look to Aboriginal peoples as practitioners of Traditional Knowledge to be active participants in the process, and to share that knowledge with the NWMO to the extent they wish to in order to help guide the decisions involved in site selection and ensure safety and the long-term well-being of the community. The NWMO will seek to engage in discussions with Traditional Knowledge holders to ensure that the factors and approaches used to assess the site appropriately interweave Traditional Knowledge and western science throughout the steps in the siting process.

1.5.6 International Guidance

The development and safety of deep geological repositories has been the subject of international attention by the IAEA and the Nuclear Energy Agency for many years.

A number of technical documents are available that provide guidance on best international practices with respect both to achieving safety, and on the demonstration of safety. Particular international documents relevant to development and safety for a repository are listed in Table 1-2.

Table 1-2: International Guidance Applicable to the APM Project

Document Number	Title
IAEA SSR-5	Disposal of Radioactive Waste
IAEA SSG-23	The Safety Case and Safety Assessment for Radioactive Waste Disposal
ICRP 103	The 2007 Recommendations of the International Commission on Radiological Protection
ICRP 122	Radiological Protection in Geological Disposal of Long-lived Solid Radioactive Waste
Case Study	European Pilot Study on the Regulatory Review of the Safety Case for Geological Disposal of Radioactive Waste – Case Study: Uncertainties and their Management (Vigfusson et. al 2007)

Note: The latest version of international guidance can be found on the associated agency's website (www.iaea.org, www.icrp.org).

1.6 Safety Case

CNSC Guide G-320 states "*Demonstrating long term safety consists of providing reasonable assurance that waste management will be conducted in a manner that protects human health and the environment. This is achieved through the development of a safety case, which includes a safety assessment complemented by various additional arguments*".

The safety case has been defined in Section 1.1 as: the integration of arguments and evidence that describe, quantify and substantiate the safety, and the level of confidence in the safety, of the deep geological repository and associated facilities. It includes the collection of scientific and technical arguments and evidence in support of the safety of the repository covering the site characterization and geosynthesis, the design, construction and operation of the repository, the assessment of risk during operation and postclosure, and quality assurance of all safety-related work associated with the repository.

This report documents components of a safety case, but not a full safety case, as discussed later, representing information at a very early stage before a site has been selected. The report contains a description of these various components, and in some cases, an illustration of how the design of the repository will meet Canadian regulatory requirements and will be consistent with international practice.

CNSC Guide G-320 (CNSC 2006) recommends following a structured approach for preparing a safety case and safety assessment. The safety assessment is defined as: the process of systematically analyzing the hazards associated with the facility, and the ability of the site and design to provide the safety functions and meet technical requirements.

The most recent international guidance is included in the IAEA's SSG-23 (IAEA 2012). This guidance is used to present the safety case components for this study. The guidance also acknowledges applying the concept of defence in depth to disposal facilities by stating that: *"the host environment shall be selected, the engineered barriers of the disposal facility shall be designed… to ensure that safety is provided by means of multiple safety functions. Containment and isolation of the waste shall be provided by means of a number of physical barriers of the disposal system. The performance of these physical barriers shall be achieved by means of diverse physical and chemical processes…The capability of the individual barriers…shall be demonstrated. The overall performance of the disposal system shall not be unduly dependent on a single safety function."* It further recommends that the number and extent of required barriers depends on the type of waste and should be commensurate with the hazard potential of the waste, in accordance with the graded approach.

The components of a postclosure safety case are illustrated in Figure 1-4 and are largely consistent with IAEA (2012). This figure is used to illustrate the current phase and to identify the future work that will be included as part of a project at the final selected site. The discussion of each of these components is included in this section.

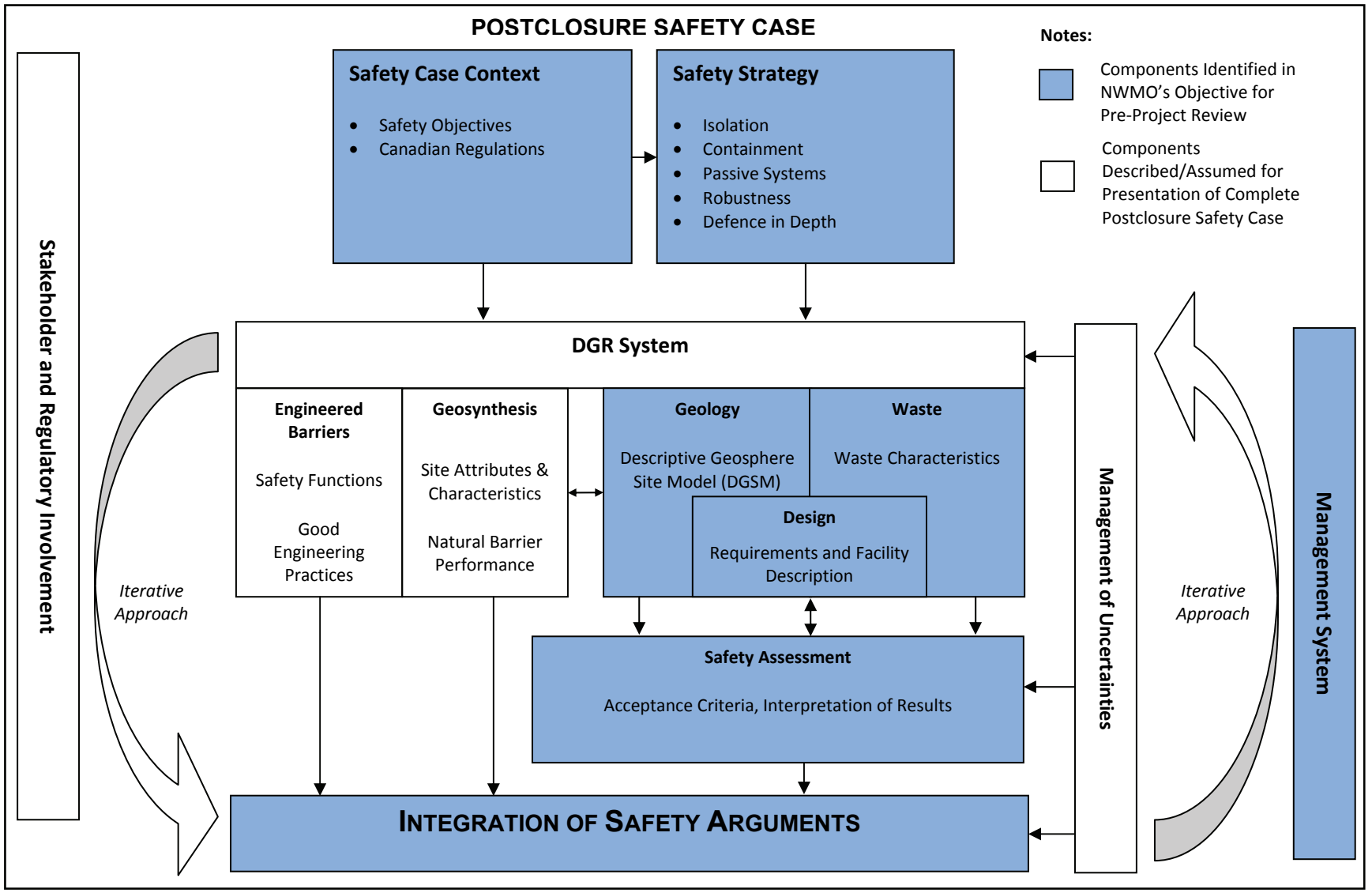

Figure 1-4: Components of the Safety Case

1.6.1 Safety Case Context

The Canadian regulatory framework presented in Section 1.5 provides the regulatory context for a deep geological repository safety case.

The primary *safety objective* of the deep geological repository is:

> to provide safe long-term management of used fuel without posing unreasonable risk to the environment or health and safety of humans.

This objective is consistent with the *Nuclear Safety and Control Act* (subparagraph 9(a) (i)) and IAEA guidance (IAEA 2011), which notes that the geological disposal of radioactive waste is aimed at:

- Containing the waste until most of the radioactivity, and especially that associated with shorter-lived radionuclides, has decayed;
- Isolating the waste from the biosphere and substantially reducing the likelihood of inadvertent human intrusion into the waste;
- Delaying any significant migration of radionuclides to the biosphere until a time in the far future when much of the radioactivity will have decayed; and
- Ensuring that any levels of radionuclides eventually reaching the biosphere are such that possible radiological impacts in the future are acceptably low.

As described in Section 1.1, this study presents a conceptual design and illustrative safety assessment for a deep geological repository at a hypothetical site. The level of detail is consistent with the pre-project stage, i.e., before a final site has been selected, and sufficient to support a CNSC review with respect to the approach and methodology. It is not a full safety case. It considers a hypothetical site, and therefore does not include a geosynthesis. It identifies and analyzes key scenarios, but does not assess all relevant scenarios.

1.6.2 Safety Strategy

The safety strategy is to provide long-term containment and isolation of used nuclear fuel through the use of multiple barriers and passive systems, including in particular a stable and robust geosphere. The geosphere has characteristics that will also delay significant migration of radionuclides to ensure that the impacts of any releases in the future are acceptably low.

In this study, a set of safety relevant features are assumed to be present at a hypothetical site. The geological features will need to be affirmed at any future candidate site as part of the Site Selection Process (NWMO 2010). The design concept includes engineered barriers that have properties that also allow a set of safety functions to be fulfilled.

The geological characteristics and the engineered barrier's safety functions identified in this report are consistent with the concept of defence in depth and are further described in the following section on the deep geological repository system.

1.6.3 Deep Geological Repository System

The DGR system includes the DGR facility, its geological setting, and the surrounding surface environment. The system includes the engineered and the natural barriers that provide

containment and isolation of the waste. The repository system includes the waste, containers, sealing systems and the near-field geosphere around the repository.

Figure 1-4 represents the system across three main areas for which safety arguments are presented: 1) the geology, 2) the waste characteristics, and 3) the design. This section includes a summary of the assumptions that are made and the type of information that needs to be considered in a safety case.

In this study for a hypothetical site, no specific description of communities is considered, although that will be important for any candidate site.

1.6.3.1 Geology

The information that describes the geological setting of the repository is used to guide the design of the DGR facility and as an input into the safety assessment. The geoscience program for a future candidate site will be designed to support the safety case and to produce:

- A Descriptive Geosphere Site Model (DGSM) that will describe, assess and interpret geoscientific data as it relates to site-specific geologic, geochemical, hydrogeologic and geomechanical characteristics and attributes; and
- A Geosynthesis that will provide a geoscientific explanation of the overall understanding of site characteristics, attributes and evolution as they relate to demonstrating long-term performance and safety.

The DGSM is defined as: a description of the present day three-dimensional physical and chemical characteristics of a specific site as they relate to implementation of the repository concept. For the purpose of the pre-project report and for conducting the illustrative safety assessment, this type of information is presented in Chapter 2.

The safety strategy identified that long-term containment and isolation is provided through the use of multiple barriers and passive systems, including in particular a stable and robust geosphere. The evidence to support the safety case arguments will be presented in the Geosynthesis for a candidate site that examines the past, present, and future evolution of the site. The Geosynthesis is defined as: the assembly of all the geologically-based evidence relevant to the repository safety case; the integration of multi-disciplinary geoscientific data relevant to the development of a descriptive conceptual geosphere model; and explanation of a site-specific descriptive geosphere model within a systematic and structured framework.

The NWMO's siting process (NWMO 2010) includes technical evaluations of a candidate site. The factors (listed in Section 1.6.8) in this process include the following key geological considerations.

- The depth of the host rock formation should be sufficient for isolating the repository from surface disturbances and changes caused by human activities and natural events.
- The volume of available competent rock at repository depth should be sufficient to host the repository and provide sufficient distance from active geological features such as zones of deformation or faults and unfavourable heterogeneities.

- The mineralogy of the rock, the geochemical composition of the groundwater and rock porewater at repository depth should not adversely impact the expected performance of the repository multi-barrier system.
- The hydrogeological regime within the host rock should exhibit low groundwater velocities.
- The mineralogy of the host rock, the geochemical composition of the groundwater and rock porewater should be favourable to retarding radionuclide movement.
- The host rock should be capable of withstanding mechanical and thermal stresses induced by the repository without significant structural deformation or fracturing that could compromise the containment and isolation functions of the repository.
- Current and future seismic activity at the repository site should not adversely impact the integrity of the repository system during operation and in the very long term.
- The expected rates of land uplift, subsidence and erosion at the repository site should not adversely impact the containment and isolation functions of the repository.
- The repository should not be located within rock formations containing economically exploitable natural resources such as minerals and other valuable commodities as known today.
- The repository is not located within geological formations containing groundwater resources at repository depth that could be used for drinking, agriculture or industrial uses.

It is noted that site characterization activities for an actual site in sedimentary rock would include a thorough and systematic assessment of such features as, for example, major fractures and natural resource potential in the proximity of the repository. The assessment findings would be documented in the DGSM and in the Geosynthesis prepared for a candidate site, described above. For the purpose of the pre-project report, the key attributes assumed for the hypothetical site in southern Ontario are:

- The repository is located at a depth of 500 m;
- There is sufficient volume of rock at the site and depth to host the repository;
- Groundwater and porewater at the repository horizon is saline;
- Groundwater at repository depth provides a chemically reducing environment and a low concentration of potentially corrosive agents;
- No large-scale transmissive fractures in close proximity to the repository site;
- The host rock is capable of withstanding mechanical and thermal stresses;
- Seismic activity is low, consistent with general Michigan Basin conditions;
- Rates of land uplift, subsidence and erosion at the site are low enough that they will not adversely impact the isolation of the repository; and
- The host rock formations do not contain groundwater or economically exploitable natural resources at repository depth.

1.6.3.2 Waste Characteristics

The waste characteristics are an input to the safety assessment and guide the design of the DGR facility. In addition, the waste has safety features that are identified in the safety case as follows:

- The used nuclear fuel is a durable uranium oxide (UO_2); it will dissolve very slowly under the chemical conditions within a failed container.
- Most of the initial radioactivity is held within the UO_2 grains, where it can only be released as the used fuel dissolves.

The waste characteristics are further described in Chapter 3.

1.6.3.3 Design

The design is largely guided by the geological characteristics and features of a candidate site and also by the characteristics of the waste that will be placed in the repository. For the pre-project report, a hypothetical sedimentary site in southern Ontario is considered. Representative characteristics of the sedimentary site are used to guide specific repository design requirements which include engineered barriers to fulfill specific safety functions. Design requirements are used as an input to the safety assessment.

The safety strategy acknowledges that properties of the engineered barriers will allow safety functions to be fulfilled. This includes the following design characteristics:

- The used fuel container has a design life of at least 100,000 years under the geomechanical and chemical repository conditions expected to exist within the repository; and
- The container is surrounded by a layer (approximately 60 cm) of dense bentonite-based clay that inhibits groundwater movement, has self-sealing capability, inhibits microbial activity near the container, and retards contaminant transport.

The repository design is described in Chapter 4 at a conceptual level of detail. The description focuses on the underground portions relevant to postclosure safety.

The purpose of the design concept presented here is to provide information to support the postclosure safety assessment. This design concept is expected to be further refined once a site has been selected and site specific information becomes available.

1.6.3.4 Institutional Controls

Institutional controls have been described in Section 1.4.2 where it is stated that institutional controls are assumed for a period of time. The safety feature associated with this assumption includes: institutional controls will limit the potential for human encounter with the repository in the near term after closure.

1.6.3.5 Long-Term Evolution of Repository

And finally, Chapter 5 discusses the evolution of the deep geological repository system, including how the different components of the system will interact with each other and the environment in the long term, consistent with CNSC Guide G-320 (CNSC 2006).

1.6.4 Safety Assessment

The safety assessment has been defined as: the process of systematically analyzing the hazards associated with the facility, and the ability of the site and design to provide the safety functions and meet technical requirements. As noted in the scope of this report, it focuses on the illustrative postclosure safety assessment, which is discussed in detail in Chapters 6, 7 and 8. The scenarios, assessment tools and methods and assessment results are presented. Both radiological and non-radiological impacts are assessed and the safety assessment results are compared against interim acceptance criteria.

1.6.5 Management of Uncertainties

The report describes the assessment of uncertainties associated with numerical analyses at a level that is reasonable for a conceptual design at a hypothetical site. The discussion is consistent with the CNSC guidance for analyzing uncertainties and addresses such things as: degree of conservatism, conceptual model uncertainty, parameter value uncertainty, and scenario uncertainty. The illustrative safety assessment provides examples of approaches used to assess and understand the relevance of uncertainties in scientific knowledge, data or analysis that support statements of reliability in calculated repository performance.

As described throughout Section 1.6.3, a number of assumptions have been made for the purpose of illustrating the safety assessment approach at this early stage of implementing APM. These assumptions are often characterized in the assessment process as “realistic” or “conservative”.

Realism is defined as: the representation of an element of the system (scenario, model or data), made in light of the current state of system knowledge and associated uncertainties, such that the safety assessment incorporates all that is known about the element under consideration and leads to an estimate of the expected performance of the system attributable to that element (IAEA 2006).

Conservatism is defined as: the conscious decision, made in light of the current state of system knowledge and associated uncertainties, to represent an element of the system (scenario, model or data) such that it provides an under-estimate of system performance attributable to that element and thereby an over-estimate of the associated radiological impact (i.e., dose or risk) (IAEA 2006).

As noted in Section 1.6.3.1, the geoscience program for a future candidate site will be designed to support the safety case and to produce a Descriptive Geosphere Site Model and a Geosynthesis.

The site model and geosynthesis will be developed in the phased site characterization work program. The work program will allow for the iterative development, testing and refinement of a

site-specific model that will contribute to managing uncertainties in scientific understanding, data or models. The design is also expected to be further refined once a site has been selected and site specific information becomes available.

The iterative approach described below also highlights how the assessment of uncertainties will be incorporated in the process of developing a safety case for a future candidate site.

1.6.6 Iterative Approach

Consistent with international guidance, the NWMO plans to use an iterative approach in the strategies for management, site characterization, design and assessments of a candidate site. The documentation process to support this iterative approach is included in Figure 1-5. On the left hand side of this figure, two key documents that will support licence applications and that will document the safety case are identified as the Preliminary Safety Report and Final Safety Report.

As noted in Section 1.6.3.3, the design concept presented is illustrative and intended for the safety assessment methodology to be demonstrated. The actual design is expected to be refined once a specific site has been selected, site-specific information becomes available, and design optimization is implemented.

Furthermore, once a site has been selected, Figure 1-5 assumes that the characterization and engineered design programs will go through iterations based on increased knowledge of site characteristics and safety assessment input during detailed site investigations. A few iterations are expected during the phase of detailed investigations.

Some of the key activities in this approach include:

- National and international peer reviews;
- Using site characterization results as an input to repository design and safety assessment, and in building the safety case;
- Conducting complementary geoscience analogue studies to assist with the explanation of geoscience phenomena related to, and to enhance confidence in, the understanding of long-term repository safety;
- Using proven technology in the design;
- Using the results of safety assessment, in particular the preclosure safety assessment and occupational radiation dose ALARA[2] assessment and conventional safety considerations in the design;
- Continuing to make use of a range of safety and performance indicators in safety analyses; and
- Assessing associated uncertainties and identification of any significant deficiencies in scientific understanding, data or analysis that might affect the analysis results that are presented.

[2] ALARA: As low as reasonably achievable, social and economical factors taken into account.

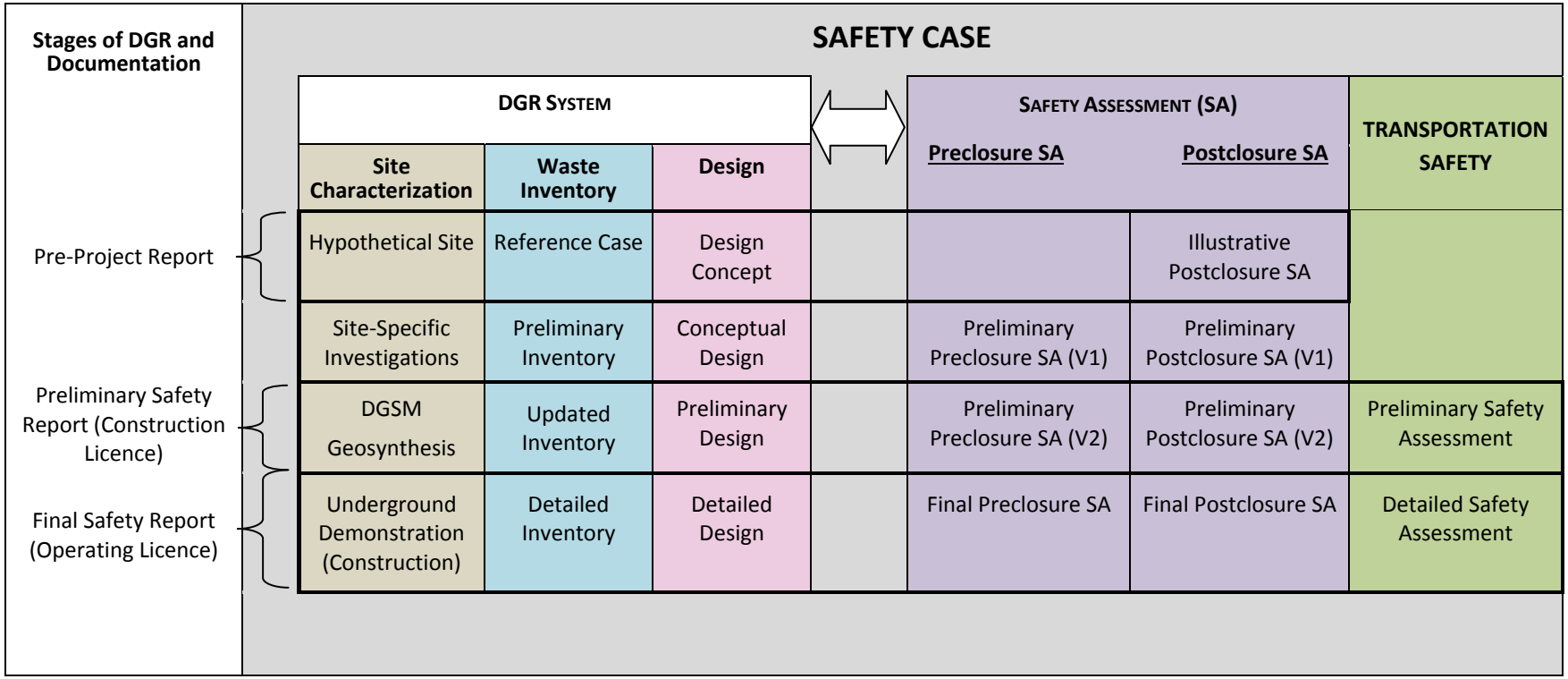

Figure 1-5: Iterative Process for Developing the Safety Case

1.6.7 Integration of Safety Arguments

The safety arguments will be integrated as part of a complete safety case. These arguments will be supported by evidence and multiple lines of reasoning gathered in the site characterization work program and documented in a Geosynthesis for a candidate site.

For the purpose of this report and to present the illustrative safety assessment, a number of assumptions are identified in Section 1.6.3. These assumptions are made to show how site characteristics or attributes and safety functions are used to illustrate the robustness of a multi-barrier system.

The assessment results presented in Chapters 7 and 8 will be used to support safety arguments resulting from the postclosure assessment.

1.6.8 Stakeholder and Regulatory Involvement

As noted in Section 1.1, the purpose of this report is to present a case study involving an illustrative safety assessment of a deep geological repository in a representative sedimentary setting for a pre-project regulatory review. This is being conducted under a special project arrangement between the CNSC and the NWMO (CNSC and NWMO 2008).

This report considers a hypothetical site, so there are no direct stakeholders. However, it will be available to the public and may be of interest to communities as part of the site selection process.

This report and illustrative safety assessment have been conducted in parallel with activities in the NWMO APM site selection process. This section shows how both of these activities are consistent and also confirms that technical evaluation stages are built into the process to select a candidate site.

As noted in the project overview, a site selection process was designed to identify an informed and willing host community for a deep geological repository for the long-term management of Canada's used nuclear fuel. It is a nine-step process developed to reflect the values, concerns and priorities expressed by Canadians, which are detailed by the NWMO (2010). The guiding principles that are embedded in the site selection process include:

- Focusing decision-making on safety;
- Meeting or exceeding regulatory requirements;
- Finding an informed and willing host community;
- Focusing siting on the provinces directly involved in the nuclear fuel cycle; and
- Acknowledging the right for a community to withdraw from the process.

Furthermore, it identifies site evaluation factors with which the suitability of a candidate site to host an APM repository will be assessed (see Figure 1-6). These factors include the list of geoscientific attributes identified in Section 1.6.3.1 and the following attributes:

- The containment and isolation characteristics (e.g., geological, hydrogeological, chemical, and mechanical) of the host rock;

- The long-term stability of the site to ensure that containment and isolation of the repository will not be unacceptably affected by future geological processes and climate changes including earthquakes and glacial cycles;
- Surface and underground characteristics of the site are favourable for the repository's construction, operation, closure, and long-term performance;
- Future human activities are not likely to disrupt containment and isolation of the repository;
- The characteristics of the site should be amenable to site characterization and site data interpretation activities; and
- The site should have a route that exists or is amenable to being created that enables the safe and secure transportation of used fuel from storage sites to the repository site.

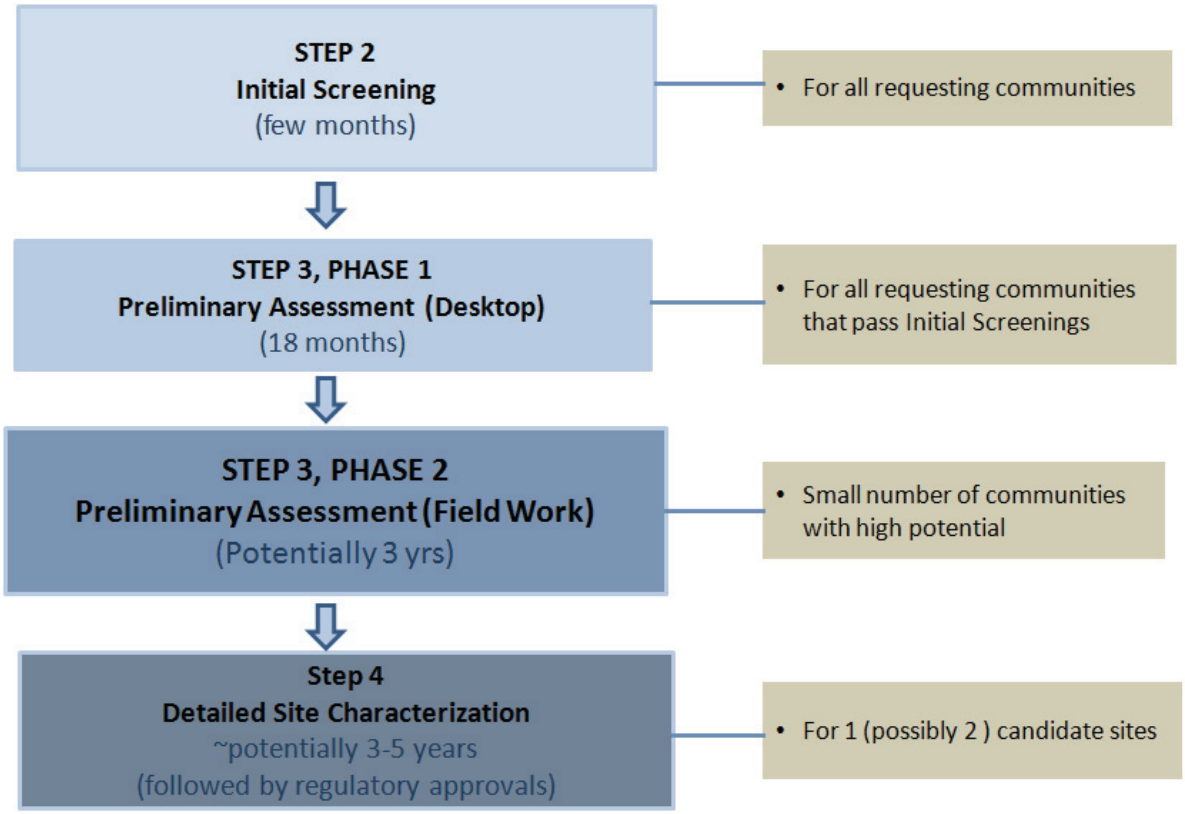

Figure 1-6: Site Evaluation Process

The stakeholder and regulatory involvement activities associated with the siting process were initiated in 2010 and are ongoing.

1.6.9 Management System

The management system includes a project quality plan under which the APM safety assessment has been executed. The project quality plan was developed specifically for this phase of the work. The plan includes the following elements:

- The project organization and responsibilities;
- NWMO and project-specific governance;
- Quality requirements;
- Verification requirements;
- Requirements for consultant or contractor quality management system;
- Records requirements;
- Program's periodic assessment activities; and
- Annual assessment activities.

Chapter 11 describes the elements of the project quality plan in more detail.

1.7 Development of National Deep Geological Repositories

The concept of using a deep geological repository for long-term management of used fuel is consistent with other national plans for high-level waste as summarized in Table 1-3.

Table 1-3: Status of National Plans for High-Level Waste

Country	National Plan for High-Level Waste	Potential Rock Type	Repository Status
Finland	Geological Repository	Crystalline Rock	- Willing host community selected - Underground demonstration facility operating at repository site
Sweden	Geological Repository	Crystalline Rock	- Willing host community selected - Underground demonstration facility operating at generic site
France	Geological Repository	Sedimentary Rock	- General geological region identified - Underground demonstration facility operating at generic site
UK	Geological Repository	To be decided	- Siting process underway
Germany	Geological Repository	Salt, Crystalline, and Sedimentary Rock	- Plans under development
Japan	Geological Repository	Crystalline and Sedimentary Rock	- Siting process underway - Generic underground research facilities under construction
Switzerland	Geological Repository	Sedimentary Rock	- Siting process underway - Underground demonstration facility operating at generic site
USA	Geological Repository	To be decided	- Blue Ribbon Panel recommendations issued
China	Geological Repository	Crystalline Rock	- Siting process underway

1.8 Report Structure and Content

The structure of this pre-project review report is as follows:

Chapter 1 Introduction: An overview of the APM project and the context for the report.

Chapter 2 Description of a Hypothetical Site: Information related to a hypothetical site is presented.

Chapter 3 Used Fuel Characteristics: Information on the reference fuel bundle adopted in the postclosure safety assessment is presented.

Chapter 4 Repository Facility – Conceptual Design: Description of conceptual design for a deep geological repository.

Chapter 5 Long-Term Evolution of the Multiple Barrier System: Description of the deep geological repository system, including the interaction of different components of the system.

Chapter 6 Scenario Identification and Description: Description of the systematic scenario identification process used to identify Normal Evolution and Disruptive Event Scenarios.

Chapter 7 Postclosure Safety Assessment – Contaminant Transport: Provides an evaluation of potential impacts during Normal Evolution and Disruptive Event Scenarios for water-borne transport.

Chapter 8 Postclosure Safety Assessment – Gas Generation and Transport: Provides an evaluation of potential impacts during the Disruptive Event Scenario for gas-borne transport.

Chapter 9 Treatment of Uncertainties: Description of scenario, model and data uncertainties.

Chapter 10 Natural Analogues: Description of natural analogues that illustrate material integrity and identification of the role of site-specific analogues.

Chapter 11 Quality Assurance: Description of the APM quality assurance plan.

Chapter 12 Summary and Conclusions: Summary of information presented in the pre-project report and overall conclusion on meeting the pre-project report objective.

Chapter 13 Special Terms: Includes units, abbreviations and acronyms.

Appendix A Design Optimization: Description of observations on sedimentary rock considerations for a used fuel repository in other countries.

The IAEA's structured approach presented in the recent guidance on the Safety Case and Safety Assessment for the Disposal of Radioactive Waste (IAEA 2012) was used to describe

the components of a safety case in Section 1.6. This guidance is complimentary to the CNSC Guide G-320 and its structure is used to present the information in this report. To illustrate how the content of G-320 is captured in this report, a mapping of the pre-project report sections to the content in G-320 is included in Table 1-4.

Table 1-4: Pre-Project Report Content Mapped to CNSC Guide G-320

G-320 Content	Relevant Section(s) in Report
Developing a Long-Term Safety Case	
Safety Assessment	Chapters 7 and 8
Use of Different Assessment Strategies	Sections 7.2 and 8.2
Robustness and Natural Analogues	Chapters 7, 8 and 10
Use of Complementary Indicators to Safety	Section 7.11.1
Defining Acceptance Criteria	
Overview	Section 7.1
Criteria for Protection of Persons and the Environment	Section 7.1
Performing Long-Term Assessments	
Selection of Appropriate Methodology	Section 7.4, 8.4
Assessment Context	Section 7.2, 8.2
System Description	Chapters 2, 3, 4, and 5
Assessment Time Frames	Section 1.4
Assessment Scenarios	Chapter 6
Developing and Using Assessment Models	Sections 7.5-7.9, 8.5-8.7
Interpretation of Results	
Comparing Assessment Results with Acceptance Criteria	Section 7.12, 8.7, 8.8
Analyzing Uncertainties	Chapter 9

1.9 References for Chapter 1

CEAA. 1998. Report of the Nuclear Fuel Waste Management and Disposal Concept Environmental Assessment Panel. Canadian Environmental Assessment Agency. Ottawa, Canada.

CNSC. 2004. Regulatory Policy P-290: Managing Radioactive Waste. Canadian Nuclear Safety Commission. Ottawa, Canada.

CNSC. 2006. Regulatory Guide G-320: Assessing the Long Term Safety of Radioactive Waste Management. Canadian Nuclear Safety Commission. Ottawa, Canada.

CNSC and NWMO. 2008. Special Project Arrangement between the Canadian Nuclear Safety Commission and the Nuclear Waste Management Organization. Canadian Nuclear Safety Commission and Nuclear Waste Management Organization. April 1, 2008.

Gierszewski, P., J. Avis, N. Calder, A. D'Andrea, F. Garisto, C. Kitson, T. Melnyk, K. Wei and L. Wojciechowski. 2004. Third-Case Study – Postclosure Safety Assessment. Ontario Power Generation Report 06819-REP-01200-10109-R00. Toronto, Canada.

Hare, F.K., A.M. Aikin and J.M. Harrision. 1977. The Management of Canada's Nuclear Wastes. Report for Energy, Mines and Resources Canada EP77-6. Minister of Energy, Mines and Resources. Ottawa, Canada.

IAEA. 1970. Treaty on the Non-Proliferation of Nuclear Weapons. International Atomic Energy Agency INFCIRC/140. Vienna, Austria.

IAEA. 1972. Agreement Between the Government of Canada and the International Atomic Energy Agency for the Application of Safeguards in Connection with the Treaty on the Non-Proliferation of Nuclear Weapons. International Atomic Energy Agency INFCIRC/164. Vienna, Austria.

IAEA. 1995. IAEA Safety Series: The Principles of Radioactive Waste Management. International Atomic Energy Agency. Safety Fundamentals IAEA 111-F. Vienna, Austria.

IAEA. 2000. Protocol Additional to the Agreement between Canada and IAEA for the Application of Safeguards in Connection with the Treaty on the Non-Proliferation of Nuclear Weapons. International Atomic Energy Agency INFCIRC/164/Add. 1. Vienna, Austria.

IAEA. 2006. Safety Requirements: Geological Disposal of Radioactive Waste. International Atomic Energy Agency Safety Requirements WS-R-4. Vienna, Austria.

IAEA. 2011. IAEA Safety Standards: Disposal of Radioactive Waste. International Atomic Energy Agency. Specific Safety Requirements IAEA SSR-5. Vienna, Austria.

IAEA. 2012. IAEA Safety Standards: The Safety Case and Safety Assessment for the Disposal of Radioactive Waste. International Atomic Energy Agency. Specific Safety Guide IAEA SSG-23. Vienna, Austria.

ICRP. 2007. The 2007 Recommendations of the International Commission on Radiological Protection. International Commission on Radiological Protection Publication 103, Annals of the ICRP (W2-4). Vienna, Austria.

ICRP. 2013. Radiological Protection in Geological Disposal of Long-lived Solid Radioactive Waste. International Commission on Radiological Protection Publication 122, Annals of the ICRP 42(3). Vienna, Austria.

MoEE. 1994. Water Management Policies Guidelines Provincial Water Quality Objectives of the Ministry of Environment and Energy. Ministry of Environment and Energy. Ontario, Canada.

MoE. 2011. Soil, Ground Water and Sediment Standards for Use under Part XV.1 of the Environmental Protection Act. Ontario Ministry of Environment. Ontario, Canada.

NWMO. 2010. Moving Forward Together: Process for Selecting a Site for Canada's Deep Geological Repository for Used Nuclear Fuel. Nuclear Waste Management Organization. Toronto, Canada.

NWMO. 2012. Used Fuel Repository Conceptual Design and Postclosure Safety Assessment in Crystalline Rock, Pre-Project Report. Nuclear Waste Management Organization NWMO TR-2012-16. Toronto, Canada.

Vigfusson, J., J. Maudoux, P. Raimbault, K.-J. Röhlig and R.E. Smith. 2007. European Pilot Study on the Regulatory Review of the Safety Case for Geological Disposal of Radioactive Waste – Case Study: Uncertainties and their Management.

THIS PAGE HAS BEEN LEFT BLANK INTENTIONALLY

2. DESCRIPTION OF A HYPOTHETICAL SITE

2.1 Introduction

The purpose of this chapter is to describe the characteristics of a hypothetical sedimentary rock site that could be encountered during geoscientific site characterization activities on the margin of the Michigan Basin in southern Ontario. The description is provided in-lieu of geoscientific information that would be derived through site-specific surface and sub-surface investigations. The intent is to provide information necessary to support an illustrative safety assessment, the focus of which is to demonstrate the methodology to assess the postclosure safety of a deep geological repository for Canada's used nuclear fuel in a sedimentary rock geosphere at an approximate depth of 500 metres below ground surface (mBGS).

Although the data represent a hypothetical sedimentary basin site, the information is consistent with reported values obtained from both regional and site-specific investigations for Ontario Power Generation's Deep Geological Repository for Low & Intermediate Level Waste (INTERA 2011, Sykes et al. 2011). The following sections describe typical site features through the presentation of descriptive geologic (Section 2.2.1), hydrogeologic (Section 2.2.2) and geochemical (Section 2.2.3) site models. The site models are supported by numerical groundwater simulations, presented in Section 2.3.

2.1.1 Site Attributes

There are several key site attributes that relate to demonstrating the geoscientific suitability of the hypothetical sedimentary site and these attributes are described below:

- Site Predictability – near-horizontally layered, undeformed sedimentary shale and limestone formations of large lateral extent;
- Multiple Natural Barriers – multiple low permeability bedrock formations enclose and overlie the repository site;
- Low rates of Contaminant Transport – the deep groundwater flow system is stagnant, with long travel times and no indication of perturbations from glaciation;
- Shallow Groundwater Resources are Isolated – near-surface groundwater aquifers are isolated from the deep saline groundwater system;
- Rock Strength – the host rock should be capable of withstanding mechanical and thermal stresses induced by the repository without significant structural deformation or fracturing that could compromise the containment and isolation functions of the repository;
- Rock Volume – the volume of available competent rock at repository depth should be sufficient to host the repository and to provide sufficient distance from active geological features such as zones of deformation or faults and unfavourable heterogeneities; and
- Seismically quiet - comparable to a Canadian Shield setting.

These attributes would be tested and confirmed through a site characterization and Geosynthesis program at a real candidate site.

2.1.2 Modelling Strategy

The behaviour and stability of the geosphere at repository depth are illustrated through the use of a reference case contrasted with comparative sensitivity cases, based upon the conceptual

model described in Section 2.2. In the sensitivity cases, key geosphere parameters are varied to illustrate the role they play in influencing groundwater flow and transport. The reference case and the geosphere parameters varied in the sensitivity cases are described in Section 2.3.

The reference case simulates current site conditions at the regional scale and includes groundwater salinity distributions to allow simulation of density-dependent flow.

Sensitivity cases, in which the distribution of total dissolved solids are varied, are conducted to examine the role of spatially variable groundwater density (salinity) distributions in governing hydraulic gradients, groundwater velocities, groundwater system stability and dominant mass transport processes. The permeability of the rock mass is also varied within an expected range of uncertainty to illustrate the sensitivity of estimated groundwater performance measures and, in particular, designation of mass transport regimes.

The purpose of the paleohydrogeologic scenarios is to assess the influence of a glacial event on groundwater system stability. In particular, the simulations explore transient hydraulic gradients, groundwater velocities and the depth of penetration by glacial recharge, which are relevant to illustrating long-term DGR safety. The paleohydrogeologic boundary conditions are varied to include cold and warm based glaciers in order to illustrate groundwater system response to external perturbations. The effect of hydromechanical coupling during paleohydrogeologic scenarios is investigated.

2.2 Conceptual Model for Hypothetical Site

The following section describes the geosphere model for the hypothetical sedimentary site, including information on the site and regional scale geology, surface features (topography and hydrology), hydrogeological and geochemical conditions, and natural resource potential.

2.2.1 Descriptive Geological Model

The geologic site model describes the geologic composition and structural features of the geosphere, and provides the basis for geoscientific understanding of the current conditions as well as its past evolution.

2.2.1.1 Geologic Description

The geology of the site is comprised of a layer of Quaternary-aged glacial drift, overlying thick sequences of Paleozoic-aged sedimentary rock, which sits upon basement bedrock of Precambrian-aged granitic gneiss. Fractures within the regional study area are expected to be sparse and infrequent, and will not penetrate Paleozoic sedimentary rocks younger than Ordovician in age (NWMO, 2011). The stratigraphic column for the sedimentary rock found at the centre of the hypothetical repository site is shown in Table 2-1. Table 2-1 also includes geologic formations that are not present at the repository site, but are found within the regional modelling area (described in Section 2.3). Formation thicknesses will vary across the regional modelling area, and a total of 15 formations pinch-out within 10 km of the repository site.

Table 2-1: Formation Thicknesses at the Hypothetical Site

Period	Geological Unit	Unit Top Depth (mBGS)	Thickness (m)
Quaternary	Drift	0.0	29.4
Devonian	Hamilton Group	-	-
	Dundee	-	-
	Detroit River Group	-	-
	Bois Blanc	-	-
Silurian	Bass Islands	-	-
	Unit G	-	-
	Unit F	-	-
	Unit F Salt	-	-
	Unit E	-	-
	Unit D	-	-
	Unit B and C	29.4	52.3
	Unit B Anhydrite	-	-
	Unit A-2 Carbonate	81.7	27.0
	Unit A-1 Upper Carbonate	108.7	3.0
	Unit A-1 Carbonate	111.7	22.1
	Unit A-1 Evaporite	133.8	2.0
	Unit A0	135.8	2.3
	Guelph	138.1	71.4
	Goat Island	-	-
	Gasport	-	-
	Lions Head	-	-
	Reynales/Fossil Hill	209.5	6.8
	Cabot Head	216.3	15.8
	Manitoulin	232.1	15.6
Ordovician	Queenston	247.7	77.6
	Georgian Bay/Blue Mountain	325.3	154.3
	Cobourg	479.6	46.4
	Sherman Fall	526.0	47.3
	Kirkfield	573.3	39.5
	Coboconk	612.8	8.0
	Gull River	620.8	53.4
	Shadow Lake	674.2	7.6
Cambrian	Cambrian	-	-
Precambrian	Upper Precambrian	681.8	20.0
	Precambrian	701.8	-

Note: Repository location at the hypothetical site is in the Cobourg Formation.

2.2.1.1.1 Basement Geology

The basement geology at the repository site is found at a depth of 682 mBGS. The Precambrian bedrock beneath the repository site is composed of metamorphic rock types ranging from felsic gneiss to mafic metavolcanics to marble.

2.2.1.1.2 Sedimentary Bedrock Geology

The sedimentary rock overlying the Precambrian basement at the repository site has a thickness of 682 m and comprises a thick sequence of limestones and dolostones, as well as shales and evaporites.

Cambrian

The Cambrian lithologies include fine- to medium-grained crystalline dolostones, sandy dolostone, argillaceous dolostone, as well as fine and coarse sandstone. The Cambrian pinches-out against the Precambrian surface and is assumed not to be present at the repository site.

Ordovician

The Ordovician rocks beneath the repository site are composed of a thick sequence of shales overlying carbonates. The Ordovician shales include the Queenston and the Georgian Bay/Blue Mountain Formations, and have a total thickness 232 m. The Ordovician carbonates include the argillaceous limestone of the Cobourg Formation, as well as the limestones of the Sherman Fall and Kirkfield formations. At the base of the Ordovician sequence is the Black River Group, which is comprised of the Shadow Lake, Gull River and Coboconk formations. The Shadow Lake Formation is made up of poorly sorted shales, sandstones and argillaceous dolostones, with rare conglomerates (Armstrong and Carter 2006). The overlying Gull River Formation is composed of limestone. At the top of the Black River Group, the Coboconk is composed of bioclastic limestone.

Overlying the Black River Group is the Trenton Group, which is comprised of the Kirkfield, Sherman Fall and Cobourg formations. The Kirkfield Formation is composed of limestone with thin shale interbeds. The overlying Sherman Fall Formation ranges from argillaceous limestone at its base to fossiliferous limestone in its upper section.

The Cobourg Formation is composed of fine-grained to argillaceous limestone. The Cobourg Formation is the proposed host rock for the repository discussed herein.

The upper part of the Ordovician sequence at the repository site is made up of a thick sequence of shale, and is comprised of the Blue Mountain, Georgian Bay and Queenston formations. The Blue Mountain Formation is composed of non-calcareous shale. The Georgian Bay Formation is composed of shale with intermittent siltstone and limestone interbeds. The Queenston Formation is composed of shale and minor amounts of siltstone, sandstone and limestone (Armstrong and Carter 2010).

Silurian

The Silurian lithologies can be grouped into three sets of formations, the Lower, Middle and Upper Silurian. The Lower Silurian rocks unconformably overlie the Queenston Formation and

are comprised of the Manitoulin and Cabot Head formations. The Manitoulin Formation is composed of argillaceous dolostone with minor shale. The overlying Cabot Head Formation is composed of noncalcareous shale with minor sandstone and carbonate interbeds (Armstrong and Carter 2010).

The Middle Silurian rocks are composed of the Fossil Hill, Lions Head, Gasport, Goat Island and Guelph formations. The Fossil Hill Formation is composed of a fossiliferous dolostone. Lying overtop of the Fossil Hill, the Lions Head, Gasport, Goat Island and Guelph formations form the Niagaran Group, which is included within the regional geologic framework model (Section 2.3.3.2). The Lions Head is a sparsely fossiliferous dolostone with minor chert nodules (Armstrong and Carter 2010). The Gasport Formation is composed of dolostone. The Goat Island is lithologically similar to the Gasport, but is more argillaceous. The Guelph Formation is composed of reefal to inter-reefal dolostones (Armstrong and Goodman 1990). Reefal facies represent pinnacle, patch and barrier reefs.

The Upper Silurian rocks are composed of the Salina Group, which include a thick sequence of carbonates and evaporites. The Salina Group at the repository site includes the following units: Unit A0 (carbonate), Unit A1-Evaporite, Unit A1-Carbonate, Unit A1-Upper Carbonate, Unit A2 Carbonate and Unit B and C (carbonate).

In addition to the Salina units described above, the following units are found regionally: Unit D (carbonate and evaporite), Unit E (carbonate and shale), Unit F (carbonate, shale and evaporite), and Unit G (carbonite, shale, evaporite).

Lying on top of the Salina Group, and at the top of the Silurian lithologies, the Bass Island Formation is composed of microcrystalline dolostone.

Devonian

Overlying the Silurian strata are the Devonian formations and groups, which include the Bois Blanc Formation, the Detroit River Group, the Dundee Formation and the Hamilton Group. These strata are found regionally, but are not present at the hypothetical repository site. The Bois Blanc Formation is composed of cherty dolostone. The Amherstburg and the Lucas formations comprise the Detroit River Group, which is made up of mixed limestones and dolostones. Overlying the Detroit River Group is the Dundee Formation, which is composed of fossiliferous limestones with minor dolostones (Armstrong and Dodge 2007).

Quaternary

The Quaternary cover found at the repository site is composed of a thick sequence of glacial till, glaciofluvial sands and gravels, and glaciolacustrine clays and silts.

2.2.1.2 Surface Features

2.2.1.2.1 Topography

A representative regional area encompassing a watershed was selected for this case study, and is shown in Figure 2-1 with an area of 18,000 km^2. The lateral boundaries for the regional domain were selected to correspond with surface and groundwater divides, which represent planes across which groundwater flow is not expected.

The top surface of the domain was defined by a Digital Elevation Model (DEM) from the Shuttle Radar Topography Mission (SRTM) and a river network in ArcGIS. Based on the assumption that the water table is a subdued reflection of surface topography, the topographic divides representing no-flow boundaries are a reasonable choice for the upper flow regime. The higher permeability Niagaran Group, within the intermediate flow regime, subcrops within the modelling domain, while the western boundary occurs at a groundwater divide beneath Lake Huron. The modelling domain includes the local topographic high in southern Ontario and the domain extends to the deepest portions of both Lake Huron and Georgian Bay. The bathymetric data of both water bodies, provided by National Oceanic and Atmospheric Administration (NOAA), was combined with the DEM to provide a continuous surface for the top of the Earth's solid surface.

The regional watershed and hydrogeologic conditions are described in Section 2.3.

2.2.1.2.2 Surface Hydrology

The regional domain contains two major lakes and is located in the western and northern portions of the regional area, as shown in Figure 2-1. Smaller rivers flowing into the two major lakes can also be found in Figure 2-1.

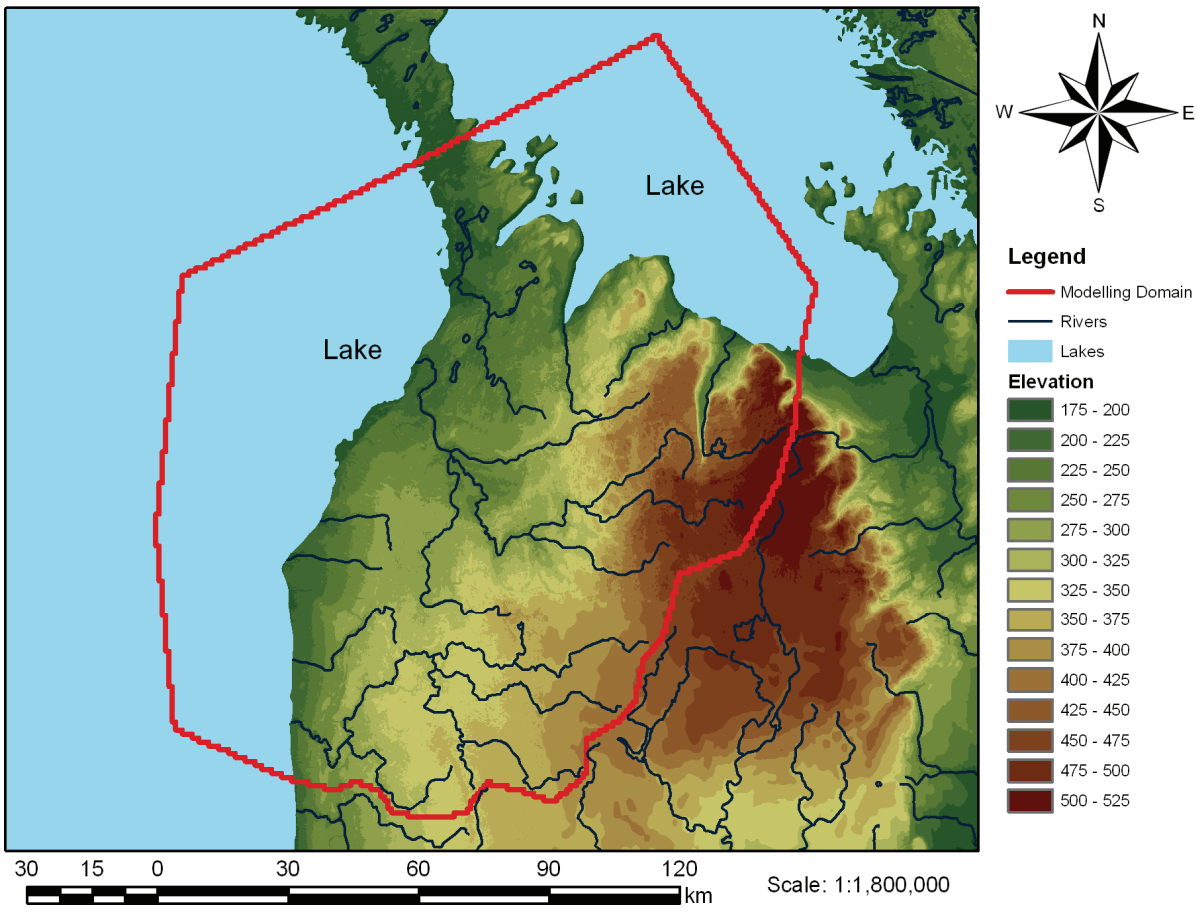

Note: Elevation is measured in metres above sea level (mASL). The elevation for the lakes shown is 176 mASL.

Figure 2-1: Regional Scale Topography

2.2.2 Descriptive Hydrogeologic Model

2.2.2.1 Groundwater Systems

Three groundwater systems are considered for the site. The groundwater systems are identified, in part, by the regional distribution of hydraulic conductivities, as well as groundwater total dissolved solids (TDS) concentrations and redox conditions (a detailed geochemical conceptual model is presented in Section 2.2.3). The primary characteristics of the three groundwater systems are described below.

Shallow Groundwater System (0 - 215 mBGS)

The shallow groundwater system, located near surface, is predominately driven by local- and sub-regional scale topographic changes. Meteoric water, in the form of rain or snowmelt, initially recharges the groundwater system by infiltration in near surface weathered zones, and flows from topographic highs near the surface before discharging into streams, rivers, lakes or swamps and bogs associated with local topographic lows. The average travel time for groundwater to recharge, and then subsequently discharge, in the shallow groundwater zone is typical less than 1,000 years. The groundwater in the shallow groundwater zone is fresh and oxygen-rich, with low TDS concentrations (further discussion can be found in Section 2.2.3).

Intermediate Groundwater System (215 - 250 mBGS)

The groundwater in the intermediate groundwater system transitions from fresh and oxygen-rich, to more mineralized and chemically reducing with depth. At the hypothetical site, the shift from oxidizing to reducing conditions occurs within this system. In the intermediate groundwater system, larger domains of low permeability rock tend to decrease mass transport rates.

Deep Groundwater System (> 250 mBGS)

In contrast to the shallow and intermediate groundwater zones, groundwaters in the deep system have higher total dissolved solids concentrations and, hence, higher fluid densities. The geochemical redox potential is reducing. The increased fluid density will influence both energy gradients within the groundwater regime and vertical upward movement of groundwater between the shallow/intermediate and deep groundwater zones (Park et al. 2009).

2.2.2.2 Hydraulic Parameters

The key hydraulic parameters, including the horizontal and vertical hydraulic conductivities (K_H, and K_V respectively), anisotropy ratio for the hydraulic conductivity ($K_H : K_V$), porosity, specific storage (S_s), tortuosity (τ), fluid density, and loading efficiencies (ζ) for the hypothetical site are shown in Table 2-2.

Table 2-2: Regional Hydrogeologic Parameters

Formation	Unit Top Depth (mBGS)	Thickness (m)	K_H (m/s)	K_V (m/s)	$K_H : K_V$	Porosity	Fluid Density (kg/m^3)	Initial TDS (g/L)	S_s [1] (m^{-1})	ζ [1]	τ [2]
Drift	0	29.4	$1x10^{-7}$	$5x10^{-8}$	2:1	0.2	1,000	0	$1x10^{-4}$	0.99	$4.00x10^{-1}$
Hamilton Group	-	-	$2x10^{-11}$	$2x10^{-12}$	10:1	0.1	1,008	12	$2x10^{-6}$	0.8	$1.19x10^{-1}$
Dundee	-	-	$8x10^{-8}$	$8x10^{-9}$	10:1	0.1	1,005	8	$2x10^{-6}$	0.8	$1.19x10^{-1}$
Detroit River Group	-	-	$6x10^{-7}$	$2x10^{-8}$	30:1	0.077	1,001	1.4	$1x10^{-6}$	0.84	$1.56x10^{-1}$
Bois Blanc	-	-	$1x10^{-7}$	$1x10^{-8}$	10:1	0.077	1,002	3.2	$1x10^{-6}$	0.84	$1.56x10^{-1}$
Bass Islands	-	-	$5x10^{-5}$	$2x10^{-6}$	25:1	0.056	1,004	6	$2x10^{-6}$	0.92	$1.07x10^{-1}$
Unit G	-	-	$1x10^{-11}$	$1x10^{-12}$	10:1	0.172	1,010	14.8	$1x10^{-6}$	0.55	$3.01x10^{-3}$
Unit F	-	-	$5x10^{-14}$	$5x10^{-15}$	10:1	0.1	1,040	59.6	$1x10^{-6}$	0.68	$4.93x10^{-2}$
Unit F Salt	-	-	$5x10^{-14}$	$5x10^{-15}$	10:1	0.1	1,040	59.6	$1x10^{-6}$	0.68	$4.93x10^{-2}$
Unit E	-	-	$2x10^{-13}$	$2x10^{-14}$	10:1	0.1	1,083	124	$7x10^{-7}$	0.51	$5.66x10^{-2}$
Unit D	-	-	$2x10^{-13}$	$2x10^{-14}$	10:1	0.089	1,133	200	$6x10^{-7}$	0.53	$6.35x10^{-2}$
Unit B and C	29.4	52.3	$4x10^{-13}$	$4x10^{-14}$	10:1	0.165	1,198	296.7	$1x10^{-6}$	0.38	$8.75x10^{-2}$
Unit B Anhydrite	-	-	$3x10^{-13}$	$3x10^{-14}$	10:1	0.089	1,214	321	$7x10^{-7}$	0.53	$1.04x10^{-3}$
Unit A-2 Carbonate	81.7	27	$3x10^{-10}$	$3x10^{-11}$	10:1	0.12	1,091	136	$7x10^{-7}$	0.46	$1.20x10^{-2}$

Table 2-2: Regional Hydrogeologic Parameters (Continued)

Formation	Unit Top Depth (mBGS)	Thickness (m)	K_H (m/s)	K_V (m/s)	$K_H : K_V$	Porosity	Fluid Density (kg/m^3)	Initial TDS (g/L)	S_s [1] (m^{-1})	ζ [1]	τ [2]
Unit A-2 Evaporite	-	-	$3x10^{-13}$	$3x10^{-14}$	10:1	0.089	1,030	45.6	$6x10^{-7}$	0.53	$1.04x10^{-3}$
Unit A-1 Upper Carbonate	108.7	3	$2x10^{-7}$	$2x10^{-7}$	1:1	0.07	1,019	28.6	$5x10^{-7}$	0.59	$1.17x10^{-1}$
Unit A-1 Carbonate	111.7	22.1	$9x10^{-12}$	$9x10^{-13}$	10:1	0.019	1,128	192	$4x10^{-7}$	0.84	$1.14x10^{-2}$
Unit A-1 Evaporite	133.8	2	$3x10^{-13}$	$3x10^{-14}$	10:1	0.007	1,217	325	$4x10^{-7}$	0.94	$5.16x10^{-3}$
Unit A0	135.8	2.3	$3x10^{-13}$	$3x10^{-14}$	10:1	0.032	1,240	360	$5x10^{-7}$	0.76	$1.13x10^{-3}$
Guelph	138.1	71.4	$3x10^{-8}$	$3x10^{-8}$	1:1	0.057	1,247	370	$4x10^{-7}$	0.47	$6.12x10^{-1}$
Goat Island	-	-	$2x10^{-12}$	$2x10^{-13}$	10:1	0.02	1,200	300	$3x10^{-7}$	0.72	$9.03x10^{-3}$
Gasport	-	-	$2x10^{-12}$	$2x10^{-13}$	10:1	0.02	1,200	300	$3x10^{-7}$	0.72	$9.03x10^{-3}$
Lions Head	-	-	$5x10^{-12}$	$5x10^{-13}$	10:1	0.031	1,200	300	$3x10^{-7}$	0.62	$4.66x10^{-1}$
Rochester	-	-	$5x10^{-12}$	$5x10^{-13}$	10:1	0.031	1,200	300	$3x10^{-7}$	0.62	$4.66x10^{-1}$
Reynales/Fossil Hill	209.5	6.8	$5x10^{-12}$	$5x10^{-13}$	10:1	0.031	1,200	300	$3x10^{-7}$	0.62	$1.67x10^{-3}$
Cabot Head	216.3	15.8	$9x10^{-14}$	$9x10^{-15}$	10:1	0.116	1,204	306	$1x10^{-6}$	0.6	$3.22x10^{-2}$

Formation	Unit Top Depth (mBGS)	Thickness (m)	K_H (m/s)	K_V (m/s)	$K_H : K_V$	Porosity	Fluid Density (kg/m^3)	Initial TDS (g/L)	S_s [1] (m^{-1})	ζ [1]	τ [2]
Manitoulin	232.1	15.6	$9x10^{-14}$	$9x10^{-15}$	10:1	0.028	1,233	350	$8x10^{-7}$	0.86	$6.45x10^{-3}$
Queenston	247.7	77.6	$2x10^{-14}$	$2x10^{-15}$	10:1	0.073	1,207	310	$9x10^{-7}$	0.71	$1.65x10^{-2}$
Georgian Bay/Blue Mountain	325.3	154.3	$4x10^{-14}$	$3x10^{-15}$	13:1	0.07	1,200	299.4	$1x10^{-6}$	0.79	$1.41x10^{-2}$
Cobourg	479.6	46.4	$2x10^{-14}$	$2x10^{-15}$	10:1	0.015	1,181	272	$3x10^{-7}$	0.8	$2.97x10^{-2}$
Sherman Fall	526	47.3	$1x10^{-14}$	$1x10^{-15}$	10:1	0.016	1,180	270	$5x10^{-7}$	0.88	$1.65x10^{-2}$
Kirkfield	573.3	39.5	$8x10^{-15}$	$8x10^{-16}$	10:1	0.021	1,156	234	$5x10^{-7}$	0.85	$2.41x10^{-2}$
Coboconk	612.8	8	$4x10^{-12}$	$4x10^{-15}$	1,000:1	0.009	1,170	255	$5x10^{-7}$	0.93	$3.61x10^{-2}$
Gull River	620.8	53.4	$7x10^{-13}$	$7x10^{-16}$	1,000:1	0.022	1,135	203	$5x10^{-7}$	0.85	$1.42x10^{-2}$
Shadow Lake	674.2	7.6	$1x10^{-9}$	$1x10^{-12}$	1,000:1	0.097	1,133	200	$7x10^{-7}$	0.56	$1.61x10^{-2}$
Cambrian	-	-	$3x10^{-6}$	$3x10^{-6}$	1:1	0.071	1,157	235	$4x10^{-7}$	0.34	$2.88x10^{-1}$
Upper Precambrian	681.8	20	$1x10^{-10}$	$1x10^{-10}$	1:1	0.038	1,200	300	$3x10^{-7}$	0.49	$9.50x10^{-3}$
Precambrian	701.8	-	$1x10^{-12}$	$1x10^{-12}$	1:1	0.005	1,200	300	$2x10^{-7}$	0.88	$7.22x10^{-2}$

Notes: For this study, the permeability of the upper 50 m of the domain is set to $1.0x10^{-7}$ m/s in order to reflect weathering of the geologic units near surface.
[1] S_s represents specific storage and ζ represents loading efficiencies.
[2] The estimated tortuosities for formations below the drift are based upon a free solution diffusion coefficient for NaI of 1.662E-9 m^2/s (Weast 1983), porosity values specified above, the effective diffusion coefficients ($D_{e,v}$) for NaI in Table 1 of APM-REF-01900-29841, assuming a diffusion accessible porosity factor of 0.5 for NaI (INTERA 2011). The tortuosity for the drift was adopted from Sykes et al. (2011).

2.2.2.3 Paleohydrogeology Boundary Conditions

Paleohydrogeological simulations are used to illustrate the long-term evolution and stability of the geosphere to external perturbations. Glaciation is expected to be the largest external perturbation to which the repository would be subjected.

Over the last one million years, the sedimentary rocks chosen for the host rock at the repository site have been subjected to nine glacial cycles, each lasting for a period of approximately 100,000 years (Peltier 2002). During the last glacial advance and retreat, up to three kilometres of ice overrode the hypothetical repository site. In assessing the long-term stability and evolution of groundwater systems at depth in sedimentary rock, the loading and unloading of the geosphere by the glacier will represent one of the most significant perturbations from the current conditions.

The University of Toronto (UofT) Glacial Systems Model (GSM) provides the hydraulic and mechanical paleoclimate boundary conditions and permafrost depths for the paleohydrogeologic simulations (Peltier 2011). Peltier (2011) describes eight models that "span the apparent range of model characteristics that provide acceptable fits to the totality of the observational constraints." Of these eight models, nn9921 and nn9930 are two of the best models based on aggregate misfit, and both include high-resolution permafrost development. Paleoclimate simulation nn9930 represents a single realization of a glacial cycle, as predicted by the GSM. A plot of various nn9930 GSM outputs for the grid cell containing the sub-regional modelling domain is shown in Figure 2-2. These outputs include ice thickness, meltwater production rate, lake depth, permafrost depth, and ice-sheet basal temperature relative to the pressure melting point of ice. Only the ice thickness, lake depth, and permafrost depth outputs are applied to the paleohydrogeologic groundwater simulations. The isostatic movement of the ground surface due to ice loading is not considered; applied hydraulic boundary conditions are stated in terms of elevation, assuming the grid does not move vertically. The application of lake depth is also a relative term independent of isostatic movement, although isostatic depression is required for a proglacial lake to form. Although lake depth could be interpolated across the TIN (Triangulated Irregular Network) in a similar manner to permafrost depth and vertical stress due to ice, large gradients could be created across the domain which would not exist in the presence of a large proglacial body of water because isostatic movement is not considered. Due to this, lake depth is added to the existing lake elevation and the hydraulic boundary conditions are adjusted accordingly.

The alternate paleoclimate simulation, nn9921, GSM model outputs for the grid cell containing the sub-regional modelling domain are shown in Figure 2-3. The paleoclimate simulation nn9921 represents a cold-based ice sheet, whereas paleoclimate simulation nn9930 represents a warm-based ice sheet. The main difference between the two glaciation scenarios is the duration of permafrost during the 121,000 years GSM simulation; the length of time nn9930 is subject to permafrost and glaciated conditions is less than that of nn9921. In addition, more frequent glacial advances and retreats occur in paleoclimate simulation nn9921. The paleoclimate boundary conditions presented in Figure 2-2 and Figure 2-3 are applied to the paleoclimate simulations described in Section 2.3.4.3. Permafrost hydraulic conductivity is discussed in Section 2.3.3.2.1.

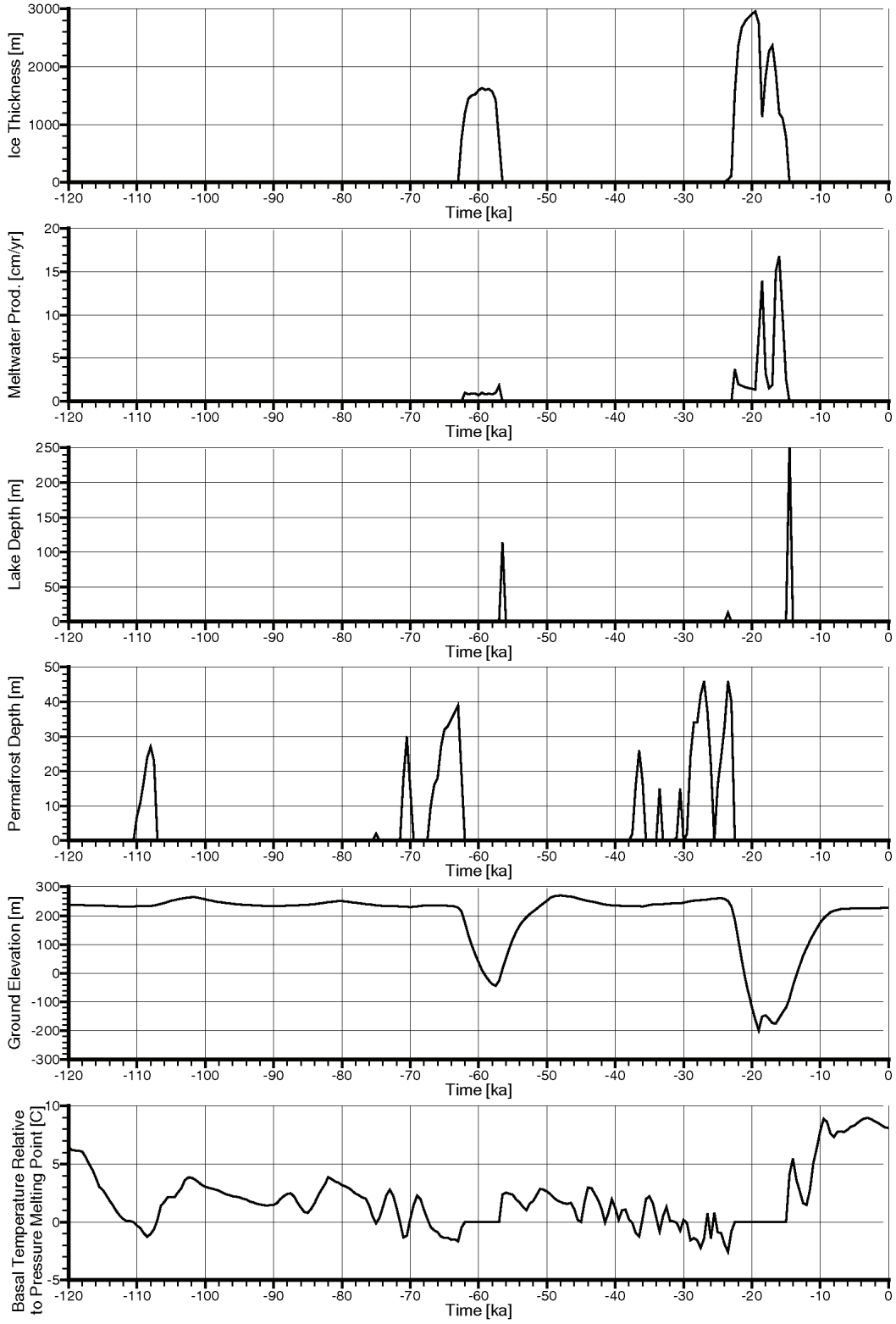

Figure 2-2: nn9930 GSM Model Outputs for the Grid Block Containing the Repository Footprint for this Study

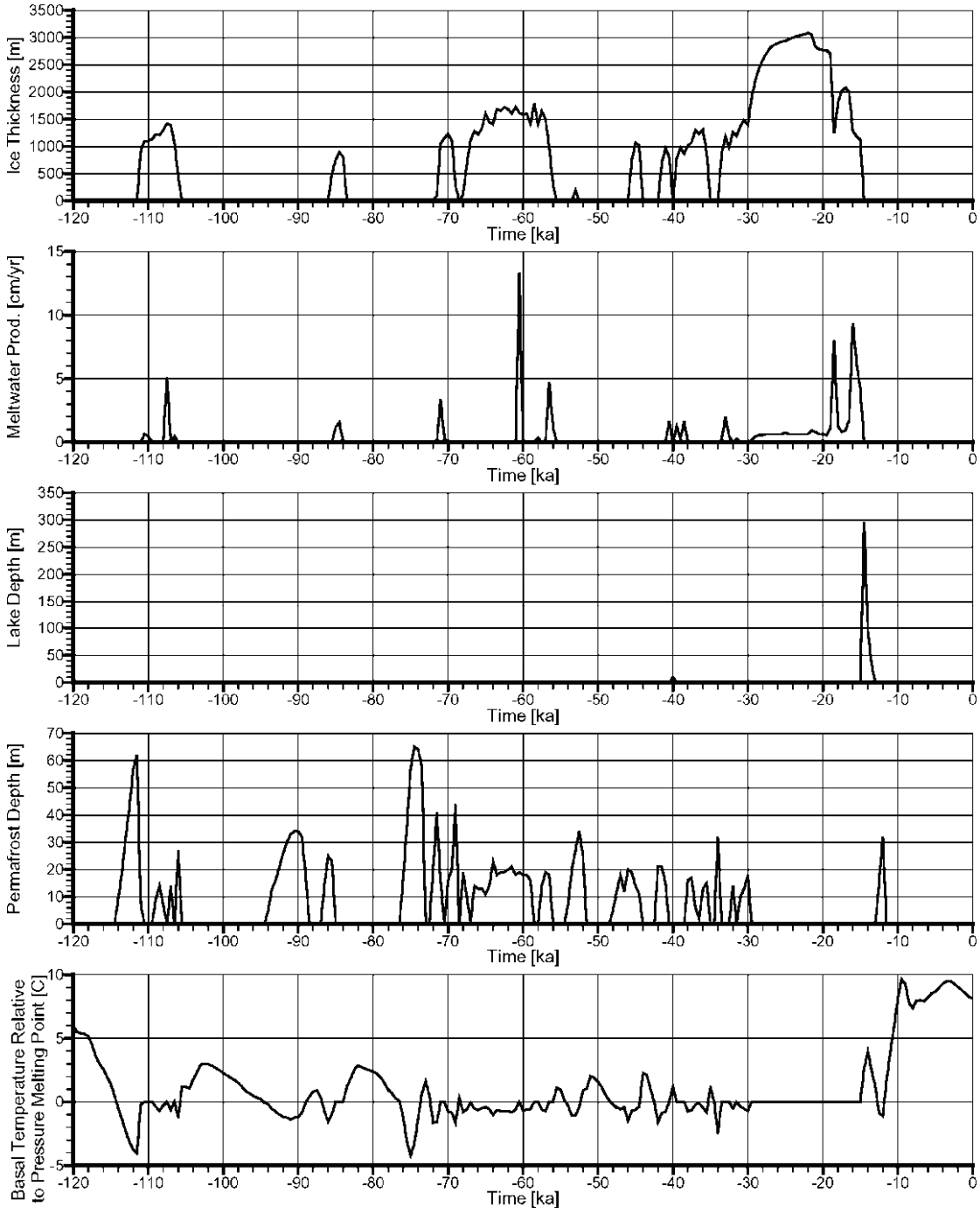

Figure 2-3: nn9921 GSM Model Outputs for the Grid Block Containing the Repository Footprint for this Study

2.2.2.4 Abnormal Pressure Distributions

Within the Michigan Basin, abnormal pressure distributions have been observed. Where the Cambrian Formation is present within the regional area, overpressures with respect to ground elevation have been observed in the formation (NWMO 2011). However, the Cambrian Formation is not present at the hypothetical site. For the purpose of this study, hydrostatic pressure with depth is assumed at the repository site.

2.2.2.5 Unsaturated Groundwater Flow

Although there is evidence of residual gas phases in some formations in the Michigan Basin, the geoscience scenarios investigated for this study only consider fully-saturated groundwater flow.

2.2.3 Descriptive Geochemical Model

Groundwaters and porewaters in sedimentary basin environments can often be typified by the following characteristics.

- $\delta^{18}O$ and $\delta^{2}H$ signatures are enriched relative to the Global Meteoric Water Line (GMWL), typically plotting to the right and below the GMWL on a plot of $\delta^{18}O$ versus $\delta^{2}H$.
- Formation waters are attributed to an ancient seawater or evaporated seawater origin, with relatively high concentrations of sodium (Na), calcium (Ca) and chloride (Cl).
- Variations in formation water chemistry from a seawater or evaporated seawater signature are often attributed to a variety of natural processes, such as water-rock interaction, mixing with other waters, dilution, and microbially-mediated reactions. Groundwater and porewater geochemistry is modified over both time and space by such processes.
- High total dissolved solids (TDS) concentrations which are typical of sedimentary formations as a result of the aforementioned processes.

The regional hydrogeochemical data (presented in Hobbs et al. 2011) generally indicates increasing salinity with depth below ground surface in southwestern Ontario. A vertical salinity profile, between ground surface and a depth of 865 m, collected at the Bruce site (presented in NWMO 2011; Figure 4.6), located near Tiverton, Ontario, is consistent with the regional trend.

Numerous geochemical processes have been proposed to account for the high salinity of sedimentary brines. In the context of southern Ontario, processes that are considered possible include:

1. The evaporation of seawater (e.g., Carpenter 1978, Kharaka et al. 1987);
2. The dissolution of halite or other evaporites (e.g., Rittenhouse 1967, Land and Prezbindowski 1981);
3. Membrane filtration (Bredehoeft et al. 1963, Berry 1969, Kharaka and Berry 1973, Graf 1982); and/or
4. Ingress of concentrated brines from crystalline shield-type rocks (e.g., Land 1997).

It is generally agreed that most chloride in sedimentary basin brines has been derived from some combination of entrapped and/or infiltrated evaporated seawater and dissolved, subsurface evaporites (e.g., Kharaka and Hanor 2005, Hanor 2001).

Sedimentary formation waters typically have chemistries that vary considerably from what would be expected of evaporated meteoric water or seawater. During the diagenetic evolution of the brines, calcium and strontium concentrations can increase by up to an order of magnitude compared to evaporated seawater, whereas magnesium and potassium concentrations may decrease by as much as an order of magnitude (Kharaka and Hanor 2005). Variations in the chemistry of brines from that expected for evaporated seawater are often explained using water-rock reaction processes, including:

1. Dissolution or precipitation of evaporite minerals, including halite and gypsum and/or anhydrite;
2. Calcite precipitation or dissolution;
3. Dolomitization;
4. Dissolution or precipitation of aluminosilicates; and
5. Ion exchange reactions with clays (e.g., McIntosh and Walter 2006).

Dolomitization is the most extensive diagenetic process to have influenced the sedimentary sequence underlying southern Ontario (Hobbs et al. 2011).

Information on the geochemical conditions collected as part of detailed site characterization activities would be combined with available regional information to define site-specific conditions. The geochemical conditions in the shallow, intermediate and deep groundwater systems assumed for the hypothetical site are described below. Microbiology, sorption, and the anticipated gas species in groundwaters within the sedimentary setting at the proposed repository horizon are also described in Sections 2.2.3.1 to 2.2.3.3, respectively.

For the site, a hypothetical TDS profile (presented in Section 2.3.4.1), suggests the presence of three distinct groundwater systems within the sedimentary package: a shallow system (0-215 m), consisting of relatively fresh water, with TDS of ≤ 5 g/L; an intermediate system (215-250 m); and, a deep system (>250 m) with significantly elevated groundwater and porewater salinities (200-300 g/L TDS). The transition zone between the shallow and deep systems is loosely termed the intermediate system, which is marked by a change in salinity from ~5 g/L TDS to ~275 g/L over a vertical distance of approximately 35 m.

Table 2-3 shows the average TDS (g/L) values, which are based on the modelled salinity profile presented in Section 2.3.4.1. The groundwaters and porewaters in the sedimentary formations at the site show the following general salinity distribution trends with depth. The TDS values are indicative of relatively fresh water (<5 g/L) in the shallow system between ground surface and 215 m depth. The TDS values begin to increase at the base of the Fossil Hill Formation (215 m). Between the base of the Fossil Hill Formation and the top of the Manitoulin Formation, TDS values increase from ~5 g/L to ~260 g/L. Maximum salinity (~290 g/L) is projected to occur near the contact between the Queenston Formation and the Georgian Bay/Blue Mountain Formation at a depth of approximately 330 m. Salinity values are relatively consistent with depth through the remainder of the shales until just above the Georgian Bay/Blue

Mountain-Cobourg Formation contact, where TDS values begin to decrease steadily with depth to a value of 200 g/L in the Shadow Lake Formation (680 m).

The geochemical conditions described below pertain to the overall properties of both the groundwaters and porewaters present within the shallow, intermediate and deep groundwater systems at the hypothetical site.

Shallow Groundwater System (0 - 215 mBGS)

The shallow groundwater system extends from ground surface to approximately 215 m depth. The shallow groundwater system is characterized by relatively fresh waters (<5 g/L TDS) and includes the Quaternary, Late Silurian and Middle Silurian groundwaters and porewaters. Based on regional observations, as well as data collected at the Bruce site, the shallow groundwater system is expected to be oxidizing.

Intermediate Groundwater System (215 - 250 mBGS)

The intermediate groundwater system is characterized by a transition in salinity from approximately 5 g/L TDS at the top of the Cabot Head Formation to a salinity of approximately 275 g/L TDS at the base of the Manitoulin Formation, over a vertical distance of ~35 m. The intermediate groundwater system represents a transition zone from oxidizing to reducing conditions as well (NWMO 2011). Although no site-specific data exists, similar conditions are anticipated for the hypothetical site. Such conditions would be verified during site characterization activities.

Deep Groundwater System (>250 mBGS)

The deep groundwater system is characterized by high salinity, ranging between 200 and 300 g/L TDS. Based on regional data, as well as data collected at the Bruce site, reducing conditions are expected at all depths below 250 m.

Table 2-3: Average TDS Values for Sedimentary Formation Groundwaters and Porewaters

Formation	Average TDS (g/L)
Drift	0.1
Unit B and C	0.3
Unit A-2 Carbonate	0.6
Unit A-1 Upper Carbonate	0.8
Unit A-1 Carbonate	2
Unit A-1 Evaporite	3
Unit A-0	3
Guelph	3
Reynales/Fossil Hill	4
Cabot Head	12
Manitoulin	142
Queenston	294
Georgian Bay/Blue Mountain	298
Cobourg	279
Sherman Fall	260
Kirkfield	244
Coboconk	235
Gull River	219
Shadow Lake	204
Upper Precambrian	203
Precambrian	250

Saline groundwater conditions are expected at the depth of the hypothetical repository (500 mBGS). Groundwater chemistry at this depth in sedimentary formations of southern Ontario is typically Na-Ca-Cl or Ca-Na-Cl water under reducing conditions (Hobbs et al. 2011). A reference composition has been defined for the porewaters anticipated to be found within the proposed repository horizon. The composition is presented in Table 2-4.

Table 2-4: Reference SR-270-PW Composition

Composition	SR-270-PW
Water Type	Na-Ca-Cl
pH	5.8
Environment Type	Reducing
Eh	-200 mV
Density	1,181
Solutes (mg/L)	
Na	50,100
K	12,500
Ca	32,000
Mg	8,200
HCO_3	110
SO_4	440
Cl	168,500
Br	1,700
Sr	1,200
Li	5
F	1
I	3
B	80
Si	4
Fe	30
NO_3	<5
PO_4	-
TDS	275,000

Based on diffusion experiments performed on core collected during site investigations at the Bruce site, effective diffusion coefficients (D_e) for iodide and tritiated water (HTO) were estimated for the proposed host rock, and for the surrounding Silurian and Ordovician shale and carbonate rocks. The D_e values obtained with HTO are on average 1.9 times greater than the D_e values obtained with an iodide tracer. The D_e values at the hypothetical site are anticipated to be similar to those measured for the Bruce site (see below), but would have to be verified during site characterization activities:

Silurian carbonate: 10^{-13} to 10^{-10} m^2/s, and

Ordovician shale and carbonate: 10^{-13} to 10^{-11} m^2/s (INTERA 2011).

2.2.3.1 Microbial Conditions in Sedimentary Environments

A number of studies have been performed on sedimentary rock in attempts to characterize microbial populations and activities. Microbial metabolism requires a carbon source, a terminal electron donor and terminal electron acceptor. Additional nutrients are required for growth and maintenance, including nitrogen (N), phosphorous (P), sulfur (S), potassium (K), magnesium (Mg), sodium (Na), calcium (Ca) and iron (Fe), as well as a suite of other trace elements. Subsurface microbial communities are capable of using an array of terminal electron accepting processes. The dominant species in a given environment tend to be those bacteria that generate the most energy from the available nutrient sources.

Some of the most extensive work on microbial activity in low permeability sedimentary systems has been performed on the Opalinus Clay Formation at the Mont Terri Rock Laboratory in Switzerland. Clay-rich formations, such as the Opalinus Clay, have been the focus of significant attention as possible host formations for nuclear waste repositories due to their low permeability, diffusion-dominated transport regimes, geochemical stability and capacity for self-sealing (Wersin et al. 2011, Stroes-Gascoyne et al. 2011). Due to the low salinity of the waters at Mont Terri, application of the results of such studies to the hypothetical site is somewhat limited. However, aspects of the Mont Terri work are relevant to the hypothetical site in the context of repository safety. A key result of the work indicated that contamination during drilling could promote anaerobic microbial activity (in particular, NO_3-, Fe- and SO_4- reducers and methanogens; Wersin et al. 2011, Stroes-Gascoyne et al. 2011) and that the effects of drilling and excavation disturbances are both temporary and spatially limited. In a state-of-science review documenting the role of microorganisms in relation to the design and performance of a DGR, Sherwood Lollar (2011) concluded that hydrology, geochemistry, and resident microbial populations may be sensitive to changes (i.e., perturbations) in any given system, but that many systems possess a geochemical buffering capacity to counter the effects of perturbations. In the context of the hypothetical site, properties of the deep system, such as low porosity and very high salinity, are anticipated to provide a natural buffering capacity to the proposed host and surrounding rock.

Microbial analyses were performed on samples of Queenston Formation shale and Cobourg Formation limestone from drill core collected during site characterization activities at the Bruce nuclear site (Stroes-Gascoyne and Hamon 2008). Samples of crushed and powdered Cobourg limestone, and samples of crushed Queenston shale, were analyzed for microbial activity. Crushed or powdered rock samples were suspended in a buffering solution or a synthetic porewater solution and plated on regular agar. The synthetic porewater solutions were intended to simulate geochemical conditions (e.g., high salinity, low water activity) at depth and the results used to assess the likelihood of a sustainable microbial community under such conditions. The results of the analyses indicate only the presence of common near-surface aerobic and anaerobic microorganisms, which were attributed to contamination of the rock samples after core recovery. Samples were analyzed for the presence of phospho-lipid fatty acid (PLFA), neutral-lipid fatty acid (NLFA) and glycol-lipid fatty acid (GLFA) as a means to measure microbial activity. The presence of PLFA is used to indicate viable (live) microbial cells, while NLFA and GLFA are indicators of dead cells. In the Cobourg Formation powdered limestone sample, no viable biomass was identified and only NLFA and GLFA were identified, indicating a lack of on-going microbial activity. Based on the existing microbiological data for deep sedimentary formations, it is anticipated that similar conditions – i.e., low water activity,

low microbial activity – would occur at the hypothetical site at the proposed repository depth of 500 m.

2.2.3.2 Sorption

The sorption of radionuclides onto mineral surfaces within the geosphere is a potential mechanism for slowing the transport of radionuclides from the repository to the surface environment. There are many factors that impact radionuclide sorption processes in the geosphere, such as rock type, mineral surface area, groundwater salinity, pH, redox conditions, temperature, the presence or absence of complexing ligands and radionuclide concentration.

Sorption of radionuclides is generally reduced in groundwaters with high salinity (Vilks 2009). Experiments to develop a further understanding of sorption processes in Na-Ca-Cl brine solutions within Canadian sedimentary rocks were initiated in 2009 (Vilks et al. 2011). Sorption of several elements on shale and limestone was tested in Na-Ca-Cl brine solutions with TDS values as high as 300 g/L. The results demonstrated that some elements will not sorb, notably elements such as Sr(II) that sorb by ion exchange. The results showed that sorption of other elements, including Eu(III) (an analogue to trivalent actinides), and U(VI) to shale and limestone is measurable in brine solutions (Vilks et al. 2011). The formation of complexes with carbonate was observed to reduce the sorption of Eu(III) and U(VI).

2.2.3.3 Gas Characterization

Natural gases commonly encountered in deep sedimentary formations include methane, helium and carbon dioxide. Both concentrations and isotopes of methane, helium and carbon dioxide can be helpful in assessing fluid origin and solute transport.

Sherwood Lollar et al. (1994) examined natural gases from within Ordovician and Cambrian reservoirs in southwestern Ontario, and characterized the gases using isotopic and compositional indicators. Consistent with the findings of Barker and Pollock (1984), gases from the Cambrian and Ordovician reservoirs are composed predominantly of CH_4. The Cambrian and Ordovician gases were found to be thermogenic in origin, with no evidence of bacterial CH_4 contributions. Where the sedimentary rocks were in direct contact with the Precambrian basement, the gases sampled had elevated helium concentrations (Sherwood Lollar et al. 1994). The elevated helium concentrations, and associated high $^3He/^4He$ ratios, may reflect mixing between gases generated in-situ (in the Cambrian and Ordovician strata) and an end-member enriched in helium. Possible sources for the helium-rich end-member include gas deep within the Precambrian basement rock or an external helium-enriched fluid that migrated from deeper within the sedimentary system along pathways controlled by basement-structures (Sherwood Lollar et al. 1994).

Data collected at the Bruce site is generally consistent with regional scale findings. Thermogenic methane has been identified in the Ordovician Trenton and Black River Groups, while the overlying shales and Cobourg Formation are characterized by the presence of biogenic methane (NWMO 2011; Section 4.4.3.1). There is little evidence of mixing between the biogenic and thermogenic gas, and it is hypothesized that the thermogenic methane may have been generated in-situ in association with peak burial and/or has been transported from a deeper basinal or Precambrian source. $^3He/^4He$ ratios in the Trenton and Black River groups are observed to be elevated relative to the overlying Ordovician shales, and also relative to

values estimated for in-situ formation due to natural decay processes in the rock, which suggests an enriched end-member for mixing, possibly of deep basin or Precambrian origin. Carbon dioxide was also analyzed for both concentration and isotopic composition, but only the isotopic data is considered to be reliable for interpretation purposes. The isotopic composition ($\delta^{13}C$ and $\delta^{18}O$ of CO_2) of the carbon dioxide is consistent with the assessment of biogenic gas formation in the Ordovician shales and thermogenic (non-biotic) gas formation in the Trenton and Black River groups.

At the hypothetical site, which, like the Bruce site, is located along the eastern margin of the Michigan Basin, it is anticipated that similar gas distributions and signatures would be observed. This would require verification during site characterization activities.

2.3 Regional Scale Hydrogeologic Modelling

The primary objective of the analyses of this section is to investigate the role of key geosphere parameters and processes, such as sedimentary rock permeabilities and groundwater salinity, on geosphere stability at repository depth. The following sections describe the suite of regional scale numerical groundwater models that were developed.

2.3.1 Computational Models

The numerical groundwater modelling was performed using FRAC3DVS-OPG v1.3.0 (Therrien et al., 2010). This computational model is designed to solve the equation for three-dimensional variably-saturated groundwater flow and solute transport in discretely-fractured media. The numerical solution to the governing equations is based on implementations of both the control volume finite element method and the Galerkin finite-element method. The FRAC3DVS-OPG model couples fluid flow with salinity transport through fluid density, which is dependent on the total dissolved solids concentration. Details of the model that are pertinent to the study are described in Therrien et al. (2010) and in Normani et al. (2007). FRAC3DVS-OPG was developed and is maintained as nuclear grade software in a Quality Assurance framework. Details on the validation of FRAC3DVS-OPG are found in Therrien et al. (2010).

Important attributes of FRAC3DVS-OPG include:

1. Its ability to describe arbitrary combinations of porous, discretely fractured and dual porosity media;
2. Its flexible pre- and post-processing capabilities;
3. The accurate handling of fluid and mass exchanges between fracture zones and matrix, including matrix diffusion effects and solute advection in the matrix;
4. Fluid and solute mass balance tracking; and
5. Adaptive time-stepping schemes with automatic generation and control of time steps.

Additional attributes added in previous work supported by the NWMO and OPG includes sub-gridding and sub-timing capabilities (Park et al. 2008). Additionally, algorithms to estimate performance measures of groundwater age and life expectancy for the domain groundwater are available also (Cornaton and Perrochet 2006a, 2006b).

2.3.2 System Performance Measures

The safety case for a potential deep geologic repository relies, in part, on the ability of the geosphere to provide a long-term barrier to solute transport. The behaviour and stability of the groundwater flow and transport regimes found at repository depth can be illustrated by determining and quantifying what impact, if any, the variability of model parameters will have upon the model results. By demonstrating and determining the sensitivity of the model to perturbations in model parameters, a more rigorous understanding of the groundwater system at depth can be achieved.

Common measures of the performance of a groundwater system include the flow state variables of equivalent freshwater head or environmental head and the derived porewater velocity, the solute concentration for a conservative tracer, the Péclet number of molecular diffusion (Bear 1988, Huysmans and Dassargues 2005) and, as shown in Normani et al. (2007), mean lifetime expectancy (MLE) and groundwater age. Lifetime expectancy can be estimated by determining the Probability Density Function (PDF) for the time required for water particles at a spatial position in a groundwater system to reach potential outflow points. Particles can migrate to the boundary by both advection and hydrodynamic dispersion; particles at a given point in the system will not follow the same path to the boundary due to hydrodynamic dispersion. In this case study, the first moment of the PDF for lifetime expectancy is estimated with the value being expressed as the MLE. MLE correctly replicates the transport processes, but is subject to the classical problems of numerical instability. For a model with large grid blocks and, hence, a large numerical dispersivity that meets grid or cell Péclet number criteria, MLE tends to underestimate the average time for particles to reach discharge points.

2.3.3 Regional Scale Conceptual Model

2.3.3.1 Model Domain and Spatial Discretization

The regional scale modelling domain boundary was chosen by Sykes (2007). The southeastern portion of the boundary follows the regional surface water divides. These divides were determined using a Digital Elevation Model (DEM) from the Shuttle Radar Topography Mission (SRTM) and a river network in ArcGIS. Based on the assumption that the water table is a subdued reflection of surface topography, topographic divides are chosen as no-flow boundaries for the upper flow regime, as well as for the higher permeability Niagaran Group within the intermediate flow regime. The eastern boundary of the modelling domain is at a topographic high (west of the Algonquin Arch) and the domain extends to the deepest portions of both the lakes to the north and west. The bathymetric data of both water bodies, provided by National Oceanic and Atmospheric Administration (NOAA), was combined with the DEM to provide a continuous surface for the top of the Earth's solid surface.

The reference case data set for the conceptual model consists of 32 stratigraphic units, as defined by the 3DGF geologic framework model (Table 2-2 from ITASCA CANADA and AECOM 2011). In this case study, the Niagaran Group in the 3DGF model was divided into the Guelph, Goat Island, Gasport, and Lions Head (Rochester) formations; the A-1 Carbonate unit in the 3DGF was divided into the A1-Upper Carbonate and the A1-Carbonate. Some stratigraphic units are sub-divided into multiple model layers, as shown in Table 2-5. In total, 102 model layers were developed for the regional scale domain.

Table 2-5: Sub-divisions of Geologic Formations

Period	Formation	Model Layers
Quaternary	Drift	1
Devonian	Hamilton Group	1
	Dundee	2
	Detroit River Group	6
	Bois Blanc	1
Silurian	Bass Islands	2
	Unit G	1
	Unit F	1
	Unit F Salt	1
	Unit E	1
	Unit D	1
	Units B and C	4
	Unit B Anhydrite	2
	Unit A-2 Carbonate	6
	Unit A-2 Evaporite	6
	Unit A-1 Upper Carbonate	6
	Unit A-1 Carbonate	6
	Unit A-1 Evaporite	4
	Unit A0	4
	Guelph	6
	Goat Island	2
	Gasport	2
	Lions Head/Rochester	2
	Reynales/Fossil Hill	1
	Cabot Head	1
	Manitoulin	1
Ordovician	Queenston	2
	Georgian Bay/Blue Mtn.	3
	Cobourg	1
	Sherman Fall	1
	Kirkfield	1
	Coboconk	1
	Gull River	1
	Shadow Lake	4
Cambrian	Cambrian	6
Precambrian	Upper Precambrian	4
	Precambrian	6

A two-dimensional square grid (1 km × 1 km) was developed to fit within the conceptual model boundary. The grid has an east-west extent of 152 km, a north-south extent of 179 km, and covers an area of 18,887 km^2. The two-dimensional grid forms a horizontal template to develop the three-dimensional grid by interpolating the vertical position of each node from the 32 interfaces provided by ITASCA CANADA and AECOM (2011). Four additional interfaces are generated by the refinement of both the Niagaran Group and the A-1 Carbonate.

A block-cut view of the assigned FRAC3DVS-OPG geologic layer zone identifiers within the model domain are shown in Figure 2-4. Each zone identifier is associated with a specific geologic layer or geologic grouping. Note that the vertical exaggeration is 40:1 in this and other figures showing the regional scale spatial domain (152 km × 179 km). A view of all geologic units and the spatial variation in their thickness is shown in Figure 2-5. The inset block in the Cobourg represents a 20 km x 20 km area around the hypothetical site.

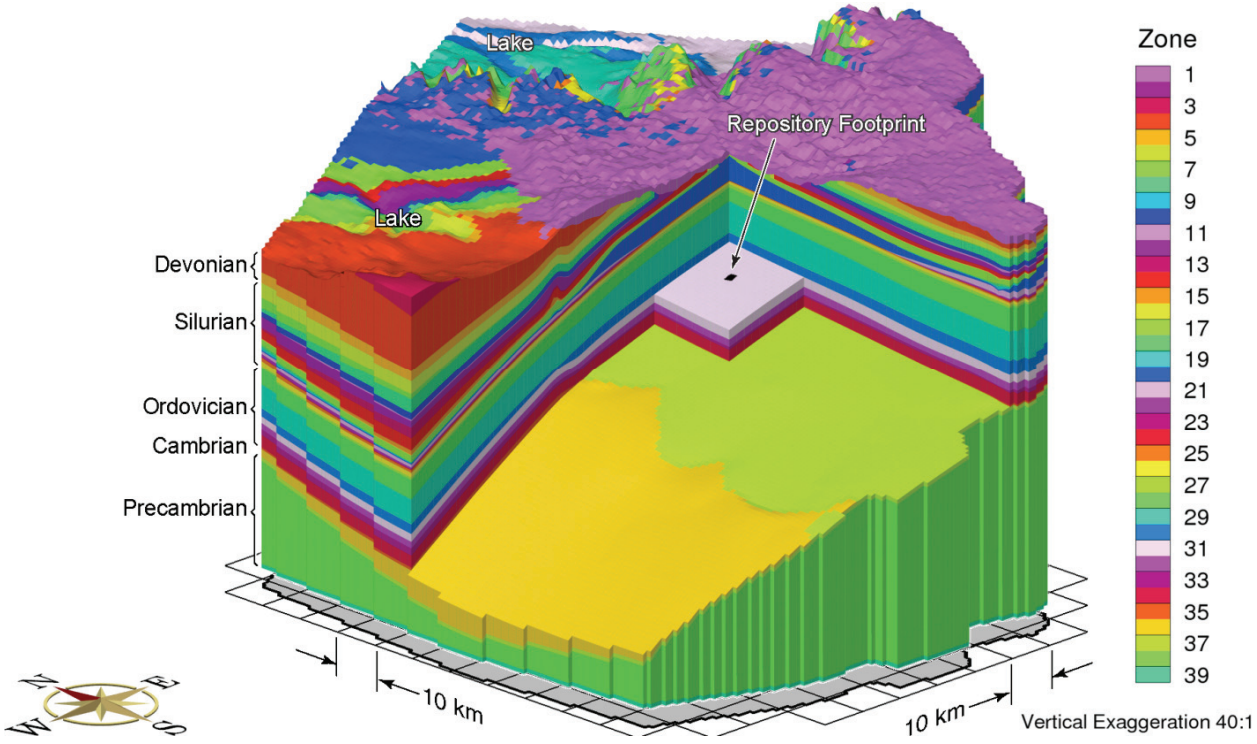

Figure 2-4: Block Cut View of FRAC3DVS-OPG Zone Identifiers for Regional Scale Domain

2.3.3.2 Model Parameters

The physical hydrogeological parameters defined in this section are applied to the regional scale numerical models. All groundwater flow parameters summarized in Table 2-2 are consistent with parameters used for regional modelling for the OPG Low & Intermediate Level Waste Deep Geologic Repository (Sykes et al. 2011). For the scenario with a Biot coefficient of 0.5, alternate computed loading efficiency and specific storage values for each geologic unit are listed in Table 2-6.

2.3.3.2.1 Hydraulic Conductivity of Permafrost

For paleohydrogeologic simulations, the interpolated permafrost depths from the Glacial Systems Model (GSM) simulations (Peltier 2011) were used to select any FRAC3DVS-OPG grid block whose top face was within the permafrost zone for each time step. A detailed description of selected paleoclimate simulations is discussed in Section 2.3.4.3. A permafrost hydraulic conductivity of 5×10^{-11} m/s is applied (McCauley et al. 2002). Permafrost within a grid block would limit vertical flow in and out of the groundwater system due to its very low effective hydraulic conductivity.

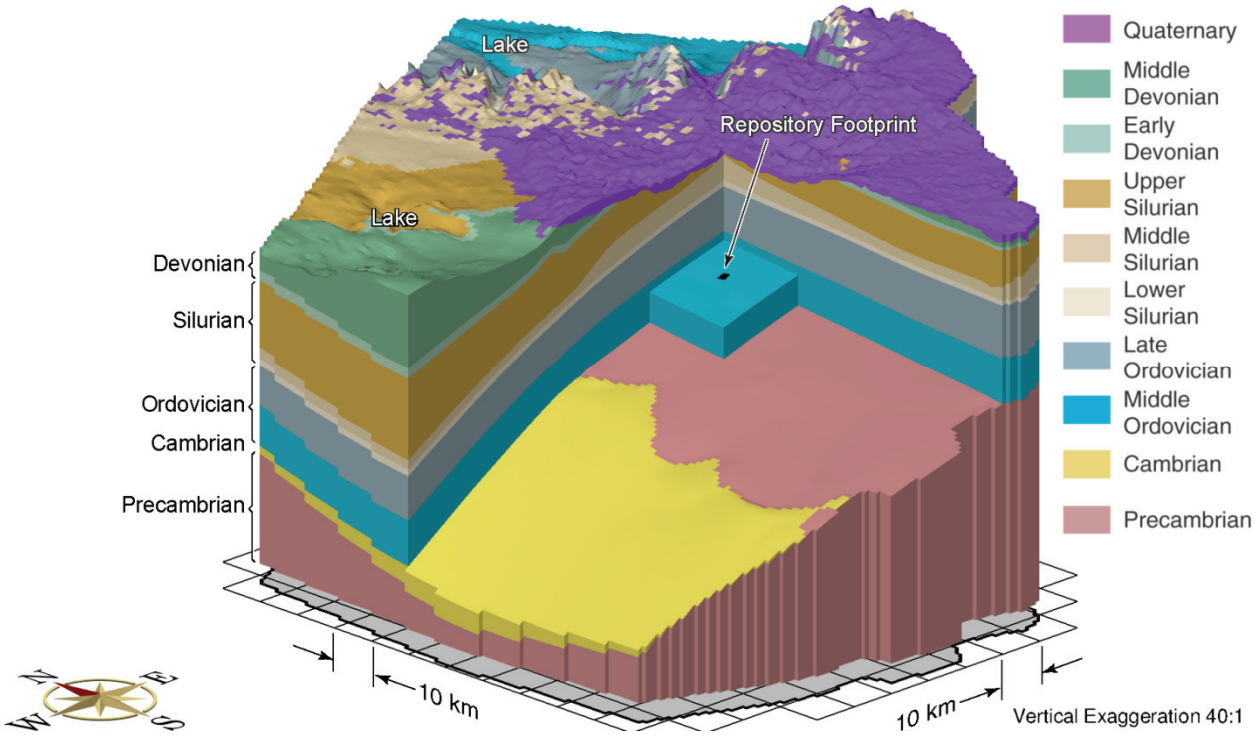

Figure 2-5: Block Cut View Showing Spatial Extent of the Bedrock Units

2.3.3.2.2 Precambrian Hydraulic Conductivity

Horizontal and vertical permeabilities for the Precambrian units, as a function of depth, are expressed following Normani (2009), as determined for data from various Canadian field studies at the Whiteshell Research Area (WRA):

$$\mathbf{k_H} = \mathbf{10^{-14.5-4.5\left(1-e^{-0.002469d}\right)}} \tag{2-1}$$

$$k_V = \begin{cases} 10k_H, & \text{for } d \leq 300 \text{ m;} \\ [0.09(400-d)+1]k_H, & \text{for } 300 < d \leq 400 \text{ m;} \\ k_H, & \text{for } d > 400 \text{ m.} \end{cases} \tag{2-2}$$

where k_H is the horizontal permeability [L^2];

k_V is the vertical permeability [L^2]; and

d is the depth relative to a constant reference elevation of 176 m for the top of the Precambrian [L].

As shown in Figure 2-6, the matrix permeabilities decrease exponentially with increasing depth.

2.3.3.2.3 Groundwater Transport Parameters

Table 2-2 lists various transport parameters that are used in this study to simulate the movement of variably dense pore fluids, for tracer movement to determine the depth of recharge water penetration, and for mean life expectancy calculations. The large grid spacing used for the regional scale domain necessitates relatively large dispersivity values employed in the modelling phase of this case study, in order to maintain numerically stable results. The dispersivity values used for MLE calculations are triple the values listed in Table 2-7.

Table 2-6: Loading Efficiency (ζ) and Specific Storage (S_s) for Scenario (fr-base-paleo-biot05) with a Biot Coefficient of 0.5

Formation	S_s (m^{-1})	ζ
Drift	9.9×10^{-5}	0.99
Hamilton Group	1.1×10^{-6}	0.54
Dundee	1.1×10^{-6}	0.54
Detroit River Group	1.0×10^{-6}	0.56
Bois Blanc	1.0×10^{-6}	0.56
Bass Islands	1.3×10^{-6}	0.71
Unit G	8.7×10^{-7}	0.36
Unit F	7.2×10^{-7}	0.45
Unit F Salt	7.2×10^{-7}	0.45
Unit E	5.1×10^{-7}	0.32
Unit D	4.9×10^{-7}	0.35
Unit B and C	7.7×10^{-7}	0.24
Unit B Anhydrite	5.3×10^{-7}	0.35
Unit A-2 Carbonate	5.7×10^{-7}	0.29
Unit A-2 Evaporite	4.5×10^{-7}	0.35
Unit A-1 Upper Carbonate	3.9×10^{-7}	0.39
Unit A-1 Carbonate	2.8×10^{-7}	0.62
Unit A-1 Evaporite	2.6×10^{-7}	0.71
Unit A0	3.5×10^{-7}	0.54
Guelph	3.1×10^{-7}	0.30
Goat Island	1.8×10^{-7}	0.51
Gasport	1.8×10^{-7}	0.51
Lions Head	2.1×10^{-7}	0.42
Rochester	2.1×10^{-7}	0.42
Reynales/Fossil Hill	2.1×10^{-7}	0.42
Cabot Head	7.7×10^{-7}	0.41
Manitoulin	5.1×10^{-7}	0.63
Queenston	6.4×10^{-7}	0.50
Georgian Bay/Blue Mountain	8.0×10^{-7}	0.58
Cobourg	1.8×10^{-7}	0.58
Sherman Fall	3.7×10^{-7}	0.59
Kirkfield	3.8×10^{-7}	0.56
Coboconk	3.4×10^{-7}	0.62
Gull River	3.7×10^{-7}	0.56
Shadow Lake	5.9×10^{-7}	0.35
Cambrian	3.2×10^{-7}	0.19
Upper Precambrian	2.2×10^{-7}	0.29
Precambrian	1.1×10^{-7}	0.60

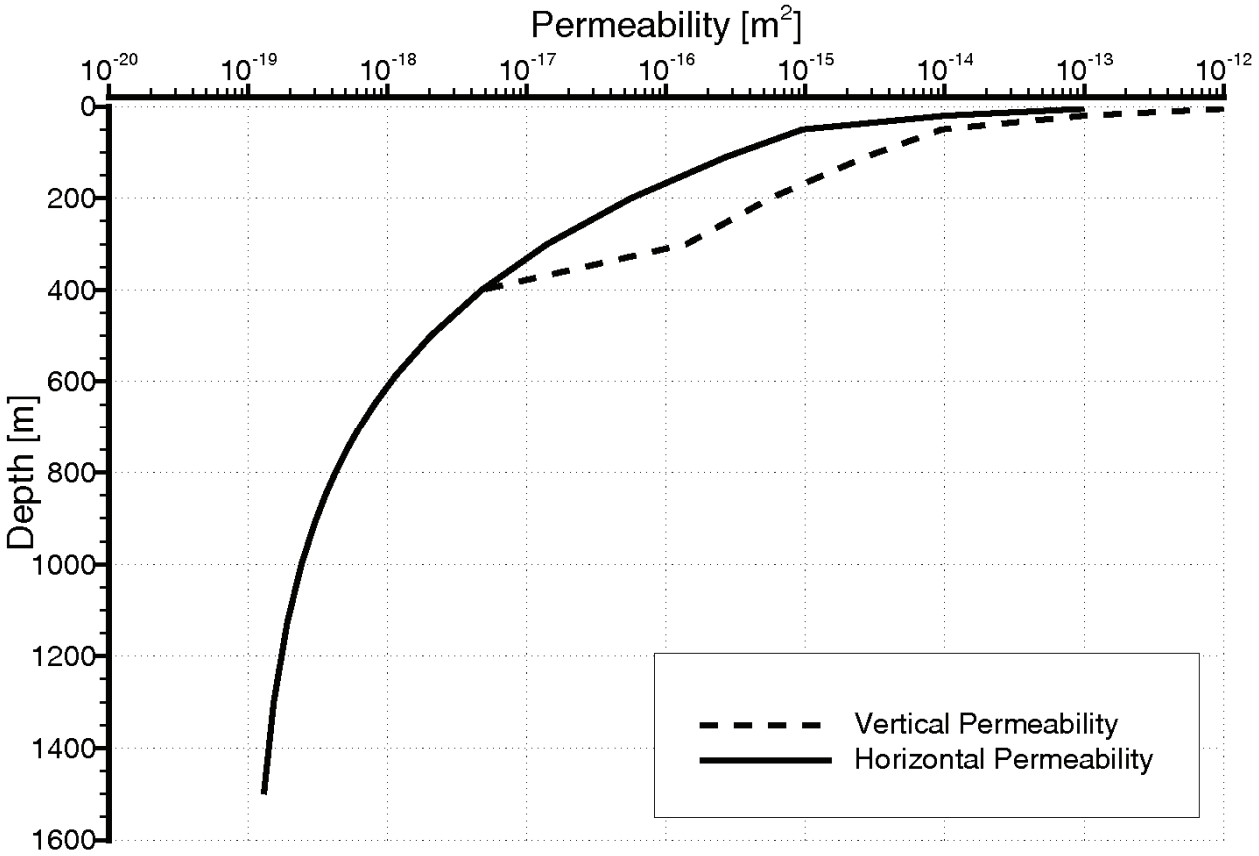

Note: Figure from Normani (2009).

Figure 2-6: Precambrian Horizontal and Vertical Matrix Permeabilities as a Function of Depth

Table 2-7: Groundwater Transport Parameters

Parameter	Value	Reference
Brine diffusion coefficient	1.484×10^{-9} m^2/s	Weast (1983, p. F-46)
Tracer diffusion coefficient	2.66×10^{-9} m^2/s	Singh and Kumar (2005, p. 37)
Longitudinal dispersivity	500 m	
Horizontal transverse dispersivity	50 m	
Vertical transverse dispersivity	5 m	

2.3.3.3 Flow Boundary Conditions

For the solution of the groundwater flow equation, a specified head (Dirichlet) boundary condition is applied to all surface nodes to set the water table 3 m below ground surface, regardless of streams or other inland water bodies such as lakes or wetlands, but not less than the elevation of the larger lakes which were set to a mean water elevation of 176 m. Zero flux boundary conditions are applied to both the lateral and bottom boundaries of the modelling domain. Based on results of sensitivity analyses conducted by Sykes et al. (2011) for a regional modelling domain of similar lateral extent, the assigned lateral and bottom boundary conditions are not expected to impact rates of mass transport at the location of the proposed repository. For simulations involving coupled density-dependent flow and transport of brine, a Dirichlet boundary condition equal to the TDS value at the bottom of the modelling domain is applied to all bottom nodes and a mixed (Cauchy) boundary condition with zero concentration for recharging waters is applied to all surface nodes.

A tracer representing recharge waters is used in the paleohydrogeologic simulations and its boundary conditions are set to zero concentration for all bottom nodes and a concentration of unity using a Cauchy boundary condition for all surface nodes. Lateral boundary conditions for both brine and tracer transport are zero-gradient.

2.3.3.4 Initial Conditions and Solution of Density-Dependent Flow

Salinity plays an important role with regard to fluid flow at depth. An increase in the concentration of TDS will result in an increase in the fluid density, which will then act as an inhibiter of active flow at depth (Park et al. 2009). The method for developing a solution for density-dependent flow is described in the following paragraphs.

In the absence of a source term for salinity, a transient analysis is required to determine an equilibrium solution at a time, *t,* for density-dependent flow. The analysis requires the specification of an initial distribution throughout the spatial domain for both freshwater heads and total dissolved solids concentrations. In a transient analysis, the initial prescribed salinity distribution is allowed to equilibrate to a new state that reflects the boundary conditions, hydraulic properties and transport properties of the regional scale domain. For the coupled density-dependent flow and transport system, fresh water can recharge at the surface, reducing the TDS concentration in the shallow groundwater system. The time to flush TDS from a unit is a function of the permeability of the unit and the energy potential of the displacing fluid as compared to the energy potential of the fluid being displaced. Fluids with lower total dissolved solids, such as recharging water, will have a lower energy potential when compared to water with higher total dissolved solids at the same elevation and pressure. Therefore, for low-permeability regions with a relatively high total dissolved solids concentration, the time to flush the region or displace the fluids can be very long (i.e., millions of years). Complete flushing may only occur as a result of diffusion because energy gradients and/or low permeabilities may yield low fluid fluxes that may not be sufficient for advective displacement to occur. In using this method to synthesize a spatial salinity distribution, the total mass of dissolved solids, and its distribution in the model domain, is assumed to be known and will be a maximum initially because there are no internal sources to generate dissolved solids resulting from rock-water interaction. With this approach, as time progresses, the dissolved solids will gradually decrease as the groundwater discharges from the system.

The initial condition for total dissolved solids must specify concentrations for all lithologies at all locations in the regional scale domain. Field data are not available for the spatial distribution of TDS in the shallow low permeability units, such as the Queenston shale where it outcrops, or for the spatial distribution in the deeper units. The values from Table 2-2 for a given lithology were assigned to all areas of the spatial domain assigned to that zone. For the model zones representing the Precambrian, a depth-dependent initial TDS distribution was determined using the data described by the dashed line in Figure 2-7, and represented by Equation 2-3, where *TDS* is in units of g/L.

$$TDS = \begin{cases} 10^{0.001981697d}, & \text{for } d \leq 1250 \text{ m}; \\ 300, & \text{for } d > 1250 \text{ m}. \end{cases} \quad (2\text{-}3)$$

The depth, *d,* is the depth relative to a constant reference elevation of 176 m for the top of the Precambrian; there is no Precambrian above this elevation in the regional scale domain. If the concentration from the dashed line in Figure 2-7 at a given depth was lower than that assigned to the lowest sedimentary rock at the location (Shadow Lake or Cambrian sandstone, where present), the higher zone TDS concentration was assigned. The initial TDS distribution developed for this study is shown in block-cut view in Figure 2-8. A linear relationship is assumed between fluid density and TDS such that a fluid density of 1200 kg/m^3 is equal to 300 g/L. Further discussion of the linear relationship between fluid density and TDS can be found in Normani et al. (2007).

For this study, the final freshwater head distribution for the reference case analysis was calculated using the following three-step process:

1. The steady-state solution was calculated for a density-independent groundwater flow system;
2. The total dissolved solids concentration distribution in Figure 2-8 was assigned throughout the domain as an initial condition using the procedure described in the preceding paragraph. The density-independent freshwater heads were allowed to equilibrate to the assigned TDS distribution in a transient analysis, while fixing the TDS distribution;
3. A further transient analysis was performed to allow evolution of the TDS distribution over a one million year time interval.

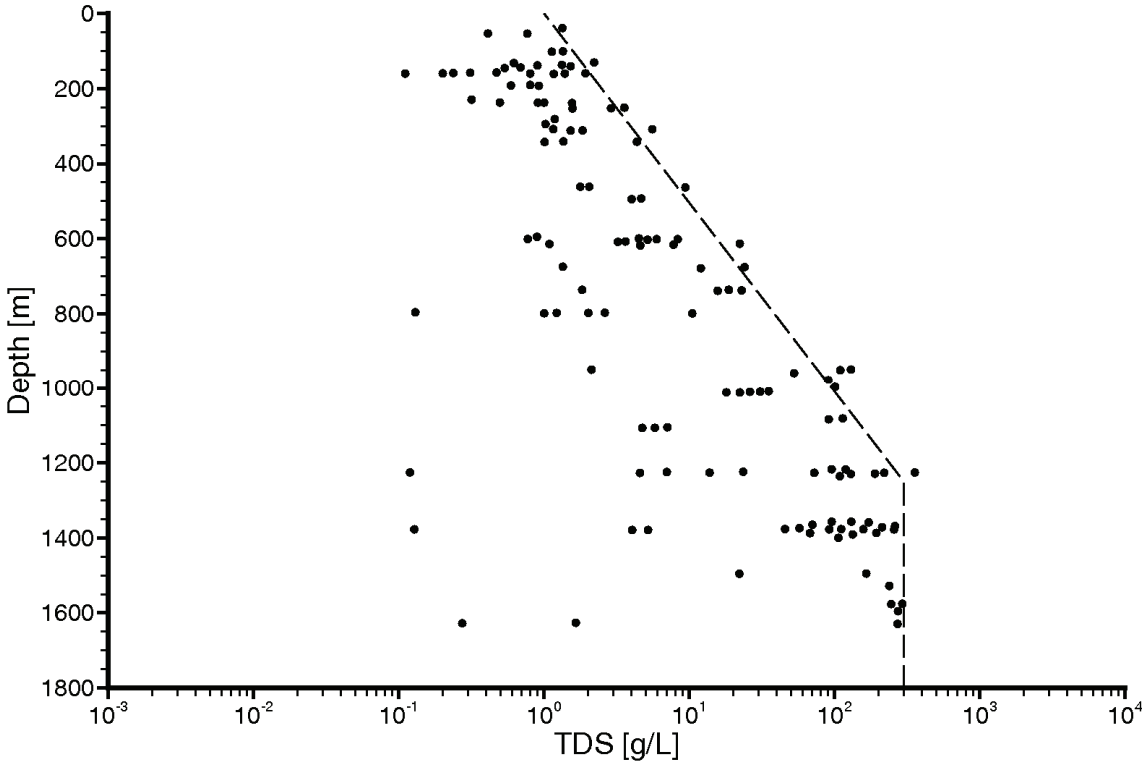

Note: Figure adapted from Figure 2b in Frape and Fritz (1987).

Figure 2-7: Plot of TDS versus Depth for Groundwater from the Canadian Shield

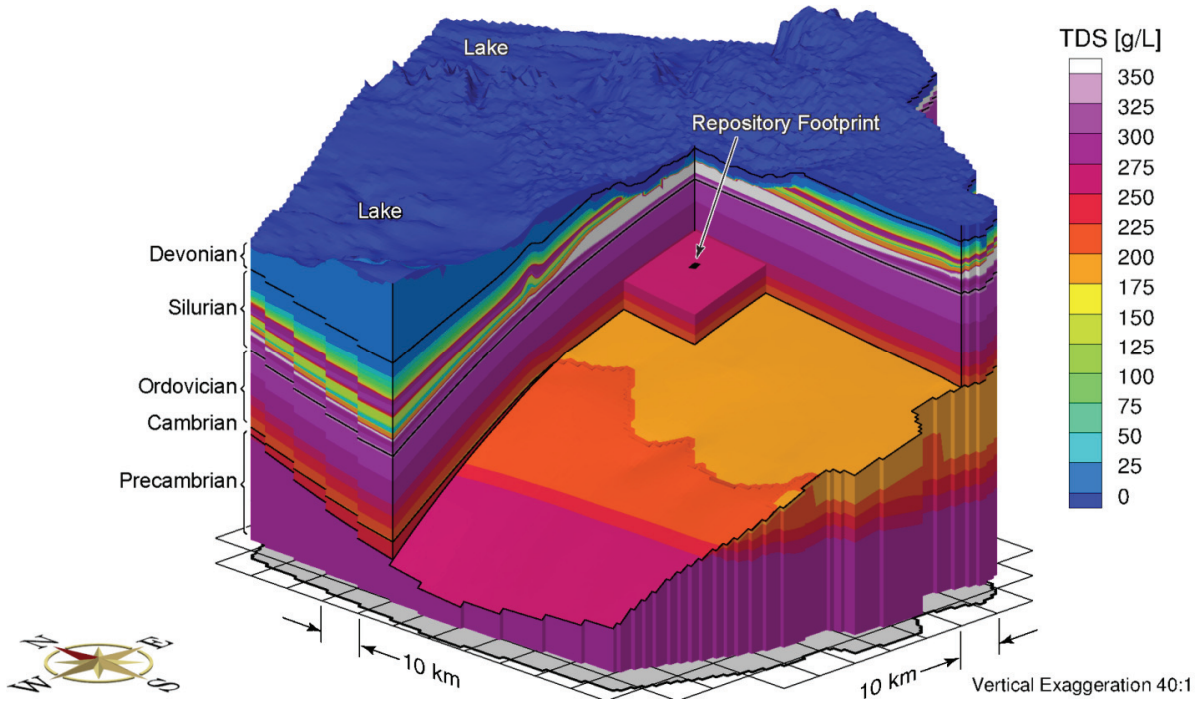

Figure 2-8: Block Cut View of Initial Total Dissolved Solids Concentration Distribution

After one million years, the model, having been allowed to reach pseudo-equilibrium between freshwater heads and TDS distribution, produces a salinity distribution that is compatible with the boundary conditions, geochemical framework and, hence, the flow domain. Generally, pseudo-equilibrium is reached when the model TDS reasonably matches field measurements (for detailed discussion, see Normani 2009). Note that in this study, no field data were available for comparison. In recharge areas, brine will be flushed because of a combination of the absence of a source term for brine and the effect of meteoric recharge. This is contrasted with discharge locations, which tend to transport higher concentration brines from deeper in the groundwater system. Both the freshwater heads and brine concentrations at one million years are used as the initial conditions for the paleohydrogeologic simulations.

2.3.3.5 Model Uncertainties and Sensitivities

Uncertainty is unavoidable and inherent to groundwater models, due to uncertain estimates of model parameter values. System performance measures, such as mean life expectancies, porewater velocities, Péclet number, and recharge water tracer migration, are monotonically related to model parameters through the governing equations describing groundwater flow and solute transport. As such, model parameter bounding scenarios are used in this study to investigate groundwater system behaviour.

In addition to the regional scale reference case analysis, two temperate sensitivity cases were developed. An increase in fluid density by salinity tends to retard groundwater flow at depth (Park et al. 2009). The regional scale reference scenario accounts for pore fluid density effects by assuming a linear relationship between fluid density and salinity, expressed as TDS. A conservative bounding case regarding pore fluid density is represented by a steady-state freshwater groundwater flow simulation. The second sensitivity case included enhanced hydraulic conductivities of one order of magnitude to evaluate the impact of enhanced advection on the system performance measures. Additionally, a conservative bounding case was simulated by increasing hydraulic conductivities by three orders of magnitude (see Section 2.3.5).

In terms of paleohydrogeologic simulations, additional uncertain model parameters include alternate paleoclimate simulations, paleohydrogeologic surface boundary conditions, one-dimensional loading efficiencies and Biot coefficients. In addition to the warm-based paleoclimate simulation used for the paleohydrogeologic reference case, an alternate cold-based paleoclimate simulation includes greater permafrost extent and more frequent glacial episodes. The bounding scenarios for paleohydrogeologic surface hydraulic boundary conditions include 100% of ice-sheet thickness expressed as equivalent freshwater heads and a free draining surface boundary condition. The impacts of no hydro-mechanical coupling and full hydro-mechanical coupling were investigated by setting the one-dimensional loading efficiencies to zero and unity, respectively. Incompressible mineral grains are assumed for the reference paleohydrogeologic scenario, resulting in a Biot coefficient of 1.0. To investigate the effects of compressible mineral grains, as suggested by ITASCA (2011), an alternate Biot coefficient of 0.5 is assumed for all lithologic layers. The resulting changes to both specific storage and loading efficiency are listed in Table 2-6.

2.3.4 Regional Scale Analyses

2.3.4.1 Reference Case Simulation

As described in Section 2.3.3.4, the reference case is comprised of a three-step simulation procedure: steady-state groundwater flow, transient groundwater flow equilibrated to a static TDS distribution, and a transient groundwater simulation with temporally varying TDS distribution for one million years. The steady-state freshwater head distribution, as a block-cut view, is shown in Figure 2-9. The freshwater steady-state heads shown are calculated without the influence of density. The freshwater heads for the shallow groundwater regime above the Salina Formation (within the Silurian) are dominated by the prescribed Dirichlet boundary condition representing local topography. Beneath the shallow groundwater zone, the heads are not controlled to the same extent by local topography.

The pseudo-equilibrium at one million years is taken to represent the present day state of the density-dependent groundwater flow system. The equivalent freshwater heads at a pseudo-equilibrium time of one million years are shown in Figure 2-10. For a density-dependent flow system, freshwater heads increase with an increase in fluid density and include the effects of both topographic and density gradients. However, the plot of freshwater heads can only be used to interpret horizontal head gradients, not vertical gradients. The main control for the horizontal head gradients at depth is the elevation difference between the lakes and the topographic high at the escarpment.

The distribution of total dissolved solids concentrations at a pseudo-equilibrium time of one million years is shown in Figure 2-11. Meteoric water recharging into the shallow groundwater zone above the Salina will dilute any salinity that diffuses upward through the Silurian or Ordovician formations, resulting in relatively fresh groundwater within the shallow groundwater regime. High TDS concentrations for the deep groundwater zone, including the Ordovician formations and below, are attributed to the initial high TDS concentration and the low permeability layers. The TDS transitional zone occurs in the Silurian, specifically where most of the Salina units pinch out. A TDS distribution plot shown as an east-west cross-section through the hypothetical repository in Figure 2-12 clearly displays the sharp transition of TDS concentrations in the vicinity of the hypothetical repository footprint due to significantly varying lithology. Within 10 km of the hypothetical repository footprint, a total of 15 units pinch out, based on the three-dimensional regional geologic framework model (see Section 2.3.3.2). In addition, a total of 7 units pinch out west of the 20 km by 20 km inset block shown in Figure 2-5.

The reference case porewater velocity magnitudes at a pseudo-equilibrium time of one million years are presented in Figure 2-13. Relatively high velocities occur in the shallow groundwater zone and permeable geologic units, including the Guelph and Cambrian formations. The reduction of velocities beneath the lake in the northeastern part of the domain are the result of the absence of a horizontal gradient. The low velocities in the Salina units and the Ordovician result from the low permeability of each unit. Within the Ordovician in the vicinity of the hypothetical repository footprint, the majority of porewater velocity magnitudes are less than 1×10^{-6} m/a. For a brine diffusion coefficient of 1.484×10^{-9} m^2/s and a characteristic length of 1 m, the Péclet number of molecular diffusion (Bear 1988) is less than 2.13×10^{-5}, indicating solute transport in the Ordovician is diffusion dominated.

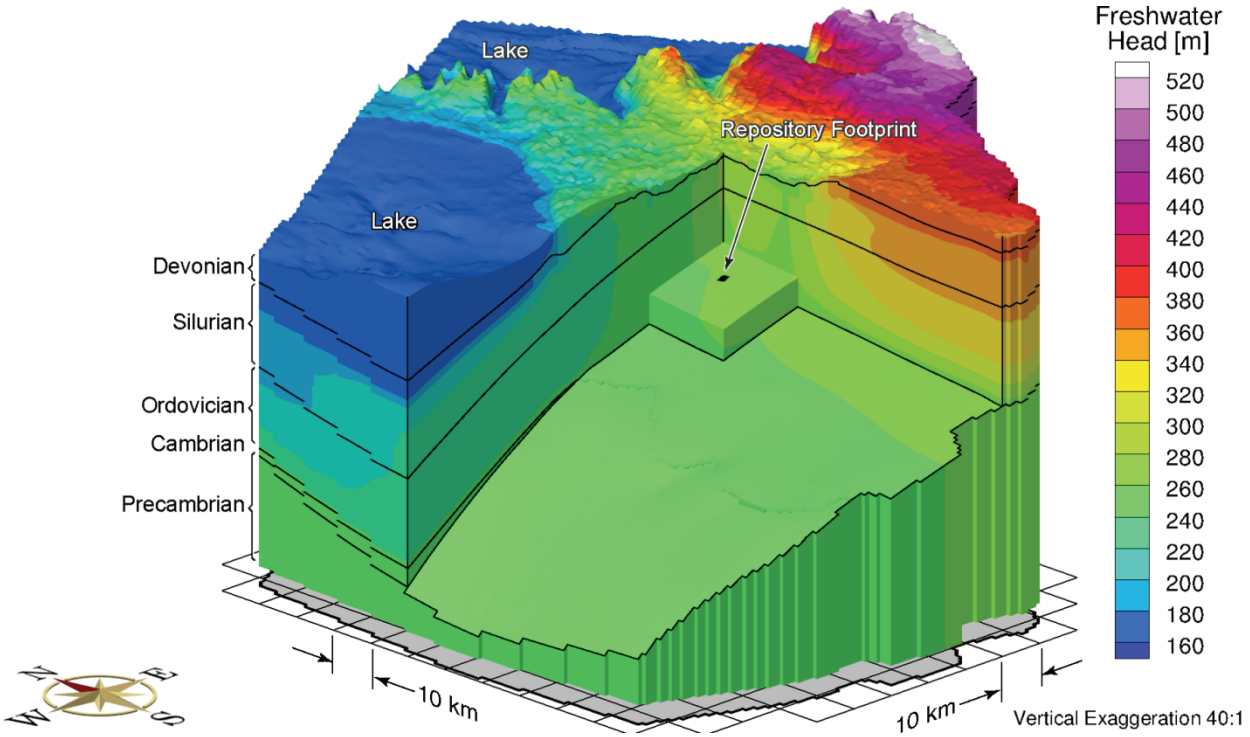

Figure 2-9: Block Cut View of Steady-State Density-Independent Freshwater Heads

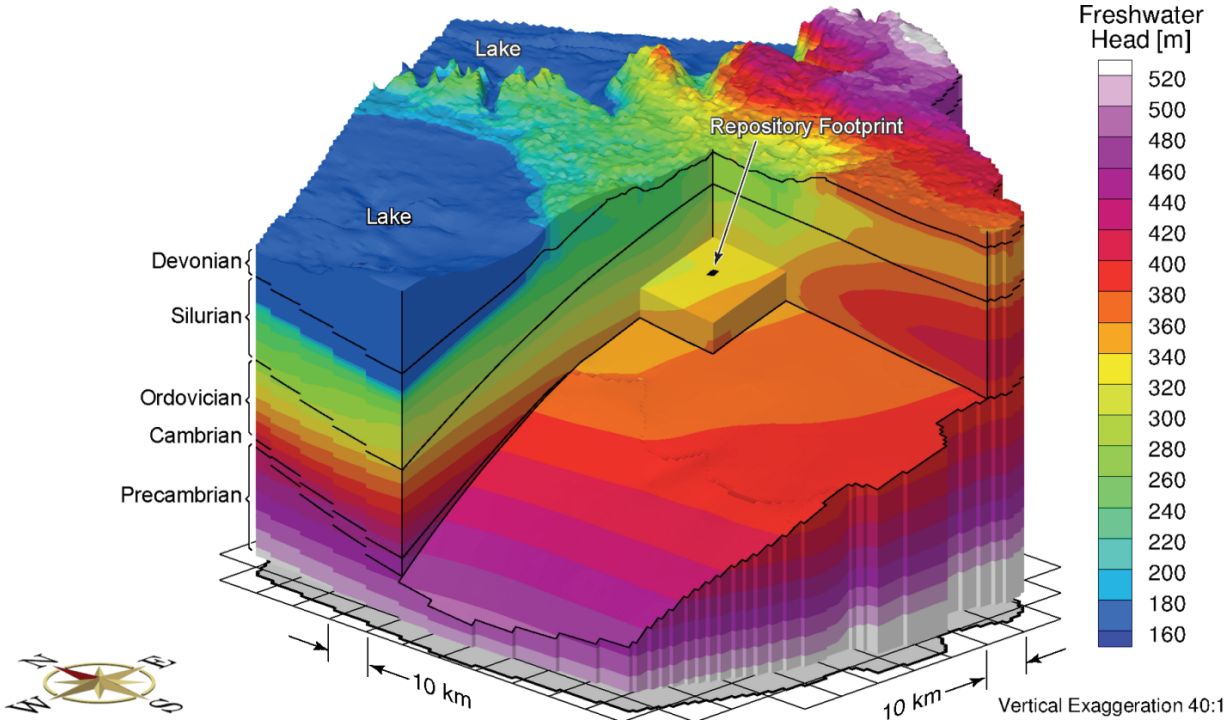

Figure 2-10: Block Cut View of Freshwater Heads at Pseudo Equilibrium Time of One Million Years with Temporally Varying TDS Distribution

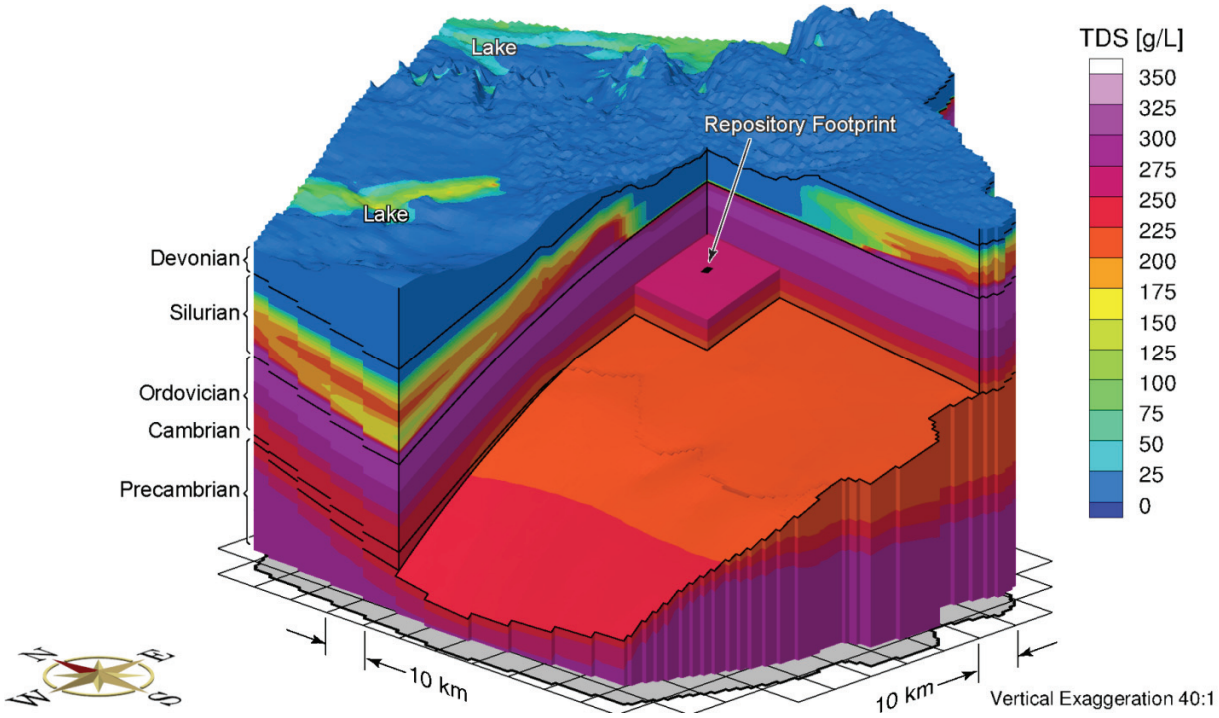

Figure 2-11: Block Cut View of Total Dissolved Solids Concentration at Pseudo Equilibrium Time of One Million Years with Temporally Varying TDS Distribution

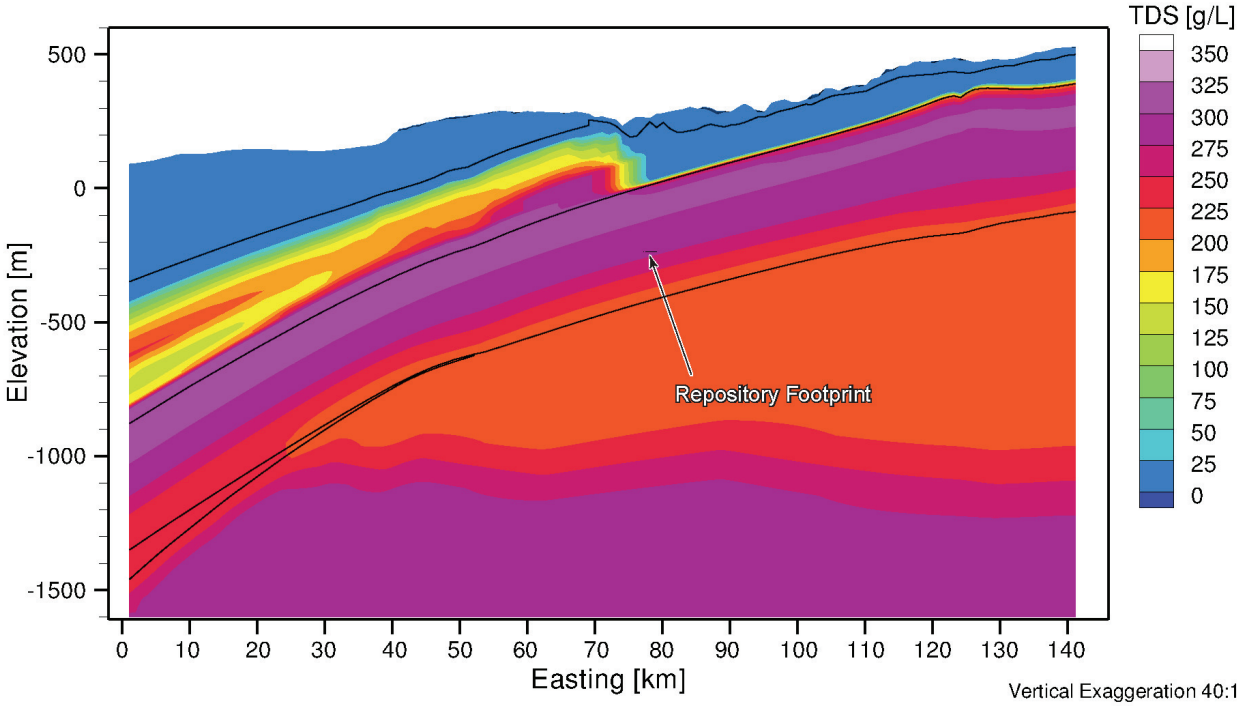

Figure 2-12: Base Case Total Dissolved Solids Concentration at Pseudo Equilibrium Time of One Million Years at East-West Cross-Section through the Hypothetical Repository Footprint

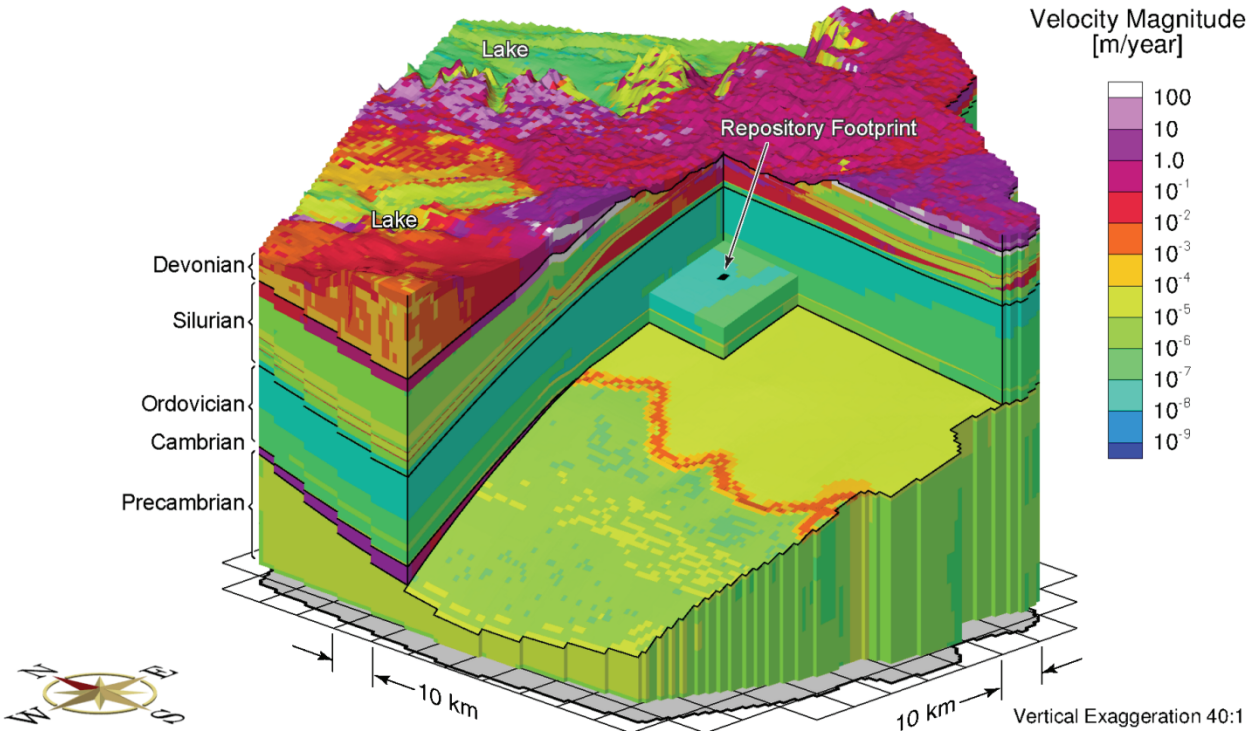

Figure 2-13: Block Cut View of Reference Case Porewater Velocity Magnitude at Pseudo Equilibrium Time of One Million Years

The ratio of the vertical component of velocity to velocity magnitude for the regional scale domain is shown in Figure 2-14. The figure can be used to determine the predominant direction of the calculated velocity vectors in the hydrostratigraphic units of the regional scale model. The vertical component of the velocity vector will equal the velocity magnitude only when there are no horizontal components to the velocity vector; the ratio of the vertical component of the velocity vector to the velocity magnitude will be positive 1.0 for solely upward velocity and negative 1.0 for solely downward velocity. In the figure, blue corresponds to zones where the vertically downward velocity component dominates, white to zones where horizontal velocity components dominate the velocity vector, and red to zones where the velocity vectors are dominated by the vertically upward component. Transition zones are evident in the figure. It is important to note that the figures cannot be used to interpret velocity magnitude; they can only be used to interpret the direction of the calculated velocity vectors at a given location. This figure should be referred to in conjunction with Figure 2-13, which shows the porewater velocity magnitudes. In the upper Precambrian, sharp transitions in flow direction over relatively short distances, in combination with low velocity magnitude, indicate stagnant flow where subtle changes in topography and total dissolved solids concentration impact the direction of the velocity vectors.

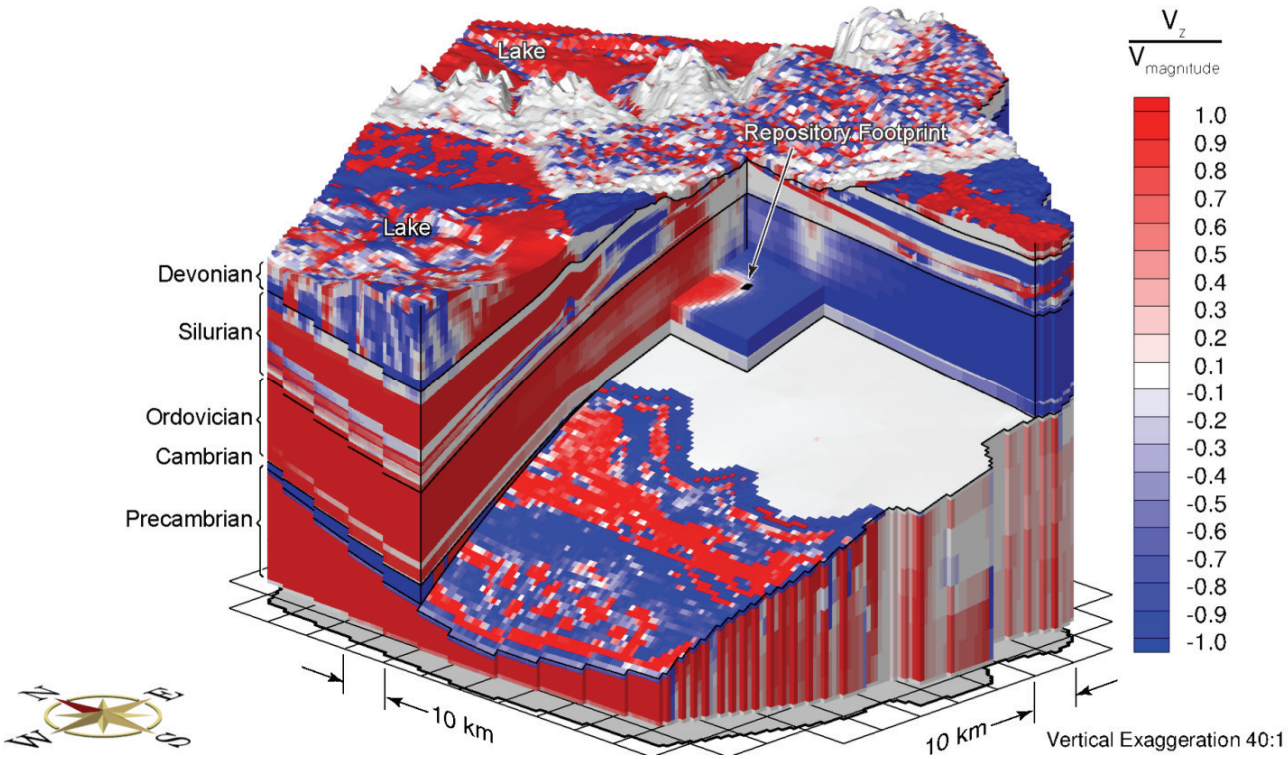

Figure 2-14: **Block Cut View of Reference Case Ratio of Vertical Velocity to Velocity Magnitude at Pseudo Equilibrium Time of One Million Years**

The performance measure selected for the evaluation of the groundwater system is mean life expectancy (MLE), as shown in Figure 2-15. The shallow groundwater zone has significantly shorter mean life expectancies compared to the deep groundwater system. The areas of recharge versus discharge can be noted in the figure as the recharge areas have high MLEs while the discharge areas have low MLEs. As a result of many geologic units pinching out, the sharp MLE transition zones in the Silurian, as shown in Figure 2-16, correspond with the behavior of the TDS distribution shown in Figure 2-12. The MLEs in the vicinity of the hypothetical repository footprint are greater than 100,000,000 years for the reference case simulation.

2.3.4.2 Temperate Transient Sensitivity Cases

The attributes of the sensitivity cases investigated in this study are summarized in Table 2-8. This section provides a comparison of two temperate sensitivity cases to the reference case. The first comparison investigates the role of fluid density between a steady-state freshwater simulation and the density-dependent reference case. The second comparison investigates the effects relative to the reference case of enhanced hydraulic conductivity on porewater velocities, TDS and MLE for all geologic units, excluding the upper 50 m of bedrock.

The impact of assuming groundwater flow is independent of density is shown by comparing porewater velocity magnitudes and mean life expectancies between a steady-state groundwater flow simulation (fr-base-nobrine) and the reference transient density-dependent flow simulation (fr-base). Figure 2-17 shows the ratio or quotient of porewater velocity magnitudes between scenarios fr-base-nobrine and fr-base on a logarithmic scale. In the figure, blue corresponds to zones where the density-independent groundwater flow from the steady-state simulation has lower velocity magnitudes than those of the reference case. Red zones indicate porewater velocities in the steady-state model are greater than in the density-dependent reference case model.

Porewater velocities are generally about the same or less without brine present; in some portions of the domain, the velocities can be slightly greater, for instance, in the close vicinity of the hypothetical repository footprint. The reduced velocities in the density-independent case are caused by the attainment of an equilibrium state, while the groundwater flow system of the reference case with salinity is experiencing slow evolution even after one million years of simulated time. A slight change in TDS distribution will have an impact on the magnitude and direction of porewater velocities, especially in the high permeability units.

Within the Ordovician formation containing the hypothetical repository footprint, the velocity magnitude ratio is close to unity due to the dominance of diffusive solute transport. Calculating the ratio of MLE between a steady-state freshwater system without brine and the pseudo-equilibrium transient brine simulation, as shown in Figure 2-18, shows order-of-magnitude changes across the domain. The mean life expectancies are generally similar or greater in the freshwater simulation, except for the portion beneath the lake, where the MLEs are reduced by one order of magnitude. At the location of the hypothetical repository footprint, a MLE of 183 Ma was estimated for the case of density-independent flow when compared to a MLE of 177 Ma for the reference case including salinity. It is non-intuitive that MLE is less in the density-independent system, as density usually retards active groundwater flow at depth and results in a smaller value of MLE. The reason lies in the fact that the groundwater movement attained in the freshwater simulation is steady-state and purely driven by topography.

Table 2-8: Table of Regional Scale Simulations for this Study

Attribute	Sensitivity Case	fr-base	fr-sens	fr-base-nobrine		fr-base-paleo	fr-base-paleo-sens	fr-base-paleo-nobrine	fr-base-paleo-cold	fr-base-paleo-80	fr-base-paleo-30	fr-base-paleo-0	fr-base-paleo-lbiot05	fr-base-paleo-le1	fr-base-paleo-le0	fr-base-paleo-0-le1
Conductivity	Reference	•		•		•		•	•	•	•	•	•	•	•	•
	Sensitivity		•				•									
Surface BC	Dirichlet at surface	•	•	•												
Density	Brine	•	•			•	•		•	•	•	•	•	•	•	•
	no brine			•				•								
Paleo Simulation	nn9930					•	•	•		•	•	•	•	•	•	•
	nn9921								•							
Paleo Surface BC	Dirichlet 100%					•	•	•	•				•	•	•	
	Dirichlet 80%									•						
	Dirichlet 30%										•					
	Dirichlet 0%											•				•
Hydro-mechanical Coupling	Biot 1.0					•	•	•	•	•	•	•		•	•	•
	Biot 0.5												•			
Loading Efficiency	Actual					•	•	•	•	•	•	•	•			
	1.0													•		•
	0.0														•	

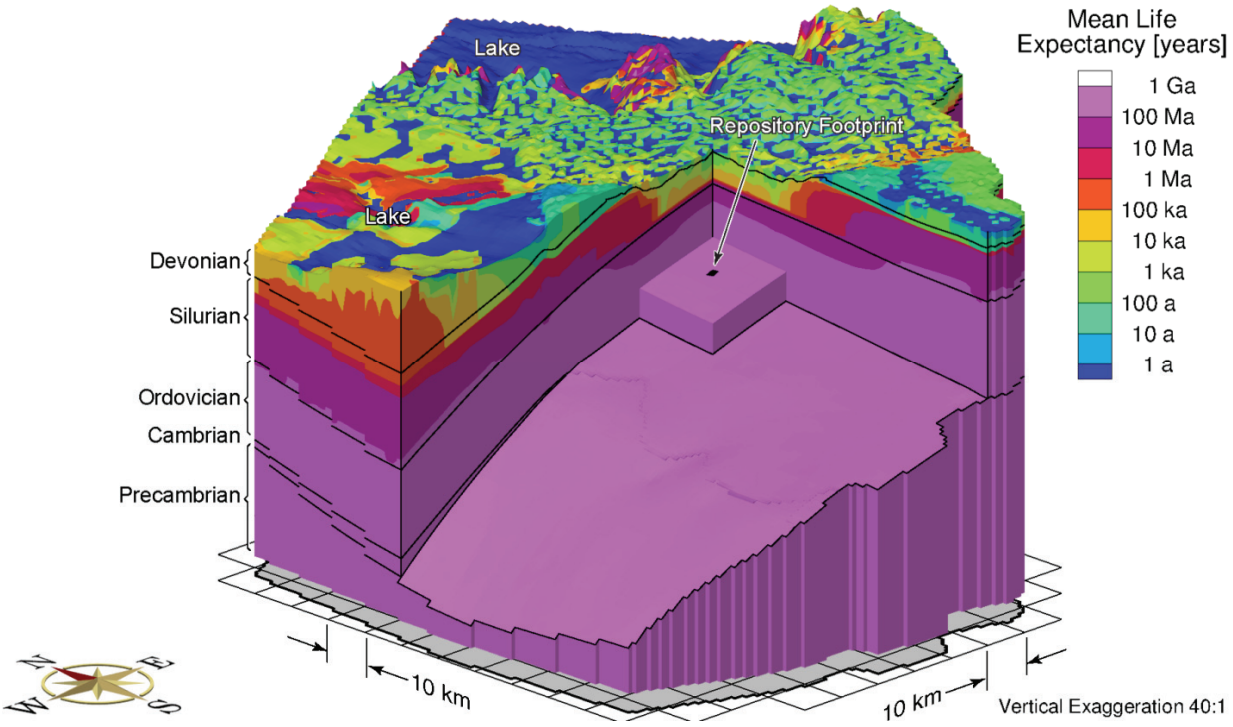

Figure 2-15: Block Cut View of Base Case Mean Life Expectancy at Pseudo Equilibrium Time of One Million Years

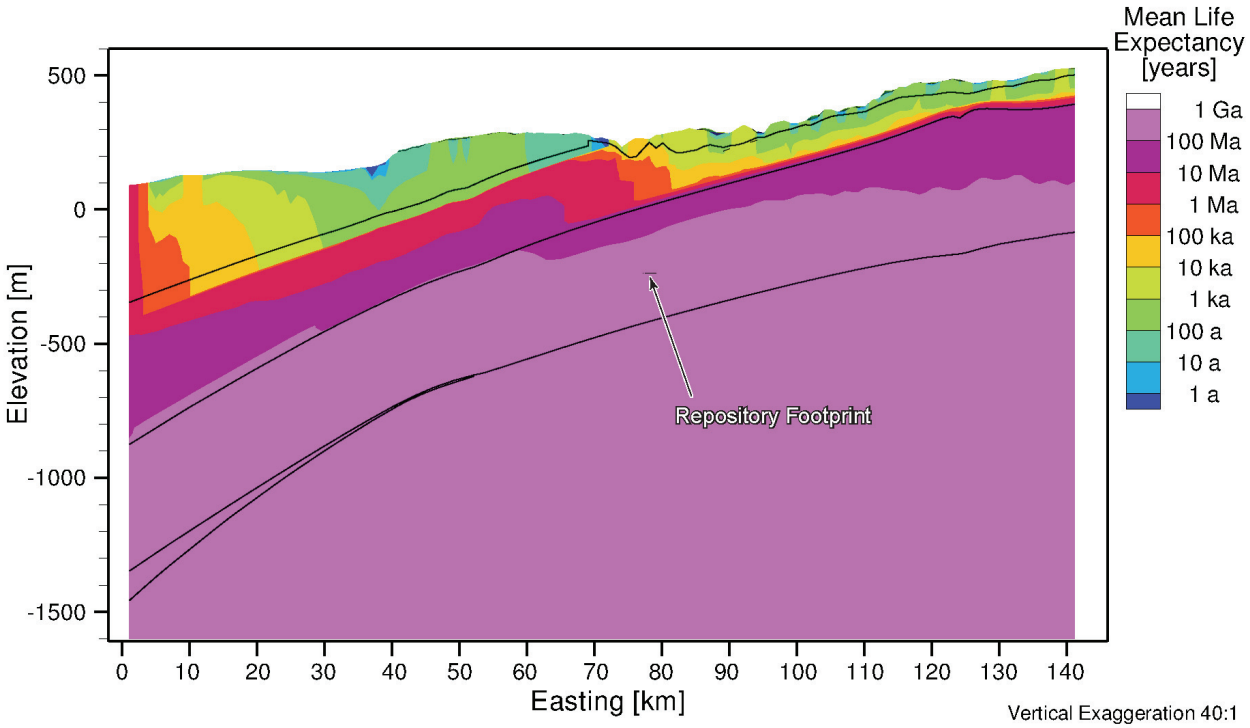

Figure 2-16: Reference Case Mean Life Expectancy at Pseudo Equilibrium Time of One Million Years at East-West Cross-Section through the Hypothetical Repository Footprint

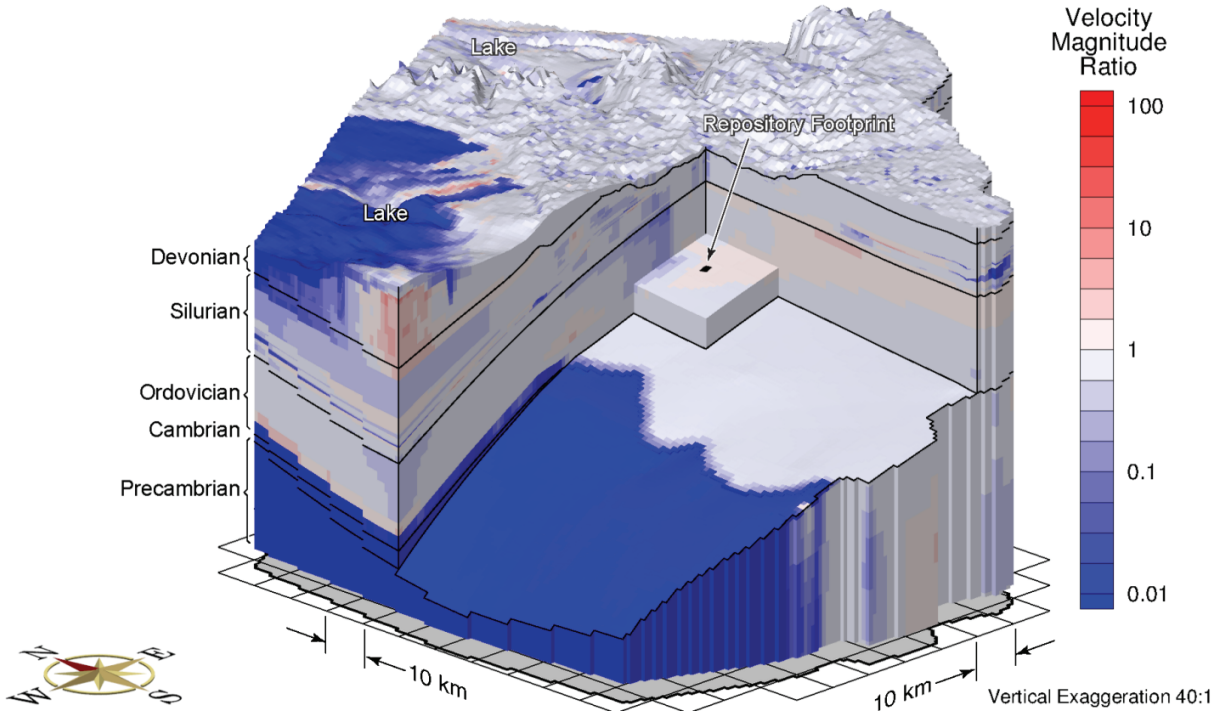

Figure 2-17: Ratio of Velocity Magnitudes of Steady-State Groundwater Flow to Density-Dependent Flow Reference Case

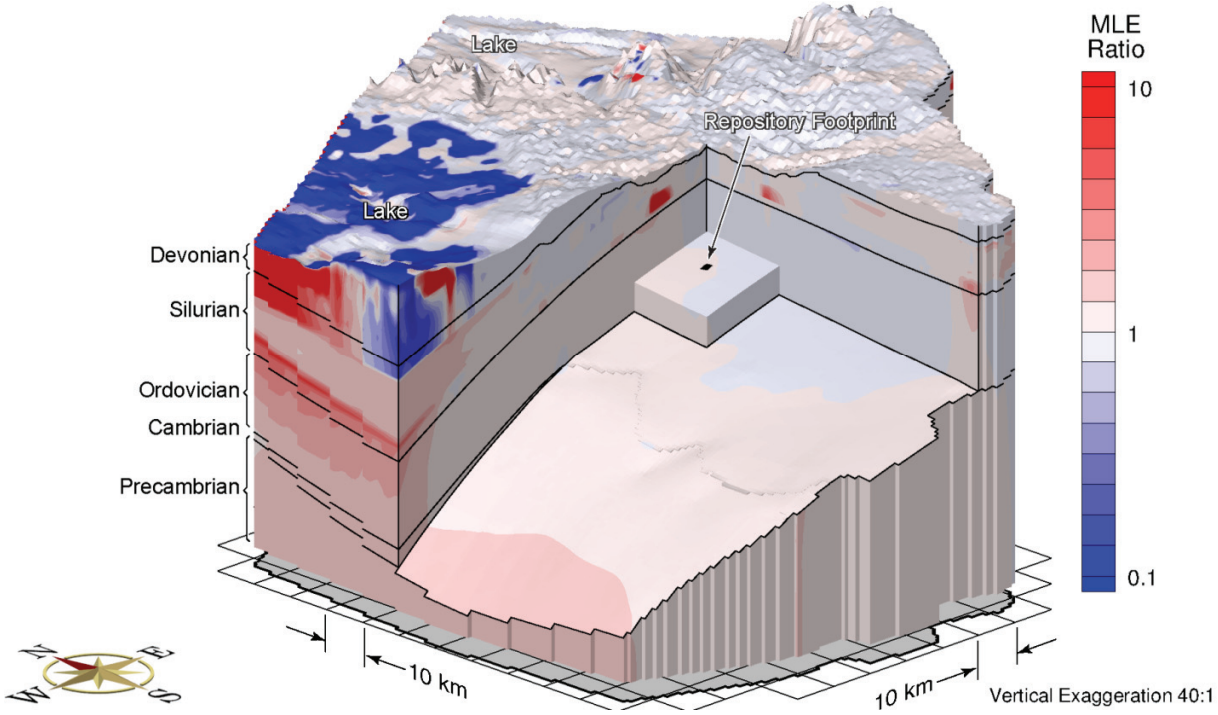

Figure 2-18: Ratio of MLEs of Steady-State Groundwater Flow to Density-Dependent Flow Reference Case

In contrast, the density-dependent solution is also affected by the evolving TDS distribution even at one million years of simulation time. In this case study, the groundwater flow induced by non-equilibrated TDS gradients is more significant than the inhibition of the groundwater flow system by density effect, which leads to a lower MLE. The relative difference in the MLE for the two cases is considered to be trivial. For a system dominated by low permeability units, the MLE is not sensitive to fluid density effects.

To investigate the impact of enhanced hydraulic conductivities on the groundwater flow system, the permeability profiles for all geologic units were increased by one order-of-magnitude, except for the upper 50 m of bedrock scenario (fr-sens). Higher hydraulic conductivities allow the groundwater system to transport TDS from the Salina group to the shallow groundwater system and then to flush the TDS from the system in a shorter period of time. Figure 2-19 shows the total dissolved solids at one million years for the sensitivity case. A comparison of the results to those of the reference case (fr-base), shown in Figure 2-11, reveals that the TDS concentrations in the Salina group are much lower than those from the reference case. The difference in freshwater heads between the sensitivity case and the reference case are shown in Figure 2-20. In the Silurian and below, freshwater heads are generally decreased as a result of lower TDS when compared to TDS values in the reference case.

The ratio of porewater velocities between the sensitivity case and the reference case is shown in Figure 2-21. Due to the enhancement of hydraulic conductivities, the porewater velocities are consistently greater throughout the modelling domain, excluding portions of upper layers beneath the lake. Higher hydraulic conductivities allow the groundwater system to equilibrate to a more stable state quicker than for the reference case at one million years. Therefore, an increase in hydraulic conductivity by a given factor under similar hydraulic gradients will result in an increase in porewater velocities and a decrease in travel times by a similar factor. The MLE ratios shown in Figure 2-22 generally indicate a decrease in the MLE values for the sensitivity case, resulting in an MLE for the hypothetical repository of 114 Ma. At the location of the hypothetical repository footprint, the corresponding mean life expectancy for the sensitivity case decreases by a factor of 1.6, significantly less than the one order-of-magnitude increase in the hydraulic conductivities. This highly nonlinear relationship between MLE and hydraulic conductivities indicates the dominance of molecular diffusion in the transport mechanism.

2.3.4.3 Paleohydrogeologic Sensitivity Cases

A total of eleven paleohydrogeologic simulations were performed to investigate the role of varying paleoclimate boundary conditions and the characterization of hydro-mechanical coupling. These simulations are summarized in Table 2-8. The reference case model (fr-base) is used as the basis for all simulations and the initial conditions for both freshwater heads and brine distribution come from the transient brine simulation at one million years, as described in Section 2.3.3.4. A conservative tracer of unit concentration is applied as a Cauchy boundary condition at the top surface of the model domain. This tracer represents the migration of recharge water, including glacial meltwater, which occurs during a paleohydrogeologic simulation. The tracer migration at 120,000 years for the paleohydrogeologic reference case simulation (fr-base-paleo) is shown in Figure 2-23. The 5% isochlor is considered conservative because it represents a pore fluid containing 5% recharge water and provides an indication of recharge water migration into the subsurface. For the reference case, the 5% isochlor migrates to the top of the Ordovician in the vicinity of the hypothetical repository footprint. The model units in the Salina and the Ordovician are of comparatively low hydraulic conductivity and tend

to retard the downward advective migration of the tracer, which indicates that diffusion is the dominant transport mechanism. Furthermore, Figure 2-24 shows the tracer concentration with depth at the location of the hypothetical repository footprint. Tracer penetration depth can be determined by the intersection of tracer concentration with a vertical line representing the 5% isochlor concentration. All paleohydrogeologic simulations are plotted on the same figure for comparison. The tracer concentrations do not reach formations below the Queenston in any of the paleoclimate scenarios.

To apply the same logic as the temperate transient sensitivity cases, the analysis of a no density scenario (fr-base-paleo-nobrine) in Table 2-8 investigates the impact of assuming that groundwater flow is independent of density. Additionally, the impact of enhanced hydraulic conductivities on the paleohydrogeologic groundwater flow system (fr-base-paleo-sens) is investigated by increasing the permeability profiles for all the geologic units by one order-of-magnitude, except for the upper 50 m of bedrock. The initial conditions for these two paleohydrogeolgic simulations are from the density-independent steady-state and enhanced hydraulic conductivities sensitivity case simulations, respectively. The importance of fluid density and enhanced hydraulic conductivities in impacting the paleogeologic groundwater flow system is revealed in a comparison of the results obtained from these scenarios with the reference case (see Figure 2-24). The increase in density of the deeper fluids will act as an inhibiter of active flow at depth (Park et al. 2009); higher hydraulic conductivity leads to deeper tracer migration, as confirmed by Figure 2-24 which shows slightly higher tracer concentration profiles and deeper penetration depth than does the reference case.

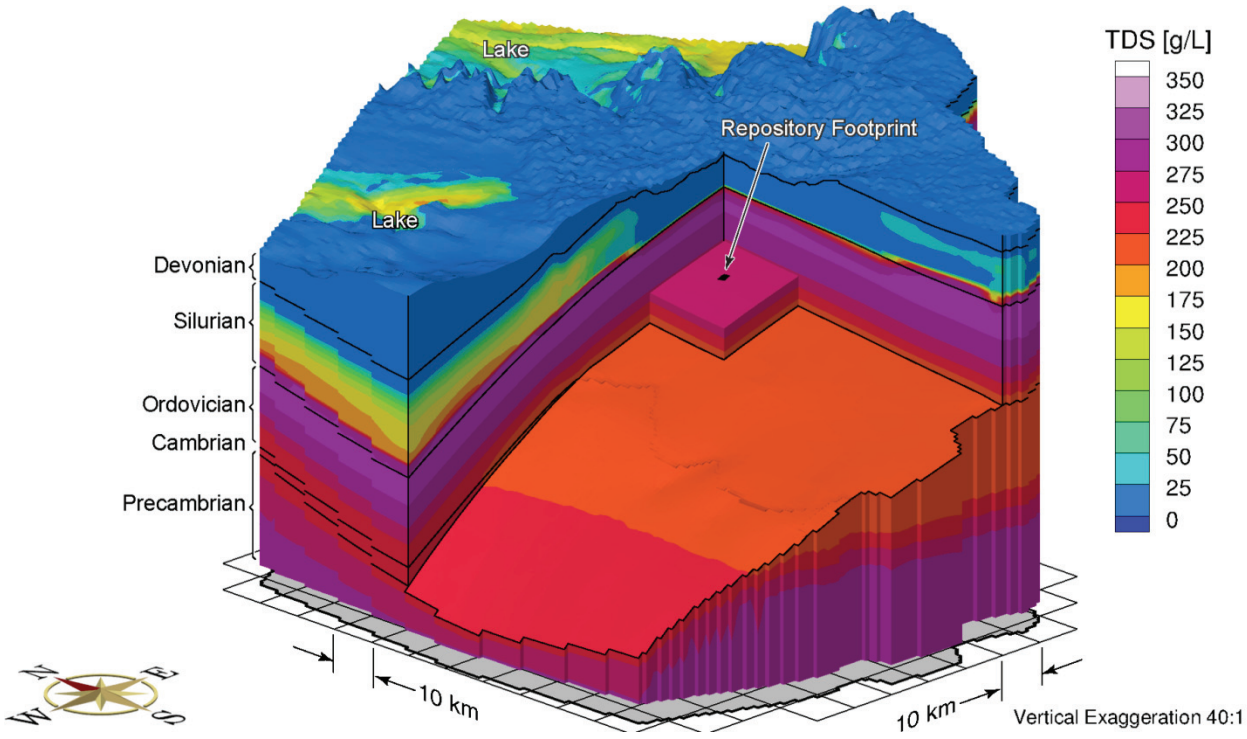

Figure 2-19: The Total Dissolved Solids Concentrations at Pseudo Equilibrium Time of One Million Years for an Increased Rock Mass Hydraulic Conductivity

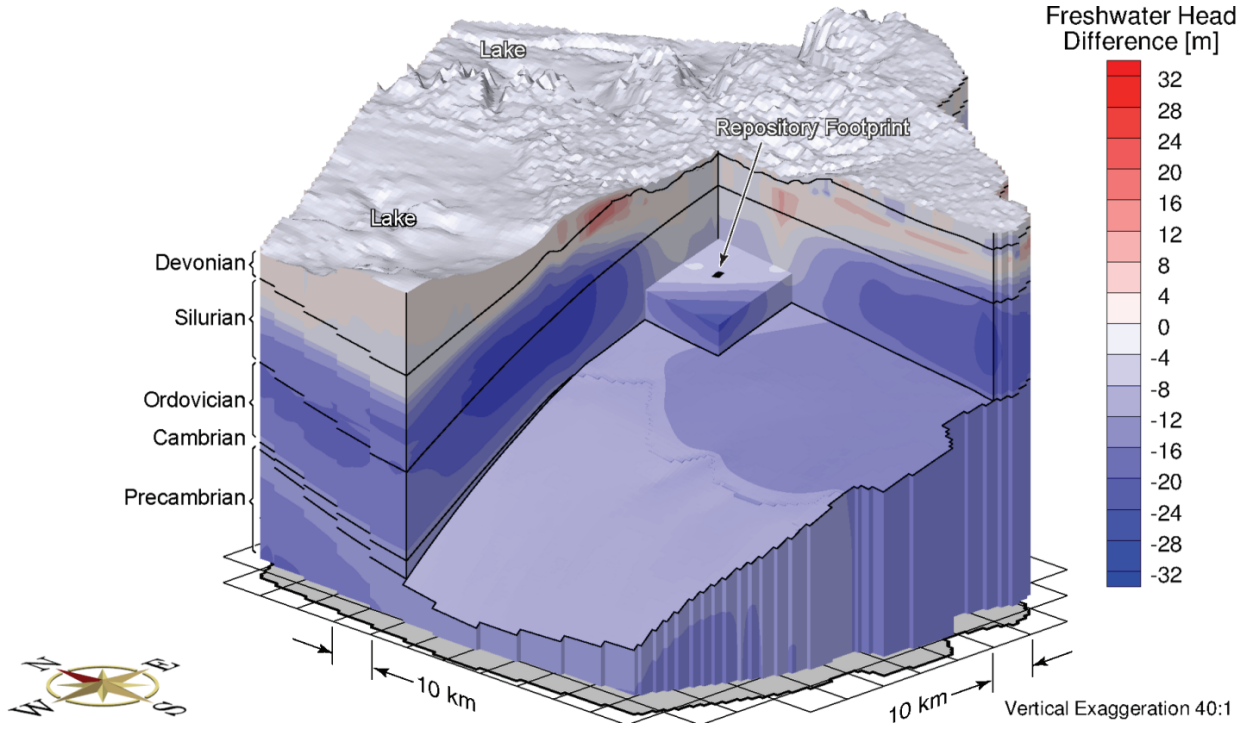

Figure 2-20: Difference in Freshwater Heads between a Simulation Using an Increased Rock Mass Hydraulic Conductivity and Reference Case

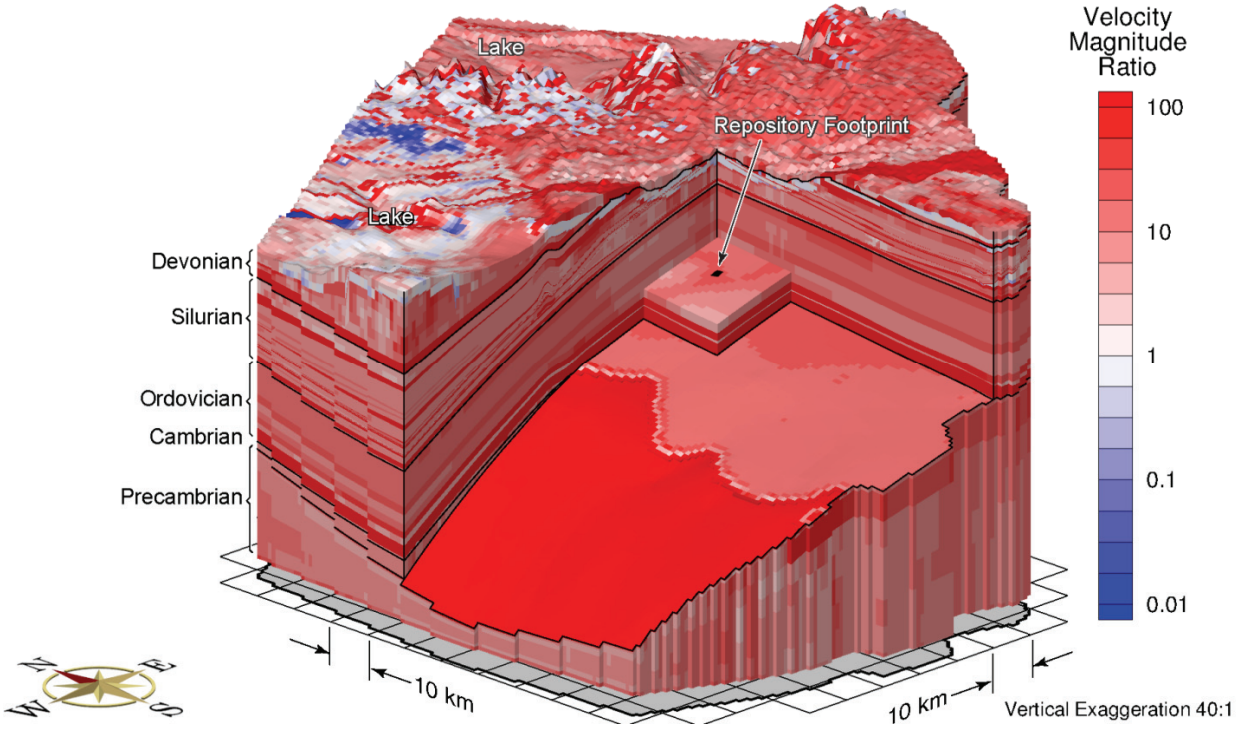

Figure 2-21: Ratio of Pore Velocity Magnitudes of Sensitivity Case using an Increased Rock Mass Hydraulic Conductivity to Reference Case

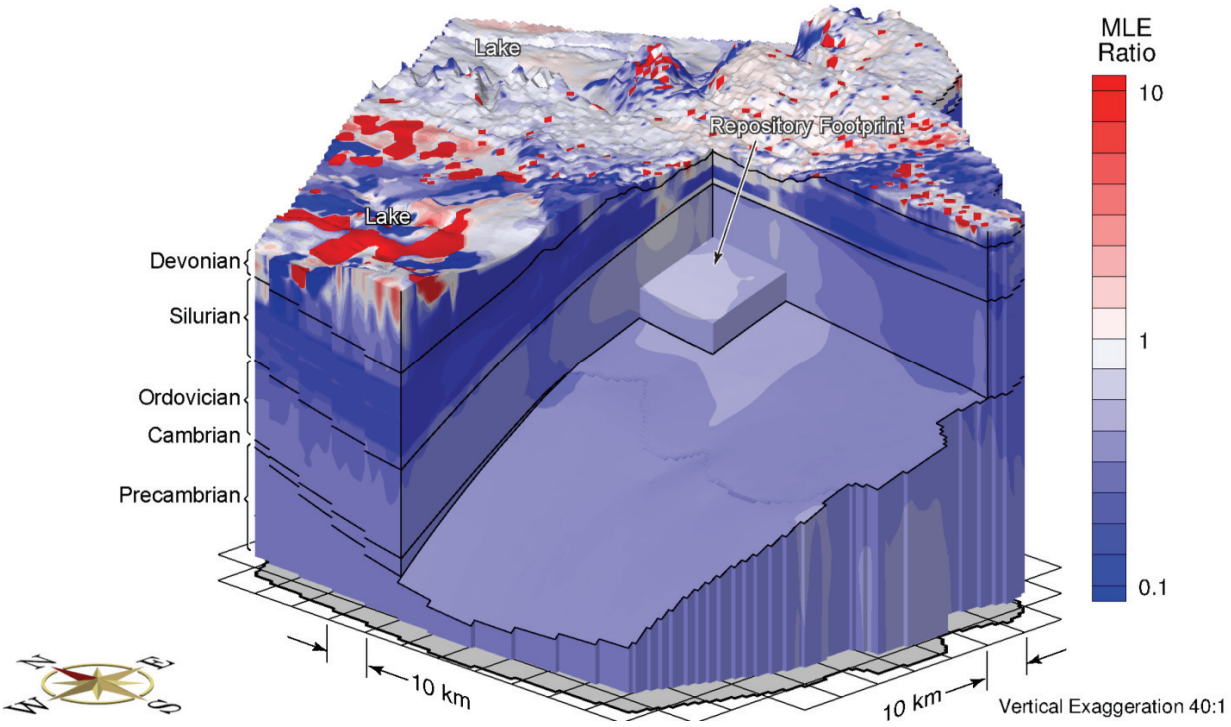

Figure 2-22: MLE Ratio of Increased Rock Mass Hydraulic Conductivities Simulation to Reference Case Simulation

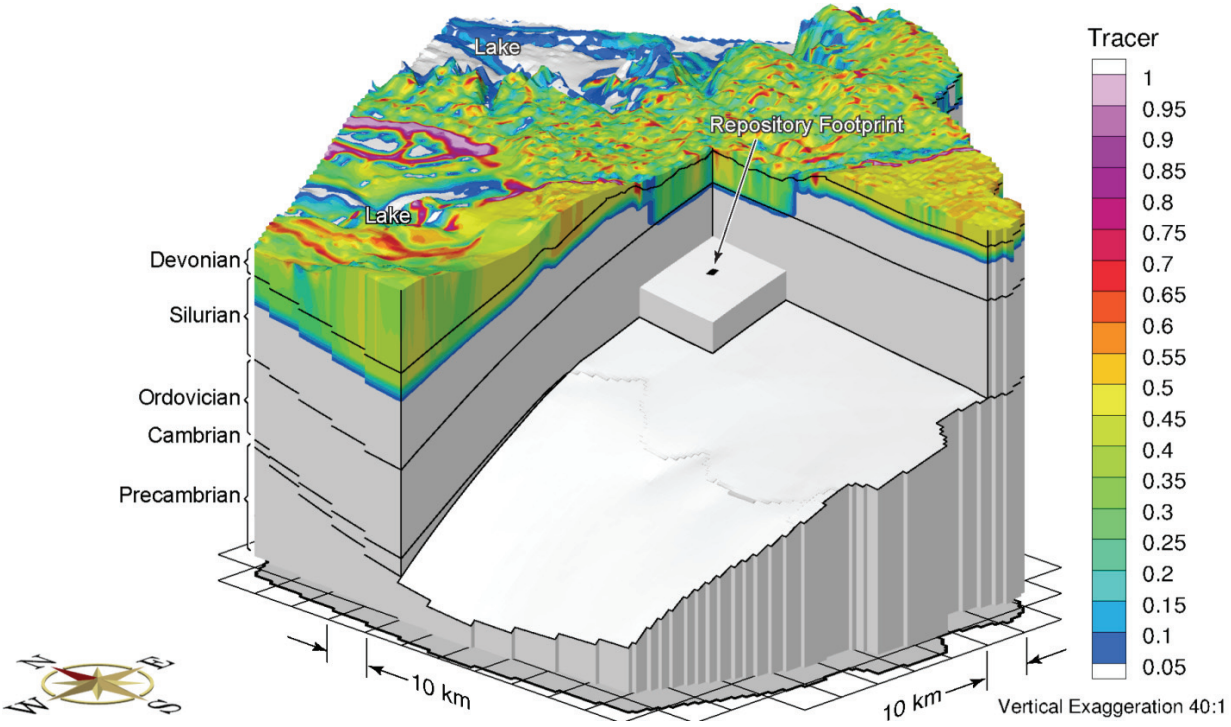

Figure 2-23: Block View Showing the Depth of Penetration of a Tracer after 120,000 Years for a Reference Case Paleohydrogeologic Scenario

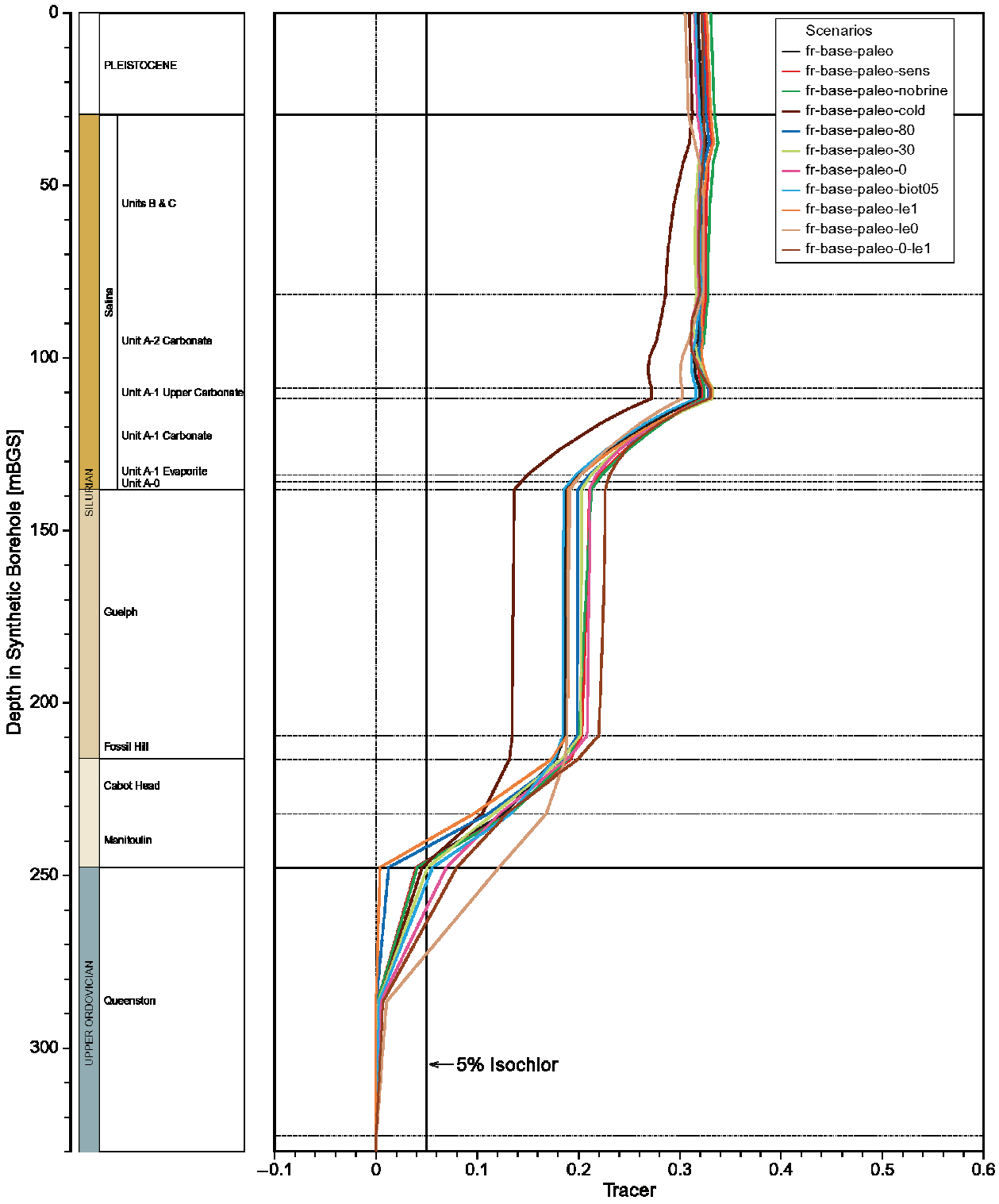

Figure 2-24: Vertical Profile Plots of Tracer Concentrations for the Paleohydrogeologic Simulations at the Location of the Hypothetical Repository Footprint at 120,000 Years

Peltier (2011) reconstructs eight paleoclimate glacial systems models (GSM). The reference case paleohydrogeologic simulation (fr-base-paleo) uses paleoclimate simulation nn9930, representing a warm-based ice-sheet condition. An alternate paleoclimate simulation, nn9921 (fr-base-paleo-cold), represents much more extensive permafrost over the 120,000 year paleoclimate time span and more ice-sheet advance/retreat cycles than nn9930. Both of the GSM models provide ice thickness, lake depth and permafrost depth over the 120,000 year simulation period, as shown in Figure 2-2 and Figure 2-3, respectively. These outputs are applied to the paleohydrogeologic groundwater flow simulations.

Figure 2-25 shows the tracer migration at 120,000 years for the nn9921 paleoclimate boundary conditions. In comparison to the reference case simulation, there is a significant decrease of tracer concentrations in the Silurian formations, as shown in Figure 2-24. Decreased tracer migration is a result of the longer duration of permafrost conditions.

The top surface hydraulic boundary condition can be varied using different percentages of ice-sheet thickness. The reference case uses 100% of ice-sheet thickness in calculating the equivalent freshwater head. Paleohydrogeologic scenarios with equivalent freshwater heads of 0%, 30%, and 80% (named fr-base-paleo-0, fr-base-paleo-30, and fr-base-paleo-80, respectively) of ice-sheet thickness were performed to allow for some reduction in heads beneath the ice-sheet. The 30% and 80% cases result in a tracer concentration profiles that are very similar to the reference case. For the 0% case, representing zero fluid pressure at the top surface, upward flow occurs during glacial loading, and downward flow occurs during glacial unloading due to in situ pore fluid pressure changes resulting from hydromechanical coupling. Higher tracer concentrations occur for the fr-base-paleo-0 case than for the reference case.

In addition to the surface hydraulic boundary condition, an equally important parameter is the one-dimensional loading efficiency. The loading efficiency is calculated based on the pore fluid and rock matrix compressibilities. In the reference case simulation, the one-dimensional loading efficiencies use this computed value for each geologic unit in Table 2-5. In two paleohydrogeologic sensitivity scenarios, the one-dimensional loading efficiencies are set to zero (fr-base-paleo-le0) to investigate the role of neglecting hydro-mechanical coupling, and unity (fr-base-paleo-le1) to evaluate the impact of full hydro-mechanical coupling on the groundwater flow system at depth. Both the loading efficiency and specific storage values are affected by the choice of Biot[1] coefficient. An additional sensitivity case investigates the role of the Biot coefficient on hydro-mechanical coupling. For a Biot coefficient of 0.5 (fr-base-paleo-biot05), alternate one-dimensional loading efficiencies and specific storages for each unit are listed in Table 2-6. The final simulation (fr-base-paleo-0-le1) uses a loading efficiency of unity and a 0% of ice-sheet thickness equivalent freshwater head for the surface hydraulic boundary condition. Of the paleohydrogeologic simulations with nn9930 paleoclimate boundary conditions, two extreme scenarios are represented by fr-base-paleo-le0 (having the most downward flow) and fr-base-paleo-0-le1 (having the most upward flow) during the loading portion of ice-sheet advance.

[1] According to Wang (2000), "The Biot-Willis parameter α is the ratio of increment of fluid content to change in bulk volume when the pore fluid remains at constant pressure [...]. It would be exactly one if all of the bulk strain were due to pore volume change (i.e., the solid phase is incompressible). It is less than one for a compressible solid phase because the change in bulk volume is greater than the change in pore volume by the amount of the change in the solid volume."

For the nn9930 paleoclimate boundary conditions, fr-base-paleo-le1 (Figure 2-26) represents the shallowest predicted tracer depth, while fr-base-paleo-le0 (Figure 2-27) represents the deepest penetration depth of tracer. As the one-dimensional loading efficiency is decreased, vertical gradients increase because in situ pore pressures are reduced during ice-sheet loading for the same 100% of ice-sheet thickness equivalent freshwater head surface hydraulic boundary condition. Similar to the comparison between fr-base-paleo-0 and fr-base-paleo, higher tracer concentrations occur in the fr-base-paleo-0-le1 (Figure 2-28) simulation as compared to fr-base-paleo-le1, as shown in Figure 2-24. Deeper tracer migration is attributed to larger downward vertical gradients resulting from the combination of a zero pressure hydraulic surface boundary condition with full hydromechanical coupling and a loading efficiency of unity.

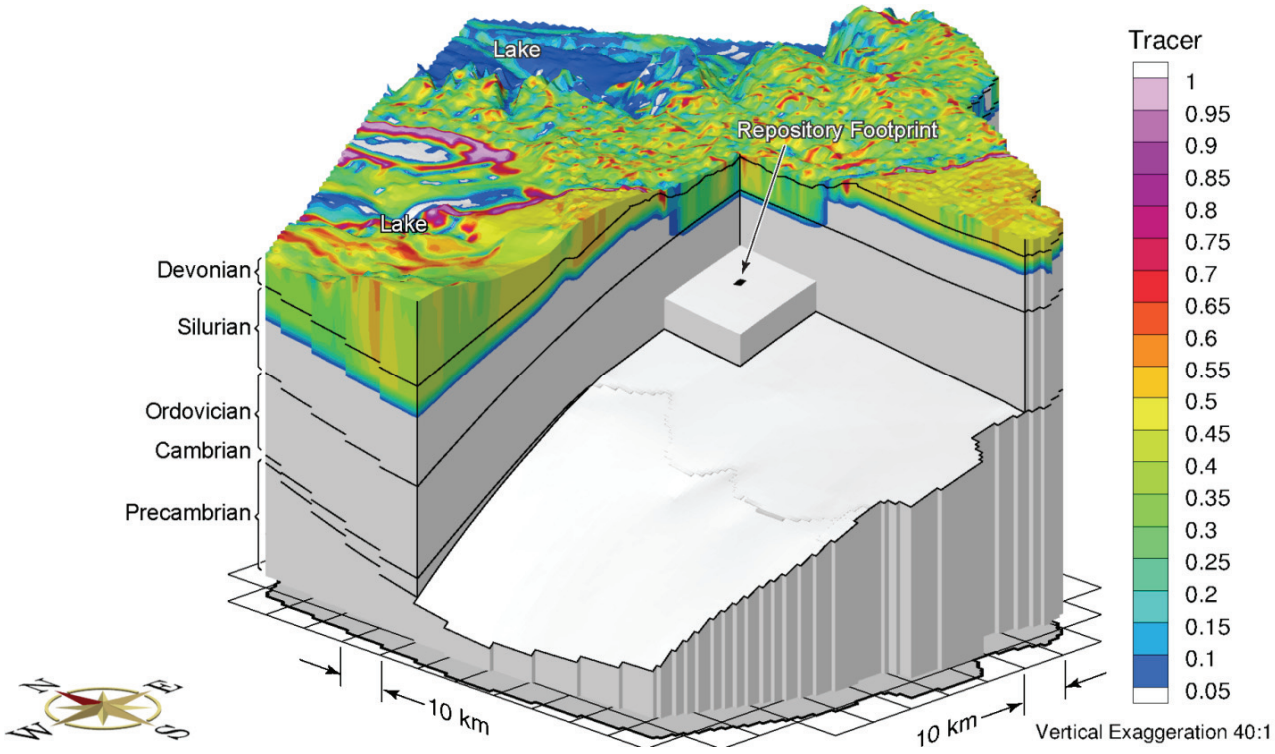

Figure 2-25: Block View Showing the Depth of Penetration of a Tracer after 120,000 Years for the nn9921 Paleoclimate Boundary Conditions (fr-base-paleo-cold)

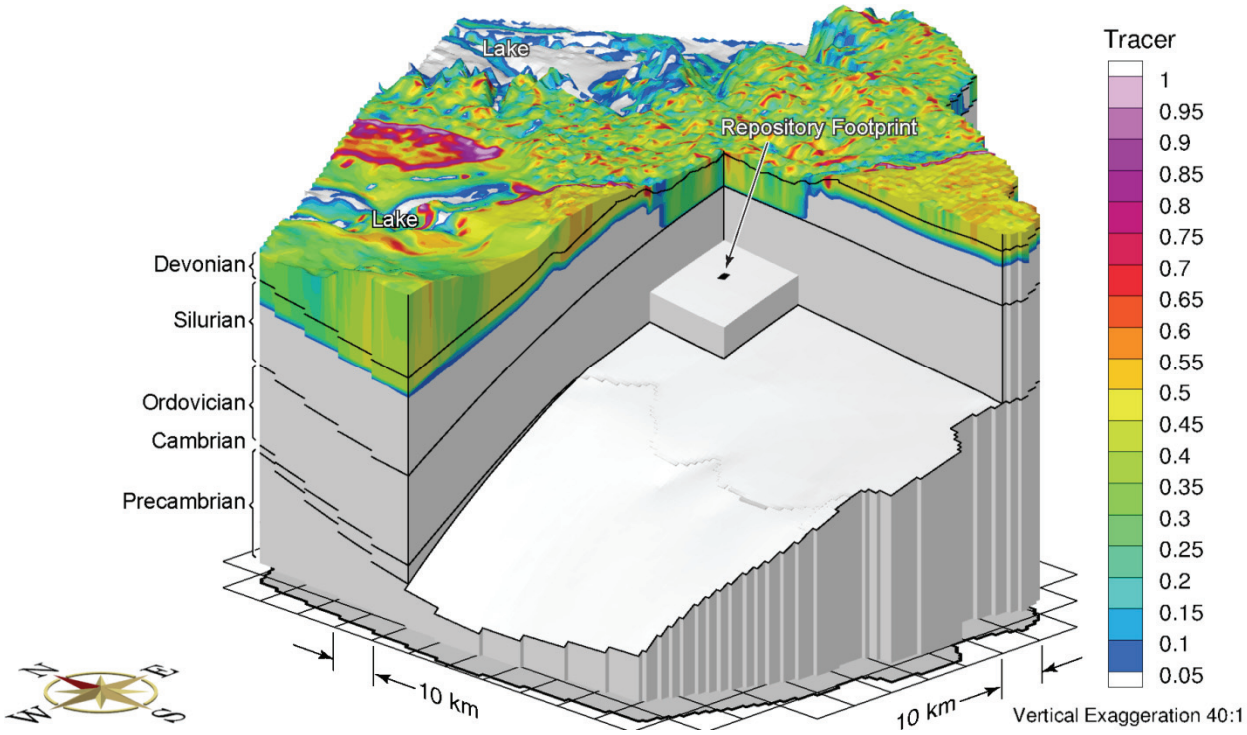

Figure 2-26: Block View Showing the Depth of Penetration of a Tracer after 120,000 Years for the nn9930 Paleoclimate Boundary Conditions and a Loading Efficiency of 1 (fr-base-paleo-le1)

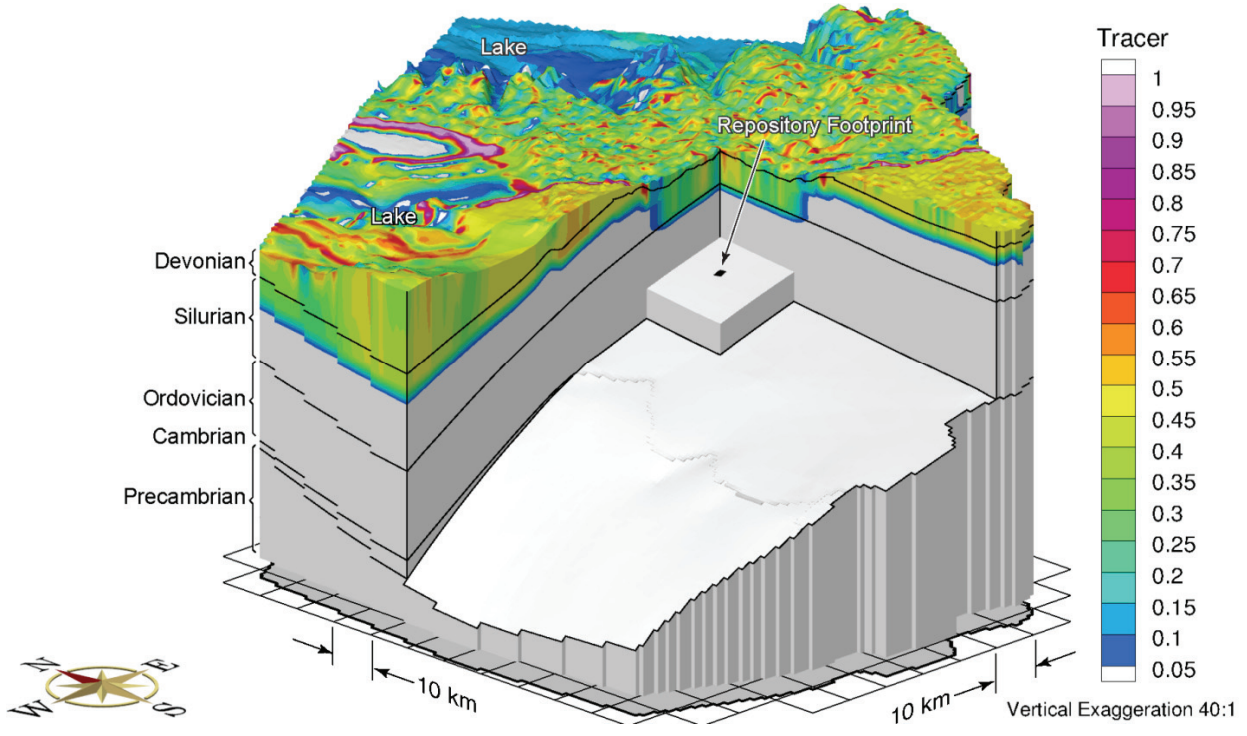

Figure 2-27: Block View Showing the Depth of Penetration of a Tracer after 120,000 Years for the nn9930 Paleoclimate Boundary Conditions and a Loading Efficiency of 0 (fr-base-paleo-le0)

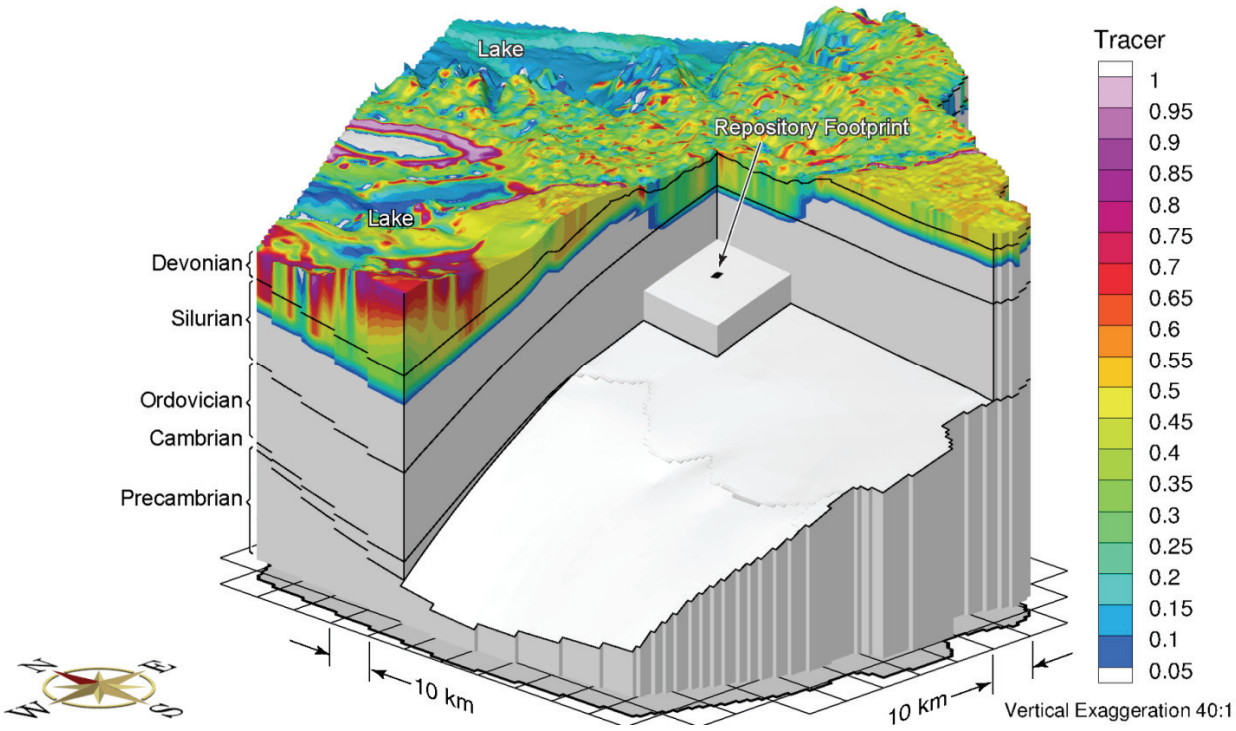

Figure 2-28: Block View Showing the Depth of Penetration of a Tracer after 120,000 Years for the nn9930 Paleoclimate Boundary Conditions, a Loading Efficiency of 1, and a 0% of Ice-Sheet Thickness Equivalent Freshwater Head for the Surface Hydraulic Boundary Condition (fr-base-paleo-0-le1)

The Péclet number, calculated as a ratio of the product of the porewater velocity and a characteristic length to the effective diffusion coefficient (Bear 1988), serves as an indicator for the dominance of advection or diffusion in mass transport processes. A plot of the Péclet number of molecular diffusion versus time for the reference case paleohydrogeologic scenario (fr-base-paleo), with a characteristic length of unity, is shown in Figure 2-29, and illustrates the stability of the geosphere during glacial advances and retreats. Five time series curves of the Péclet number are extracted at the center, west corner, north corner, east corner, and south corner of the hypothetical repository footprint, respectively. The grey regions in the figure represent upward groundwater movement, while the white regions represent downward groundwater movement. Through the duration of the glacial cycle, the Péclet number is well below the transition region, which indicates diffusion as the dominant transport mechanism for the reference case.

Select sensitivity cases illustrating the Péclet numbers versus time for scenarios fr-base-paleo-sens, fr-base-paleo-le0, and fr-base-paleo-0-le1, are shown in Figure 2-30, Figure 2-31, and Figure 2-32, respectively. These scenarios were chosen based upon porewater velocities, which are governed by hydraulic conductivities and head gradients. The Péclet numbers for the scenario with enhanced rock mass hydraulic conductivities (fr-base-paleo-sens), as illustrated in Figure 2-30, are slighter greater than for the reference case, but are still far below the transition zone. Thus, diffusion remains the dominant transport mechanism for the duration of the glacial cycles.

Scenarios fr-base-paleo-le0 and fr-base-paleo-0-le1 have the greatest downward and upward hydraulic gradients during glacial loading, however, their Péclet numbers versus time curves show less variation than the reference case, which can be explained by two main reasons. Firstly, the uniform loading efficiencies for these two cases means that inter-formational vertical gradients will not be generated during the glacial cycles. Secondly, the hydraulic conductivities of the Salina and Ordovician sediments are so low that the hydraulic boundary conditions at the top surface will not propagate into the deep groundwater flow system at the hypothetical repository footprint level. Both of the scenarios have Péclet numbers consistently far less than 0.4, which indicates that solute transport is dominated by molecular diffusion (Bear 1988).

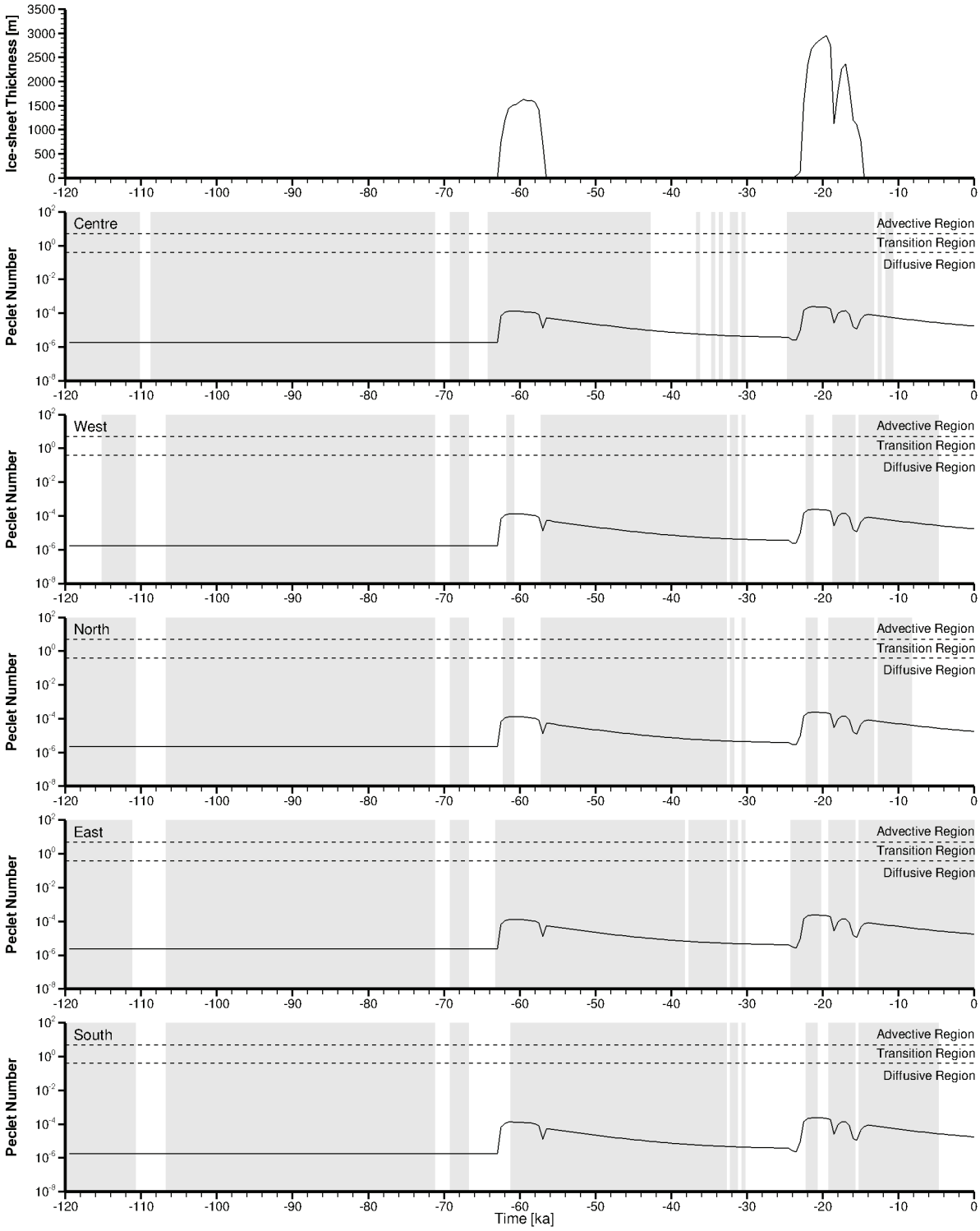

Note: Grey regions represent upward flow and white regions represent downward flow.

Figure 2-29: Péclet Number of Molecular Diffusion versus Time at the Hypothetical Repository Footprint for the Reference Paleohydrogeological Scenario (fr-base-paleo)

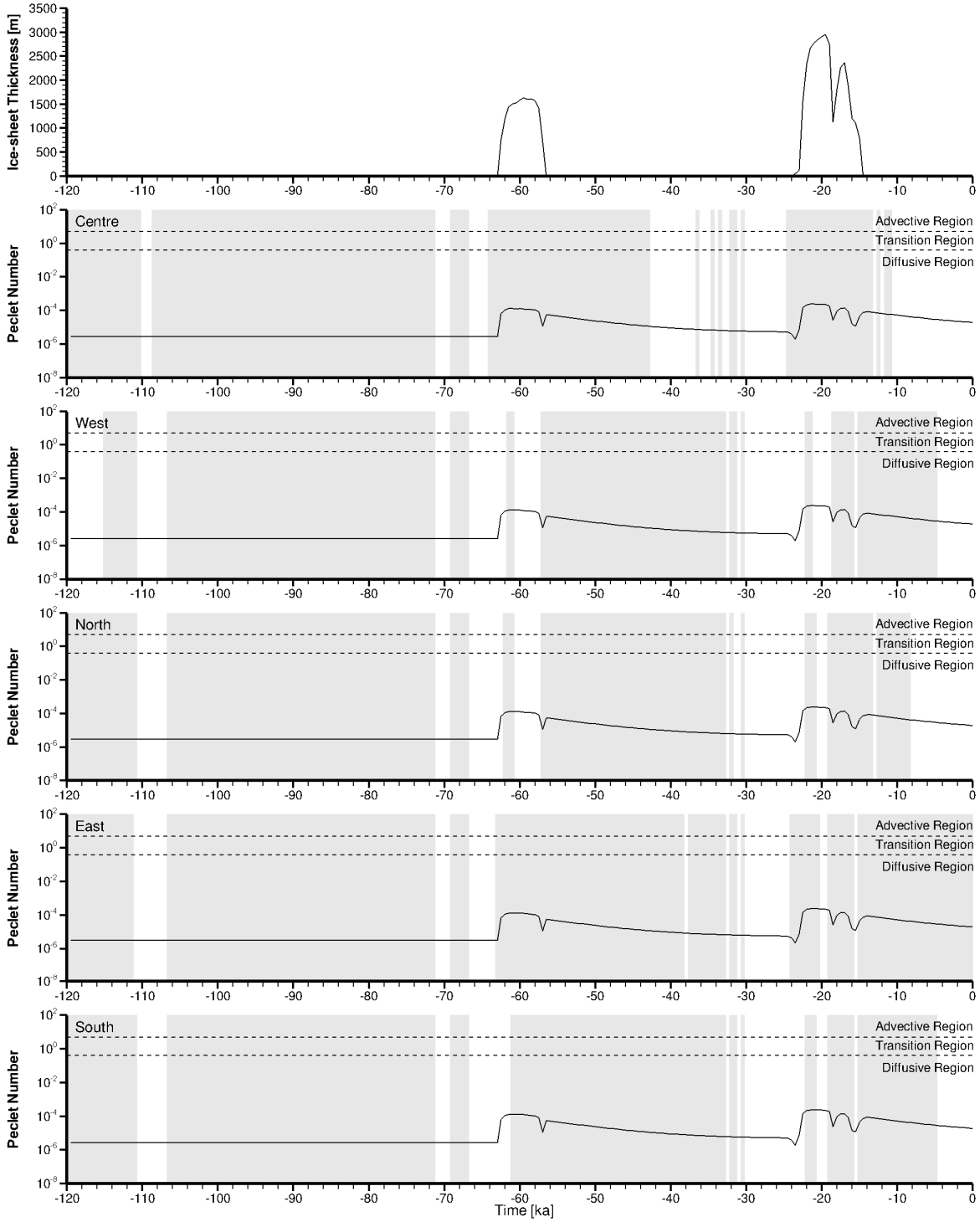

Figure 2-30: Péclet Number of Molecular Diffusion versus Time at the Hypothetical Repository Footprint for the Paleohydrogeological Scenario with Increased Rock Mass Hydraulic Conductivity (fr-base-paleo-sens)

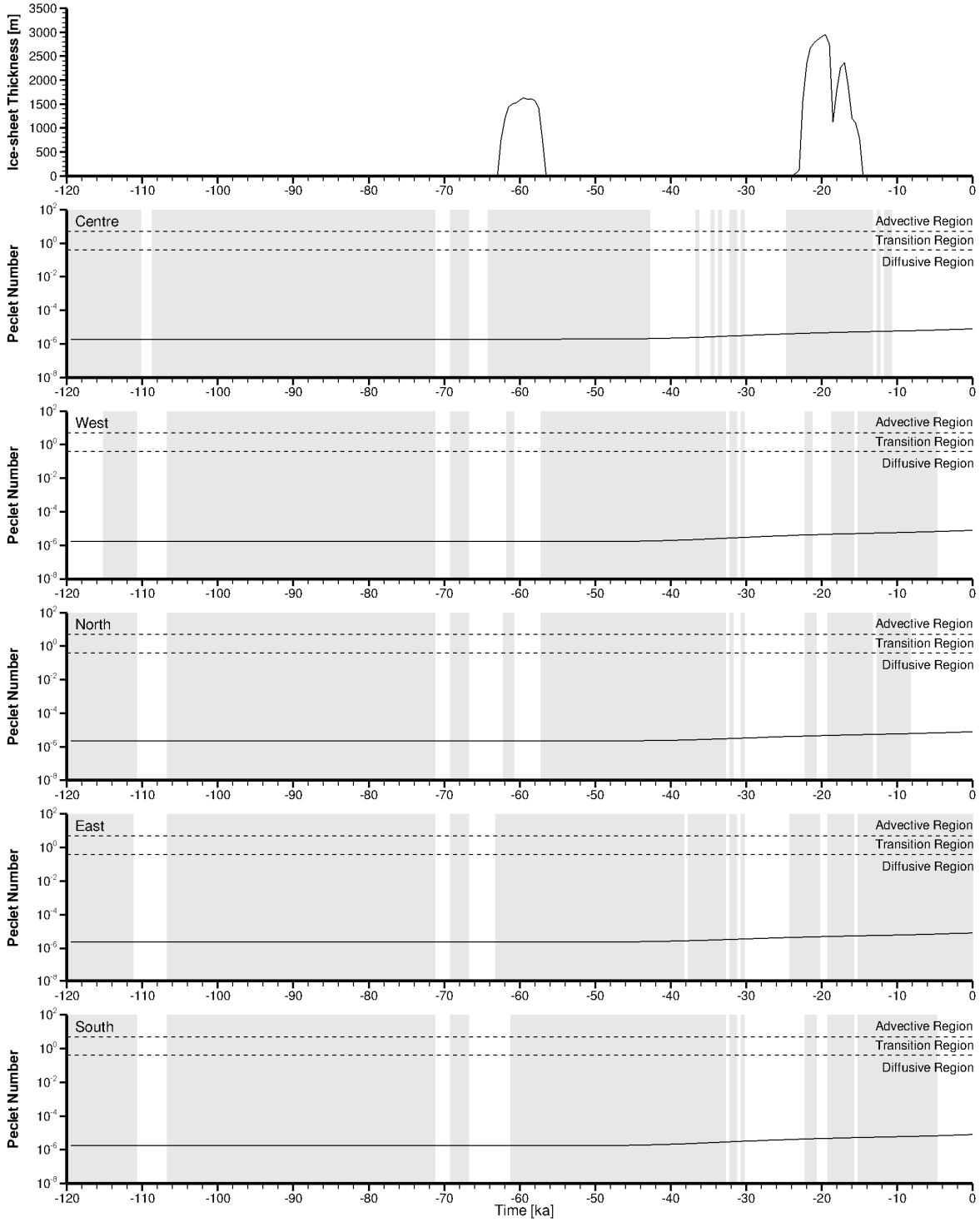

Figure 2-31: Péclet Number of Molecular Diffusion versus Time at the Hypothetical Repository Footprint for nn9930 Paleoclimate Boundary Conditions and a Loading Efficiency of 0 (fr-base-paleo-le0)

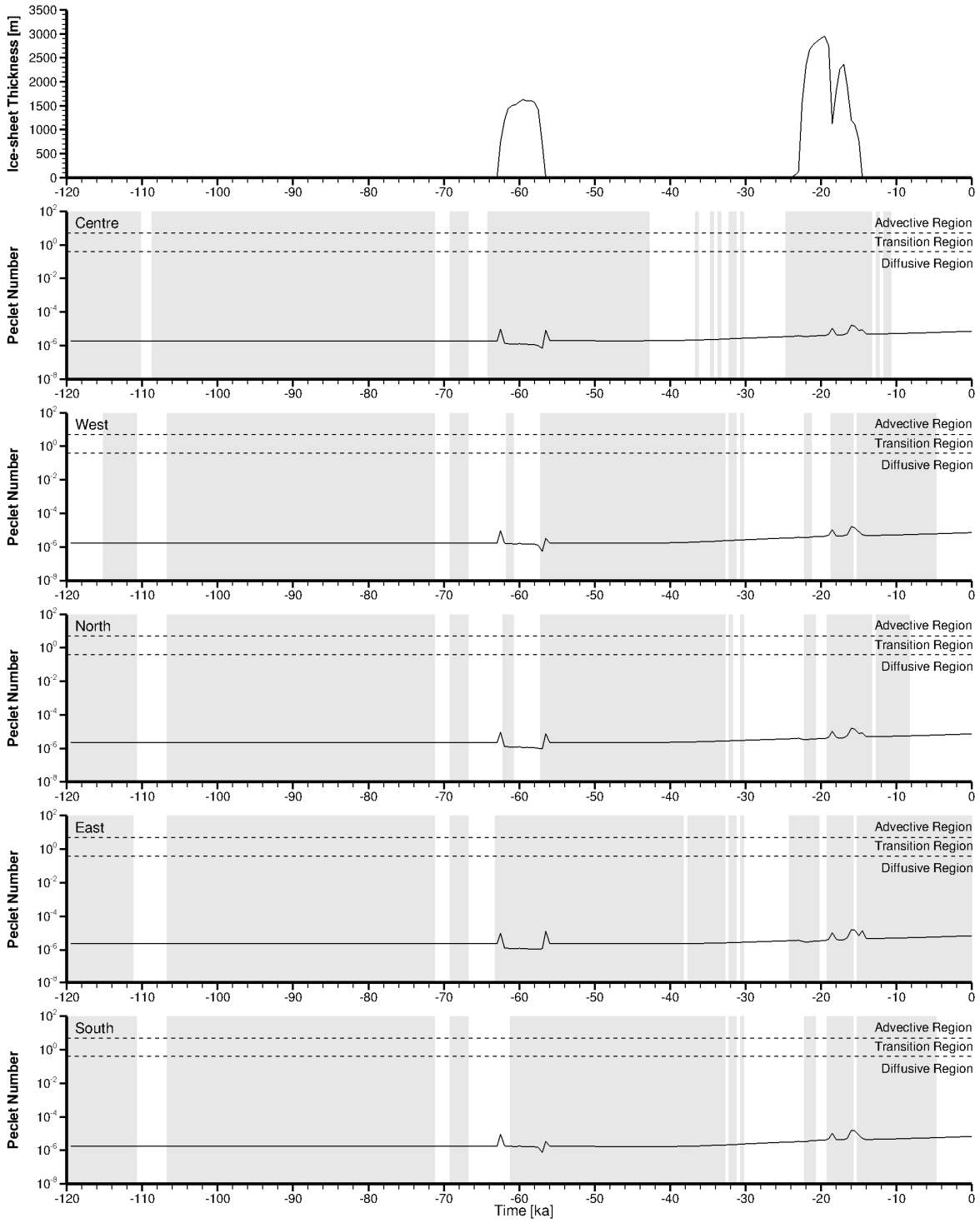

Figure 2-32: Péclet Number of Molecular Diffusion versus Time at the Hypothetical Repository Footprint for nn9930 Paleoclimate Boundary Conditions, a Loading Efficiency of 1, and a 0% of Ice-Sheet Thickness Equivalent Freshwater Head for the Surface Hydraulic Boundary Condition (fr-base-paleo-0-le1)

In a density-dependent groundwater flow system, freshwater head can only be used to determine hydraulic gradients along a horizontal plane; and environmental heads define hydraulic gradients along a vertical line (Lusczynski 1961). For the reference case paleohydrogeologic scenario (fr-base-paleo), a plot of environmental head versus time for various formations (Figure 2-33) indicates vertical gradients due to head differences across formations at the hypothetical repository footprint during the nn9930 glacial cycle. A large portion of the hydraulically conductive Guelph Formation is exposed to the Quaternary drift layer, which creates a hydraulic connection between the Guelph Formation and the top surface of the model. Therefore, Figure 2-33 shows that minimal vertical hydraulic gradients exist between the top surface and Guelph Formation throughout the 120,000 years paleohydrogeologic simulation. The very low hydraulic conductivities in the Salina units and Ordovician sediments ensure the deep groundwater flow system is not hydraulically connected to the surface boundary conditions, even during ice-sheet advance and retreat. The variations of heads over time are caused by one-dimensional hydro-mechanical coupling. The vertical hydraulic gradients at depth are mainly determined by the relative magnitude of loading efficiency for each formation. The Queenston Formation has the smallest loading efficiency and the value for the Precambrian is the largest. The resulting vertical hydraulic gradients from the Queenston to the Precambrian are mostly upward during the loading and unloading intervals. Figure 2-34 and Figure 2-35 show the time series plots of environmental heads for fr-base-paleo-le0 and fr-base-paleo-0-le1, respectively. The same conclusion can be drawn (as for the preceding section) that uniform loading efficiencies result in zero vertical hydraulic gradients in this case. Additionally, it is worth noting that the environmental heads in the Queenston Formation behave differently. At the location of hypothetical repository footprint, most of the Salina units pinch out west of the site such that the heads above the Ordovician sediments will be affected by the surface boundary conditions during the glacial cycles to some degree.

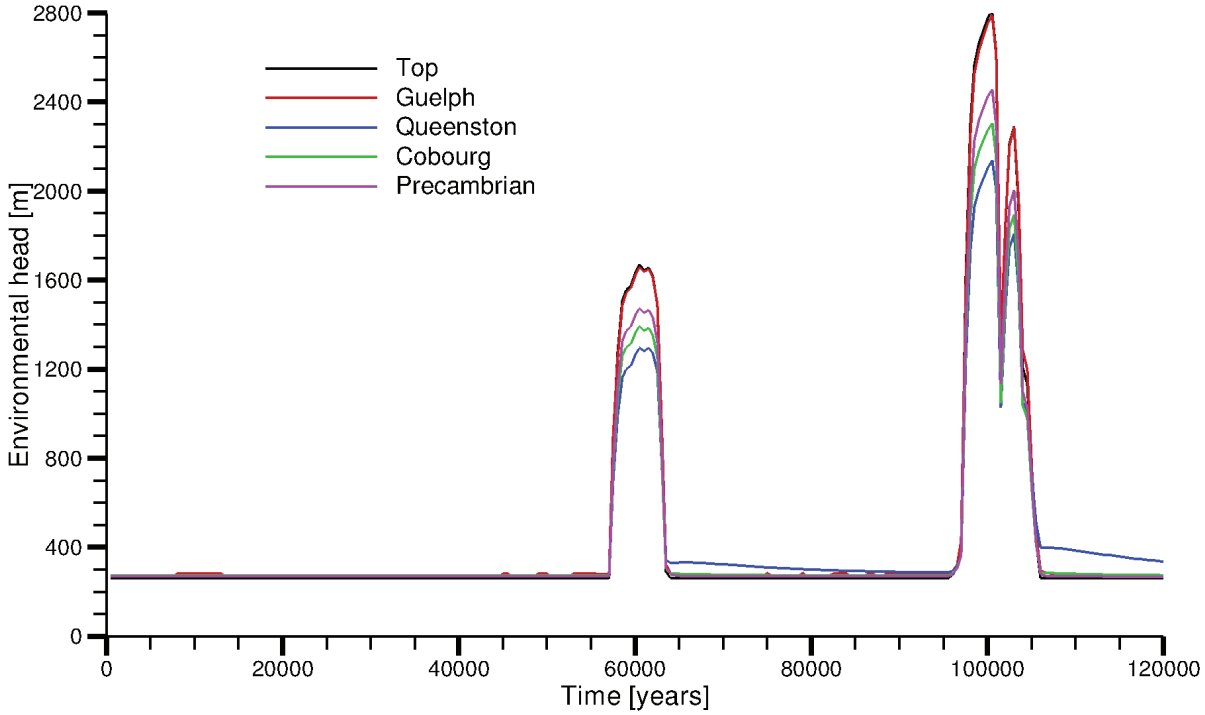

Figure 2-33: **Environmental Head versus Time for the Reference Paleohydrogeological Scenario (fr-base-paleo)**

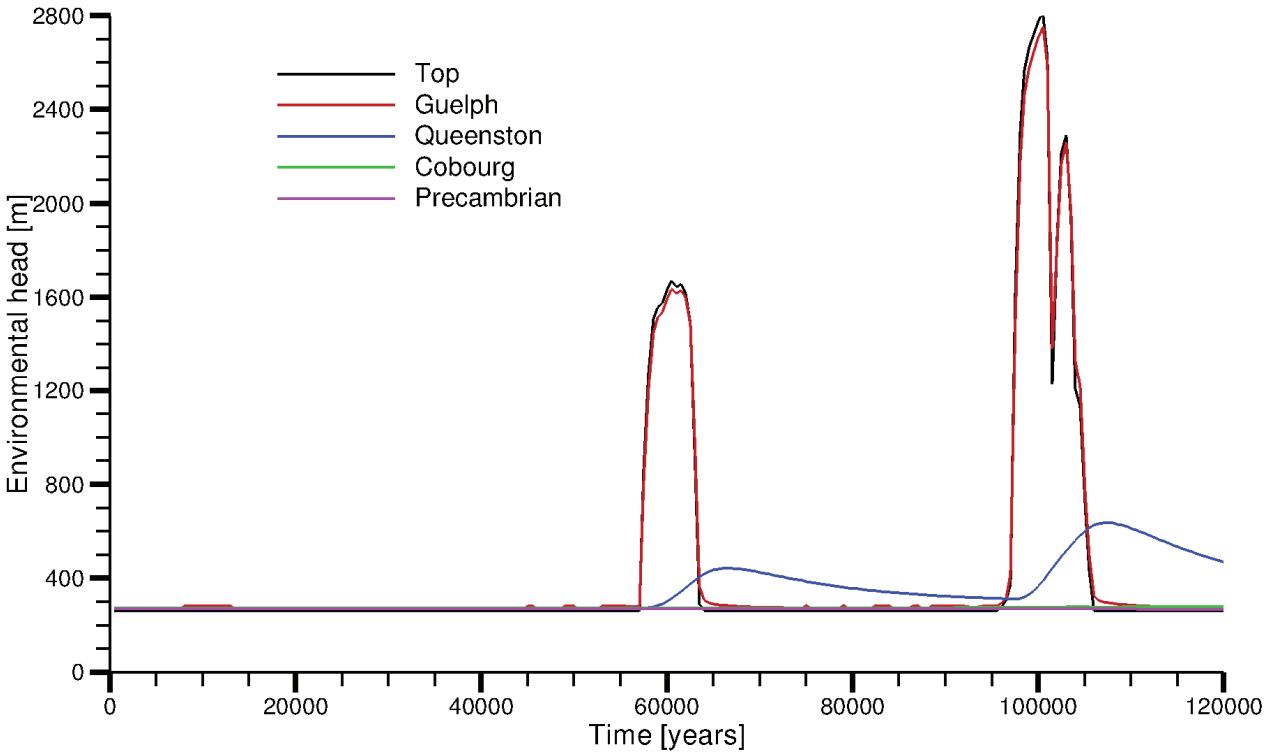

Figure 2-34: Environmental Head versus Time for nn9930 Paleoclimate Boundary Conditions and a Loading Efficiency of 0 (fr-base-paleo-le0)

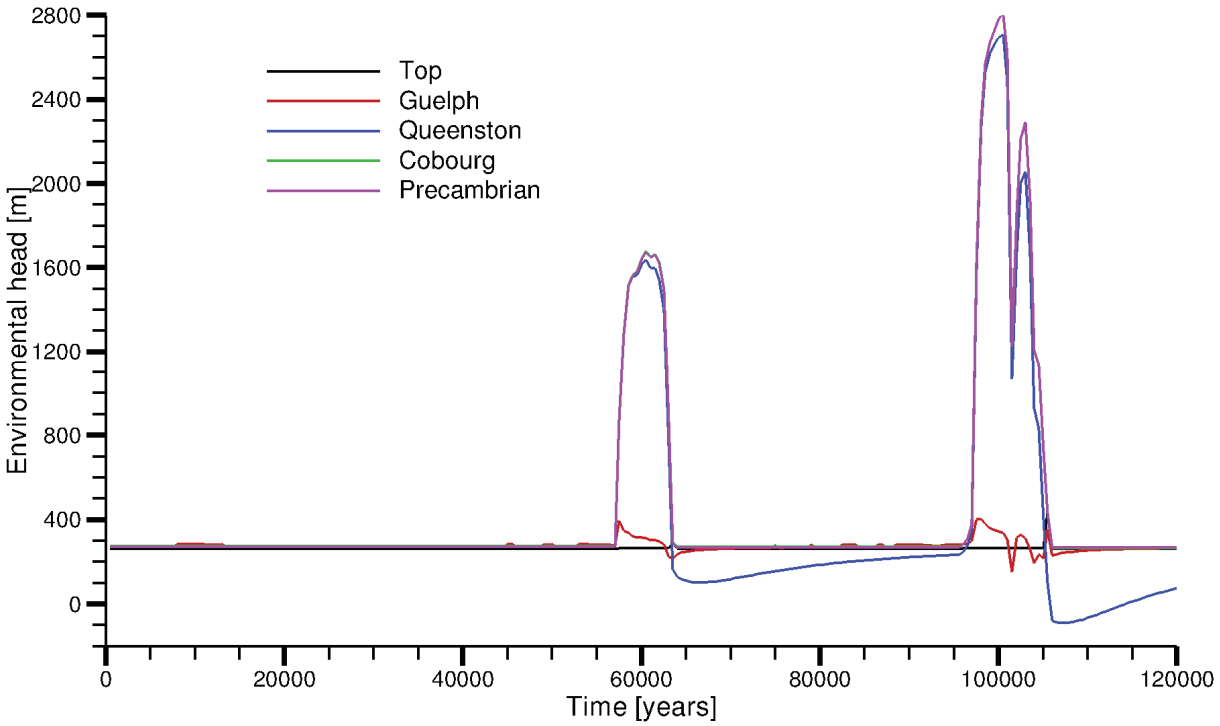

Figure 2-35: **Environmental Head versus Time for nn9930 Paleoclimate Boundary Conditions, a Loading Efficiency of 1, and a 0% of Ice-Sheet Thickness Equivalent Freshwater Head for the Surface Hydraulic Boundary Condition (fr-base-paleo-0-le1)**

2.3.4.4 Groundwater System Behaviour

2.3.4.4.1 Glaciation

The role of using a different paleoclimate model was investigated by scenario fr-base-paleo-cold using the nn9921 paleoclimate simulation. Through a comparison of Figure 2-25 to Figure 2-26, nn9921 includes more glaciation episodes, and longer glacial duration and permafrost presence at the hypothetical repository footprint within a 120,000 years period than paleoclimate model nn9930. Glacial presence tends to induce downward tracer migration and groundwater dilution by recharge water. Permafrost presence, on the contrary, tends to retard these processes by reducing the effective hydraulic conductivity of the layer. Figure 2-24 shows that the tracer migration for model nn9921 is still largely contained within the Silurian, and tracer concentrations are largely less than the tracer profile of the reference case. Figure 2-36 indicates that TDS concentrations in the Silurian are consistently greater for model nn9921 (fr-base-paleo-cold) than TDS concentrations in the reference scenario. Therefore, the impact of permafrost presence on the tracer migration outweighs the role of glaciation.

The reference case uses 100% of ice-sheet thickness in calculating the equivalent freshwater head. Alternate hydraulic boundary conditions applied to the surface of the modelling domain are analyzed in this study. These hydraulic boundary conditions are set to 80%, 30%, and 0% of the ice thickness equivalent freshwater head. For the reference scenario, glaciation generally results in downward flow during the loading phase and upward groundwater flow during the unloading phase. In the shallow units, the tracer migrates from surface and is then flushed out within one glacial episode. For the 0% case, representing zero fluid pressure at the top surface, upward flow occurs during glacial loading, and downward flow occurs during glacial unloading, primarily due to increased pore fluid pressures resulting from hydromechanical coupling. Thus, slightly deeper tracer migration occurs when compared to the reference case (as shown in Figure 2-24). The 30% case results in the tracer profiles situated between the reference case (100%) and the 0% case. The 80% case demonstrates a lower tracer concentration than the reference case, primarily due to loading efficiencies in the upper formations close to a value of 0.8 (see Table 2-2); a loading efficiency of 0.8 would result in no vertical gradients from glacial loading or unloading. The different TDS distributions in Figure 2-36 for these four scenarios are attributed to the relative magnitude of ice-sheet loading and unloading rates, in addition to the relative proportion of the surface hydraulic boundary condition to the one-dimensional loading efficiency for various formations.

2.3.4.4.2 Permafrost

Permafrost develops in advance of the ice-sheet because the ground surface is directly exposed to climate variations, whereas ice-sheets thermally insulate the underlying geosphere from climate influences (Peltier 2002). Permafrost with very low permeability often acts as the inhibitor of surface water migration downward and groundwater discharge. By a comparison of tracer migration in Figure 2-24 and TDS distribution at 120,000 years in Figure 2-36 (between the reference case with the nn9930 paleoclimate condition and fr-base-paleo-cold with the nn9921 paleoclimate condition), it is found that the cold-based paleohydrogeologic simulation has higher TDS concentrations in the shallow regime and less penetration depth of recharge water. In fact, Figure 2-26 demonstrates that the more frequent glacial cycles and longer permafrost presence in the nn9921 model, as compared to the nn9930 model, will inhibit both surface recharge water migration downward and the dilution of brines with fresh water.

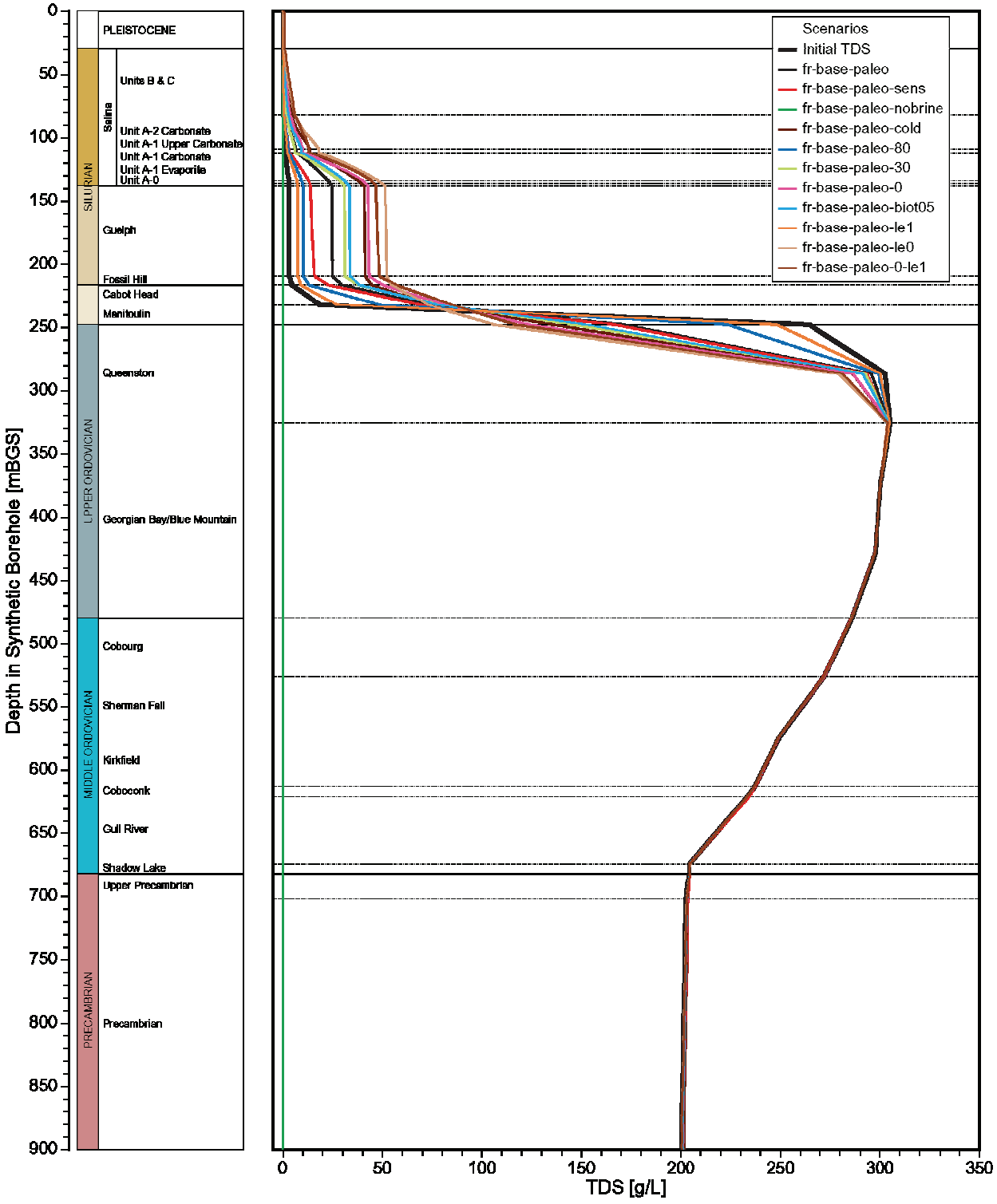

Figure 2-36: Vertical Profile Plots of TDS Concentrations for the Paleohydrogeologic Simulations at 120,000 Years at the Location of Hypothetical Repository Footprint

2.3.4.4.3 Depth of Surficial Recharge and Pathways

A tracer summary plot at 120,000 years for all paleohydrogeologic simulations is shown in Figure 2-24. The penetration depths of surficial recharge are represented by the intercepts between a straight line at a concentration of 0.05 and tracer concentration profiles at the hypothetical repository footprint at 120,000 years. The tracer for all the simulations only migrates into the bottom of the Silurian or the top of the Queenston Formation at 120,000 years. Thus, the downward migration of tracer is largely retarded by the low permeable Ordovician formations, which indicates the dominance of diffusion as a transport mechanism in the Ordovician. The greatest downward tracer migration occurs for the scenario fr-base-paleo-le0 with zero loading efficiency and 100% of ice-sheet thickness equivalent freshwater head for the surface hydraulic boundary condition. This tends to induce the greatest downward hydraulic gradient during the glacial loading phase. Scenario fr-base-paleo-le1 has the shallowest penetration depth, as the additional in-situ head induced by the mechanical coupling always equilibrates to the hydraulic surface boundary conditions with 100% of ice-sheet thickness equivalent freshwater head. Thus, for this scenario, negligible vertical hydraulic gradients exist throughout the paleohydrogeologic simulation period, including during glaciation cycles. The tracer in this case migrates downward mostly by diffusion.

2.3.4.4.4 The Role of Density

The increase in density of fluids at depth tends to slow down active flow in the deep groundwater system because resistance to driving forces increases with denser groundwater at depth (Park et al. 2009). However, the comparison of porewater velocities between steady-state and density-dependent simulation results in Figure 2-17 show that the velocity magnitude at depth in the steady-state model without brine (fr-base-nobrine) is slightly less than that in the reference model (fr-base). This can also be verified by the MLE comparison plot in Figure 2-18. Except for the portion beneath the lake, the mean life expectancies are generally higher in the freshwater simulation, which indicates a more stagnant groundwater system. The apparent contradiction can be explained by factors that influence fluid movement. A steady-state solution can be derived from the freshwater model, where the groundwater flow is purely driven by topography. The groundwater flow system of the reference case (with salinity) is still experiencing slow evolution at one million years of simulation time. Groundwater movement is not only driven by topography, but also is affected by the evolving TDS distribution.

For the paleohydrogeologic simulations, Figure 2-24 shows that no major difference in tracer profiles is observed between the reference case and the sensitivity case without salinity (fr-base-paleo-nobrine). Tracer only migrates into the shallow groundwater regime, which has low TDS concentrations in Figure 2-36. The groundwater system with high salinity at depth is diffusion dominant. The impact of density on the tracer migration cannot be evaluated based on these two paleohydrogeologic simulations. A plot of environmental head versus time for the paleohydrogeologic scenario without brine (in Figure 2-37) shows the vertical gradients at the hypothetical repository footprint. The direction and magnitude of the vertical gradients at depth are almost identical throughout the simulation period, as in the reference case shown in Figure 2-33.

2.3.4.4.5 Anomalous Heads

A summary plot of freshwater heads versus depth at 120,000 years for all paleohydrogeologic simulations is shown in Figure 2-38. At the Upper Ordovician, including the Queenston and Georgian Bay/Blue Mountain formations, no under or over-pressures are simulated for the scenario (fr-base-paleo-le1) with a loading efficiency of unity and a 100% ice-sheet thickness as equivalent freshwater head for the surface hydraulic boundary condition. The increase or decrease of hydraulic heads, due to hydro-mechanical coupling, always equilibrates to the surface hydraulic boundary condition; no vertical gradients are imposed by glacial loading and unloading.

Three scenarios (fr-base-paleo-0, fr-base-paleo-30, and fr-base-paleo-0-le1) result in under-pressured head distributions, owing to the reduced surface boundary heads. Among them, fr-base-paleo-0-le1 has the greatest under-pressures in the Upper Ordovician, as the loading efficiency of unity, combined with a free surface boundary condition, causes the largest upward hydraulic gradient during glacial loading. Discharge of groundwater during glacial loading leads to a deficit of water and the formation of under-pressures during glacial unloading. As compared to the reference case with a slight over-pressure, a reduction of surface boundary heads can shift the head distribution in the Upper Ordovician from over-pressured to under-pressured. Simulations with 80%, 30%, and 0% of ice-sheet thickness as equivalent freshwater heads result in less over-pressure than the reference case, slight under-pressure and more under-pressure in the Upper Ordovician, respectively.

Scenario fr-base-paleo-le0 has the greatest over-pressures due to the lack of hydro-mechanical coupling, which does not allow for an increase in in-situ pore pressures throughout the domain as a result of glacially induced hydro-mechanical coupling. The increase in pore pressure tends to diminish the vertical hydraulic gradient from the surface boundary condition for a non-zero loading efficiency. The increased downward gradients lead to the greatest residual heads of all the paleohydrogeologic simulations.

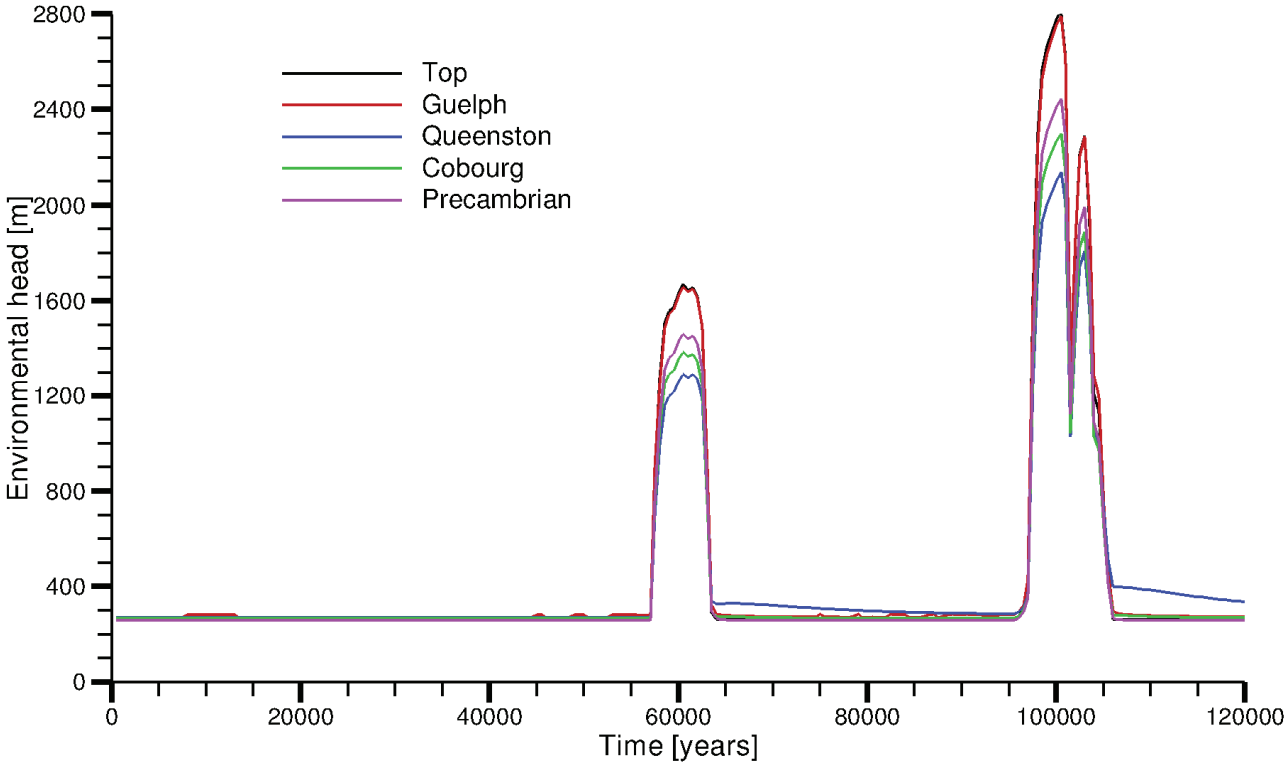

Figure 2-37: Environmental Head versus Time for the Paleohydrogeological Scenario without Salinity (fr-base-paleo-nobrine)

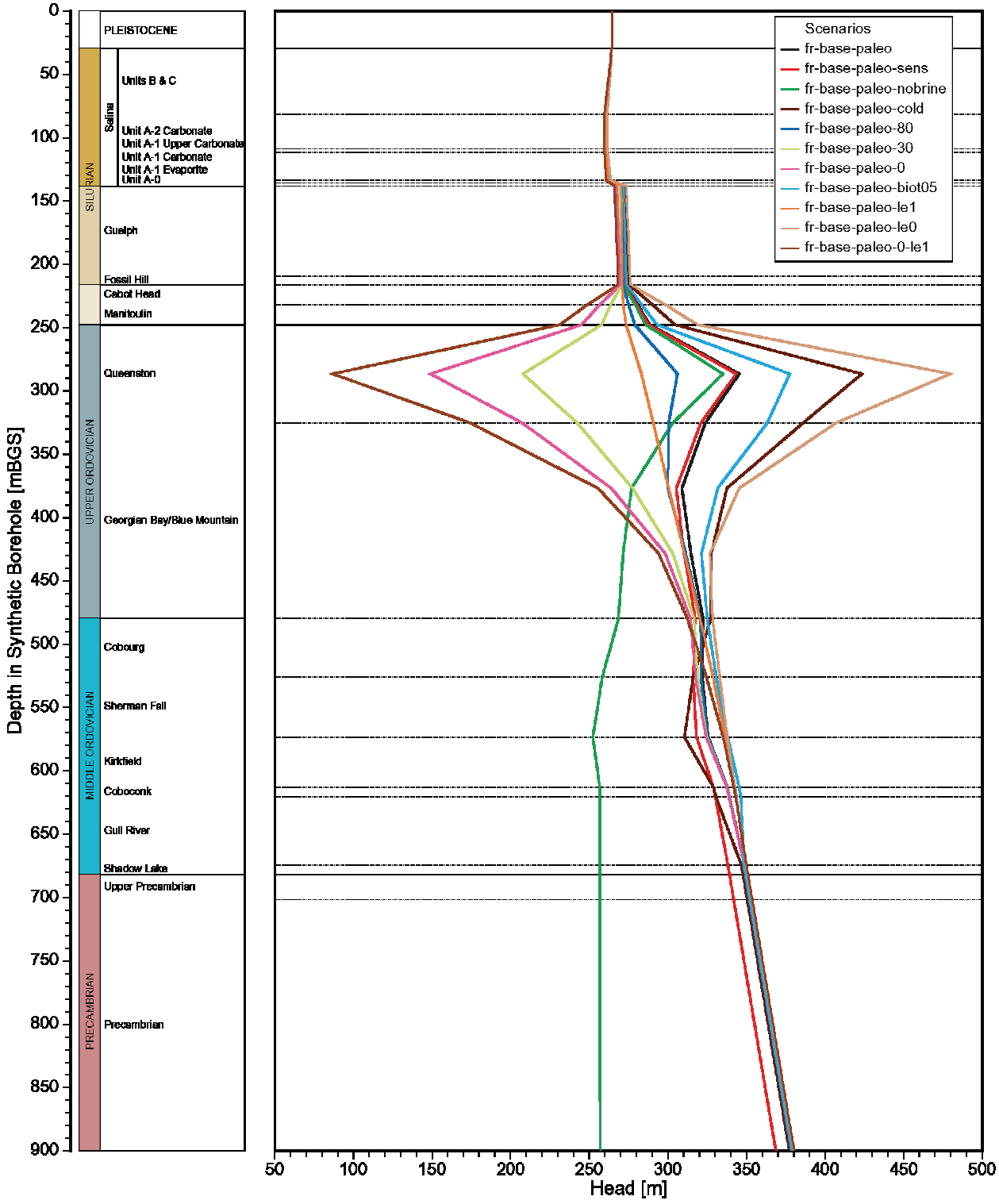

Figure 2-38: Vertical Profile Plots of Freshwater Heads for the Paleohydrogeologic Simulations at 120,000 Years at the Location of Hypothetical Repository Footprint

2.3.5 Additional Temperate Transient Sensitivity Analyses

Additional temperate scenarios were developed to determine the sensitivity of system performance to parameters including diffusion coefficients, dispersivities and hydraulic conductivities. Generally, an increase in diffusion or dispersion leads to mean life expectancy (MLE) spreading and overall reductions in MLE values. Similarly, total dissolved solids (TDS) are more uniformly distributed. At pseudo-equilibrium times of one million years, the groundwater system state is closer to equilibrium and can result in higher MLE values. The sensitivity of MLE to parameter changes is represented using dimensionless or normalized local sensitivities.

The base case (fr-base) MLE value at the repository footprint is 177 Ma. Table 2-9 lists MLE values at the center of the repository footprint for the reference case and for the additional temperate scenarios. Free solution diffusion coefficients for both brine and mean life expectancy were increased by one order of magnitude, resulting in an MLE value of 19.1 Ma at the repository footprint, nearly one-tenth the MLE of the base case. The local sensitivity was determined by perturbing the diffusion coefficients by 1%; the normalized local sensitivity (the percentage change in computed MLE divided by the percentage change in diffusion coefficients) is -0.74 at the repository footprint. In this case, MLEs are considered sensitive and negatively correlated to diffusion coefficients; increasing diffusion coefficients will yield lower MLEs.

Increasing the free solution diffusion coefficients affects both brine and MLE transport. In coupled density-dependent groundwater systems, a change to TDS distributions throughout the domain also affects the flow system and porewater velocities; changes to the flow system affect MLE transport. To separate the combined effects of changes to both MLE and to the flow system, resulting from modified transport parameters, further simulations were performed using the base case velocity fields to compute MLE, and are listed in Table 2-9. MLE values at the repository footprint for scenarios with diffusion coefficients increased by 1% and increased by one order of magnitude are 175 Ma and 19.0 Ma, respectively. These values are slightly lower than their counterpart MLE values because the base case velocity fields are further from equilibrium, due to the lower diffusion coefficients for brine transport. By comparing the differences in MLE values, it can be concluded that the direct impact of MLE diffusion coefficients on MLE values is more important than the brine diffusion coefficients, which have an indirect influence on MLEs through a more evenly distributed TDS field and a more equilibrated velocity field.

Figure 2-39 and Figure 2-40 show the vertical MLE and TDS profiles, respectively, at the repository footprint for the reference case and the additional scenarios. TDS and MLE profiles for scenarios with a 1% increase in diffusion coefficients (fr-de1p) are almost indistinguishable from the reference case. A one order of magnitude increase (fr-de10) in diffusion coefficients significantly increases solute transport by diffusion, forcing high initial TDS in the upper Ordovician to dissipate upward to the Silurian and downward to the lower Ordovician much faster than in the reference case. The resulting MLE profiles are well below the reference case. Additionally, because the correlation coefficient of -0.74 is near to -1, this indicates that MLE transport is dominated by molecular diffusion.

The second set of analyses increased dispersivity values by 1%, 10%, and 100% and are identified as scenarios fr-disp1p, fr-disp10p, and fr-disp2. The local sensitivity analysis of dispersivities, determined by perturbing dispersivities by 1%, indicates that MLEs are positively correlated to dispersivities with a coefficient of 0.62 and an increase in MLE values relative to the base case. Further increases in dispersivity tend to yield similar MLE values within 5% of the base case (see Table 2-9); MLEs at the repository footprint are, therefore, not deemed to be sensitive to changes in dispersivity, and are largely attributed to the diffusion dominant transport regime below the Guelph Formation. Figure 2-39 and Figure 2-40 demonstrate that TDS and MLE profiles for scenarios with alternate dispersivities are either very close to or almost indistinguishable from the reference case. In doubling dispersivities (100% increase) for both brine and MLE, the MLE value at the repository footprint decreases to 171 Ma with a normalized sensitivity of -0.036.

Scenarios using the reference case porewater velocity field (fr-base prefix) and enhanced dispersivities for MLE were performed for two purposes: to evaluate the direct impact of MLE dispersivities on performance measures; and separately, to evaluate the indirect influence of brine dispersivities. Increasing MLE dispersivities always contributes to lower MLEs at the repository footprint, as shown in Table 2-9. Brine dispersivity enhancement leads to greater equilibration in TDS distribution and the groundwater flow field, leading to greater MLEs. For the 1% and 10% alternate dispersivity scenarios, brine dispersivities contribute to increased MLE, while the 100% cases result in decreased MLE at the repository footprint. For the third sensitivity analysis, hydraulic conductivities were enhanced by three orders-of-magnitude for the low permeability units between the Guelph and the Cambrian formations. The substantial increase in hydraulic conductivities results in more brine and TDS being flushed from the groundwater system, as shown in Figure 2-41. Compared to the reference case (Figure 2-13), Figure 2-42 shows that the velocity magnitude in those units with enhanced hydraulic conductivities is approximately increased by three orders-of-magnitude. The solute transport at the repository footprint is still dominated by diffusion; the Peclet number of molecular diffusion of 0.05 for a characteristic length of unity is well below 0.4 (Bear 1988). The mean life expectancy at the repository footprint is 6.3 Ma. Solute transport, by both advection and diffusion, from the upper Ordovician, with high initial TDS upward to the Silurian and downward to the lower Ordovician, is greatly enhanced during the one million year pseudo-equilibrium simulation. This results in lower TDS in the upper Ordovician shales and higher TDS in the Silurian formations and in the Ordovician carbonate formations, due to advective transport, than are observed in the reference case (Figure 2-40). Figure 2-39 and Figure 2-40 demonstrate that higher TDS concentrations in the shallow groundwater flow regime within the Silurian formations contributes to lower groundwater flow velocity magnitude and larger MLEs than in the reference case. As noted by Park et al. (2009), the increase in pore fluid density often acts to retard active flow. The MLEs in the Ordovician are significantly less than in the reference case due to higher velocity magnitudes caused by the increase of hydraulic conductivities in these units. In the Precambrian, the same profiles of MLE versus depth are observed, as the properties of this portion of the model domain remain unchanged.

Table 2-9: Computed MLE Values at the Repository Footprint for Alternate Temperate Scenarios

Scenario	Transport Parameter Application	
	Brine and MLE*	MLE**
Base case (fr-base)	177 Ma	177 Ma
Increase diffusion coefficient by 1% (prefix-de1p)	176 Ma	175 Ma
Increase diffusion coefficient by 1 order of magnitude (prefix-de10)	19.1 Ma	19.0 Ma
Increase dispersivities by 1% (prefix-disp1p)	178 Ma	177 Ma
Increase dispersivities by 10% (prefix-disp10p)	177 Ma	176 Ma
Increase dispersivities by 100% (prefix-disp2)	171 Ma	169 Ma
Increase hydraulic conductivity by 3 orders of magnitude (fr-hc1000)	6.34 Ma	N/A

Note: * prefix = ‘fr‘ in Column 1, ** prefix = ‘fr-base‘ in Column 1

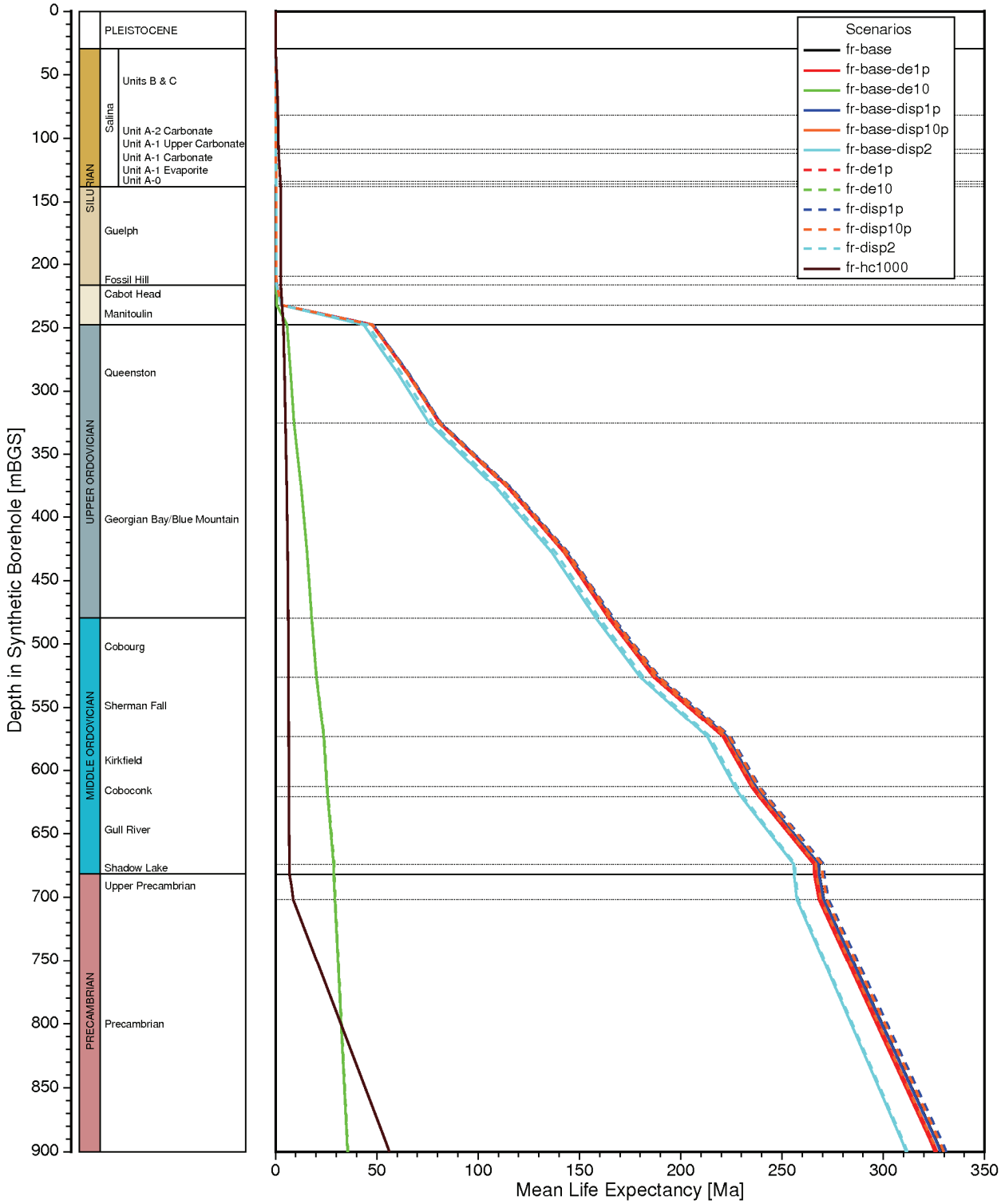

Notes: Solid lines represent scenarios which use the base case porewater velocity field.
Scenarios fr-base-de10 and fr-de-10 overlap.

Figure 2-39: Vertical Profile Plots of Mean Life Expectancies at One Million Years for the Reference Case and Additional Sensitivity Scenarios

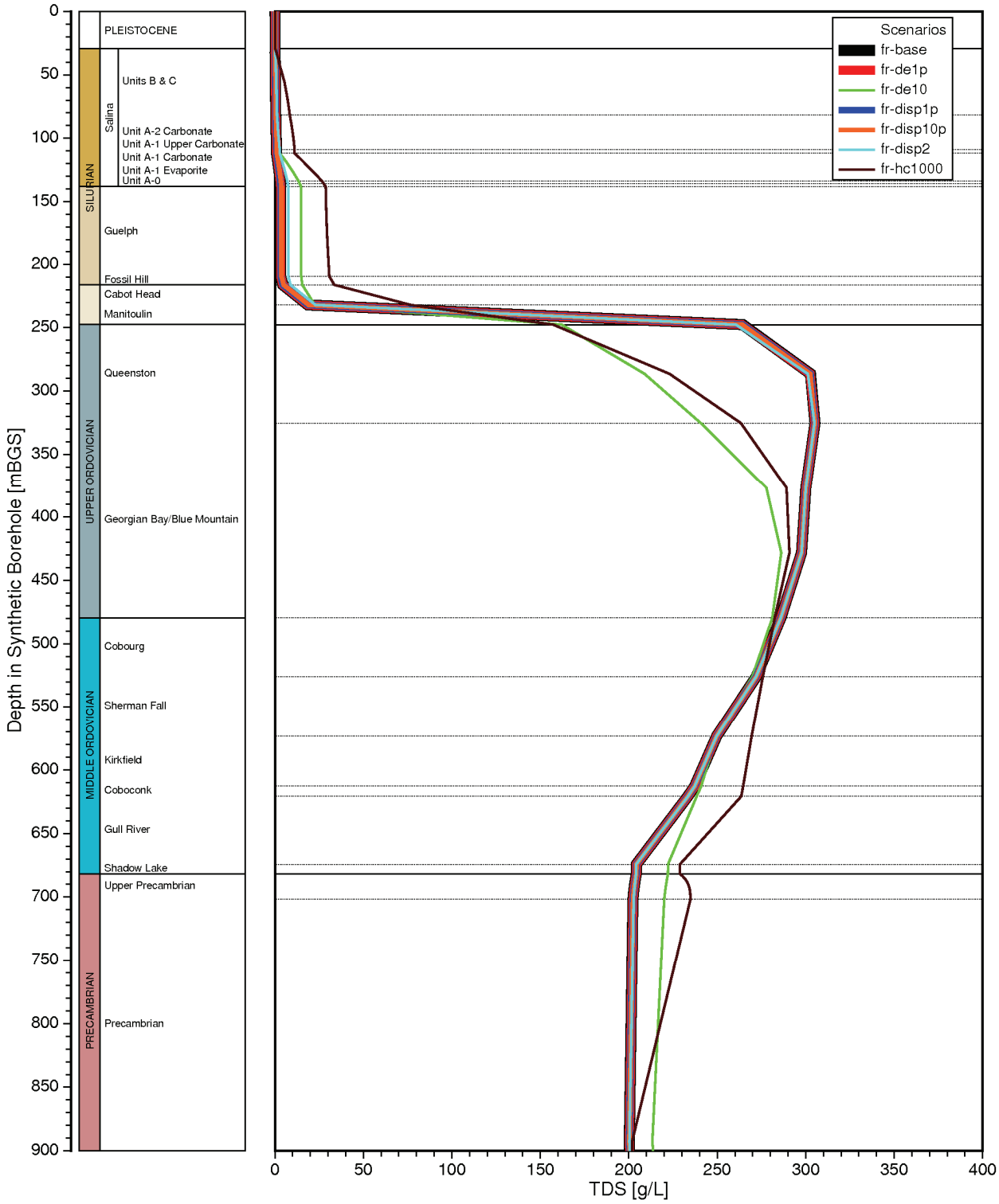

Figure 2-40: **Vertical Profile Plots of Total Dissolved Solids Concentrations at One Million Years for the Reference Case and Additional Sensitivity Scenarios**

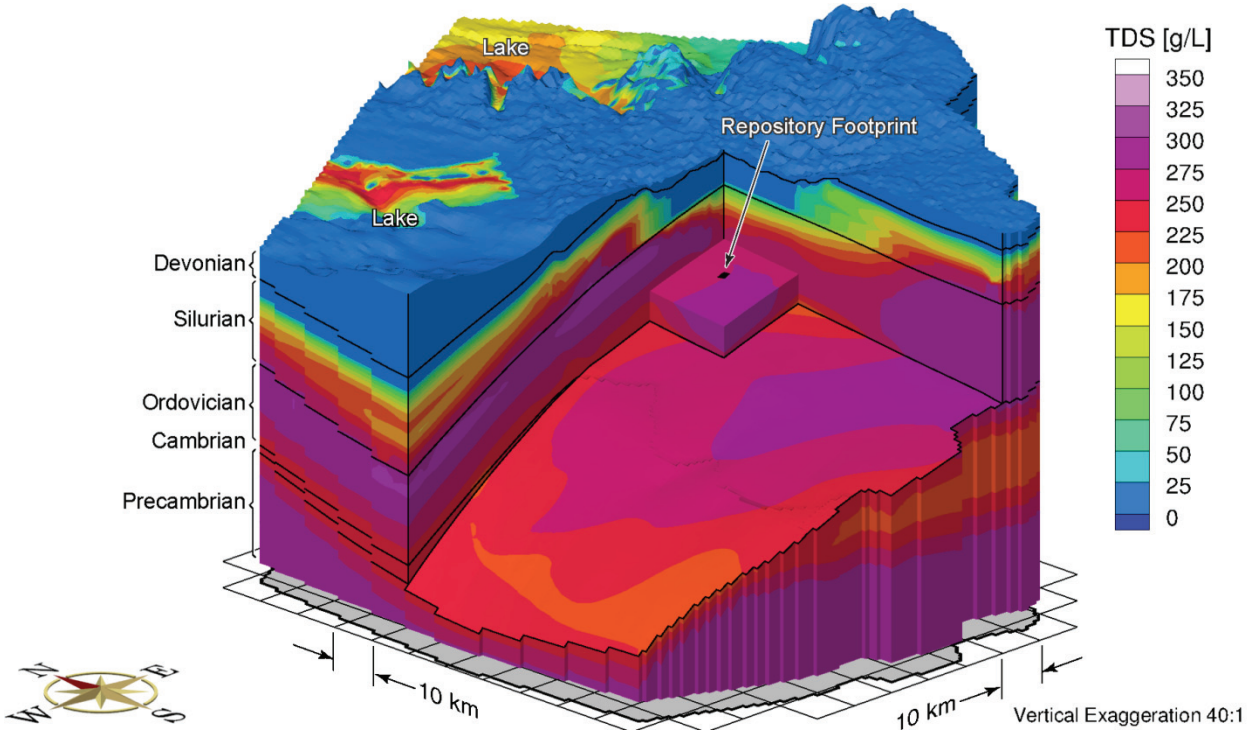

Figure 2-41: **Total Dissolved Solids Concentrations at One Million Years for a Three Order of Magnitude Enhancement in Hydraulic Conductivities**

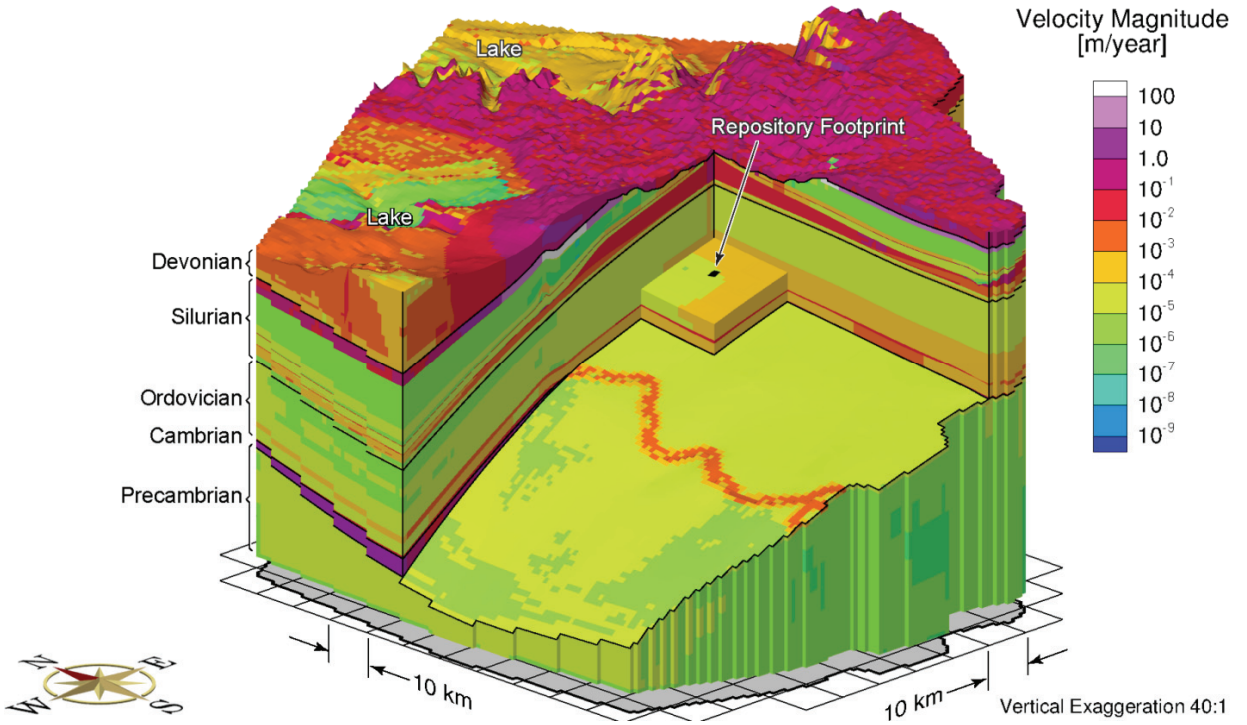

Figure 2-42: **Porewater Velocity Magnitude for a Three Order of Magnitude Enhancement in Hydraulic Conductivities**

2.4 Summary and Conclusions

This chapter describes a geosphere dataset for a hypothetical sedimentary rock site. The geosphere data set described in this chapter was provided for the purpose of performing an illustrative postclosure safety assessment. Three groundwater systems are considered: shallow, intermediate and deep. The behaviour of the groundwater systems during temperate and glacial conditions was explored through a suite of sensitivity cases.

The sedimentary rock overlying the hypothetical repository contains a thick sequence of low permeability limestones and shales. Temperate hydrogeologic modelling illustrates the role played by the low permeability limestones and shales as natural barriers to groundwater movement and contaminant transport.

The hydrogeological domain for the geosphere described in this chapter is divided into three groundwater systems: shallow (0- 215 mBGS), intermediate (215-250 mBGS) and deep (>250 mBGS). These systems are identified, in part, by rock mass hydraulic conductivities, as well as groundwater total dissolved solids (TDS) concentrations and redox conditions. The shallow groundwater zone occurs in the upper 215 m and comprises glacial sediment overlying a relatively permeable sequence of limestone and dolostone. In the shallow system, groundwater is considered to be fresh, oxygen-rich and isolated from the deeper groundwater systems. The intermediate groundwater system is a transition zone in which the groundwater becomes progressively more mineralized and reducing with depth. Within the deep groundwater system, groundwater conditions are saline and reducing. With increasing depth, the general increase in salinity and decreased rock mass hydraulic conductivities leads to improved groundwater system stability at time frames relevant to repository safety.

Péclet numbers and MLEs were used as illustrative performance measures to gain insight into the processes most influencing mass transport. For an assumed reference case, the shallow groundwater system is advective, whereas at greater depths, the low permeability rock mass results in low rates for mass transport. Further groundwater system stability occurs as a result of salinity gradients within the intermediate and deep groundwater systems.

Paleohydrogeological simulations were used to illustrate the long-term evolution and stability of the geosphere and groundwater systems to external perturbations. The distribution and duration of permafrost at the repository location play a role in governing the depth to which meltwater penetrates. Paleohydrogeologic simulations suggest that glacial meltwaters will not reach the repository horizon, due to the low hydraulic conductivity of the overlying shales dolostones and evaporites of the Salina Group. Glacial recharge penetrating below the shallow groundwater system is not expected to be oxygenated or to influence redox conditions at the repository horizon. For the paleohydrogeologic sensitivity cases performed, the glacial perturbations did not materially change mass transport rates at repository depth and mass transport remained diffusion dominated throughout the glacial cycle.

2.5 References for Chapter 2

Armstrong, D.K. and T.R. Carter. 2010. The Subsurface Paleozoic Stratigraphy of Southern Ontario. Ontario Geological Survey, Special Volume 7.

Armstrong, D.K. and J.E.P. Dodge. 2007. Paleozoic geology of southern Ontario. Ontario Geological Survey, Miscellaneous Release-Data 219.

Armstrong, D.K. and T.R. Carter. 2006. An Updated Guide to the Subsurface Paleozoic Stratigraphy of Southern Ontario. Ontario Geological Survey, Open File Report 6191.

Armstrong, D.K. and W.R. Goodman. 1990. Stratigraphy and depositional environments of Niagaran carbonates, Bruce Peninsula, Ontario. Field Trip No. 4 Guidebook. American Association of Petroleum Geologists, 1990 Eastern Section Meeting, hosted by the Ontario Petroleum Institute. London, Ontario.

Barker, J.F. and S.J. Pollock. 1984. The Geochemistry and Origin of Natural Gases in Southern Ontario. Bulletin of Canadian Petroleum Geology 32, 313-326.

Bear, J. 1988. Dynamics of Fluids in Porous Media. Dover Publications Inc., New York, USA.

Berry, F.A.F. 1969. Relative factors influencing membrane filtration effects in geologic environments. Chemical Geology 4, 293-301.

Bredehoeft, J.D., C.R. Blyth, W.A. White and G.G. Maxey. 1963. Possible mechanism for concentration of brines in subsurface formations. American Association of Petroleum Geologists Bulletin 47, 257-269.

Carpenter, A.B. 1978. Origin and chemical evolution of brines in sedimentary basins. Oklahoma Geological Survey Circular 79, 60-77.

Cornaton, F. and P. Perrochet. 2006a. Groundwater age, life expectancy and transit time distributions in advective–dispersive systems: 1. Generalized reservoir theory. Advances in Water Resources 29(9), 1267–1291.

Cornaton, F. and P. Perrochet. 2006b. Groundwater age, life expectancy and transit time distributions in advective–dispersive systems: 2. Reservoir theory for sub-drainage basins. Advances in Water Resources 29(9), 1292–1305.

Frape, S.K. and P. Fritz. 1987. Geochemical trends for groundwaters from the Canadian Shield. In Saline Water and Gases in Crystalline Rocks (P. Fritz and S.K. Frape, eds.). Number 33 in Geological Association of Canada Special Paper, 19–38.

Graf, D.L. 1982. Chemical osmosis and the origin of subsurface brines. Geochimica et Cosmochimica Acta 46, 1431-1448.

Hanor, J.S. 2001. Reactive transport involving rock-buffered fluids of varying salinity. Geochimica et Cosmochimica Acta 65(21), 3721-3732.

Hobbs, M.Y., S.K. Frape, O. Shouakar-Stash and L.R. Kennell. 2011. Regional Hydrogeochemistry – Southern Ontario. Nuclear Waste Management Organization Report NWMO DGR-TR-2011-12 R000. Toronto, Canada.

Huysmans, M. and A. Dassargues. 2005. Review of the use of Péclet numbers to determine the relative importance of advection and diffusion in low permeability environments. Hydrogeology Journal 13, 895–904.

INTERA. 2011. Descriptive Geosphere Site Model. Nuclear Waste Management Organization Report NWMO DGR-TR-2011-24 R000. Toronto, Canada.

ITASCA. 2011. Long Term Geomechanical Stability Analysis. Nuclear Waste Management Organization Report NWMO DGR-TR-2011-17 R000. Toronto, Canada.

ITASCA CANADA and AECOM. 2011. Three-Dimensional Geological Framework Model. Nuclear Waste Management Organization Report NWMO DGR-TR-2011-42 R000. Toronto, Canada.

Kharaka, Y.K. and J.S. Hanor. 2005. Deep fluids in the Continents: 1. Sedimentary Basins. In: J.I. Drever (Ed.). Treatise on Geochemistry, Surface and Groundwater, Weathering, and Soils 5, 499-540.

Kharaka, Y.K., A.S. Maest, W.W. Carothers, L.M. Law, P.J. Lamothe and T.L. Fries. 1987. Geochemistry of metal-rich brines from central Mississippi Salt Dome Basin, U.S.A. Applied Geochemistry 2, 543-561.

Kharaka Y.K. and F.A.F. Berry. 1973. Simultaneous flow of water and solutes through geological membranes I: Experimental investigation. Geochimica et Cosmochimica Acta 37, 2577-2603.

Land, L.S. 1997. Mass transfer during burial diagenesis in the Gulf of Mexico sedimentary basin: an overview. Society for Sedimentary Geology 57, 29-39.

Land, L.S. and D.R. Prezbindowski. 1981. The origin and evolution of saline formation water, Lower Cretaceous carbonates, south-central Texas, U.S.A. Journal of Hydrology 54, 51-74.

Lusczynski, N.J. 1961. Head and flow of ground water of variable density. Journal of Geophysical Research 66(12), 4247–4256.

McCauley, C.A., D.M. White, M.R. Lilly and D.M. Nyman. 2002. A comparison of hydraulic conductivities, permeabilities and infiltration rates in frozen and unfrozen soils. Cold Regions Science and Technology 34(2), 117–125.

McIntosh, J.C. and L.M. Walter. 2006. Paleowaters in Silurian-Devonian carbonate aquifers: Geochemical evolution of groundwater in the Great Lakes region since the late Pleistocene. Geochimica et Cosmochimica Acta 70, 2454-2479.

NWMO. 2011. Geosynthesis. Nuclear Waste Management Organization Report NWMO DGR-TR-2011-11 R000. Toronto, Canada.

Normani, S.D. 2009. Paleoevolution of Pore Fluids in Glaciated Geologic Settings. Ph.D. thesis, University of Waterloo. Ontario, Canada.

Normani, S.D., Y.J. Park, J.F. Sykes, and E.A. Sudicky. 2007. Sub-regional Modelling Case Study 2005-2006 Status Report. Nuclear Waste Management Organization Report NWMO TR-2007-07. Toronto, Canada.

Park, Y-J., E.A. Sudicky and J.F. Sykes. 2009. Effects of shield brine on the safe disposal of waste in deep geologic environments. Advances in Water Resources 32, 1352–1358.

Park. Y.-J., E.A. Sudicky, S. Panday, J.F. Sykes, and V. Guvanasen. 2008. Application of implicit sub-time stepping to simulate flow and transport in fractured porous media. Advances in Water Resources, 31(7), 995-1003.

Peltier, W.R. 2011. Long-Term Climate Change. Nuclear Waste Management Organization Report NWMO DGR-TR-2011-14 R000. Toronto, Canada.

Peltier, W.R. 2002. A design basis glacier scenario. Ontario Power Generation Report 06819-REP-01200-10069-R00. Toronto, Canada.

Rittenhouse, G. 1967. Bromine in oil-field waters and its use in determining possibilities of origin of these waters. American Association of Petroleum Geology Bulletin 51(12), 2430-2440.

Sherwood Lollar, B. 2011. Far-field Microbiology Considerations Relevant to a Deep Geological Repository – State of Science Review. Nuclear Waste Management Organization Report NWMO TR-2011-09.

Sherwood Lollar B., S.M. Weise, S.K. Frape and J.F. Barker. 1994. Isotopic constraints on the migration of hydrocarbon and helium gases of southwestern Ontario. Bulletin of Canadian Petroleum Geology 42, 283-295.

Singh, B.P. and B. Kumar. 2005. Isotopes in Hydrology, Hydrogeology, and Water Resources. Narosa Publishing House Pvt. Ltd., New Delhi, India.

Stroes-Gascoyne, S., C. Sergeant, A. Schippers, C.J. Hamon, S. Nèble, M.-H. Vesvres, V. Barsotti, S. Poulain and C. Le Marre. 2011. Biogeochemical processes in a clay formation *in situ* experiment: Part D - Microbial analyses - Synthesis of results. Applied Geochemistry 26, 980-989.

Stroes-Gascoyne, S. and C.J. Hamon. 2008. Preliminary Microbial Analysis of Limestone and Shale Rock Samples. Nuclear Waste Management Organization Report NWMO TR-2008-09. Toronto, Canada

Sykes, J.F., S.D. Normani and Y. Yin. 2011. Hydrogeologic Modelling. Nuclear Waste Management Organization Report NWMO DGR-TR-2011-16 R000. Toronto, Canada.

Sykes, E.A. 2007. Hydrogeologic modelling to assess conditions related to OPG's proposed Deep Geologic Repository in Tiverton, Ontario. Master's thesis, University of Waterloo. Ontario, Canada.

Therrien, R., R.G. McLaren, E.A. Sudicky, S.M. Panday, and V. Guvanasen. 2010. FRAC3DVS_OPG: a three-dimensional numerical model describing subsurface flow and solute transport. User's Guide. Groundwater Simulations Group, University of Waterloo, Ontario, Canada.

Vilks. P., N.H. Miller and K. Felushko. 2011. Sorption Experiments in Brine Solution with Sedimentary Rock and Bentonite. Nuclear Waste Management Organization Report NWMO TR-2011-11. Toronto, Canada.

Vilks, P. 2009. Sorption in Highly Saline Solutions – State of the Science Review. Nuclear Waste Management Organization Report NWMO TR-2009-18. Toronto, Canada.

Weast, R.C. (Ed.). 1983. CRC Handbook of Chemistry and Physics. 64th edition. CRC Press, Inc., Boca Raton, Florida, USA.

Wersin, P., S. Stroes-Gascoyne, F.J. Pearson, C. Tournassat, O.X. Leupin and B. Schwyn. 2011. Biogeochemical processes in a clay formation *in situ* experiment: Part G - key interpretations and conclusions. Implications for repository safety. Applied Geochemistry 26, 1023-1034.

THIS PAGE HAS BEEN LEFT BLANK INTENTIONALLY

3. USED FUEL CHARACTERISTICS

3.1 Used Fuel Description

3.1.1 Used Fuel Type and Amount

The used fuel waste form is a post-discharge natural uranium UO_2 CANDU fuel bundle.

The hypothetical repository is assumed to contain 4.6×10^6 bundles, which is the total reference used fuel inventory projected over the expected lifetime of the current fleet of Canadian CANDU power reactors (Garamszeghy 2012)[1].

There are a few variant CANDU fuel bundle designs, in particular the 28-element bundle, the 37-element standard bundle, the 37-element long length bundle, and the 37m bundle[2]. Some older bundles do not have CANLUB, which is a thin graphite coating between the fuel pellet and the fuel sheath. Sensitivity studies by Tait et al. (2000) indicate that the radionuclide inventory per unit mass of fuel is not sensitive to these different designs, and so the standard 37-element (Bruce) fuel bundle is selected as the reference as it will be the most common bundle.

The age of the fuel when placed in the repository will vary. Because the earliest bundles date back to 1970 and because the repository is unlikely to open before 2035, some fuel will be over 60 years old. The older the fuel, the lower the residual thermal power and the lower the radiation fields. For this pre-project review, all fuel bundles are assumed to have an out-of-reactor decay time of 30 years.

Table 3-1 summarizes the characteristics of the reference used fuel. These are further discussed below.

[1] Includes refurbishment of Bruce A, Darlington, Point Lepreau and Gentilly-2. No further refurbishment of Pickering or Bruce B. No new build reactors. Because Gentilly-2 has decided to not proceed with refurbishment, the projected used fuel inventory is reduced to about 4.4×10^6 bundles.

[2] A modified 37-element bundle (37m) will be entering service in some stations; however, the changes are minor and do not significantly affect inventory.

Table 3-1: Used Fuel Parameters

Parameter	Value	Comment
Waste Form	37-element UO_2 fuel bundle	Standard fuel bundle from Bruce and Darlington stations
Mass U/bundle	19.25 kg	Initial mass (before irradiation)
Mass Zircaloy/ bundle	2.2 kg	Includes cladding, spacers, end plates
Initial U-235	0.72 wt%	Natural uranium is used in OPG CANDU fuel
Burnup	220 MWh/kgU	Highest OPG station-average burnup in Tait et al. (2000). More recent data indicate this exceeds the median value recorded for each station for each decade of operation (Wilk 2013)
Power Rating	455 kW/bundle	Nominal mid-range value
Fuel Age (when placed in repository)	30 years	e.g., 10 years in pools, 20 years in dry storage
Fuel Pellet Geometric Surface Area	8.47 cm^2	Surface area of undamaged pellet (37 element design)

Note: From Tait et al. (2000).

3.1.2 Geometry

Fuel pellets formed from natural uranium UO_2 are placed inside a fuel sheath made of a zirconium-tin alloy (Zircaloy-4) with a thin CANLUB graphite coating on the inside. The ends of the sheath are closed by a welded zirconium alloy plug to produce a sealed fuel element. Fuel elements are welded to zirconium alloy end plates to form a fuel bundle as shown in Figure 3-1.

The number of pellets in a fuel element, and the number and dimensions of the fuel elements in a fuel bundle depend on the particular CANDU reactor. The most common bundle contains 37 fuel elements, each of which is 13.1 mm diameter and 486 mm long. This fuel bundle weighs 23.9 kg, of which 21.7 kg is UO_2 and 2.2 kg is Zircaloy (Tait et al. 2000).

Upon discharge, less than 0.1% of the bundles have minor damage or defects (such as pinhole failures in the fuel sheaths) (Tait et al. 2000). Analysis of the integrity of used fuel bundles indicates that they are unlikely to fail during storage (Freire-Canosa 2011). A small percentage may have increased susceptibility to integrity failure during subsequent transport to permanent storage. While the specific value may be relevant to the packaging plant design, the postclosure safety assessment is not sensitive to this value since no credit is taken for fuel integrity.

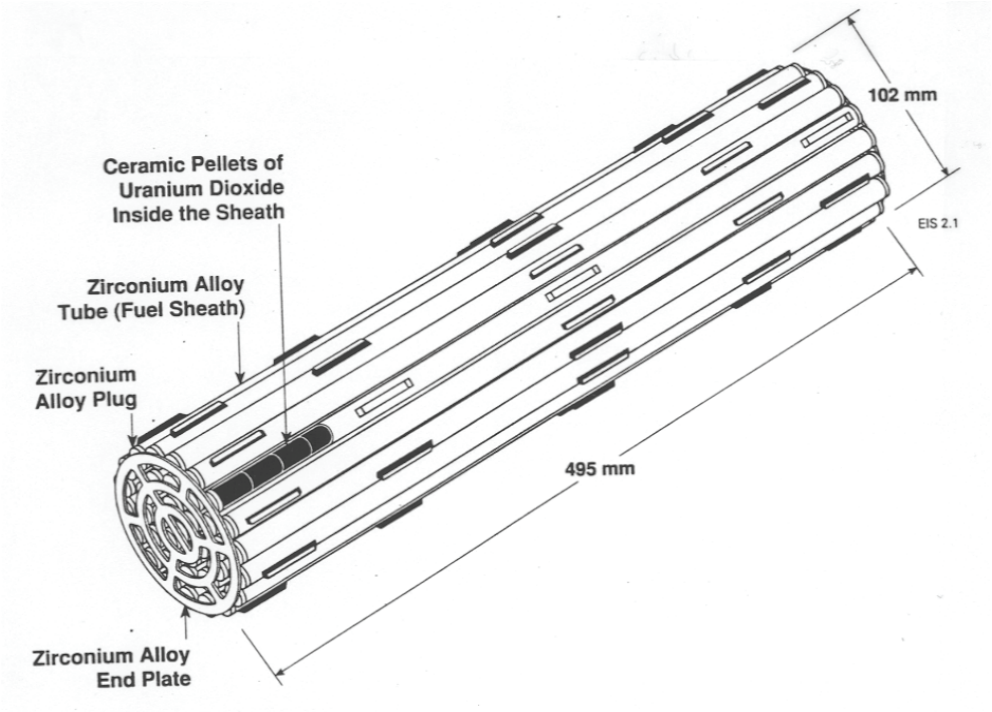

Figure 3-1: Typical CANDU Fuel Bundle

3.1.3 Burnup and Linear Power

The radioactivity level, heat generation rate, and bundle composition are all affected by the fuel burnup. This in turn depends on many factors including the type of reactor, the location of the bundle in the core, the bundle residence time, and bundle shifts that occur during fuelling operations. Although each bundle has a unique irradiation history, used fuel from all CANDU reactors is similar enough that it is not necessary to know individual detailed characteristics to assess the overall behaviour of the used fuel assemblies in the repository.

The aggregate 95th percentile burnup value for CANDU fuel is 254 MWh/kgU with some exceptional fuel elements experiencing burnups as high as 706 MWh/kgU (Wilk 2013). On a per station per decade basis, the 95th percentile values vary between 224 MWh/kgU and 286 MWh/kgU (Wilk 2013). A 220 MWh/kgU burnup exceeds the median value recorded for all stations for all decades and is well above the aggregate median value of about 190 MWh/kgU (Wilk 2013). At this level, about 2% of the initial uranium is converted into other elements.

The other major irradiation parameter that characterizes used fuel is linear power, which is the energy production rate per unit length. Tait et al. (2000) considered a power range of 200 to 900 kW/bundle (10-50 kW/m) as typical for the power range within which most CANDU bundles operate during their reactor lifetimes. The power level primarily affects the operating temperatures, which typically range from around 400°C on the outside of the fuel sheath to between 800°C and 1700°C in the fuel centreline, well below the melting temperature of 2800°C.

Tait et al. (2000) have calculated that the differences in radionuclide inventories between typical minimum and maximum power levels (200 and 900 kW/bundle) are generally less than about 2% for the same burnup. Tait et al. (2000) therefore used a mid-range value of 455 kW/bundle for reference inventory calculations.

In summary, a burnup level of 220 MWh/kgU and a power level of 455 kW/bundle are used to calculate radionuclide inventories.

3.1.4 Effect of Irradiation

The fuel undergoes a number of microstructural changes during irradiation, as illustrated by the sequence of photographs in Figure 3-2. Unirradiated fuel has a cohesive, interlocking microstructure and many grains have some internal sintering porosity from the fuel fabrication process. During irradiation, the sintering porosity is largely eliminated, boundaries between individual grains become more distinct, and some volatile elements diffuse out of the fuel grains to form fission gas bubbles at the interfaces between grains. At linear power ratings higher than approximately 50 kW/m (i.e., higher than achieved in most CANDU bundles), the fission gas bubbles enlarge and begin to coalesce, leading in some cases to the formation of gas tunnels along grain boundaries.

Unirradiated fuel pellets are very fine-grained, but at linear power ratings higher than approximately 50 kW/m equiaxial grain growth occurs in the pellet interior where temperatures are highest (Figure 3-3). Grain growth is typically accompanied by the diffusion and segregation of non-volatile fission products, some of which form small metallic particles at grain boundaries as shown in Figure 3-4.

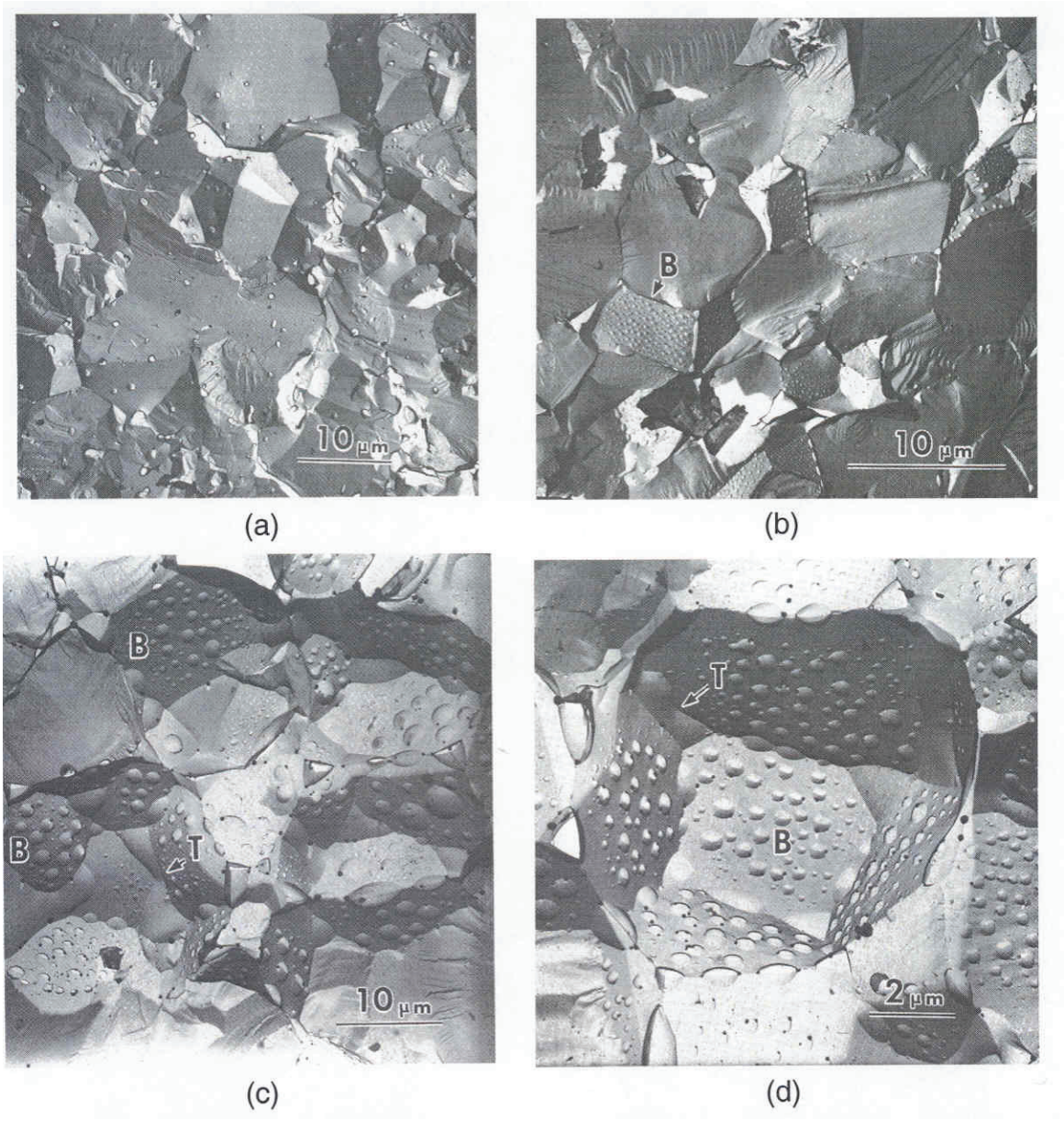

Notes: a) Typical microstructure of unirradiated UO_2. Small inclusions = sintering porosity.
b) Irradiated at low power (< 45 kW/m). Note loss of sintering porosity and development of small intergranular fission gas bubbles (B).
c) Irradiated at higher power (≥ 50 kW/m), showing growth of fission gas bubbles (B) and initiation of tunnels (T).
d) Magnified view of irradiated higher power fuel. Note the grain-edge tunnels (T) and the development of fission gas bubbles (B) on all faces of the "pull-out" of a single grain.
Ref.: Hastings (1982).

Figure 3-2: Typical Microstructure of Unirradiated and Irradiated UO_2 Fuel

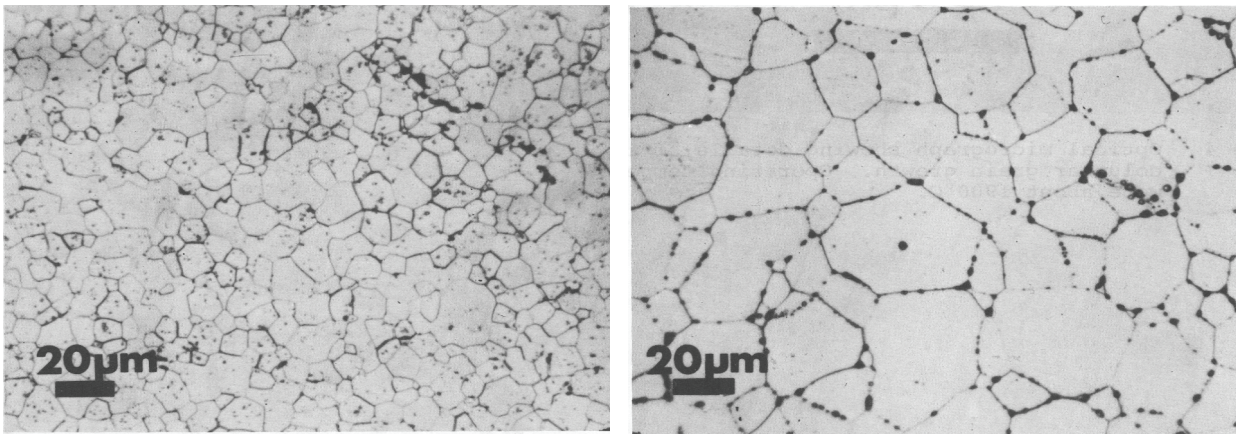

(a) **(b)**

Notes: a) Unirradiated UO_2. Note sintering porosity in grain interiors.
b) Irradiated UO_2 at low burnup and high power (20 MWh/kgU at 50 kW/m). Note increase in grain size, loss of sintering porosity, and formation of fission gas bubbles and tunnels along boundaries.
Ref.: Hastings (1982).

Figure 3-3: Grain Growth in Irradiated UO_2 Fuel

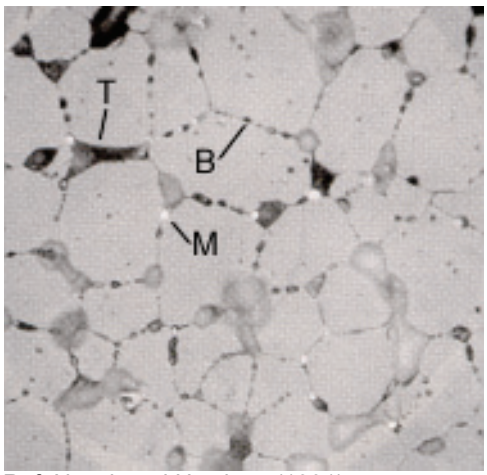

Ref: Novak and Hastings (1991)

Notes: Optical micrograph of polished and etched UO_2 fuel irradiated to very high burnup (770 MWh/kgU at 52 kW/m), showing small white particles at grain boundaries (M) that are formed from incompatible metals such as Mo, Ru, and Pd that have diffused out of the UO_2 grains. Well-developed fission gas bubbles (B) and tunnels (T) are also present at grain boundaries. Scale is approximately same as shown for Figure 3-3.

Figure 3-4: Segregation of Metallic Fission Products from UO_2 Fuel

Compared to fresh bundles, used bundles contain new elements (approximately 2% by mass), including fission products, activation products and actinides other than uranium. Of these, more than ~95% remain within the UO_2 lattice very close to the location of their formation (Gobien et al. 2013, and references therein).

As indicated in Figure 3-5, the species produced can be grouped according to their chemical behaviour into the following categories (Kleykamp 1985):

1. Species such as He, Kr, Ar, Cs and I that are gaseous or somewhat volatile at fuel operating temperatures (i.e., 400-1700^{o}C). Due to their relatively high diffusion coefficients, during reactor operation a small fraction of each species migrates out of the fuel grains and into fuel element void spaces (i.e., into the fuel sheath gap and into cracks in the fuel pellets). At the same time, another small fraction moves to the grain boundaries within the fuel pellets and forms fission gas bubbles. The remainder (roughly 95%) of the fission gases are held in the UO_2 crystal lattice.

2. Species such as the metals Mo, Ru, and Pd that are non-volatile but have a low solubility in UO_2. At high in-reactor temperatures, small quantities of these species can diffuse from the fuel grains and segregate as metallic alloy phases at grain boundaries, particularly in areas of UO_2 grain growth. The majority of incompatible species remain trapped within the fuel grains due to their low diffusion coefficients in UO_2 at fuel operating temperatures.

3. Species that are compatible with UO_2, including the lanthanide elements and actinides such as Pu, Am, Np. These elements can substitute chemically for uranium in UO_2, and the atoms are then structurally bound as trace elements in the UO_2 crystal lattice.

The Zircaloy-4 fuel sheath consists of more than 98 wt% Zr and approximately 1.5 wt% Sn, with a number of other elements present as impurities (Tait et al. 2000). During irradiation, the cladding receives a neutron fluence of around 10^{25} n/m^2 (Truant 1983). The irradiated metal cladding is a fine-grained material (grain size typically 10 μm, thickness typically 0.4 mm) with neutron activation products, such as C-14, Ni-59 and Ni-63, present at concentrations less than 1 mg/kg Zr. Due to the low temperature of the cladding during irradiation (< 400^{o}C), activation products in the Zircaloy cannot diffuse any significant distance from the site of their formation, and they are therefore likely to be distributed uniformly throughout the metal. While in-reactor, coolant pressure causes the fuel cladding to collapse onto the fuel pellets, the heat generated in the fuel causes the pellets to expand slightly into an hourglass shape, which leads to the formation of minor cylindrical ridges in the cladding. This effect is more pronounced at high linear power and when fuel is in the reactor for long times.

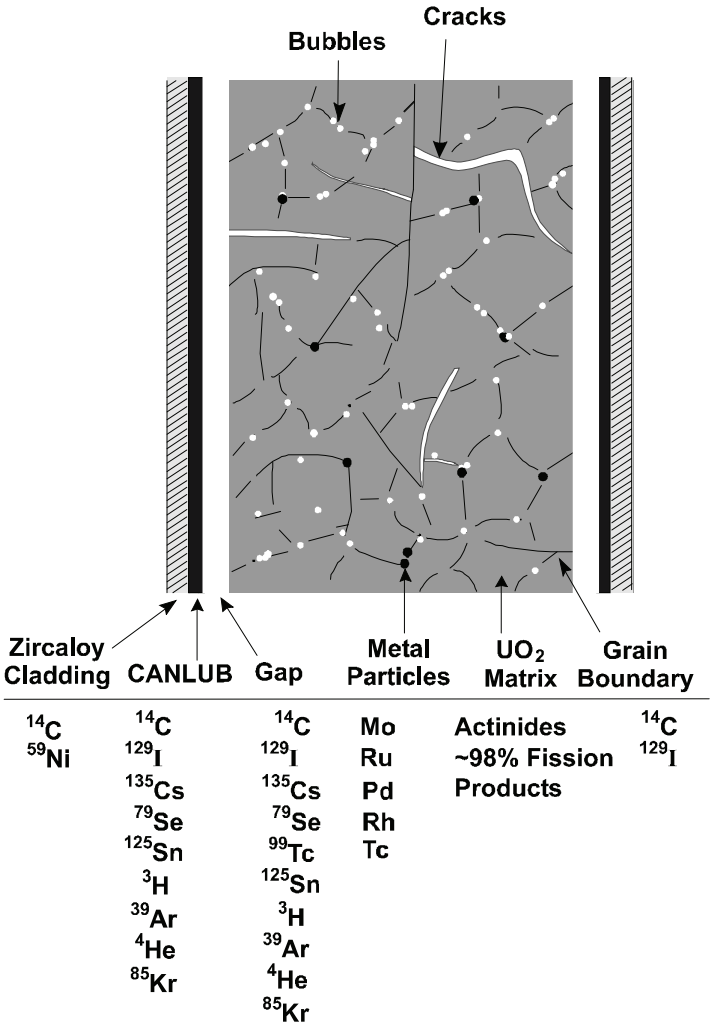

Figure 3-5: Illustrative Distribution of Some Fission Products and Actinides within a Used-Fuel Element

3.2 Radionuclide and Chemical Element Inventory

At the time of discharge the used fuel contains hundreds of different radionuclides; however, following placement in a deep geological repository only a small fraction poses a potential radiological risk to humans or the environment. The subset of radionuclides of potential concern for safety assessment is identified via a screening analysis.

The screening analysis for the groundwater-transport scenarios, described in Chapter 7, analysis identifies 31 radionuclides from the UO_2 fuel as potentially important. The gas-transport scenario, described in Chapter 8, considers C-14, Cl-36 Se-79, and I-129 as

potentially important, with C-14 releases from both the UO_2 fuel and the Zircaloy included. Parents and progeny of the screened in radionuclides are also included to ensure ingrowth is properly accounted for. In all, a total of 38 radionuclides are represented.

Table 3-2 shows the included radionuclides and their associated decay chains.

Table 3-2: Radionuclides Included in the Radiological Assessment

Fuel	
Single Nuclides	C-14, I-129, Cl-36, Cs-135, Pd-107, Se-79, Sm-147, Tc-99
Chains	
Neptunium Series	Am-241 → Np-237 → Pa-233 → U-233 → Th-229 → Ra-225 → Ac-225
Uranium Series	Pu-242 → U-238 → Th-234 → U-234 → Th-230 → Ra-226 → Rn-222 → Pb-210 → Bi-210 → Po-210
Actinium Series	Pu-239 → U-235 → Th-231 → Pa-231 → Ac-227 → Th-227 → Ra-223
Thorium Series	Pu-240 → U-236 → Th-232 → Ra-228 → Th-228 → Ra-224

At the time of discharge the used fuel also contains essentially the entire periodic table of elements from hydrogen to californium; however, only a small fraction of these could pose a non-radiological hazard to humans or to the environment. As is the case for radionuclides, the subset of chemical elements of potential concern is identified via a screening analysis.

This screening analysis is also described in Chapter 7. The analysis identifies 26 elements of potential concern arising from the fuel, where multiple isotopes of an element (i.e., U, Pb, and Ba) are considered as one element. To ensure that ingrowth is properly accounted for in the system model, an additional 33 radionuclides are also included. The analysis also shows seven elements of potential concern arising from the Zircaloy sheath, to which an additional three parent radionuclides have been added due to include ingrowth.

Table 3-3 shows the included chemical elements and their associated decay chains.

Table 3-3: List of Potentially Significant Chemically Hazardous Elements and Associated Radionuclide Decay Chains Included in the Hazardous Substance Assessment

Fuel	
Elements	Al, Cd, Ce, Co, Cr, Cu*, Hg, La, Mo, Nd, Ni, P, Pr, Sb, Se, Sm, V, Y
Chains	
Neptunium Series	Am-241 → Np-237 → Pa-233 → U-233 → Th-229 → Ra-225 → Ac-225 → Bi
Uranium Series	Pu-242 → U-238 → Th-234 → U-234 → Th-230 → Ra-226 → Rn-222 → Pb-210 → Bi-210 → Po-210 → Pb
Actinium Series	Pu-239 → U-235 → Th-231 → Pa-231 → Ac-227 → Th-227 → Ra-223 → Pb
Thorium Series	Pu-240 → U-236 → Th-232 → Ra-228 → Th-228 → Ra-224 → Pb
Misc	Sn-126 → Sb-126 → Te Sr-90 → Y-90 → Zr Cs-135 → Ba Cs-137 → Ba Pd-107 → Ag Sm-151 → Eu
Zircaloy	
Elements	Be, Cr, Cd, Sb, V
Chains	Pd-107 → Ag Sr-90 → Y-90 →Zr

Note: * Cu arising from the fuel is screened out in Chapter 7. It is included here because of the copper containers.

Note that it is the total concentration of a potentially chemically hazardous element that is important for the hazardous substance assessment. For example, the total uranium concentration in a particular biosphere medium is the sum of the concentrations of all the uranium isotopes.

Table 3-4 and Table 3-5 list all the radionuclides included in either Table 3-2 or Table 3-3 together with their half lives, their inventories at the assumed time of placement in the repository, and various uncertainties associated with the inventories. The inventories are taken from Tait and Hanna (2001); however, corrections were made to account for the difference in the bundle average and "ring sum[3]" inventories if differences exceeded +1%, as described in Gobien et al. (2013).

It should be emphasized that what is important for the safety assessment is the uncertainty in the total radionuclide inventory in a container with 360 fuel bundles which (based on the central limit theorem) would be much smaller than the uncertainly in the inventory of a single fuel bundle. Thus, it is the uncertainties in total inventory in the container that are shown in Table 3-4.

[3] "Ring sum" refers to a separate radionuclide inventory calculation performed with different burnup assumptions in the individual fuel bundle 'rings'

Uncertainty arises due to the accuracy of the ORIGEN-S calculations when compared against measurements (σ_{OR}), and due to the use of an average power rating (σ_{PR}) in the calculation of initial radionuclide inventories. The latter uncertainty is small for the radionuclides of interest except for Cs-135 (Gobien et al. 2013).

There is no need to account for the uncertainty arising from calculating the inventories at a burnup of 220 MWh/kgU because this burnup is greater than the average burnup from any of the generating stations (Wilk 2013). Thus, since inventories generally increase with burnup (Tait et al. 2000), the calculated inventories are conservative.

Validation studies (Tait et al. 1995) indicate that ORIGEN-S predictions generally agree with measured actinide and fission product inventories, with the residual uncertainty in many cases related more to the accuracy of the measurements. A comparison of measured and predicted values for a Pickering fuel bundle is shown in Table 3-6. Pickering is used because more comprehensive data are available.

More recent comparisons by SKB (2010) for PWR fuel, indicates that the ratio of measured to ORIGEN calculated inventories is 1.01 for U and Pu isotopes, 1.01 for fission products and 1.11 for actinides other than U and Pu. Again, the agreement is good and within the uncertainty of the measured data.

Further information on the derivation of the uncertainties is available in Gobien et al. (2013).

Table 3-7 and Table 3-8 list the chemical elements included in Table 3-3 together with their inventories, at the assumed time of placement in the repository, and with the various uncertainties associated with the inventories. The inventory of an element shown in Table 3-7 excludes the concentration of all short-lived isotopes of the element as well as the concentrations of the long-lived isotopes of the element shown in Table 3-4.

The inventories are from Tait and Hanna (2001). However, corrections to the inventories were made to account for the difference in the bundle average and “ring sum” inventories if differences exceeded +1%, as described in Gobien et al. (2013). Also, for Eu, the inventory includes the inventory of a short-lived precursor (Sm-151).

Table 3-4: Inventories of Radionuclides of Interest in UO_2 Fuel for 220 MWh/kgU Burnup and 30 Years Decay Time

Nuclide	Half-life* [a]	Inventory [moles/kgU initial]	σ_{OR} [%]	σ_{PR} [%]	σ_{Total} [%]
Ac-225	2.738E-02	1.662E-14	-	-	NA1
Ac-227	2.177E+01	1.573E-11	2.5	-	2.5
Am-241	4.326E+02	1.155E-03[&]	15	-	15
Bi-210	1.372E-02	5.296E-18	-	-	NA1
C-14	5.700E+03	5.60E-06	-	-	NA2
Cl-36	3.010E+05	5.42E-06	-	-	NA2
Cs-135	2.300E+06	2.675E-04	7	3	7.6
Cs-137	3.008E+01	1.287E-03	5	-	5.0
I-129	1.570E+07	4.228E-04	7	-	7.0
Np-237	2.144E+06	1.708E-04	20	-	20
Pa-231	3.276E+04	3.820E-08	2.5	-	2.5
Pa-233	7.385E-02	5.901E-12	-	-	NA1
Pb-210	2.220E+01	8.604E-15	55	-	55
Pd-107	6.500E+06	6.901E-04	7	-	7
Po-210	3.789E-01	1.463E-16	-	-	NA1
Pu-239	2.411E+04	1.123E-02	3	-	3
Pu-240	6.561E+03	5.339E-03	4	-	4.0
Pu-242	3.735E+05	4.257E-04	7	-	7.0
Ra-223	3.129E-02	2.243E-14	-	-	NA1
Ra-224	1.002E-02	1.099E-12	-	-	NA1
Ra-225	4.079E-02	2.460E-14	-	-	NA1
Ra-226	1.600E+03	2.354E-12	55	-	55
Ra-228	5.750E+00	8.370E-13	-	-	NA1
Rn-222	1.047E-02	1.541E-17	-	-	NA1
Sb-126	3.381E-02	2.462E-12	-	-	NA1
Se-79	2.950E+05	1.762E-05	7	-	7.0
Sm-147	1.060E+11	6.551E-04	7	-	7.0
Sm-151	9.000E+01	1.455E-05	7	-	7.0
Sn-126	2.300E+05	5.182E-05	7	-	7.0
Sr-90	2.879E+01	7.561E-04	4	-	4.0
Tc-99	2.111E+05	2.409E-03	10	-	10
Th-227	5.114E-02	3.620E-14	-	-	NA1
Th-228	1.912E+00	2.097E-10	-	-	NA1
Th-229	7.340E+03	4.783E-09	20	-	20

Nuclide	Half-life* [a]	Inventory [moles/kgU initial]	σ_{OR} [%]	σ_{PR} [%]	σ_{Total} [%]
Th-230	7.538E+04	1.636E-08	55	-	55
Th-231	2.911E-03	2.944E-14	-	-	NA1
Th-232	1.405E+10	2.095E-03	4	-	4
Th-234	6.598E-02	6.091E-11	-	-	NA1
U-233	1.592E+05	3.608E-05	20	-	20
U-234	2.455E+05	2.089E-04[&]	50	-	50
U-235	7.038E+08	7.238E-03	2.5	-	2.5
U-236	2.342E+07	3.501E-03	4	-	4
U-238	4.468E+09	4.125E+00	0	-	0
Y-90	7.301E-03	1.965E-07	-	-	NA1

Notes:
NA1 = Nuclide assigned a constant inventory because it has a short half-life.
NA2 = Nuclide inventory is assigned a uniform distribution. For C-14, the inventory is between 2.45×10^{-6} and 8.75×10^{-6} moles/kgU and for Cl-36 the inventory is between 9.86×10^{-7} and 9.86×10^{-6} moles/kgU. Table shows the median value, which is not from Tait et al. (2000).
NA3 = Nuclide assigned a constant inventory because it is formed by activation of impurity in the fuel, and impurity levels were assigned high values in Tait et al. (2000).
*Half-life from ENDF/B VII.1 (Chadwick et al. 2011) and converted as required using 365.25 days = 1 year.
[&]Includes inventory of short-lived precursor: Am-241 (Pu-241, 2.737E-4 mol/kgU) and U-234 (Pu-238, 2.259E-5 mol/kgU). Since the uncertainty is expressed as a percentage, it is affected by addition of the precursor inventory.

Table 3-5: Inventories of Radionuclides of Interest in Zircaloy for 220 MWh/kgU Burnup and 30 Years Decay Time

Nuclide	Half-life* [a]	Inventory [moles/kgZr initial]	σ_{OR} [%]	σ_{PR} [%]	σ_{Total} [%]
C-14	5.700E+03	1.903E-05			NA2
Pd-107	6.500E+06	6.222E-08	7	-	7.0
Sr-90	2.879E+01	4.776E-11	4	-	4.0
Y-90	7.301E-03	1.241E-14	-	-	NA1

Notes:
NA1 = Nuclide assigned a constant inventory because it has a short half-life.
NA2 = Nuclide assigned a constant inventory because it is formed by activation of impurity in Zircaloy, and impurity levels were assigned high values in Tait et al. (2000).
*Half-life from ENDF/B VII.1 (Chadwick et al. 2011) and converted as required using 365.25 days = 1 year.

Table 3-6: ORIGEN-S: Pickering Fuel Inventory Comparison

Isotope	Measured[1] (Bq/kgU)	ORIGEN-S (Bq/kgU)	Ratio (meas/calc)
Cm-244	7.12E+08 ± 15%	7.44E+08	0.96 ± 0.14
Am-241	1.86E+10 ± 20%	1.92E+10	0.97 ± 0.19
Np-237	1.00E+05 ± 20%	8.51E+05	1.17 ± 0.23
H-3	2.07E+09 ± 7%	2.23E+09	0.92 ± 0.06
Sr-90	4.86E+11 ± 4%	5.03E+11	0.97 ± 0.04
Tc-99	1.08E+08 ± 10%	1.50E+08	0.72 ± 0.07
Ru-106	8.72E+07 ± 5%	2.52E+08	0.35 ± 0.02
Sb-125	2.20E+09 ± 18%	2.56E+09	0.86 ± 0.16
I-129	2.44E+05	3.62E+05	0.67
Cs-134	4.16E+09 ± 7%	4.03E+09	1.03 ± 0.07
Cs-137	8.05E+11 ± 5%	7.88E+11	1.02 ± 0.05
Eu-154	8.14E+09 ± 5%	9.07E+09	0.90 ± 0.04
Eu-155	3.35E+09 ± 8%	3.13E+09	1.07 ± 0.09
Isotope	**Measured (g/kgU)**	**ORIGEN-S (g/kgU)**	**Ratio (meas/calc)**
U-233	< 0.01	2.22E-07	--
U-234	0.0339 ± 55%	0.0423	0.8 ± 0.44
U-235	1.64 ± 2.4%	1.64	1.00 ± 0.02
U-236	0.802 ± 3.7%	0.813	0.99 ± 0.04
U-238	983.5 ± 0.01%	983.5	1.00 ± 0.0
Pu-238	0.0058 ± 5.6%	0.0053	1.10 ± 0.06
Pu-239	2.69 ± 2.5%	2.72	0.99 ± 0.03
Pu-240	1.22 ± 37%	1.25	0.98 ± 0.04
Pu-241	0.134 ± 9%	0.142	0.95 ± 0.09
Pu-242	0.094 ± 6.8%	0.0972	0.97 ± 0.07

Notes:

From Tait et al. (1995), Pickering fuel bundle with average burnup of 221 MWh/kgU and average outer-element linear power of 43 kW/m.

[1] Analytical uncertainty expressed as a percentage.

Table 3-7: Inventories of Chemical Elements of Interest in UO_2 Fuel for 220 MWh/kgU Burnup and 30 Years Decay Time

Element	Main Source[1]	Inventory* [moles/kgU initial]	σ_{OR} [%]	σ_{PR} [%]	σ_{Total}[2] [%]
Ag	FP	3.348E-4	7	-	7.0
Al	Imp	3.702E-3	-	-	NA1
Ba	FP	4.738E-3	7	-	7.0
Bi	Imp	9.595E-5	-	-	NA1
Cd	FP	1.928E-4	7	-	7.0
Ce	FP	4.766E-3	7	-	7.0
Co	Imp	3.099E-4	-	-	NA1
Cr	Imp	9.635E-4	-	-	NA1
Cu	Imp	3.121E-4	-	-	NA1
Eu	FP	1.895E-4	6.5	-	6.5
Hg	Imp	6.719E-6	-	-	NA1
La	FP	2.459E-3	7	-	7.0
Mo	FP	9.488E-3	7	-	7.0
Nd	FP	7.562E-3	7	-	7.0
Ni	Imp	1.044E-3	-	-	NA1
P	Imp	1.935E-3	-	-	NA1
Pr	FP	2.181E-3	7	-	7.0
Pb	Imp	4.824E-4	-	-	NA1
Pr	FP	2.181E-3	7	-	7.0
Sb	FP	2.977E-5	7	-	7.0
Se	Imp	4.185E-4	-	-	NA1
Sm	FP	1.063E-3	7	-	7.0
Te	FP	1.048E-3	7	-	7.0
V	Imp	3.892E-4	-	-	NA1
Y	FP	1.327E-3	7	-	7.0
Zr	FP	1.021E-2	7	-	7.0

Notes:

*The inventories shown here exclude the concentrations of all short-lived isotopes of the element and the concentrations of the long-lived radionuclides in Table 3-4.

[1] Source of chemical element in fuel is either fission product (FP) or impurity in fuel (Imp).

[2] NA1 = Nuclide assigned a constant inventory because it is formed by activation of impurity in the fuel, and impurity levels were assigned high values in Tait et al. (2000).

Table 3-8: Inventories of Chemical Elements of Interest in Zircaloy for 220 MWh/kgU Burnup and 30 Years Decay Time

Element	Main Source[1]	Inventory [moles/kgZr initial]	σ_{OR} [%]	σ_{PR} [%]	σ_{Total} [%]
Ag	Imp	7.644E-5	-	-	NA1[2]
Be	Imp	1.111E-2	-	-	NA1[2]
Cd	Act	2.327E-5	7	-	7.0
Cr	Imp	2.495E-2	-	-	NA1[2]
Sb	Imp	1.098E-4	-	-	NA1[2]
V	Imp	1.008E-3	-	-	NA1[2]
Zr	MM	1.064E+1	-	-	NA2[3]

Notes:

[1] Source of chemical element in Zircaloy is either an activation product (Act) or impurity in Zircaloy (Imp) or the matrix material (MM).

[2] NA1 = Nuclide assigned a constant inventory because it is formed by activation of impurity in the fuel, and impurity levels were assigned high values in Tait et al. (2000).

[2] NA2 = Zr assigned a constant inventory because the inventory of the matrix material is well known.

3.3 References for Chapter 3

Chadwick, M.B., M. Herman, P. Obložinský, M.E. Dunn, Y. Danon, A.C. Kahler, D.L. Smith, B. Pritychenko, G. Arbanas, R. Arcilla, R. Brewer, D.A. Brown, R. Capote, A.D. Carlson, Y.S. Cho, H. Derrien, K. Guber, G.M. Hale, S. Hoblit, S. Holloway, T.D. Johnson, T. Kawano, B.C. Kiedrowski, H. Kim, S. Kunieda, N.M. Larson, L. Leal, J.P. Lestone, R.C. Little, E.A. McCutchan, R.E. MacFarlane, M. MacInnes, C.M. Mattoon, R.D. McKnight, S.F. Mughabghab, G.P.A. Nobre, G. Palmiotti, A. Palumbo, M.T. Pigni, V.G. Pronyaev, R.O. Sayer, A.A. Sonzogni, N.C. Summers, P. Talou, I.J. Thompson, A. Trkov, R.L. Vogt, S.C. van der Marck, A. Wallner, M.C. White, D. Wiarda, P.G. Young. 2011. ENDF/B-VII.1 Nuclear data for science and technology: Cross section, covariances, fission product yields, and decay data. *Nuclear Data Sheets*: 112-12, 2887-2996 (2011).

Freire-Canosa, J. 2011. Used Fuel Integrity Program: Summary Report. Nuclear Waste Management Organization Report NWMO TR-2011-04. Toronto, Canada.

Garamszeghy, M. 2012. Nuclear Fuel Waste Projections in Canada - 2012 Update. Nuclear Waste Management Organization Report NWMO TR-2012-13. Toronto, Canada.

Gobien, M., F. Garisto, E. Kremer and C. Medri. 2013. Fifth Case Study: Reference Data and Codes. Nuclear Waste Management Organization Report NWMO TR-2013-05. Toronto, Canada.

Hastings, I.J. 1982. Structures in Irradiated UO_2 Fuel from Canadian Reactors. Atomic Energy of Canada Limited Report AECL-MISC-249. Chalk River, Canada.

Kleykamp, H. 1985. The chemical state of the fission products in oxide fuels. Journal of Nuclear Materials 131, 221-246.

Novak, J. and I.J. Hastings. 1991. Ontario Hydro Experience with Extended Burnup Power Reactor Fuel. Atomic Energy of Canada Limited Report AECL-10388. Chalk River, Canada.

SKB. 2010. Spent nuclear fuel for disposal in the KBS-3 repository. Swedish Nuclear Fuel and Waste Management Company Report SKB TR-10-13. Stockholm, Sweden.

Tait, J.C., I.C. Gauld and A.H. Kerr. 1995. Validation of the ORIGEN-S code for predicting radionuclide inventories in used CANDU fuel. Journal of Nuclear Materials 223, 109-121.

Tait, J.C. and S. Hanna. 2001. Characteristics and radionuclide inventories of used fuel from OPG nuclear generating stations, Volume 3 - Radionuclide inventory data. Ontario Power Generation Report 06819-REP-01200-10029-R00. Toronto, Canada.

Tait, J.C., H. Roman and C.A. Morrison. 2000. Characteristics and Radionuclide Inventories of Used Fuel from OPG Nuclear Generating Stations, Volumes 1 and 2. Ontario Power Generation Report 06819-REP-01200-10029. Toronto, Canada.

Truant, P.T. 1983. CANDU Fuel Performance: Power Reactor Experience. Atomic Energy of Canada Limited Report AECL-MISC-250, Rev. 1. Chalk River, Canada.

Wilk, L. 2013. CANDU Fuel Burnup and Power Rating – 2012 Update. Nuclear Waste Management Organization Report NWMO-TR-2013-02. Toronto, Canada.

THIS PAGE HAS BEEN LEFT BLANK INTENTIONALLY

4. REPOSITORY FACILITY – CONCEPTUAL DESIGN

4.1 General Description

The APM facility is a self-contained complex that includes an underground repository for used CANDU fuel and a number of surface facilities designed to support the construction and operation of the repository. The primary function of the surface facilities is to receive used fuel that is shipped from reactor-site storage facilities, place it in durable used fuel containers and transfer the containers to the underground repository. The reference used fuel container is designed with a corrosion-resistant copper barrier and an inner supporting steel vessel to provide long-term containment of the fuel in the repository (SNC Lavalin 2011).

Since a repository site has not been selected, the assumptions made for development of the site model reflect the properties of typical sedimentary rock found in Canada. Therefore, a generic repository design is described here for the purpose of preparing an illustrative postclosure safety assessment for a hypothetical APM facility in sedimentary rock. Two key safety concepts on which the repository design is based are the multiple barrier system for containment of the fuel, and passive safety. In this case, passive safety means that once the operational phase is complete and the repository is backfilled and sealed, no further actions will be required to ensure its safety.

For the purpose of this study, the repository is assumed to be constructed in sedimentary rock at a depth of 500 m. In the repository, the used fuel containers will be surrounded by an engineered barrier consisting of clay-based sealing materials that will provide protection against mechanical, chemical and biological agents that could cause container damage. The function of the repository engineered barriers also includes creating both a chemical and physical environment that would limit the mobility of contaminants. The used fuel container, the sealing systems surrounding the container and the rock mass in which the repository is constructed constitute a multiple barrier system that is capable of containing and isolating the used fuel indefinitely.

The underground repository consists of several panels of used fuel container placement rooms, which are connected to the surface via a network of access tunnels and three vertical shafts. The containers are placed horizontally, supported by a compacted bentonite pedestal, along the axis of the placement room.

An illustration of an APM facility in sedimentary rock is shown in Figure 4-1.

Monitoring systems for verification of safety performance are provided as part of the repository system design. Retrievability of the fuel containers is another design feature of the APM repository. These two capabilities of the repository design are discussed further by SNC Lavalin (2011) and Villagran (2012).

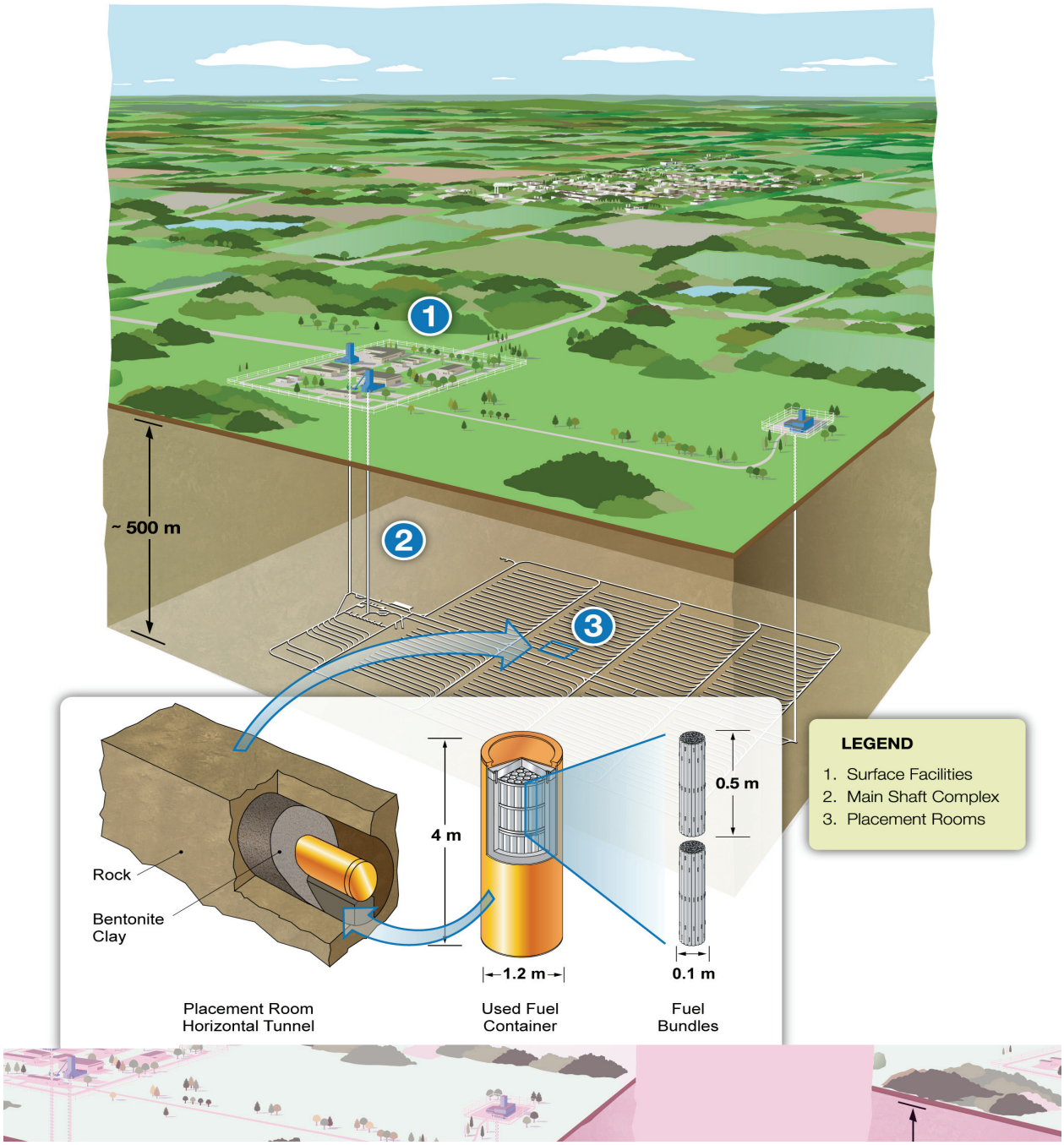

Figure 4-1: Illustration of an APM Facility in Sedimentary Rock

4.2 Surface Facilities

The APM facility requires a dedicated surface area of about 600 m by 550 m for the surface buildings and about 100 m by 100 m for the ventilation exhaust shaft located about 2 kilometres from the main facility. The APM facility also requires an off-site storage area of about 700 m by 700 m for the excavated rock; its location would be selected in consultation with the community and surrounding region. The surface water run-off from the excavated rock will be monitored and appropriate effluent control procedures will be implemented based on the monitoring results.

The site layout is shown in Figure 4-2; individual buildings and other surface facilities are listed Table 4-1. The site is surrounded by a perimeter fence; and the facilities within this perimeter are arranged into two areas:

1. The Protected Area, which is a high-security zone; and
2. The Balance of Site, a zone which includes facilities that do not require high security.

The main facilities included in the Protected Area are the Used Fuel Packaging Plant (UFPP), the main shaft and service shaft buildings as well as the auxiliary building, quality control offices, laboratory, radioactive waste handling facilities, switchyard, transformer area and powerhouse. All activities pertaining to handling and storage of used nuclear fuel are conducted in the UFPP. A detailed description of the UFPP and its operation is given in Section 4.4.

The Balance of Site zone includes the administration building, the fire hall, the ventilation shaft building, as well as ancillary facilities such as the cafeteria, garage, warehouse, water and sewage treatment plants, and helicopter pad. Fuel and water storage tanks and an air compressor building are also found in the Balance of Site, as well as the aggregate plant, concrete batch plant and the sealing materials compaction plant.

The aggregate plant will produce material for the concrete batching plant and sealing materials compaction plant. The concrete batching plant will produce the concrete mixes required for specific functions in the repository, including the Low-Heat, High-Performance Concrete (LHHPC) required for the bulkheads used for closing the filled container placement rooms and as components of other repository seals. At the sealing materials compaction plant, raw materials from the aggregate plant and externally sourced lake clay and bentonite will be mixed to produce dense backfill blocks, light backfill, compacted bentonite blocks and gap-fill material required for used fuel container placement and for sealing of the placement rooms.

A number of other support buildings and structures including offices, laboratory facilities and the common services required in a self-sufficient industrial site are also included in the site; a complete list is given in Table 4-1.

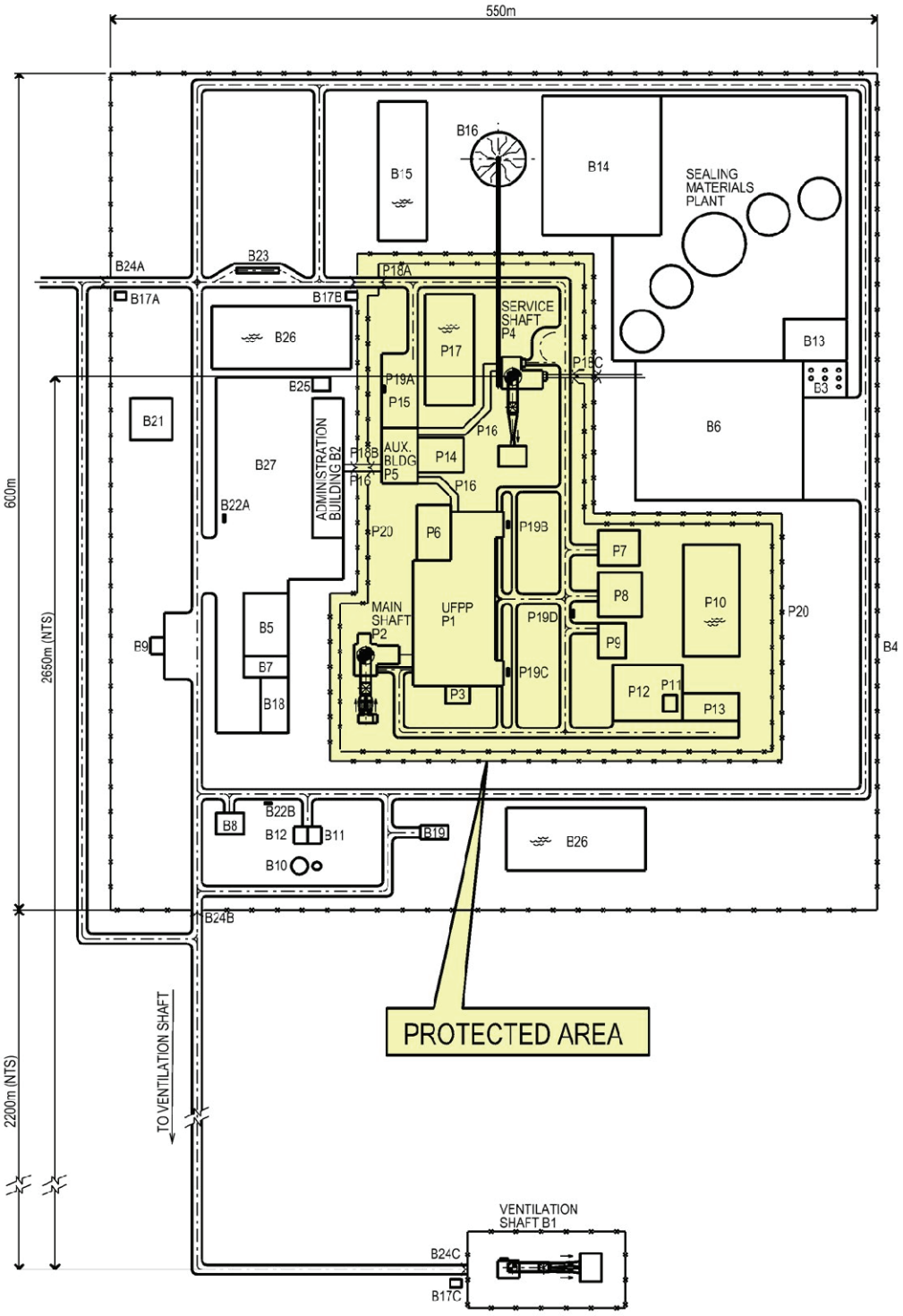

Figure 4-2: APM Surface Facilities Layout

Table 4-1: APM Facility Number and Description

Area	Protected Area	Area	Balance of Site
P1	Used Fuel Packaging Plant	B1	Ventilation Shaft Complex
P2	Main Shaft Complex	B2	Administration Building including Firehall and Cafeteria
P3	Stack	B3	Sealing Material Storage Bins
P4	Service Shaft Complex	B4	Perimeter Fence
P5	Auxiliary Building	B5	Garage
P6	Active Solid Waste Handling Facility	B6	Sealing Materials Compaction Plant
P7	Waste Management Area	B7	Warehouse and Hazardous Materials Storage Building
P8	Active Liquid Waste Treatment Building	B8	Air Compressor Building
P9	Low-Level Liquid Waste Storage Area	B9	Fuel Storage Tanks
P10	Stormwater Retention Pond	B10	Water Storage Tanks
P11	Switchyard	B11	Water Treatment Plant
P12	Transformer Area	B12	Pump House
P13	Powerhouse	B13	Concrete Batch Plant
P14	Quality Control Offices and Laboratory	B14	Aggregate (Rock Crushing) Plant
P15	Parking Area	B15	Process Water Settling Pond
P16	Covered Corridor / Pedestrian Routes	B16	Waste Rock Stockpile
P17	Mine Dewatering Settling Pond	B17	Guardhouse
P18	Security Checkpoint	B18	Storage Yard
P19	Bus Shelters	B19	Sewage Treatment Plant
P20	Double Security Fence	B20	Not Used
		B21	Helicopter Pad
		B22	Bus Shelters
		B23	Weigh Scale
		B24	Security Checkpoints
		B25	Security Monitoring Room
		B26	Storm water Retention Ponds
		B27	Parking Area

4.3 Used Fuel Container

The reference used fuel container design used for this study is the IV-25 copper container. It consists essentially of two vessels: an inner carbon-steel vessel that provides the required mechanical strength and outer copper vessel that provides a durable corrosion barrier. The capacity of the IV-25 copper container is 360 used CANDU fuel bundles with a mass of 8,640 kg. The inner vessel wall thickness is 102.5 mm and it is designed to sustain a maximum external isotropic pressure of 45 MPa, which is a conservative estimate of the maximum load the container would experience in the repository during a glaciation cycle, as a result of a 3 km thick ice sheet above the repository site.

The IV-25 container has been designed with a 25 mm thick outer copper shell for corrosion, fabrication and handling purposes. Under repository conditions, corrosion of the copper barrier is predicted to be less than 2 mm over a period of one million years (Kwong 2011), which is approximately the time required for the radioactivity of the used CANDU fuel to decay to levels comparable to those of natural uranium deposits.

The used fuel bundles are arranged inside the container in six layers of 60 bundles each. They are loaded into the container in three baskets holding two layers of 60 fuel bundles. The container and basket are illustrated in Figure 4-3. The design parameters of the copper and the steel vessels are given in Table 4-2 and Table 4-3, respectively. The total mass of a loaded used fuel container is approximately 26,700 kg.

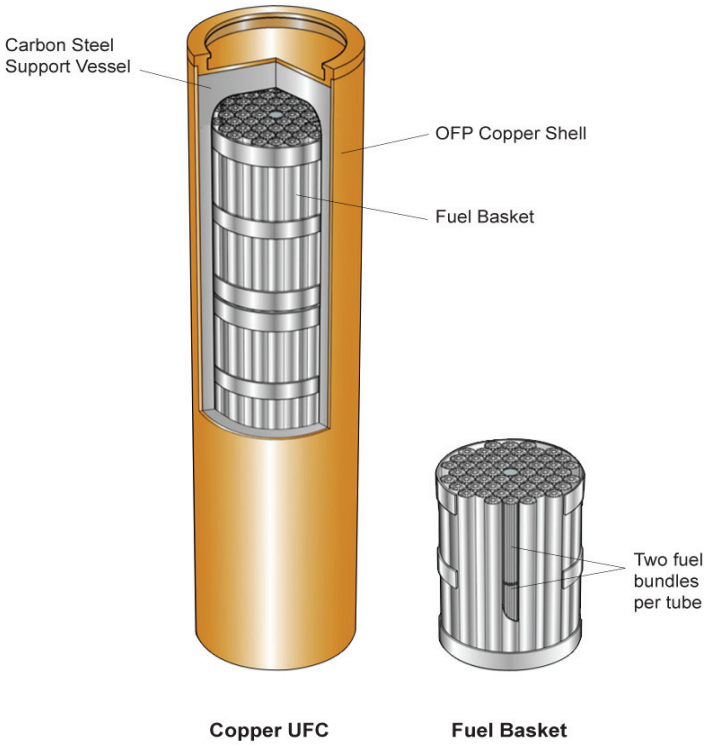

Figure 4-3: Copper Used-fuel Container and Fuel Basket

Table 4-2: Reference Copper Vessel Parameters

IV-25 Outer Copper Vessel	
Material	Oxygen-free, phosphorus-doped, high purity copper
Height	3,842 mm
Outside diameter	1,247 mm
Thickness (minimum)	25 mm
Mass of copper vessel	4,170 kg

Table 4-3: Reference Steel Vessel Parameters

IV-25 Inner Steel Vessel	
Material	ASTM[1] A516 Gr 70 steel
Height	3,700 mm
Outside diameter	1,195 mm
Thickness (minimum)	102.5 mm
Mass of steel vessel	12,650 kg
Mass of 3 fuel baskets	1,240 kg

4.4 Used Fuel Packaging Plant

The Used Fuel Packaging Plant (UFPP) is a multi-storey building designed to receive the used fuel shipped from interim storage facilities, transfer the fuel bundles into long-lived used fuel containers, seal and inspect the containers for subsequent transfer to the underground repository. The UFPP concrete structure contains a number of cells where specialized operations requiring shielding and containment capability are conducted. The plant conceptual design is illustrated in a cross-section and two layout plans inserted towards the end of this section. These drawings are useful to visualize both fuel handling operations, and the loading and processing of used fuel containers.

[1] American Society for Testing and Materials.

The used fuel containers are assumed to be manufactured at a dedicated plant, separate from the APM facility and shipped to the UFPP, where they will be received at a dedicated receiving hall for empty used fuel containers.

The used nuclear fuel is assumed to be shipped from interim storage facilities at the reactor sites in a used fuel transportation package (UFTP). The reference UFTP has a capacity of 192 fuel bundles, held in two used fuel storage modules containing 96 bundles each (NWMO 2013). The casks are received at the dedicated UFTP receiving and shipping hall. The process for transferring the used fuel from transport casks and placing it into used fuel containers consists of several major steps:

1. Receiving, unloading, decontamination and return of the UFTP;
2. Moving the received used fuel storage modules to the module handling cell and then to the fuel handling cell or, alternatively, placing them in a module storage pool;
3. Receiving and preparing new used fuel containers for loading;
4. Transferring the used fuel bundles from fuel storage modules to used fuel baskets;
5. Loading the fuel baskets into new used fuel containers;
6. Sealing and machining the container closure seal;
7. Inspecting the quality of the container closure seal; and
8. Placing used fuel container in a shielded transfer cask for transfer to the underground repository.

These operations and the associated features of the UFPP are described in the following sub-sections of this report.

4.4.1 Transport Cask Receiving and Unloading

The transport cask receiving and shipping hall is a dedicated area for transport cask handling and temporary storage provided with an overhead crane, which is initially used to unload the cask from the transport vehicle. Subsequently the transport cask impact limiter is removed and the cask is placed on a transfer pallet, which will move the cask along one of two processing lines. These two processing lines are identical and allow parallel unloading of casks and transfer of the used fuel storage modules either directly to the fuel handling cell or into a wet storage pool.

Transfer pallets that move on rails are used to move the transport casks from the cask receiving and shipping hall to a cask vent cell, and then to a docking position below the module handling cell (Figure 4-10 through to Figure 4-12). The transfer pallets are equipped with a scissors lift that enables the cask to be raised and docked at the module handling cell port.

The cask vent cell permits safe removal of the lid bolts and venting of the transport casks in a containment space. The vent cells are used also during dispatch of empty casks for replacing and fastening lid bolts, pressure testing lid seals and monitoring the cask surface for contamination. If necessary the transport casks can be decontaminated at the cask vent cell.

4.4.2 Module Handling Cells

From the vent cell the transport cask is moved to a cask docking cell, where it is connected to one of the two (parallel) module handling cells. Once docked, the cask lid is removed and

placed on the cell floor. The module handling cells are equipped with lead glass windows and remotely-operated manipulators. They provide the required radiation shielding and containment to safely unload the fuel storage modules from the transport cask. An overhead crane is used in each module handling cell for lifting and transferring modules between different positions in the cell.

A module drying booth is included in the fuel processing line to permit drying of the used fuel before it is transferred to the fuel handling cell, where the fuel is placed into used fuel baskets. Alternatively, a fuel storage module in either of the two module handling cells can be moved into a module storage pool for interim storage before processing. The module storage pool provides buffer storage so that the fuel transfer and container loading operations can proceed without interruption.

4.4.3 Empty Used Fuel Container Receiving

Receiving and storage of new, empty used fuel containers takes place in a dedicated receiving hall located at ground floor level that includes storage positions for 40 empty used fuel containers and 126 empty fuel baskets. The receiving hall has a dedicated truck bay for unloading the new used fuel containers arriving at the UFPP.

The hall is equipped with a 30 tonne crane and a used fuel container preparation platform. The platform contains two parallel positions for inspection, installation of used fuel containers into sleeves, required to load the used fuel container into a shielded frame. Adjacent to the preparation platform are eight storage positions for sleeves, eight positions for empty baskets and four positions for pallets with empty used fuel containers in sleeves. The pallets are moved within the hall using an air-cushion transporter. Three new used fuel baskets are placed inside each fuel container prior to placing it in its docking position under the Fuel Handling Cell port.

4.4.4 Used Fuel Container Transport within the Plant

Both empty and full used fuel containers are moved in a Shielded Frame consisting essentially of a steel frame holding two telescopic, cylindrical shields vertically mounted on a steel platform. The bottom shield section can be raised and lowered by screw jacks, enabling a used fuel container to be raised and docked at the processing stations docking ports.

The top section is equipped with a gamma gate and is designed for airtight docking to the container ports at the used fuel container loading and processing stations. The shielded frame provides the required radiation shielding and effective isolation of the Fuel Handling Cell and the container processing stations from the used fuel container transfer area.

The shielded frames are moved between stations using an air-cushion transporter. The air-cushion transporter is equipped with steering wheels that remain in contact with the floor while the transporter is in the raised position, and can be controlled both manually and remotely. This technology is routinely used in industry as a safe and efficient means of moving heavy equipment. A shielded frame on an air-cushion transporter being used at SKB's Canister Laboratory in Sweden is shown in Figure 4-4.

Figure 4-4: Shielded Frame and Air-cushion Transporter

Using air-cushion technology for moving the shielded frames allows the containers to be transported independently of each other and allows simultaneous, independent operation of all the processing stations. Other operational advantages of this used fuel container transport method include easy maintenance and faster recovery from equipment failure, minimizing the risk of production stops.

4.4.5 Fuel Handling Operations

The fuel handling cell is a shielded containment cell used for transferring used fuel bundles from storage modules into fuel baskets and for loading the filled fuel baskets into used fuel containers. To fulfill these tasks the cell is equipped with three fuel handling machines, lead glass windows, remote manipulators and vacuum cleaners. All equipment in the fuel handling cell is remotely operated. To enable loading of filled baskets into a container, the fuel handling cell has a docking port that connects it to the used fuel container transfer area.

During the fuel transfer operation from a module to a basket, the fuel bundle serial number is recorded for safeguard purposes. Damaged bundles can be placed in cans and/or loaded into baskets specially designed to accommodate damaged fuel.

The cell is also equipped with a crane for lifting used fuel modules and baskets. Within the cell, there are four positions for the temporary storage of modules, and one position for parking the containment door and inner vessel lid. The cell also has a dedicated area for the temporary storage of up to 12 filled or empty baskets. In the floor of the fuel handling cell, there is a port with a gamma gate leading to a waste management facility, which includes provisions for the decontamination and compaction of empty fuel storage modules.

4.4.6 Used Fuel Container Processing

Once three fuel baskets are loaded into the used fuel container, the container inner lid is bolted on and the container is moved to other processing stations where a sequence of operations takes place to seal and test the container prior to its transfer to the underground repository. These operations, which take place at four separate processing stations, include backfilling the container with an inert gas, welding of the outer copper lid, machining the weld surface and non-destructive testing (NDT) of the weld. These processing stations are described below.

4.4.6.1 Inerting Station

The inerting station is a radiation shielded cell that contains provisions for remotely bolting the inner vessel lid to the inner steel vessel. The station also houses equipment for removing the air contained in the inner vessel and backfilling the volume with an inert gas. This process is done via a valve in the inner vessel lid that can also be used for testing the leak-tightness of the lid. Containers are docked to the station in the same manner as described for the fuel handling cell. The inerting station is also equipped with a hatch and a crane for importing and moving container lids and any required equipment. Figure 4-5 shows a conceptual illustration of the inerting station.

After its inner volume is backfilled with an inert gas the container is moved to the welding station, illustrated in Figure 4-6, which has the required equipment for placing the copper lid on the container and welding it to the copper shell.

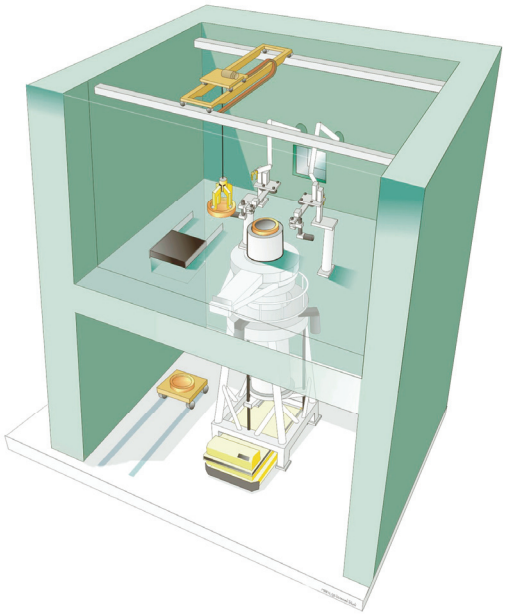

Figure 4-5: Inerting Station

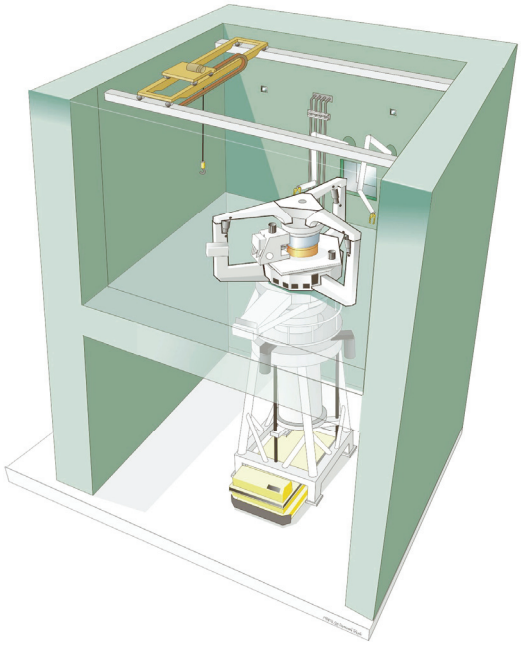

Figure 4-6: Welding Station

4.4.6.2 Welding Station

The selected method for welding the container copper lid to the container is Friction-Stir Welding (FSW). This method was originally developed for various industrial applications by The Welding Institute (TWI) in the United Kingdom, and adapted to this specific use by SKB. The process essentially consists of inserting a rotating metal tool in the lid-body joint at a perpendicular angle to the container surface and moving the tool along the circumference of the joint (Figure 4-7). The rotation of the welding tool around its own axis generates heat that effectively joins the lid and body of the container without melting of the metal. To execute this operation the container is held in a fixed position while the welding head assembly rotates around the container axis. Non-destructive testing (NDT) methods will be used to examine and verify the quality of the welds.

FSW has been extensively tested at SKB's Canister Laboratory and selected as the reference welding method for the Swedish spent fuel canisters after a thorough comparison with Electron-Beam Welding (EBW). FSW was found to be a more reliable process resulting in more uniform weld quality, and the properties of the resulting weld material were very close to those of the original OFP copper material. The FSW development program and the assessment results are documented in SKB 2007 and SKB 2008.

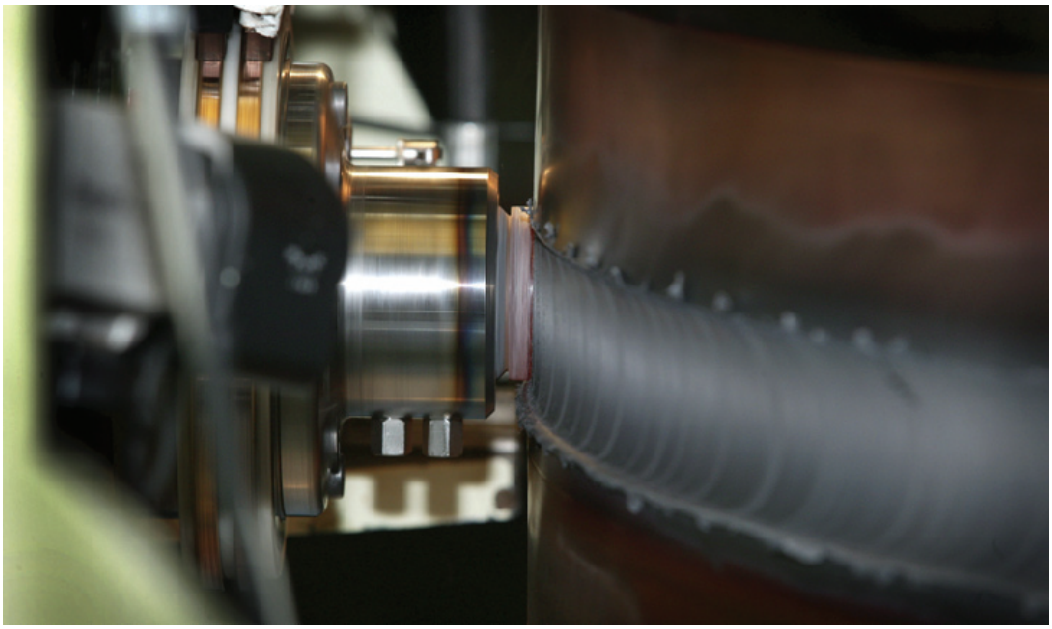

Figure 4-7: Friction Stir Welding of a Copper Lid

4.4.6.3 Machining and NDT Stations

Following welding of the copper lid, the used fuel container is moved to a station where the weld surface is machined to achieve a finish similar to that of the rest of the container surface. This is required to ensure that the weld surface has a corrosion behaviour consistent with the rest of the copper shell as well as to facilitate non-destructive testing of the weld.

During machining, the equipment is rotated and the used fuel container is held in a fixed position (see Figure 4-8). The docking arrangements in the machining station are similar to those in the welding station (see Figure 4-9). After this operation the container is moved to the non-destructive testing station, which contains equipment to conduct a visual examination of the weld plus two other independent NDT examinations using different testing methods. Two methods being considered are radiography (tomography) and ultrasonic testing. High-energy X-ray sources with very small focal spots and fast detectors with good time and spatial resolution allow the construction of good 3-D images in practical times. These weld examination methods are currently being assessed by Posiva (Finland) and SKB (Sweden), whose spent fuel container designs include a thick copper shell as corrosion barrier.

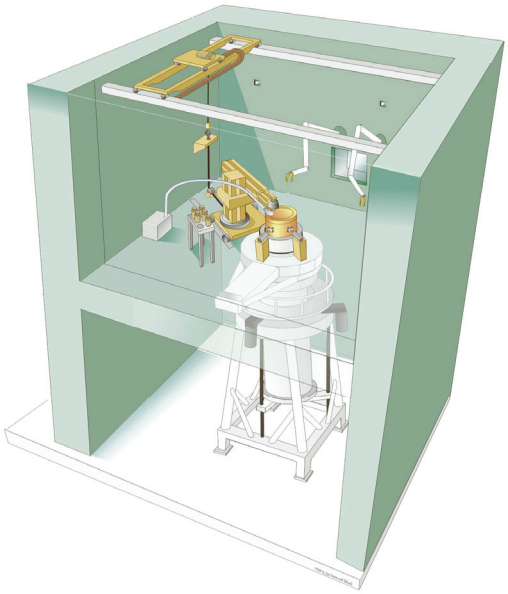

Figure 4-8: Machining Station

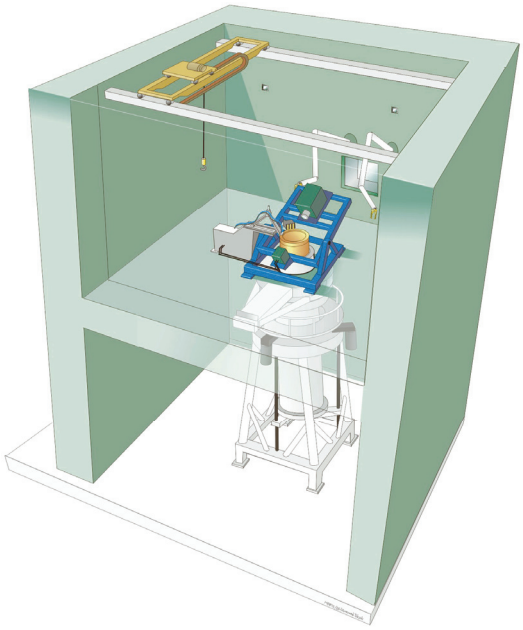

Figure 4-9: Non-destructive Testing Station

Both the stereoscopic radiography and ultrasound testing methods appear to provide satisfactory results (Sandlin 2010a, 2010b, 2010c). The stereographic radiography method has some limitations for detection of thin, planar defects; in this case ultrasonic testing is used to overcome the radiographic method's limitations. Further tests on a larger sample of welds will be needed to achieve the required level of precision. Both SKB and Posiva are continuing work in the testing of full-scale container welds (Pitkanen 2010).

For design (logistics) purposes, it is assumed that one out of 100 containers are found to not meet the specified weld quality requirements during non-destructive testing in the UFPP (SNC Lavalin 2011). The handling of defective containers is outlined below.

For postclosure safety assessment, it is assumed that one out of 5,000 containers placed in the repository have undetected through-wall defects. Effectively, this requires that both a substantive defect exists and that it is not detected by three NDT examinations using different methods. This rate is based on a review of failure statistics for other nuclear components (Maak et al. 2001). The assumed undetected weld defect rate is considered to be conservative for safety assessment purposes, although a lower probability of undetected defects could likely be achieved. The achievable failure rate would need to be confirmed by studies and testing of prototype containers.

Recently, an International Review Team was established by the Nuclear Energy Agency (NEA) to review SKB's postclosure safety case for a used fuel repository in Sweden (NEA 2012). The review was conducted by the NEA Secretariat on behalf of the Swedish Government. The International Review Team reviewed the methods developed by SKB for non-destructive testing of the container and the weld, and concluded that those methods have been verified to be able to detect inconsistencies and failures below the design limits of the safety case.

4.4.6.4 Handling of Defective Containers

Upon detecting a defect in a sealed used fuel container, the container processing at the UFPP is stopped and two separate actions are taken:

1. The cause for the weld defects is investigated and resolved before loading and processing of new containers is allowed to proceed; and
2. Depending on the nature of the defect, the defective container is either repaired and re-inspected or the defective container is opened (copper shell cut open only), the loaded steel core is retrieved and put into a new copper shell, which is then welded and inspected. The original (defective) copper shell is decontaminated and returned to the container factory for recycling of the materials.

To implement this second action, the container with the defective weld is moved from the NDT station back to the machining station where the container weld is cut. Subsequently the copper lid is removed and the container is docked at the module handling cell where the three fuel baskets are extracted from the container, then both the lid and the container body are decontaminated and returned to the container factory for recycling.

After the cause for the weld defect is identified and the problem corrected, used fuel container processing is allowed to resume. As data is acquired through both development and

implementation of the weld examination process, more sophisticated methods can be used to improve the statistics of the NDT data (Holmberg and Kuusela 2011).

4.4.7 Filled Used Fuel Container Storage Cell

At the end of the used fuel container processing area opposite to the module handling cell there is a shielded area where full used fuel containers can be monitored and placed in temporary storage. This cell has 40 storage positions and is located above the container transfer area; it is equipped with four ports and a 30 tonne overhead crane capable of handling both empty and full used fuel containers.

Containers that have been successfully loaded, welded and inspected are then brought to an entrance port dedicated to the import/export of full containers. After a container is brought into the storage area it is either placed in a storage spot or monitored, decontaminated if required, and then transferred to the filled container dispatch cell. Containers requiring decontamination can be lowered using the overhead crane into a decontamination cell located below the floor level of the storage area.

4.4.8 Used Fuel Container Dispatch Hall

Adjacent to the loaded used fuel container storage cell is a dispatch hall, where the filled used fuel containers are placed into a shielded transfer cask for transfer to the repository. In the dispatch hall there is an airlock for the transfer casks arriving and departing on a rail wagon.

The used fuel container dispatch hall is equipped with an 80 tonne overhead crane and a working platform for inspection and cask preparation operations. The hall is also equipped with an air-cushion transporter and pallet for the transfer of a cask between the working platform and the filled used fuel container dispatch hall (see Figure 4-10 and Figure 4-12).

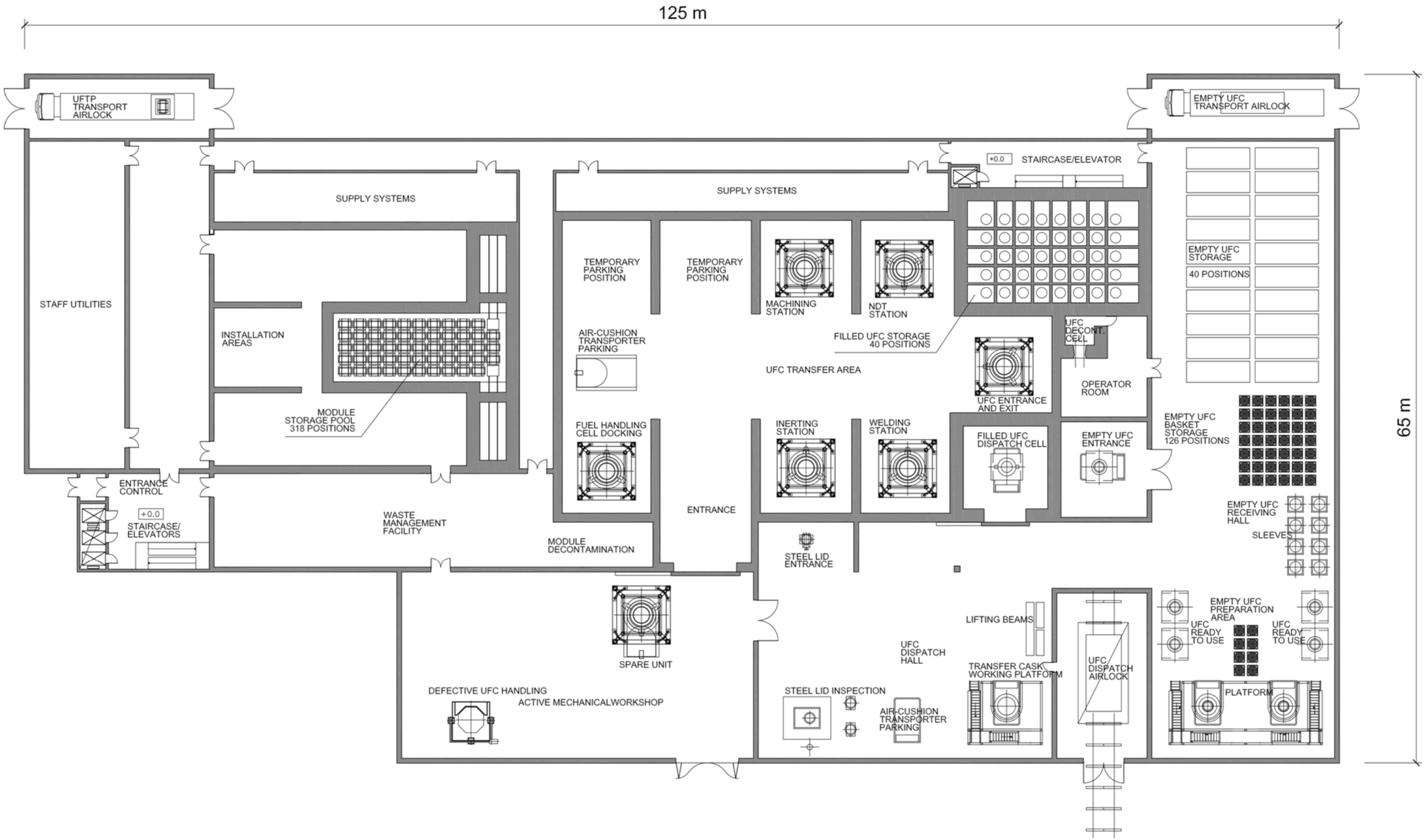

Figure 4-10: Used Fuel Packaging Plant – Container Transfer Level

THIS PAGE HAS BEEN LEFT BLANK INTENTIONALLY

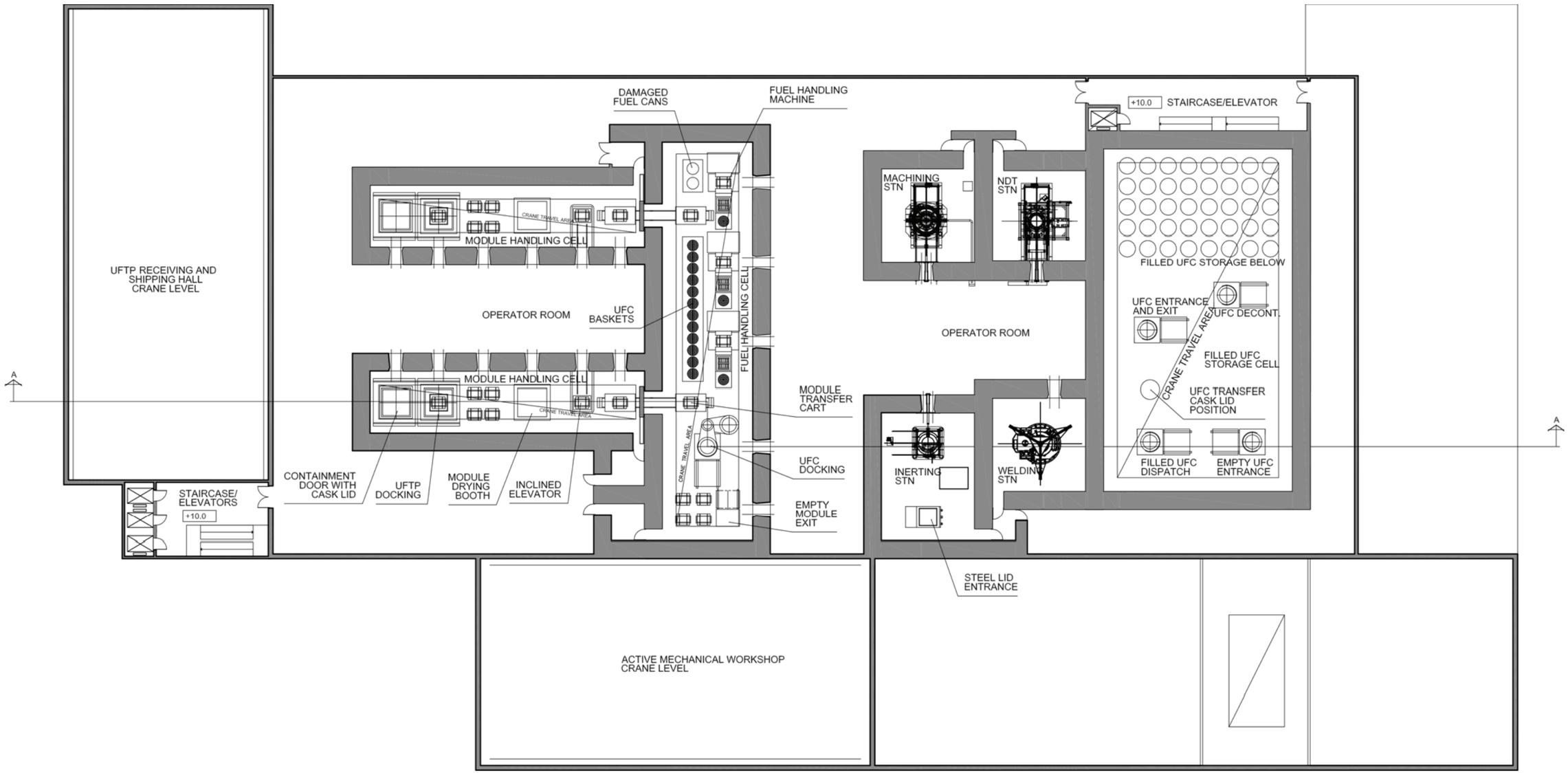

Figure 4-11: Used Fuel Packaging Plant – Operation Level

THIS PAGE HAS BEEN LEFT BLANK INTENTIONALLY

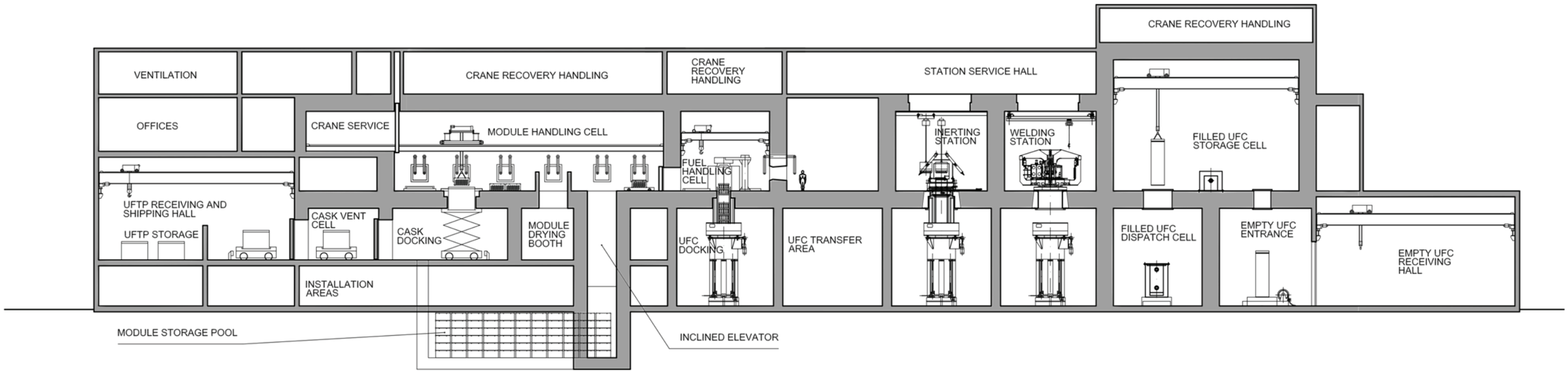

Figure 4-12: Used Fuel Packaging Plant – Cross-Section

THIS PAGE HAS BEEN LEFT BLANK INTENTIONALLY

4.5 Seals and Sealing Materials

4.5.1 General Description

The engineered barriers system concept presented in this report is based on previous Canadian and international studies. This concept uses a highly compacted bentonite (HCB) pedestal to support the used fuel container in its assigned position and bentonite pellets, placed by pneumatic methods, to fill all the remaining voids in the container placement room.

After a placement room has been filled, it will be closed off by means of a Low-Heat High-Performance Concrete (LHHPC) bulkhead. The concrete bulkhead will counteract the swelling pressure of the bentonite components and keep the tunnel backfill materials in their intended position. The room closure would also provide physical isolation of the filled container placement rooms from the ongoing operations in the rest of the repository.

The use of compacted bentonite blocks and in-situ compacted bentonite in tunnel and shaft sealing applications has been demonstrated during the past several years in various repository programs (Dixon et al. 2009, 2012 and Pusch et al. 2004). Research is currently underway on the manufacturing and installation methods of bentonite pellets in order to optimize both the as-placed and final density of the material when used as backfill in horizontal tunnels (Kim et al. 2012).

Other sealing materials of potential use in the repository include grouts that may be used to seal possible rock fractures or any areas of higher rock permeability that may intersect tunnels, and compacted bentonite blocks that may be used as a component of placement room closure seals or shaft seals. Concrete may also be used as a component of repository seals.

After the repository operational period, during decommissioning, the access tunnels and shafts also would be backfilled and sealed. Seals will be required at locations where tunnels or shafts intersect hydraulically active regions in the rock and also along the shafts, to interrupt potential transport paths to the surface.

Shaft seals designs would use durable, well understood materials, and proven placement methodologies. The shaft seals would likely consist of multiple components placed in series that may include a column of in-situ compacted bentonite/sand mixture, or pre-compacted bentonite blocks, and/or an asphalt column. The intent will be to suit the configuration and rock characteristics of the geological layers intersected by the shaft and provide redundant, low permeability sealing components to prevent water movement. Concrete bulkheads could be used to provide structural support and confinement to the column of shaft sealing materials (Dixon et al. 2009, 2012).

Siting, construction, and operation of a repository would require the drilling of exploratory and monitoring boreholes, including those drilled from the surface as well as boreholes drilled from tunnels and shafts into the adjacent rock. As part of repository closure, these boreholes will eventually be decommissioned and sealed. Composite seals made of similar materials as those used for the sealing of tunnels and shafts would be used for this purpose.

4.5.2 Placement Room Backfill Materials

The materials used in the container placement room consist of a highly-compacted bentonite (HCB) pedestal designed to support the used fuel container, and bentonite pellets, which will be pneumatically placed to fill the remaining spaces surrounding the containers. Both the pedestal and the pelletized backfill are made of 100% bentonite and have properties as described in Dixon et al. (2009, 2012). The main mineral phase in bentonite is montmorillonite, a smectitic clay mineral that has expandable layers when allowed access to free water, as well as a high cation-exchange capacity. As a consequence, bentonite can significantly increase its original volume when it becomes in contact with water. When compacted bentonite placed in a confined space comes in contact with water it will incorporate water and develop a substantial swelling pressure. This makes it an excellent material to seal fractures and produce tight contacts with interfacing materials. Bentonite-based materials also have the advantage of having a very low permeability, reducing advective transport, and, when placed at high density, bentonite also has the capability of limiting microbial activity. For the purposes of this design it is assumed that the pneumatically placed bentonite pellets backfill will achieve the required density to inhibit bacterial life (Kim et al. 2012).

4.5.3 Placement Room Configuration

The placement rooms are essentially circular cross-section tunnels 2.5 m in diameter. The used fuel containers are positioned horizontally, supported by the HCB pedestal, in a coaxial configuration with the placement tunnel. The container configuration in the tunnel is shown in Figure 4-13.

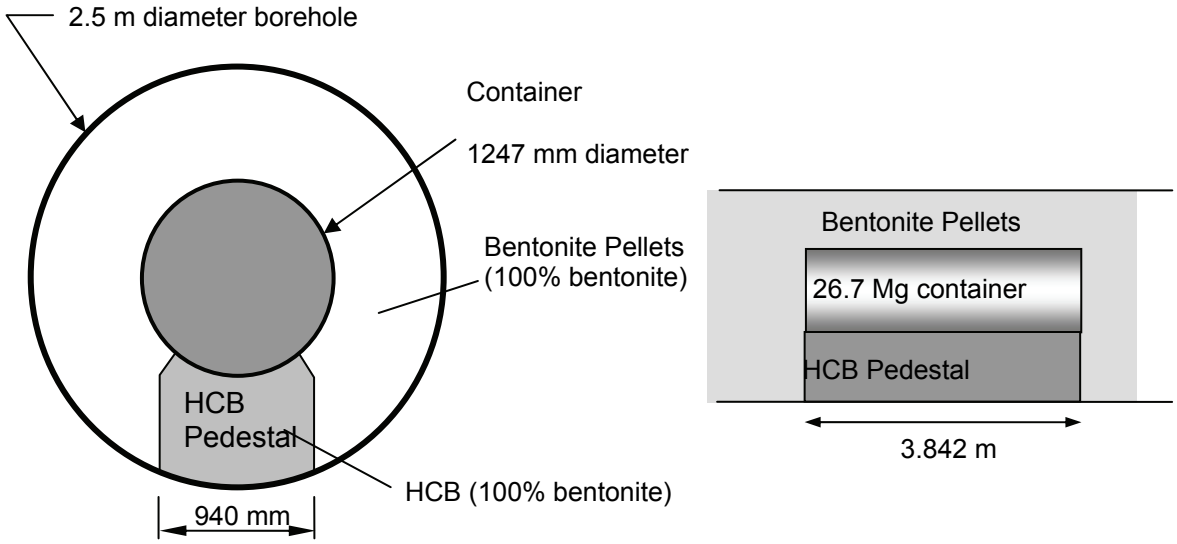

Figure 4-13: Container and Pedestal Configuration

The functions of the bentonite components in the container placement tunnel include:

- Maintaining the container position and geometry in the tunnel;
- Providing mechanical protection by acting as a buffer between the container and the rock;
- Providing a counter pressure that will tend to close EDZ fractures and reduce their transmissivity
- Facilitating heat transfer between the container and the rock;
- Limiting the container corrosion rate by inhibiting the movement of corrosion agents and influencing the chemistry of groundwater around the container; and
- Inhibiting the viability of bacteria near the container, reducing the potential for microbially induced corrosion of the container surface.

In the event of a breach of the container barrier, the bentonite components would also:

- Limit the solubility of certain contaminants by maintaining the pH of the groundwater around neutral conditions; and
- Retard or prevent the migration of dissolved contaminants by restricting their movement to diffusion transport, and to a lesser extent, by sorption. In this case study, only a few elements are assumed to be retained by sorption in the sealing materials because of the assumed high salinity of the groundwater.

4.5.4 Access Tunnels Backfill

Man and Martino (2009) identify two types of backfill that are used in the repository tunnels: dense backfill and light backfill, which are manufactured in the form of pre-compacted blocks. These materials will be used for backfilling the repository longitudinal drifts, as well as the cross-cuts that provide access to the placement rooms. However, these materials will not be used as backfill in the container placement rooms. The general composition and properties of materials considered at this preliminary design stage are given in Table 4-4. In order to provide a method for comparison of sealing materials performance, their properties are expressed in terms of their “effective montmorillonite dry density”, a parameter that normalizes bentonites and bentonite-sand mixtures based of the content of montmorillonite clay.

Dense backfill as formulated in Table 4-4 is a mixture of crushed rock, naturally-occurring glacial lake clay, and bentonite. It is manufactured and installed in the form of pre-compacted blocks to fill the majority of the tunnel volume. Important functions of the dense backfill are to provide load-bearing support to the rock openings by filling most of the excavated space in tunnels, and to slow the movement of groundwater within the repository excavated spaces.

Light backfill has similar functions to dense backfill, but it contains less crushed rock and more bentonite than dense backfill, as indicated in Table 4-4. Light backfill blocks are also made of different shapes in order to fill the sides and upper (crown) regions of tunnels where for geometric reasons it is not possible to place dense backfill blocks. Depending on the application, light backfill can also be compacted in-situ.

Table 4-4: Composition and As-Placed Properties of Clay-Based Sealing System Components

	Dry density [kg/m^3]	Saturation [%]	Porosity [%]	Bulk density [kg/m^3]	Water content [kg/kg]	Effective montmorillonite dry density [kg/m^3]
HCB (100% bentonite)	1,610	65	41.3	1,880	0.167	1,470
Gap Fill (100% bentonite)	1,410	6	48.6	1,439	0.021	1,260
Light backfill (50:50 bentonite/ sand)	1,240	33	53.7	1,418	0.143	692
70% bentonite (70:30 bentonite/ sand)	1,600	80	41.1	1,930	0.205	1,220
Dense backfill (5:25:70 bentonite/clay/crushed rock aggregate)	2,120	80	19.4	2,276	0.074	376

Note: Dry densities and saturations of the clay-based sealing materials are taken from SNC Lavalin (2011); other properties are determined using calculations illustrated in Baumgartner (2006).

4.5.5 Concrete

Concrete is used throughout the repository for sealing components and tunnel closure bulkheads and in the concrete components of repository seals. It is also used for tunnel floors where required. The concrete used to support tracks in the placement rooms will be removed as container placement progresses. The concrete floors installed in drifts and cross-cuts will be removed as a part of the repository decommissioning process. The only concrete that will remain in the repository is the concrete used in repository seals.

Interactions between concrete and water in a repository have the potential to produce alkaline chemical conditions that are detrimental to the swelling properties of bentonite, therefore LHHPC (Dixon et al. 2009, 2012) will be used, in repository seal components. LHHPC has a lower lime content than regular concrete, which results in a lower pH in reactions with water. The lower alkalinity limits the potential for adverse chemical reactions within the repository. In addition, the LHHPC generates less heat than regular concrete during the curing process, so the poured concrete is less likely to develop cracks during curing.

4.5.6 Grout

Grouting will be used during excavation and construction in any localized areas with higher rock permeability, or in order to limit seepage around engineered structures. Clay-based grouting materials may be an option under some conditions in a repository, but cement or silica-based grouts are more likely to be used. A sample grout specification for use in a repository environment is included in Table 4-5 (Dixon et al. 2009).

Table 4-5: Composition and Properties of a Cement Grout for Repository Use

Mix Composition	
Solids	90% Canadian Type HS* cement, 10% Silica fume by dry mass
	The cement Blaine fineness needs to be specified for the specific application (e.g., 600 m^2/kg).
Water/cement ratio	0.4 to 0.6 by mass
Superplasticizer	Sodium sulphonate naphthalene formaldehyde
Selected Properties	
Viscosity	Modified by water/cement ratio and superplasticizer content
Setting time	Initial: varies with temperature 10 to 16 hours
	Final: varies with temperature 12 to 20 hours
Strength	Varies with water to cement ratio, time and temperature: 20 to 60 MPa at 28 days
Hydraulic Conductivity	< 10^{-12} m/s

Note: * Type HS cement is the designation for sulphate resistant cement in Canada.

4.5.7 Asphalt

An asphalt column may form part of the shaft seals. Asphalt has the ability to flow and make good contact with host rock, and will create an effective barrier to water flow immediately upon placement. The reference asphalt mixture is based on a mix of asphalt compounds and combined aggregates with a small porosity fraction to ensure low permeability, including also lime to reduce microbial activity.

4.6 Sealing Materials Production Plants

A number of engineered barriers are used as part of the repository system to isolate the used fuel containers from the rock and to inhibit the mobility of water and contaminants within the repository. These engineered barriers are manufactured on site, using bentonite clay, sand and crushed rock as their main components, and are globally referred to as sealing materials. The primary barriers placed around the used fuel container consist of: a) a pedestal made of compacted bentonite that is placed on the tunnel floor and supports the used fuel container in its designated position, and b) placement tunnel backfill, in the form of bentonite pellets, that fills the remaining spaces in the placement room, including the space between the containers and the rock and the space between containers.

Other sealing materials used to construct seals at strategic points in the repository or used as backfill for the repository access tunnels include highly-compacted bentonite (HCB) blocks, used to construct tunnel and shaft seals, and backfill blocks used to fill the repository excavated spaces (other than the container placement rooms) at the time of repository decommissioning.

The backfill blocks are of two general types, dense backfill, and light backfill. Their composition is given in Table 4-6. The concrete components of repository seals are made of LHHPC, described by Dixon et al. (2009).

Table 4-6: Sealing Materials Attributes

Material	Attributes
Pedestal Composition and Density	Monolithic blocks, made from 100% bentonite clay (MX-80 or equivalent) and compacted to 1,610 kg/m^3 dry density
Dense Backfill Composition and Density	5% bentonite, 25% lake clay, 70% crushed rock aggregate, 2,120 kg/m^3 dry density
Light Backfill Composition and Density	50/50 bentonite clay/ sand, compacted in-situ to 1,240 kg/m^3 dry density
Tunnel and Shaft Seals Composition and Density	70:30 bentonite clay/sand, either in pre-compacted blocks, or in-situ compacted to1,600 kg/m^3 dry density
Concrete	Low-heat high-performance concrete (LHHPC)

The repository surface facilities used to produce sealing materials include an aggregate plant and rock crushing plant (Area B14), a concrete batch plant (Area B13) and a sealing material compaction plant with associated material storage bins (Areas B6 and B3), as shown in Figure 4-2.

The aggregate plant uses a portion of the excavated rock to manufacture products suitable for the concrete batch plant, including sand and stone. Modified granular A (a graded crushed stone commonly used on roads) and fine sand for the compaction plant are also produced in the aggregate plant and used as a component of the sealing materials. Externally sourced raw materials required in the production of the various sealing materials include binders (Type 50 cement, silica fume and flour) as well as bentonite and glacial lake clay. The concrete batch plant produces two different types of LHHPC mixes, one for the placement room floor and the other for the placement room closure bulkhead.

During decommissioning, the plant will produce the bentonite shaft seal materials. Asphalt seal mixes that may be required for sealing of shafts are assumed to be produced externally.

4.7 Shafts and Hoists

Access to the repository is via shafts serviced by hoisting facilities. Three shafts will be constructed: the main shaft, the service shaft, and the ventilation shaft (Figure 4-14); each serving specific functions during construction, operations and decommissioning of the repository facility. Their primary functions are the transport of materials and personnel, and providing ventilation to the repository. The shafts will be constructed using techniques that minimize host rock damage, to enhance the effectiveness of postclosure repository seals. The finished

diameter of each shaft is: main shaft 7.0 metres, service shaft 6.5 metres; and ventilation shaft 6.5 metres.

The headframes for the three shafts will be of slip-formed concrete construction for a durable and easily maintainable structure. All the shafts will be concrete lined; the lining will be removed during decommissioning and closure of the facility. The three shaft structures (including head frames and hoisting plants) provide a number of support functions during underground development, repository operation and decommissioning:

- The main shaft serves as the exclusive means for transfer of used fuel containers from the surface to the underground repository. It could also be used for transfer of a retrieved used fuel container from the repository to the surface, if this was required. The main shaft also provides the fresh air supply to the underground.
- The service shaft serves as the principal conveyance for personnel, materials and equipment to the underground as well as for transport of excavated rock to the surface. It also provides some ventilation exhaust.
- The ventilation shaft, located about 2 km outside the main surface facilities fence is the primary exhaust shaft and serves also as emergency exit from the repository.

4.8 Underground Facility Design

For the purpose of preliminary design and safety studies for a hypothetical site in sedimentary rock, the used fuel repository is assumed to be developed on a single level, at a depth of approximately 500 m. A possible layout of a repository designed to accommodate a reference inventory of 4.6 million used fuel bundles is shown in Figure 4-14. The actual layout for a selected repository site will be adapted to suit the specific site conditions. The geology of the hypothetical site used in this study is described in Chapter 2.

The layout of the repository reference design, shown in Figure 4-14, has a rectangular configuration, with two central access drifts and two perimeter access drifts connected by perpendicular tunnels (cross-cuts) that provide access to the used fuel container placement rooms.

The container placement rooms are a series of parallel tunnels arranged in ten panels. Within each panel, the placement rooms have a centre-to-centre spacing of 20 m, and each room has a single access from the corresponding cross-cut tunnel. The entrance to the room has a 50 m turning radius to facilitate the movement of the container transfer cask and related systems. The length of the rooms in the reference design is specified as 412 m and the used fuel containers are placed along the tunnel axis with a center-to-center spacing of 8.0 m. The longitudinal section of a container placement room is illustrated in Figure 4-15.

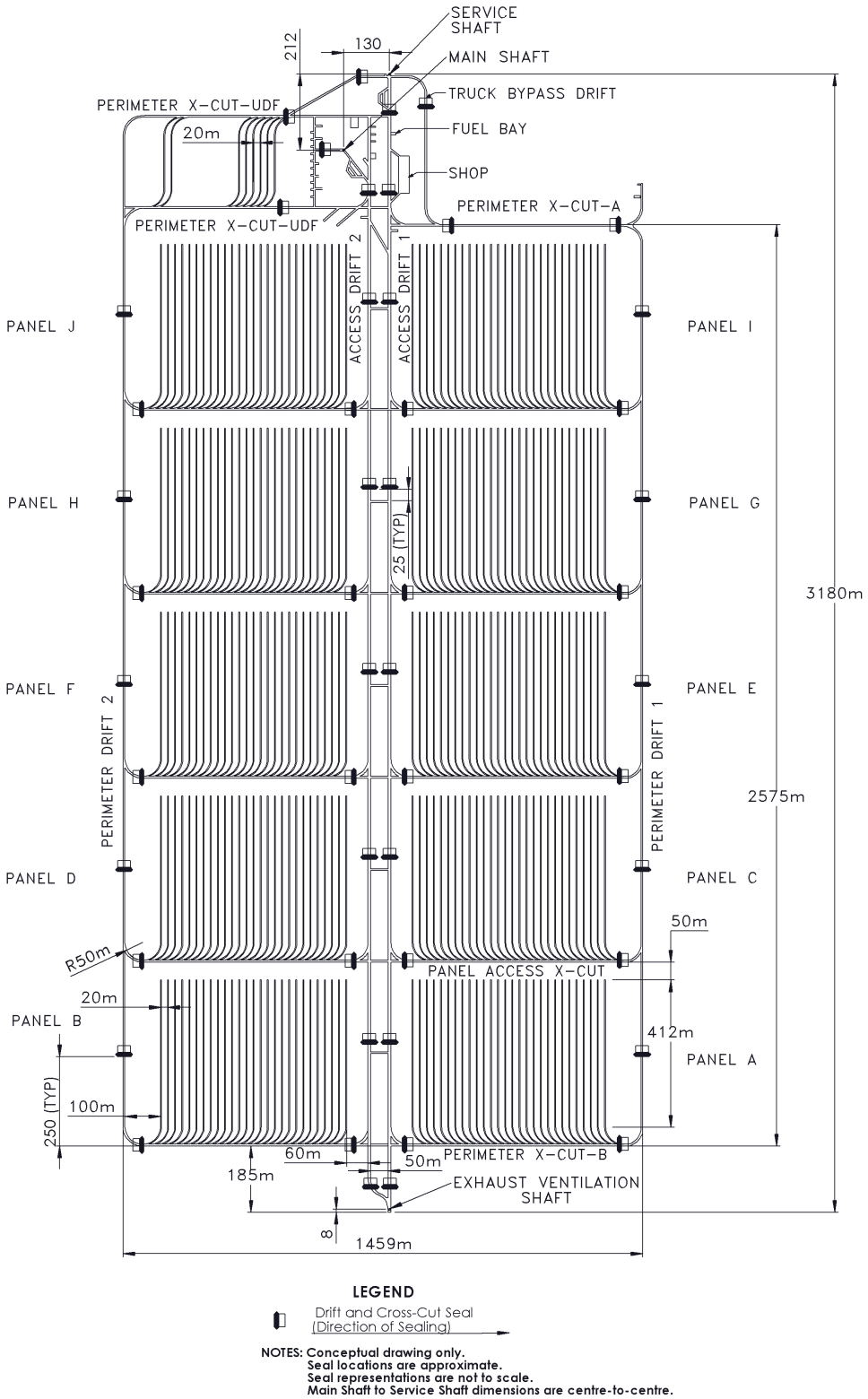

Figure 4-14: Underground Repository Layout

The used fuel container density is designed to minimize the repository underground footprint while satisfying thermal design requirements as described in Chapter 5. The repository includes provision for an underground demonstration facility located near the main and service shafts. This facility may be used to support long-term testing and demonstration of repository technology.

In each placement room, as used fuel container placement operations advance, the rails and concrete floor are removed and the room is backfilled with pneumatically placed bentonite pellets. The pellets will fill the spaces between the container and the tunnel wall as well as the space between containers. After a placement room is full, a 12 m concrete bulkhead will be placed to seal the entrance to the room. The major components of a placement room are illustrated in Figure 4-15 (SNC Lavalin 2011).

Both repository development (excavation) and used fuel container placement will be conducted on a panel by panel basis and, in a sequence that will provide suitable separation of these two major activities. The repository development/operation strategy will optimize efficiency while considering both, safety and operating factors (e.g., vehicle traffic and ventilation) as well as the potential interactions between repository development and operations.

4.8.1 Ventilation System

The repository ventilation system utilizes the three shafts and a combination of parallel airways for intake and exhaust. Underground booster fans, ventilation doors and dampers are used to control the airflow distribution. Since the primary repository ventilation system consists of relatively large airways, the overall circuit has relatively low resistance characteristics in a push-pull type network. Two parallel, surface fresh air fans supply air (heated as required) to the main shaft. The fresh air supply reaches the repository level at the main shaft station and is split to the underground demonstration facility and the main repository itself. A portion of the exhaust air flow is routed to the service shaft by an exhaust booster fan.

Exhaust air from the repository area is routed to the ventilation shaft by two exhaust booster fans, installed underground in a parallel configuration at the shaft station. Return air is exhausted to atmosphere by two parallel exhaust fans installed on the surface in the ventilation shaft area. Air distribution in the repository is promoted through the use of fans and regulators. Fresh air will be distributed to the individual panels through axial flow fans. Individual placement rooms will also be ventilated by axial flow fans that will remove air from the rooms and direct it into the exhaust circuit.

The ventilation fans will work with a duct network to provide a design flow of 37.8 m^3/s of air to the room during excavation. During used fuel container placement activities, the required supply flow per room will be 14 m^3/s. The exhaust air flow from these ventilation fans will be routed to the panel exhaust drift, and then to underground booster exhaust fans (SNC Lavalin 2011).

The system will be operated to ensure that the underground work is performed in a fresh air supply stream with the exhaust being directed through unoccupied areas. High-efficiency particulate air (HEPA) filtration systems could be installed in the service shaft and ventilation shaft stations as stand-by systems that would be activated as required. Subsurface ventilation systems could also be equipped with air filtration systems if required. For the purpose of this conceptual design, stand-by HEPA filtration systems are assumed to be installed at the service shaft and ventilation shaft stations.

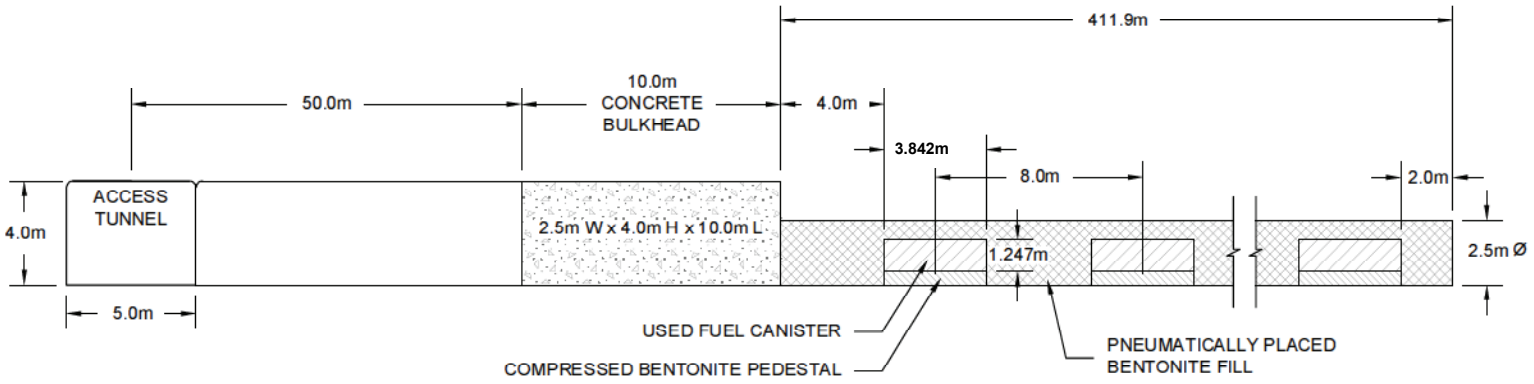

Figure 4-15: Longitudinal Section of Placement Room

4.9 Repository Construction

Repository construction will be initiated after both a safety assessment and an environmental assessment have been completed and a construction licence has been obtained for the site. Initial site preparation activities, including clearing and grading, establishing access roads and the installation of basic infrastructure systems may be conducted in advance under a site preparation licence. The site infrastructure required to support excavation, such as electrical systems, headframes, ventilation and excavated rock management systems would follow after the construction licence is obtained.

Controlled construction methods will be used to minimize disturbances to the area surrounding the facility. The three shafts will be developed using a controlled drill and blast shaft sinking approach specifically designed to minimize the excavation damage zone (EDZ).

Conventional blasting operations include drilling blast holes in a converging pattern designed to minimize the quantity of detonated explosive per volume of rock. In order to reduce damage to the perimeter of the opening, a larger number of blast holes with smaller explosive charges will be used in the outer region of the shaft. This method, usually referred to as contour wall blasting, will be used to minimize the thickness of the excavation damage zone. Between the blasting cycles, fumes will be vented, scaling will be done to remove loose rock and ground support is applied as required. This excavation method is expected to result in a rate of advance of approximately 2.5 m to 3.5 m per day.

Upon completion of the three shafts, the perimeter drifts will be excavated, defining the outline of the underground facility. The underground development required as support infrastructure will precede the development of used fuel container placement rooms. Then, development of placement room panels will be initiated along the cross-cut near the ventilation shaft and will continue in a retreating fashion towards the main shaft end of the repository. This strategy is designed to minimize any possible effects of the excavation activities on container placement operations.

Both, panel development and used fuel placement operations will move from the ventilation shaft end towards the main shaft end of the repository. Retreating towards the main shaft will minimize the need for personnel to enter or pass by completed repository areas and will ensure that all ventilation air from operating areas is routed directly to the exhaust shaft. Each placement room panel will require about 3 years for development to be completed. Placement activities in each panel are expected to require from 3.5 to 4 years. Since development and container placement operations (in different panels) will largely overlap the estimated duration of the repository operating phase is expected to be of the order of 40 years.

4.10 Repository Operation

The first step of the used fuel container placement operation will be the installation of a concrete floor and tracks that will be used to move on rails heavy equipment such as the container transfer cask. It is envisaged that the track system will be modular, consisting in rail segments pre-mounted on a steel bottom plate that will be bolted to the concrete floor. The equipment required for the container placement operations is schematically illustrated in Figure 4-16, and the sequence of operations is shown in Figure 4-17. Note that in these figures and in the description

below “used fuel container” is abbreviated as UFC and highly-compacted bentonite is abbreviated as HCB.

4.10.1 Container Placement

A thin layer of bentonite will be placed at the pedestal location and compacted into place to fill any irregularities left by the excavation process. For the purpose of this description, the pedestal is considered to be a monolithic block of HCB. In practice handling requirements may require that the pedestal be made of three monolithic HCB segments. In either case, the pedestal will be transported into the placement room by rail and installed in place using a specially designed crane, which is part of the Pedestal Placement trolley.

Once the first pedestal is installed, the UFC placement cart and the shielding barrier are moved into place. A loaded UFC transfer cask will then be brought by rail from the Main Shaft area to the placement room and coupled to the shielding barrier. The doors of the transfer cask and the shielding barrier will then be opened and the UFC will be pushed, using a ram, from the transfer cask onto the UFC placement cart, which is equipped with a set of roller beds that can be adjusted to receive, raise or lower the UFC as required.

The placement cart holding the UFC will then be moved into place over the pedestal and the UFC will be lowered onto its designated position. The ram will then be retracted, the shield doors and transfer cask doors will be closed, and the empty UFC transfer cask will be returned to the shaft area. The outer shielding door will subsequently be moved into place to allow the safe backfilling of the tunnel around the UFC (see Figure 4-17, Phase 20). The current logistics for the container placement operation require that the pedestal for the next UFC be installed before the backfill is placed around the last placed UFC. The step-by-step UFC placement operation is graphically described in Figure 4-17.

4.10.2 Backfilling Operation

Once a UFC has been placed and the placement equipment removed, a segment of the bottom plate and rails will be removed to allow placement of the next pedestal. The next pedestal will then be transported to the placement room and lowered into place. Following this, the bentonite blowing equipment will be moved into the placement room and connected to services. A locomotive will be attached to the UFC placement barrier, pedestal shielding barrier and UFC placement frame. Bentonite will be continuously blown to the far end of the placement room, retreating towards the entry of the room. As bentonite injection retreats, the locomotive will retreat the shielding barrier and placement frame. These operations are described step by step in Figure 4-17.

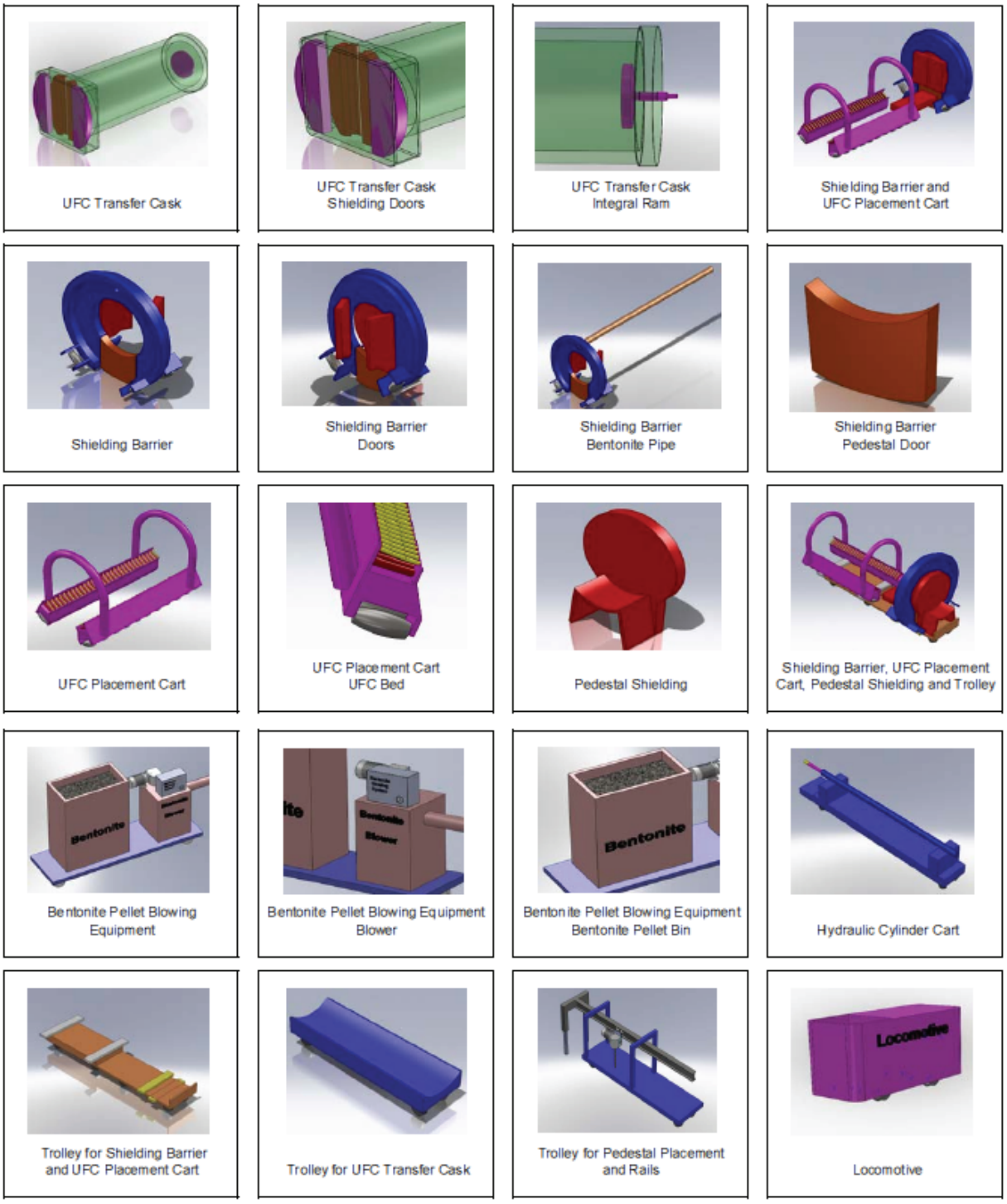

Figure 4-16: Legend for Container Placement Equipment

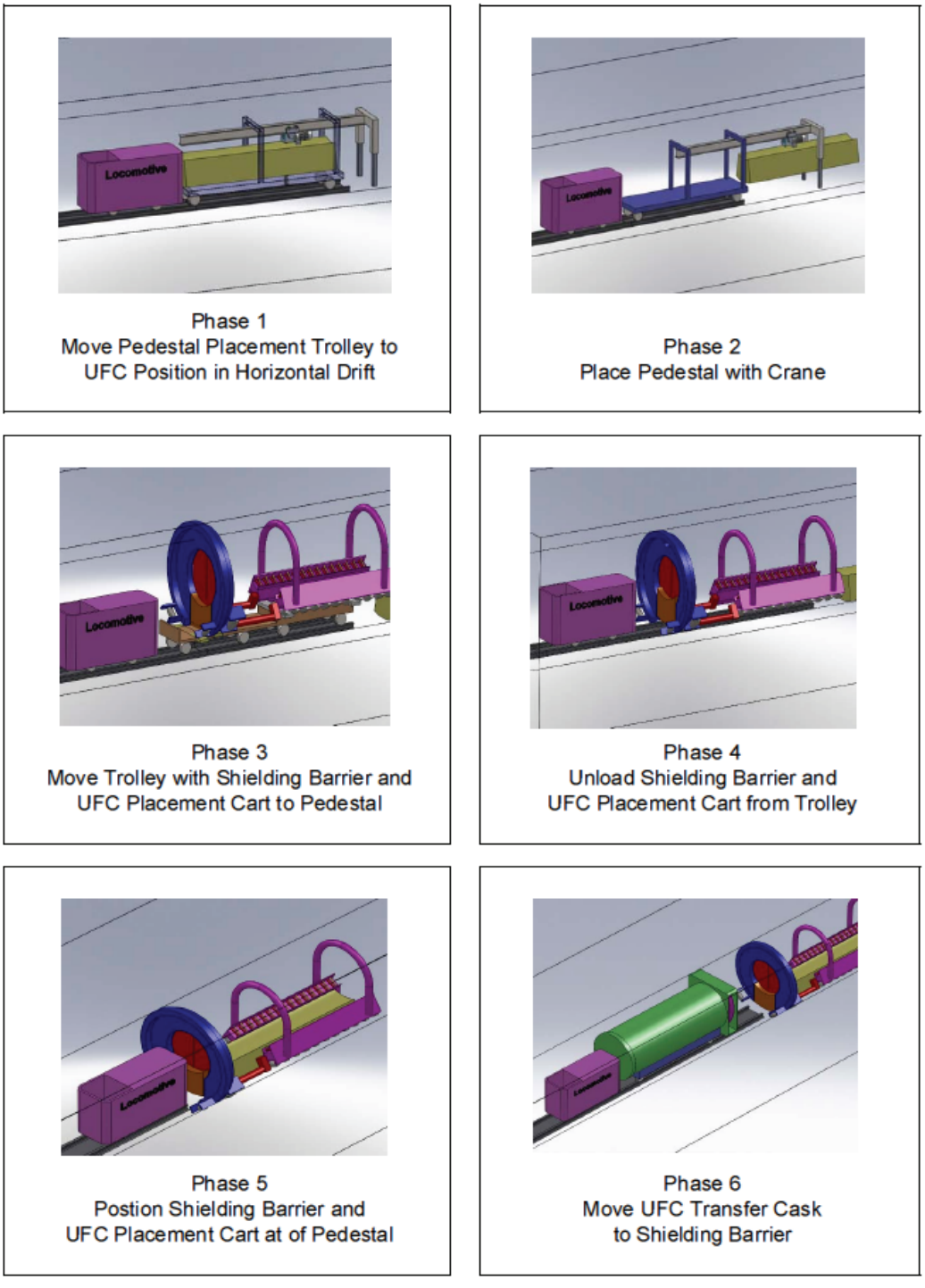

Figure 4-17: Container Placement – Sequence of Operations

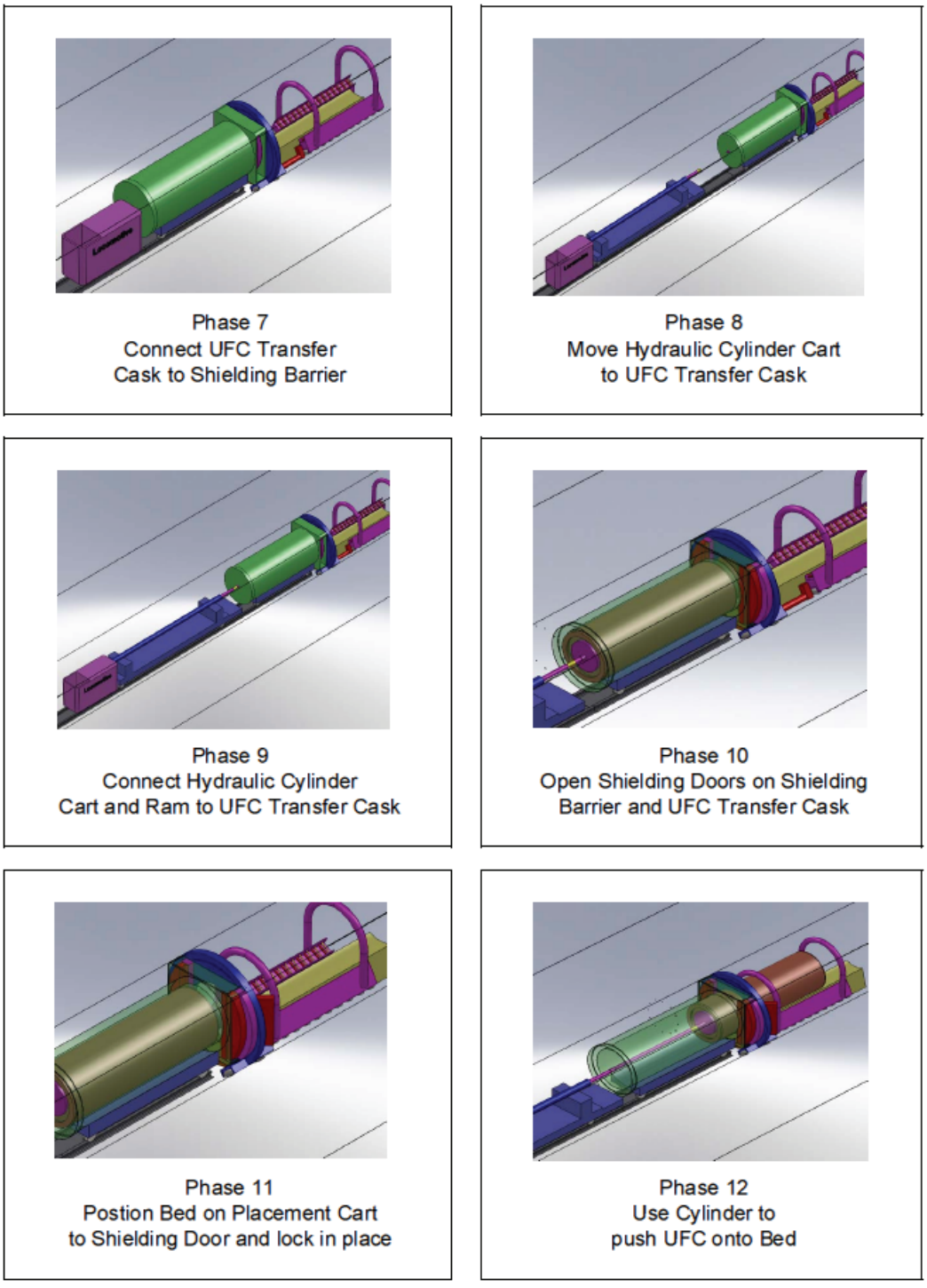

Figure 4-17: Container Placement – Sequence of Operations (Continued)

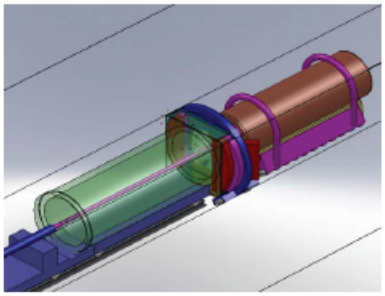

Phase 13
Unlock Placement Cart Bed and push UFC and Bed into position over Pedestal

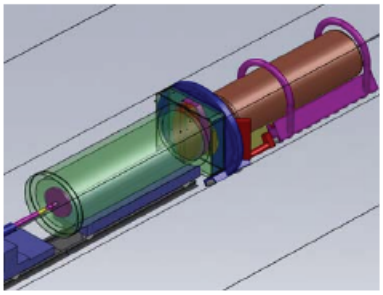

Phase 14
Retract Cylinder and close Shielding Doors on Barrier and UFC Transfer Cask

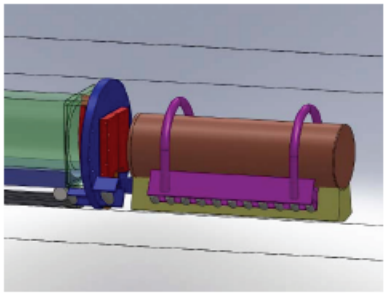

Phase 15
Lower Placement Cart Bed so UFC is placed on Pedestal

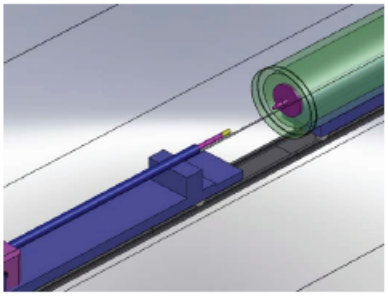

Phase 16
Remove Coupling between Cylinder and Ram

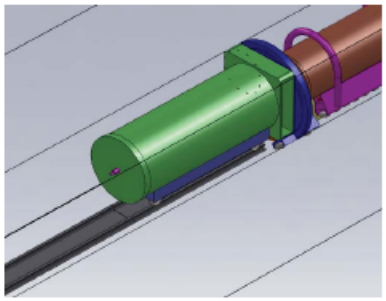

Phase 17
Remove Hydraulic Cylinder Cart

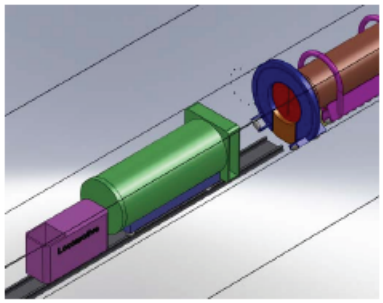

Phase 18
Disconnect UFC Transfer Cask from Shielding Barrier

Figure 4-17: Container Placement – Sequence of Operations (Continued)

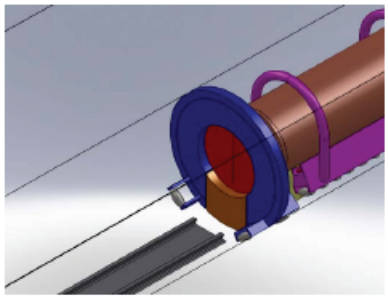

Phase 19
Move UFC Transfer Cask
and Trolley to Storage

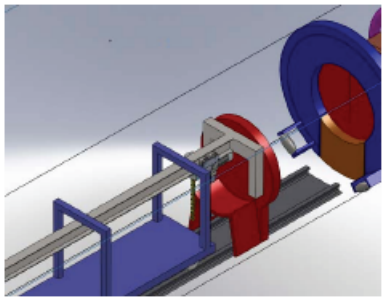

Phase 20
Using Pedestal Placement Trolley move
Outer Shielding Door to Shielding Barrier

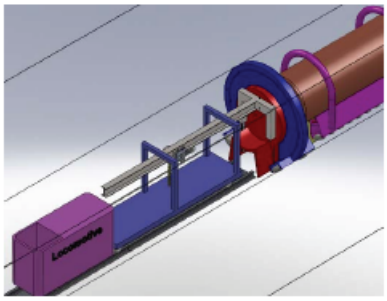

Phase 21
Attach Outer Shielding
Door to Shielding Barrier

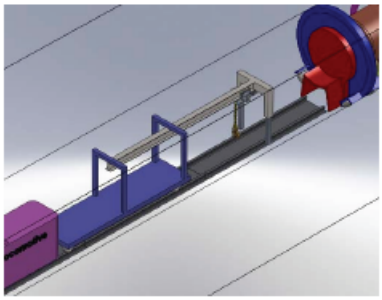

Phase 22
Position Pedestal Placement Trolley
to remove Rails and Bottom Plate

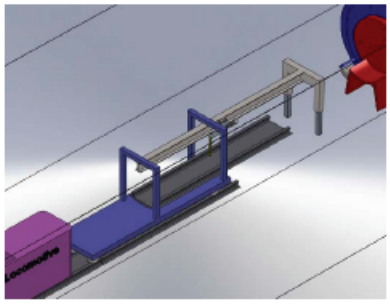

Phase 23
Lift Rails and Bottom Plate
into Cart and transfer to Storage

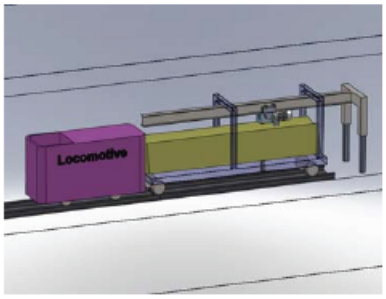

Phase 24
Move Pedestal Placement Trolley to
next UFC Position in Horizontal Drift

Figure 4-17: Container Placement – Sequence of Operations (Continued)

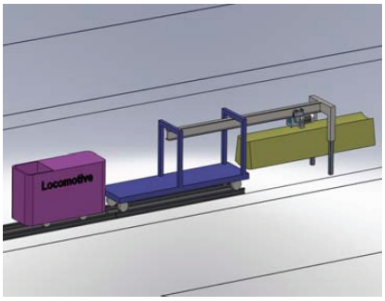

Phase 25
Place Pedestal with Crane and move
Pedestal Placement Trolley to Storage

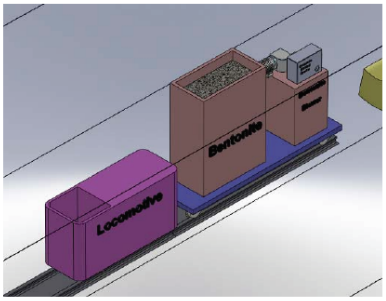

Phase 26
Move Bentonite Blowing Equipment
Cart to Shielding Barrier

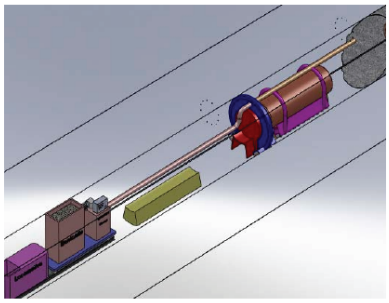

Phase 27
Connect Bentonite Blowing Equipment to
Services and blow in Bentonite Pellets

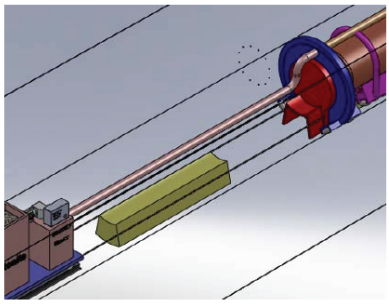

Phase 28
Connect Locomotive to
Shielding Barrier with Cable

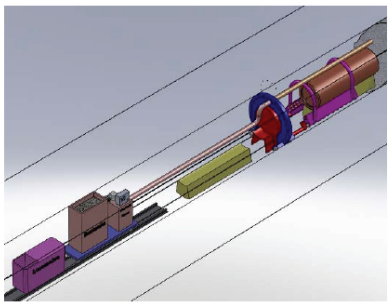

Phase 29
Move Barrier and Placement
Cart to Pedestal with Locomotive

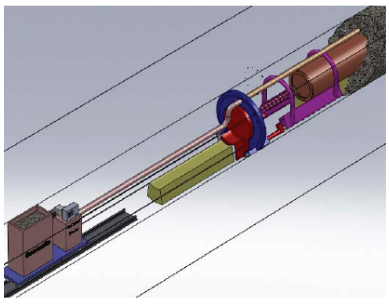

Phase 30
Continue Blowing Bentonite Pellets

Figure 4-17: Container Placement – Sequence of Operations (Continued)

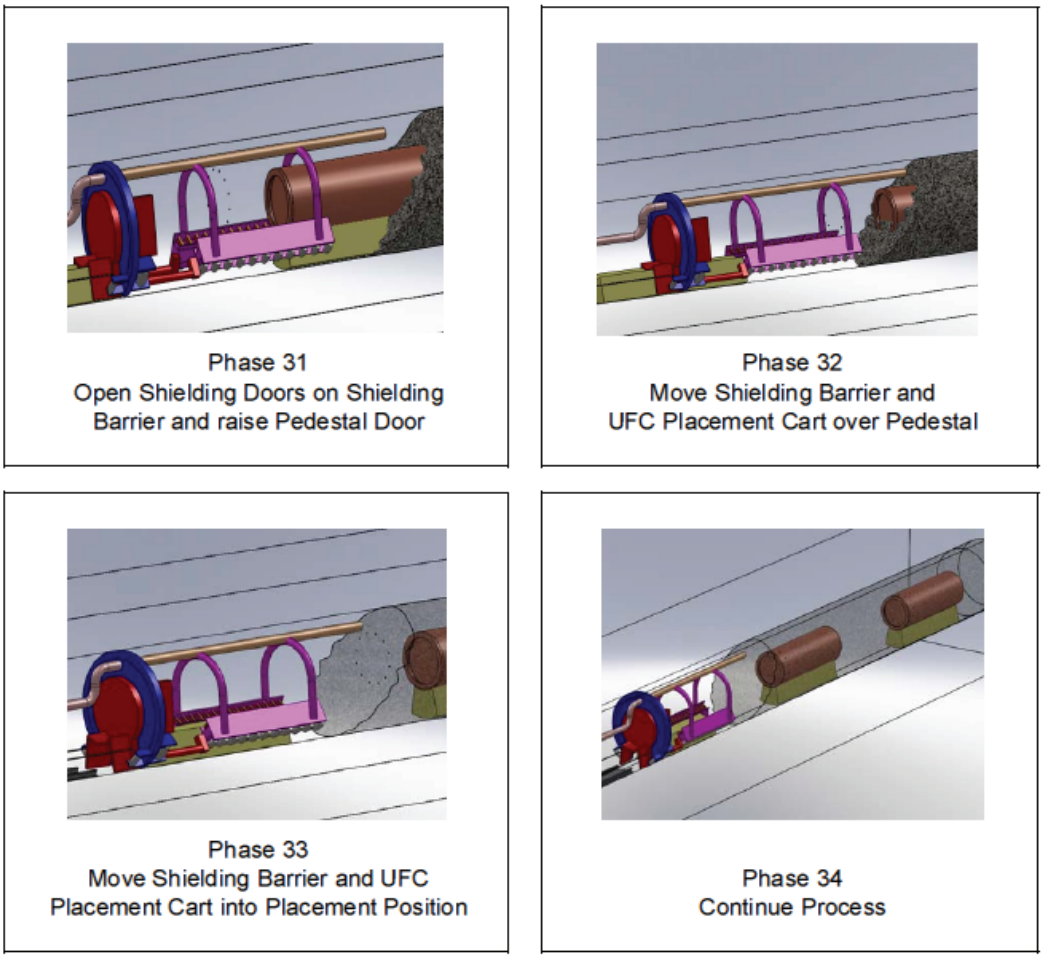

Figure 4-17: Container Placement – Sequence of Operations (Continued)

The repository operations will continue until all used fuel has been repackaged in used fuel containers, all used fuel containers are placed into placement rooms and all placement rooms sealed. The duration of the repository operational phase is expected to be approximately 40 years.

4.11 Extended Monitoring

Upon completion of all used fuel container placement activities, all placement rooms will have been sealed and closed, but the access tunnels and shafts will remain open. The facility will be placed in an extended care and maintenance program during which monitoring of the repository and surrounding geosphere will continue to confirm the performance of the repository system. The extended monitoring period could have a duration of several decades.

4.12 Decommissioning

Once the extended monitoring period has been completed, the facility will formally enter a decommissioning phase where the underground facilities will be prepared for backfilling and then backfilled and sealed from the surface. Subsequently, the surface facilities will be decommissioned and the site will be returned to a green-field condition. The repository decommissioning phase is discussed below.

4.12.1 Sealing of Underground Horizontal Openings

The sealing of underground horizontal openings consists of closing off access drifts and ancillary facilities. Such activities will commence with the preparation of exposed rock surfaces by removing loose rock before backfilling and sealing. This will be followed by removal of all remaining equipment and installations. Cross-cuts access drifts will then be backfilled, with sealing bulkheads installed at strategic locations.

The tunnels and underground openings will be backfilled using a combination of dense backfill blocks and light backfill, as specified in Section 4.6 and Table 4-6. The clay-based backfill will be complemented by strategically placed composite seals consisting of a concrete bulkhead and a clay component consisting of highly-compacted bentonite blocks (see Table 4-6) to provide a barrier to groundwater movement.

The sequence for the closure of tunnels will see first the sealing of cross-cuts and perimeter tunnels in a retreating manner from the ventilation shaft to the service shaft while maintaining open a central access tunnel. Bulkheads will be installed near access drift intersections and also near intersections with significant zones (as appropriate). The purpose of the bulkheads is to provide mechanical restraint against the forces exerted by swelling clay seals and other repository sealing systems. The bulkheads will further act to keep the sealing materials isolated in their intended positions.

4.12.2 Sealing of Shafts

Sealing of the shafts will be the last step in the decommissioning of the underground repository. This activity will start when the sealing of underground tunnels and ancillary areas is complete. At that time, the following activities will take place:

- Removal of shaft services including compressed air lines, water lines, power supply, lighting and communication cables;
- Removal of instruments and sealing from any impacted geological investigation boreholes;
- Removal of furnishings including all of the shaft guides and sets, steel support brackets, brattice and lower crash beam assemblies from bottom to top while backfilling; and
- Reaming of the shafts (as required) to remove the concrete linings and any degraded wall rock.

It is assumed that approximately 0.5 m of rock will be removed from the shaft walls to expose the sound rock. After this operation, each shaft will be re-equipped with services and staging, and backfilling will be initiated with sealing bulkheads installed at strategic locations. The proposed design for a shaft seal system is described in Table 4-7. The final design for the shaft seals will depend on the geological conditions of the site.

The purpose of removing monitoring wells and then sealing the geological borehole is to inhibit groundwater movement and contaminant transport. A combination of cement-based materials and clay-based materials with low permeability and a high swelling potential will be used as required to isolate fractured and highly permeable zones and prevent the geological boreholes from becoming preferential transport paths.

Table 4-7: Proposed Sealing System for Shafts

Depth from Surface	Material
0 – 20 m	Low-heat high-performance concrete– concrete cap at surface
20 – 150 m	70/30 bentonite / sand shaft seal compacted in-situ
150 – 170 m	Low-heat high-performance concrete for concrete bulkhead keyed into rock / overburden to a distance of 0.5 times the original radius of the shaft
170 – 330 m	70/30 bentonite / sand shaft seal compacted in-situ
330 – 380 m	Asphalt or highly-compacted bentonite seal
380 – 480 m	70/30 bentonite / sand shaft seal compacted in-situ
480 – 500 m	Concrete monolith – Low-heat high-performance concrete

4.12.3 Decommissioning of Monitoring Wells and Sealing of Geological Boreholes

A minimized administration area will be maintained during the end of decommissioning to support the post-decommissioning monitoring systems. If at that time it is felt that permanent facilities are no longer required, the monitoring systems could be supported by small enclosures for the electrical equipment, and all other remaining facilities could be removed and the site fully returned to greenfield conditions.

The facility's environmental monitoring carried out during the operational and extended monitoring periods as well as throughout the decommissioning stage may be continued following decommissioning and closure. The scope and duration of such tasks will be decided at the appropriate time by both regulatory entities and society at large.

4.13 References for Chapter 4

Baumgartner, P. 2006. Generic Thermal-Mechanical-Hydraulic (THM) Data for Sealing Materials – Volume 1: Soil-water Relationships. Ontario Power Generation Report 06819-REP-01300-10122-R00. Toronto, Canada.

Dixon, D.A., J.B. Martino and D.P. Onagi. 2009. Enhanced Sealing Project (ESP): Design, Construction and Instrumentation Plan. Nuclear Waste Management Organization Report APM-REP-01601-0001. Toronto, Canada.

Dixon, D.A., D.G. Priyanto and J.B. Martino. 2012. Enhanced Sealing Project (ESP): Project Status and Data Report for Period Ending 31 December 2011. Nuclear Waste Management Organization Report APM-REP-01601-0005. Toronto, Canada.

Holmberg, Jan-Erik, and P. Kuusela. 2011. Analysis of Probability of Defects in the Disposal Canisters. Posiva Working Reprt 2011-36. Posiva Oy, Eurajoki, Finland.

Kim, C.S., A. Man, D. Dixon, E. Holt and A. Fritzell. 2012. Clay-based Pellets for use in tunnel backfill and as gap fill in a deep geological repository: characterization of therma-mechanical properties. Nuclear Waste Management Organization Report NWMO TR-2012-05. Toronto, Canada.

Kwong, G. 2011. Status of Corrosion Studies for Copper Used Fuel Containers under Low Salinity Conditions. Nuclear Waste Management Organization Report NWMO TR-2011-14. Toronto, Canada.

Maak, P., P. Gierszewski and M. Saiedfar. 2001. Early Failure Probability of Used-Fuel Containers in a Deep Geological Repository. Ontario Power Generation Report 06819-REP-01300-10022-R00, Toronto, Canada.

Man, A. and J.B. Martino. 2009. Thermal, Hydraulic and Mechanical Properties of Sealing Materials. Nuclear Waste Management Organization Report NWMO TR-2009-20. Toronto, Canada.

NEA. 2012. The Post-Closure Radiological Safety Case for a Spent Fuel Repository in Sweden. An International Peer Review of the SKB License-Application Study of March 2011 (Final report). Nuclear Energy Agency Report NEA/RWM/PEER(2012)2. Paris, France.

NWMO. 2013. Used Fuel Transportation Package Safety Analysis Report. Nuclear Waste Management Report APM-SR-00531-0001 R000. Toronto, Canada.

Pitkänen, Jorma. 2010. Inspection of Bottom and Lid Welds for Disposal Canisters. Posiva Report 2010-04. Posiva Oy Olkiluoto, Finland.

Pusch, R. L. Börgesson and C. Svemar. 2004. Prototype Repository - Final Report (Deliverable D36). Svensk Kärnbränslehantering AB, International Progress Report IPR-04-27. Stockholm, Sweden

Sandlin, S. 2010a. X-Ray Inspection Setups for the Disposal Canister Welds. Posiva Oy Report 2009-98. Olkiluotto, Finland.

Sandlin, S. 2010b. High-Energy Radiography for Inspection of the Lid Weld in Disposal Canisters. Posiva Oy Report 2009-82. Olkiluoto, Finland.

Sandlin, S. 2010c. Defect Detectability in the Disposal Canister Lid-Weld using the 9 MeV Linear Accelerator. Posiva Oy Report 2009-84. Olkiluoto, Finland.

SKB. 2007. RD&D Programme 2007. Programme for Research, Development and Demonstration of Methods for the Management and Disposal of Nuclear Waste. Swedish Nuclear Fuel and Waste Management Company Report SKB TR-07-12. Stockholm, Sweden.

SKB. 2008. Inspection of Copper Canister for Spent Nuclear Fuel by means of Ultrasound. FSW Monitoring with Emission, Copper Characterization and Ultrasonic Imaging. Swedish Nuclear Fuel and Waste Management Company Report SKB TR-08-12. Stockholm, Sweden.

SNC Lavalin. 2011. Deep Geological Repository Design Report Sedimentary Rock Environment Copper Used Fuel Container. SNC Lavalin Nuclear Report APM-REP-00440-0002. Toronto, Canada.

Villagran, J. 2012. Used Fuel Container Retrieval from a Deep Geological Repository in Sedimentary Rock. Horizontal Tunnel Configuration. Nuclear Waste Management Organization Report NWMO TR-2012-17. Toronto, Canada.

THIS PAGE HAS BEEN LEFT BLANK INTENTIONALLY

5. LONG-TERM EVOLUTION OF THE MULTIPLE BARRIER SYSTEM

Chapters 2, 3, and 4 of this report describe aspects of the hypothetical sedimentary site, the used fuel waste form and the engineered repository design sufficient to support the presentation of an illustrative postclosure safety assessment. This chapter considers how these multi-barrier components of the system are expected to interact with each other and with the environment in the long term, consistent with CNSC Guide G-320 (CNSC 2006). Additional Features, Events and Processes (FEPs) were assessed and excluded for the reasons outlined in the FEPs report (Garisto 2013) and thus are not part of the expected evolution described in this chapter.

As noted in Chapter 1, a geosynthesis will be required as part of a safety case for a repository at a selected site. The geosynthesis provides a description of the site's past geologic evolution, its current state and potential future evolution as influenced by repository construction and external perturbations (i.e., glaciations and earthquakes). In this respect, the geosynthesis provides evidence to support an understanding of the natural geologic barriers and, in particular, their function and long-term integrity at timeframes relevant to demonstrating repository safety. In the absence of a real site and therefore a geosynthesis, a number of assumptions have been made in this report to illustrate the safety assessment approach and methodology.

The evolution of certain site parameters and conditions are presented herein to allow illustration of the type of considerations that would be given to specific aspects of the site. Table 5-1 presents general information for the key repository components, many of which were described in Chapters 2, 3, and 4. The evolution of these components are discussed in separate sections of this chapter.

The preparation of this report is consistent with the expectations of CNSC Guide G-320, which states:

> *"Early in the licensing lifecycle, it may be necessary to rely on design specifications, waste acceptance criteria, generic or default data, and assumptions to describe the waste management system in sufficient detail that its performance can be predicted. At later stages in the facility's development, as-built information and operational data should be used to refine the model of the system for assessment purposes. As with the site model, the model of the waste management system should evolve to become more realistic, and less conservative, based on real data."*

The NWMO continues technical work in a number of areas that are summarized in the NWMO's research, development and demonstration program as detailed in Crowe et al. (2013) and Villagran et al. (2011). The technical program's objectives include increasing knowledge and reducing uncertainties associated with components described in this chapter.

Table 5-1: General Parameters

PROPERTY	REFERENCE VALUE
Used Fuel	
Waste form	Used CANDU fuel bundles
Bundle	37-element standard bundle length of 495 mm (e.g., Bruce, Darlington)
Initial mass U	19.25 kg/bundle
Initial mass Zircaloy	2.2 kg/bundle
Average burnup	220 MWh/kgU
Average bundle power rating	455 kW/bundle
Minimum fuel age at placement	30 years (out of reactor)
Container	
Design	Copper outer vessel, with steel load-bearing inner vessel, bundles held in steel sleeves
Outer shell material	Oxygen-free, phosphorus-doped high-purity copper
Inner shell material	Carbon steel
Container fill gas	Inert gas installed at atmospheric pressure
Container capacity	360 bundles
Container dimensions	1.25 m outer diameter x 3.84 m long
Outer shell thickness	25 mm
Container mass	26.7 Mg loaded
Thermal output	1270 W at 30 years, 220 MWh/kgU
Temperature (outer surface)	Up to 120^{o}C
Buffer/Backfill	
Buffer design	UFC is placed on a 0.63 m high, 0.94 m wide Highly Compacted Bentonite (HCB) buffer pedestal, with the remainder of placement tunnel backfilled with 100 % bentonite gap fill (GF) pellets
Buffer material	100% bentonite clay, MX-80 or equivalent
HCB buffer density	1,610 kg/m^3 dry density
Gap fill buffer density	1,410 kg/m^3 dry density
Backfill design	Backfill is used to fill access drifts and perimeter drifts. It is primarily a dense backfill material, with gap fill used to fill remaining gaps
Dense backfill material	5% bentonite, 25% lake clay, 70% granite aggregate, 2,120 kg/m^3 dry density
Concrete	Low-heat, high-performance concrete
Buffer temperature	At a minimum, 0.3 m of buffer under 100°C
Repository	
Depth	500 m
Footprint	~6 km^2
General design	Horizontal tunnel placement, single row of containers along room centre

PROPERTY	REFERENCE VALUE
Total number of bundles	4.6 million
Total number containers	12,800
Operation phase	40 years
Extended monitoring phase	Up to 70 years (following placement of all containers)
Geosphere	
Predominant rock type	Sedimentary
Rock structure at depth	Limestone/Shale
Geothermal gradient	14°C/km
Temperature at depth	12°C (assuming land surface temperature of 5°C)
Hydraulic conductivity	$2x10^{-14}$ m/s horizontally and with $2x10^{-15}$ m/s vertically at repository horizon
Porosity	0.015 at repository horizon
Total Dissolved Solids	275 g/L at repository horizon
Surface/Biosphere	
Land surface temperature	+5°C annual average (present)
Air surface temperature	+5°C annual average (present)
Ecosystem	Temperate deciduous (present)

5.1 Long-Term Evolution of Used Fuel

A detailed description of the used fuel waste form when placed in the repository is provided in Chapter 3. The used fuel assemblies remain isolated and dry within the container. The main long-term process is radioactive decay, as long as there is no container failure, as outlined in Table 5-2. The processes in a failed container are described later.

Table 5-2: Processes with a Potential Influence on the Evolution of Used Fuel Bundles

PROCESS	POTENTIAL INFLUENCE
RADIATION	
Radioactive decay	• Production of heat, radiation and helium • Decay of radionuclides
THERMAL	
Heat transfer from fuel to container	• Change in fuel temperature
HYDRAULIC & PNEUMATIC	
None	• None
MECHANICAL	
None	• None
CHEMICAL	
None	• None
BIOLOGICAL	
None	• None

Notes: Processes listed are those that are most likely to have a notable effect on the used fuel bundles, over a time scale of one million years.

5.1.1 Radioactive Decay

When the used fuel is first removed from the reactor it is highly radioactive. This activity decreases rapidly over the first year and more slowly thereafter as shown in Figure 5-1.

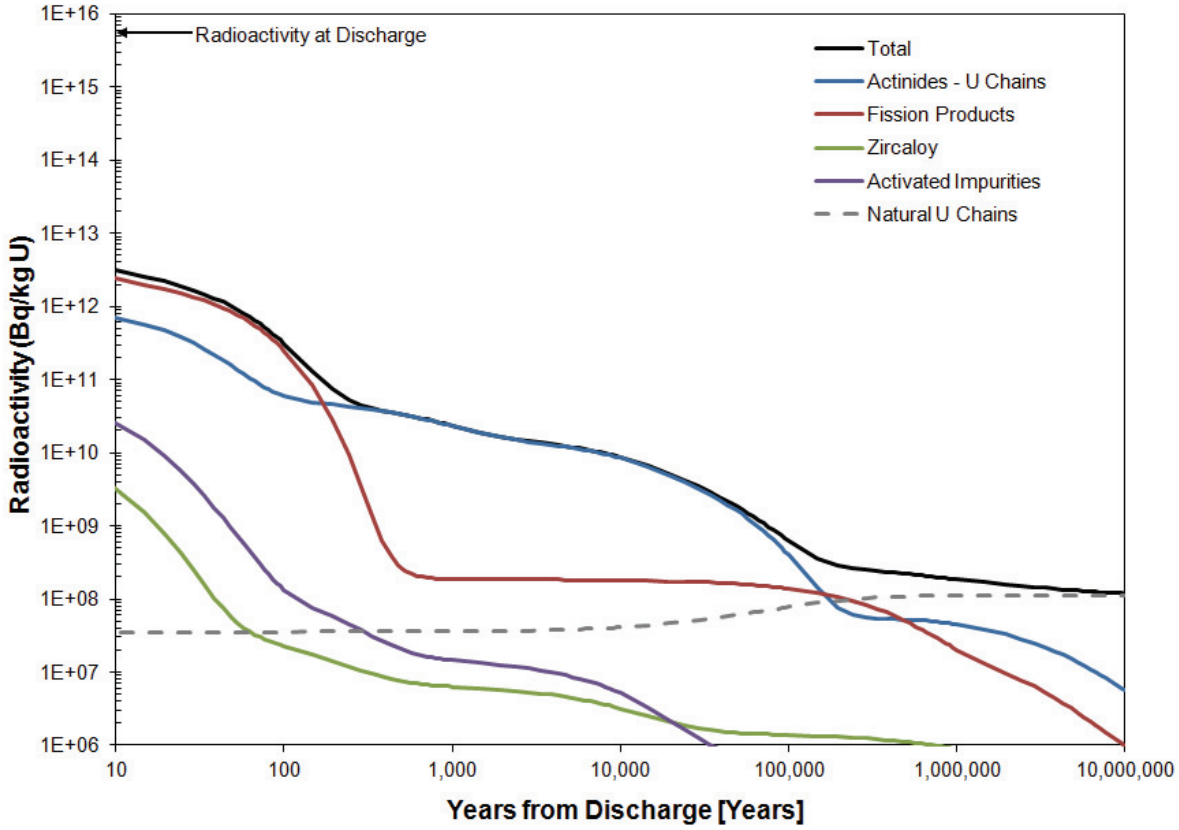

Note: U Chains represents radioactivity from uranium in fuel, including all progeny.

Figure 5-1: Radioactivity of Used CANDU Fuel (220 MWh/kgU burnup)

During the first year out of the reactor, the overall radioactivity decreases to about 1% of its initial value, and after about 100 years it decreases to 0.01% of its initial value. For the first 500 years, the total radioactivity of the fuel would be dominated by numerous short-lived fission products, most of which are gamma emitters; thereafter, it would be dominated by long-lived actinides, including uranium, many of which decay by emission of alpha particles. After about a million years, the total radioactivity in fuel would have declined to levels that are equivalent to that found in naturally occurring uranium.

Radioactive decay would gradually change the radionuclide composition of the used fuel. The radionuclide inventory, radiation output and heat output can be calculated as a function of time, as illustrated in Figure 5-2 for the radionuclide inventory. The greatest change in the

composition of the used fuel is a pronounced decrease in fission products after about 500 years. Nevertheless, over a million-year timeframe all of the changes resulting from radioactive decay would represent only a modest change in the composition of the fuel, of which about 98% would persist as uranium and oxygen.

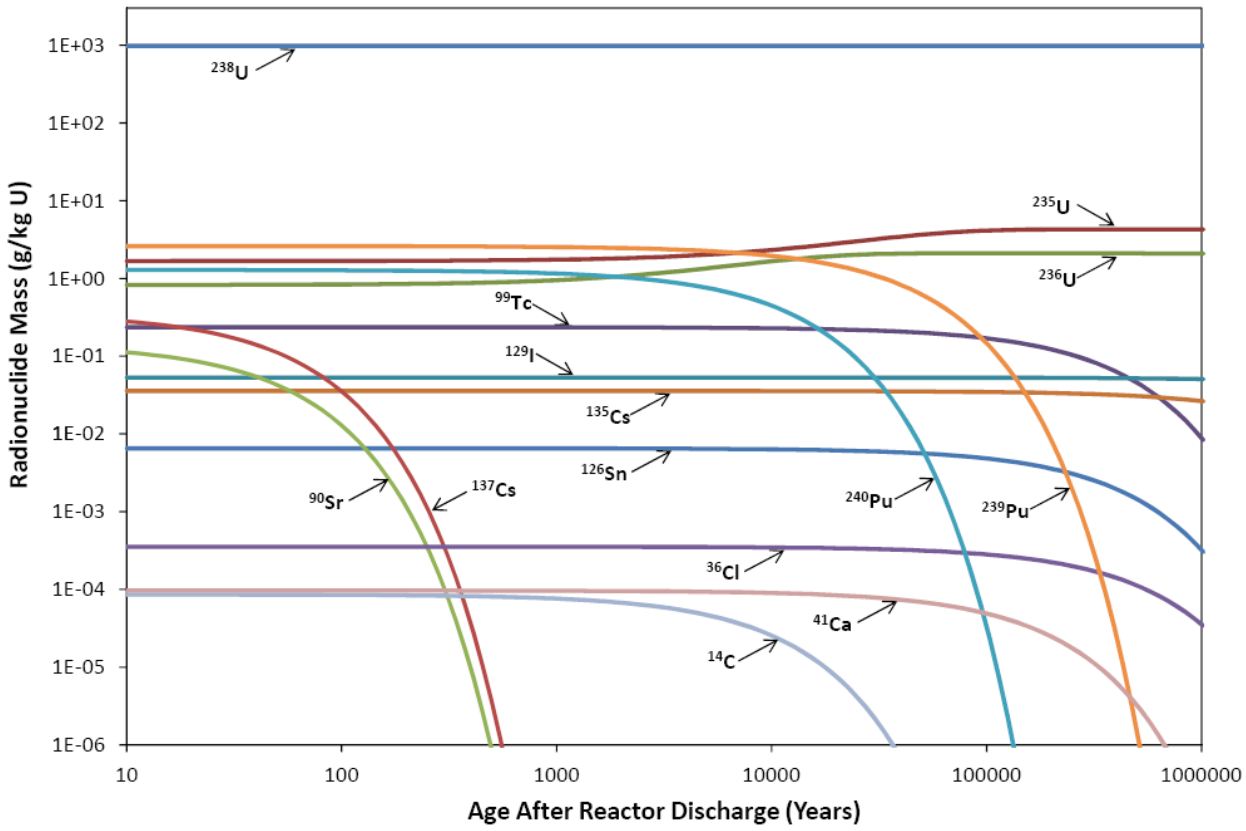

Note: Figure is based on data taken from Tait et al. (2000).

Figure 5-2: Amounts of Key Long-Lived Radionuclides in Used Fuel (220 MWh/kg U burnup)

5.1.2 Changes in Temperature

Radioactive decay of the fuel is accompanied by alpha, beta and gamma radiation that is largely absorbed by the fuel itself and converted to heat. Immediately after being removed from a power reactor, a reference used fuel bundle would release about 27,000 watts of heat. This heat output rapidly decreases. After 10 years, the thermal output has decreased to 5.4 watts and after 30 years about 3.5 watts. The minimum used fuel age at the time of placement is 30 years out of reactor.

Figure 5-3 illustrates the time dependence of thermal power for a container with 360 fuel bundles. Around 10,000 years after placement, the heat output of the entire container would be approximately that of a single 60-watt light bulb. It may be noted that the heat output of the used fuel after 10 years is low enough that the containers can be passively cooled; that is, they do not require active water cooling.

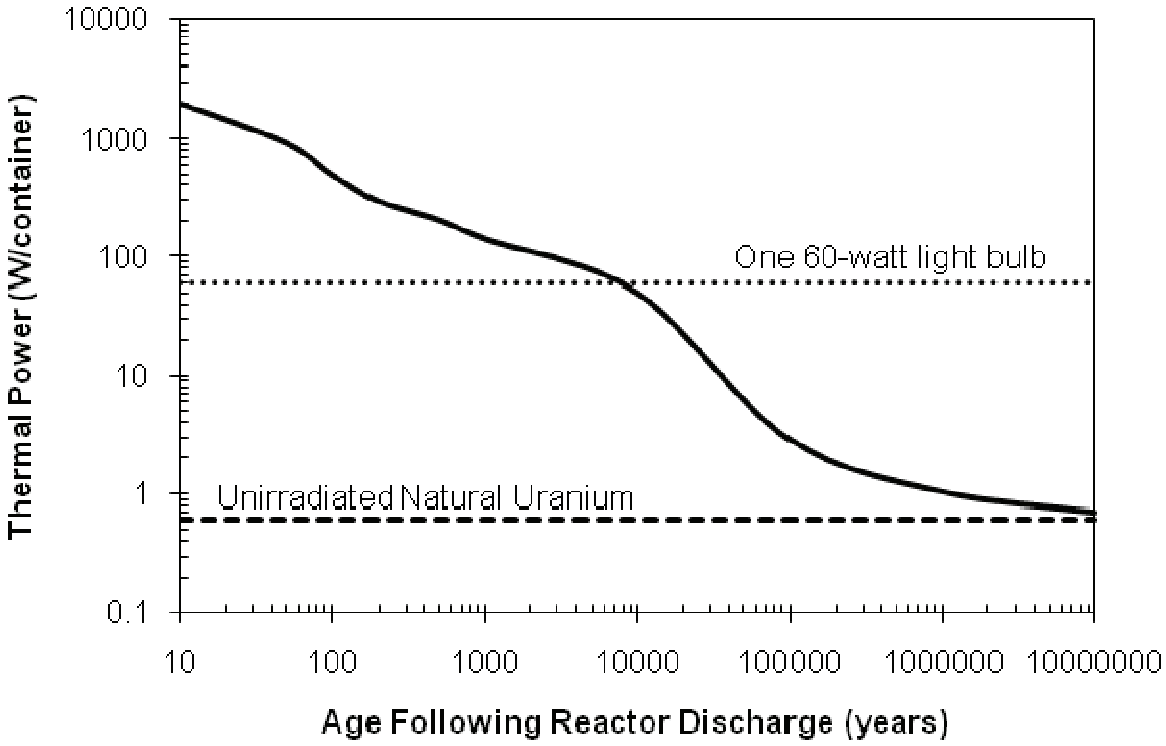

Figure 5-3: Heat Output of a Used Fuel Container with 360 Used Fuel Bundles

The temperature of the container's outer surface will increase up to 120°C after placement (see Section 5.2.4). The temperature of the used fuel bundles inside the container is determined largely by the internal container design, which transfers heat from the bundles to the container surface. The used fuel temperature inside the reference container, loaded with 30-year-cooled used CANDU fuel, would not exceed 200°C. Temperature measurements of used fuel inside concrete storage containers suggest that, more likely, the interior temperature would be less than about 150°C. The maximum temperature of the used fuel bundles would be attained within about 30 years after placement in the repository.

5.1.3 Changes in the UO_2

In the dry, inert gas environment inside the sealed containers, there are few processes that would significantly alter the condition of the used fuel assemblies, even over long times.

5.1.3.1 Radionuclide Diffusion

The crystalline structure of the UO_2 would experience radiation damage due to alpha-recoil during storage and after placement in a repository, and temperatures would not be high enough to ensure annealing of the damage. Radiation damage has the potential to increase the rate at which gaseous species diffuse through the UO_2 fuel; however, theoretical and experimental assessments (Ferry et al. 2008) indicate that this effect is small and there is little redistribution of radionuclides within the fuel under repository conditions.

5.1.3.2 Changes in the Oxidation State of Fuel

In some cases, radioactive decay results in the formation of an element with a higher oxidation valence than that of the parent radionuclide. In principle this could modify the oxygen potential and oxidation state of the UO_2 matrix, in turn affecting diffusion coefficients for radionuclides. Thermal diffusion coefficients of radionuclides are small at repository temperatures, but increase as the oxygen/metal (O/M) ratio of the fuel increases. However, any changes in CANDU fuel are expected to be quite small, from O/M ~ 2.001 to 2.010 or less, and this would not significantly affect thermal diffusion coefficients.

The oxidation state of the fuel potentially could also be changed by the reaction of UO_2 and Zr to produce ZrO_2, which is more stable thermodynamically than UO_2. Where the cladding and UO_2 are in direct contact, the Zr eventually would reduce UO_2 to U by solid-state diffusion of oxygen atoms. This process is unlikely to be significant for used fuel due to the small amount of Zr present (10% of UO_2) and very slow solid-state diffusion rates at repository temperatures (McMurry et al. 2003).

5.1.3.3 Build-Up of He Gas

Alpha decay results in the formation of helium (He) atoms in the used fuel. Because helium is stable (non-radioactive) and unreactive with other elements, the total amount of helium gas in the fuel elements would increase over time. Figure 5-4 compares the effective volume of helium gas that would be produced in a CANDU fuel element with the volume of fission gases (essentially the radionuclides of the noble gases Kr and Xe) present in the same element, assuming that none of the gases are retained in the UO_2 matrix. The fission gases formed during irradiation in the nuclear reactor, and their amount (except for radioactive decay) would be constant over time. In contrast, after about 30,000 years, the amount of helium would be equal to that of the fission gases, so that the total amount of gas present would be double that of the initial conditions. After about one million years, the rate at which helium was being produced in the fuel would slow to a value corresponding to the decay of natural uranium and its progeny, but the total amount of helium within the fuel element would continue to increase.

Under repository temperatures, He release from the UO_2 grains to the grain boundaries would be relatively low, so that helium would accumulate within the grains. For low burnup fuel (like CANDU fuel), the quantity of He produced is not sufficient to induce micro-cracking of grains (Ferry et al. 2008), which is the first step before any significant He release to grain boundaries occurs. Thus, the microstructure of CANDU fuel should not significantly evolve with He accumulation, and build-up of He gas within the void volume of the fuel element would not occur (see also Section 5.1.4.1).

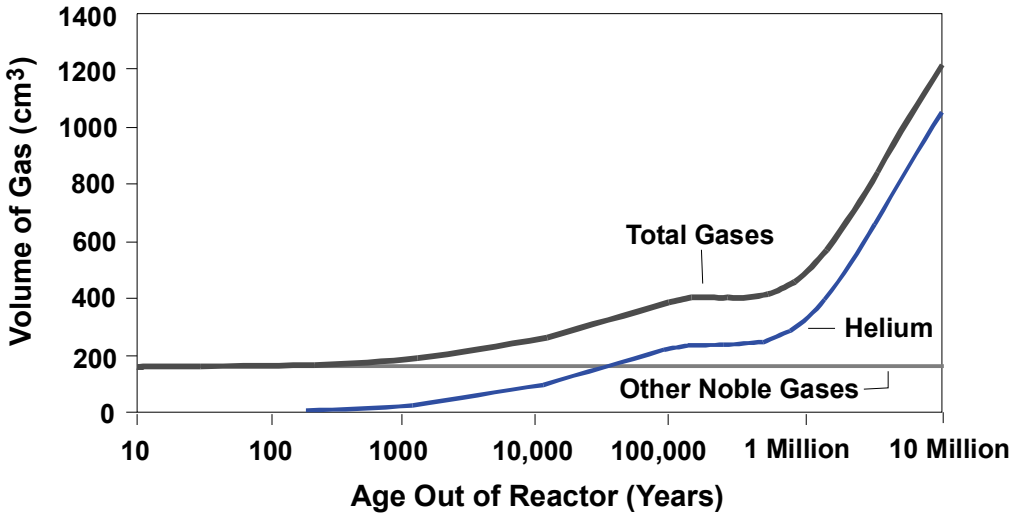

Note: Figure from McMurry et al. (2003).

Figure 5-4: Equivalent Volume of Gas at Standard Temperature and Pressure Produced in a CANDU Fuel Element (220 MWh/kgU burnup)

5.1.3.4 Alpha Radiation Damage

During radioactive decay, the crystalline matrix of the used fuel would experience localized damage to the crystal lattice from the emission of alpha particles, which travel only short distances from the nucleus but have high energy and a relatively large mass. The implications for radionuclide diffusion have been discussed above.

Natural analogue evidence suggests that alpha irradiation damage would not cause used fuel to crumble, even after extremely long times. At Oklo in western Africa, uraninite (UO_2) ore deposits underwent spontaneous nuclear fission reactions more than two billion years ago. Although affected by brecciation during fission and by subsequent hydrothermal alteration in some cases, the uraninite is still granular and massive (Jensen and Ewing 2001).

5.1.4 Changes in the Zircaloy Cladding

Intact cladding would provide a further barrier to water contacting the fuel or to radionuclide release. A summary of relevant work associated with changes in the Zircaloy cladding is presented below. Some of the changes could lead to cracking or rupture of the cladding. However, even if it occurred, the cracking or rupture of the cladding inside a sealed container would have few consequences. Helium from alpha decay and fission gases would, for example, merely be released into the larger volume of the container interior, and the fuel pellets would be exposed to the inert gas atmosphere inside the container. Although cracked, the cladding itself would continue to provide physical support to most of the used fuel pellets in the fuel element.

5.1.4.1 Zircaloy Creep and Rupture

The most significant physical process potentially affecting the cladding over time is likely to be long-term creep of the Zircaloy, as caused by stresses created by pressure build up inside the sealed fuel elements due to the decay-related production of helium gas. The mechanisms and extent of creep processes in Zircaloy are uncertain. Most creep data for cladding are from high stress, short-term experiments (McMurry et al. 2003).

Conservative calculations, assuming the He gas migrates to the fuel-cladding gap, suggest that given sufficient time, the gas pressure inside the sealed fuel element would increase to the point that the Zircaloy cladding would rupture. However, as indicated in Section 5.1.3.3, it is unlikely that the He would escape from the fuel grains and increase the pressure within the cladding. Hence, He generation should not lead to rupture of the Zircaloy cladding on relevant time scales.

5.1.4.2 Uniform Corrosion (Oxidation) of Cladding

The corrosion properties of Zircaloy cladding have been determined from almost 50 years of experience with reactor operation, pool storage, and dry storage of used fuel. When Zircaloy is exposed to air, a thin passive zirconium oxide film forms rapidly on its surface which then inhibits further corrosion. Experiments were conducted that examined the condition of used CANDU fuel under dry storage conditions over several decades. It was found that the average outer and inner surface zirconium oxide thickness, after 19 years of dry air storage at seasonally varying temperatures, was about 6 μm, slightly more than an average pre-storage oxide layer thickness of about 4 μm. Therefore, most of the uniform corrosion of the Zircaloy would have occurred prior to placement (McMurry et al. 2003). Shoesmith and Zagidulin (2010) also indicate that passive corrosion rates of Zircaloy would be very low.

The fuel containers are filled with an inert gas. In the absence of oxygen, further growth of a uniform oxidation film on the cladding cannot occur.

5.1.4.3 Hydrogen Absorption and Zircaloy Embrittlement

As-fabricated Zircaloy cladding has a residual hydrogen concentration of about 25 μg/g. After use in a CANDU reactor, the cladding also contains up to about 100 μg/g of deuterium, absorbed in-reactor from the heavy water coolant, in addition to trace amounts of tritium. The hydrogen precipitates as zirconium hydrides in the Zircaloy after the fuel is removed from the reactor and cools. The hydrides result in a less ductile (more brittle) Zircaloy that is more susceptible to fracturing (McMurry et al. 2003).

In intact used fuel containers that had been dried and backfilled with an inert gas prior to sealing, little or no hydrogen would be available for reaction with the cladding after placement. Small amounts of H_2O may be present as residual humidity or as liquid water (e.g., in defected fuel elements). Hydrogen would be released from this water via radiolysis or as the water was consumed by corrosion of the steel interior of the container, which could be absorbed by the Zircaloy and also increase the amount of hydrides present.

5.1.4.4 Delayed Hydride Cracking

The main factors required for delayed hydride cracking are sufficient tensile stress, a defect site to concentrate the stress, and sufficient hydrogen in the metal. Even where hydrogen is distributed in relatively low concentrations in Zircaloy, under certain conditions of stress and temperature the hydrogen can diffuse through the metal to form locally high hydrogen concentrations that lead to the precipitation of zirconium hydrides. These hydrides are brittle and tend to crack.

Detailed examination of used CANDU fuel stored in dry air at 150°C for 15 years indicates that highly stressed areas in the cladding must be present for delayed hydride cracking to occur. Generally, the most stressed areas in cladding are the heat-affected zones at and near welds. The timing and extent of delayed hydride cracking in a repository would be controlled by diffusion of hydrogen to the crack tip. The susceptibility of cladding to delayed hydride cracking is unlikely to be significant at temperatures inside the container (Freire-Canosa 2011).

5.1.4.5 Stress Corrosion Cracking

Stress corrosion cracking of zirconium metal occurs in oxidizing environments, in strongly oxidizing neutral saline solutions, and in the presence of some metals and gases such as cesium and iodine. Little work has been directed towards the study of stress corrosion cracking of Zircaloy under conditions such as would occur in a deep geological repository. However, the dry environment inside an unbreached container would not contain sufficient quantities of strongly oxidizing agents (such as nitric acid or hydrogen peroxide) or of iodine gas from fuel elements to induce stress corrosion cracking (McMurry et al. 2003). Moreover, CANLUB inhibits the diffusion of iodine into the Zircaloy. In addition, in CANDU fuel almost all of the iodine in the fuel gap is present as cesium iodide (CsI) and so is unable to form the zirconium iodides that are thought to be the chemical precursors of stress corrosion cracking (OPG 2002).

5.1.4.6 Pellet Swelling and Cladding “Unzipping”

Cladding “unzipping” is driven by the expansion of a fuel pellet (pellet swelling) in proximity to a defect in the cladding, causing a strain in the cladding that extends the size of the defect. If the two processes (i.e., swelling and rupture) perpetuate each other, the deformation would propagate in increments over time (“unzipping”). One example of this phenomenon occurs when water enters a fuel element through a pinhole defect and reacts with the fuel, transforming the UO_2 into the less-dense phase U_3O_8. The additional stress exerted on the defect site by the expansion in the volume of the pellet then leads to further cracking of the cladding. More water is then able to enter the fuel element, which in turn leads to more alteration, more swelling, and further deformation of the cladding. In intact containers, there would be no source of water to initiate pellet swelling, so unzipping by this process can be disregarded.

5.1.5 Other Processes

Several other processes expected to have minimal or no effects on the evolution of the used fuel are indicated below.

5.1.5.1 Criticality

Criticality is not an issue for several reasons, the most important of which is that CANDU fuel cannot become critical without the presence of heavy water, regardless of the density or age of the fuel. Ordinary water is insufficient to induce criticality. Moreover, water would have no access to the used fuel in intact containers and so it could not act as a moderator.

5.1.5.2 Hydraulic Processes

As long as the containers remain intact, there are no hydraulic processes affecting the used fuel assemblies.

5.1.5.3 Mechanical Stresses

As long as the fuel bundles are supported by baskets in intact containers, they are not subjected to significant load-bearing stresses. If tremors associated with earthquakes caused the fuel bundles to vibrate sufficiently, presumably some of the fuel pellets or the cladding could be damaged. The damaged material would remain in an intact container, and the overall evolution of the used fuel bundles would not be significantly changed.

5.1.5.4 Biological Processes

No changes arising from biological processes are expected because the combination of high temperatures, significant radiation fields, and the absence of water and organic carbon would exclude any biological reactions inside a container.

5.1.6 Confidence

At the time of placement in a deep geological repository, the physical properties of the used fuel and the inventory of radionuclides would be well characterized. Radionuclide decay constants are generally well defined, and so the changes in the inventory and the related changes in decay heat over time can be calculated with a high degree of confidence.

The rates of several processes, such as the diffusion of helium in UO_2 and of hydrogen in Zircaloy, are influenced by temperature. These rates would be low since the temperature inside the container would be at most several tens of degrees hotter than the exterior container surface, which would only increase up to 120°C, and drop to ambient host rock temperatures on a 100,000 year timeframe.

In the dry and closed-system environment provided by an intact and load-bearing container, the physical condition of the fuel is not expected to change significantly over long periods of time. The only significant factor would be container failure, which is discussed later.

5.2 Long-Term Evolution of the Repository Environment

5.2.1 Repository-Induced Disturbances

Disturbances to the geosphere as a result of construction and operation of a repository include those induced by excavation (damage to surrounding host rock and development of unsaturated conditions within the host rock) and due to placement of the waste and engineered systems, including temperature changes, changes to near-field chemistry and potential gas generation. These processes are summarized in Table 5-3.

Table 5-3: Processes with a Potential Influence on the Near-Field Geosphere

PROCESS	POTENTIAL INFLUENCE
RADIATION	
None	• None
THERMAL	
Heat transport from repository	• Increased porewater pressure in rock around repository • Altered hydraulic conductivity around repository
HYDRAULIC & PNEUMATIC	
Excavation-related drawdown along shaft and access tunnels	• Temporary desaturated, oxygenated zone around vault
Groundwater flow	• Saturation of repository • Mass transfer of aqueous chemical species at repository interface
MECHANICAL	
Excavation of shaft and rooms	• Formation of higher permeability excavation damaged zone in shaft and rooms
Thermal stresses	• Microcracking
CHEMICAL	
Reactions with redox-sensitive minerals	• Initial partial oxidation of some minerals • Long-term maintenance of reducing conditions at repository depth
Reactions with repository porewater	• Precipitation of secondary minerals near interface • Steel corrosion and gas generation
BIOLOGICAL	
Microbial activity	• Maintenance of redox conditions at repository depth

Notes: Processes listed are those that are most likely to have a notable effect on the near-field geosphere, over a time scale of one million years.

5.2.2 Excavation Damaged Zone

The zone of rock immediately surrounding the placement rooms, tunnels, shafts and other underground openings that is mechanically disturbed during excavation is referred to as the excavation damaged zone (EDZ). This zone is characterized by structural changes in the rock, such as the formation of microcracks, along with a potential increased permeability. The shape, extent and properties of this zone depend on factors such as the nature of the host rock, the ground stress regime, the geometry of the excavation, the excavation method and the strength of the rock. A summary of EDZ classification and in-situ observations in sedimentary rock is described in a literature review conducted by Fracture Systems (2011).

In tunnels constructed using drill-and-blast techniques, the explosive charge density has been shown to influence the extent and severity of damage in the near-field. There is evidence to suggest that connected permeability associated with blast-induced damage may not be continuous across blast rounds in environments with a high strength to stress ratio (Fracture Systems 2011, Simmons 1992). This is also supported by recent in-situ work in crystalline rock (Posiva 2010). Because the EDZ behaves hydraulically as a serial system, a local increase in EDZ permeability does not translate to a continuous zone of connected high permeability along the axes of shafts and tunnels.

For the sedimentary sequence considered in this report (Chapter 2), the maximum EDZ is expected to occur in the weak Cabot Head shale and is anticipated to be about a half of the shaft excavation diameter (NWMO 2011). Fracture Systems (2011) found that regardless of the damage mechanism, the extent of EDZ measured around underground openings is typically less than 1.5 times the radius of the openings. Smaller EDZ extent would occur around the emplacement rooms within the stronger host rock of the Cobourg Formation.

Perturbations to the geosphere, such as glaciation and earthquakes (see Section 5.5), are not expected to have any major structural effects on the long-term behaviour of the EDZ due the confining pressure of the backfill materials. The EDZ may also have some tendency to seal itself over time in rock formations with high clay content - several mechanisms, including the impact of increased stress on the EDZ due to swelling of backfill materials, are discussed in Bock et al. (2010). These mechanisms would be assessed for a specific site.

5.2.3 Repository Saturation

During the construction and operational phases, groundwater inflows into the excavations will be managed through pumping. At a depth of 500 m below the surface, the hydrostatic pressure within a water-saturated rock mass is about 6 MPa. A sharply defined hydraulic gradient would exist between the geosphere at repository depth and the excavated openings (rooms, cross-cuts and drifts), which would be at atmospheric pressure. This difference would tend to draw porewater through the host rock into the open spaces of the repository. However, porewater movement through the low permeability, low porosity host rock considered in this study is expected to be extremely slow.

Any groundwater seeping into the repository from the surrounding rock will be pumped away to maintain dry conditions within excavated openings. Evaporation would tend to keep the rock surfaces in the excavated openings dry, and may induce partial desaturation of the rock immediately adjacent to the openings (i.e., within the excavation damaged zone and host rock

near the repository). Any dewatering during operation and monitoring of the repository will be of relatively short duration and will result in groundwater flow(s) toward the repository until pumping activities cease following repository closure. In the postclosure phase, water will move towards the repository and the near-field will slowly resaturate.

The process of saturation may require a long time, as ingress of water may be restricted because of low host rock permeabilities and the use of grouting and seals. Furthermore, the rate of resaturation will likely vary at different locations within the repository. In particular, local heating from the containers, swelling of buffer materials, and local gas generation could delay resaturation. A "pre-saturated period" can be defined, which covers the time period from when the containers are first placed in a repository until their exterior surface comes in contact with fully saturated sealing materials. In low permeability sedimentary rock, it is likely that this pre-saturated period would last at least 10,000 years (see Section 5.4.1).

At the time that the placement rooms are backfilled and sealed, they would contain partially saturated buffer. Voids (porosity) in the sealing materials would contain trapped air. Heat from the container would cause the nearby buffer to dry out, and condensation of the water vapour would occur in cooler portions of the buffer near the rock. The relative humidity of the trapped air in the sealing materials near a container is of interest because corrosion of copper and iron in air is observed to be slow or nonexistent at relative humidities of less than about 60%.

5.2.4 Temperature

Among the first changes to occur in a repository after container placement is an increase in temperature of the sealing materials around the containers. The exact distribution and time dependence of temperatures in a repository depends on design details and site-specific conditions.

Figure 5-5 shows an example of thermal profiles for a region around a used fuel container placed in a limestone setting (horizontal tunnel placement). A range of points from the exterior surface of a container out through the buffer and into the near-field rock is illustrated.

Key points to note in Figure 5-5 are:

- The temperature of sealing materials adjacent to the surface of the container increases rapidly at first, within days or weeks of placement.

- The maximum temperature of the buffer occurs within the first 30 years and remains below 120^{o}C. More than 0.3 m of the buffer remains below 100^{o}C.

- Within about one hundred years, reflecting in part the decay of the heat source, there is an appreciable reduction in peak temperatures.

- After several thousand years, the thermal evolution is marked by a slow, steady cooling. Temperatures return to near-ambient conditions within about 100,000 years.

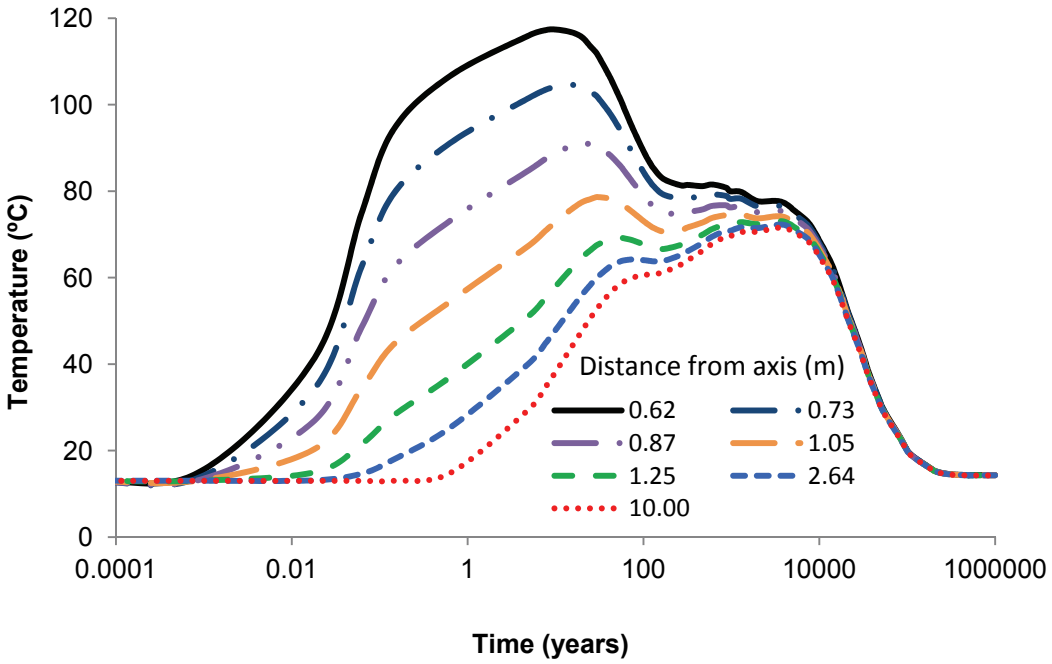

Note: Figure from Guo (2010). The solid black line is the container surface and the dashed green line is the rock wall.

Figure 5-5: Illustrative Example of the Range of Temperature Variation over Time in a Placement Room

5.2.5 Near-Field Chemistry

During repository excavation and operations, oxidizing conditions would develop in the porewaters of the adjacent rock due to exposure to the air in the repository. This could result in some oxidizing reactions, such as partial conversion of sulphides in the rock into sulphates.

However, after the rooms are closed and sealed, the redox conditions within the near-field will evolve back to an anaerobic state. Oxygen is consumed by a number of reactions, including reactions with residual iron in the rooms (e.g., rock bolts) and with copper on the containers (Reaction (5-1)), as well as by reactions with microbes and with redox-sensitive materials throughout the buffer.

$$\mathrm{Cu} + \mathrm{Air} \rightarrow \mathrm{Cu_2O}, \mathrm{CuO} \qquad (5\text{-}1)$$

Most of the repository-related changes in groundwater chemistry would occur at or near the interface between the geosphere and the sealing materials. The diffusion of porewater components, or the mixing of fluids at the repository-geosphere interface, may result in the precipitation of secondary mineral phases at the interface or in nearby fractures in the geosphere. A broader effect would be due to heat from the repository, which would raise the temperature of water in the geosphere. This could result in a slightly greater dissolution rate for some minerals. Later, as the waters cool, the precipitation of secondary phases, such as amorphous silica and calcite, would occur. The extent and significance of the precipitation would depend on site-specific characteristics, such as the distribution and dimensions of the fractures. In the long term, the geosphere, as a whole, would act as a strong buffer in response to chemical and thermal perturbations from a repository. As the pore fluids in the repository evolve to a composition more similar to that of the surrounding groundwater, and as temperatures in the geosphere gradually return to ambient levels, the chemical conditions in the geosphere would be diminishingly affected by the presence of a repository.

5.2.6 Steel Corrosion and Gas Generation

In principle, corrosion of carbon steel (C steel) in underground facilities has a number of potential impacts on the performance of the repository system. Dissolved ferrous species produced as a result of corrosion reactions can interact with bentonite and convert swelling smectite clays to non-swelling illitic forms, resulting in a partial loss of swelling capacity (Wersin et al. 2007). Anaerobic corrosion will result in the generation of hydrogen that may form a gaseous H_2 phase in the repository, which will affect repository pressures and may impact the migration of radionuclides. This latter effect may impact the viability of some microbial species, favouring anaerobic species that can use hydrogen as an energy source.

Accordingly, this section is focussed primarily on the estimation of the rate of H_2 generation due to corrosion of the carbon steel in the repository. In the normal evolution of a repository, this process is relevant because of the presence of steel structures such as rock bolts, supports or other infrastructure that is necessary for the safe construction of a repository; clearly, this presumes that such steel is left behind after used fuel container placement.

Owing to the very low gas transport that can occur in Canadian sedimentary environments, the steel corrosion processes have been examined in great detail below. The volume of steel available for corrosion within the normal evolution scenario is sufficiently small that the relatively small quantiy of hydrogen gas produced does not have the potential to alter the repository characteristics. However, because of the use of carbon steel as a container material, the impact of hydrogen generation on the repository is considered within the All Containers Fail scenario in Chapter 8.

The corrosion behaviour of the steel components will change with time as the environment in the repository evolves. From a corrosion perspective, the most important environmental factors are the temperature, the redox conditions, the degree of saturation of the repository material, and the composition of the pore water in contact with the steel components. For a DGR in low-permeability sedimentary host rock, saturation of the DGR may take tens of thousands of years. This slow saturation has led to the definition of four phases in the evolution of the environment, as described below, as well as in detail within other NWMO references (Suckling et al. 2012 and King 2013).

Phase 1

An early aerobic period prior to the onset of aqueous corrosion. Immediately following closure of the repository, it is assumed that saturation of the Engineered Barrier System (EBS) has not yet occurred, that no liquid water is available for corrosion, and that the EBS near the UFCs remains unsaturated due to high temperatures and gas generation. Oxygen is initially present in the in the unsaturated pore space when the EBS is emplaced. If relative humidity is also low, corrosion will be limited to slow air oxidation. This unsaturated aerobic corrosion is modelled as follows:

$$4Fe + 3O_2 \rightarrow 2Fe_2O_3 \tag{5-2}$$

$$R_1 = \frac{A_1 \exp\left(-\frac{5864}{T}\right)}{t^{1/2}} \mu m \cdot a^{-1} \tag{5-3}$$

where R_1 is the rate of corrosion in microns per year, T is the Kelvin temperature, and t is the time in years and the pre-exponential term A_1 is assigned a best-estimate value, as well as lower and upper bounds. Although there are relatively few data available, it is not unreasonable to expect that the lower and upper bound corrosion rates might differ by a factor of ten. In the absence of other information, it is assumed here that the best-estimate value is the (geometric) mean of the lower and upper bound values. Thus, the values of A_1 for the lower and upper bound estimates are 4.279 x 10^5 μm/a and 4.279 x 10^6 μm/a, respectively (King 2013). Aqueous corrosion is possible above a critical or threshold relative humidity (RH) that is determined by the nature of the surface and the presence of surface contaminants. As relative humidity increases above a lower threshold value, the consumption of carbon steel by Phase 1 corrosion will decrease until an upper RH threshold is reached, upon which Phase 1 corrosion stops. For this work, the lower RH threshold was set to 60% and the upper RH threshold was 80% (Suckling et al. 2012).

Phase 2

An unsaturated aerobic phase following the condensation of liquid water on the steel surface. During Phase 1, if relative humidity rises above 60-80%, aerobic aqueous corrosion may instead proceed according to the following relationships:

$$4Fe + 3O_2 + 2H_2O \rightarrow 4FeOOH \tag{5-4}$$

$$R_2 = A_2 \exp\left(-\frac{1340}{T}\right) \ \mu m \cdot a^{-1} \tag{5-5}$$

where A_2 has a best-estimate value of 4,168 μm/a, and values of 1,042 μm/a and 10,420 μm/a for the lower and upper bound fits, respectively. As relative humidity increases above a lower threshold value (60%), the consumption of carbon steel by Phase 2 corrosion will gradually increase until an upper RH threshold is reached (80%), at which point full Phase 2 corrosion is calculated. Note that Phase 1 and Phase 2 corrosion overlap as the relative humidity increases from 60% to 80%.

Phase 3

An unsaturated anaerobic phase will occur following the consumption of the oxygen and prior to the full resaturation of the repository; the gaseous phase will be predominantly N_2, H_2 and H_2O vapour. Corrosion during this period is supported by the cathodic reduction of water accompanied by the evolution of hydrogen. Detailed surface analysis indicates that corrosion under unsaturated anaerobic conditions forms magnetite as the predominant corrosion product, which is represented in the model as follows:

$$3Fe + 4H_2O \rightarrow Fe_3O_4 + 4H_2 \tag{5-6}$$

$$R_3 = A_3 \exp\left(-\frac{5332}{T}\right) \ \mu m \cdot a^{-1} \tag{5-7}$$

where the pre-exponential term A_3 is assigned a best-estimate value, as well as lower and upper bounds. The best-estimate value for the pre-exponential term A_3 is equal to 8.89×10^6 μm/a. Although there are relatively few data available, it is not unreasonable to expect that the lower and upper bound corrosion rates under anaerobic unsaturated conditions might differ by a factor of ten. In the absence of other information, it is assumed here that the best-estimate value is the (geometric) mean of the lower and upper bound values. Thus, the values of A_3 for the lower and upper bound estimates are 2.81×10^6 μm/a and 2.81×10^7 μm/a, respectively (King 2013).

The rate of reaction is affected by relative humidity (RH), which has upper and lower bounding conditions, $RH_{CRIT,U}$ and $RH_{CRIT,L}$:

for $RH \leq RH_{CRIT,L}$ Rate = 0 (5-8)

for $RH_{CRIT,L} < RH \leq RH_{CRIT,U}$ $$\text{Rate} = R_3\left(\frac{RH - RH_{CRIT,L}}{RH_{CRIT,U} - RH_{CRIT,L}}\right) \tag{5-9}$$

and

for $RH > RH_{CRIT,U}$ Rate = R_3 (5-10)

where the values of best-estimate and upper- and lower-bound values for $RH_{CRIT,L}$ and $RH_{CRIT,U}$ are dependent on the cationic content of the buffer system, but may be as low as 0.1 and 0.2, respectively, for highly saline systems. Thus, for RHs as low as 20%, the reaction could proceed at its maximum rate.

Phase 4

A long-term saturated anaerobic phase once the EBS material has become completely saturated by groundwater. As with Phase 3, corrosion during Phase 4 is supported by the cathodic reduction of water accompanied by the evolution of hydrogen. In the presence of compacted bentonite under saturated conditions, in addition to the reaction shown in (5-6),

where magnetite (Fe_3O_4) is the corrosion product, carbon steel corrodes with the formation of a carbonate-containing corrosion product. The source of carbonate is calcite and other carbonate minerals assumed to be present in the EBS material. The overall stoichiometry of the corrosion reaction and the corrosion rate for Phase 4 are modelled according to the following relationships:

$$Fe + CO_3^{2-} + H_2O \rightarrow FeCO_3 + H_2 + 2OH^- \quad (5\text{-}11)$$

$$R_4 = A_4 \exp\left(-\frac{2435}{T}\right) \ \mu m \cdot a^{-1} \quad (5\text{-}12)$$

For the best-estimate corrosion rate, A_4 = 8,200 µm/a; A_4 = 16,400 µm/a for the upper bound and A_4 = 2,050 µm/a for the lower bound (King 2013).

It is important to note that these four phases do not necessarily occur sequentially. Phases 1 and 2 both occur under aerobic conditions and the degree to which the Phase 1 and Phase 2 corrosion processes are active depends on the relative humidity. The Phase 3 and 4 corrosion processes proceed under anaerobic conditions after Phase 1 and Phase 2. The degree to which the Phase 3 and Phase 4 corrosion processes are active depends on whether or not liquid water has moved through to the steel components or not. As noted above, the Phase 3 process also depends on relative humidity.

The vast majority of H_2 that will be produced in the repository will result from the uniform corrosion of C steel during the (unsaturated and saturated) anaerobic phase. Hydrogen can be produced under aerobic conditions due to the reduction of H^+ in acidic environments in pits, crevices, or porous corrosion products formed as a result of the hydrolysis of Fe(III) species (Akiyama et al. 2010, Tsuru et al. 2005). Local reduction of H^+ may lead to enhanced hydrogen absorption and environmentally assisted cracking (King 2009a) but will not lead to the generation of significant H_2 and is not considered further here.

Hydrogen generated by corrosion can undergo a number of subsequent processes. The H_2 that is evolved could be consumed by microbes (Pedersen 2000) in those parts of the near- and far-fields in which the environment is conducive to microbial activity (namely a water activity greater than 0.96, Stroes-Gascoyne et al. 2006, Stroes-Gascoyne and Hamon 2008). Another fraction of the hydrogen will be absorbed by the C steel as atomic H, either from adsorbed H atoms prior to their evolution as H_2 or via the dissociative absorption of gaseous H_2; however, eventually this hydrogen will be released as the steel continues to corrode.

In addition to the evolution of the redox conditions and the degree of saturation, the temperature will also change during these different phases. The precise time dependence of the repository temperature will depend on the rate of saturation, which is not known a priori. However, in general, it is clear that Phases 1 and 2 will be warmer than Phase 3 and 4, with Phase 3 and 4 encompassing the period of long-term ambient conditions.

The rate of oxidation of carbon steel in dry air (Phase 1) is low at the temperatures of interest (maximum of approximately 120°C) and will result in only a few microns of corrosion. Although the rate of aerobic corrosion in the presence of moisture under unsaturated conditions (Phase 2) is higher, the extent of corrosion is limited by the initial inventory of trapped oxygen in the repository. Therefore, upon the establishment of high humidity Phase 2 conditions, the

duration of aerobic corrosion is predicted to be less than 1 year. This has been confirmed in all model results to date.

Of most interest is the rate of anaerobic corrosion under first unsaturated (Phase 3) and subsequently saturated (Phase 4) conditions. Based on the review of published corrosion studies, these rates are temperature dependent; the corrosion rate decreases with time as the container cools.

A number of other environmental parameters, in addition to the temperature, relative humidity, and redox conditions, also affect the uniform corrosion behaviour, including:

Pore-water chemistry: Under saturated conditions, the steel will be in contact with EBS pore water. At least initially, the composition of the pore water may differ from that of the groundwater. Eventually, however, the pore water will equilibrate with the ground water.

pH: Calcite minerals in the bentonite may effectively buffer the pH in the range pH 7-8.

Mass transport: During the aerobic phase, the rate of corrosion may be limited by the rate of transport of O_2 to the steel surface through low permeable EBS materials.

Radiation: Gamma radiolysis of water will produce oxidizing and reducing radiolysis products. However, the maximum surface absorbed dose rate for a 10-cm-thick C steel UFC will be <1 Gy/a, for which there is no significant effect on the corrosion rate (Shoesmith and King 1999). Steel components more distant from the UFC will certainly see no effect of radiation/radiolysis.

Microbial activity: Microbial activity is suppressed by the presence of saline solutions in compacted bentonite (Stroes-Gascoyne et al. 2006, Stroes-Gascoyne and Hamon 2008). However, since rock bolts and other steel components will reside outside the UFC engineered barrier system, it is possible that halophilic microbial species may accelerate corrosion versus a non-microbially active region of the engineered barrier system.

Stress: Applied and residual stresses affect the environmentally assisted cracking behaviour of the steel but have no effect on uniform corrosion.

Mineral impurities: Mineral impurities in the host rock (e.g., pyrite) will have an insignificant effect on the uniform corrosion behaviour of the container.

As described above, for a repository with intact containers, the only steel available for reaction is material from repository construction and operations, such as rock bolts, that remain in the placement rooms after closure. Little hydrogen would be produced by corrosion of these metals. A quantitative discussion of the effects of gas generation for the All Containers Fail scenario appears in Chapter 8.

5.2.7 Confidence

Excavation Damaged Zone: Estimates of the extent and permeability of the excavation damaged zone are based on investigative findings for other sedimentary rocks; however, actual repository specific data will not be known until in-situ measurements are obtained. Once available, these data will be incorporated into the various assessments together with appropriate allowances for residual uncertainties.

Sensitivity studies indicate that long-term repository performance is not especially sensitive to reasonable variations in EDZ assumptions.

Repository Saturation: The resaturation rate depends on properties of the host rock and engineered barrier materials, temperature, hydraulic gradients, and gas or vapour transport, and so requires coupled models. The modelling would be supported in part through engineering demonstration tests or monitoring of early placement rooms. While there is some inherent uncertainty, long-term repository performance is not particularly sensitive to the actual time of resaturation.

Additional discussion on repository saturation is provided in Section 5.4.1.

Temperature: There is good confidence in results obtained from thermal models over long periods of time and in conservative estimates at shorter times. Some uncertainties exist in temperature predictions for pre-saturation conditions due to varying physical parameters (such as shrinkage or cracks) and moisture content (affecting thermal conductivity) of the material surrounding the container.

Additional discussion on temperature effects is provided in Section 5.1.2, Section 5.3.1.2 and Section 5.4.2.

Near-Field Chemistry: The time at which reducing conditions will be re-established following repository closure is uncertain due to specifics of the complex interactions between groundwater, repository components, and microbial processes.

Regardless of the amount of time required, the total amount of oxygen is limited and it is a given that reducing conditions will be re-established at some point in the postclosure period. Conservative assumptions can be applied in the repository design and analysis process to bound the associated uncertainties to ensure appropriate conclusions concerning repository performance are made.

Additional discussion on chemistry is provided in Section 5.3.1.4, Section 5.3.1.5 and Section 5.4.3.

Steel Corrosion and Gas Generation: Gas generation and migration depends upon host rock properties, the rate at which water enters the repository, the quantity of organic material present, the number and distribution of rock bolts, the degree to which radiolysis of water occurs, the timing and number of container failures, and the corrosion rates. For the bounding case considered in Chapter 8, gas generation from corrosion of all steel inner containers far exceeds that from other sources, so that some of the related uncertainties are not of special concern.

Confidence in the predictions is gained through modelling, comparison of models with international experience and the use of bounding assumptions. The remaining uncertainties can be reduced through the use of improved modelling codes and the adoption of repository designs that cater to gas migration. Research and model development activities continue in Canada and elsewhere with this objective in mind.

5.3 Long-Term Evolution of a Used Fuel Container

As described in Chapter 1, the design of the reference container is consistent with lifetimes in excess of 100,000 years. To achieve such lifetimes, a container must be able to withstand the expected geological evolution from hot, dry and aerobic, to cool, water saturated anaerobic conditions. Within this context, specific effects have been examined as they pertain to the evolution of the used fuel container in a deep geological repository; these are summarized in Section 5.3.1, below. In addition, and in keeping with the safety arguments described in Chapter 1, specific conditions that pertain to a breached container are described in Section 5.3.2, below.

5.3.1 Evolution of Intact Containers

As described in Section 4.3, the reference copper container design for sedimentary rock consists of a copper outer vessel that encloses a steel inner vessel. Upon placement in the repository, the copper outer vessel protects the inner steel vessel from corrosion. The copper outer vessel is not designed to be load-bearing. When the normal 7 MPa load from hydrostatic and swelling pressures is applied to the container, the copper shell would compress onto the steel inner vessel, transferring the external load to the steel inner vessel (Poon et al. 2001). The container is designed to withstand an external isotropic pressure of 45 MPa at 50°C; this value indicates that the container could withstand the additional hydrostatic load exerted at repository depth by a 3,800 m glacier above the repository connecting the container's surface to the top of the glacier by a continuous column of water. Thus, in the analysis of intact containers, many of the specific effects of placement of the containers within the repository are limited to processes that affect the outer copper shell and inner steel vessel. The main processes experienced by the container over time are listed in Table 5-4 and discussed in the succeeding sections.

Table 5-4: Processes with a Potential Influence on the Evolution of Containers

PROCESS	POTENTIAL INFLUENCE
RADIATION	
None	• None
THERMAL	
Heat transfer from fuel to container	• Change in container temperature
HYDRAULIC & PNEUMATIC	
Saturation of repository	• Pressure applied to container • Initiation of aqueous corrosion on container surface
MECHANICAL	
Hydrostatic load and swelling of the buffer	• Stresses on container
Glacial loading	• Stresses on container
Creep	• Deformation of copper shell onto steel inner vessel
CHEMICAL	
Reactions with water and oxygen in sealing materials or chlorides/sulphides in water	• Thin layer of corrosion products on container surface • Corrosion of container
BIOLOGICAL	
Aerobic microbial activity in vault	• Consumption of oxygen • Production of sulphide

Notes: Processes listed are those that are most likely to have a notable effect on the containers, over a time scale of one million years.

5.3.1.1 Irradiation of Container Materials

The radioactivity inside the container is at its maximum value when the fuel is first loaded. The radiation field around the container is dominated by the gamma emission from short-lived fission products, which decay almost completely within the first 500 years after placement (see Figure 5-1). Thereafter, the residual radiation field would be very low because most of the remaining radioactivity would be from the alpha emission of long-lived actinides. Alpha particles do not penetrate beyond the fuel cladding.

High levels of neutron radiation, as found in nuclear reactors, can lead to hardening and embrittlement of reactor parts. The neutron flux inside a reactor is on the order of 4×10^{13} n/cm^2·s (neutron per centimetre squared, per second). In comparison, the neutron flux from used fuel is much smaller (~10^2 - 10^3 n/cm^2·s initially in a container of used CANDU fuel) and is mainly lower-energy neutrons. Over a million-year timeframe, the total neutron fluence experienced by the container would be less than 10^{15} n/cm^2 (based on Tait et al. 2000), whereas a neutron fluence greater than 10^{22} n/cm^2 would be required to produce measurable

displacement effects in metal. Defect formation from thermal neutrons would require neutron fluences of 10^{19} - 10^{21} n/cm^2 in copper and iron at 70 - 80°C to result in significant hardening. Consequently, it is unlikely that the container metals would be significantly affected by radiation over a million year exposure to used fuel (McMurry et al. 2003).

Radiation would be more likely to have a small indirect influence on container properties, in terms of changes to the chemical environment that would result from the decomposition (radiolysis) of air and water in the vicinity of the container.

5.3.1.2 Changes in Container Temperature

Thermal analyses are performed to determine thermally acceptable layouts of a repository using computer codes such as CODE_BRIGHT (Guo 2010). Various heated field experiments have been conducted and modelled (e.g., the full-scale Canister Retrieval Test at the Äspö Hard Rock Laboratory in Sweden, Guo 2009). The findings indicate that thermal responses were successfully modelled. There is good confidence that the evolution of temperatures of the container surface and surrounding bentonite buffer materials can be well estimated by existing computer models.

In this case study, the exterior surface temperature of the reference copper container after placement reaches a maximum value of 120°C (see Figure 5-5), considering the reference horizontal tunnel placement concept at a depth of 500 m in sedimentary rock and the repository layout presented in Chapter 4. This is higher than the 100°C value reached in crystalline rock because of the slightly lower thermal conductivity of sedimentary rock, as well as the horizontal placement adopted in the present study. Both temperature values are ensured by the container spacing within the repository such that the heat can be conducted away through the buffer and rock.

The purpose of determining the maximum temperature value is to understand the effect of elevated temperatures on the physical properties of the buffer sealing material surrounding the container. Only a fraction of the containers in a repository (those with the youngest fuel and / or the highest burnup values) would approach this maximum temperature. In the case of containers that otherwise are identical, those near the edges of a repository would have lower maximum temperatures than those in the centre of a repository because they would be less affected by heat from adjacent containers as illustrated in Figure 5-6.

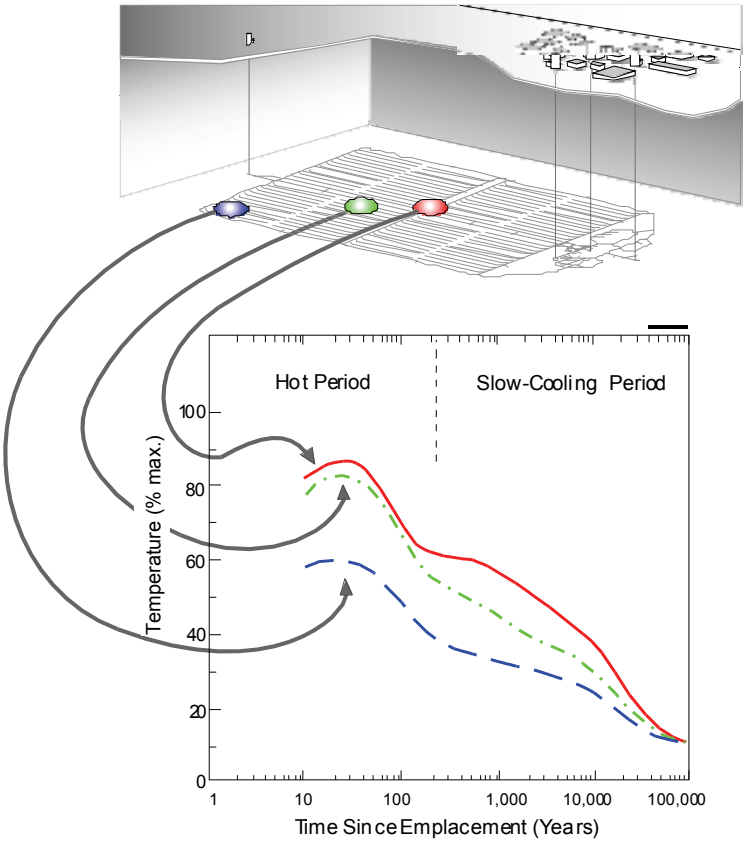

Notes: Figure is adapted from McMurry et al. (2003). Although otherwise identical, containers near the repository margin would remain cooler than those near the centre. The maximum temperature reached is 117°C, as shown in Figure 5-5.

Figure 5-6: Illustrative Container Temperature Profiles at Three Generalized Locations within a Repository

The thermal profile for a reference container near the centre of the repository (red position in Figure 5-6) is shown in Figure 5-5. Some key points are:

1. The maximum container surface temperature is reached relatively soon after placement (i.e., within 30 years). In general, the greater the heat flux for the container, the sooner the peak temperature is attained.
2. There is a subsequent plateau or slow decline in the container temperature. The specific shape of this region is influenced by repository design and site conditions.
3. The containers cool to near-ambient conditions after approximately 100,000 years.

5.3.1.3 Changes to Mechanical Integrity

Containers would experience a range of stress conditions over time. The structural design of the container is determined largely by the requirement to provide adequate mechanical strength throughout its design life.

5.3.1.3.1 Early Conditions

As soon as the steel lid is bolted onto the steel vessel, heat from the used fuel bundles would increase the pressure of the inert gas inside the vessel. For example, at a temperature of 120°C inside the container, the internal gas pressure would increase by about 40%. This internal pressure would have a negligible effect on container stresses and would decrease with time as the container cooled.

Another early heat-related stress effect would be the differential expansion of the metals in the container. The coefficient of thermal expansion of steel is about 3.7×10^{-6} mm/mm/ ^{o}C at 100°C, whereas that of copper is about 5.4×10^{-6} mm/mm/°C. Over a period of hours to days after the used fuel bundles are loaded, the temperature increase would result in a slight differential thermal expansion of the two container materials, causing the small gap between the outer and inner vessels to increase by less than a tenth of a millimetre. This effect would not be significant.

After the containers are loaded and sealed, they would be transferred from the fuel loading and container assembly area to a placement room in the repository. Depending on the facility design, the transportation and placement process would involve multiple stages of handling of the containers, possibly including several rotations from vertical to horizontal orientations during transfer from the surface facilities to a final position in a placement room. This handling would impose various short-term loads on the container that would be within its design basis.

5.3.1.3.2 Effects of Hydrostatic and Buffer Swelling Pressures

After placement, the external load on the containers initially would consist of little more than the weight of the overlying sealing materials. The load would gradually increase during saturation of the repository. The swelling of the bentonite in the sealing materials is likely to occur unevenly on a local scale because the swelling would be controlled by the supply of water from the rock, by the shape of the room, and by the pathway of water along interfaces. The heterogeneous development of swelling pressures would result initially in non-uniform external loads on the containers, an effect that is expected to diminish as full saturation is achieved. The container design is robust enough to account for this.

By the time a repository is fully saturated, the hydrostatic pressure would have increased to about 6 MPa at the repository depth of 500 m. Buffer swelling pressures would contribute up to another 0.4 to 1 MPa to the load on the containers, depending on groundwater salinity and buffer density. Under these loading conditions the copper shell would be expected to compress onto the steel load-bearing inner vessel. The resulting load is within the container design basis.

5.3.1.3.3 Effects of Glacial Loading

Additional compressive stresses would be applied to the container by glaciation. It is unlikely that an ice sheet would develop over the repository until at least several tens of thousands of years had elapsed. By this time, the buffer saturation-related pressure loads would be fully applied. The increased stresses associated with glacial loading are likely to recur several times over a million-year timeframe because of successive glaciation events (Figure 5-7).

The container is designed to withstand a load of 45 MPa. In this case study, the container could withstand an increase in hydrostatic pressure of 38 MPa from glacial loading (in addition to the 7 MPa due to pre-glaciation hydrostatic and swelling pressures), a value that corresponds to a loading from a 3,800-metre thick ice sheet above the repository location. Recent studies have indicated that a glacial loading estimate of 38 MPa is likely to be conservative, i.e., the additional hydrostatic pressure at repository depth is likely to be considerably less than this (see Chapter 2).

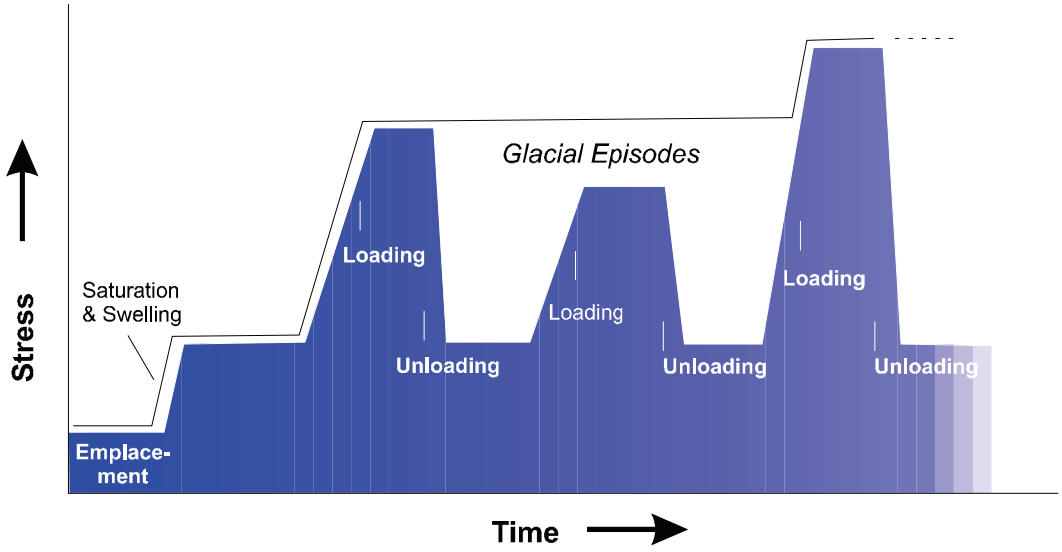

Figure 5-7: Schematic Representation of the Loading History in a Repository

5.3.1.3.4 Effect of Seismic Stresses

In general, the Michigan Basin is characterized by low levels of seismic activity as it is located within the tectonically stable center of the stable North America continent (Hayek et al. 2010). Most earthquakes in the regional area, although rare, are deep and occur in pre-existing faults within the Precambrian basement. Seismic events with focal depths in the Paleozoic sequence are not known to occur. During glaciation, an increase in the frequency of earthquakes is expected during a glacial retreat, however the magnitude of these events is expected to remain low. Within the sedimentary rock in the Michigan Basin below the Bruce nuclear site, this is supported by the lack of apparent evidence for cross formational mixing of groundwaters and the lack of neotectonic deformation (NWMO 2011).

To further improve confidence in long-term stability regarding seismic hazards, there is a considerable body of evidence to show that earthquakes, in general, are less destructive at depth than at the surface, diminishing the impact of any seismic activity (including proximal events) on a deep geological repository (Bäckblom and Munier 2002, Atkinson and Kraeva 2011). In addition, an analysis conducted for an in-floor placement in crystalline rock design by the Swedish repository program (Raiko et al. 2010) concluded that there would be no significant effect on containers even if an earthquake resulted in shearing over a distance of 0.05 m in the rock directly across the container location.

5.3.1.3.5 Effect of Creep

Creep is the slow deformation of a material under an applied stress that results in a permanent change in shape. The process of creep in copper is governed by properties of the metal (e.g., grain size, impurities at grain boundaries, crystallographic structure), temperature, stress level, and time. To maintain the mechanical integrity of the copper shell, the container is designed so that the total of the elastic, plastic, and creep strains developed in the metal does not exceed its creep-rupture strain over the design lifetime. A number of research and development studies have been carried out in the Canadian, Swedish, and Finnish nuclear fuel waste management programs to assess the creep lifetime of dual-vessel containers that have a copper outer shell. These studies have included the development of oxygen-free phosphorus-doped (OFP) copper materials with improved creep ductility, and container designs that limit the amount of creep deformation. While recent analysis of this data has revealed some uncertainty in the long-term creep fracture performance of OFP copper (SSM 2012a), as well as a need to supplement modelling capability with respect to creep ductility (SSM 2012b), a long-term study is ongoing to improve confidence in these areas. The upper bound of the creep rates for a copper vessel in a deep geological repository is presently estimated to be in the range of 3×10^{-13} to 1×10^{-10} /s.

During the saturation period, when hydrostatic and swelling pressures begin to apply stress to the container, the copper shell would have a surface temperature of about 120°C at most. The copper would compress onto the steel vessel, closing the small assembly gap (1 mm) that was initially present between the two parts of the container. At the expected temperature and pressure, the main process by which this deformation takes place is creep, since the maximum stresses that develop in the copper shell would be below the yield stress limit of the copper, preventing plastic yielding from taking place.

In certain areas (e.g., around the lid), some gap is likely to remain between the copper and steel, and localized creep of copper would be likely to continue. First-order analyses have suggested that the additional creep strain developed in these areas would be negligible because of the low stresses and low temperatures at long times (Saiedfar and Maak 2002).

Under isotropic loading, independent creep of the copper would cease after the copper compresses against the steel vessel. If any further creep of copper were to occur, it would be in response to deformation of the steel vessel. However, the thick-walled steel vessel would be designed to remain load-bearing over the design lifetime for a container (Werme 1998, Saiedfar and Maak 2002). For example the maximum stresses developed in the reference steel vessel are only about 30% of its yield strength under saturation-related pressures, and approaches the yield strength under peak design-basis glaciation pressures. The creep rate of steel under the anticipated loading conditions (20% of its ultimate tensile strength under

saturation-related pressures) and temperature (20% of melting temperature) is insignificant. The exact rate is uncertain, but it is expected that it would take at least 100,000 years for any appreciable amount of creep deformation to develop in the steel vessel (Dutton 2006).

5.3.1.4 Effect of Chemical Processes Inside the Container

The containers remain intact throughout the timeframe of the study. Chemical changes over time involving those processes that affect the interior of the container (a closed system) may therefore be considered separately from those that affect its exterior surface.

At the time of packaging, the container interior is dry, as are the used fuel assemblies. Most water vapour is eliminated from the container interior during packaging operations because the air inside the container is replaced by an inert gas before the container is sealed. The small amount of residual air and water vapour would provide some oxygen to react with the metals in the container interior, and the irradiation of any air present would produce small quantities of nitrogen oxides by radiolysis. For the anticipated "dry" conditions inside the container, aggressive corrosive agents such as nitric acid would not form (McMurry et al. 2003).

The zirconium alloy in the fuel bundles would already have a surface film of ZrO_2 that formed at high temperatures in a reactor. This resistant ZrO_2 surface layer on the cladding would inhibit any further reaction with the small amount of air initially available inside the container. In contrast, the more porous iron oxide layer on steel would slow but not prevent further reaction. Thermodynamic arguments predict that reaction between the iron and oxygen would occur even at a very low oxygen partial pressure. The steel inner vessel and the steel baskets holding the fuel bundles would tend to react rapidly with any available oxygen, forming iron oxides/hydroxides as corrosion products. Corrosion of the steel would effectively remove any gaseous oxygen from the interior of the container, so that conditions in the interior would become anoxic. An upper bound on the amount of corrosion from residual air can be obtained by assuming that the container is filled with air instead of with an inert gas. For a container design as indicated in Table 5-1, the total internal void volume is about 1.58 m^3. The total consumption of oxygen from air trapped in this space would result in 0.01 mm of corrosion of the steel basket walls. This indicates that there would be more than enough iron present to consume any oxygen.

Fuel elements with defective cladding would release some fission gases to the container interior, particularly if the cladding fails after the container is sealed. Iodine, which assists stress corrosion cracking of metals under some conditions, is the most noteworthy of these gases. The partial pressure and total quantities of any released gases would be small, (e.g., $<10^{-40}$ MPa for oxygen and $<10^{-17}$ MPa for iodine), and the CANLUB coating within the fuel element would tend to absorb any gaseous iodine. Most of the other released gases would be adsorbed onto the internal surfaces of the steel structure, or they would be distributed among the exposed iron, zirconium and copper surfaces, not resulting in any significant changes to the interior of the container (McMurry et al. 2003).

In summary, the scarcity of oxygen and water inside the inert gas-filled sealed containers would greatly limit the chemical changes that would take place there. Water radiolysis, accompanied by reactions with the metal interior of the container, would quickly consume the small amount of gaseous oxygen that would be present (SKB 2011). The interior of the container thereafter

would have a dry, reducing chemical environment that would persist as long as the container remains intact.

5.3.1.5 Effect of Chemical Processes Outside the Container

This section summarizes the current understanding of the corrosion behaviour of copper used fuel containers in a deep geological repository. This understanding has been developed on the basis of an extensive experimental program carried out in Canada and elsewhere over the past 30 years and on the results of mechanistically based mathematical modelling of various corrosion processes.

The corrosion behaviour of copper depends on the nature of the environmental conditions. For this discussion, the following attributes of the container and reference repository design are important:

- The container corrosion barrier is manufactured from an oxygen-free grade of copper;
- The container is placed in the room and sealed immediately afterwards;
- The containers are surrounded by a buffer material comprising dense bentonite pellets with an average dry density of at least 1.4 Mg/m^3;
- The groundwater is a Ca-Na-Cl solution, with small amounts of sulphate and low levels of carbonate;
- The available O_2 is limited to that trapped initially in the pores of the buffer and backfill materials, the groundwater itself is O_2-free;
- The container includes a thick inner steel vessel resulting in a maximum surface absorbed dose rate of <1 Gy/a;
- The container surface temperature will reach a value of up to 120°C;
- There is a period of unsaturated conditions immediately following container placement and prior to saturation of the repository;
- There is no sulphide (HS^-) present in the groundwater; and
- The container is subject to external loading from a combination of the hydrostatic load and bentonite swelling pressure, assuming that the relaxation of the surrounding rock has completed prior to container placement.

Experimental research and modelling has considered uniform corrosion, pitting corrosion, stress corrosion cracking (SCC) and microbial-induced corrosion (MIC). A list of studies conducted in the Canadian copper corrosion program is tabulated in Kwong (2011), and reviewed in Scully and Edwards (2013).

Overall, these studies conclude that a copper-shelled used fuel container in a deep geological repository will be primarily subject to general corrosion. The degree of localized attack (pitting), MIC and SCC will be negligible and can be controlled using standard engineering design and practice. All forms of corrosion will be stifled as the repository environment becomes anoxic. The various corrosion mechanisms are discussed in more detail in the following sections.

The important characteristics of the corrosion of copper containers in a deep geological repository are:

- The corrosion behaviour changes with time, largely as a result of the evolution of the repository environment (King and Shoesmith 2010). This environment evolves from an

initial period of warm, aerobic conditions to an indefinite period of cool, anoxic conditions. From a corrosion perspective, this environmental evolution means that localized corrosion processes are limited to the early period, with corrosion becoming more uniform in nature as time progresses;

- The nature of the environment at the container surface determines the corrosion behaviour. The surface environment can be different from that in the host rock as a result of the chemical conditioning of the groundwater by the bentonite clay and the slow mass transport of reactants to, and of corrosion products away, from the container surface due to the presence of the bentonite;

- In general, groundwater chloride promotes the uniform dissolution of copper and suppresses localized corrosion and SCC (King et al. 2010, 2011a); and

- The dense bentonite clay buffer and high groundwater salinity around the container suppresses microbial activity.

5.3.1.5.1 Uniform Corrosion

The uniform corrosion of copper in the environment expected in a deep geological repository has been extensively studied and the corrosion mechanism is well understood and summarized in Kwong (2011). Figure 5-8 illustrates the mechanism developed to describe the uniform corrosion of copper in compacted bentonite saturated with oxygen (O_2)-containing chloride (Cl^-) porewaters. The mechanism couples the interfacial electrochemical reactions that occur on the container surface to various processes occurring at or within the bentonite. These processes include: the diffusive mass-transport of species to and from the corroding interface (denoted by the wavy arrows in Figure 5-8); the adsorption and desorption of Cu(II) on the clay; redox reactions involving dissolved O_2, Fe(II), and Cu(I) and Cu(II) species; the dissolution and precipitation of various solid mineral phases and corrosion products; the partitioning of O_2 between the gaseous and aqueous phases, and, in a simplistic manner, the microbial consumption of dissolved O_2. This reaction scheme applies equally to both the buffer and backfill materials, as well as the host rock, and further details are included in this section.

Copper can react in dry air as shown in Reaction (5-13). The rate of copper oxidation in dry air at temperatures below 150°C is of the order of nm/a, and, therefore, effectively negligible.

$$2Cu + \tfrac{1}{2}O_2 \rightleftarrows Cu_2O \qquad (5\text{-}13)$$

The corrosion behaviour of copper in O_2-containing Cl^- solution has been well studied. A detailed reaction mechanism exists that accounts for the various electrochemical, chemical, redox, adsorption/desorption, precipitation/dissolution, and mass transport processes involved in the corrosion process in compacted bentonite. The behaviour of copper over a range of chloride concentrations has also been experimentally evaluated. Kinetic rate constants, equilibrium constants and other thermodynamic parameters required for modelling are available, as summarized in Kwong (2011).

Copper will corrode in solutions containing O_2 and Cl^- and under atmospheric conditions providing the relative humidity is above that required to form a thin surface water film,

i.e., approximately 50 to 70% relative humidity. The rate of corrosion will depend on the presence of atmospheric contaminants, such as SO_2, NO_2, and CO_2. The ion-containing water film acts as an electrolyte to support electrochemical reactions and the dissolved impurities will further enhance the corrosion process. For instance, the SO_2 forms H^+ and HSO_3^-; the latter species can be oxidized to sulphate by oxidants in the air, and NO_2 can be absorbed in the water film as HNO_3, which dissociates to H^+ and NO_3^-.

Copper dissolves in Cl^--containing solutions as the cuprous (Cu(I)) complex ion $CuCl_2^-$; this process is of particular importance for the expected high salinity of the Canadian sedimentary environment, see Table 2-4. The anodic dissolution is coupled to the cathodic reduction of an oxidant, either dissolved O_2 or Cu^{2+}. Cupric species are produced by homogeneous oxidation of Cu(I) by O_2 (Reaction (5-14)).

$$4\mathrm{Cu(I)} + \mathrm{O_2} + 2\mathrm{H_2O} \rightarrow 4\mathrm{Cu(II)} + 4\mathrm{OH^-} \quad (5\text{-}14)$$

Both Cu(I) and Cu(II) can precipitate as Cu_2O and $CuCl_2 \cdot 3Cu(OH)_2$, respectively (Reactions (5-15) and (5-16)). Such a duplex corrosion product layer would comprise an inner layer of Cu_2O and an outer layer of basic Cu(II) salts such as $CuCl_2 \cdot 3Cu(OH)_2$) or $Cu_2CO_3(OH)_2$, depending on the specific composition of the porewater.

$$2\mathrm{CuCl_2^-} + \mathrm{H_2O} \rightleftarrows \mathrm{Cu_2O} + 2\mathrm{H^+} + 4\mathrm{Cl^-} \quad (5\text{-}15)$$

$$2\mathrm{Cu_2O} + \mathrm{O_2} + 2\mathrm{Cl^-} + 4\mathrm{H_2O} \rightleftarrows \mathrm{CuCl_2 \cdot 3Cu(OH)_2} + 2\mathrm{OH^-} \quad (5\text{-}16)$$

The precipitated surface film blocks surface electrochemical reactions and does not sustain the permanent separation of anodic and cathodic reactions that would be required for localized corrosion to occur. As the repository environment becomes anaerobic, the $CuCl_2 \cdot 3Cu(OH)_2$ layer dissolves with further corrosion supported by the cathodic reduction of Cu(II).

In the absence of oxygen, corrosion would require a reaction with water to produce hydrogen gas (H_2):

$$2\mathrm{Cu} + \mathrm{H_2O} \rightleftarrows \mathrm{Cu_2O} + \mathrm{H_2} \quad (5\text{-}17)$$

or

$$\mathrm{Cu} + \mathrm{H_2O} \rightleftarrows \mathrm{CuOH} + \tfrac{1}{2}\mathrm{H_2} \quad (5\text{-}18)$$

Known thermodynamic relationships (Puigdomenech and Taxén 2000) indicate that the equilibrium shown in Reaction (5-17) is very strongly biased towards the reactants: metallic copper and water. Accordingly, upon formation of a very small amount of Cu_2O (i.e. a single layer), only a very small amount of hydrogen, with a partial pressure on the order of 10^{-11} mbar, is necessary to suppress the corrosion reaction; i.e., Reaction (5-17) becomes unfavourable in the forward direction. In addition, the corrosion product in Reaction (5-18) has not been shown to be stable. Therefore, Reactions (5-17) and (5-18) are considered very improbable in water.

Under anaerobic conditions, copper corrosion accompanied by the evolution of H_2 does occur in the presence of sulphide (Reaction (5-19)).

$$2Cu + H^+ + HS^- \rightleftarrows Cu_2S + H_2 \quad (5\text{-}19)$$

Sulphide is not widely found in groundwaters in sedimentary rock in Canada (INTERA 2011). In Sweden and Finland, however, deep groundwaters do contain small amounts of HS^- (typically ~1 mg/L, King et al. 2010, 2011a), resulting in corrosion rates of the order of nm/year due to the slow transport of sulphide to the container surface through the compacted bentonite buffer (SKB 2011).

Researchers from the Royal Institute of Technology (Sweden) have published experimental results that they claim indicate that copper can corrode in pure, oxygen-free water. Their research claims that water is reduced in the anaerobic corrosion process to form hydrogen atoms (Szakálos et al. 2007, Hultquist et al. 2009, 2011), and that a hydroxyl-containing copper corrosion product may be produced. Subsequent expert review (Swedish National Council 2010) concluded that it was necessary to demonstrate that the proposed corrosion product was thermodynamically stable before it could be justifiably claimed that copper could corrode in oxygen and sulphide-free water. An SKB review also concluded that there were possible errors in the original experiments (SKB 2010).

Further studies are underway in Sweden, as well as by NWMO, to address these topics. Preliminary results are reported in SSM (2011a) and Hultquist et al. (2013). These have found extremely small quantities of hydrogen in similar experiments, although the tests were not definitive. In addition, careful analysis of the thermodynamics of the reactions between copper, pure water, and sulphide (SSM 2011b) has indicated that copper-water interactions as described by (5-17) and (5-18) are theoretically possible, but would only produce very small quantities of hydrogen, and that reactions with sulphide species are much more important (SSM 2011b).

In summary, while this topic is still being studied, it appears that the hydrogen produced from a copper-water interaction would be self limiting, and not a significant corrosion mechanism within a repository. Assuming the corrosion mechanism via reaction (5-18) occurs, then at temperatures of 73°C and 45°C, hydrogen partial pressures of ~1 mbar (Szakálos et al. 2007) and 0.5 mbar (Hultquist et al. 2009), respectively, would suppress the corrosion reaction. This hydrogen could be present either from the copper-water reaction, if it occurs, or more likely from the anaerobic corrosion of steel components or reactions between copper or steel with trace levels of sulphides or from native hydrogen levels (SKB 2010). For example, measurements at depth within crystalline formations have demonstrated hydrogen concentrations between 2 and 1,600 µmol/L (Sherwood Lollar 2011), equivalent to partial pressures of 2.6 to 2,000 mbar.

The rate controlling process for the uniform corrosion of copper changes as the environmental conditions evolve. Under aerobic conditions, there is evidence that the transport of dissolved Cu away from the corroding interface is rate controlling (King et al. 2010, 2011a) (i.e., the corrosion reaction is anodically transport limited). As the repository environment becomes anoxic, the corrosion rate must eventually become cathodically transport limited as a result of the slow diffusion of oxidant to the container surface. In the presence of sulphide, if such species were to be found in Canadian groundwaters or produced from sulphates by microbes, then the corrosion rate is limited by the rate of transport of HS^- to the container surface (Chen et al. 2011, King et al. 2011b).

Overall, the uniform corrosion behaviour of copper in conditions expected for a deep geological repository in sedimentary rock is well understood. Both the mechanism of copper corrosion in oxygen-containing chloride (as high as 5 mol/L) and kinetic and thermodynamic parameters required for modelling are available.

In addition to the extensive experimental studies on which the mechanism in Figure 5-8 is based, a detailed reactive-transport model has been developed to predict the long-term uniform corrosion behaviour of copper containers in the repository. The model, referred to as the Copper Corrosion Model for Uniform Corrosion (CCM-UC), is based on the mechanism in Figure 5-8 and couples the corrosion behaviour of the container to the various processes occurring in the near- and far-fields of the repository, specifically the evolution of the environmental conditions. The corrosion behaviour is modelled using electrochemical mixed-potential principles. As a result, the model not only predicts the time-dependent corrosion rate (as a corrosion current density), but also the time-dependent corrosion potential (E_{CORR}). As discussed below, E_{CORR} is a useful parameter for assessing the probability of localized corrosion and stress corrosion cracking, as well as providing information about uniform corrosion.

Various methods have been developed to predict the rate or extent of the uniform corrosion of copper containers. Because uniform corrosion is limited by the availability of oxidant, the rate of corrosion is of less importance than the extent of corrosion. The maximum depth of corrosion can be assessed based on mass-balance principles (SKB 2011) or using the detailed mechanistically based CCM-UC model (King et al. 2008).

The total amount of O_2 trapped in the repository at the time of closure, expressed per unit area of the container surface, is of the order of 1-10 mol_{O2}/m^2. The exact amount depends on the volume and porosity of buffer and backfill materials and, crucially, the initial degree of saturation (since the majority of the trapped O_2 is present as gaseous O_2 in the air-filled pores of the buffer and backfill). If all of this oxygen is consumed by corrosion of the container, King et al. (2010) estimate that the maximum wall penetration for a copper container in a deep geological repository would be 0.17 mm. In reality, some of the O_2 will be consumed by aerobic microbial activity in the backfill material and the oxidation of ferrous species, so that the actual depth of uniform corrosion will be lower. Depending upon the relative rates of the different microbial and redox reactions, the model predictions suggest that more than 50% of the trapped O_2 could be consumed by processes other than corrosion. A consequence of the limited availability of oxidant is that once all of the O_2 (or the Cu^{2+} produced by the oxidation of $CuCl_2^-$ by O_2) has been consumed, and there is sufficient generation of H_2, corrosion of the container ceases.

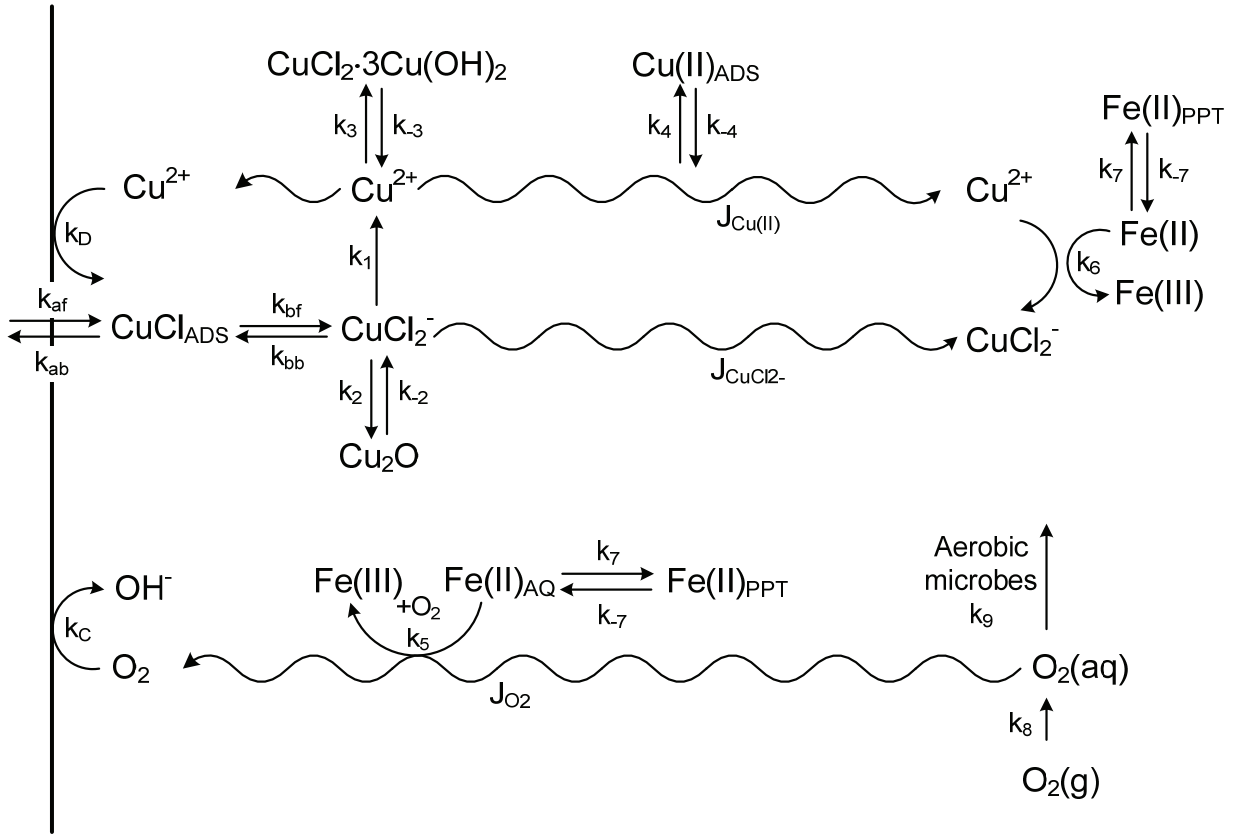

Notes: From King and Kolář (2000) and King et al. (2008, 2010, 2011a). The k's denote rate constants for the various interfacial electrochemical and homogeneous reactions and the J's denote diffusive fluxes.

Figure 5-8: Reaction Scheme for the Uniform Corrosion of Copper in Compacted Bentonite Saturated with O_2-Containing Chloride Solution

5.3.1.5.2 Localized Corrosion

Kwong (2011) and Scully and Edwards (2013) identify that studies designed to specifically examine the surface profile of copper corroded in groundwater-saturated, compacted buffer materials have been completed. Results showed that the copper will only undergo a form of surface roughening as a result of the non-permanent separation of anodic and cathodic processes. Evaluations of the distribution of precipitated corrosion products and surface morphology on the coupon surface (i.e., distribution of peaks and valleys on the surface) indicated an "under-deposit" corrosion. A mechanism to account for the observed surface profile, which involved the periodic separation of anodic and cathodic processes through the formation of temporary occluded cells has since been proposed (King and Kolář 2000).

Experiments were carried out to assess the possibility of localized corrosion of copper for the situation in which there are differences in the flux of O_2 to different parts of the container surface, for example, in the case where bentonite blocks of different density might be used around the container. In this situation, the temporary spatial separation of anodic and cathodic processes is possible. It was shown that the localized corrosion rates would decrease with decreasing oxygen concentration and decreasing container surface temperature. The corroded copper surface showed only general corrosion with minor surface roughening and no distinct pitting. It was concluded that the rate and extent of localized corrosion in a deep geological repository would be very small since there will only be a limited supply of oxygen. It was expected that the corrosion products on the container surface would further limit the rate and extent of localized corrosion.

The long-term localized corrosion behaviour of copper has also been extensively studied in the Swedish / Finnish nuclear waste management programs. They predicted the depth of localized corrosion based on pitting factors and an analysis of empirical pitting data from archaeological artifacts subject to long-term burial in natural environments. Extreme-value statistics developed by Ontario Power Generation for the Canadian program have also been applied to estimate the maximum pit depth on a container as a function of exposure time in the repository (King 2006). A pit propagation model was developed for reducing conditions assuming the pit growth was limited by the transport of HS^- to the copper surface.

Based on these various measurements and models, it was generally agreed that a copper container in a deep geological repository will not undergo classical pitting corrosion, but only a surface roughening or under-deposit corrosion. Corrosion occurs under deposits on the surface, with the resultant temporary spatial separation of the anodic and cathodic sites accounting for the roughened surface. Surface roughening, or under-deposit corrosion, may add a maximum of 0.1 mm to the depth of general corrosion.

5.3.1.5.3 Stress Corrosion Cracking

This section summarizes the considerations for stress corrosion cracking (SCC) of the copper shell that are explored in Kwong (2011). The occurrence of SCC requires a susceptible metal to be exposed to sufficient tensile stress and an active SCC agent. Copper is known to be susceptible to SCC in environments containing ammonia, nitrite ions, acetate, or, possibly, high concentrations of sulphide. Studies focussed on SCC have concluded that the SCC of copper requires the prior formation of a thin oxide or tarnish film. When this film does not form, SCC is not observed.

While SCC agents are not normally found in natural groundwater, they could be introduced by either mining activities or microbial activity. Numerous tests have, therefore, been performed to assess the SCC behaviour of copper in nitrite-, ammonia- and acetate-containing environments. Results indicate that copper SCC susceptibility would decrease with decreasing concentrations of the SCC agents. These studies also suggest a threshold concentration level for each agent below which SCC would not occur. Also observed in these studies is the inhibiting effect of chloride on copper SCC in nitrite, ammonia and acetate environments, the SCC susceptibility decreasing with increasing chloride concentration. The ability of chloride to inhibit SCC also appears to be enhanced by elevated temperatures, as exhibited in tests conducted at 100 to 130^{o}C (in nitrite only and nitrite/chloride solutions). This effect can be attributed to the ability of chloride ions to promote general dissolution of copper, which results in more uniform corrosion at the expense of the formation of the required thin oxide film.

Surface defects on the used fuel container surface can act as stress concentrators (notch-like defects) or stress intensifiers (crack-like defects) and may increase the probability of crack initiation or growth, respectively. A literature review and engineering analyses were performed to assess the effect of surface discontinuities on the initiation and propagation of localized corrosion and SCC of copper welds. The findings indicate no evidence that weld discontinuities would adversely affect the localized corrosion and SCC behaviour of copper containers. The predicted service life of the containers is not affected by the presence of the surface discontinuities.

A number of mechanisms have been proposed for the SCC of copper, including film-rupture/anodic dissolution, tarnish rupture, film-induced cleavage, and surface mobility mechanisms. Taking into account the pre-requisites for crack initiation and crack growth, a conceptual SCC model was defined for copper containers in a repository based on predicting whether the necessary environmental conditions will exist or co-exist. The model is mechanistically based and defines various absolute and conditional criteria for SCC. This model also addresses each of the environmental parameters that control the initiation and growth of SCC.

Research results have suggested SCC under aerobic conditions in a deep geological repository is unlikely as the pre-requisite conditions of corrosion potential, interfacial pH, and concentration of SCC agents do not exist simultaneously at the container surface. According to mechanistic arguments, there is also no evidence to indicate that SCC of copper is possible under anaerobic conditions at the sulphide levels expected at the container surface. Based on the nature of the repository environment, SCC does not appear to be a threat to the integrity of a copper used fuel container.

Despite the low risk of SCC on copper, suitable engineering procedures can be effectively applied to further minimize the probability of SCC. For instance;

1. The level of airborne ammonia and nitrite formed during blasting operations can be controlled to below the threshold concentration in order to preclude the possibility of cracking;
2. The residual tensile stress following container shell and bottom manufacturing can be thermally relieved; and
3. The residual stress on the final closure weld can be controlled and/or reduced using a suitable welding technique.

With regard to the later, it is often good engineering practice to perform a post-weld stress relief of the final closure weld, regardless of the apparent SCC susceptibility of the material. The introduction of a surface compressive stress has proven to be an effective way of preventing the initiation of SCC on various industrial structures. Ambient temperature techniques, such as laser peening and low plasticity burnishing have been developed in the Yucca Mountain Project for this purpose (DOE 2008).

5.3.1.5.4 Microbiologically Influenced Corrosion

The microbiologically-influenced corrosion (MIC) program is summarized in Kwong (2011). Similar to other engineering materials, copper is susceptible to this type of corrosion. Microbial metabolic by-products may affect the SCC behaviour of copper as microbial activity may form SCC agents, namely ammonia, nitrite, and acetate ions. Ammonia and nitrite are produced (and also consumed) by different types of microbe as part of the nitrogen cycle. Acetate is produced by the fermentation of organic molecules. Another species often considered is HS^- produced by the reduction of sulphate by sulphate-reducing bacteria. This last reaction occurs under anaerobic conditions and requires the presence of simple organic molecules or H_2 as electron donors. Without the formation of biofilms on the container surface, the only form of MIC possible is that due to the diffusion of remotely-produced metabolic by-products through the bentonite to the container surface. Sulphide ions produced at a location away from the container surface must diffuse through the bentonite sealing materials to have any effect on container corrosion. The corrosion rate is, therefore, limited by the rate of diffusion of sulphide (HS^-) to the container surface, a continued supply of which is required to sustain MIC.

The Canadian microbial experimental program has demonstrated that a water activity of ≤ 0.96 will be readily achieved within the Canadian sedimentary system, as the pore-water salinity may approach 300 g/L total dissolved salts (see Table 2-4).

A reactive-transport corrosion model to predict the extent of MIC of copper containers has also been developed in the Canadian corrosion program. This model indicates that microbial activity in the repository will not result in shorter container lifetimes. The amount of sulphide ions provided by the microbial reduction of sulphate that reach the container surface is predicted to be insignificant over a million year timeframe. The amount of nitrite and acetate ions, both of which are associated with SCC of copper, are similarly insignificant. Although a higher maximum concentration of ammonia (another known SCC agent) of ~10^{-6} mol/L is predicted at the container surface, cracking is unlikely because of the relatively low concentration and because ammonia is only formed after all oxidants in the repository have been consumed.

Based on the assumption that sulphate-reducing bacteria activity would occur in the host rock near the placement room wall and would, conservatively, produce a continuous concentration of 3 ppm of hydrogen sulphide, the corrosion rate was estimated at 1 nm per year and the corrosion allowance for MIC was estimated to be 1 mm after one million years.

5.3.1.6 Summary

Research work over the past 20 years has established a good understanding of the long-term performance of copper used fuel containers in a deep geological repository.

In the high salinity environments anticipated in sedimentary rock groundwater (i.e., > total dissolved solids of ≈ 300 g/L), copper will begin to corrode under early atmospheric conditions

provided the relative humidity is above ~ 50 - 70%. The rate and mechanism of corrosion will be affected by the presence of atmospheric contaminants such as SO_2 and NO_2. Over time, as the repository environment evolves, the copper container will experience an initial aerobic period of uniform corrosion and some form of surface roughening, before establishing a long-term condition of thermodynamic stability. Uniform corrosion is associated with active copper dissolution in the presence of chloride, which causes the copper container to corrode uniformly, thereby avoiding localized corrosion. Stress corrosion cracking on the copper container is unlikely owing to the lack of the pre-requisite conditions for SCC; namely, the required threshold concentration of SCC agents, a suitable interfacial pH, and the required corrosion potential on the copper surface. Microbiologically influenced corrosion of copper will be controlled by the use of compacted bentonite around the copper container and the high salinity of native groundwater to suppress microbial activity in the near field and to limit the migration of any corrosive agents produced by microbial activity in the far field.

Although there have been measurements of water acting as an oxidant for copper, the available evidence is not entirely reproducible. Within experiments, early measurements are complicated by the presence of air-formed oxides, which may explain some reproducibility concerns; however, there appears to be a gradual coalescence among researchers. Within the most recent Hultquist work (Hultquist et al. 2013), corrosion rates below 10 nm/a have been observed in bulk solutions; this particular value presumes a significant, unproven loss of hydrogen during experimentation has occurred: up to three times what is detected. Without this factor, the Hultquist et al. (2013) corrosion rates are in the 3 nm/yr range in the absence of mass-transfer restrictions from bentonite; this would project to be much lower when the effects of bentonite and ambient hydrogen are included. It is expected that continued experimentation will also decrease uncertainty of such measurements. Regardless of such uncertainty, there is significant evidence that the hydrogen produced from a copper-water interaction or steel corrosion within the repository, would compel any such mechanism to be self limiting, and not a significant corrosion mechanism within a repository. In addition, any effects of water corroding copper would be overwhelmed by the corrosive interaction of copper and microbially produced sulphide, which allows for 1 mm corrosion in one million years.

The knowledge gained over the past 20 years from studies on the corrosion of copper has allowed improved and more realistic predictions to be made for the lifetime of a copper container in a deep geological repository. Under the expected saline groundwater conditions, a realistic estimate of the total extent of copper corrosion from all processes is a loss of wall thickness of about 1.27 mm, i.e., 0.17 mm (uniform corrosion) + 0.1 mm (under-deposit corrosion) + 1 mm (MIC) in one million years.

Therefore, the lifetime of a copper used fuel container is expected to exceed one million years in a deep geological repository in Canada. This finding is comparable with the predicted container lifetime for the Swedish deep geological repository in crystalline rock.

5.3.2 Evolution of a "Breached Used Fuel Container"

Containers for a repository would be manufactured according to a process that includes careful design, fabrication, closure welding, and a series of inspections to avoid significant defects.

Based on defect statistics for a variety of pressure vessels and nuclear components, it was estimated that the probability of a used fuel container having a undetected through-wall

manufacturing or installation defect was on the order of 1 defect per 5000 containers (range 1:1,000 to 1:10,000) (Maak et al. 2001).

More recent SKB (2011) analysis of sample welded containers with a similar design but 50 mm thick copper shell, states that the likelihood of an undetected copper weld defect longer than 20 mm is negligible, and the likelihood of a 10-20 mm defect is one per 1,000 containers. As a result, they do not expect any initial through-wall defects within their 6,000 container repository. However, their weld defect statistics are roughly consistent with an estimate that, for a 25-mm thick container, the likelihood of an undetected through wall defect is somewhat less than 1 in 1,000 containers. In a Canadian repository with 12,800 containers, therefore it is statistically estimated that there would be about three containers emplaced with an undetected through-wall defect.

The defect size would be constrained by the fact that it must be large enough to penetrate a sheet of copper that is about 25 mm thick but small enough that it escapes detection. For example, the area exposed by a defect was assumed to be 5 mm^2 in early SKB models, and 0.07 to 7 mm^2 in AECL models associated with the Second Case Study. In the current study, the size of the assumed initial defect is approximately 3 mm^2.

5.3.2.1 Repository Conditions Prior to Saturation for a "Breached Container"

The pre-saturated period covers the time from when the containers are first placed in a repository until the time their exterior (copper) surface is in contact with fully saturated sealing materials (i.e., the time at which the buffer is saturated and is exerting a swelling pressure on the container surface). In low permeability rock, it is likely that this pre-saturated period would last at least 10,000 years.

At the time that the placement rooms are backfilled and sealed, they would contain partially saturated (moistened) buffer. Voids (porosity) in the sealing materials would contain trapped air. Heat from the container would cause the nearby bentonite to dry out. Condensation of the water vapour would occur in cooler portions of the sealing materials.

The relative humidity of the trapped air in the sealing materials near a container is of interest because corrosion of copper and iron in air is observed to be slow or nonexistent at relative humidities less than about 60%. Above this value, copper is subject to aerobic uniform corrosion. Corrosion of steel under the same conditions produces hydrated iron oxides ("rust").

In a breached container, air would initially be present in the narrow assembly gap between the copper and steel vessels (Figure 5-9). The void space in the interior of the steel vessel would be filled with an inert gas (i.e., helium), held in place by a gasket seal beneath the bolted-on lid of the steel vessel. By the end of the pre-saturated period, the gas in the interior of the steel vessel would consist mainly of a mixture of oxygen-depleted air (largely N_2) and helium (Figure 5-9).

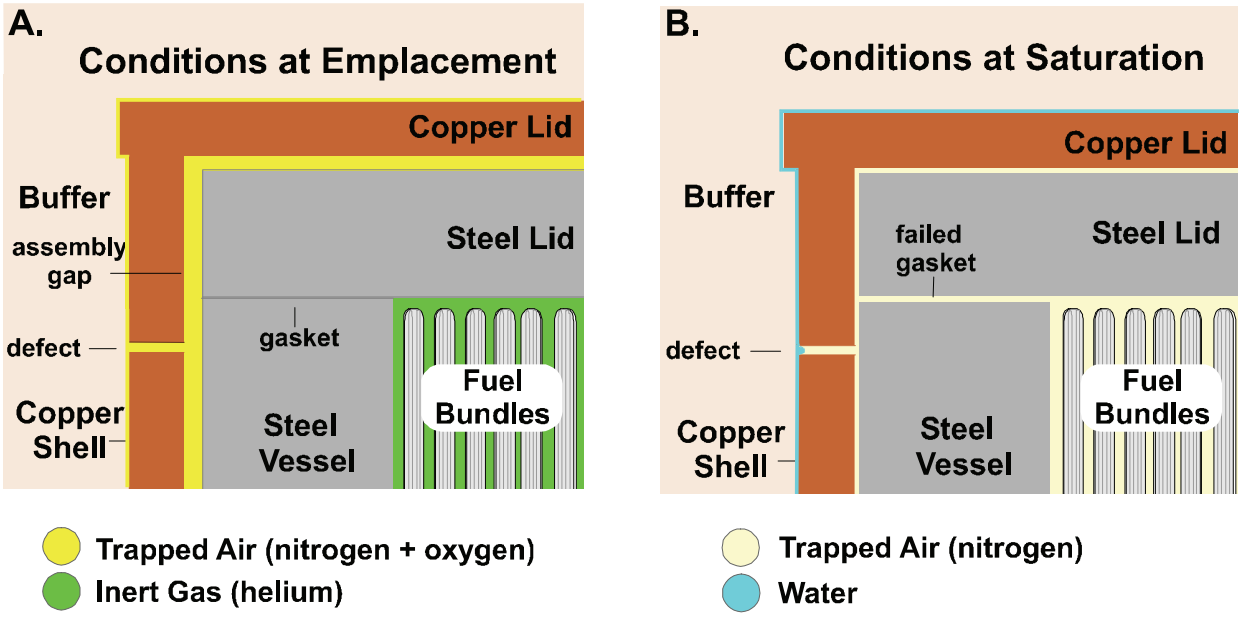

Note: Figure from McMurry et al. (2004).

Figure 5-9: Early Evolution of Conditions in a Container with a Small Defect in the Copper Shell

At saturation, the hydrostatic pressure in the water-filled pores of the sealing materials would be 6 MPa; however, it is likely that the air pressure inside a breached container at this point would be less. This is because the internal free volume (void space) of a container is approximately 1.58 m^3. Filling this volume to 6 MPa would require 75 m^3 of air at 0.1 MPa (i.e., atmospheric pressure); however, this volume is a significant fraction of all of the air that was originally trapped in the room. Given other constraining factors, such as the low permeability of saturated buffer, it is likely that a pressure differential will develop between the interior and exterior of the breached container. As a result, water vapour or liquid would be drawn from the wet buffer into the container interior via the defect in the copper shell.

5.3.2.2 Description of Post-Saturation Processes for a "Breached Container"

The description of post-saturation processes begins when the clay buffer surrounding the breached container is saturated, and liquid water is able to enter the defect in the container (Figure 5-9). A minimum of 10,000 years will have passed after placement of the container in the repository. The assembly gap between the copper and steel vessels (about 1 mm in the reference design) will be almost completely squeezed closed except near the corner of the copper lid and shell. The temperature of the container at this time would be likely in the range of 60 to 90°C.

5.3.2.3 Anaerobic Corrosion of the Steel Vessel

By the time that the repository is saturated, virtually all of the free oxygen in the sealing materials would have been consumed, and anaerobic conditions would prevail. A thin layer of corrosion products (mostly iron oxides or hydroxides from aerobic corrosion of the steel vessel) would be sandwiched between the copper and steel of the breached container. Compared to the metals, the corrosion products would be more porous and less dense. Gases may preferentially diffuse through them, and liquid water may be able to permeate them. Porewater would move from the buffer through the defect in the copper shell, and come into contact with the inner steel vessel. The copper itself would be chemically resistant under anaerobic conditions and would not be significantly affected by contact with water. In contrast, the steel vessel would undergo anaerobic corrosion as long as it was in contact with water; although the corrosion rate would be slower than under oxygenated conditions, and would also decrease as corrosion products were generated.

Where water is in contact with the steel, Reaction (5-6) will occur forming an iron corrosion product and, in the absence of oxygen, hydrogen.

An amorphous or poorly crystalline solid would be likely to form first, which would gradually transform into a more crystalline phase, likely magnetite, and possibly siderite, should sufficient carbonate be carried into the breached container, as discussed in Section 5.2.6.

Initially, iron corrosion products would form only on the outside surface of the steel. After water leaked into the interior of the steel vessel along the space between lid and body, anaerobic corrosion would also occur on the inside steel surfaces. Literature values for the anaerobic corrosion rate of steel vary over a wide range, between 0.1 and 50 μm/a. The corrosion rate in a breached container likely would be at the lower end of the range, given that the water would be chemically buffered by clay and given that the water would be supplied at a limited rate to the steel; this same limitation would likely mitigate any radiolysis reactions that could potentially impact corrosion. Among other factors, the water ingress would be restricted by the low permeability of the bentonite clay around the container, by the small aperture of the defect in the copper shell which may be blocked by swelling bentonite, by slow passage through the porous corrosion products in the narrow copper-steel gap, and possibly by blockage of the opening by the build-up of a hydrogen gas backpressure from the corrosion reaction inside the container. For a steel corrosion rate of 0.1 μm/a, the corresponding H_2 production rate would be about 0.1 to 1 mol/a for one container (equivalent to approximately 0.04 to 0.4 L/a at 6 MPa) depending on what fraction of the inner vessel surface was corroding.

5.3.2.4 Galvanic Corrosion

Although the design of the container puts the copper shell and inner steel container in physical contact, galvanic corrosion will not occur as long as the copper shell is intact. While this condition persists, corrosion reactions and rates will be defined by the outer copper shell. However, for a “breached container”, galvanic corrosion may exist, where one metal performs/catalyzes the cathodic electrochemical reactions, while the other metal performs/catalyzes anodic reactions. In the case of steel (iron) coupled to copper, oxidation of iron at the container breach would be enhanced if the very large intact copper surface could sufficiently support reduction reactions: either oxygen reduction during the aerobic period or hydrogen reduction during the long anaerobic period.

Experiments conducted by Smart et al. (2004, 2005) have examined both conditions and measured galvanic currents: with the copper behaving as a cathode and the iron behaving as an anode. In aerated conditions, galvanic corrosion rates of iron (coupled to copper) are as high as 100 µm/a. Other research has revealed that copper-steel couples in aerated seawater can cause an enhancement in corrosion of steel (Chen et al. 2007). However, the actual depth of corrosion from this process would be significantly limited by the repository oxygen volume, as described in Section 5.3.1.5. When their system was dearated, galvanic currents measured by Smart et al. were much lower: typically 0.1 µm/a at 30°C and 1 µm/a at 50°C (Smart et al. 2005). These values are no different from those measured on iron in dearated groundwater that is not coupled to copper; in effect, the copper couple does not alter the corrosion properties of iron in this medium. The interpretation of this result is that the couple between iron and copper does not sufficiently polarize the copper negatively to support enhanced water reduction (King et al. 2010). Accordingly, the copper shell would be largely inactive to the iron corrosion process, as well as having the additional benefit of protecting the remainder of the steel container from corrosion processes.

The low importance of galvanic corrosion is also supported by results from the SKB Minican experiment. Post-test examination of the first experiment after 4 years in-situ have indicated extensive corrosion by sulphide present in the groundwater, but no evidence of galvanic corrosion (Smart et al. 2012).

5.3.2.5 Deformation of the Copper Shell

As the iron exposed through the copper defect is corroded, it will form corrosion products. Iron corrosion products are less dense than the metal itself. Thus, the volume of Fe_3O_4 formed by Reaction (5-6) is about twice the volume of the Fe metal consumed in its formation (McMurry et al. 2004). As a result of this volume change, the formation of corrosion products in a confined space has the potential to exert a force on the adjacent solids. These stresses would have little preliminary effect on the steel vessel, due to its thick walls (100 mm) and high mechanical strength. However, the copper shell and the surrounding clay buffer would deform more easily. The build up of corrosion products could eventually cause the copper shell to open further around the defect. The opening of the copper shell at the defect site would allow more water to enter the container. Eventually, water also would begin to seep between the steel vessel and the steel lid and into the interior of the container.

This would be limited by the rate of water access through the defect and through the corrosion product. Furthermore, the iron corrosion reactions would also produce hydrogen. This could be at a rate exceeding the ability of the gas to diffuse into the buffer. In this case, hydrogen gas would accumulate in and around the container and form a pressure build-up that would block liquid water from moving into the container through the defect. Then, only water vapour could diffuse through the opening to sustain the steel corrosion. In these analyses, the “bubble” of hydrogen gas blanketing the steel vessel would slow the rate of steel corrosion and expansion of corrosion product thereby delaying rupture of the copper shell for time scales of the order of 200,000 years. The hydrogen blanketing scenario is plausible, but the long time delay requires that there be complete blanketing of the steel.

Experimental evidence shows that high stresses will not be produced by iron corrosion products (Smart et al. 2003, 2006). During analysis of stresses produced during anaerobic corrosion, no detectable expansion was observed over a two year period for bentonite-equililbrated

groundwaters under compressive loads (Smart et al. 2006). In addition, the anaerobic corrosion products are easily deformable, and are incapable of producing expansion under simulated repository conditions. Only for aerobic conditions, and low applied loads were expansions measureable due to corrosion products. Similarly, observations from the first MiniCan experiment after 4 years in-situ indicates no expansion in the outer copper shell due to corrosion of the cast iron insert, and apparent extrusion of iron corrosion products through the defect (Smart et al. 2012). As a result, it is likely that the copper shell deformation/rupture described above would occur very slowly.

5.3.2.6 Deformation of the Steel Vessel

The container design for normal loading conditions (i.e., prior to glaciation) would have a significant margin of mechanical strength. For example, the reference container design with 100 mm of steel can meet the reference maximum 7 MPa external pressure with a safety factor of about six. At an anaerobic corrosion rate of 0.1 to 1 μm/a (including corrosion of inner, as well as outer surfaces of the steel vessel), it would take 10,000 to 100,000 years before a 20 mm thickness of steel would be consumed.

Another factor to consider is the additional stress from glacial loading, which would be expected to first occur in about 60,000 years (see Chapter 2, Figure 2-2). At the full design-basis glaciation load, there may be little margin for thinning of the steel vessel walls. If significant corrosion had occurred already, collapse or brittle fracture of the steel vessel would be likely in response to the glacial loading stresses. It is also plausible that the glaciation load would be less than the design basis. For example, if the ice thickness is less than the design-basis maximum, if the load transmitted to depth is less than the hydrostatic loading equivalent to the ice thickness, or if the container was full of water (which would provide hydrostatic balancing of the glacial load). In such cases, the container would be more likely to tolerate further corrosion before plastic deformation and buckling. Regardless of the specific timing and processes the key point is that at some point the steel vessel in a breached container would become sufficiently weakened by corrosion that it would cease to be load-bearing, and it would collapse by buckling inwards.

The stresses causing the steel vessel to collapse would produce a corresponding deformation of the copper shell around it. During this movement, the strain limit for copper would be exceeded in portions of the copper shell, and the copper would crack, but in a general sense the copper metal would continue to conform to the shape of the steel vessel. Similarly, as the copper and steel compressed inwards, the surrounding buffer would expand around the new configuration of deformed metal.

Even after the breached container collapsed, the overall change in its volume would not be substantial compared to the volume that was originally occupied by the container. Initially (at the time of placement), the open or void space in a container, into which the collapse would occur, would be roughly 1.58 m^3, which is about 30% of the container's total volume. Moreover, it is likely that much of this initially open volume would have become filled with iron corrosion products, further restricting the amount of collapse.

After the breached container buckled and the buffer around it expanded to conform to the change in shape, the copper shell would remain essentially unchanged in appearance for the remainder of the million-year timeframe. Complete corrosion of the copper is estimated to take

several million years or longer, as indicated by sheets of natural copper that have persisted in sedimentary rocks for more than a hundred million years. In contrast to the copper, anaerobic corrosion of the steel vessel would continue in-situ until all of the steel was consumed.

5.3.2.7 Corrosion and Deformation of the Zircaloy Cladding

At the time of placement in a repository, virtually all of the used fuel elements would have intact Zircaloy cladding. A few of the cladding sheaths would have become defective during their use in a reactor (estimates of this number range from approximately 1 per 10,000 to 1 per 100,000 fuel elements) (Frescura and Wight 1979). Some others may have developed defects during post-reactor storage, during transportation, or during packaging into containers. In a breached container, one of the most significant changes in the used fuel bundles over time would be mechanical failure of the cladding, mainly in association with corrosion of the steel vessel. In addition, the cladding would be subjected to hydrogen embrittlement, corrosion, and creep, as described below.

Over time, hydrogen gas would be produced inside a breached container by two separate processes - the anaerobic corrosion of steel and the radiolysis of water. Hydrogen-induced cracking is a potential failure mechanism for Zircaloy cladding. Studies of the durability of used fuel bundles in dry or moist air have found no evidence of cladding failures (Lovazic and Gierszewski 2005). Given that significant partial pressures of hydrogen gas would not develop in a container until saturation of the repository had occurred, lifetimes of the Zircaloy cladding in a breached container could exceed thousands of years.

On observable time scales, the uniform corrosion of Zircaloy cladding is negligible, likely between 1 and 5 nm/a, and with an upper limit of 20 nm/a, even in contact with water, due largely to the corrosion resistance of a passive oxide film on the Zircaloy surface (Shoesmith and Zagidulin 2010). In a breached container, pitting and crevice corrosion of cladding would be inhibited by the rapid consumption of oxidizing agents (residual oxygen and radiolysis products) by the iron and copper container materials. In addition, iodine-induced stress corrosion cracking would be inhibited because most of the iodine in the fuel gap in CANDU fuel exists as cesium iodide, preventing it from forming the zirconium iodides that are thought to be the chemical precursors to stress corrosion cracking in Zircaloy. Using the above values, a general corrosion lifetime for a 0.5 mm cladding could be calculated to exceed 25,000 years presuming the highest corrosion rate of 20 nm/a, and with a more realistic expectation above 100,000 years for the expected corrosion rates at or below 5 nm/a.

Ultimately, any used fuel bundles that otherwise remained unruptured would be likely to fail during the corrosion-induced collapse of the steel vessel. As discussed previously, the timing of this event is uncertain, but a reasonable estimate would be within 10,000 to 100,000 years after a defect is created in the copper shell.

5.3.2.8 Dissolution of the Used Fuel Matrix

After the cladding is breached and the fuel pellets exposed to water, the next barrier against radionuclide release is the UO_2 fuel matrix, which contains most of the radionuclides and has a very low solubility. Dissolution of the UO_2 matrix of the used fuel would progress according to two general methods: oxidative dissolution (i.e., corrosion) and chemical dissolution. Radiolysis of water in contact with the fuel pellets would produce oxidizing conditions at or near the used fuel surface, contributing initially to oxidative dissolution of the UO_2. To the

extent that water is able to contact the fuel while radiation fields are high, this process would tend to promote the dissolution of the used fuel at a higher rate than would be expected solely on the basis of the chemical solubility of UO_2 in the near-field porewater. The production rate of oxidants by radiolysis would decrease with time as the strength of the radiation field decreases (Gobien et al. 2013).

At the fuel-water interface, the alpha dose rate exceeds the gamma and beta dose rates for most of the fuel history (Figure 5-10) and is the main contributor to radiolysis, producing molecular oxidants such as H_2O_2. Other potential sources of oxidants, such as any O_2 trapped inside the container when it was sealed, would already have been consumed by Fe and Cu corrosion processes before the fuel cladding was breached because these corrosion reactions are much faster than the reaction with UO_2. In principle, the radiolytically produced oxidants also would be consumed by reaction with container materials rather than by reaction with used fuel; however, for alpha radiolysis, the oxidants would only be produced within 20 μm of the fuel-water interface and they would have difficulty diffusing through openings in the cladding to react with container materials.

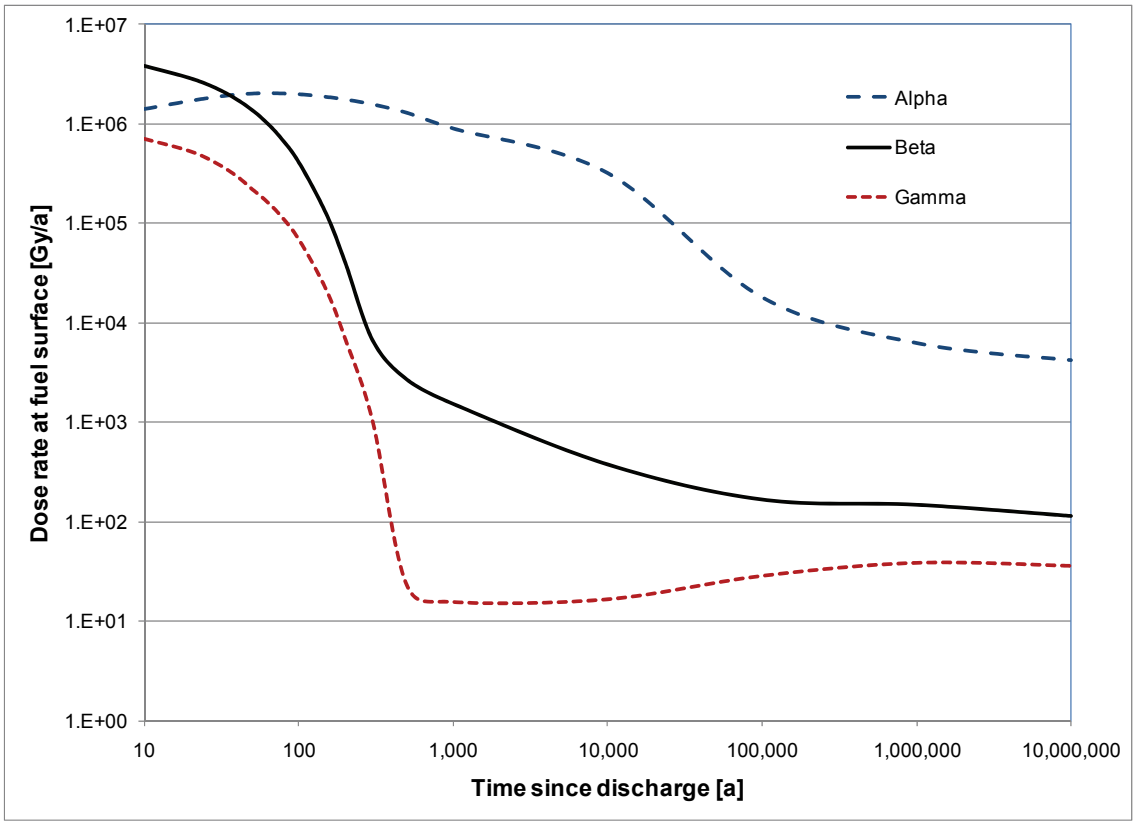

Figure 5-10: Radiation Dose Rate in Water at the Fuel Surface (220 MWh/kgU burnup)

Oxidative dissolution of the fuel continues as long as the alpha radiation field is sufficiently high. However, the actual dissolution rate decreases as the alpha field decreases due to decay. Experiments and mechanistic models have been developed to describe this corrosion rate, and

indicate that the dissolution of the used fuel would take more than one million years (Gobien et al. 2013).

Furthermore, in UO_2 and used fuel dissolution experiments the dissolution rate dropped by several orders of magnitude in the presence of even modest pressures of hydrogen gas (Shoesmith 2008) that would certainly be present due to corrosion of the iron vessel. A number of mechanisms have been either demonstrated or proposed to explain these effects, all of which involved the activation of hydrogen to produce the strongly reducing $H^{\bullet}$ radical, which scavenges radiolytic oxidants and suppresses fuel oxidation and corrosion (Shoesmith 2008).

After the alpha radiation field has decreased substantially, chemical dissolution of the fuel, proceeds according to the reaction,

$$UO_2 + 2H_2O \rightarrow U(OH)_4 \qquad (5\text{-}20)$$

under the anaerobic conditions expected in the repository. This reaction occurs very slowly, as is illustrated by the age of uraninite ore (largely UO_2) deposits, including northern Saskatchewan.

5.3.2.9 Radionuclide Release from the Fuel Pellets

Extensive studies of the interactions between used fuel and groundwater have established that radionuclide release from the used fuel occurs by two main processes. Initially, there would be a comparatively rapid release of a small fraction (typically a few percent) of the inventory of a selected group of radionuclides, that are either very soluble (such as ^{137}Cs, ^{129}I, ^{14}C and ^{36}Cl) or gaseous (such as Xe), and that are residing in the fuel sheath gap or at grain boundaries which are quickly accessed by water. This release process is referred to as “instant-release”. The second and slower release process comprises release of radionuclides from the UO_2 fuel matrix as the matrix itself corrodes or dissolves (called "congruent dissolution").

The instant-release fractions for various important radionuclides in used CANDU fuel are given in Gobien et al. (2013) and typical values for selected radionuclides are presented in Table 5-5. Note that the use of the term “instant release” with reference to the gap and grain boundary inventories is a simplification. In reality, it would take a finite time for water to penetrate into the grain boundaries and for the radionuclides located there to diffuse out. However, compared to the much longer time required for dissolution of the UO_2 matrix itself, grain boundary releases are so much faster that they can be considered “instantaneous”. Therefore, in conceptual models of radionuclide release, both locations - the gap and grain boundary inventories - are considered to contribute to the instant-release fraction.

Table 5-5: Typical Instant-Release Fractions for Selected Radionuclides

Radionuclide	Instant-Release Fraction (% of Inventory)
Cs	4
I	4
Cl	6
Tc	1
Actinides (Pu, Am, etc.)	0

Note: From Gobien et al. (2013).

Ferry et al. (2008) have shown that the instant release fractions do not change with time due to, for example, athermal diffusion of radionuclides induced by alpha-particle recoil displacements.

In addition to the bulk of the radionuclides in the used fuel pellets, there would be a small quantity of radionuclides present in the irradiated Zircaloy cladding from neutron activation. These radionuclides are generally distributed uniformly through the cladding and would only be released as the cladding itself dissolves. (However, evidence suggests that some of the C-14 in the Zircaloy is present within the zirconium oxide film (Gobien et al. 2013). This C-14 is released as soon as water contacts the Zircaloy. Zircaloy is corrosion-resistant in water due to the stability of its oxide coating, as described in Section 5.3.2.7. The strong adherence of the ZrO_2 corrosion layer to the metal surface suggests that radionuclides would be incorporated into the ZrO_2 as it forms and would only be released to solution when the oxide itself dissolves. Given the low solubility of ZrO_2, the rate of dissolution of the oxide and hence the release rate of the nuclides in the Zircaloy can be described using a solubility-limited dissolution model in which the rate of dissolution of the ZrO_2 is determined by the rate of diffusion of Zr away from the cladding.

5.3.2.10 Fate of Released Radionuclides

As radionuclides are released to solution, some would become oversaturated and secondary radionuclide-bearing phases would precipitate (e.g., ThO_2) on the fuel surface or on other surfaces nearby, such as provided by the metal corrosion products. Besides the low overall amount of such nuclides in a container, it is expected that their concentration in a precipitate would be diluted by the co-precipitation of other elements. Precipitation of a large mass of fissile nuclides in particular would be hindered by the intergrowth of such mixed-isotope precipitates along with iron corrosion products or buffer clays.

The radionuclides that remained in solution as aqueous species, and solids suspended in colloidal form, would diffuse through the various metal corrosion products inside the container. The corrosion products would also provide a surface for sorption of many of the radionuclides. In some cases, the sorption would be irreversible because the radionuclides would be incorporated into the crystal lattice of the corrosion product if it undergoes a transformation to a more stable solid phase.

Dissolved radionuclides would diffuse by a tortuous path through what was left of the steel container, through the cracks in the copper shell, through the low-permeability sealing materials, and finally through the rock around the repository. Migration of radionuclides away from the repository and their transport rate through the geosphere as a whole would be controlled by the local hydrogeological conditions. For the current hypothetical geosphere, groundwater velocities are low and transport is diffusion controlled. Radionuclides in colloid form or sorbed to colloids would be filtered by the buffer and not reach the geosphere.

5.3.3 Confidence

Extensive corrosion experiments have been carried out to improve the confidence for predicting the corrosion behaviour and lifetime of copper used fuel containers in a deep geological repository in Canada.

Container Corrosion: Because of the extensive experimental database on the corrosion of copper, the level of mechanistic understanding that has been developed over the past 30 years, and the existence of natural and archaeological analogues (discussed in Chapter 10), there is a significant confidence in the prediction of the long-term corrosion behaviour of copper containers. Both the predictive models for corrosion processes that are expected to occur, such as uniform corrosion and localized surface roughening, and the reasoned arguments against those that are not thought to be possible, such as stress corrosion cracking, are robust. Where uncertainty exists, such as the mechanism and exact corrosion rate that describe copper corrosion in anaerobic water or brine solutions, the total corrosion possible from these processes is very small over the container design life.

The evidence from natural and man-made analogues builds confidence in the conclusions drawn from experimental and modelling studies. Man-made analogues, such as Bronze Age artifacts or more-recent anthropogenic objects (discussed in Chapter 10), also provide useful supporting evidence that copper corrodes slowly, even in near-surface aerobic environments. The existence of native metallic copper deposits indicates that, under certain environmental conditions, metallic copper is stable over geological time scales. The fact that the majority of copper deposits in the Earth's crust are in the form of sulphide minerals is also evidence of the potential role of HS^- species in the corrosion of copper containers. Although it is not a pre-requisite that the groundwater at repository depth be free of sulphide, as the programs in Sweden and Finland demonstrate, there are clear advantages to selecting a site with no or low sulphide groundwater levels, as appears to be the case in southern Ontario sedimentary rock.

Confidence in long-term predictions is also supported by the robustness of those predictions and on the underlying information on which they are based. This confidence can stem from achieving the same result from different modelling approaches. For example, the conclusion that the maximum depth of uniform corrosion is of the order of a few hundred micrometres is predicted by both simple mass-balance models (SKB 2011) and from detailed mechanistically based reactive-transport modelling (King et al. 2008). These detailed reactive-transport models have been validated against experimental data and evidence from archaeological analogues (King et al. 2001).

Confidence also results from having a sound mechanistic understanding of corrosion processes. For example, the proposed mechanism to explain observations discussed in Section 5.3.1.5.2 is strong evidence that under repository conditions the localized corrosion of copper containers will

take the form of surface roughening rather than pitting. This understanding is equally important for processes that are not considered likely to occur, such as stress corrosion cracking. The approach for stress corrosion cracking provides multiple lines of argument against this behaviour and it is not considered feasible that all of the pre-requisite conditions for cracking would exist in the repository at the same time.

There are also multiple lines of argument for why microbiologically induced corrosion will have a minimal impact on the container (King 2009b, Sherwood Lollar 2011 and Wolfaardt and Korber 2012). However, uncertainties regarding the potential for microbial growth and activity under unsaturated conditions and at component interfaces requires further investigations. Since the possibility of remote microbial activity cannot be excluded, a corrosion allowance is made for this in lifetime assessments (Kwong 2011 and Scully and Edwards 2013).

The multi-barrier repository system represents a robust system that is capable of withstanding upset or unexpected conditions whilst still maintaining a high degree of containment. For example, the predicted container lifetimes are insensitive to the groundwater salinity and, in fact, higher Cl^- concentrations promote uniform rather than localized corrosion (King et al. 2010, 2011a). Information from site investigations in sedimentary rock in Canada suggest that the there is little or no sulphide in deep groundwaters (INTERA 2011). Experience from the Swedish and Finnish programs demonstrates that the combination of a copper container and dense bentonite buffer provides long-term containment even if sulphide were to be present. Similarly, there is no geological evidence that O_2-containing water has never reached repository depths even through glaciation events (see Chapter 2).

Copper Creep: Creep tests and modelling studies indicate that the copper creep deformation would stop once it has collapsed onto the inner steel vessel since the estimated creep deformation is extremely small. This also means that the amount of creep deformation of the copper vessel would depend on the gap width between the copper vessel and steel vessel. Recent analysis of data has revealed some uncertainty in the long-term creep fracture performance of oxygen-free phosphorus doped copper, and a need to supplement modelling capability with respect to creep ductility and mechanical integrity models. Accordingly, a long-term study is ongoing to improve confidence in these areas.

Container Temperature: The container surface temperature is affected by the container power, placement method, chemical composition, water content and thickness of sealing materials, distance between containers, distance between the placement rooms and tunnels, etc. The thermal responses were successfully modelled and there is good confidence that the evolution of temperatures of the container surface and surrounding bentonite buffer materials can be well estimated by existing computer models.

Container Structural Integrity: To maintain long-term structural integrity during its design life, the repository container is designed to withstand a load of 45 MPa. This includes an external isotropic pressure of up to 7 MPa during the pre-glaciation period, which accounts for the 6 MPa hydrostatic pressure up to a 500 m depth together with 1 MPa bentonite swelling pressure. The container could also withstand an external pressure load of 38 MPa during the glaciation period (which corresponds to a 3,800 m thick ice sheet) with full load applied as hydrostatic head (i.e., no load carried by the rock matrix). These are conservative assumptions. While glaciation would be a significant load, the earliest site coverage due to an ice sheet would be thousands of years in the future, probably at least another 60,000 years.

The copper container would be subjected to uneven bentonite swelling loads during the transient period before the completion of full water saturation and also, possibly, after saturation (though to a reduced extent) because of density differences that do not entirely homogenize because of internal friction. It is expected that the uneven swelling pressure loads would not cause container failure, based on the results of analyses for similar SKB and Posiva containers (Werme 1998, Raiko 2005). This will be verified by further engineering analyses.

Overall, there is high confidence in the structural integrity of the inner steel container for at least 100,000 years, and probably for as long as the copper shell maintains its integrity.

5.4 Long-Term Evolution of Buffer, Backfill and Seals

Each used fuel container along the centerline placement tunnel rests on a highly-compacted bentonite pedestal, with the remaining void spaces filled with gap-fill pellets. Bentonite is a type of clay that swells on contact with water, providing a natural self-sealing ability. Bentonite is a durable natural material that is expected to maintain its properties over the long term.

The safety strategy acknowledges that properties of the engineered barriers will allow safety functions to be fulfilled. This includes the design characteristics of surrounding the container by a buffer layer (approximately 60 cm) of dense bentonite-based clay pellets that will swell on contact with water. This clay layer will inhibit groundwater movement, has self-sealing capability, will inhibit microbial activity near the container, and retard contaminant transport.

The main processes with potential influence on the evolution of the sealing systems are listed in Table 5-6 and discussed in the following sections.

Table 5-6: Processes with a Potential Influence on the Evolution of Buffer/Backfill/Seals

PROCESS	POTENTIAL INFLUENCE
RADIATION	
None	• None
THERMAL	
Heat transport from container	• Change in temperature of sealing materials and rock • Redistribution of moisture prior to saturation • Temperature increases across gap or interface
HYDRAULIC & PNEUMATIC	
Saturation of repository	• Expansion of bentonite to close gaps • Chemical reactions between water and sealing materials • Development of swelling and hydrostatic pressure • Changes in thermal conductivity of buffer

PROCESS	POTENTIAL INFLUENCE
Groundwater flow	• Rate of water supply for saturation • Erosion/piping under excessive amounts of inflow in the preclosure period
MECHANICAL	
Swelling pressure	• Density redistribution in clay-based sealing materials • Sealing of cracks and gaps in clay • Stresses in concrete/bulkhead
Thermal strains in concrete	• Fracturing in concrete; increased permeability
CHEMICAL	
Diffusion of chemical species	• Changes in porewater composition/salinity
Ion exchange in clays	• Changes in porewater composition • Change in hydraulic conductivity and swelling pressure of clay-based seals
Reactions with redox-sensitive minerals	• Consumption of oxygen in repository
Increase in salinity	• Changes in hydraulic conductivity and swelling pressure of clay-based seals
BIOLOGICAL	
Aerobic microbial activity in backfill	• Consumption of oxygen in repository
Anaerobic microbial activity in backfill	• Generation of sulphide which is a potential corrosion risk to copper container

Notes: Processes listed are those that are most likely to have a notable effect on the buffer/backfill/seals, over a time scale of one million years.

5.4.1 Changes during Saturation

After the buffer pellets are installed, the water seeping into the repository would begin to wet them, and the bentonite in the buffer would expand. As this expansion progresses, it will fill the space between the pellets and restrict water movement. Moreover, the swelling pressure would in due course provide mechanical resistance to the local effects of large-scale flexing and crustal rebound processes associated with glacial loading, reducing the severity of damage to the near-field rock surrounding the backfilled openings of the repository. The swelling capacity of the bentonite decreases at high salinity, but the performance requirements for swelling pressures are met for salinities expected at 500 m depth, i.e., a total dissolved solids content of around 275 g/L (Figure 5-11).

The Effective Montmorillonite Dry Density (EMDD) is a parameter that allows a comparison of the behaviour of different types and densities of clay-based materials (Man and Martino 2009, Dixon et al. 2011) (see Table 4-4). For the reference gap fill material, using dense pellets of MX-80 clay and emplaced at an effective dry density of 1,410 kg/m^3, the EMDD will be around 1,260 kg/m^3.

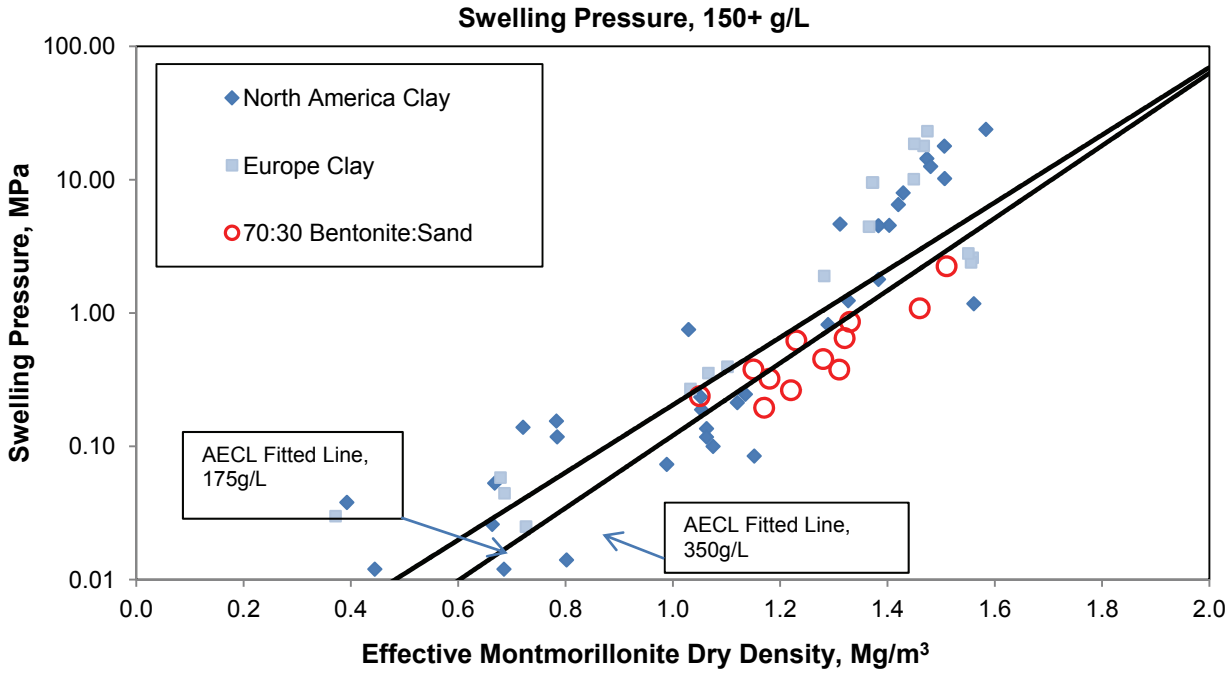

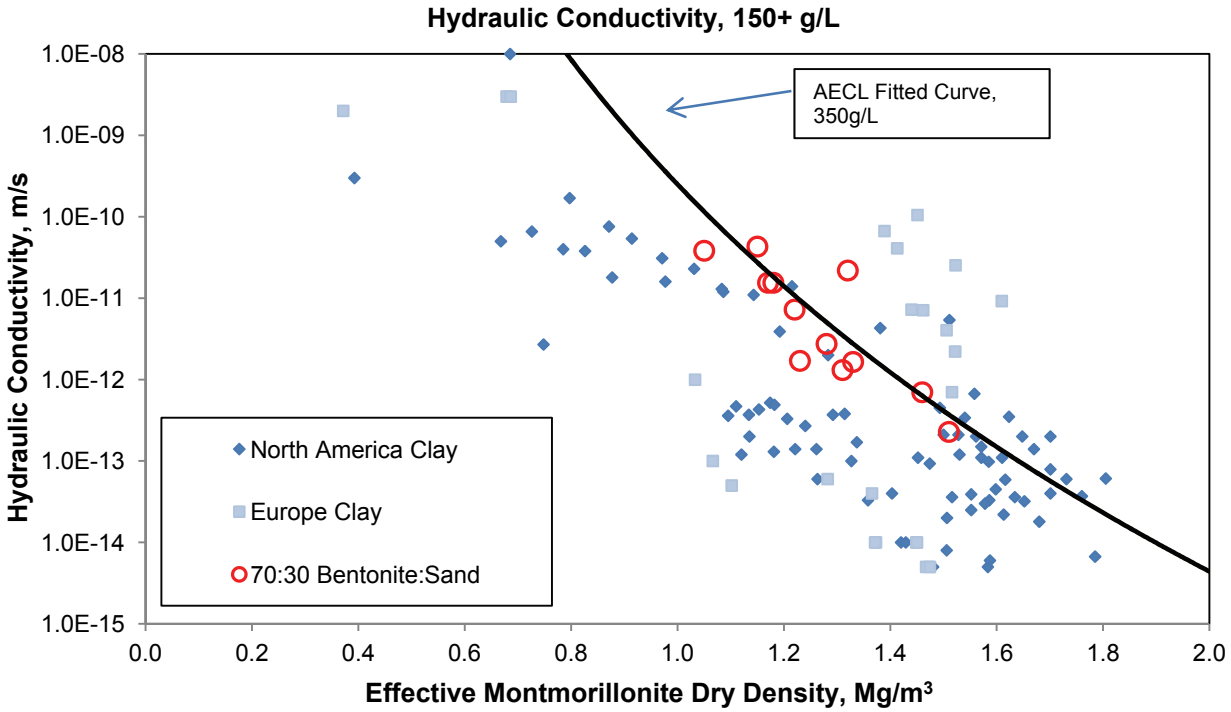

Note: Recent measurements of 70:30 Bentonite:Sand under relevant sedimentary rock conditions are shown in red circles.

Figure 5-11: Hydraulic Conductivity and Swelling Pressure under Saline Water Conditions: Variation with Effective Montmorillonite Dry Density

The timing and rate of saturation of a repository depends on a number of site-specific conditions. In the Cobourg Formation, the limestone has a very low hydraulic conductivity and porosity; as such, ingress of water into the repository will be very slow and the bentonite buffer will take a considerable amount of time to saturate. In addition, other factors such as the thermal gradient from the containers would counter the resaturation process. In order to estimate the saturation time of the repository, the saturation process was modelled using the coupled thermal-hydro-mechanical code T2GGM (Suckling et al. 2013). The minimum saturation time was estimated to be 10,000 years (Gobien et al. 2013, Section 5.2) accounting for the availability of water in the rock, the suction potential of the bentonite and the thermal gradient of the container.

5.4.2 Temperature Changes

The thermal conductivity of the various clay-based sealing system components changes with their degree of water saturation. Figure 5-12 illustrates this relationship for bentonite-only and bentonite-sand compositions. This figure illustrates the effects of sealing material composition and water content on its heat-transfer characteristics. Initially considered for use as the buffer material in the repository concept developed by AECL, a mixture of equal dry weight proportions of sand and bentonite was defined as the reference bentonite-sand buffer for use in filling the region between the container and the surrounding rock. Subsequent review identified bentonite-only clay as the preferred buffer material, such as the 100% bentonite gap fill pellets with a dry density of 1,410 kg/m^3.

From Figure 5-12, it can be seen that in the region nearest the containers, the thermal conductivity of the buffer will decrease as heat from the containers drives moisture away. In contrast, buffer thermal conductivity will gradually increase as the degree of saturation increases. Good agreement is obtained in modelling of thermal profiles in field experiments like the SKB Container Retrieval Test when the thermal conductivity characteristics provided in Figure 5-12 were used (Guo 2009).

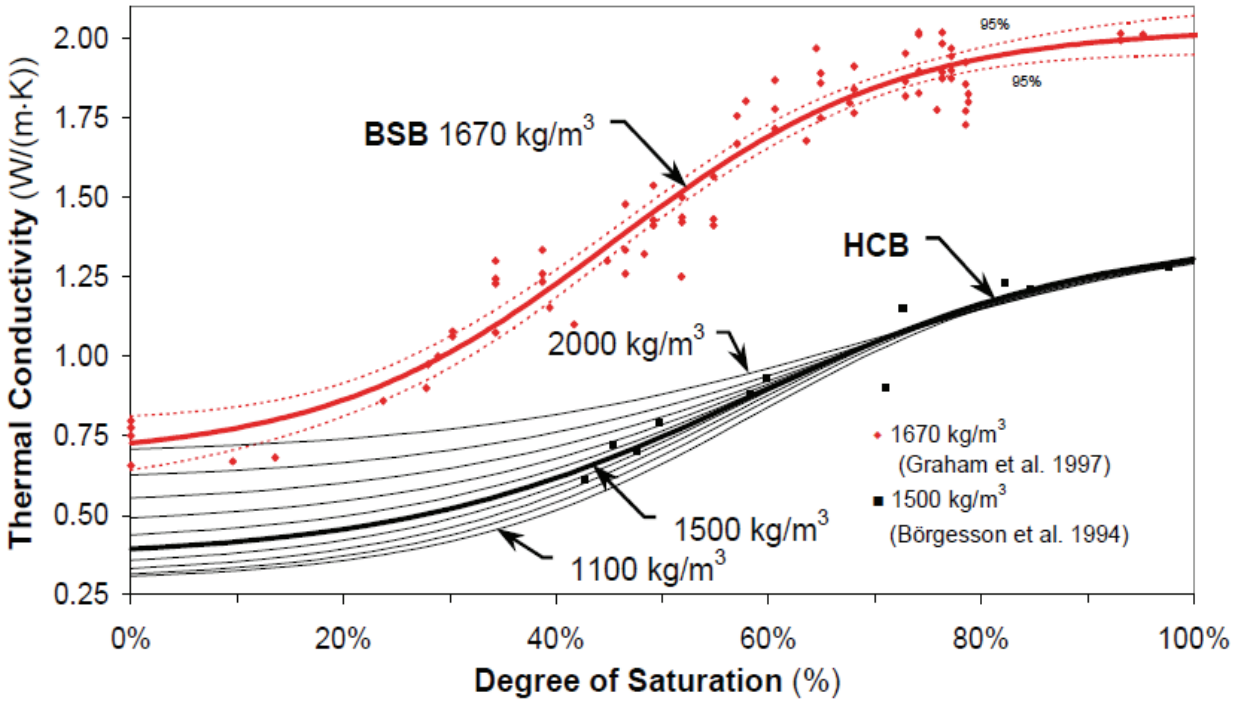

Notes: From Man and Martino (2009). Label units are dry densities.

Figure 5-12: Thermal Conductivity of 50:50 wt% Bentonite-Sand Buffer (BSB) and of 100 wt% MX-80 Bentonite

The maximum near-field temperature is predicted to occur within the first 30 years following placement as shown in Figure 5-5 (Guo 2010), when the buffer will be unsaturated.

The main sealing material that would potentially be affected by thermal expansion is the concrete bulkheads at the ends of placement rooms (Figure 4-15), which could also be affected by heat released during their curing process. These would be installed using low-heat concrete and in a manner that minimized contraction during the concrete curing process.

Later, as the temperature of the repository declines (Figure 5-5), thermal contraction of the concrete bulkhead is likely to cause some rejuvenation of cracks or the production of new cracks at the rock-concrete interface. This process was observed in the concrete seal portion of the AECL URL Tunnel Sealing Experiment (Chandler et al. 2002). The concept of using a composite HCB-concrete structure in a repository anticipates that by the time temperatures decrease significantly in this region, the clay gasket that was installed as part of the composite seal should be fully saturated. The clay would expand providing a tight contact with the concrete and rock and if water flow is occurring from the backfilled tunnel past the concrete it is expected that some of the clay will move/intrude into the open interface and reduce mass-transport along this feature.

5.4.3 Chemical Changes

An important function of the buffer is to produce/maintain a chemical environment in the repository, which will inhibit corrosion of the containers and, in the case of a breach in a container, would limit the solubility of the used fuel and the subsequent migration of radionuclides. Conversely, the composition of porewater in the repository will affect the mechanical and hydraulic properties of the buffer. The evolution of porewater chemistry in the sealing materials is complex as it is influenced by many parameters, including the compositions and proportions of minerals in the buffer and backfill, the composition of the saturating groundwater, the repository temperature, the relative rates of movement through the clay, the initial proportions of exchangeable cations in the clay minerals, and the composition of the water used during wetting and compaction of the sealing materials. Eventually the porewater in the buffer would resemble the groundwater entering the repository and the Na in the bentonite would have exchanged with Ca in the groundwater, potentially causing a reduction in the swelling pressue and an increase in the hydraulic conductivity of the buffer. However, such potential effects are accounted for in the design of the repository.

5.4.4 Changes due to Biological Processes

Aerobic biodegradation of concrete is a well-known microbial process (Humphreys et al. 2010). Initially, conditions in the vicinity of the concrete seals and floors in the deep geological repository may be moist and aerobic enough that pyrite or other sulphide minerals present in the sealing materials (as part of the concrete aggregate or as minor components in buffer or backfill) could be converted to sulphuric acid by sulphate-producing bacteria. The extent of this corrosion would be minor, however, given the relatively short duration of oxidizing conditions in the repository and the likely low abundances of sulphide accessory minerals in the sealing materials.

Clay-based materials have been shown to contain indigenous aerobic and anaerobic microorganisms. Microorganisms could also enter the sealing materials during the operating phase of a repository from the air and human activities in the short term and from the host rock in the long term. The current understanding of microbiology in the context of a repository is summarized by Wolfaardt and Korber (2012).

Specific biogeochemical processes in the buffer, backfill and seals pertain to:

1. Consumption of oxygen and creation of an anaerobic environment;
2. Gas production and consumption; and
3. Microbiologically-influenced corrosion (MIC).

As the geosphere of a deep geological repository is nutrient-poor, microbial activity at depth is limited compared to the near-surface environment.

During the time that a repository is open, the engineered barrier system and adjacent rock would be exposed to air. This would facilitate the growth of aerobic bacteria. After the repository is closed, the aerobic bacteria in this zone are expected to actively promote reducing conditions by consuming the remaining oxygen. Anaerobic bacteria, which were likely to have been the main forms of life in the deep subsurface environment prior to repository excavation,

would eventually dominate again, and reducing groundwater conditions would be maintained far into the future. Upon establishment of anaerobic repository conditions, a variety of organisms with the capabilities to utilize alternate electron acceptors have the potential to become active. Anaerobic bacteria can both produce and consume gases, which have limited potential to impact both the physical and chemical aspects of the repository. Of particular interest, is the potential for microbial activity to cause microbiologically influenced corrosion, as discussed in Section 5.3.1.5.4. As a result, a substantial amount of research has been conducted on ability of clay buffer to inhibit microbial activity (e.g., Stroes-Gascoyne 2010).

In the current Canadian EBS design, 100% highly-compacted bentonite buffer material surrounding the waste containers is proposed to prevent or minimize potential negative consequences of microbial activity, such as damage to the container or barrier integrity. Numerous studies have evaluated the survival and activity of microorganisms in clay-based sealing materials under relevant environmental conditions, as summarized in Wolfaardt and Korber (2012). The activity and abundance of microbes in a repository are affected by three main factors: the supply of usable nutrients and energy sources, the availability of water, and elevated temperatures. Radiation fields are not expected to be significant due to the shielding provided by the thick-walled containers.

Sources of nutrients in the sealing materials would include organic matter associated with the clays, as well as nitrates and fuel oil from blasting residues, and hydrocarbons from diesel oils and exhaust gases, introduced during repository excavation and operation. As the organic matter in such clays has already persisted in the presence of indigenous microbial assemblages for thousands to millions of years, it is probably unrealistic to assume that all of the organic carbon would be accessible to microbes. It is likely, therefore, that “available” organic carbon would be the limiting nutrient for microbial activity in a repository.

The second factor that would have an important influence on microbes in clay-based sealing materials is the availability of water. Microbiologists generally use a thermodynamic parameter, water activity (a_w), to express water availability in a quantitative sense. This term corresponds to the ratio of a solution’s vapour pressure to that of pure water at a given temperature. The activity of porewater in sealing materials is affected in particular by the salinity of the water, as well as by the affinity of the clay for water. For example, while the water activity in pure water is 1, the water activity in a 2 mol/kg solution of $CaCl_2$ is about 0.85 within the buffer material (King and Stroes-Gascoyne 1997). Bacteria must expend extra effort to grow in a habitat with a low a_w because they must maintain a high internal solute concentration to retain water within their cells. Most bacteria flourish only at or above an a_w of approximately 0.98, the a_w for seawater (see Figure 5-13). In order for the buffer to inhibit bacterial growth, it has been established that bentonite would need to meet one or both of the following criteria:

- A water activity of less than or equal to 0.96, resulting from a bentonite dry density of at least 1,600 kg/m^3 or a porewater salinity greater than 60 g NaCl/L (Stroes-Gascoyne et al. 2006, 2007a, 2007b); or
- A swelling pressure of at least 2 MPa (Pusch 1999). Swelling of clay is expected to restrict the mobility of microbes and of nutrients, causing starvation.

The third major factor affecting the viability of microbes in the sealing materials is temperature, which would range from ambient (10 - 20^{o}C) to ~120^{o}C adjacent to the container. Temperatures within this range would have some impact on the viability of most microbes indigenous to the

sealing materials. The bacteria in buffer closest to the container would be subjected to the most intense heat and also the related buffer desiccation. Experiments assessing the effect of temperature suggest that microbes were not particularly sensitive to a temperature of 60°C and some culturability remained after exposure to 80°C at all dry buffer densities studied (0.8 to 2.0 Mg/m^3), whereas at temperatures ≥ 121°C, culturability was reduced (Stroes-Gascoyne and Hamon 2010). Importantly, the effect of temperature on culturability in low dry density bentonite was reversible once the heat source was removed and re-saturation was allowed to occur, highlighting the importance of maintaining high dry density to keep microbial activity to a minimum (Stroes-Gascoyne and Hamon 2010).

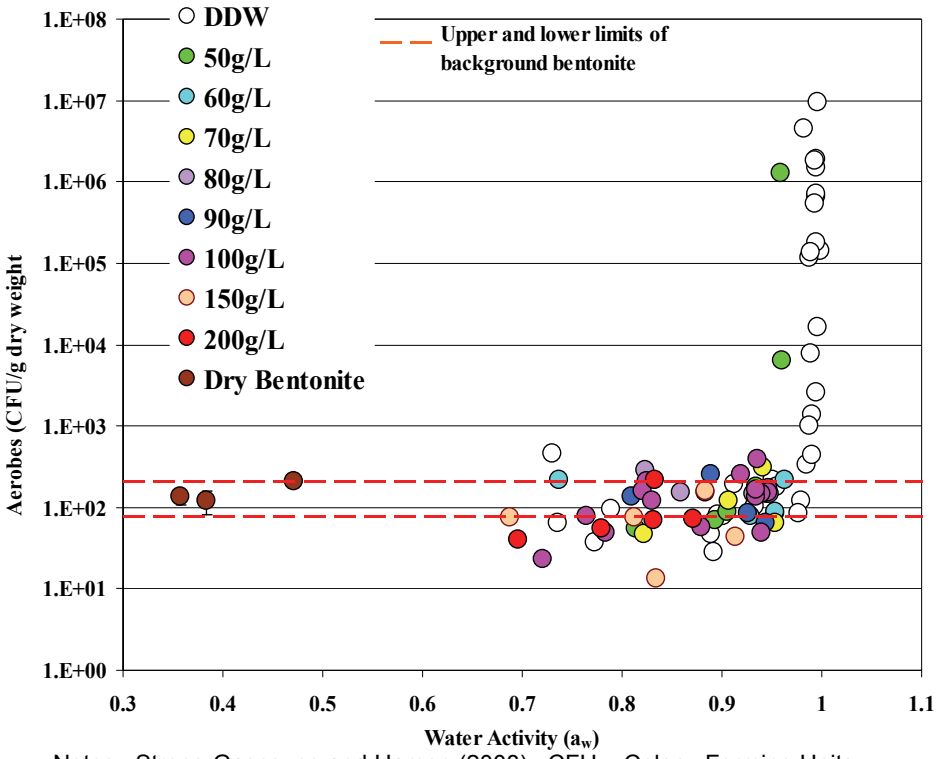

Notes: Stroes-Gascoyne and Hamon (2008). CFU – Colony Forming Units.

Figure 5-13: Effect of Water Activity on Aerobic Culturability in Compacted Bentonite

In summary, in a high-salinity repository environment, with porewater salinities ≥ 50 g/L, salinity will suppress microbial activity over a wider range of bentonite dry densities (~ 800 to 1,800 kg/m^3) (Stroes-Gascoyne et al. 2010a, 2011). In contrast, experimental evidence indicates that in a low-salinity environment, a highly compacted bentonite with a dry density of 1,600 kg/m^3 will suppress microbial aerobic culturability below background levels (Stroes-Gascoyne et al. 2010b).

5.4.5 Radiation

Radiation would have little effect on the sealing materials, even near the container surfaces, because the thick-walled containers are largely self-shielding. It was estimated that for the reference container, the initial surface gamma dose rate would be approximately 0.05 Gy/a.

Radiation may restrict biological processes in the immediate vicinity of the container, and it may result in minor chemical changes in gas and porewater composition due to radiolysis, but none of these effects are expected to be major (McMurry et al. 2003).

5.4.6 Sorption

An important function of the clay-based buffer is to provide a substrate for the sorption of contaminants if there is a breach of containment. Sorption is a general term for surface-related processes that involve the transfer of ions from a solution in which they have freedom of movement to a fixed position on a surface. In addition to ion exchange, sorption includes surface complexation, in which ions form a strong chemical bond with a reactive surface group at the mineral surface without the displacement of any other ions, and surface precipitation, in which a chemical reaction occurs on the surface because conditions there differ from those in solution. Under highly saline conditions, ion exchange will not be an important sorption mechanism, and only species that react through surface complexation will be significantly sorbed (Vilks 2009, Vilks et al. 2011).

5.4.7 Vertical Movement of Containers

In the horizontal tunnel placement concept, used fuel containers rest on a highly-compacted bentonite pedestal, with the remaining void space filled with gap-fill bentonite pellets. One of the design requirements of this buffer is to prevent containers from shifting from the centre of the placement tunnel, which would reduce the buffer thickness.

Upon closure, water is expected to slowly enter the placement rooms, wetting, swelling and compressing the blocks and pellets. The rate of resaturation will depend on the rate and location of water inflow and the actual evolution of the saturation and homogenisation of the buffer. Variability in resaturation is expected to lead to an uneven distribution of swelling pressures within the placement rooms. In addition, some upwards swelling is expected since the gap-fill pellets have a lower swelling pressure than the bentonite pedestal and a certain degree of compressibility. Such small movements of the containers would not affect repository evolution.

5.4.8 Buffer Erosion and Colloid Formation

Colloids are small solid particles between 1 nm and 1 μm in diameter that are suspended and dispersed in groundwater. Colloids may form by microbial activity or as precipitates due to a change in porewater chemistry. Colloids are of interest in a repository primarily because they have the potential to sorb radionuclides if containers have failed, at which point the transport of the contaminant is controlled by the mobility of the colloid, rather than by the chemical speciation of the radionuclide. These are not expected to be important due to the very low permeability host rock, such that transport is by diffusion not advection. Also, the high salinities will tend to minimize microbial activity (and potential colloid formation) as well as formation of bentonite colloids.

5.4.9 Confidence

The engineered sealing system components would be installed subject to design, manufacturing, and construction specifications, and so their properties would be known with a high degree of confidence. Nevertheless, there are uncertainties about the long-term behaviour of the materials and the processes that would affect them.

Temperature: There is confidence in the results of thermal models over long timeframes. Temperatures in the near-field are generally well-predicted in modelling of prototype repository design experiments over a range of repository saturation levels. Uncertainties would tend to be localized, and due to spatial variability in properties.

Repository Resaturation: Considerable confidence exists in the ability to describe repository performance in a saturated state, but there would exist a period of potentially thousands of years in which saturation has not yet been achieved in this very low permeability host rock. It is therefore during this pre-saturation stage of repository evolution that many of the interactions between repository components would occur. The resaturation of a repository involves coupling of thermal-hydraulic-mechanical processes. Current numerical models are able to broadly explain the evolution of saturation conditions.

Swelling Pressures and Stresses: The swelling pressures generated by the buffer would depend on the buffer composition, buffer density, and groundwater conditions. The swelling characteristics of a wide range of bentonite based sealing materials have been determined through testing but would need to be confirmed for site-specific conditions. The manner in which stresses develop within a repository would also influence the swelling pressure. Strains within one component of the repository sealing system may affect the density and hence the swelling pressure development of another component. The development of thermal stresses in conjunction with the hydraulic and swelling stresses within a multi-component system is complex. Numerical models are presently weakest in explaining the evolution of the stress field in the near-field.

Evolution of Material Properties: The properties of the pellet gap fill are not yet thoroughly characterized with respect to their performance under repository conditions. Further studies on the long-term evolution of these materials under interaction with adjacent materials and saline groundwater are warranted.

Mineralogical Stability of Montmorillonite: Under the expected repository conditions (temperatures less than 120^{o}C, moderate pH levels, moderate potassium concentrations in groundwater), it is very unlikely that substantial conversion of montmorillonite to illite would occur over a million-year timeframe. The effect of high salinities, however, needs more assessment.

Microbial Processes: Although viable microbes would initally inhabit at least some portions of a deep geological repository, there are a number of uncertainties associated with the extent of changes that would result from their presence. For example, although experimental data indicate it is unlikely that bacteria would become active or able to recolonize saturated, highly compacted buffer material, their behaviour in gap fill material needs to be demonstrated. Nevertheless, in the long run, the salinity of the groundwater would limit microbial activity in the repository.

Redox Conditions: There is some uncertainty about when reducing conditions would be established in the sealing materials. It has also been noted that estimates of the time required to reach anaerobic conditions vary, depending on assumptions made in the calculations, from approximately tens of thousands of years to hundreds of thousands of years. Regardless of the amount of time required for oxygen in the repository to be consumed, the total amount of oxygen available for reaction is limited. There are no processes (including radiolysis) that are likely to introduce significant additional quantities of oxygen after closure.

5.5 Long-Term Evolution of the Geosphere

As noted in Chapter 1, the Geoscience program for a future candidate site will be designed to support the safety case. As part of geosynthesis activities, both regional and site-specific information from site characterization activites would be integrated to provide improved understanding of the natural processes that might affect the performance of a repository over one million years. These processes include climate change (specifically glaciation) and geologic processes such as glacial erosion, seismicity, fault rupture/reactivation and volcanism (Table 5-7). To capture the potential degradation of the rock mass, the long-term strength of the rock would be used to analyze the stability of the opening in the host rock at a future candidate site.

Table 5-7: Processes with a Potential Influence on the Geosphere

PROCESS	INFLUENCE
THERMAL	
Glaciation-related cooling	• Permafrost formation • Development of thick ice sheet
HYDRAULIC & PNEUMATIC	
Glaciation and permafrost formation	• Regional changes in groundwater flow pattern • Depth-related changes in groundwater composition
MECHANICAL	
Glacial loading and unloading	• Glacial erosion • Repository rock mass stability
CHEMICAL	
Glaciation-related changes in groundwater flow	• Depth-related changes in groundwater composition • Potential precipitation of secondary mineral phases due to depth-related changes in groundwater composition, and potential dissolution of soluble vein infilling minerals (e.g., gypsum, halite).
BIOLOGICAL	
Glaciation-related changes in groundwater flow	• Potential changes in microbial activity due to depth-related changes in groundwater composition

Notes: Glaciation is the most significant process likely to disturb the geosphere at repository depths over a time scale of one million years.

5.5.1 Geological Disturbances

The following sections describe, in general terms, the likely effects of seismicity, fault rupture/reactivation and volcanism on a repository located within the Michigan Basin.

5.5.1.1 Seismicity and Seismic Hazard Assessment

In general, the Michigan Basin is characterized by low levels of seismic activity as it is located within the tectonically stable center of the stable North America continent (Hayek et al. 2010). Most earthquakes in the regional area, although rare, are deep and occur in the Precambrian

basement. Seismic events with focal depths in the Paleozoic sequence are not known to occur. During glaciation, an increase in the frequency of earthquakes is expected during a glacial retreat, however the magnitude of these events is expected to remain low. This is supported by the lack of apparent evidence for cross formational mixing of groundwaters and the lack of neotectonic deformation (NWMO 2011).

To further improve confidence in long-term stability regarding seismic hazards, there is a considerable body of evidence to show that earthquakes, in general, are less destructive at depth than at the surface, diminishing the impact of any seismic activity (including proximal events) on a deep geological repository (Bäckblom and Munier 2002, Atkinson and Kraeva 2011).

Although beyond the scope of the current study, it is noted that for an actual deep geological respository site (or sites), a probabilistic seismic hazard assessment would be conducted for the area as part of site characterization/geosynthesis activities. This assessment would be done following the guidance of the Senior Seismic Hazard Advisory Committee (SSHAC 1997). Seismic monitoring would also be conducted as part of site characterization activities to capture additional information on low-magnitude seismic events.

5.5.1.2 Fault Rupture and Reactivation

Seismicity within a sedimentary basin environment is expected to be confined to regions containing pre-existing features (e.g., faults, fractures) within the Precambrian basement. Damage to intact rock is not expected to occur because in-situ tectonic and glacially induced stresses are not considered sufficient to generate the forces required to create rupture (Lund 2006). For this case study, it is assumed that the repository is sited in an area where no faults have been observed, and it would require earthquakes to propagate faults into previously unfaulted rock. As previously stated, most earthquakes in the region are deep, occur on pre-existing basement faults, and are very rare in this area. There are no known seismic events in the region with a focal depth in the Paleozoic sequence.

5.5.1.3 Volcanism

Volcanoes are primarily found at plate boundaries. Because the Michigan Basin is located several thousands of kilometres from the nearest plate boundary, the risk to a repository from a volcano is considered insignificant. Another mechanism that might create a volcano is a mantle plume, or “hot spot”. The closest active “hotspot” is located in the Snake River Plain and Yellowstone area of the western United States, at a distance of over 3,000 km away.

The lack of active orogenic activity in southern Ontario under the currently stable tectonic regime suggests strongly that volcanic activity is not expected to influence the hypothetical repository site.

5.5.2 Climate Change (Glaciation)

The past 2 million years of Earth’s history has been marked by periods of glaciation. Ice coverage was not continuous over the Michigan Basin, but was marked by many cycles of glacial ice sheet advance and retreat, separated by ice-free periods of warmer climate (interglacials), lasting from thousands to hundreds of thousands of years. Nine glacial cycles occurred over the past million years. During the last glaciation, starting approximately 120,000 years before present, more than 97% of Canada was repeatedly covered by ice. The final retreat of the ice sheet occurred between about 9,000 and 6,500 years ago. Discussion on

the current understanding of glaciation, and the processes that cause glaciations, can be found in Peltier (2002, 2011).

If a reglaciation of the Canadian land mass should occur again, it is most likely to occur 60,000 years from present (Peltier 2011). If, at that time, the concentration of carbon dioxide and other greenhouse gases in the atmosphere were similar to present levels, it is unlikely that a renewed episode of glaciation could occur. Because our ability to predict the CO_2 level that will exist at a time so far into the future is difficult, we cannot discount the possibility of a renewed glacial event and, therefore, must take glacial processes into account when developing the safety case for a used fuel repository.

The numerous characteristics of the glaciation process that are relevant to the understanding of repository performance include:

- Erosion, related to ice sheet movement across the land surface.

- Mechanical properties, such as the time dependence of the thickness of glacial ice that could develop over the site and the normal stress regime associated with the weight of the ice load. Also relevant is the evolution of temperature at the base of the ice sheet. Periods of thickest ice cover are associated with the warmest basal temperatures, which is a consequence of the degree of thermal insulation provided by the thick ice and the continuing flow of heat from the Earth's interior into the base of the ice sheet.

The subsurface thermal regime is important to repository performance as well, in particular the depth to which frozen ground (permafrost) may extend. This issue is important not only in the regions that are episodically ice-covered, but also in exterior regions where the influence of permafrost may be even more extreme. In regions within which the base of the ice sheet is temperate (i.e., having temperatures above the freezing point), meltwater is continually generated by the outflow of geothermal heat, and the rate of such generation is crucial to understanding the extent to which such meltwater may be forced to infiltrate into the subsurface and potentially impact deep groundwater systems.

The phenomena associated with glaciation potentially affecting a repository and/or the geologic setting at the repository site can be grouped into three broad categories: glacial erosion, glacial loading and permafrost formation. These are discussed under the headings below.

5.5.2.1 Glacial Erosion

The predominant geosphere process that will result in erosion over the next million years is glaciation. Glacial meltwater can erode sediment and rock by abrasion, quarrying, and mechanical erosion. Regardless of the mechanism, the rate of surface erosion can be limited by the ability of the meltwater to remove debris (e.g., due either to an insufficient hydraulic head gradient to carry debris-laden subglacial water out of the basin, or the lack of adequate subglacial pathways for water). In terms of erosion at a local level, the basal sliding velocity is the primary factor controlling the rate of erosion. However, rapid basal sliding velocity does not necessarily correlate with rapid erosion at the base of the glacier, as the glacier may be decoupled from the bedrock surface by a thin layer of basal melt water, or by a layer of deformable sediment.

Hallet (2011) conducted a glacial erosion assessment in which several independent types of geological evidence were examined to assess the magnitude of erosion which would likely occur over one glacial cycle at different scales, from regional to local. In total, thirteen estimates (eleven of which are independent of one another) were presented which support the conclusion that erosion would not exceed many tens of metres in the Bruce region of southern Ontario over one glacial cycle; no erosion and net deposition of sediments in the region is also possible. For the hypothetical site considered in this study, it is assumed that net erosion is likely on the order of tens of metres over one million years. This assumption is supported by local erosion estimates reported by Hallet (2011) for the Bruce nuclear site. As part of site characterization activities, an investigation would be conducted of topographic features or other known factors that might tend to localize erosion at a potential site.

5.5.2.2 Glacial Loading

Climate modelling of the late Quaternary ice advances and retreats has predicted ice thicknesses of up to 4 km of ice over northern Canada and approaching 2.5 km of ice in southern Ontario (Peltier 2002). The last glacial episode had a duration of approximately 120,000 years, and involved multiple glacial advances and retreats, resulting in loading and unloading cycles on the underlying rock with each advance and retreat.

The weight of the thick ice sheet acts to depress the Earth's crust and removal of the ice load by melting leads to crustal rebound, a process known as isostacy, which continues today. Peltier (2011) has predicted that the maximum crustal depression from the equilibrium level occurred at the Last Glacial Maximum (LGM) and reached values in excess of 500 m.

The University of Toronto Glacial Systems Model (UofT GSM), which is a model of continental-scale glaciation events, was used by Peltier (2011) to develop a description of glaciation of the Canadian landmass. A maximum glacial event time profile for ice loading was developed based on Peltier (2011), as shown in Figure 5-14, and indicates that the vertical stress reaches a maximum value of approximately 30 MPa. In addition to changing the vertical stress at depth, glaciation can also cause the horizontal stress to increase due to both Poisson's effect and plate bending. The horizontal stress increase due to Poisson's effect is:

$$\Delta\sigma_h = \frac{\nu}{1-\nu}\Delta\sigma_v \tag{5-21}$$

where... σ_h is the horizontal stress;
σ_v is the vertical stress; and
ν is the poisson's ratio.

The increase in the horizontal stress due to plate bending is also proportional to the increase in vertical stress, with the maximum increase assumed to be 2 MPa. Numerical analyses carried out by Lund et al. (2009) showed that shear stresses are relatively minor compared to the vertical and horizontal normal stresses.

Numerical modelling of the effects of stress changes associated with glacial advance and retreat (as described above) on a repository is beyond the scope of this study for a hypothetical site, but would be conducted in order to support a safety case for a candidate site.

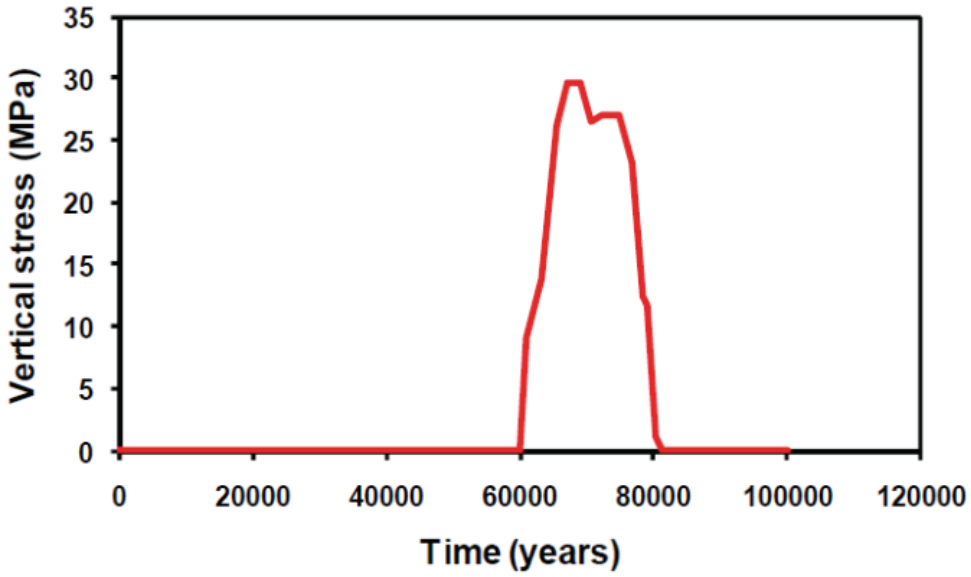

Notes: Time from present is for first event.

Figure 5-14: Simulated Evolution of Ice Sheet Load

5.5.2.3 Permafrost Formation (Changes in Groundwater Recharge)

Permafrost formation as a result of glaciation will impact the extent to which glacial meltwater will infiltrate into the subsurface. Future glacial conditions at the hypothetical repository site would be preceded by an extended period with widespread formation of permafrost. Under permafrost conditions, groundwater would freeze in the subsurface, decreasing the connected porosity and permeability and significantly decreasing recharge and altering flow system hydraulic gradients for up to tens of thousands of years.

In regions of permafrost, taliks are regions of perennially unfrozen ground that exist within otherwise continuous permafrost environments (Peltier 2004). The formation of taliks is dependent on site-specific thermal, chemical, geological and hydrological conditions (Peltier 2004). Heat emanating from the repository is unlikely to create a talik since periglacial conditions are not expected for several tens of thousands of years, after heat from the repository has already decreased.

Meltwater beneath glacial ice sheets can be pressurized, resulting in hydraulic heads far in excess of those found during interglacial periods. Two factors affecting the penetration of glacial water to depth are permafrost depth and distribution, as well as stress changes developed from the ice load.

When permafrost exists under the ice sheet (cold-based conditions), groundwater recharge to depth is inhibited, despite the high hydraulic head imposed at the ice sheet base. A warm-based ice sheet is one in which the free water at the base is at temperatures above the pressure freezing point beneath the ice (i.e., no permafrost), and enhanced recharge may occur. Subglacial groundwater flow patterns associated with warm-based conditions are likely to involve increased volumes of water and more rapid movement than pre-glacial or cold-based conditions, particularly in the shallow groundwater flow system.

Glaciation-related changes in groundwater chemistry are not expected to affect the redox or salinity conditions of groundwaters at repository depth. Paleohydrogeology and geochemical modelling studies can be used to evaluate changes associated with previous glaciation events. For example, isotopic evidence in the Michigan Basin indicates that recharge of glacial meltwater is constrained to formations above the Ordovician shales (NWMO 2011).

The depth of penetration of glacial waters into the deep groundwater system at the hypothetical sedimentary site was considered in this study. Paleohydrogeological modelling was completed for the Laurentide glacial episode (120,000 to 10,000 years before present) and presented in detail in Chapter 2 (Section 2.3.4.3). The key insights from the illustrative modelling are summarized.

A total of eleven paleohydrogeologic simulations were performed to investigate the role of varying paleoclimate boundary conditions. Details of the paleoclimate modelling scenarios can be found in Section 2.3.4.3. The performance measure of choice to compare the paleohydrogeologic simulations is the movement of a conservative unit tracer applied with a Cauchy boundary condition at the top surface of the model domain. This tracer represents the predicted migration of recharge waters into the groundwater system over the course of a 120,000 year simulation. The depth of the tracer is determined by the 5% isochlor, which is conservative in that it represents a pore fluid containing 5% recharge water. The 5% isochlor provides an indication of recharge water migration into the subsurface, which can be used to compare alternative paleohydrogeologic scenarios. The paleohydrogeologic simulations do not consider reactive transport; therefore, although the 5% isochlor provides an indication of the percentage meltwater, it does not take into account the consumption of oxygen. In addition to the tracer, Péclet numbers were estimated to assess changes in transport mechanisms during the paleohydrogeologic scenarios. The Péclet number is estimated by comparing rates of advection to diffusion.

The depth of penetration of the conservative tracer is shown in Figure 5-15. The penetration depths of surficial recharge are represented by the intercepts between a straight line at a concentration of 0.05 and tracer concentration profiles at the hypothetical repository footprint at 120 ka. As shown in Figure 5-15, the low permeability Ordovician shales and Silurian evaporites and dolostones prevent the migration of the tracer to the repository horizon. Thus, the downward migration of tracer is largely retarded by the low permeability Ordovician formations, which is indicative of low rates of mass transport in the Ordovician.

Plots of Péclet number at the repository horizon versus time are shown in Figure 5-16 for points bounding the repository, as well as at the repository centre. The glacial loading history is also included to reflect its impact on the groundwater system at the repository horizon. As illustrated by the plots, mass transport mechanisms within the repository during the 120,000 year paleohydrogeologic simulation are predicted to remain diffusive, even at the maximum ice thickness of almost 3 km.

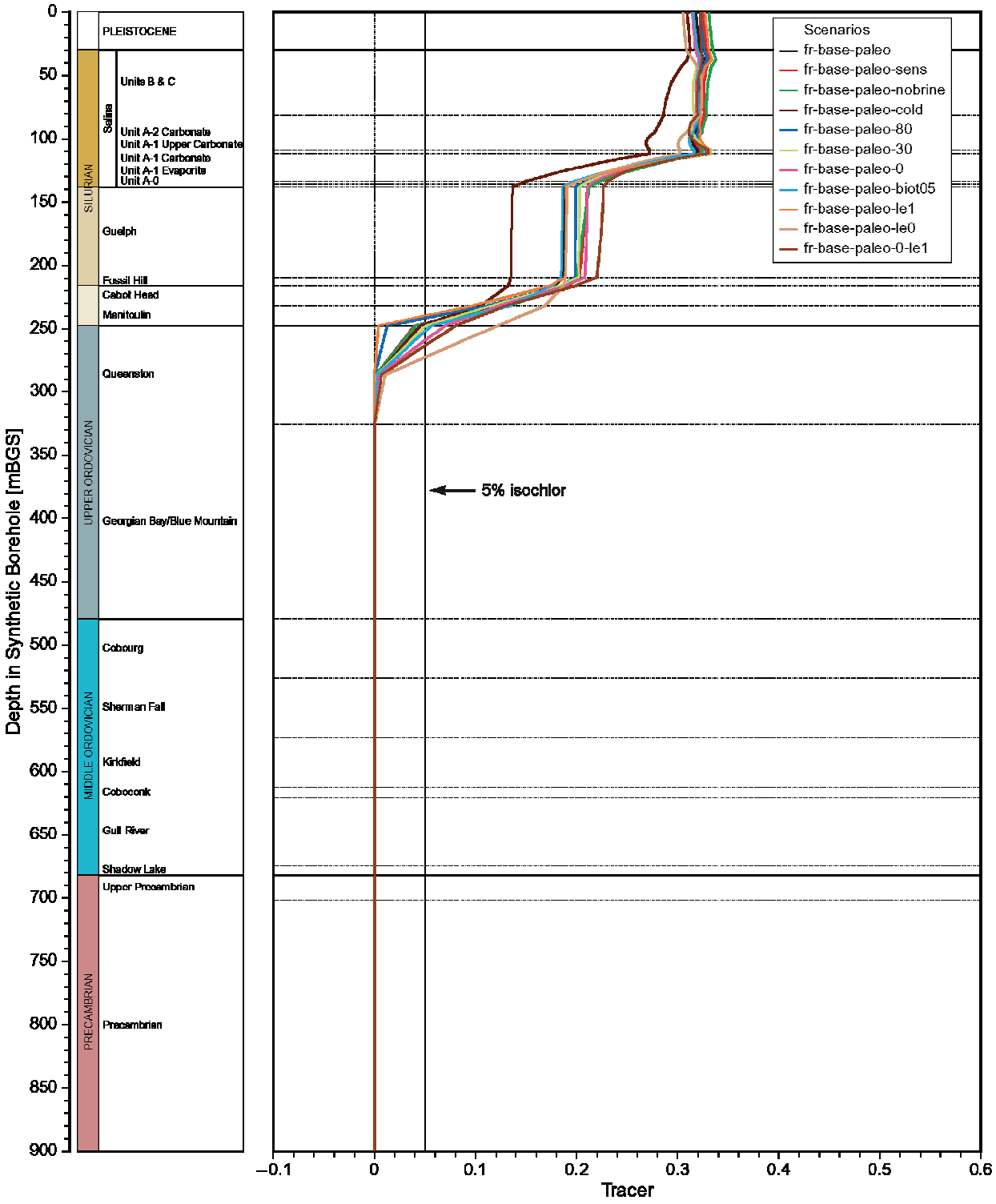

Figure 5-15: Vertical Profile Plots of Tracer Concentrations for the Paleohydrogeologic Simulations at the Location of the Hypothetical Repository Footprint at 120,000 Years

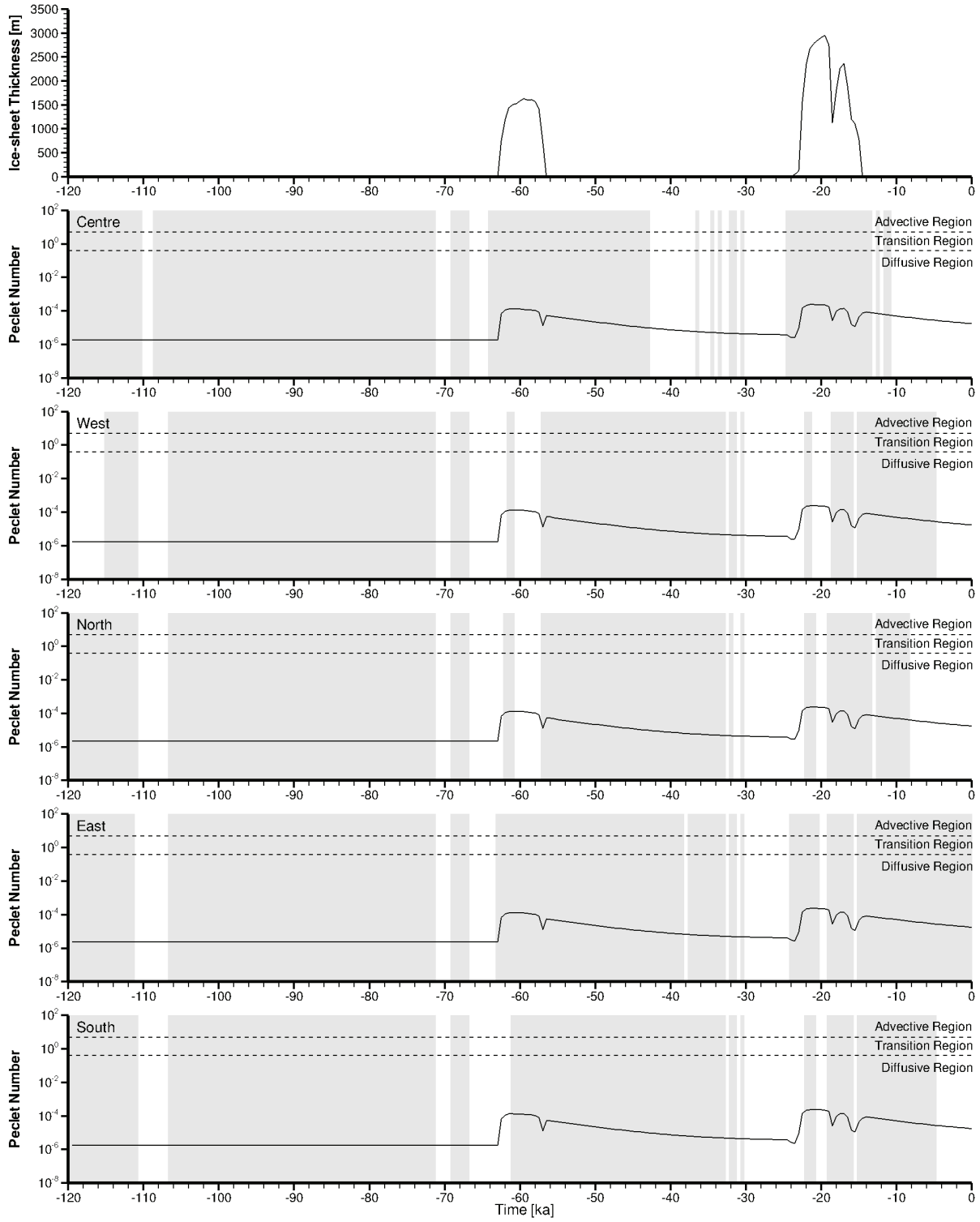

Note: grey regions represent upward flow and white regions represent downward flow

Figure 5-16: Péclet Number of Molecular Diffusion versus Time at the Hypothetical Repository Footprint for the Reference Paleohydrogeological Scenario (fr-base-paleo)

5.5.3 Confidence

As noted in Chapter 1, the geosciences program for a future candidate site will be designed to support the safety case. A site model and geosynthesis will be developed during a phased site characterization work program. The work program will allow for the iterative development, testing and refinement of a site-specific model that will contribute to managing uncertainties in scientific understanding, data and models.

Temperature: The thermal conductivity of sedimentary rock is primarily influenced by the rock composition and structure. Many of the uncertainties associated with estimates of heat transport in the geosphere would be resolved during site characterization activities. Temperature distributions in the geosphere would vary on a local scale as a result of details of repository design.

Fracture Development: A factor in repository siting is the geomechanical environment. The host rock would be demonstrably resilient to fracture development based on its history. The actual repository location would be chosen to avoid fracture zones or faults where future fracture movement or development is more likely.

Groundwater Mass Transport: Evidence gathered during site characterisation activities would attempt to minimize uncertainties through a synthesis of geologic, structural geologic, hydrogeochemical and physical hydrogeology to assess long-term groundwater system evolution and stability. Such efforts would be aided through the application of numerical methods that provide a systematic framework to integrate independent data sets. Such techniques, as supported by field data, can provide a basis to gain insight into trends (i.e., time rate of change and magnitude) of groundwater system response to external events and constrain uncertainty with regard to geosphere performance.

Glacial Processes: Peltier (2011) provides a review of what is currently known concerning the geologically recent history of long-term climate change, as background to the detailed analysis of the conditions that would be expected to develop at and below the surface of the Earth if the Canadian land mass were to be reglaciated. Results from an appropriately calibrated model of the most recent glaciation events that occurred in the Late Quaternary period of Earth history are used as a model of a future reglaciation event. The physical model employed for the purpose of this analysis is the University of Toronto Glacial Systems Model (UofT GSM).

The analyses that have been performed using the UofT GSM, for the purpose of contributing to the development of the required future glacial event predictions, are explicitly based upon the fact that it is impossible to provide a unique description of the detailed characteristics of such an event. The approach used is to apply Bayesian methods to examine the range of models that would be compatible with the constraints that can be brought to bear upon the detailed characteristics of the most recent North American glaciation event of the Late Quaternary ice-age. It is thereby shown that the spread of model characteristics is rather broad, sufficiently broad, it is believed, to encompass the characteristics of any similar event that could occur in the future (Peltier 2011).

Geochemistry: Uncertainties in the future evolution of groundwater compositions are coupled to uncertainties about the movement of groundwater. Similarly, impacts of glaciation at repository depth will be dependent on site-specific conditions. The age of, and potential influence of

glaciation on, groundwaters and porewaters cannot be determined directly; instead, they are inferred from paleohydrogeological evidence such as fluid inclusion data and stable water isotope ratios. Together with numerical tools, such as reactive transport modelling, this information can be used to illustrate the potential evolution of geochemical conditions at repository depths.

5.6 Summary

This discussion in this chapter describes changes that would occur in the multi-barrier repository system during its lifetime. The discussion is based on reasonable expectations for conditions that are likely to be encountered in sedimentary rock.

Many properties of the repository components and the processes that would affect them are well-characterized. The system is based on durable materials and passive natural processes. Natural and archaeological analogues help to support the descriptions of system behaviour into the far future. Of the uncertainties that remain, some questions would be resolved during the site characterization. Other uncertainties about the future evolution of the system arise from the recognition that simplifying assumptions and simple models may not in all cases adequately represent the complexity or heterogeneity of an actual repository over long periods of time. These uncertainties would be addressed by further analyses, by additional experimental or field studies (including extended monitoring in the repository itself), and by using conservative or bounding assumptions in the safety assessment models.

5.7 References for Chapter 5

Akiyama, E., K. Matsukado, M. Wang and K. Tsuzaki. 2010. Evaluation of hydrogen entry into high strength steel under atmospheric corrosion. Corrosion Science 52, 2758-2765.

Atkinson, G. and N. Kraeva. 2011. Polaris Underground Project at Sudbury Neutrino Observatory (P.U.P.S.). Nuclear Waste Management Organization Report TR-2009-02. Toronto, Canada.

Bäckblom, G. and R. Munier. 2002. Effects of Earthquakes on the Deep Repository for Spent Fuel in Sweden based on Case Studies and Preliminary Model Results. Swedish Nuclear Fuel and Waste Management Company Report TR-02-24. Stockholm, Sweden.

Bock, H., B. Dehandschutter, C.D. Martin, M. Mazurek, A. De Haller, F. Skoczylas and C. Davy. 2010. Self-Sealing of Fractures in Argillaceous Formations in the Context of Geological Disposal of Radioactive Waste. Nuclear Energy Agency No. 6184. Paris, France.

Börgesson, L., A. Fredrikson and L-E. Johannesson. 1994. Heat Conductivity of Buffer Materials. Swedish Nuclear Fuel and Waste Management Company Report 94-29. Stockholm, Sweden.

Chandler, N.A, A. Cournut, D.A. Dixon, C. Fairhurst, F. Hansen, M. Gray, K. Hara, Y. Ishijima, E. Kozak, J. Martino, K. Masumoto, G. McCrank, Y. Sugita, P. Thompson, J. Tillerson and B. Vignal. 2002. The Five-year Report of the Tunnel Sealing Experiment: An International Project of AECL, JNC, ANDRA and WIPP. Atomic Energy of Canada Limited Report AECL-12727. Pinawa, Canada.

Chen, J., Z. Qin and D.W. Shoesmith. 2011. Rate controlling reactions for copper corrosion in anaerobic aqueous sulphide solutions. Corrosion Engineering, Science and Technology 46, 138-141.

Chen, Y., X.H. Wang, J. Li, J.L. Lu, F.S. Wang. 2007. Polyaniline for corrosion prevention of mild steel coupled with copper. Electrochimica Acta 52, 5392-5399.

CNSC. 2006. Regulatory Guide G-320: Assessing the Long Term Safety of Radioactive Waste Management, Canadian Nuclear Safety Commission, Ottawa, Canada.

Crowe, R., K. Birch, J. Chen, D. Doyle, F. Garisto, M. Gobien, N. Hunt, S. Hirschorn, M. Hobbs, P. Keech, L. Kennell, E. Kremer, P. Maak, J. McKelvie, C. Medri, M. Mielcarek, A. Murchison, A. Parmenter, R. Ross, E. Sykes and T. Yang. 2013. Technical Program for Long-Term Management of Canada's Used Nuclear Fuel – Annual Report 2012. Nuclear Waste Management Organization Report NWMO TR-2013-01. Toronto, Canada.

Dixon D., T. Sandén, E. Jonsson and J. Hansen. 2011. Backfilling of Deposition Tunnels: Use of Bentonite Pellets. Swedish Nuclear Fuel and Waste Management Company Report SKB P-11-44. Stockholm, Sweden.

DOE. 2008. Final Supplemental Environmental Impact Statement for a Geologic Repository for the Disposal of Spent Nuclear Fuel and High-Level Radioactive Waste at Yucca Mountain, Nye County, Nevada. Department of Energy Report DOE/EIS-0250F-S1. Nevada, USA.

Dutton, D. 2006. Preliminary Evaluation of the Creep Behaviour of the Inner Steel Vessel of a Used-fuel Container. Ontario Power Generation Report 06819-REP-01300-10108-R00. Toronto, Canada.

Ferry, C., J.-P. Piron, A. Poulesquen and C. Poinssot. 2008. Radionuclides release from the spent fuel under disposal conditions: Re-evaluation of the instant release fraction. Materials Research Society Symposium Proceedings 1107, 447-454.

Fracture Systems. 2011. Excavation Damaged Zones Assessment. Nuclear Waste Management Report NWMO DGR-TR-2011-21. Toronto, Canada.

Freire-Canosa, J. 2011. Used Fuel Integrity Program: Summary Report. Nuclear Waste Management Organization Report NWMO TR-2011-04. Toronto, Canada.

Frescura, G.M. and A.L. Wight. 1979. Fuel Management & Reactor Operation Review of Operating Experience. From Canteach Website at: https://canteach.candu.org/Content%20Library/20042116.pdf.

Garisto, F. 2013. Fifth Case Study: Features, Events and Processes. Nuclear Waste Management Organization Report NWMO TR-2013-06. Toronto, Canada.

Gobien, M., F. Garisto and E. Kremer. 2013. Fifth Case Study: Reference Data and Codes. Nuclear Waste Management Organization Technical Report NWMO-TR-2013-05. Toronto, Canada.

Graham, J., N.A. Chandler, D.A. Dixon, P.J. Roach, T. To and A.W.L Wan. 1997. The Buffer/Container Experiment: Results, Synthesis, Issues. AECL Report 11746, COG-97-46-I.

Guo, R. 2009. Coupled Thermal-Hydraulic-Mechanical Modelling of the Canister Retrieval Test. Nuclear Waste Management Organization Report NWMO TR-2009-31. Toronto, Canada.

Guo, R. 2010. Coupled Thermal-Mechanical Modelling of a Deep Geological Repository using the Horizontal Tunnel Placement Method in Sedimentary Rock using CODE_BRIGHT. Nuclear Waste Management Organization Report NWMO TR-2010-22. Toronto, Canada.

Hallet, B. 2011. Glacial Erosion Assessment. Nuclear Waste Management Organization Report NWMO DGR-TR-2011-18. Toronto, Canada.

Hayek, S.J., J.A. Drysdale, J. Adams, V. Peci, S. Halchuk and P. Street. 2010. Seismic Monitoring near the DGR - Annual Report 2009. Nuclear Waste Management Organization Report DGR-TR-2010-03. Toronto, Canada.

Hultquist G., P. Szakálos, M.J. Graham, A.B. Belonoshko, G.I. Sproule, L. Gråsjö, P. Dorogokupets, B. Danilov, T. AAstrup, G. Wikmark, G.-K. Chuah, J.-C. Eriksson and A. Rosengren. 2009. Water corrodes copper. Catalysis Letters 132, 311-316.

Hultquist G., M.J. Graham, P. Szakálos, G.I. Sproule, A. Rosengren and L. Gråsjö. 2011. Hydrogen gas production during corrosion of copper by water. Corrosion Science 53, 310-319.

Hultquist, G., M.J. Graham, O. Kodra, S. Moisa, R. Liu, U. Bexell and J.L. Smialek. 2013. Corrosion of Copper in Distilled Water without Molecular Oxygen and the Detection of Produced Hydrogen. SSM Technical Note 2013:07. Stockholm, Sweden.

Humphreys, P.N., J.M. West and R. Metcalfe. 2010. Microbial Effects on Repository Performance. Prepared by Quintessa Limited for the Nuclear Decommissioning Authority Report No. QRS-1378Q-1. Oxfordshire, United Kingdom.

INTERA. 2011. Descriptive Geosphere Site Model. Nuclear Waste Management Organization Report NWMO DGR-TR-2011-24. Toronto, Canada.

Jensen, K.A. and R.C. Ewing. 2001. The Okélobondo natural fission reactor, southeast Gabon: Geology, mineralogy, and retardation of nuclear-reaction products. Geological Society of America Bulletin 113, 32-62.

King, F. 2006. Review and Gap Analysis of the Corrosion of Copper Containers under Unsaturated Conditions. Ontario Power Generation Report 06819-REP-01300-10124-R00. Toronto, Canada.

King, F. 2009a. Hydrogen Effects on Carbon Steel Used Fuel Containers. Nuclear Waste Management Organization Report NWMO TR-2009-29. Toronto, Canada.

King, F. 2009b. Microbiologically influenced corrosion of nuclear waste container. Corrosion 65, 233-251.

King, F. 2013. Consequences of the General Corrosion of Carbon Steel Used Fuel Containers for Gas Generation in a DGR. Nuclear Waste Management Organization Report NWMO TR-2013-16. Toronto, Canada.

King, F. and S. Stroes-Gascoyne. 1997. Predicting the effects of microbial activity on the corrosion of copper nuclear waste disposal containers. Eds. J.H. Wolfram, R.D. Rogers and L.G. Gazso in Microbial Degradation Processes in Radioactive Waste Repository and in Nuclear Fuel Storage Areas. Volume 11 of NATO ASI Series. Kluwer Academic Publishers, Netherlands. 149-162.

King, F. and M. Kolář. 2000. The Copper Container Corrosion Model Used in AECL's Second Case Study. Ontario Power Generation Report 06819-REP-01200-10041-R00. Toronto, Canada.

King, F., L. Ahonen, C. Taxén, U. Vuorinen and L. Werme. 2001. Copper Corrosion under Expected Conditions in a Deep Geologic Repository. Swedish Nuclear Fuel and Waste Management Company Report SKB TR-01-23. Stockholm, Sweden.

King, F., M. Kolář and P. Maak. 2008. Reactive-transport model for the prediction of the uniform corrosion behaviour of copper used fuel containers. Journal of Nuclear Materials 379, 133-141.

King, F. and D. Shoesmith. 2010. Nuclear waste canister materials, corrosion behaviour and long-term performance in geological repository systems. Eds. J. Ahn and M.J. Apted in Geological Repository Systems for Safe Disposal of Spent Nuclear Fuel and Radioactive Waste. Woodhead Publishing, Cambridge, United Kingdom.

King, F., C. Lilja, K. Pedersen, P. Pitkänen and M. Vähänen. 2010. An Update of the State-of-the-Art Report on the Corrosion of Copper under Expected Conditions in a Deep Geologic Repository. Swedish Nuclear Fuel and Waste Management Company Report SKB TR-10-67. Stockholm, Sweden.

King, F., C. Lilja, K. Pedersen, P. Pitkänen and M. Vähänen. 2011a. An Update of the State-of-the-art Report on the Corrosion of Copper under Expected Conditions in a Deep Geologic Repository. Posiva Oy Report POSIVA 2011-01. Olkiluoto, Finland.

King, F., M. Kolář, M. Vähänen and C. Lilja. 2011b. Modelling long term corrosion behaviour of copper canisters in KBS-3 repository. Corrosion Engineering, Science and Technology 46, 217-222.

Kwong, G.M. 2011. Status of Corrosion Studies for Copper Used Fuel Containers Under Low Salinity Conditions. Nuclear Waste Management Organization Report NWMO TR-2011-14. Toronto, Canada.

Lovasic, Z. and P. Gierszewski. 2005. CANDU Fuel Long-Term Storage and Used Fuel Integrity. Paper at 9th International Conference on CANDU Fuel. Canadian Nuclear Society Bulletin Vol. 26, No. 4.

Lund B. 2006. Stress Variations during a Glacial Cycle at 500 m Depth in Forsmark and Oskarshamn: Earth Model Effects. Swedish Nuclear Fuel and Waste Management Company Report R-06-95. Stockholm, Sweden.

Lund, B., P. Schmidt and C. Hieronymus. 2009. Stress Evolution and Fault Stability during the Weichselian Glacial Cycle. Swedish Nuclear Fuel and Waste Management Company Report TR-09-15. Stockholm, Sweden.

Maak, P., M. Saidfar and P. Gierszewski. 2001. Early Failure Probability of Used-Fuel Containers in a Deep Geologic Repository. Ontario Power Generation Report 06819-REP-01300-10022 R00. Toronto, Canada.

Man, A. and J.B. Martino. 2009. Thermal, Hydraulic and Mechanical Properties of Sealing Materials. Nuclear Waste Management Organization Technical Report NWMO TR-2009-20. Toronto, Canada.

McMurry, J., D.A. Dixon, J.D. Garroni, B.M. Ikeda, S. Stroes-Gascoyne, P. Baumgartner and T.W. Melnyk. 2003. Evolution of a Canadian Deep Geologic Repository: Base Scenario. Ontario Power Generation Report 06819-REP-01200-10092-R00. Toronto, Canada.

McMurry, J., B.M. Ikeda, S. Stroes-Gascoyne, D.A. Dixon and J.D. Garroni. 2004. Evolution of a Canadian Deep Geologic Repository: Defective Container Scenario. Ontario Power Generation Report 06819-REP-01200-10127-R00. Toronto, Canada.

NWMO. 2011. Geosynthesis. Nuclear Waste Management Organization Report NWMO DGR-TR-2011-11. Toronto, Canada.

OPG. 2002. Pickering Waste Management Facility Safety Report. Ontario Power Generation Report 92896-SR-01320-10002-R02. Toronto, Canada.

Pedersen K. 2000. Microbial Processes in Radioactive Waste Disposal. Swedish Nuclear Fuel and Waste Management Company Report SKB TR 00-04. Stockholm, Sweden.

Peltier, W.R. 2002. A Design Basis Glacier Scenario. Ontario Power Generation Report 06819-REP-01200-10069-R00. Toronto, Canada.

Peltier, W.R. 2004. Permafrost Influences Upon the Subsurface. Ontario Power Generation Report 06819-REP-01200-10134-R00. Toronto, Canada.

Peltier, W.R. 2011. Long-term Climate Change. Nuclear Waste Management Organization Report NWMO DGR-TR-2011-14 R000. Toronto, Canada.

Poon, G., M. Saiedfar and P. Maak. 2001. Selection of a Primary Load-Bearing Component Conceptual Design for Used-fuel Containers. Ontario Power Generation Report 06819-REP-01200-10051-R00. Toronto, Canada.

Posiva. 2010. EDZ09 Project and related EDZ Studies in ONKALO 2008-2010. Posiva Working Report 2010-27. Olkiluoto. Finland.

Puigdomenech, I. and C. Taxén. 2000. Thermodynamic Data for Copper: Implications for the Corrosion of Copper under Repository Conditions. Swedish Nuclear Fuel and Waste Management Company Report SKB TR 00-13. Stockholm, Sweden.

Pusch, R. 1999. Mobility and Survival of Sulphate-reducing Bacteria in Compacted and Fully Water Saturated Bentonite – Microstructural Aspects. Swedish Nuclear Fuel and Waste Management Company Report SKB TR 99-30. Stockholm, Sweden.

Raiko, H. 2005. Disposal Canister for Spent Nuclear Fuel – Design Report. Posiva Oy Report POSIVA 2005-02. Olkiluoto, Finland.

Raiko H., R. Sandström, H. Rydén and M. Johansson. 2010. Design Analysis Report for the Canister. Swedish Nuclear Fuel and Waste Management Company Report SKB TR-10-28, Stockholm, Sweden.

Saiedfar, M. and P. Maak. 2002. Preliminary Assessment of the Deformation and Stresses of Copper Used-fuel Containers in a Hypothetical Deep Geologic Repository. Ontario Power Generation Report, 06819-REP-01300-10049-R00. Toronto, Canada.

Scully, J. and M. Edwards. 2013. Review of the NWMO Copper Corrosion Allowance. Nuclear Waste Management Report NWMO TR-2013-04. Toronto, Canada.

Sherwood Lollar, B. 2011. Far-Field Microbiological Considerations Relevant to a Deep Geological Repository – State of Science Review. Nuclear Waste Management Organization Report NWMO TR-2011-09. Toronto, Canada.

Shoesmith, D.W. and F. King. 1999. The Effects of Gamma Radiation on the Corrosion of Candidate Materials for the Fabrication of Nuclear Waste Packages. Atomic Energy of Canada Limited Report AECL 11999. Pinawa, Canada.

Shoesmith, D.W. 2008. The Role of Dissolved Hydrogen on the Corrosion/Dissoluton of Spent Nuclear Fuel. Nuclear Waste Management Organization Report NWMO TR-2008-19. Toronto, Canada.

Shoesmith, D.W. and D. Zagidulin. 2010. The Corrosion of Zirconium under Deep Geological Repository Conditions. Nuclear Waste Management Organization Report NWMO TR-2010-19. Toronto, Canada.

Simmons, G. R. 1992. The Underground Research Laboratory Room 209 Excavation Response Test - A Summary report. Atomic Energy of Canada Limited. Report AECL-10564, COG-92-56. Chalk River, Canada.

SKB. 2010. Critical Review of the Literature on the Corrosion of Copper by Water. Swedish Nuclear Fuel and Waste Management Company Report SKB TR-10-69. Stockholm, Sweden.

SKB. 2011. Long-term Safety for the Final Repository for Spent Nuclear Fuel at Forsmark. Main Report of the SR-Site Project. Volume I. Swedish Nuclear Fuel and Waste Management Company Report SKB TR-11-01. Stockholm, Sweden.

Smart N., A. Rance, P. Fennell and L. Werme. 2003. Expansion due to anaerobic corrosion of steel and cast iron: experimental and natural analogue studies. Eds. D. Féron and D.D. Macdonald in Prediction of Long Term Corrosion Behaviour in Nuclear Waste Systems: Proceedings of the International Workshop. Cadarache, France. London: Maney Pub. (European Federation of Corrosion Publications 36), paper 19, pp 280–294.

Smart N., P. Fennell, A. Rance and L. Werme. 2004. Galvanic corrosion of copper-cast iron couples in relation to the Swedish radioactive waste canister concept. Ed. D. Féron in Prediction Of Long Term Corrosion Behaviour in Nuclear Waste Systems: Proceedings of the 2nd International Workshop. European Federation of Corrosion, pp 52–60. Nice, France.

Smart N.R., A.P. Rance and P.A.H. Fennell. 2005. Galvanic Corrosion of Copper-Cast Iron Couples. Swedish Nuclear Fuel and Waste Management Company Report SKB TR-05-06. Stockholm, Sweden.

Smart N.R., A.P. Rance and P.A.H. Fennell. 2006. Expansion due to the Anaerobic Corrosion of Iron. Swedish Nuclear Fuel and Waste Management Company Report SKB TR-06-41. Stockholm, Sweden.

Smart N., A. Rance, B. Reddy, P. Fennell and R. Winsley. 2012. Analysis of SKB MiniCan Experiment 3. Swedish Nuclear Fuel and Waste Management Company Report SKB TR-12-09. Stockholm, Sweden.

SSHAC. 1997. Recommendations for Probabilistic Seismic Hazard Analysis. Guidance on Uncertainty and Use of Experts. Senior Seismic Hazard Advisory Committee, U.S. Nuclear Regulatory Commission, NUREG/CR-6372. Washington, USA.

SSM. 2011a. Evolution of Hydrogen by Copper in Ultrapure Water without Dissolved Oxygen. Stråal Säkerhets Myndigheten Report 2011:34. Stockholm, Sweden.

SSM. 2011b. Is Copper Immune to Corrosion when in Contact with Water and Aqueous Solutions? Stråal Säkerhets Myndigheten Report 2011:09. Stockholm, Sweden.

SSM. 2012a. 2012. A Review of the Creep Ductility of Copper for Nuclear Waste Canister Application. Stråal Säkerhets Myndigheten Technical Note 2012:13. Stockholm, Sweden.

SSM. 2012b. A Review of the Mechanical Integrity of the Canister. Stråal Säkerhets Myndigheten Technical Note 2012:15. Stockholm, Sweden.

Stroes-Gascoyne, S. 2010. Microbial occurrence in bentonite-based buffer, backfill and sealing materials from large-scale experiments at AECL's Underground Research Laboratory. Applied Clay Science 47, 36-42.

Stroes-Gascoyne, S., C.J. Hamon, C. Kohle and D.A. Dixon. 2006. The Effects of Dry Density and Porewater Salinity on the Physical and Microbiological Characteristics of Highly Compacted Bentonite. Ontario Power Generation Report 06819-REP-01200-10016 R00. Toronto, Canada.

Stroes-Gascoyne, S., C.J. Hamon, D.A. Dixon and J.B. Martino. 2007a. Microbial analysis of samples from the tunnel sealing experiments at AECL's Underground Research Laboratory. Physics and Chemistry of the Earth: Parts A/B/C 32, 219-231.

Stroes-Gascoyne, S., P. Maak, C.J. Hamon, and C. Kohle. 2007b. Potential Implications of Microbes and Salinity on the Design of Repository Sealing System Components. Nuclear Waste Management Organization Report NWMO TR-2007-10. Toronto, Canada.

Stroes-Gascoyne, S. and C.J. Hamon. 2008. The Effect of Intermediate Dry Densities (1.1-1.5 g/cm^3) and Intermediate Porewater Salinities (60-90 g NaCl/L) on the Culturability of Heterotrophic Aerobic Bacteria in Compacted 100% Bentonite. Nuclear Waste Management Organization Report NWMO TR-2008-11. Toronto, Canada.

Stroes-Gascoyne, S. and C.J. Hamon. 2010. The Effects of Elevated Temperatures on the Viability and Culturability of Bacteria Indigenous to Wyoming MX-80 Bentonite. Nuclear Waste Management Organization Report NWMO TR-2010-08. Toronto, Canada.

Stroes-Gascoyne, S., C.J. Hamon, D.A. Dixon and D.G. Priyanto. 2010a. The Effect of $CaCl_2$ Porewater Salinity (50-100 g/L) on the Culturability of Heterotrophic Aerobic Bacteria in Compacted 100% Bentonite with Dry Densities of 0.8 and 1.3 g/cm^3. Nuclear Waste Management Organization Technical Report NWMO TR-2010-06. Toronto, Canada.

Stroes-Gascoyne, S., C.J. Hamon, P. Maak and S. Russell. 2010b. The effects of the physical properties of highly compacted smectitic clay (bentonite) on the culturability of indigenous microorganisms. Applied Clay Science 47, 155-162.

Stroes-Gascoyne, S., C.J. Hamon and P. Maak. 2011. Limits to the Use of Highly Compacted Bentonite as a Deterrent for Microbiologically Influenced Corrosion in a Nuclear Fuel Waste Repository. Physics and Chemistry of the Earth 36(17-18), 1630-1638.

Suckling, P., J. Avis, N. Calder, P. Humphreys, F. King and R. Walsh. 2012. T2GGM Version 3.1: Gas Generation and Transport Code. Nuclear Waste Management Organization Report NWMO TR-2012-23. Toronto, Canada.

Suckling, P., J. Avis, N. Calder, P. Humphreys, F. King and R. Walsh. 2013. T2GGM Version 3.1: Gas Generation and Transport Code – Supporting Documentation. Quintedda Limited Report QRS-1335B-TR6. Henley-on-Thames, UK.

Swedish National Council. 2010. Nuclear Waste State-of-the-Art Report 2010 – Challenges for the Final Repository Programme. Swedish Government Official Reports SOU 2010:6. Stockholm, Sweden.

Szakálos P., Hultquist G., Wikmark G. 2007. Corrosion of copper by water. Electrochemical and Solid-State Letters 10, C63–C67.

Tait, J.C., H. Roman and C.A. Morrison. 2000. Characteristics and Radionuclide Inventories of Used Fuel from OPG Nuclear Generating Stations. Ontario Power Generation Report 06819-REP-01200-10029-R00. Toronto, Canada.

Tsuru, T., Y. Huang, Md.R. Ali and A. Nishikata. 2005. Hydrogen entry into steel during atmospheric corrosion process. Corrosion Science 47, 2431-2440.

Vilks, P. 2009. Sorption in Highly Saline Solutions – State of the Science Review. Nuclear Waste Management Organization Report NWMO TR-2009-18. Toronto, Canada.

Vilks, P., N.H. Miller and K. Felushko. 2011. Sorption Experiments in Brine Solutions with Sedimentary Rock and Bentonite. Nuclear Waste Management Organization Report NWMO TR-2011-11. Toronto, Canada.

Villagran, J., M. Ben Belfadhel, K. Birch, J. Freire-Canosa, M. Garamszeghy, F. Garisto, P. Gierszewski, M. Gobien, S. Hirschorn, N. Hunt, A. Khan, E. Kremer, G. Kwong, T. Lam, P. Maak, J. McKelvie, C. Medri, A. Murchison, S. Russell, M. Sanchez-Rico Castejon, U. Stahmer, E. Sykes, A. Urrutia-Bustos, A. Vorauer, T. Wanne and T. Yang. 2011. RD&D Program 2011 – NWMO's Program for Research, Development and Demonstration for Long-Term Management of Used Nuclear Fuel. Nuclear Waste Management Organization Report NWMO TR-2011-01. Toronto, Canada.

Werme, L. 1998. Design Premises for Canister for Spent Nuclear Fuel. Swedish Nuclear Fuel Waste Management Company Report SKB TR-98-08. Stockholm, Sweden.

Wersin, P., M. Birgersson, S. Olsson, O. Karnland and M. Snellman. 2007. Impact of Corrosion-Derived Iron on the Bentonite Buffer within the KBS-3H Disposal Concept – the Olkiluoto Site as Case Study. Posiva Oy Report POSIVA 2007-11. Olkiluoto, Finland.

Wolfaardt, G.M. and D.R. Korber. 2012. Near-Field Microbiological Considerations Relevant to a Deep Geological Repository for Used Nuclear Fuel – State of Science Review. Nuclear Waste Management Organization Report NWMO TR-2012-02. Toronto, Canada.

6. SCENARIO IDENTIFICATION AND DESCRIPTION

Postclosure safety is assessed through consideration of a set of potential future scenarios, where scenarios are descriptions of alternative possible evolutions of the repository system. However, scenarios can also be designed with the aim of illustrating the properties of natural or engineered barriers (IAEA 2012). For that purpose, it can be instructive to assign parameter values such that the barrier under consideration is influenced in an exaggerated way so that the robustness of the barriers can be more clearly exhibited. Scenarios of this sort are often called "what-if" scenarios to distinguish them from realistic scenarios.

The purpose of scenario identification is to develop a comprehensive range of possible future evolutions against which the performance of the system can be assessed. Consistent with the specification of CNSC Guide G-320 (CNSC 2006), both Normal Evolution and Disruptive Event Scenarios are considered. The Normal Evolution Scenario represents the normal (or expected) evolution of the site and facility, while Disruptive Event Scenarios examine the effects of unlikely events that might lead to penetration of barriers and abnormal degradation and loss of containment.

Scenarios of interest are identified through consideration of the various factors (see Table 6-1) that could affect the repository system and its evolution (IAEA 2012). These factors can be further categorized into Features, Events and Processes (FEPs) as shown in Table 6-1. FEPs are organized in a hierarchical structure with up to 4 levels. The finest discretization of the FEPs occurs at the lowest level. This is illustrated in Table 6-2 where the FEPs are listed down to level 3, the lowest level for these FEPs.

FEPs can be characterized as either "external" or "internal", depending on whether they are outside or inside the spatial and temporal boundaries of the repository system domain, which here includes the repository, the geosphere and the affected biosphere. The external factors originate outside these boundaries; whereas, waste package, repository, geosphere, biosphere and contaminant factors can be considered as "internal" factors. Hence, the waste package, repository, geosphere, biosphere and contaminant factors will be referred to as Internal FEPs and the external factors will be referred to as External FEPs.

The External FEPs provide the system with boundary conditions and include influences originating outside the repository system that might cause change. Included in this group are decisions related to repository design, operation and closure since these are outside the temporal boundary of the postclosure behaviour of the repository system. If these External FEPs can significantly affect the evolution of the system and / or its safety functions of isolation and containment, they are considered scenario-generating FEPs in the sense that whether or not they occur (or the extent to which they occur or the form that they take) could define a particular future scenario that should be considered.

The External FEPs are listed in Table 6-2. Those that are likely to affect the repository system and its evolution are discussed in Section 6.1. The effects of less likely External FEPs and certain Internal FEPs that might lead to abnormal degradation and loss of containment are discussed in Section 6.2.

Table 6-1: FEP List Showing FEPs Down to Level 2

FEP Number and Title	
1.	**EXTERNAL FACTORS**
1.1	Repository Issues
1.2	Geological Factors
1.3	Climatic Factors
1.4	Future Human Actions
1.5	Other External Factors
2.	**WASTE PACKAGE FACTORS**
2.1	Waste Package Characteristics
2.2	Waste Form Processes
2.3	Waste Container Processes
2.4	Contaminant Transport – Waste Package
3.	**REPOSITORY FACTORS**
3.1	Repository Characteristics
3.2	Repository Processes
3.3	Contaminant Transport – Repository
4.	**GEOSPHERE FACTORS**
4.1	Geosphere Characteristics
4.2	Geosphere Processes
4.3	Contaminant Transport - Geosphere
5.	**BIOSPHERE FACTORS**
5.1	Surface Environment
5.2	Human Behaviour
5.3	Contaminant Transport - Biosphere
5.4	Exposure Factors
6.	**CONTAMINANT FACTORS**
6.1	Contaminant Characteristics

Note: From Garisto (2013).

6.1 The Normal Evolution Scenario

The Normal Evolution Scenario is based on a reasonable extrapolation of present day site features and receptor[1] lifestyle. It includes the expected evolution of the site and repository.

[1] The receptor is a person (or persons) who may be exposed to contaminants potentially released from the repository.

6.1.1 External FEPs

The External FEPs have been reviewed to identify those that are likely to occur and could potentially affect the repository and, therefore, should be included in the Normal Evolution Scenario. The resulting list of included / excluded items is shown in Table 6-2 together with a brief justification for their inclusion / exclusion. Further details are provided in Garisto (2013).

Table 6-2 shows that the repository is largely unaffected by many External FEPs, primarily due to its depth and associated geological characteristics. The main External FEPS that are likely to have an impact are:

- Placement of some containers with undetected defects (FEP 1.1.03);
- Glaciation and its effects (FEPs 1.2.02, 1.2.03, 1.2.07, 1.3.01, 1.3.02, 1.3.04, 1.3.05, 1.3.08 and 1.3.09);
- Earthquakes (FEP 1.2.03);
- Human influence on global climate (FEP 1.4.01) delaying onset of the next glaciation; and
- Social and institutional developments leading to changes of land use at the repository site (FEP 1.4.02), and associated drilling, site development and water management (FEPs 1.4.04, 1.4.08 and 1.4.10).

The containers are robust and there are multiple inspection steps to ensure they are fabricated and placed correctly (Chapter 4). However, with the large number of containers, it is possible that some containers could be placed in the repository with defects. Consequently, for the assessment of the Normal Evolution Scenario, it is assumed that some containers with undetected defects are present in the repository.

An important external influence is glaciation. Although glaciation is likely to cause major changes in the surface and near-surface environment, as discussed below, the repository itself is intentionally isolated by its depth from these changes.

Glacial erosion at the hypothetical repository site, although slow, could progressively remove a fraction of the rock overlying the repository in the first one million years. Hence, glacial erosion is considered in the Normal Evolution Scenario; however, deep erosion is assumed not to be likely within this time frame for this hypothetical site and repository depth.

For the hypothetical repository site, the paleohydrogeologic simulations described in Chapter 2 indicate that glacial meltwaters will not reach the repository horizon, as illustrated in Figure 2-24. This is due to the low hydraulic conductivity of the overlaying shales, dolostones and Salina Group evaporites. The glacial recharge penetrating below the shallow groundwater system (i.e., depths greater than 215 m) is not expected to be oxygenated or influence the redox conditions at the repository horizon (see Section 2.4). Furthermore, for the paleohydrogeologic sensitivity cases performed, the glacial perturbations did not materially change mass transport rates at the repository depth (i.e., diffusion remains the dominant transport mechanism (see Section 2.3.4.3, particularly Figures 2-31 to 2-34)). These characteristics of the repository site are used in the scenario identification.

Table 6-2: Status of External FEPs for the Normal Evolution of the Repository System

External FEP			Status*	Remark
1.1	***Repository Issues***			
	1.1.01	Site Investigation	Included	The sedimentary rock site is hypothetical. The topography, stratigraphy and hydrological properties are typical of those found on the Michigan Basin in Southern Ontario. The site is described in Chapter 2. It is assumed that there are no fractures or faults at or near the repository site (as per Chapter 2), there are no undetected geological features at the site, and there are no identified commercially viable mineral resources at the site (as per Chapter 1).
	1.1.02	Excavation and Construction	Included	The repository is built consistent with the design basis, as described in Chapter 4. Controlled drill and blast excavation is used, which reduces but does not avoid formation of an excavation damaged zone (see Chapter 4).
	1.1.03	Placement of Wastes and Backfill	Included	The in-room container placement method is used. Rooms are backfilled as containers are placed, as described in Chapter 4. Due to the large number of containers, it is assumed that some containers are placed with initial defects that are not detected during the fabrication, inspection and placement processes.
	1.1.04	Closure and Repository Sealing	Included	The repository is closed and sealed as described in Chapter 4. This includes sealing of the shafts.
	1.1.05	Repository Records and Markers	Included	Repository records and markers (and passive societal memory) are assumed sufficient to ensure that inadvertent intrusion would not occur for at least a few hundred years.
	1.1.06	Waste Allocation	Included	The repository holds 4.6 million CANDU fuel bundles. There is no placement of other radioactive or chemically hazardous material at the site.
	1.1.07	Repository Design	Included	The repository design concept is described in Chapter 4.

External FEP			Status*	Remark
	1.1.08	Quality Control	Included	Construction, operation, monitoring and closure of the repository are all undertaken under a project quality plan that ensures that the design and safety basis is met (see Chapter 10). However, due to the large number of containers, it is assumed that some containers are placed with initial defects that are not detected during the fabrication, inspection and placement processes.
	1.1.09	Schedule and Planning	Included	The assumed schedule is ~40 years operation, 70 years extended monitoring and 30 years for decommissioning and closure.
	1.1.10	Repository Administrative Control	Included	Administrative controls ensure proper operation and closure of the repository. Institutional controls (e.g., land use restrictions) will be implemented on closure, which, while they remain effective, will prevent inadvertent human intrusion and the drilling of wells.
	1.1.11	Monitoring	Excluded	The postclosure monitoring program will not compromise the safety of the repository.
	1.1.12	Accidents and Unplanned events	Excluded	The likelihood of preclosure accidents or unplanned events that could impact the long-term safety of the repository will be minimized by good engineering practice and quality control; and the effects of any that do occur will be mitigated before the repository is closed.
	1.1.13	Retrieval of Wastes	Excluded	The repository schedule includes an extended period of monitoring after rooms have been filled but before the access tunnels and shaft are sealed, which would facilitate retrieval if required. However, retrieval after closure is not expected and is not included in this safety assessment.
1.2	***Geological Factors***			
	1.2.01	Tectonic Movement and Orogeny	Excluded	The hypothetical site is in a tectonically stable region away from plate margins, with no tectonic activity over the time scale of interest (i.e., 1,000,000 years).

External FEP			Status*	Remark
	1.2.02	Deformation (Elastic, Plastic or Brittle)	Included	The repository site is assumed to be tectonically stable; hence, deformation due to tectonic movement and orogeny is unlikely over the timescales on interest. Thus, over the next million years, the only significant deformation force is that due to ice sheet advance over the site. This could cause crustal depression in excess of 500 m, but would occur on a continental scale (Peltier 2011). Ice sheet weight could also cause local movement along existing faults or fractures zones but would not lead to creation of new fractures. As per Chapter 2, it is assumed there are no fractures or faults intersecting the repository.
	1.2.03	Seismicity (Earthquakes)	Included	Earthquakes will occur over the time scale of interest; however, since the site is assumed located in a seismically inactive region, the likely magnitude, frequency and distance of earthquakes would limit their impact at the repository location. Larger earthquakes are more likely during retreat of ice sheets. Earthquakes are in general less destructive at depth than at the surface, diminishing the impact of any seismic activity on a deep repository. Since the repository is backfilled, preventing rock fall, the main concern would be shearing along an existing fracture plane intercepting the repository, providing either a groundwater pathway or damaging containers. However, it is assumed for the Normal Evolution Scenario that, consistent with Chapter 2, there are no fracture zones or faults at or near the site and that there are no undetected geological features at the repository site.
	1.2.04	Volcanic and Magmatic Activity	Excluded	No volcanic or magmatic activity over the time scale of interest due to the site location.
	1.2.05	Metamorphism	Excluded	No processes occur over the time scale of interest that will cause metamorphism.
	1.2.06	Hydrothermal Activity	Excluded	The hypothetical repository is assumed located in a geologically stable sedimentary basin in Ontario with a low geothermal flux. Hydrothermal processes therefore act too slowly to be of concern over the time scale of interest.

External FEP			Status*	Remark
	1.2.07	Regional Erosion and Sedimentation	Included	The area is topographically relatively flat and not high above sea level so there is limited potential for large-scale denudation. However, over the past 1,000,000 years, ice-sheet erosion and deposition has shaped the topography and could continue to do so in the future. Erosion is accounted for in the definition of the Normal Evolution Scenario.
	1.2.08	Diagenesis	Excluded	Would have negligible effect on repository safety over the timescale of interest (1,000,000 years).
	1.2.09	Salt Diapirism and Dissolution	Excluded	No significant salt deposits are assumed to be located in the vicinity of the site. Historically, there could have been salt deposits but these have already been dissolved in the distant past.
	1.2.10	Hydrological Response to Geological Changes	Excluded	A severe seismic event could potentially change fracture zone permeabilities or activate a fault and therefore change local hydrology. However, it is assumed for the Normal Evolution Scenario that site characterization has not identified any fracture zones or faults at or near the hypothetical repository site. At the hypothetical site, it is assumed that the hydraulic pressure is hydrostatic - there is no pattern of over- and under-pressures in the different rock formations (see Chapter 2). Also, none of the other included geologic processes identified above are able to cause significant hydraulic changes on relevant timescales.
1.3	***Climate Factors***			
	1.3.01	Global Climate Change	Included	After a period of global warming, it is assumed that glacial / interglacial cycling will eventually resume since the solar insolation variation driving this cycling will continue.
	1.3.02	Local and Regional Climate Change	Included	In the near term, global warming is likely to cause temperature and precipitation changes, although the local / regional climate is likely to remain generally temperate due to its northerly latitude location. In the long-term, it will respond to global climate change, and in particular will cool or warm with glacial cycles.

External FEP			Status*	Remark
	1.3.03	Sea-level Change	Excluded	Changes in sea level do not affect the site due to its assumed mid-continental location.
	1.3.04	Periglacial Effects	Included	These will occur during colder climate states experienced during the glacial cycles that are likely to occur at the site over a one million year timeframe. In particular, this would include permafrost development (see Chapter 2).
	1.3.05	Local Glacial Effects	Included	Ice sheets will cause a range of local effects. These include change in rock stress (FEP 1.2.02), earthquake initiation (FEP 1.2.03), change in surface and near-surface hydrology (FEP 1.3.07), penetration of glacial waters to depth, changes in ecosystems (FEP 1.3.08) and human behaviour (FEP 1.3.09).
	1.3.06	Warm Climate Effects (Tropical and Desert)	Excluded	Climate change is unlikely to result in development of tropical or hot desert conditions at the site due to its northerly latitude. An initial period of human-induced global warming is not expected to result in extreme temperature rise resulting in tropical or desert conditions in this region.
	1.3.07	Hydrological Response to Climate Change	Excluded	Surface and near-surface groundwater systems could be altered by a climatic change to wetter or drier conditions. However, the deep groundwater system at the site would not be significantly altered by climatic change to wetter or drier conditions (within expected variation, see FEP 1.3.06), due to its low-permeability and depth (see Chapter 2). Changes in hydrology due to glaciation are discussed separately under Periglacial Effects (1.3.04) and Local Glacial Effects (1.3.05).
	1.3.08	Ecological Response to Climate Changes	Included	Flora and fauna at the site change in response to glacial / interglacial cycling.
	1.3.09	Human Behavioural Response to Climate Change	Included	Human behaviour changes in response to glacial / interglacial cycling.

External FEP			Status*	Remark
1.4	***Future Human Actions***			
	1.4.01	Human Influences on Climate	Included	Human actions are a possible cause of global climate change, which is included in expected evolution (see FEP 1.3.01, Global Climate Change).
	1.4.02	Deliberate Human Intrusion	Excluded	Deliberate human intrusion into the repository is not considered. It is assumed that any future society choosing to recover materials from the repository would have the technology to understand and manage the hazards. Note that unauthorized deliberate intrusion is unlikely due to the infrastructure needed to excavate to repository depth.
	1.4.03	Non-Intrusive Site Investigation	Excluded	Non-intrusive site investigations would not have any effect because of the repository depth.
	1.4.04	Drilling Activities (Human Intrusion)	Excluded	The drilling of deep exploration boreholes that penetrate to the repository is excluded from the expected evolution due to the repository depth (around 500 m), the relatively small repository footprint (~6 km^2), and the assumed lack of commercially viable natural resources at the site. Note that this FEP does not include drilling of shallow wells which are considered under FEP 1.4.07.
	1.4.05	Mining (Human Intrusion)	Excluded	It is assumed that there are no commercially viable mineral resources present at the site.
	1.4.06	Surface Environment, Human Activities	Excluded	Unlikely to have any direct impact on repository due to the repository depth.

External FEP			Status*	Remark
	1.4.07	Water Management (Wells, Reservoirs Dams)	Included	The drilling of shallow water wells in the area is considered once institutional controls are no longer effective (see FEP 1.1.10). Wells in the deeper groundwater zones are excluded since the groundwater in these zones is not potable. This is consistent with present-day practice in Ontario for extraction of water from shallow groundwater systems. Construction of dams and reservoirs is unlikely to have significant effects on the deep groundwater system due to the generally low topography around the site and the low permeability of the rock.
	1.4.08	Social and Institutional Developments	Included	Institutional controls ensure appropriate use and control of the site in the near term, but it is assumed that this institutional control is eventually lost. Thereafter, the site is assumed to return to land use typical of the region and the site is occupied, including drilling of wells (see FEP 1.4.07).
	1.4.09	Technological Developments	Excluded	It is assumed that the capabilities of future humans will largely resemble present-day capabilities, consistent with the International Commission on Radiological Protection's (ICRP 2000) recommendations and CNSC (2006). Thus, there is no credit taken for advances that might reduce the risk from the repository.
	1.4.10	Remedial Actions	Excluded	Remedial actions are not expected following closure of the repository.
	1.4.11	Explosions and Crashes	Excluded	Most surface explosions and crashes would have no direct impact on the repository due to its depth. Explosions large enough to affect repository depth would likely have large direct consequences that would be much more significant than any additional harm caused by damage to the repository.

External FEP			Status*	Remark
1.5	***Other External Factors***			
	1.5.01	Meteorite Impact	Excluded	Excluded due to low probability (due to relatively small repository footprint) and / or low consequence (due to depth of repository). See FEP 1.5.01 in Garisto (2013). Furthermore, meteorites large enough to affect the repository would likely have large direct consequences that would be much more significant than any additional harm caused by damage to the repository.
	1.5.02	Species Evolution	Excluded	No evolution of humans assumed, consistent with the ICRP recommendation to apply the concept of (present-day) Reference Man to the management of long-lived solid radioactive waste (ICRP 2000). Similarly, no evolution of non-human biota assumed. General characteristics of biota are assumed to remain similar to current biota.
	1.5.03	Earth Tides, Reversal of Earth's Magnetic Poles, Polar Wander and other Unusual FEPs	Excluded	Consideration of unusual FEPs such as earth tides, reversal of earth's magnetic poles, polar wander, etc. are excluded because of their low probability or because they have no significant effect on the repository.

Note: * Status – *Included* means this factor is considered in the Normal Evolution Scenario. *Excluded* means this factor is not considered in the Normal Evolution Scenario.

6.1.2 Internal FEPs

Internal FEPs are important aids in defining the expected evolution of the repository. They assist in determining which features and processes are important to include in the conceptual model and related computer codes.

The significant FEPs are accounted for in the description of the Normal Evolution Scenario which appears in the following section.

The internal FEPs are reviewed in Garisto (2013).

Internal FEPs are not usually scenario generating; however, they are considered with respect to Disruptive Scenarios in Section 6.2.1.

6.1.3 Description of the Normal Evolution of the Repository System

From consideration of the External FEPs and the Internal FEPs, the following high-level narrative of the expected evolution of the repository system can be developed. This understanding is based on many years of study, including laboratory studies, underground research studies, and observations of analogous natural and long-lived human-made structures and materials. This narrative is used to guide both the subsequent development of the conceptual model for the safety assessment and the variations to this model considered in alternative calculation cases.

The narrative summarizes the main events in the evolution of the repository in broad terms, including the long-term changes in the geosphere and biosphere due to glaciation. It is based on the reference design concept where used fuel is placed in the repository in long-lived copper-and-steel containers. These containers are designed not to fail and will be carefully fabricated and inspected. Most of these containers do not fail in the relevant time scale; however, as noted earlier there could be some containers with undetected defects in the copper shell, potentially leading to early releases of radioactivity. Since defective containers behave differently than intact containers, they are described separately in the following sections.

The possibility of failure of the copper shell at long times due to creep deformation under expected repository conditions is presently an open issue. Because of this uncertainty and others, the All Containers Fail Scenario is included as a Disruptive Event Scenario in Section 6.2. This creep failure mechanism is assumed not to occur in the Normal Evolution Scenario.

Most of the processes identified are well understood as discussed in Chapter 5. Key points are that the geosphere isolates the repository from the surface, that the groundwater around the repository level remains within its natural chemistry range and low oxygen state, and that the load-bearing capacity of the containers is sufficient to withstand the effects of glaciation and earthquakes at repository depth.

6.1.3.1 Events Occurring for Intact Containers

0-100 years

The repository is assumed to be open and actively monitored for a period of about 100 years. The 100 year period consists of the reference design assumption of ~40 years of operation and up to 70 years of monitoring during which access tunnels are kept open. Decommissioning and closure will take a further 30 years. In the operation period, 12,778 containers (containing about 4.6 million used fuel bundles, or about 90,000 Mg of uranium) are placed in the repository with the placement rooms backfilled with clay-based sealing materials. The initial radioactivity in a full repository (assuming 30 year old fuel on average) is about 10^{20} Bq and the initial thermal load is about 16 MW (Figure 6-1).

During the first 100 years after placement:

- Radioactivity drops by a factor of 10 and the thermal output drops by a factor of four. Radionuclides with short half-lives such as tritium (H-3) and Co-60 decay to negligible levels.
- Peak temperatures are reached within the repository, with values of about 120°C at the container outer surface and values less than 100ºC at distance greater than 20 cm from the container (Guo 2010).
- The copper container reacts with oxygen from the buffer to form a very thin corrosion layer.
- Recent experiments indicate that it may be possible for copper to corrode in pure, oxygen-free water (see Section 5.3.1.5). However, the hydrogen gas generated by this copper corrosion reaction suppresses further corrosion (e.g., at 73ºC, a hydrogen partial pressure of ~1 mbar (Szakálos et al. 2007) is sufficient to suppress the copper-water reaction).
- Thermal expansion and contraction of the rock and concrete combine to create near-field stresses within the low-permeability rock and the concrete bulkhead at the ends of the placement rooms, and a limited amount of microcracking occurs.
- In the rock around the repository, groundwater flow and heads are influenced by the presence of the open tunnels and the high-suction clay, which draw water towards the repository. This is countered by the container thermal power, which redistributes water away from the containers.
- Microbes in the buffer material near the containers die or become dormant because of heat, desiccation, lack of nutrients or space to be viable.

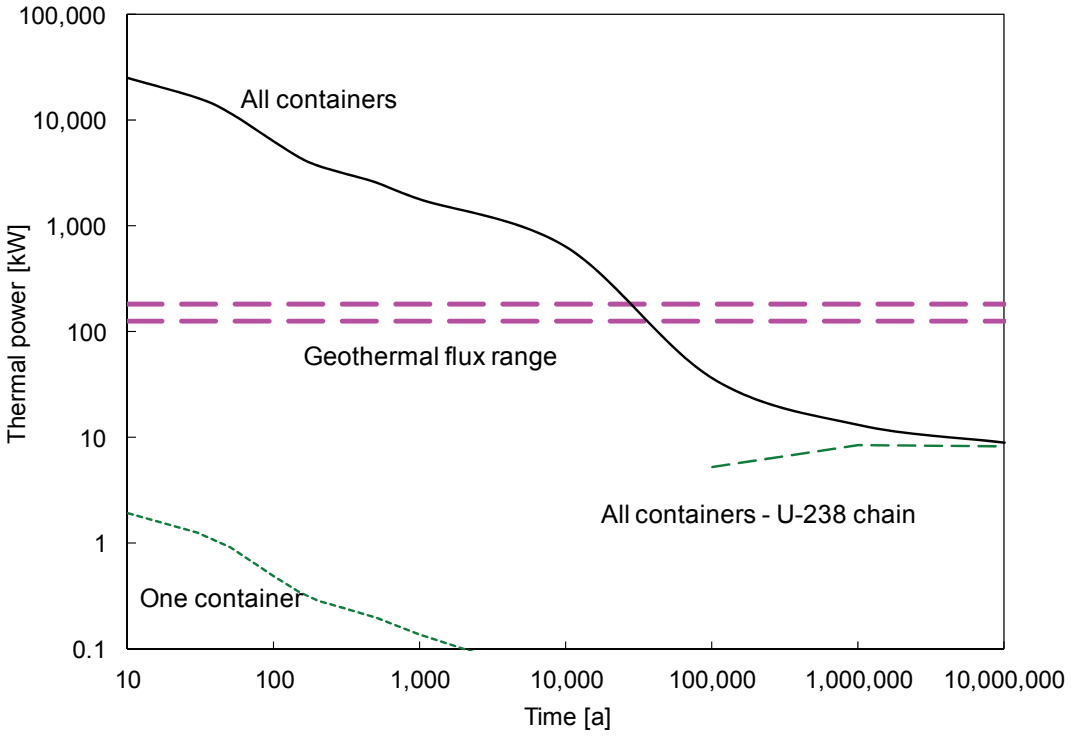

Notes: The power is similar to the natural geothermal flow (Perry et al. 2010) through the repository area after about 30,000 years. After about 1 million years, the residual power is due to radioactive decay of the decay products of uranium.

Figure 6-1: Total Thermal Power of the Repository (Average 220 MWh/kgU Burnup)

100-1,000 years

Shortly after the beginning of this time period, all access tunnels and shafts are backfilled and sealed, with particular attention paid to sealing the shafts. All intrusive monitoring systems and deep boreholes are removed or closed. For several hundred years thereafter, distinct physical and chemical differences (e.g., temperature, porewater composition) will exist between the various components of the repository, and between the repository and the geosphere. Many of the changes that occur within this timeframe are driven by these gradients. During this period:

- Radioactivity drops by a factor of 30. Most fission products decay to insignificant levels, including Sr-90 and Cs-137.
- Container thermal power drops to around 120 W per container. Residual heat comes from decay of the remaining actinides.
- Temperatures in the buffer material around the container drop to about 75^{o}C.
- The oxygen initially present in the sealing materials (as trapped air) is consumed.
- Groundwater from the geosphere enters the repository. As the clay materials begin to saturate, they start to swell and exert pressure on adjacent materials. The swelling process proceeds slowly and perhaps non-uniformly.
- Climate change may have occurred. Global warming with higher average temperatures could lead to more or less precipitation at the site. This would affect the surface waters

(lakes and rivers) and shallow groundwaters, and also the local ecosystem around the site, but deep groundwaters are unaffected.

1,000-60,000 years

- Radionuclides like C-14 have decayed.
- Thermal power drops to 6 W per container. The temperatures in and around the repository drop to approximately 10ºC above ambient rock temperatures.
- By the end of this time, the repository is saturated and anaerobic, conditions typical of deep rock environments. Peak swelling loads of clay-based seals are 0.6 to 0.7 MPa under the high salinity conditions in the repository. The swelling clay fills cracks and voids. The EDZ properties are assumed unaffected by swelling of the clay-based seals.
- Hydrostatic loads and some of the rock mechanical loads are transmitted through the clays onto the container. The copper shell is compressed onto the inner steel vessel, which is rigid and maintains its shape.
- The repository components gradually achieve equilibrium with the surrounding geosphere.
- Corrosion of the container has essentially stopped since the lack of oxygen prevents both uniform and localized corrosion.
- A fraction (< 5%) of the montmorillonite in the buffer is converted to illite due to the high potassium concentration (0.32 mol/L) in groundwater and the elevated temperatures experienced by the buffer over this period.
- The main microbial activity occurring in the repository is due to anaerobic bacteria, including sulphate-reducing bacteria, located mainly at the interfaces with the rock and in the backfill. The buffer remains largely inhospitable because of the high salinity, and high clay density and pressure, which creates adverse conditions of low water activity and small pore size.
- Locally near concrete surfaces, a more alkaline porewater develops in the clay-based sealing materials, resulting in an altered layer of clay, several centimetres thick, with a reduced swelling capacity near the interface.
- Changes continue to occur in the surface environment. Climate change due to natural or human influences would likely occur. In particular, the climate might start to cool as part of a long-term glacial cycle with possible formation of permafrost and initiation of glaciation at the site.

60,000-1,000,000 years

- Over this timeframe, the perturbations to the system will be driven by external events. The most important events will be glaciation cycles, which are likely to occur over this time period. These are likely to repeat on a period of roughly every 120,000 years.
- The residual radioactivity is dominated by the decay of actinides. By the end of this period, all plutonium has decayed.
- The onset of a glacial cycle will start with a cooling period, with mean surface temperatures over the sedimentary basin (in Ontario) dropping to approximately 0^{o}C. Permafrost develops, disrupting groundwater flow down to about 60 metres (see Chapter 2).
- Eventually, an ice sheet will form and extend across the site. The hydrological conditions at the edge of the glacier cause major perturbations to the near-surface groundwater flow system. The hydraulic heads at depth also change, but groundwater response is muted due to the low permeability of the deep rock.

- In some areas, glacially driven recharge may penetrate deeper, but reactions with minerals and microbes along the flow path of recharging meltwaters consume dissolved oxygen. Conditions at repository depth remain reducing.
- At its maximum development, the glacial ice sheet could be 2 to 3 kilometres thick above the repository, potentially increasing the hydrostatic pressure at repository depth by 20 to 30 MPa (possibly much less, depending on the rock properties and the nature of the ice sheet). This value is within the design tolerance of the containers.
- During glaciation, the land mass flexes vertically in excess of 500 m in response to the weight of the ice sheets. During glacial retreat, earthquakes may occur. Existing fracture zones may be reactivated in these locations although there is little change in terms of new fracture development.
- The advancing and retreating ice sheets and their associated meltwater both erode and deposit rock and till. The amount of additional bedrock erosion could be up to tens of metres over a one million year timeframe, but this would not adversely impact the isolation of the repository.
- The chemistry of the porewater within the sealing materials slowly changes to resemble that of the groundwater.
- Along with the porewater chemistry change, the montmorillonite component of the bentonite has lost Na and gained Ca, Mg, and Fe but has still retained its swelling capacity. Due to the lower temperatures, very little additional montmorillonite has converted to illite.
- Microbial activity in the repository is limited in general by the salinity of the groundwater (see Chapter 5). It is limited in terms of mobility by the impermeability of the dense buffer around the containers and host rock; and it is also limited metabolically by the requirement for nutrients to diffuse through the clay-based sealing materials.

Beyond 1,000,000 years

Virtually all the reactor-generated radioactivity has decayed, and most of the residual radioactivity in the used fuel comes from its natural uranium content. The amount of uranium in the repository is comparable to the large uranium ore bodies in north-central Canada. These natural deposits of uranium oxide have been stable for billions of years. Similarly, many ore deposits of metallic copper and sedimentary deposits of bentonite are known that range in age from millions to hundreds of millions of years. The ultimate fate of the repository and the materials it contains will be largely indistinguishable from these natural analogues.

6.1.3.2 Events Occurring for Defective Containers

The evolution of any defective containers will be different from that of intact containers. This evolution is summarized below (see Chapter 5 for a more detailed description).

Only the additional events that may occur in the evolution of these containers are summarized here, since most of the events occurring for the intact containers (e.g., radiation-related changes, thermal changes, etc.) also occur for defective containers. For this discussion, it is assumed that some containers are placed in the repository with small undetected defects that penetrate the copper shell. The inner steel container is therefore exposed to evolving conditions in the repository.

0-100 years

Over this period the repository is not fully saturated. Atmospheric corrosion of the steel next to the defect may occur but only to a very limited extent because the relative humidity near the copper container is low and oxygen is consumed by other processes.

100-1,000 years

As the repository saturates, water may enter the defect and contact the steel vessel. Anaerobic corrosion of the steel vessel begins, generating iron oxides and hydrogen gas. The most likely iron corrosion product is magnetite.

1,000-60,000 years

- During this period the repository becomes saturated and the buffer may swell into the defect in the container.
- Water leaks into the interior of the steel vessel through the bolted lid and the inside of the steel vessel also starts to corrode.
- Corrosion of the steel vessel continues and the hydrogen gas pressure increases near the defective container. The timing of events depends on the behaviour of the hydrogen. The corrosion rate of the steel may be limited by the availability of water due to the low hydraulic conductivity of the host rock.
- Iron corrosion products build up on the steel vessel near the defect. The build up of corrosion products causes local deformation of the copper shell and the initial defect enlarges. Formation of iron oxides however also covers the surface and inhibits the corrosion reaction.
- Hydrogen gas generated by steel corrosion forms a bubble or blanket that also inhibits water contact with the container. Once the hydrogen pressure is high enough (on the order of the hydrostatic pressure plus swelling pressure), the gas will create a channel through the buffer, and move to the interface with the rock and into the EDZ. Here, the gas would move along the interface until the gas pressure decreases sufficiently that there is no driving force for advective gas movement. The pathway through the buffer re-seals after the gas passes so the effectiveness of the buffer is not impaired.
- Water in the steel vessel contacts the fuel bundles. Local failure or corrosion of the Zircaloy cladding allows water to contact the used fuel in places. The more soluble radionuclides (typically a few percent) in the fuel / cladding gap and grain boundaries are released into the water inside the steel vessel.
- A small amount of the used fuel dissolves, releasing other radionuclides into the water. The presence of hydrogen gas from corrosion of the steel container sustains conditions that significantly decrease the rate of fuel dissolution.
- Most radionuclides have decayed, or are trapped within the used fuel. Dissolved radionuclides diffuse out of the container and into the buffer surrounding the container.

60,000-1,000,000 years

- The steel vessel continues to corrode until all of the steel is consumed.
- Corrosion of the copper vessel continues but only a small fraction of the copper corrodes over this time period.
- Hydrogen gas from steel corrosion present within the excavation damaged zone slowly dissolves in groundwater and slowly diffuses away from the repository. Hydrogen gas remaining in the container also slowly dissolves allowing full saturation of the container.

- At some point, the steel vessel is sufficiently weakened by corrosion that it is no longer load bearing and collapses. Any remaining intact fuel bundles are damaged and exposed to water.
- Most of the UO_2 is fractured but intact. About 20% of the fuel has dissolved by the end of this period.
- Some radionuclides migrate out of the container, through the buffer, and into the nearby rock. Most radionuclides decay within or near the repository and surrounding rock. Slow migration of the more mobile, soluble and long-lived species (such as I-129) through the geosphere and eventually into the shallow groundwater system and the biosphere can occur.

6.2 Disruptive Event Scenarios

Disruptive Event Scenarios postulate the occurrence of unlikely events leading to possible penetration of barriers and abnormal loss of containment.

6.2.1 Identification of Disruptive Scenarios

A set of Disruptive Scenarios has been identified by evaluating the potential for the External FEPs (Table 6-2) to compromise the safety of the repository system. Specifically, the repository system safety attributes and features identified in Chapter 1 are checked to see if they could be significantly compromised by any of the External FEPs, with the results of this assessment summarized in Table 6-3.

As a further check, the potential for the Internal FEPs to compromise the long-term safety features is also considered, and summarized in Table 6-4. Note that the FEPs considered under the “Biosphere Factors” and “Contaminant Factors” categories are not capable on their own of modifying the repository system to an extent that results in a fundamentally different evolution to that considered in the Normal Evolution Scenario. These are therefore not scenario generating and their effects can be evaluated through different calculation cases for the Normal Evolution Scenario rather than through the development of Disruptive Event Scenarios.

The failure mechanisms identified in Table 6-3 and Table 6-4 can be grouped into eight Disruptive Scenarios as discussed below and summarized in Table 6-5. Since the long-term safety of the repository is based on the strength of the geosphere and engineered barriers (including the container and the shaft seals), the scenarios focus on events in which these can be bypassed.

Table 6-3: External FEPs Potentially Compromising Arguments Relating to the Long-Term Safety

Safety Feature	Potentially Compromised by	Consider as Failure Mechanism
1. The depth of the host rock formation should be sufficient for isolating the repository from surface disturbances and changes caused by human activities and natural events.	Near-surface design adopted (FEP 1.1.02).	**No,** only a deep design is being considered for the repository.
	Meteorite impact (FEP 1.5.01).	**No,** due to low probability of meteor impact capable of compromising safety due to the relatively small repository footprint (~6 km^2) and depth of repository (~500 m). See Garisto (2013) for further discussion of probabilities.
	Exploration borehole penetrates into repository providing enhanced permeability pathway to surface environment and potential for direct exposure to waste (FEP 1.4.04).	**Yes,** although the absence of economically exploitable resources, and the depth (~500 m) and relatively small repository footprint (~6 km^2) mean that the probability of such a borehole intruding into the repository would be very low during the period of greatest potential hazard.
	Mining and other underground activities resulting in excavation in the vicinity of the repository (FEP 1.4.05).	**No,** due to assumption of the absence of commercially viable mineral resources near or below repository level. Shallow quarrying or tunnelling activities are unlikely to affect the repository because of repository depth (~500 m). Also, most underground activities would likely be preceded by exploration boreholes, as addressed above.
	Deliberate human intrusion into repository (FEP 1.4.02).	**No,** exclude deliberate human intrusion since it is expected that the intruders would take appropriate precautions. Note that unauthorized deliberate intrusion is unlikely due to the infrastructure needed to excavate to repository depth.

Safety Feature	Potentially Compromised by	Consider as Failure Mechanism
	Could discover resources that were not identified during site investigations (FEP 1.1.01) or exploit existing rocks that have become a commercially viable resource. These new resources are exploited by drilling or mining at or below repository level (FEP 1.4.04 and FEP 1.4.05).	**No,** the lack of resources at the site is assumed to be consistent with regional information. Even if the existing rocks became commercially viable, the repository site is unlikely to become a mine site because of the uniformity and large lateral extent of the host rocks that extend to shallower depths elsewhere. Also, deep mining activities would likely be preceded by an exploration borehole, which is considered under FEP 1.4.04.
	Repository and shafts not properly sealed at time of closure providing an enhanced permeability pathway to the surface environment (FEP 1.1.04).	**Yes,** although NWMO quality control and regulatory oversight will ensure that poor sealing is very unlikely. Alternatively, due to some severe societal disruption, the repository is not closed as planned but remains open and unsealed but not maintained.
	Site investigation / monitoring borehole not properly sealed at time of closure providing an enhanced permeability pathway to the surface environment (FEP 1.1.01 and FEP 1.1.11).	**Yes,** although NWMO quality control and regulatory oversight will ensure that poor sealing is very unlikely. Alternatively, due to some severe societal disruption, the repository is not closed as planned but remains open and unsealed but not maintained.
	Poor construction techniques affect the performance of the repository and shaft excavation disturbed zones providing an enhanced permeability pathway to the surface environment (FEP 1.1.02).	**Yes,** although NWMO quality control and regulatory oversight will ensure that poor sealing is very unlikely.

Safety Feature	Potentially Compromised by	Consider as Failure Mechanism
	Site investigations do not identify a permeable fracture zone or fault that provides a connection between the repository horizon and shallow groundwater system (FEP 1.1.01).	**Yes,** although very unlikely, such a feature cannot be categorically ruled out due to the limits of current technologies to identify all fracture zones, and so is considered in a "what-if" scenario.
	High magnitude seismic event results in reactivation of undetected existing structural discontinuity and / or failure of shaft seals which provides an enhanced permeability pathway to higher horizons (FEP 1.2.03).	**Yes,** the assessment time scales are such that a significant event may occur even though the annual probability is low. Even then, the probability that the earthquake could actually reactivate a nearby fracture or fail the shaft seals is very small since it would take a significant amount of energy.
	Ice sheet erosion removes a significant thickness of rock above repository (FEPs 1.2.07, 1.3.01, 1.3.02, and 1.3.05).	**Yes,** the impact of realistic rates of glacial erosion is addressed as part of the Normal Evolution Scenario; whereas, severe erosion is considered as a disruptive event scenario.
	Advance / retreat of ice sheets generate large hydraulic gradients which affect groundwater flow velocities in the deep groundwater zone (FEP 1.3.05).	**No,** the changing hydraulic head due to ice sheet advance and retreat over the repository site may affect groundwater flow at the repository level, but advective flows will remain low due to the low permeability of the deep rock (see Chapter 2, particularly the discussion of the paleohydrogeologic sensitivity cases).
	Other external geological processes disrupt the repository system, i.e., Tectonic Movement (FEP 1.2.01), Volcanic and Magmatic Activity (FEP 1.2.04), Metamorphism (FEP 1.2.05), Hydrothermal Activity (FEP 1.2.06), Diagenesis (FEP 1.2.08) and Salt Diapirism and Dissolution (FEP 1.2.09).	**No,** since precluded by site's location and assessment time scales.

Safety Feature	Potentially Compromised by	Consider as Failure Mechanism
2. The volume of available competent rock at repository depth should be sufficient to host the repository and provide sufficient distance from active geological features such as zones of deformation or faults and unfavourable heterogeneities.	Site investigations do not identify a permeable fracture zone or fault that provides a connection between the repository horizon and shallow groundwater system (FEP 1.1.01).	**Yes,** although very unlikely, such a feature cannot be categorically ruled out and so is considered in a "what-if" scenario. A nearby fracture zone could be missed due to the limits of current technologies to identify all such features in the rock.
	High magnitude seismic event results in reactivation of undetected existing structural discontinuity and / or failure of shaft seals which provides an enhanced permeability pathway to higher horizons (FEP 1.2.03).	**Yes,** the assessment time scales are such that a significant event may occur even though the annual probability is low. Even then, the probability that the earthquake could actually reactivate a nearby fracture or fail the shaft seals is very small since it would take a significant amount of energy.
	Other external geological processes disrupt the repository system, i.e., Tectonic Movement (FEP 1.2.01), Volcanic and Magmatic Activity (FEP 1.2.04), Metamorphism (FEP 1.2.05), Hydrothermal Activity (FEP 1.2.06), Diagenesis (FEP 1.2.08) and Salt Diapirism and Dissolution (FEP 1.2.09).	**No,** since precluded by site's location and assessment time scales.
3. The hydrogeological regime within the host rock should exhibit low groundwater velocities.	High magnitude seismic event results in reactivation of undetected existing structural discontinuity and / or failure of shaft seals which provides an enhanced permeability pathway to higher horizons (FEP 1.2.03).	**Yes,** the assessment time scales are such that a significant event may occur even though the annual probability is low. Even then, the probability that the earthquake could actually reactivate a nearby fracture or fail the shaft seals is very small since it would take a significant amount of energy.

Safety Feature	Potentially Compromised by	Consider as Failure Mechanism
	Advance / retreat of ice sheets generate large hydraulic gradients which affect groundwater flow velocities in the deep groundwater zone (FEP 1.3.05).	**No,** for the paleohydrogeologic sensitivity cases examined in Chapter 2, the glacial perturbations did not materially change groundwater flow rates at repository depth and diffusion remains the dominant transport mechanism in the host rock zone. Note that it is assumed that there are no fracture zones or faults at or near the site, which is consistent with Chapter2, and, furthermore, there are no undetected geological features at the repository site.
	A pattern of over- and underpressure in the groundwater and porewater hydraulic heads at the site is observed during site investigation or forms in the future due to, for example, glaciation. Such pressures would represent a state of disequilibrium.	**Yes,** such patterns have been observed at some sites in the Michigan Basin in Ontario. However, the hypothetical site is assumed to not include any significant over- or underpressure, and this would be readily detected during site characterization. No future geological mechanisms are identified that would cause this behavior on relevant timescales. Glaciation would cause pressure changes, but these are evaluated in Chapter 2 and are temporary and not significant. Nonetheless, the possibility of an overpressure forming at the boundary with the Precambrian basement is considered as a conservative sensitivity case for the Normal Evolution Scenario, even though the low hydraulic conductivity of the rock means advective flows would remain low for realistic overpressures.
	Other external geological processes disrupt the repository system, i.e., Tectonic Movement (FEP 1.2.01), Volcanic and Magmatic Activity (FEP 1.2.04), Metamorphism (FEP 1.2.05), Hydrothermal Activity (FEP 1.2.06), Diagenesis (FEP 1.2.08) and Salt Diapirism and Dissolution (FEP 1.2.09).	**No,** since precluded by site's location and assessment time scales.

Safety Feature	Potentially Compromised by	Consider as Failure Mechanism
4. The mineralogy of the rock, the geochemical composition of the groundwater and rock porewater should not adversely impact the expected performance of the repository multi-barrier system. 5. The mineralogy of the host rock, the geochemical composition of the groundwater and rock porewater should be favourable to retarding radionuclide movement.	Infiltration of glacial meltwater (without oxygen) into the repository modifies the hydrogeochemical conditions, affecting, for example, the stability of the buffer and backfill materials (i.e., leads to erosion of these materials due to colloid formation) (FEP 1.3.05).	**No,** the paleohydrogeologic simulations described in Chapter 2 suggest that glacial meltwaters will not reach the repository horizon. This is due to the low hydraulic conductivity of the overlaying shales, dolostones and Salina Group evaporites. Note that, consistent with Chapter 2, it is assumed that there are no fracture zones (or faults) at the repository site.
	Infiltration of oxygenated glacial meltwater into the repository leads to oxidizing conditions in the repository, causing relatively rapid corrosion of copper containers, rapid corrosion of used fuel in any defective containers, and enhanced mobility of redox sensitive nuclides such as U and Tc.	**No,** glacial recharge penetrating below the shallow groundwater system (i.e., depths greater than 215 m) is not expected to be oxygenated or influence the redox conditions at the repository horizon (see Chapter 2).
	Other external geological processes disrupt the repository system, i.e., Tectonic Movement (FEP 1.2.01), Volcanic and Magmatic Activity (FEP 1.2.04), Metamorphism (FEP 1.2.05), Hydrothermal Activity (FEP 1.2.06), Diagenesis (FEP 1.2.08) and Salt Diapirism and Dissolution (FEP 1.2.09).	**No,** since precluded by site's location and assessment time scales.
6. The host rock should be capable of withstanding mechanical and thermal stresses induced by the repository without significant structural deformation or fracturing that could compromise the containment and isolation functions of the repository.	Presence of repository weakens rock near repository, potentially making it susceptible to fracturing during earthquakes which could be caused by ice sheet loading / unloading (FEP 1.2.02).	**Yes,** an unknown fault or fracture zone could be reactivated due to seismic activity.

Safety Feature	Potentially Compromised by	Consider as Failure Mechanism
7. Current and future seismic activity at the repository site should not adversely impact the integrity of the repository during operation and in the very long-term.	High magnitude seismic event results in reactivation of undetected existing structural discontinuity and / or failure of shaft seals which provides an enhanced permeability pathway to higher horizons (FEP 1.2.03).	**Yes,** the assessment time scales are such that a significant event may occur even though the annual probability is low. Even then, the probability that the earthquake could actually reactivate a nearby fracture or fail the shaft seals is very small since it would take a significant amount of energy.
	Large seismic event results in shearing along an existing fracture zone that passes through a placement room of the repository. The shearing load causes failure of a used fuel container.	**Yes,** the assessment time scales are such that a significant seismic event may occur even though the annual probability is low. However, the probability that an earthquake would cause failure of a container in a placement room due to a shear load is very small due to the low seismicity, as assumed in Chapter 1; the lack of fractures in the host rock at the repository site, which is consistent with Chapter 2; and the tolerance of the design to some extent of shearing.
8. The expected rates of land uplift, subsidence and erosion at the repository site should not adversely impact the containment and isolation of the repository.	Ice sheet erosion removes a significant thickness of rock above repository (FEPs 1.2.07, 1.3.01, 1.3.02, and 1.3.05).	**Yes,** the impact of realistic rates of glacial erosion is addressed as part of the Normal Evolution Scenario; whereas, severe erosion is considered as a disruptive event scenario.
	Land uplift decreases depth of repository.	**No,** land uplift occurs on a continental scale so relative depth of repository does not change. Land uplift and large-scale erosion are also not significant factors in affecting repository depth on assessment time scale.

Safety Feature	Potentially Compromised by	Consider as Failure Mechanism
9. The repository should not be located within rock formations containing economically exploitable natural resources such as minerals and other valuable commodities as known today. 10. The repository is not located within geological formations containing groundwater resources at repository depth that could be used for drinking, agriculture or industrial uses.	Mining and other underground activities resulting in excavation in the vicinity of the repository (FEP 1.4.05).	**No,** due to the assumption of the absence of commercially viable resources near or below repository level. Other underground activities are unlikely to affect the repository (e.g., rock quarry) because of repository depth (~500 m). Also, such activities would likely be preceded by exploration boreholes, as addressed above. Even if the host rock itself became commercially viable, the repository site is unlikely to become a mine site because of the uniformity and large lateral extent of the host rock that extends to shallower depths elsewhere.
	Deliberate human intrusion into repository (FEP 1.4.02).	**No,** exclude deliberate human intrusion since it is expected that the intruders would take appropriate precaution.
	Could discover resources that were not identified during site investigations (FEP 1.1.01) or exploit existing rocks that have become a commercially viable resource. These new resources are exploited by drilling or mining at or below repository level (FEP 1.4.04 and FEP 1.4.05).	**No,** the lack of resources at the site is assumed to be consistent with regional information. Even if the host rock itself became commercially viable, the repository site is unlikely to become a mine site because of the uniformity and large lateral extent of the host rock that extends to shallower depths elsewhere. Also, the impact of drilling is already considered under exploration borehole (FEP 1.4.04).

Safety Feature	Potentially Compromised by	Consider as Failure Mechanism
11. The used nuclear fuel is a durable uranium oxide (UO_2); it will dissolve very slowly under the chemical conditions within a failed container. 12. Most of the initial radioactivity is held within the UO_2 grains, where it can only be released as the used fuel dissolves.	Infiltration of oxygenated glacial meltwater into the repository leads to oxidizing conditions in the repository, causing relatively rapid corrosion of copper containers, rapid corrosion of used fuel in any defective containers, and enhanced mobility of redox sensitive nuclides such as U and Tc.	**No,** glacial recharge penetrating below the shallow groundwater system (i.e., depths greater than 215 m) is not expected to be oxygenated or influence the redox conditions at the repository horizon (see Chapter 2).
13. The used fuel container has a design life of at least 100,000 years under the geomechanical and chemical repository conditions expected to exist within the repository.	Poor manufacturing techniques or unanticipated material problems / interactions impact on the durability of the used fuel containers (FEP 1.1.03, 1.1.07) significantly reducing the expected lifetime of some containers.	**Yes,** although application of NWMO's quality control will make it very likely that poorly manufactured containers would be discovered and not used.
	Used fuel containers fail due to increase in the isostatic load caused by a thick ice sheet passing over the repository site.	**Yes,** although the containers are designed to withstand the isostatic load from buffer swelling, hydrostatic load and a 3 km thick ice sheet over the repository site, the possibility that the design load of the container could be exceeded due to the passage of a thicker ice sheet needs to be considered. Also, given the uncertainty regarding the long-term creep behaviour of copper, container failures could occur due to this mechanism.
	Infiltration of oxygenated glacial meltwater into the repository leads to oxidizing conditions in the repository, leading to relatively rapid corrosion of the copper containers (FEP 1.3.05).	**No,** glacial recharge penetrating below the shallow groundwater system (i.e., depths greater than 215 m) is not expected to be oxygenated or influence the redox conditions at the repository horizon (see Chapter 2).

Safety Feature	Potentially Compromised by	Consider as Failure Mechanism
14. The container is surrounded by a layer (approximately 60 cm) of dense bentonite-based clay that inhibits groundwater movement, has self-sealing capability, inhibits microbial activity near the container, and retards contaminant transport.	Bentonite buffer layer not properly installed and, therefore, the density of the buffer around the container is lower than design requirement.	**Yes,** although application of NWMO's quality control will ensure that poor sealing is very unlikely.
	Infiltration of glacial meltwater (without oxygen) into the repository modifies the hydrogeochemical conditions in the repository, affecting, for example, the stability of the buffer and backfill materials (i.e., leads to erosion of these materials due to colloid formation) (FEP 1.3.05).	**No,** the paleohydrogeologic simulations described in Chapter 2 suggest that glacial meltwaters will not reach the repository horizon. This is due to the low hydraulic conductivity of the overlaying shales, dolostones and Salina Group evaporites.
	A large seismic event causes rock shear along an undetected fracture intersecting the repository at a container location, reducing the buffer thickness between the container surface and the rock.	**Yes,** the assessment time scales are such that a significant seismic event may occur even though the annual probability is low. Even then, the probability that the earthquake could actually reactivate a nearby fracture is very small since it would take a significant amount of energy.
15. Institutional Controls will limit the potential for human encounter with the repository in the near term after closure	Institutional controls on the development of the site are ineffective (FEP 1.4.08). This allows development of the site (FEP 1.4.06) and human intrusion into the repository to occur by drilling (FEP 1.4.04) and / or mining (FEP 1.4.05)	**No,** Measures are assumed to be taken in the near term to ensure that information regarding the purpose, location, design and contents of the repository is preserved so that future generations are made aware of the consequences of any actions they may choose to take. With these institutional measures as well as general societal memory, and with the absence of commercially viable natural resources at depth, inadvertent intrusion in the near term after closure is not considered. However, Human Intrusion is considered in the long-term.

Table 6-4: Internal FEPs Potentially Compromising Arguments Relating to Long-Term Safety*

Safety Feature	Potentially Compromised By	Consider as Failure Mechanism
1. The depth of the host rock formation should be sufficient for isolating the repository from surface disturbances and changes caused by human activities and natural events.	No Internal FEP could result in a significant change in the depth of the repository. Note that FEP 5.1.10 relates to the erosion of surficial deposits and not bedrock.	**No.**
2. The volume of available competent rock at repository depth should be sufficient to host the repository and provide sufficient distance from active geological features such as zones of deformation or faults and unfavourable heterogeneities.	An undetected feature (e.g., a fracture zone) in the geosphere provides a relatively high permeability connection between the repository horizon and higher horizons (FEP 4.1.02 and FEP 4.1.03)	**Yes,** a nearby fracture zone or other feature could be missed during site investigation due to the limits of current technologies to identify such features.
3. The hydrogeological regime within the host rock should exhibit low groundwater velocities.	An undetected feature (e.g., a fracture) in the geosphere provides a relatively high permeability connection n between the repository horizon and higher horizons (FEP 4.1.02 and FEP 4.1.03)	**Yes,** a nearby fracture zone or other feature could be missed due to the limits of current technologies to identify such features.
	The failure of most of the containers in the repository, due to an unexpected mechanism, leads to generation of a significant amount of hydrogen gas due to corrosion of the iron inner vessel. The hydrogen pressure could, in theory, exceed the lithostatic pressure leading to rock fracture.	**Yes,** mechanisms have been identified by which most of the containers in the repository fail (see Table 6-3). For such a scenario, it will be necessary to determine the magnitude of the peak hydrogen pressure and its impact on the repository and host rock.

Safety Feature	Potentially Compromised By	Consider as Failure Mechanism
4. The mineralogy of the rock, the geochemical composition of the groundwater and rock porewater at repository depth should not adversely impact the expected performance of the repository multi-barrier system. 5. The mineralogy of the host rock, the geochemical composition of the groundwater and rock porewater should be favourable to retarding radionuclide movement.	Various repository FEPs (e.g., FEPs 3.1.02, 3.2.01 to 3.2.05), such as temperature rise in the repository, groundwater salinity and groundwater-buffer interactions, and geosphere FEPs (e.g., FEPs 4.2.01 to 4.2.05), such as geothermal gradient and karst formation, have the potential to modify the hydrological, mechanical and chemical conditions at repository depth, affecting seal properties and / or radionuclide movement.	**No,** the effects are likely to be localized to the immediate vicinity of the repository and these FEPs can be evaluated through considering different calculation cases for the Normal Evolution Scenario (e.g., no sorption and no solubility sensitivity cases) rather than through the development of alternative Disruptive Scenarios. For conservatism, concrete seals are assumed degraded from the time of repository closure.
	Various waste package FEPs (e.g., FEPs 2.3.01 to 2.3.04) can influence the durability of the used fuel containers, potentially leading to container failures.	**Yes,** poor local conditions (e.g., low buffer density) might cause a limited number of container failures due to, for example, biofilm formation on the copper surface. Note that the Normal Evolution Scenario already includes a number of containers with pre-existing defects (e.g., welding defects) which lead to early container failures.
	Various repository FEPs (e.g., FEPs 3.2.01 to 3.2.05), such as temperature rise and groundwater interactions, and geosphere FEPs (e.g., FEPs 4.3.01 to 4.3.08), such as sorption and diffusion, can affect the rate at which contaminants are released from the repository and migrate through the shafts and geosphere.	**No,** the effects of these FEPs can be evaluated through considering different calculation cases for the Normal Evolution Scenario rather than through the development of alternative Disruptive Scenarios (e.g., no sorption and no solubility sensitivity cases). The repository and shaft excavation damaged zones are considered in the Normal Evolution Scenario. Also, concrete seals are assumed degraded from the time of repository closure.

Safety Feature	Potentially Compromised By	Consider as Failure Mechanism
	Changes in porewater chemistry in the repository due to, for example, temperature rise in the repository and presence of concrete adversely affects clay seals (FEP 3.1.02 and FEP 3.2.04).	**No,** use of low-temperature, low pH concrete in the repository minimizes interactions with clay seals. Also, the amount of concrete in the repository is small compared to the amount of clay sealing materials. Note that the Normal Evolution Scenario already includes a number of containers with pre-existing defects (e.g., welding defects) which lead to early container failures.
6. The host rock should be capable of withstanding mechanical and thermal stresses induced by the repository without significant structural deformation or fracturing that could compromise the containment and isolation functions of the repository.	Mechanical and thermal stresses induced by presence of repository are underestimated and cause greater than expected fracturing within the repository, the host rock and shaft excavation damaged zones, providing an enhanced permeability pathway to the surface environment (e.g., FEP 3.2.01 and FEP 3.2.03).	**Yes,** although application of NWMO's quality control will ensure that stresses are not underestimated and engineering calculations include safety factors.
7. Current and future seismic activity at the repository site should not adversely impact the integrity of the repository during operation and in the very long-term.	Relates to External FEPs only (see Table 6-3).	
8. The expected rates of land uplift, subsidence and erosion at the repository site should not adversely impact the containment and isolation of the repository.	Relates to External FEPs only (see Table 6-3).	

Safety Feature	Potentially Compromised By	Consider as Failure Mechanism
9. The repository should not be located within rock formations containing economically exploitable natural resources such as minerals and other valuable commodities as known today. 10. The repository is not located within geological formations containing groundwater resources at repository depth that could be used for drinking, agriculture or industrial uses.	Relates to External FEPs only (see Table 6-3).	
11. The used nuclear fuel is a durable uranium oxide (UO_2); it will dissolve very slowly under the chemical conditions within a failed container.	Various waste package FEPs (e.g., FEP 2.1.02, and FEP 2.2), such as radiation and temperature effects, and rates of used fuel dissolution in groundwater, can affect the rate at which contaminants are released from the used fuel.	**No,** the effects of these FEPs can be evaluated through considering different calculation cases for the Normal Evolution Scenario rather than through the development of alternative Disruptive Scenarios (e.g., sensitivity cases with a faster fuel dissolution rate or larger instant release fractions).
12. Most of the initial radioactivity is held within the UO_2 grains, where it can only be released as the used fuel dissolves.	Release due to criticality accident.	**No**, the used fuel is natural uranium based. . The fissile content of the used fuel is too low.

Safety Feature	Potentially Compromised By	Consider as Failure Mechanism
13. The used fuel container has a design life of at least 100,000 years under the geomechanical and chemical repository conditions expected to exist within the repository.	Containers are not fabricated to specifications and so are placed in the repository with defects (FEPs 2.3.01 to 2.3.04).	**Yes**, although the fabrication method is designed to be robust, and there would be multiple methods of inspection, there is statistically some probability of initial defects not being detected such that a few containers are placed with initial defects. The Normal Evolution Scenario assumes some containers with undetected defects are present in the repository at the time of closure, leading to early container failures.
	Various waste package and repository FEPs (e.g., FEPs 2.3.03, 2.3.04, 3.1.02, 3.2.01 to 3.2.05), such as uniform corrosion, buffer properties, temperature, and groundwater chemistry, can influence the durability of the used fuel containers, potentially leading to container failures.	**Yes,** although evidence suggests that the copper container would be thermodynamically stable under the reducing conditions expected in the repository, poor local conditions might cause a limited number of container failures. The Normal Evolution Scenario assumes some containers with undetected defects are present in the repository at the time of closure, leading to early container failures.
14. The container is surrounded by a layer (approximately 60 cm) of dense bentonite-based clay that inhibits groundwater movement, has self-sealing capability, inhibits microbial activity near the container, and retards contaminant transport.	Various repository FEPs (e.g., FEPs 3.1.02, 3.2.01 to 3.2.05), buffer properties, temperature, and groundwater chemistry, can influence the durability of the used fuel containers, potentially leading to container failures.	**Yes,** although evidence suggests that the copper container would be thermodynamically stable under the reducing conditions expected in the repository, poor local conditions might cause a limited number of container failures. The Normal Evolution Scenario assumes some containers with undetected defects are present in the repository at the time of closure, leading to early container failures.

Safety Feature	Potentially Compromised By	Consider as Failure Mechanism
	Various repository FEPs (e.g., FEPs 3.1.02, 3.1.03, 3.2.01 to 3.2.05), such as temperature, hydrothermal alteration of the buffer, and buffer-groundwater interactions, have the potential to modify the hydrological, mechanical and chemical conditions at the repository depth, affecting properties of clay-based materials.	**No,** the effects are likely to be localized to the immediate vicinity of the repository (particularly near the container surface) and these FEPs can be evaluated through considering different calculation cases for the Normal Evolution Scenario (i.e., no sorption and no solubility sensitivity cases) rather than through the development of alternative Disruptive Scenarios.
15. Institutional Controls will limit the potential for human encounter with the repository in the near term after closure	Affected by External FEPs relating to Future Human Actions (see Table 6-3) rather than the Internal FEPs relating to human behaviour that responds to the Future Human Actions.	

Note: * - the Internal FEPs are shown in Garisto (2013).

Table 6-5: Potential Failure Mechanisms and Associated Scenarios

Failure Mechanism	Associated Disruptive Scenario
Exploration borehole penetrates into the repository providing an enhanced permeability pathway to the surface environment and potential for direct exposure to waste	Human Intrusion
Poor construction techniques lead to a large excavation damaged zone around shaft seals, which provides an enhanced permeability pathway to the surface environment	Shaft Seal Failure
Repository and shafts are not properly sealed at the time of closure, providing an enhanced permeability pathway to the surface environment	Shaft Seal Failure
Long-term performance of shaft seals and excavation damaged zone deviates from that expected, due to some unexpected internal processes, resulting in an enhanced permeability pathway to the surface environment	Shaft Seal Failure
Site investigation / monitoring borehole is poorly sealed at time of closure providing an enhanced permeability pathway to the surface environment	Poorly Sealed Borehole
Long-term performance of site investigation / monitoring borehole seal deviates from that expected, due to some unexpected internal processes, resulting in an enhanced permeability pathway to the surface environment	Poorly Sealed Borehole
The repository is not closed as planned after the monitoring period and tunnels and shafts remain open.	Abandoned Repository
Site investigations do not identify a relatively high permeability fracture zone or fault that provides a connection between the repository horizon and higher horizons	Undetected Fault
Seismic event results in reactivation of an existing fracture zone and / or failure of shaft seals that provides an enhanced permeability pathway to higher horizons	Undetected Fault and Shaft Seal Failure
Glacial erosion is much more extensive than expected at the repository site over a one million year period.	Severe Erosion
Seismic event results in shearing along an existing fracture zone passing through a placement room, resulting in failure of some container(s) due to the shear load.	Container Failure
Manufacturing defect in steel vessel or unexpected high local loads lead to mechanical failure of some containers.	Container Failure
Unexpected corrosion of some copper containers due to, for example, initial defects in the copper shell, or unanticipated interaction of the copper container with groundwater in the repository.	Container Failure
Unexpected poor mechanical or chemical performance of the copper shell under repository conditions leads to failure of a significant number of containers in the repository.	All Containers Fail
Passage of thicker than expected ice sheet over repository site causes isostatic load on all containers to exceed design load of containers, resulting in failure of all containers.	All Containers Fail

The repository siting process will ensure that there are no known commercially viable natural resources near or below repository depth. Also, the repository has a relatively small footprint (~6 km^2) and the repository is at a depth of around 500 m. These factors limit the range of human activities that could directly affect the closed repository to a borehole unintentionally drilled into the repository as part of a future geological exploration program[2]. Even this situation has a low probability of occurrence. Nevertheless, once controls on the use of the site are no longer effective, the possibility of inadvertent human intrusion by this method cannot be ruled out over long time scales[3]. Such a borehole could provide an enhanced permeability pathway to the surface environment and potential for direct exposure to waste. This scenario is referred to as the **Human Intrusion Scenario**.

A second scenario by which the geosphere barrier can be bypassed is via the shafts (main, service and ventilation shafts). These are ~8 m diameter holes that penetrate the geosphere, but are placed away from the waste panels and carefully sealed in the design. The **Shaft Seal Failure Scenario** considers the possibility that the shaft seals are not fabricated or installed appropriately, or that the long-term performance of the shaft seals and shaft / repository Excavation Damaged Zones (EDZs) is poor due to unexpected physical, chemical and / or biological processes, or the shaft seals are damaged by a seismic event. While these situations could result in an enhanced permeability pathway to the surface, they are very unlikely due to quality control measures that will be applied during shaft seal closure and due to multiple durable material layers in the shaft.

In the Shaft Seal Failure Scenario, it is assumed that the other repository engineered barriers (i.e., the tunnel and room seals, and the backfill and buffer), are not degraded relative to their design properties except for the concrete component of the seals, for which degraded properties are used throughout the simulations, as in the Normal Evolution Scenario.

The geosphere barrier is also bypassed via the shafts in the "what-if" **Abandoned Repository Scenario** in which the repository is assumed not to be sealed following the monitoring period (i.e., after all containers are deposited and placement rooms are sealed), and therefore both the access tunnels and shafts remain open but not maintained at least for an extended period. Since closing the repository is clearly important and funds would have been set aside for this purpose, this scenario would require a societal collapse or abandonment of the site for other unknown reasons. The likelihood of such a scenario is unknown but is probably low.

Another way in which the geosphere barrier can be bypassed is through the site characterization / monitoring boreholes. These boreholes are located in the vicinity of the repository down to and below repository depth. These boreholes will be appropriately sealed on completion of site investigation / monitoring activities so they will have no effect on repository performance. However, if a deep borehole were not properly sealed or were to extensively degrade, then it could provide a small but relatively permeable pathway for the migration of contaminants from the repository horizon. The scenario is termed the **Poorly Sealed Borehole**

[2] The assessment excludes deliberate human intrusion since it is expected that the intruders would take appropriate precaution.

[3] The repository might appear as an anomaly in a surface / air-borne survey of the area, and this could encourage drilling at the site if all records had been lost. However, the absence of interesting minerals or geologic features in the area would argue against deliberate surveys of the area. Furthermore, a cautious approach to drilling might be used if such unexpected anomalies were identified that would minimize the consequences of any intrusion into the repository.

Scenario. Like the Shaft Seal Failure Scenario, such a situation is very unlikely due to the adoption of good engineering practice and quality control.

For the Normal Evolution Scenario, it is assumed that site investigation and geosynthesis would detect the occurrence of transmissive vertical faults / fracture zones which could provide an enhanced permeability pathway from the repository horizon to the overlying aquifer within the footprint or vicinity of the repository. However, it is possible that site characterization does not identify all existing significant fractures at the site and, therefore, a "what-if" scenario is defined to investigate the safety implications of a hypothetical transmissive fault that is either undetected or formed by the displacement of an existing structural discontinuity. The hypothetical fault is assumed to be in close proximity to the repository and to extend from below the repository level to the shallow groundwater system. This scenario is termed the **Undetected Fault Scenario**.

Glacial erosion is considered in the Normal Evolution Scenario. At this hypothetical site, a realistic amount of glacial erosion over a one million year time frame is considered as part of the Normal Evolution Scenario. However, a more severe glacial erosion rate is assessed in the **Severe Erosion Scenario**. Such a scenario is considered highly unlikely because of the absence of topographic features or other known factors that would tend to localize erosion by ice or water in the Michigan Basin (Hallet 2011). Furthermore, future glaciations would tend to repeat the actions of their predecessors, by funneling into lake basins and deepening them, and maintaining the topographic highs where the ice flow velocities and erosion rates are relatively low and where sediments tend to accumulate.

While the copper used fuel containers have a design requirement for a minimum functional life of not less than 100,000 years, they are expected to last much longer based on thermodynamic, experimental and natural analogue evidence that copper is stable for very long periods under deep geological repository conditions. Nevertheless, there are several mechanisms by which the containers could fail some time after they are installed in the repository. These container failures would be more severe than the small defects considered in the Normal Evolution Scenario (which could arise be due to, for example, undetected welding defects.) Possible failure mechanisms include the following:

- After the repository attains reducing conditions, the copper containers should be immune to further corrosion. However, unexpected interactions between the groundwater and copper container (e.g., due to higher than expected sulphide concentrations) could damage the copper container sufficiently over the time frame of interest that the steel vessel would be exposed to water, leading to weakening of the vessel due to corrosion and / or seepage of water into the container.
- A container could be damaged by a sufficiently large shear load. A large seismic event that causes the rock to slip along an undetected fracture zone intersecting a placement room could produce such a shear load. The probability of such an event depends on the likelihood of an earthquake of a sufficient magnitude, the likelihood that a placement room is intersected by a fracture zone and that a container is near the fracture zone and, finally, how the shear load is transmitted through the buffer material, which depends on the buffer thickness and density. The analysis in SKB (2011) indicates that, for their repository, less than 0.2 containers would fail due to shear load over one-million years.

The specific failure mode is not defined here, but the consequences are evaluated in the **Container Failure Scenario**. The key characteristics of this scenario are that only a few

containers are affected, that the container damage is significant, but also that the failure occurs at least 10,000 years and possibly 60,000 years after closure.

The containers are designed to be corrosion resistant and to be robust. As noted in Chapter 4, the inner steel vessel is designed to sustain an external isostatic load of 45 MPa, (i.e., the maximum load experienced by the container during passage of a 3 km thick ice sheet above the repository site). Thus, the containers are expected to have a long lifetime. However, it is possible that some unexpected event or process may occur in the future such that there are multiple container failures in the repository. For example, the copper shell of the container could fail at long times due to creep deformation. Also, the design load of the container could be exceeded if, for example, the thickness of the ice sheet passing over the repository is greater than the design basis ice sheet.

Consequently, an **All Containers Fail Scenario** is considered in which all the containers in the repository fail at 60,000 years (i.e., there are no initially defected containers), the time of the assumed first passage of an ice sheet over the site (see Chapter 2). The probability of such a scenario is likely low since, for example, the ice sheet would have to be substantially thicker than 3 km for the load exerted on the container to exceed 45 MPa, given the low buffer swelling pressure. Further, the creep behaviour of copper under repository conditions is an open issue.

Other potential Disruptive Scenarios were considered but ruled out on various grounds as discussed further in the FEPs report (Garisto 2013). No volcanic activity is anticipated in the area over the next one million years. The probability of being hit by a large meteor capable of damaging the repository is remote and the consequences of the impact itself would likely be more significant than those from the repository. Seismic activity is possible, and likely earthquakes are included in the Normal Evolution Scenario. Such seismic activity will not cause rockfall because the repository is backfilled. Large earthquakes are unlikely since it is assumed that the hypothetical site is located in a low-seismicity area. The main effects on the repository are represented by the Shaft Seal Failure, the Undetected Fault and the Container Failure Scenarios, so there is no need to consider an additional earthquake scenario. Glaciation, which could affect the repository system, is considered within the Normal Evolution Scenario.

Further confidence that an appropriate set of Disruptive Scenarios has been identified can be obtained by examining the scenarios (or sensitivity cases) considered in the postclosure safety assessments of deep repositories in other countries. The results of such an examination, summarized in Table 6-6, show that most assessments have identified a limited number of additional scenarios that consider the degradation / failure of engineered and natural barriers by natural processes (e.g., earthquakes, climate change) and human actions (e.g., drilling, poor quality control). Although there are some scenarios that are not considered in the current study, these are either not relevant for the hypothetical site (e.g., volcanic activity, sea-level rise, mining of resources) or have been included in the Normal Evolution Scenario (e.g., climate change, container failure).

Table 6-6: Additional Scenarios Considered in Other Safety Assessments

Assessment	Reference	Additional Scenarios Considered
SR-Site (Sweden)	SKB (2011)	• Canister failure due to corrosion or shear load • Disrupted buffer (due to erosion, advection) • Extended greenhouse effects • Exploratory drilling • Rock facility (e.g., quarry) • Incompletely sealed (or abandoned) repository
Olkiluoto (Finland)	POSIVA (2012)	• Defective canister (early and delayed penetration) • Earthquake/rock shear • Disrupted buffer • Exploratory drilling
Dossier Argile (France)	ANDRA (2005)	• Seal failure and defective plug • Defective waste and spent fuel containers • Borehole penetrating repository • Functioning of repository greatly degraded
H12 (Japan)[1]	JNC (2000)	• Climate and sea-level change • Exploitation drilling (water well) • Engineering defects, including poorly sealed repository
Opalinus (Switzerland)	NAGRA (2002)	• Gas pathways • Exploratory drilling • Poorly sealed repository
GPA (UK)	NIREX (2003)	• Exploratory drilling
WIPP (USA)	DOE (2004)	• Mining • Exploratory drilling
Yucca Mountain (USA)[2]	DOE (2002)	• Exploratory drilling • Seismicity • Volcanic event
SAFIR 2 (Belgium)	ONDRAF/NIRAS (2001)	• Exploratory drilling • Greenhouse effect • Poor sealing of repository • Fault activation • Severe glacial period • Failure of engineered barriers • Gas-driven transport

Notes:

[1] Isolation Failure Scenarios that involve penetration of the repository (including magma intrusion, human intrusion and meteorite impact) were also considered but screened out on the grounds that they are extremely unlikely to occur. Some 'what if' calculations were carried out instead.

[2] The term 'scenario' is used in a way that differs from the other assessments reviewed. Three Thermal Load Scenarios are discussed that are design variants, while two No-action Scenarios refer to futures in which the Yucca Mountain facility does not go ahead.

6.2.2 Description of Disruptive Event Scenarios

The identified Disruptive Event Scenarios are described below. These scenarios are evaluated separately rather than in combination since they have low probability and independent causes, and so the likelihood of simultaneous occurrence is even lower.

6.2.2.1 Inadvertent Human Intrusion Scenario

The Inadvertent Human Intrusion Scenario considers the impact of human intrusion sometime in the future. In this scenario, an exploration borehole is drilled through the geosphere and into the repository with the drill bit intersecting a used fuel container.

It is assumed that the drill crew is unaware of the facility (i.e., the intrusion occurs after institutional controls are no longer effective and societal memory of the site is lost). The investigators will most likely collect samples or conduct measurements at the repository level, due to the unusual nature of the materials. This would identify significant residual radioactivity (e.g., gamma logging is a standard borehole measurement) and the investigators would likely take precautions to prevent further exposure, including appropriate management of any materials released at the surface and sealing of the borehole. Therefore, under normal drilling, there would be little impact after the initial drill crew exposure.

Nevertheless, the Inadvertent Human Intrusion Scenario assumes:

- It is not recognized that the drill has intercepted a waste repository so no safety restrictions are applied; and
- The borehole and drill site are not managed and closed to current standards, and material from the borehole is released onto the surface around the drill site.

Contaminants can be released and humans and biota exposed via:

- Retrieval and examination of drill core contaminated with waste; and
- Uncontrolled dispersal of contaminated drill core debris on the site.

This could result in the exposure of the drill crew or other people at the time of intrusion, and people who might occupy the site subsequent to the intrusion event.

If the borehole is not properly sealed, it could provide an enhanced permeability pathway to the surface environment or even be used as a well by a future site resident. The impact of this open borehole on the future residents of the site is examined as part of the Inadvertent Human Intrusion Scenario.

6.2.2.2 Shaft Seal Failure Scenario

The shafts represent a potentially important pathway for contaminant release and therefore the repository design includes specific measures to provide good shaft seals, taking into account the characteristics of the geosphere. The Shaft Seal Failure Scenario considers the consequences of rapid and extensive shaft seal degradation. This scenario, like the other Disruptive Event Scenarios, is a bounding scenario designed to investigate the robustness of the repository system.

The groundwater transport exposure pathways are the same as those considered in the Normal Evolution Scenario.

6.2.2.3 Abandoned Repository Scenario

Another scenario by which the geosphere barrier can be bypassed via the shafts is the “what-if” Abandoned Repository Scenario. The basic assumption in the Abandoned Repository Scenario is that the repository is abandoned during the monitoring phase (i.e., after all containers are placed in the repository and all placement rooms are backfilled and sealed), but the main access tunnels and the shafts are still open. This is consistent with normal operations, in which the placement rooms are successively filled with containers and backfilled, and sealed as soon as they are filled.

Abandonment of the repository would require a significant societal breakdown because of the known importance of properly closing the repository.

The groundwater transport exposure pathways are the same as those considered in the Normal Evolution Scenario.

6.2.2.4 Poorly Sealed Borehole Scenario

Multiple deep site investigation / monitoring boreholes will be drilled in the vicinity of the repository during the site investigation phase. The Poorly Sealed Borehole Scenario considers the consequences of one of the boreholes not being properly sealed or having a seal that extensively degrades. The poorly sealed borehole provides an enhanced permeability connection between the level of the repository, the overlying groundwater zones and the biosphere, thereby bypassing some of the natural geological barriers to contaminant migration from the repository. The exposure pathways are the same as those considered in the Normal Evolution Scenario.

6.2.2.5 Undetected Fault Scenario

The Undetected Fault Scenario considers the impact of an undetected or new transmissive fault extending from around the repository level into the shallow groundwater system in close proximity to the repository. Such a fault could provide an enhanced permeability pathway that bypasses the deep groundwater system.

The groundwater transport exposure pathways are the same as those considered in the Normal Evolution Scenario.

6.2.2.6 Severe Erosion Scenario

The Severe Erosion Scenario considers the impact of severe glacial erosion on the performance of the used fuel repository.

The groundwater transport exposure pathways are the same as those considered in the Normal Evolution Scenario.

6.2.2.7 All Containers Fail Scenario

The long-lived used fuel containers are an important feature of the multi-barrier repository concept in this conceptual design. The copper containers are expected to last for a long time because copper is stable under anticipated conditions in a deep geological repository; however, the All Containers Fail Scenario considers the unlikely and hypothetical case in which all the containers simultaneously fail (i.e., water enters all containers and contacts the fuel) at 60,000 years. This timeframe corresponds to the approximate time scale for glacial cycles to resume and an ice sheet to first cover the site (see Chapter 2), which could be assumed to cause multiple container failures if the isostatic load on the containers is higher than expected. For simplicity, in this scenario, there are no initially defected containers as in the Normal Evolution Scenario

A variant case in which all containers are assumed to fail at 10,000 years is also investigated to determine the sensitivity to the assumed failure time.

The groundwater transport exposure pathways are the same as those considered in the Normal Evolution Scenario. However, the failure of all containers also leads to the generation of significant amounts of hydrogen gas due to corrosion of the inner steel vessel. Consequently, the impact of gas generation on the performance of the repository and the transport of contaminants is also addressed.

6.2.2.8 Container Failure

The Container Failure Scenario considers the impact of container failure due to several possible mechanisms.

- Corrosion of the container due to unexpected chemical interactions with the groundwater or installation of a defective (i.e., low density) buffer which allows formation of biofilms on the copper surface.
- A large seismic event (earthquake) in the vicinity of the repository that causes slip along a fracture zone that intersects a placement room. The rock slip along the fracture zone is assumed to be so large that it causes complete failure of a container. The shear is also assumed to significantly increase the transmissivity of the fracture. Although the shear movement should not affect the buffer properties, the amount of buffer between the container and the shearing fracture zone would likely be reduced.

The exposure pathways are the same as those considered in the Normal Evolution Scenario.

6.3 References for Chapter 6

ANDRA. 2005. Dossier 2005 Argile Tome Evaluation de Sûreté du Stockage Géologique. Paris, France.

CNSC. 2006. Regulatory Guide G-320: Assessing the Long Term Safety of Radioactive Waste Management. Canadian Nuclear Safety Commission. Ottawa, Canada.

DOE. 2002. Final Environmental Impact Statement for a Geologic Repository for the Disposal of Spent Nuclear Fuel and High-level Radioactive Waste at Yucca Mountain, Nye

County, Nevada. United States Department of Energy, Office of Civilian Radioactive Waste Management, DOE/EIS-0250. Nevada, USA.

DOE. 2004. 2004 WIPP Compliance Recertification Application (CRA) - Main Volume. US Department of Energy Report DOE/WIPP 04-3231. Available at: http://www.wipp.energy.gov/library/CRA/CRA_Index.htm. Accessed January 2011.

Garisto, F. 2013. Fifth Case Study: Features, Events and Processes. Nuclear Waste Management Organization Report NWMO TR-2013-06. Toronto, Canada.

Guo, R. 2010. Coupled Thermal-Mechanical Modelling of a Deep Geological Repository using the Horizontal Tunnel Placement Method in Sedimentary Rock using CODE_BRIGHT. Nuclear Waste Management Organization Technical Report NWMO TR-2010-22. Toronto, Canada.

Hallet, B. 2011. Glacial Erosion Assessment. Nuclear Waste Management Organization Report NWMO DGR-TR-2011-18 R000. Toronto, Canada.

IAEA. 2012. The Safety Case and Safety Assessment for the Disposal of Radioactive Waste. IAEA Safety Standards. Specific Safety Guide No. SSG-23. International Atomic Energy Agency. Vienna, Austria.

ICRP. 2000. Radiation Protection Recommendations as Applied to the Disposal of Long-lived Solid Radioactive Waste. International Commission on Radiological Protection Publication No. 81, Annals of the ICRP 28(4).

JNC. 2000. H12: Project to Establish the Scientific and Technical Basis for HLW in Japan. Japan Nuclear Cycle Development Institute Report JNC TN1410 2000-004. Tokai, Japan.

NAGRA. 2002. Project Opalinus Clay: Safety Report, Demonstration of the Disposal Feasibility for Spent Fuel, Vitrified HLW and Long-lived ILW. Nagra Technical Report 02-05. Wettingen, Switzerland.

NIREX. 2003. Generic Repository Studies: Generic Post-closure Performance Assessment. Nirex Report N/080. Harwell, United Kingdom.

ONDRAF/NIRAS. 2001. SAFIR 2: Safety Assessment and Feasibility Interim Report 2. ONDRAF/NIRAS Report NIROND 2001-06E. Brussels, Belgium.

Perry, C., C. Rosieanu, J.-C. Mareschal and C. Jaupart. 2010. Thermal Regime of the Lithosphere in the Canadian Shield, Canadian Journal of Earth Sciences 47, 389-408.

Peltier, W.R. 2011. Long-Term Climate Change. Nuclear Waste Management Organization Technical Report NWMO DGR-TR-2011-14 R000. Toronto, Canada.

POSIVA. 2012. Safety Case for the Disposal of Spent Nuclear Fuel at Olkiluoto – Synthesis 2012. Posiva Report 2012-12. Olkiluoto, Finland.

SKB. 2011. Long-term Safety for the Final Repository for Spent Nuclear Fuel at Forsmark, Main Report of the SR-Site Project. Swedish Nuclear Fuel and Waste Management Report SKB TR-11-01. Stockholm, Sweden.

Szakálos, P., G. Hultquist, and G. Wikmark. 2007. Corrosion of Copper by Water. Electrochemical and Solid-State Letters, 10, pp C63–C67.

7. POSTCLOSURE SAFETY ASSESSMENT – CONTAMINANT TRANSPORT

This chapter, together with Chapter 8, presents an illustrative postclosure safety assessment for a used fuel repository located in the sedimentary rock of the Michigan Basin. This chapter focusses on liquid-borne contaminant transport, where 'contaminant' includes both radionuclides and stable elements. Chapter 8 focusses on gas transport.

The purpose of a postclosure safety assessment is to determine the potential effects of the repository on the health and safety of persons and the environment during the postclosure period. The assessment timeframe is one million years based on the time period needed for the radioactivity of the used fuel to decay to essentially the same level as that in an equivalent amount of natural uranium. This timeframe is also within a reasonable extrapolation of the geological stability of these rocks. However, due to the very good retention properties of the sedimentary rock, the peak impacts may occur beyond one million years. Analyses presented here include an approximate extension beyond one million years to demonstrate that the peak impacts remain well below the interim acceptance criteria.

The assessment is conducted by applying computer models to a range of analysis cases. The analysis cases here examine the Normal Evolution Scenario and some of the Disruptive Scenarios identified in Chapter 6, together with a series of sensitivity studies performed to examine the importance of various model features and assumptions.

The assessment is arranged as follows:

- Section 7.1 – Interim Acceptance Criteria: four sets of interim acceptance criteria are presented against which the radiological and non-radiological impacts on persons and the environment assessed.
- Section 7.2 – Scope: provides a detailed description of the analysis cases together with the rationale for their selection. Included is a brief discussion of items excluded from the scope but which might otherwise be included in a licence submission.
- Section 7.3 – Conceptual Model: discusses the conceptualization of the repository evolution.
- Section 7.4 – Computer Code: introduces the main computer codes used.
- Section 7.5 – Analysis Methods and Key Assumptions: the computer code representations created for this study are described in detail. Some numerical data are presented to provide context.
- Section 7.6 – Results of Radionuclide and Chemical Toxicity Screening Analysis: discusses the set of potentially significant radionuclides and chemical elements included in the study.
- Section 7.7 – Results of Detailed 3D Groundwater Flow and Transport Analysis: discusses 3D simulations of groundwater flow and radionuclide transport for I-129, Cs-135, U-234 and U-238.
- Section 7.8 – Results of System Model: discusses deterministic and probabilistic (i.e., Monte Carlo) simulations of radionuclide release, transport and impact for all radionuclides of potential interest identified in Section 7.6.

- Section 7.9 – Disruptive Scenarios: describes the analysis and presents results for those Disruptive Scenarios included in the scope of this study.
- Section 7.10 – The Effects of Glaciation on the Normal Evolution Scenario: uses results of the regional glaciation modelling studies described in Chapter 2 to draw conclusions on the likely effects of glaciation on the dose consequences for the Normal Evolution Scenario.
- Section 7.11 – Other Considerations: describes two complementary indicators for radiological safety, results for the radiological protection of the environment, and results for the protection of persons and the environment from hazardous substances (including results for one complementary indicator).
- Section 7.12 – Summary and Conclusions.

7.1 Interim Acceptance Criteria

This section presents interim acceptance criteria applicable to the postclosure safety assessment. These criteria are used to judge the acceptability of analysis results.

CNSC Guide G-320 (CNSC 2006) identifies the following categories of acceptance criteria:

1. Radiological protection of persons;
2. Protection of persons from hazardous substances;
3. Radiological protection of the environment; and
4. Protection of the environment from hazardous substances.

Interim acceptance criteria defined for each category are discussed in the following sections. These criteria are consistent with current Canadian and international practice; however, it is recognized that the criteria used in a licence application will need to be accepted by the CNSC at that time, and may be different from the specific values identified here.

7.1.1 Interim Acceptance Criteria for the Radiological Protection of Persons

The main objective of the postclosure safety assessment is to provide reasonable assurance that the regulatory radiological dose limit for public exposure (1 mSv/a) will not be exceeded. To account for the possibility of exposure to multiple sources, a dose constraint below the regulatory limit is adopted.

For the Normal Evolution Scenario, the interim dose acceptance criterion is:

- An annual individual effective dose rate of 0.3 mSv/a with the calculation performed to encompass the time of maximum predicted impact to the average adult member of the critical group.

The 0.3 mSv/a dose constraint is consistent with recommendations of the International Commission on Radiation Protection (ICRP) and IAEA guidance (ICRP 2007, ICRP 2013, IAEA 2006) and is significantly less the average Canadian individual dose rate of 1.8 mSv/a received from background radiation (Grasty and LaMarre 2004).

At this dose level, there is no clear evidence for adverse health effects (NRC 2006, CNSC 2011). However, the Linear-No-Threshold model recommended by international agencies (ICRP 2013) and adopted by Canadian regulators assumes that any dose exposure results in some increase in health risk, notably cancer. This dose constraint ensures that the health risks are small in comparison to the risk from natural background radiation, and to the risk of cancer from all causes.

Calculating the exposure of an adult member of the critical group is consistent with ICRP recommendations which recognize that any exposures are expected to occur in the distant future, any exposure would be associated with levels of radionuclides in the environment that change slowly over the time scale of a human life time, and the calculated exposures at long times have inherent uncertainties (ICRP 2013). Effective dose rates are calculated using the dose coefficients from ICRP 72 (ICRP 1995), which are based on a human model that includes male and female organs to ensure it includes all radionuclide sensitivities.

For Disruptive Scenarios, the interim acceptance criteria are:

- An annual individual effective dose rate target of 1 mSv/a for credible chronic[1] release scenarios with the calculation performed for the average adult member of the critical group; and
- Acceptability of any scenario with the calculated annual individual effective dose rate for chronic releases exceeding 1 mSv/a to be examined on a case-by-case basis taking into account the likelihood and nature of the exposure, uncertainty in the assessment and conservatism in the dose criterion. Where the probability of exposure can be quantified without excessive uncertainty, a measure of risk will be calculated based on the probability of exposure and the consequent health effects. This is compared with a reference risk value of 10^{-5}/a.

A dose rate of 1 mSv/a corresponds to the current radiological limit for exposure of the public. This is less than the 1.8 mSv/a. average natural background dose rate for Canadians.

The reference health risk value of 10^{-5}/a is consistent with ICRP (2013) and IAEA (2006). Based on the ICRP probability coefficient of 0.057 per Sv for stochastic effects (e.g., cancers or hereditary effects) (ICRP 2007), this corresponds to a health risk about a factor of 10 lower than the risk from the natural background dose rate.

Regulatory document G-320 (CNSC 2006) and ICRP (2013) recognize that inadvertent human intrusion into a repository could result in doses greater than 1 mSv/a since human intrusion by definition bypasses the repository barriers. The risk from human intrusion is made low by the site selection criteria which require the facility to be located deep underground in an area known not to have economically exploitable natural resources or potable groundwater resources at repository depth. Institutional controls will also reduce risk in the short-term, when the hazard is highest.

[1] Chronic refers to a release that is sustained over many years.

7.1.2 Interim Acceptance Criteria for the Protection of Persons from Hazardous Substances

For this category, the interim acceptance criteria are based on Canadian guideline values for concentrations in environmental media relevant to human health and environmental protection, supplemented as needed.

The values are shown in Table 7-1. The criteria are based on federal and provincial guideline concentrations for surface water, groundwater, soil and sediment, and in particular Canadian Council of the Environment (CCME 2007 a, b, c and CCME 2002). In cases where federal guidelines do not currently exist, Ontario Ministry of the Environment guidelines (MoE 2011a, MoEE 1994) and Oregon Department of Environmental Quality (ODEQ, 2001) have been adopted as interim acceptance criteria. Depending on the actual site location, the applicable provincial guidelines would be used.

The values have been reviewed to determine the effect of updates to the original source documents. All values remain conservative.

Estimated environmental concentrations of contaminants are compared with the above interim acceptance criteria. Additive effects are not considered in this stage. If any concentrations exceed the criteria in the Normal Evolution Scenario, these contaminants are assessed further in a tiered approach with decreased conservatism in the models. If any concentrations exceed these criteria for Disruptive Scenarios, acceptability is judged on a case-by-case basis taking into account the likelihood and nature of the exposure, uncertainty in the assessment and conservatism in the criteria.

Table 7-1: Interim Acceptance Criteria for the Protection of Persons and the Environment from Non-Radiological Impacts

Chemical Hazard Criteria					
Element	**Background Groundwater [µg/L]**	**Potable Groundwater [µg/L]**	**Surface Water* [µg/L]**	**Soil [µg/g]**	**Sediment [µg/g]**
Ag	0.3	1.2	0.1	0.5	0.5
Al	-	-	5	50	-
Ba	610	1000	4	210	-
Be	0.5	4	11+	2.5	-
Bi	-	-	150	20	-
Cd	0.5	2.1	0.017	1	0.6
Ce	-	-	22	53	19000
Co	3.8	3.8	0.9	19	50
Cr	11	50	1	0.4	26
Cs	-	-	450	-	-
Cu**	5	69	5	62	16
Eu	-	-	10.1	50	4700
Hg	0.1	0.29	0.004	0.16	0.17
La	-	-	10.1	50	4700
Mo	23	70	40	2	-
Nd	-	-	1.8	50	7500
Ni	14	100	25	37	16
P	-	-	4	-	-
Pb	1.9	10	1	45	31
Pd	-	-	200	-	-
Pr	-	-	9.1	50	5800
Sb	1.5	6	20+	1	3
Se	5	10	1	1	-
Sm	-	-	8.2	5	-
Sr	-	-	1500	33000	-
Te	-	-	20	250	-
U	8.9	20	5	1.9	-
V	3.9	6.2	6	86	-
Y	-	-	6.4	50	1400
Zr	-	-	4	97	-

Notes: '-' indicates that there are no defined criteria for that element in the given medium.

* Surface water values differ from groundwater values because the surface water values protect biota and humans, whereas groundwater values protect humans only (i.e., biota (other than microbes) do not live in groundwater). Differences arise for Be and Sb because different references are used for different values.

** The Cu value is for water with a $CaCO_3$ content > 20 mg/L

+: These values are greater than their associated groundwater values because of different source documents.

Detailed information on the individual source documents is available in Gobien et al. (2013)

7.1.3 Interim Acceptance Criteria for the Radiological Protection of the Environment

For radiological protection of the environment, the interim acceptance criteria are based on dose benchmarks developed for the assessment of priority substances in relation to discharges of radionuclides from nuclear facilities.

No-Effect Concentrations are derived from Estimated No Effect Values (ENEVs) for the most limiting indicator species relevant to the Southern Canadian Deciduous Forest ecosystem, the Boreal Forest ecosystem and the Inland Tundra ecosystem. For every indicator species, the radionuclide concentration that corresponds to the ENEV is calculated for each medium (i.e., surface water, soil, and sediment) assuming zero radionuclide concentration in other media. The lowest concentration from all indicator species is then selected as the No-Effect Concentration for that radionuclide. The interim acceptance criteria are shown in Table 7-2.

If any radionuclide concentration exceeds the No-Effect Concentration in the Normal Evolution Scenario, an Ecological Risk Assessment will be carried out for that radionuclide, taking into account uncertainties and potential need for the effect of several radionuclides to be summed into account. If any concentration exceeds the No-Effect Concentration in Disruptive Scenarios, then acceptability will be judged on a case-by-case basis taking into account the likelihood and nature of the exposure, uncertainty in the assessment and conservatism in the dose criterion.

The ENEVs are based on the dose benchmarks from Environment Canada / Health Canada (EC/HC 2003) or lower; and the transfer factors are based on literature review. The analysis is summarized in Garisto et al. (2008). It is recognized that there has been a substantive effort over the past few years to obtain new data in this area, and that the parameter values will need to be reconsidered as new information becomes available. Criteria will also need to be provided for other radionuclides of potential interest; however, the basic concept of comparing media concentrations with benchmark values remains a plausible approach for non-human biota. Note that the NWMO has an ongoing work program in which different methods, including the ERICA method (Brown et al. 2008), are being investigated for defining these criteria. When this work matures, the acceptance criteria will be updated.

Table 7-2: Interim Acceptance Criteria for the Radiological Protection of the Environment

Radionuclide	Media		
	Water (Bq/L)	Soil (Bq/kg)	Sediment (Bq/kg)
Cl-36	2.8×10^{0}	3.8×10^{-1}	4.1×10^{4}
I-129	3.2×10^{0}	2.4×10^{3}	1.2×10^{6}
Cs-135	2.1×10^{-3}	8.5×10^{0}	3.5×10^{5}
Tc-99	8.0×10^{-1}	4.3×10^{1}	3.0×10^{6}
Ra-226	5.9×10^{-4}	2.5×10^{2}	9.3×10^{2}
Np-237	5.8×10^{-2}	5.0×10^{1}	1.1×10^{3}
U-238	2.3×10^{-2}	4.2×10^{1}	1.1×10^{4}
Pb-210	4.3×10^{0}	3.7×10^{3}	6.3×10^{3}
Po-210	7.0×10^{-3}	3.0×10^{1}	5.6×10^{3}

7.1.4 Interim Acceptance Criteria for the Protection of the Environment from Hazardous Substances

For this category the criteria defined in Section 7.1.2 also apply because the values selected are the lowest values relevant to either human health or the environment.

7.2 Scope

This section presents the scope of work addressed in this chapter.

The scope is developed for consistency with the objectives of the pre-project review. As such, analysis cases are limited to those needed to provide a demonstration of the overall approach and the main analysis needed to reach possible conclusions for the hypothetical site. Items excluded from the scope but which might be included in a licence submission as part of a more comprehensive assessment are discussed in Section 7.2.4.

The scope is defined taking into account the discussion of the Normal Evolution Scenario and the Disruptive Scenarios in Chapter 6 together with experience gained from previous postclosure studies performed for other hypothetical sites and conceptual designs.

Results for all scenarios and their associated sensitivity cases are measured against the interim acceptance criteria for the radiological protection of persons provided in Section 7.1.1.

Results for the Reference Case (see below) of the Normal Evolution Scenario and selected sensitivity cases are also measured against the criteria for the protection of persons from hazardous substances provided in Section 7.1.2, the criteria for the radiological protection of the environment provided in Section 7.1.3, and the criteria for the protection of the environment

from hazardous substances provided in Section 7.1.4. Comparisons are also done for the Disruptive Scenario with the most significant consequences.

7.2.1 Analysis Cases for the Normal Evolution Scenario

The Normal Evolution Scenario is based on a reasonable extrapolation of the site and repository. It accounts for anticipated significant events, in particular glaciation.

Chapter 5 presents information describing why the used fuel containers are expected to remain intact over the time scale of interest. No releases are anticipated for very long times, during which radioactivity in the used fuel decays to levels similar to that of a natural uranium ore body.

However, given the large number of containers, it is possible that some containers could be placed with undetected defects. In particular, a simple estimate of the likelihood of undetected defects arising in the copper shell welding and inspection process (i.e., 1/5000, Maak et al. 2001), indicates that statistically there could be three containers with defects placed in the repository. While these statistics have been conservatively estimated, for the Normal Evolution Scenario it is assumed that three containers with undetected defects are present.

Recognizing that the geosphere characteristics at a candidate site and the design of the repository may be different from the assumed reference conditions, a number of sensitivity cases are also examined to illustrate the function of the various engineered and natural barriers. Both deterministic and probabilistic simulations are performed.

In the deterministic simulations, parameters are varied about a Reference Case of the Normal Evolution Scenario, where the Reference Case has the following attributes:

- Geosphere properties as per Chapter 2;
- Used fuel inventories as per Chapter 3;
- Repository design as per Chapter 4;
- Three containers each with an undetected defect placed in the repository at the position with the shortest groundwater transport time to the well;
- Defect radius = 1 mm, no evolution of the defect size with time;
- No other container failures occur;
- Groundwater fills the defective containers 10,000 years after the containers are placed in the repository (Gobien et al. 2013);
- Constant temperate climate and steady-state groundwater flow;
- Self-sufficient farming family growing crops and raising livestock on the surface above the repository;
- Drinking and irrigation water for the family obtained from a 219 m deep well that penetrates the entire thickness of the Guelph formation located along the main pathway for contaminants released from the defective containers;
- The well is pumping at a rate of 1307 m^3/a. This is sufficient for drinking water and irrigation of household crops;

- A small amount (tens of metres) of surface erosion occurs in the first one million years[2]
- Input parameters that are represented by probability distributions are set to either the most probable value (when there is one) or to the median value otherwise.

The sensitivity cases are shown in Table 7-3 and listed below. The table includes a description of the variation from the Reference Case assumptions for each case together with a brief rationale for the case selection.

The sensitivity cases are:

- Fuel dissolution rate increased by a factor of 10;
- Instant release fractions set to 0.10 for all radionuclides;
- Container defect area increased by a factor of 10;
- No solubility limits in the container;
- No sorption in the Engineered Barrier System (EBS);
- Geosphere hydraulic conductivities increased by a factor of 10;
- Geosphere diffusivities increased by a factor of 10;
- No sorption in the geosphere;
- 100 m surface erosion in the first one million years (Hallet 2011);
- Overpressure in the Shadow Lake formation;
- Hydraulic conductivity of the excavation damaged zones (EDZ) increased by a factor of 10; and
- Low sorption in the geosphere with coincident high solubility limits in the container.

For the probabilistic simulations, random sampling is used to simultaneously vary all input parameters for which probability distribution functions are available. The radionuclide release and transport parameters are varied with the fixed reference geosphere adopted in the system model. This case is also described in Table 7-3.

An assessment based on the results of the regional glaciation modelling studies described in Chapter 2 is used to discuss the anticipated effects of glaciation.

Results are developed for one complementary radiological indicator.

Results are also generated to address the radiological protection of the environment, and the protection of persons and the environment from hazardous substances. A complementary indicator of safety for hazardous substances is also evaluated.

[2] This amount of erosion is neglected in the analysis simulations because of its anticipated negligible effect. A sensitivity case considers the effect of 100 m of surface erosion.

Table 7-3: Sensitivity Cases for the Normal Evolution Scenario

Uncertainty	Reference Case Assumption*	Sensitivity Case Assumption	Rationale
Fuel			
Dissolution Rate	Generated via a model that takes into account the effects of radiolysis and chemical dissolution. No credit for the effect of H_2 gas on suppressing dissolution. With this model, ~22% of the fuel dissolves in the first one million years.	The dissolution rate is increased by a factor of 10. With this increase, all of the fuel dissolves in the first one million years.	The fuel is an important barrier to the release of radionuclides because most radionuclides are contained within the fuel matrix. As the fuel dissolves in the long term these radionuclides become available for transport. The factor of 10 increase roughly corresponds to the 95th percentile value, thereby accounting for uncertainties.
Instant Release Fractions	Most radionuclides have no instant release. Instant release fractions for selected radionuclides are: Cl = 0.06 Cs = 0.04 I = 0.04 Np, Pu, Th, U = 0.00	Instant release fractions for all radionuclides are set to 0.10.	Some radionuclides in the used fuel are present initially in the fuel sheath gap and grain boundaries and are therefore available for release early after contact with water. This fraction of the inventory is referred to as the instant release fraction. Assigning an instant release fraction to all radionuclides (including actinides) ensures the results are bounding.
Container			
Defect Area	Defect Radius = 1.0 mm Defect Area = 3.14 mm^2	The defect area is increased by a factor of 10.	The container is an important barrier to the release of radionuclides. The size of the defect can influence the rate at which radionuclides escape the container and enter the buffer. Since the Reference Case assumes a constant defect size, this case provides information on the sensitivity of results to a larger defect. Defects of greater size (~ 30 mm^2) are unlikely to be missed during inspection.

Uncertainty	Reference Case Assumption*	Sensitivity Case Assumption	Rationale
Solubility Limits	Solubility limits are determined externally from thermodynamic data and specified as input. Solubility limits (mol/m^3) for selected radionuclides are: Np = 1.7×10^{-6} Se = 3.4×10^{-6} Th = 1.4×10^{-4} U = 4.5×10^{-6} Cl, Cs, I = no limit The solubility limits are increased in the Reference Case by a factor of ten above the values listed here to account for uncertainties in groundwater chemistry and thermodynamic data.	Solubility limits for all radionuclides are set to 2000 mol/m^3. This is equivalent to having no solubility limit.	The concentration of a dissolved radionuclide is one of the parameters that affect the rate of radionuclide release from the defective container. While some radionuclides are highly soluble (e.g., I and Cl), others are not (e.g., Pu and U). Removal of all solubility limits provides information on the importance of this parameter to the overall dose consequence.
Buffer, Backfill and Seals (i.e., the Near Field)			
Sorption in the EBS	Use of linear equilibrium sorption model. Sorption coefficients from SKB reviews and Vilks (2011) have been adopted where similar materials and conditions exist. Some elements are non-sorbing (e.g., Cl and I) while others are highly sorbing in the saline reducing environment (e.g., Np, Th, and U). Sorption on iron oxides, from corrosion of the steel inner vessel of the container, is conservatively neglected.	Sorption coefficients for all near field barrier components including the shafts are set to zero. Sorption coefficients in the geosphere are maintained at their Reference Case values.	The clay-based seals have a high surface area and can sorb radionuclides released into the groundwater from the containers. Under saline conditions, ion exchange absorption is not important, but surface complexation sorption is still active. Disregarding sorption provides information on the importance of this process to the overall dose consequence.

Uncertainty	Reference Case Assumption*	Sensitivity Case Assumption	Rationale
Geosphere			
Geosphere Conductivity	Reference Case hydraulic conductivity profile as defined in Chapter 2.	A factor of 10 increase relative to the Reference Case.	Geosphere hydraulic conductivity is an important parameter controlling groundwater flow and advective radionuclide transport in the sedimentary rock formations. The sensitivity case examines the effect of higher hydraulic conductivity on the advective component of radionuclide transport.
Sorption in the Geosphere	Use of linear equilibrium sorption model. Limestone and shale sorption coefficients based on Vilks (2011). Some elements are non-sorbing (e.g., Cl and I) while others are highly sorbing in the saline reducing environment (e.g., Np, Th, and U). Colloid transport is not important under diffusion-dominant and highly saline transport conditions, so it is not included.	The geosphere sorption coefficients for all elements are set to zero. All other near field sorption coefficients (i.e., buffer, backfill and seals) are maintained at their Reference Case values.	Radionuclides can be sorbed onto the surfaces of the host rock minerals, thereby retarding their transport to the surface. Under saline conditions, ion exchange absorption is not important, but surface complexation sorption is still active. Setting the sorption coefficients to zero provides information on the relative importance of sorption in the geosphere.
Geosphere Diffusivity	Reference Case effective diffusion coefficients vary from layer to layer. Anion and neutral species are assumed to have the same diffusion coefficients. This conservatively ignores anion exclusion. Cations are assumed to have an effective diffusion coefficient three times greater than neutral and anions due to surface diffusion.	A factor of 10 increase relative to the Reference Case.	Geosphere diffusivity is an important parameter controlling radionuclide transport in low hydraulic conductivity sedimentary rock formations. The sensitivity case examines the effect of higher diffusion coefficients on radionuclide transport.

Uncertainty	Reference Case Assumption*	Sensitivity Case Assumption	Rationale
Hydraulic Conductivity of EDZ	The excavation damaged zones, which also consider potential thermal damage, are defined with higher hydraulic conductivity than the surrounding rock. Hydraulic Conductivity (K/K_{rock}) for selected areas are: Rooms and drifts: Inner EDZ = 1000; Seal EDZ = 1000; Outer EDZ = 100 Shafts: Inner EDZ = 100; Seal EDZ = 100; Outer EDZ = 10	Hydraulic conductivity of all excavation damaged zones increased by a factor of 10.	The excavation damaged zone is a region of rock damaged during the construction process; potential thermal damage is also taken into account. The EDZ has higher hydraulic conductivity than the surrounding intact rock and could be a pathway for radionuclide transport. EDZ values reflect the likelihood of connected damage paths aligned with bedding planes. There is a possibility of some self-sealing due to shale swelling or salt precipitation. Increasing the hydraulic conductivity provides information on the importance of these damage zones to the transport and subsequent release of radionuclides to the surface.
Erosion	Tens of metres of erosion in the first one million years. This is neglected in the Reference Case due to its anticipated negligible effect.	100 m erosion in the first one million years.	Repeated glaciations over one million years could remove a significant amount of the formations closest to the surface.
Overpressure in the Shadow Lake Formation	No overpressure.	158 m above hydrostatic conditions.	Overpressure in formations below the repository could result in increased advective flow to the surface. This case examines the significance of this effect.
Low Sorption Geosphere with Coincident High Solubility Limits	Geosphere sorption is as described above in the “Sorption in the Geosphere” sensitivity case. Solubility limits are as described above in the Fuel “Solubility Limits” sensitivity case.	“Low” / “High” means the values are set to three sigma values in the conservative direction.	This case determines the effect of simultaneous pessimistic assumptions affecting the solubility and geosphere barrier.

Uncertainty	Reference Case Assumption*	Sensitivity Case Assumption	Rationale
Combined			
Simultaneous Variation of all Probabilistically Defined Parameters	Input parameters represented by probability distributions are set to either the most probable value (when there is one) or to the median value otherwise.	Monte Carlo analysis in which all input parameters represented by probability distributions are simultaneously varied. An important caveat is that these probabilistic simulations are performed in the fixed geosphere of the system model.	Many of the modelling parameters are uncertain or have a natural degree of variability and as such are more generally characterized by a range or distribution of values. Varying all such parameters simultaneously provides information on the overall range or uncertainty in the results.

Note: * A detailed description of the input data is available in Gobien et al. (2013).

7.2.2 Analysis Cases for Disruptive Scenarios

Disruptive Scenarios postulate the occurrence of unlikely events leading to possible penetration of barriers and abnormal loss of containment.

Chapter 6 describes the set of Disruptive Scenarios applicable to the conceptual design and hypothetical geosphere in this study. These have been identified through consideration of the features, events and processes that are important to this repository system, and through consideration of the key barriers. The scenarios are:

- Inadvertent Human Intrusion;
- All Containers Fail. A base case with failure at 60,000 years is considered together with a sensitivity case with failure occurring at 10,000 years;
- Shaft Seal Failure;
- Abandoned Repository;
- Poorly Sealed Borehole;
- Undetected Fault;
- Severe Erosion; and
- Container Failure[1].

The first three scenarios are within the scope of this illustrative safety assessment. Table 7-4 describes each of these three scenarios and includes a description of the parameters changed from the Reference Case and the rationale for the scenario selection. It is recognized that for an actual site, the full set of scenarios would need to be evaluated.

The consequences of gas generation caused by corrosion of steel in the defective containers are assessed for the All Containers Fail scenario because this event produces the greatest amount of gas. This assessment is described in Chapter 8.

With respect to the Undetected Fault Scenario, it is anticipated that any large fractures intercepting the repository not identified during site characterization would be discovered during construction such that appropriate mitigating measures could be taken. These measures could include grouting and possible rerouting of the repository layout to avoid large transmissive features.

The Abandoned Repository scenario considers the consequences if the repository is abandoned and the shafts are not sealed. It implies a near-future loss-of-society.

The Poorly Sealed Borehole scenario is a Disruptive Scenario because it creates a pathway that bypasses the low-permeability geosphere. However, as long as the boreholes are kept sufficiently far from the repository footprint, this scenario is unlikely to be important due to the small size of the borehole and the limits of diffusive transport. It would be analyzed as part of a real site, when the borehole distances are known.

---

[1] This considers delayed but substantive failure of a few containers due to unexpected in-situ conditions, and is different from the Normal Evolution Scenario which considers a small defect initially present in some containers.

The Severe Erosion scenario considers the possibility of high erosion at the repository due to glaciation. The Normal Evolution Scenario evaluated in this report assumes a small amount of net erosion (tens of metres) in the Reference Case, with a sensitivity case examining the effect of 100 m erosion. Whether a case with more erosion should be considered would need to be assessed in the context of a specific site, and would be factored into the selection of repository depth.

Although a detailed analysis of the Container Failure Scenario is outside the scope of this study, the peak dose arising from this event is anticipated to be significantly less than that associated with the All Containers Fail Scenario due to the much reduced number of affected containers.

All scenarios are analysed with deterministic methods only since the basic parameters defining the scenarios are chosen conservatively.

7.2.3 Analyses for Miscellaneous Modelling Parameters

Some additional cases were simulated in the course of the analysis to check various FRAC3DVS-OPG modelling parameters. These cases are discussed in Table 7-5 and listed below:

- Increased spatial resolution to confirm model convergence. This is achieved by comparing contours and mass fluxes between the Site-Scale and Repository-Scale models.
- Increased and decreased number of time steps to confirm that model results are not sensitive to temporal resolution.

As will be discussed in later sections, changes to spatial and temporal resolution have no material effect on the results.

Table 7-4: Analysis Cases for Disruptive Scenarios

Disruptive	Reference Case Assumption*	Disruptive Case Assumption	Rationale
Inadvertent Human Intrusion	Not Applicable	The engineered and natural barriers are bypassed via the drilling of a borehole into the repository. The borehole intersects a used fuel container and used fuel material is brought to the surface. The variant case, in which the borehole thereafter remains open, is not considered.	Institutional controls and knowledge of the repository can be lost in the future. This scenario examines the potential consequences to the drill crew and a future resident on the site for a stylized intrusion event.
All Containers Fail	Three containers each with an undetected defect (radius = 1 mm) are placed in the repository at the location with the shortest groundwater transport time to the well. Groundwater fills the defective containers 10,000 years after the containers are placed in the repository.	*Base Case* All containers fail 60,000 years after repository closure and no containers fail prior to this time. The radionuclide release model takes no credit for the presence of the container. As such, the release of radionuclides from the slowly dissolving fuel to the near field is limited only by the buffer properties. *Extreme Case* Identical to the above, except the time of container failure is 10,000 years.	The containers are anticipated to last for a period in excess of one million years, based on the copper corrosion barrier, sturdy mechanical design and favourable site attributes, including geochemical stability. This scenario considers common cause failure of all containers. The base case considers failure at 60,000 years. This corresponds to the likely timeframe for an ice sheet to cover the site, and it is possible that some unanticipated effect of the ice sheet might cause failure, such as beyond-design mechanical loading or unexpected changes in groundwater chemistry. An extreme case with failure at 10,000 years provides information on the sensitivity of results to the assumed failure time.

Disruptive	Reference Case Assumption*	Disruptive Case Assumption	Rationale
Shaft Seal Failure	The shaft is filled with a combination of bentonite / sand (70:30), concrete and asphalt with the following hydraulic conductivities (m/s): Bentonite / Sand = 1.6×10^{-11} Concrete = 1.0×10^{-10} Asphalt = 1.0×10^{-12}	*Base Case* The hydraulic conductivity of all shaft seal materials is set to 10^{-9} m/s from the time of repository closure. *Extreme Case* The hydraulic conductivity of all shaft seal materials is further increased by an additional factor of 100. A hydraulic conductivity of 10^{-7} m/s is about equivalent to that of fine silt and sand. An important caveat is that the locations of the defective containers and the well are the same as in the Reference Case. In future studies these locations may need to be moved to ensure the most conservative consequence is obtained.	This scenario examines the effects of significant degradation in shaft seal. For conservatism, this degradation is assumed to occur at the time of repository closure.

Note: * A detailed description of the input data is available in Gobien et al. (2013).

Table 7-5: Modelling Parameter Cases

Modelling Parameter	Description	Modelling Case Assumption	Rationale
Spatial Resolution and Time Step Size	User determined in the Reference Case.	Spatial resolution in the FRAC3DVS-OPG model is increased by over 10-fold. Time step control in the FRAC3DVS-OPG model is adjusted to change the number of time steps, with the changes resulting in a factor of 2 decrease in one simulation and a factor of 3 increase in another.	Increasing the spatial resolution and the number of time steps provides information on whether the model results are numerically converged.

7.2.4 Analysis Exclusions

As noted earlier in Section 7.2, the scope of the postclosure safety assessment is defined for consistency with the objectives of the pre-project review. As such, the analysis cases are limited to those needed to provide a demonstration of the overall approach and to those needed to reach preliminary conclusions for the hypothetical site.

This section lists scope items that do not appear in this report but which might otherwise be included in a postclosure safety assessment for a licence submission. These are:

- Fracture Uncertainty. In principle a sedimentary rock site may have features that provide high confidence that there are no significant fractures near the repository. For a real site, there will be some uncertainty regarding the existence (and location) of any such fractures. These uncertainties can be reduced through site selection and repository location and depth, and any residual uncertainties can be handled through the adoption of conservative assumptions and / or Disruptive Scenarios (such as the Undetected Fault Scenario) within the postclosure analysis.

- Variable Climate Analysis. The effects of permafrost and glaciation are not explicitly determined in this assessment. Instead, the results of regional glaciation modelling studies described in Chapter 2 are used to draw inferences about the likely effects of glaciation on the dose assessment for the Normal Evolution Scenario.

- Additional Disruptive Scenarios. As described in Section 7.2.2, a reduced number of Disruptive Scenarios is evaluated here. However, the full list of Disruptive Scenarios anticipated for a licence submission is identified.

- Alternative Critical Groups. Other potential critical groups may be considered for a candidate site depending on communities nearby that could be interested in potential impacts - for example, downstream communities and / or First Nation lifestyles.

7.3 Conceptual Model

This section describes the conceptual model associated with key processes occurring in the repository with defective containers present. The presence of defective containers leads to releases of contaminants that eventually enter the biosphere. These biosphere releases have potential impacts on humans and non-human biota living nearby.

The conceptual model describes the release, migration and fate of contaminants through the identification of key features, events and processes. The model is used to guide the development and application of the computer codes used in the postclosure safety assessment.

Figure 7-1 illustrates the general conceptual model. There are four main elements:

- The used fuel containers;
- The engineered barrier system;
- The geosphere; and
- The biosphere.

Each of these is discussed below. The discussion is aligned with the Reference Case of the Normal Evolution Scenario which, as noted in Section 7.2.1, assumes a constant temperate climate.

For simplicity, the descriptions of conceptual models are given in terms of radionuclides but the models also can be applied to simulate the behaviour of potentially hazardous chemical elements, except that for chemical elements there is no radioactive decay and in the biosphere there is no food chain and no dose rate calculations. Instead, protection of the environment is ascertained by comparison of calculated chemical element concentrations in various biosphere media to the criteria outlined in Table 7-1.

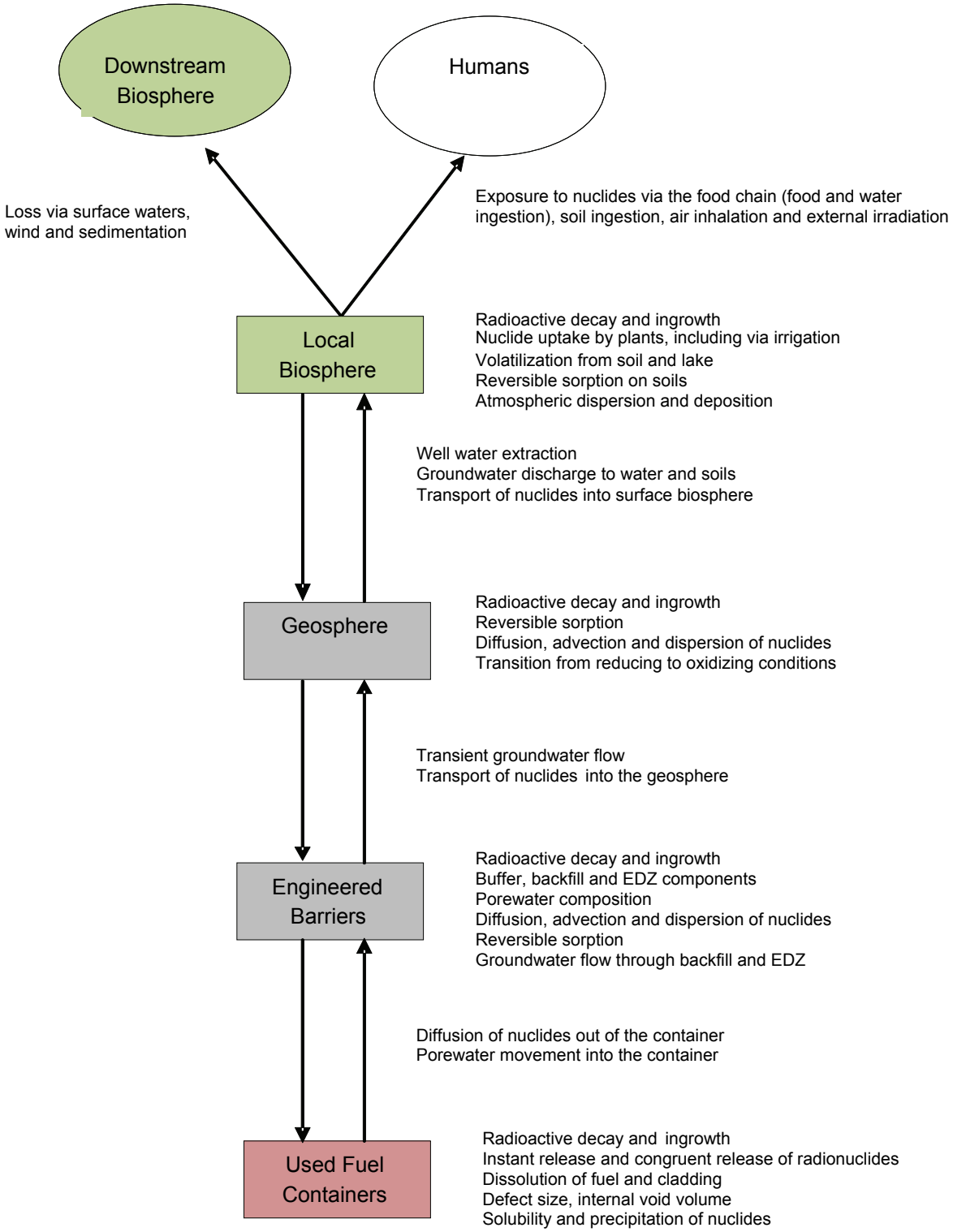

Figure 7-1: General Conceptual Model for Defective Containers

7.3.1 Used Fuel Containers

The principal fuel components and processes for the used fuel containers and waste form are shown in Figure 7-2.

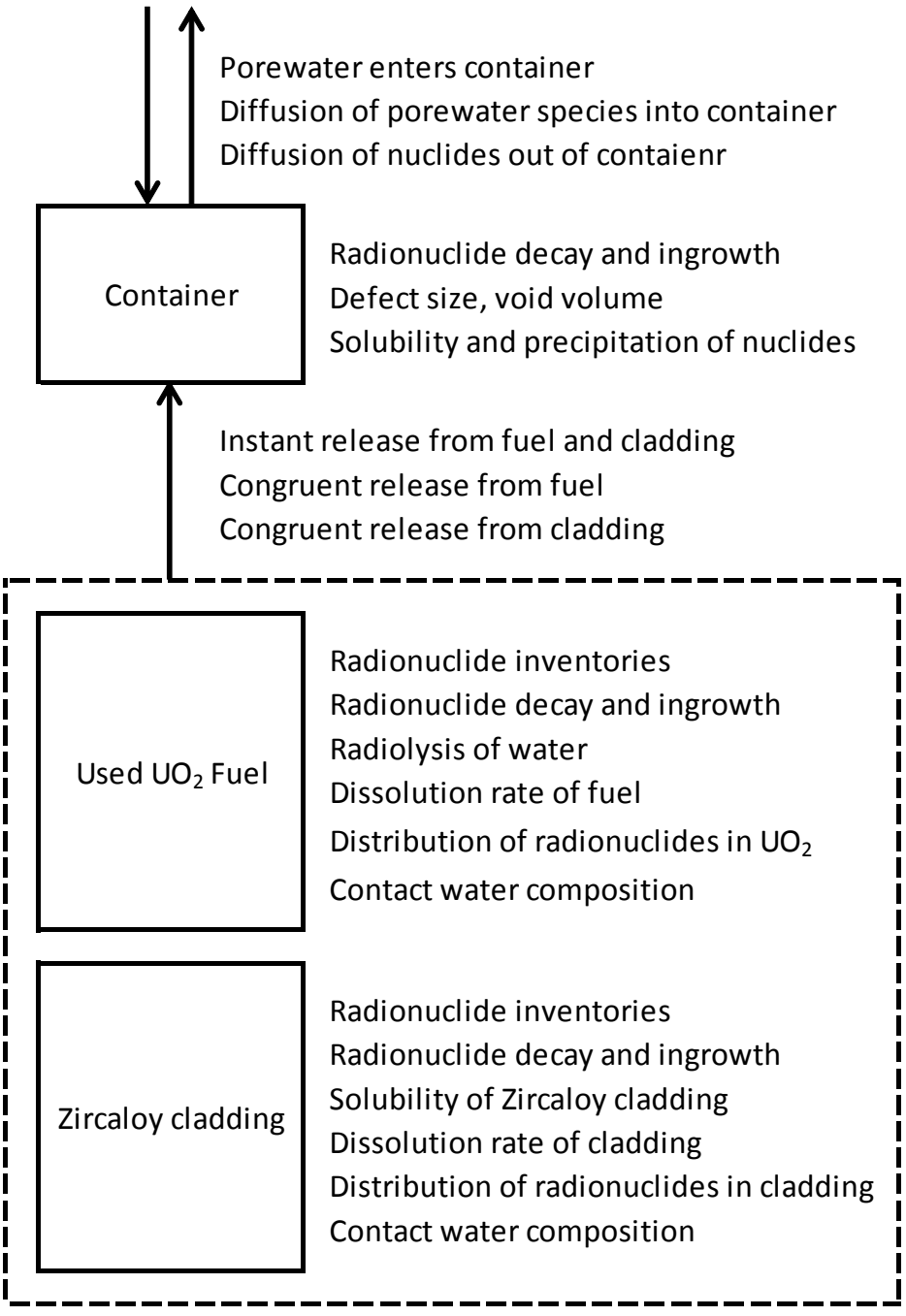

Figure 7-2: Conceptual Model for the Waste Form and Container

The container has a copper outer shell with a steel inner vessel for structural support.

The inner steel vessel is not specifically included in the conceptual model, except that it is assumed present to maintain the void volume inside the container. In practice, the steel components in any breached container would corrode, producing H_2 gas and iron oxides. Although H_2 could substantially reduce the dissolution rate of the UO_2 fuel, this effect is conservatively ignored. Similarly, formation of iron oxides would provide a high surface area for adsorption of some of the radionuclides released from the fuel. These effects are also ignored.

The reference waste form is a standard CANDU 37-element fuel bundle with a burnup of 220 MWh/kgU and an average fuel power during operation of 455 kW as discussed in Chapter 3. The repository holds 4.6 million bundles.

After water enters the container, the Zircaloy cladding could prevent water from contacting the fuel for some time. However, the cladding is neglected in the fuel dissolution model and it is assumed that water contacts all the fuel as soon as the container fills with water.

The temperature at the container surface reaches a peak value of about 120ºC at 10 years after container placement, decreases to about 80ºC at 100 years, decreases slowly to about 70ºC at 10,000 years and reaches ambient conditions at around 100,000 years (Guo 2010). To account for uncertainties in chemical element solubility values at these higher temperatures, reference solubility values are increased by a factor of 10.

The waste form has two distinct components: the UO_2 fuel and the Zircaloy cladding. Releases of radionuclides from these two waste forms are modelled separately.

Radionuclides within the UO_2 fuel are released by two mechanisms which operate on very different time scales (Grambow et al. 2010) as discussed immediately below.

Instant Release from Fuel

Initially, there will be a comparatively rapid release of a small fraction (typically a few percent) of the inventory of a selected group of radionuclides that are either very soluble (such as C-14, Cl-35, Cs-137 and I-129) or gaseous (such as Xe), and that are residing in the fuel sheath gap or at grain boundaries which are quickly accessed by water. This release process is referred to as “instant-release”; and is modelled assuming a certain fraction of the radionuclide inventory in the fuel is released at the time water contacts the fuel.

Ferry et al. (2008) have shown that the instant release fractions do not change with time due to, for example, athermal diffusion of radionuclides induced by alpha-particle recoil displacements.

The instant release fractions used in this assessment are given in Section 7.5.4.1.

Fuel Dissolution

The second and slower release process comprises release of radionuclides from the UO_2 fuel matrix as the matrix itself corrodes or dissolves (called "congruent dissolution").

At the fuel-water interface the alpha dose rate, which exceeds the gamma and beta dose rates for most of the fuel history (Figure 7-3), is the main contributor to radiolysis, producing molecular

oxidants such as H_2O_2. Other potential sources of oxidants, such as any O_2 trapped in the porewater, will already have been consumed by corrosion processes (e.g., corrosion of the Cu shell) before the fuel cladding is breached because these corrosion reactions are relatively fast (King and Kolar 2006). In principle, the radiolytically produced oxidants will also be consumed by reaction with container materials rather than by reaction with used fuel; however, for alpha radiolysis, the oxidants (e.g., H_2O_2) are only produced within 20 μm of the fuel-water interface (Garisto 1989), so they are much closer to the fuel than to the container and thus more likely to react with the fuel.

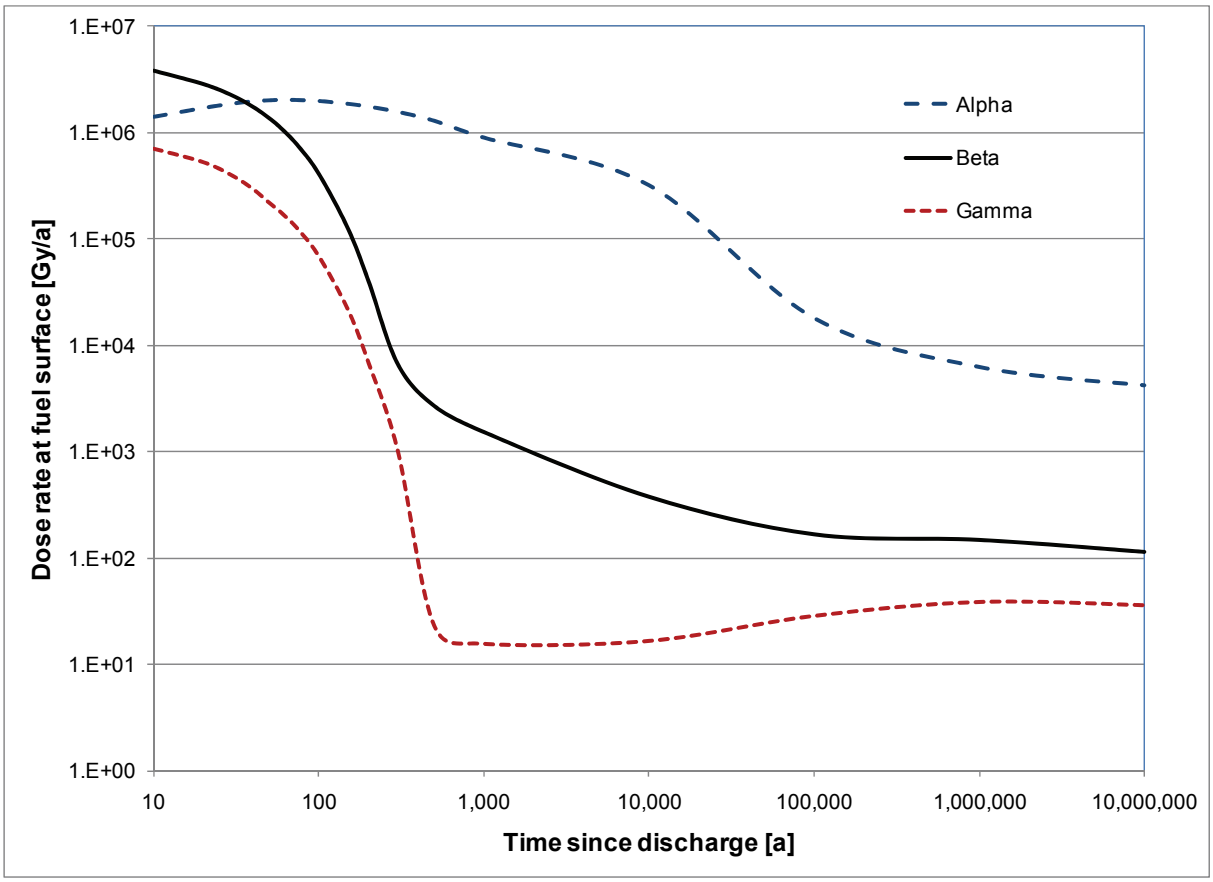

Figure 7-3: Radiation Dose Rate in Water at the Fuel Surface (220 MWh/kgU Burnup)

Oxidative dissolution of the fuel continues as long as the alpha radiation field is sufficiently high. Eventually, after about 10 million years (Gobien et al. 2013), chemical dissolution of the fuel dominates according to the reaction,

$$UO_2 + 2H_2O \rightarrow U(OH)_4 \qquad (7\text{-}1)$$

This is a very slow process, as illustrated by the existence of uranium ore bodies that are millions or billions of years old.

The UO_2 dissolution rate would be affected by build up of hydrogen gas inside the steel vessel generated by anaerobic corrosion of the steel. Experimental evidence shows that the dissolution rate drops by several orders of magnitude in the presence of even modest pressures of hydrogen gas (Shoesmith 2008). This is likely due to the activation of hydrogen by various mechanisms to produce the strongly reducing $H^{\bullet}$ radical, which in turn scavenges radiolytic oxidants and suppresses fuel corrosion (Shoesmith 2008 and references therein). While this hydrogen effect will suppress fuel dissolution, it is conservatively ignored in the current assessment.

The fuel dissolution rate used in this assessment is shown in Section 7.5.4.1.

Radionuclide Releases from Zircaloy

All radionuclides trapped in the Zircaloy cladding, except for C-14, are assumed to be released congruently as the cladding dissolves. The cladding dissolution rate is calculated using a solubility-limited dissolution model, and dissolution continues until the cladding completely dissolves. For C-14, there is evidence that a fraction of the C-14 in the Zircaloy is released as soon as water contacts the cladding (Gobien et al. 2013).

Section 7.5.2 shows that C-14 is not a potentially significant radionuclide for liquid-borne contaminant transport. The dose consequences associated with gaseous transport are described in Chapter 8.

7.3.2 Engineered Barrier System

Chapter 4 provides a detailed description of the conceptual repository and engineered barriers assumed in this study.

The dense 100% bentonite layer that surrounds the container:

1. Prevents groundwater flow near the container;
2. Mechanically supports the container; and
3. In conjunction with the high groundwater salinity, prevents microbial activity that could cause corrosion of the copper shell.

The buffer has a sufficiently low hydraulic conductivity that transport through it is diffusion dominant (i.e., the advective velocity is negligible). In contrast, advection is possible in the access tunnel backfill if sufficient hydraulic gradients are present, as it has a higher hydraulic conductivity.

The excavation damaged zone (or EDZ) extends around the perimeter of excavated spaces and is modelled as a uniform porous medium. Excavation damaged zones along placement rooms, which are narrower, may be less permeable than damage zones along the larger drifts and cross-cuts. As a conservative estimate, the placement room EDZ has been assigned the same hydraulic conductivity as the drift and cross-cut EDZ.

The design includes seals at the entrance of each placement room and seals spaced throughout the access drifts and cross cuts. These seals are composed of concrete and clay bulkheads that interrupt the tunnel and placement room EDZs. An additional smaller EDZ associated with excavation of the seals is also assigned the same hydraulic conductivity as the drifts and cross-cut EDZ. These features are modelled as uniform porous media.

Groundwater contacting the fuel must pass through the buffer. Initially, the composition of this contact water is similar to the buffer porewater composition which depends strongly on the minor mineral components of the buffer (e.g., the calcite and gypsum contents (Muurinen and Lehikoinen 1999, Curti and Wersin 2002)). After some time, these minor mineral components are all dissolved and the contact water composition resembles the geosphere porewater composition.

This time evolution in contact water composition is not explicitly taken into account; rather, two contact water compositions are defined. The first composition is geosphere porewater equilibrated with buffer minerals, and the second composition is geosphere porewater equilibrated with buffer minerals and the steel insert of the container. These compositions are used for the calculation of chemical element solubilities and the highest calculated solubility is used in the safety assessment calculations.

The composition of the groundwater and the diffusion and sorption coefficients for the buffer and backfill material assumed in this assessment are shown in Section 7.5.

7.3.3 Geosphere

Chapter 2 provides a description of the hypothetical geosphere assumed in this study.

The principal components of the conceptual model are shown in Figure 7-4. The geosphere is assumed to be continuous and relatively uniform, lacking the presence of permeable fractures or fault zones. The rock mass is assigned an effective hydraulic conductivity in accordance with properties for the different geological units assumed to be present.

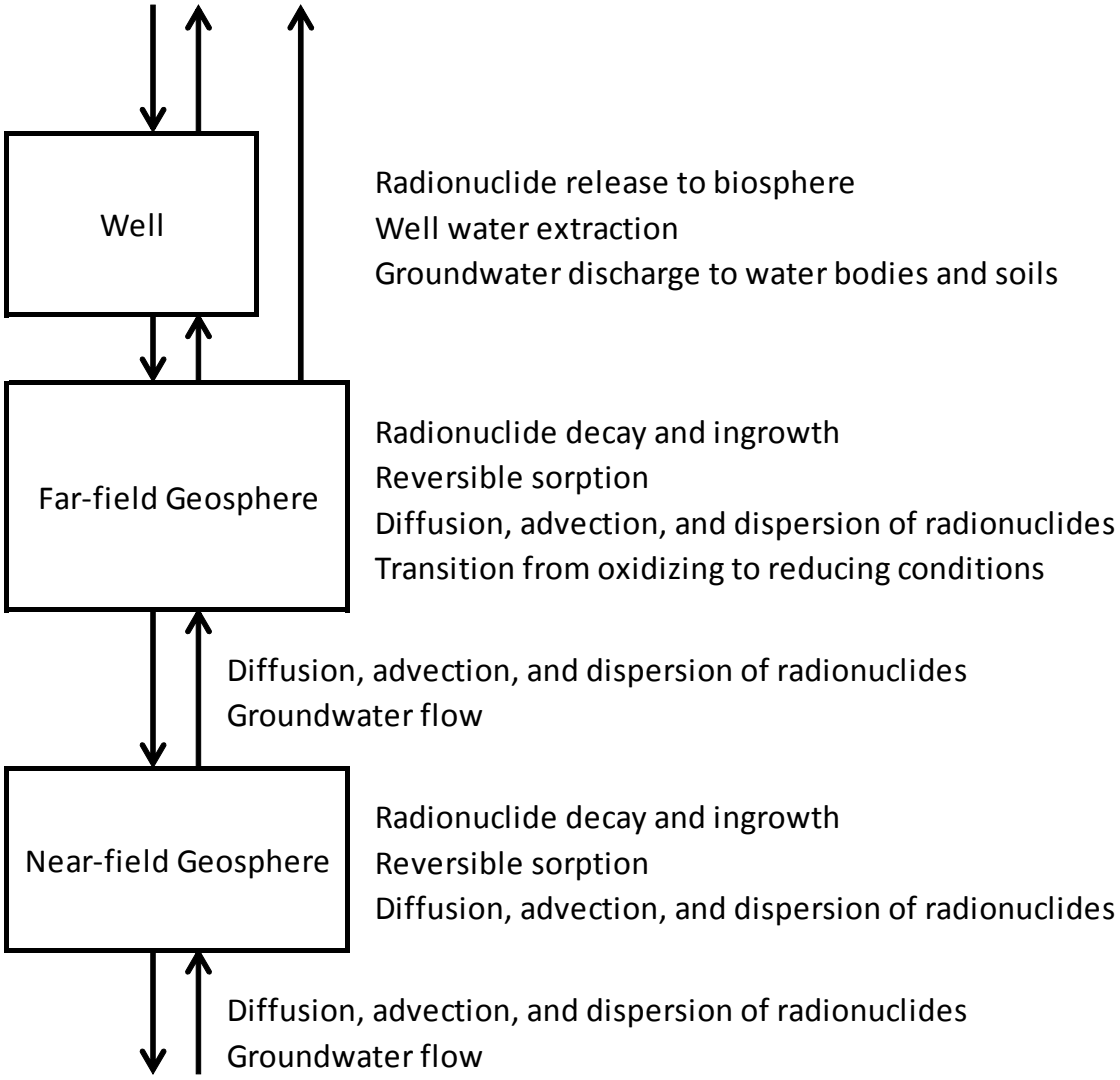

Figure 7-4: Conceptual Model for the Geosphere

Flow boundary conditions are derived from the Regional Model described in Chapter 2. The Regional Model includes the representation of density driven flow to account for the effect on the flow field of highly saline brines at greater depths. Section 7.5.3.1 contains a detailed discussion of how the model boundary conditions are obtained.

The hydrogeological model includes a 219 m deep well spanning the entire 71 m thickness of the Guelph formation, supplying water at the specified reference rate of 1307 m^3/year (i.e., the rate required to meet the needs of the critical group). At this flow rate, the influence of the well on the overall groundwater flow field is small, although the flow field near the well is affected by drawdown. According to the Regional Model (Chapter 2), groundwater in the Guelph formation

is slightly saline, so using a deep well in this formation, rather than the shallower permeable formations, is conservative with respect to contaminant uptake at the well.

In the near-field geosphere (i.e., around the repository), chemically reducing conditions prevail. The temperature in the near field will initially be warmer than in the surrounding geosphere due to radioactive decay, with the maximum temperature reached within about 5,000 years (Guo 2010) and with ambient temperatures returning within about 100,000 years. Generally, the rock mass around the repository would be about 40^{o}C for about 10,000 years. For the contaminant transport times estimated in this study, however, the bulk of the transport occurs under close to ambient conditions. Therefore 25^{o}C values are used for transport parameters.

The physical properties of the rock are described in Chapter 2. The diffusion and sorption coefficients assumed for the rock at repository level are given in Section 7.5.

7.3.4 Biosphere

The main features of the biosphere model are illustrated in Figure 7-5.

The model includes only the local biosphere near the repository, since doses to the critical group living near the repository should be higher than for any individual living further away. In general, radionuclides are lost from the local biosphere by outflow with water, by radioactive decay, by atmospheric dispersion and by leaching into deep soil or sediments.

The local biosphere has the characteristics of a temperate climate region of Southern Ontario. As noted earlier in Section 7.2.4, a constant temperate climate is assumed. While the properties of the biosphere could vary with time due to global warming in the near term, or due to other natural or human-induced changes, the assumption of a constant biosphere provides a convenient and clear measure of the potential impacts, which can be readily related to what is currently acceptable.

In the long term, it is assumed that glaciation will resume with consequent significant effects as a result of the glaciation itself and the related climate change. The anticipated effects of glaciation on the dose assessment for the Normal Evolution Scenario are discussed in Section 7.10.

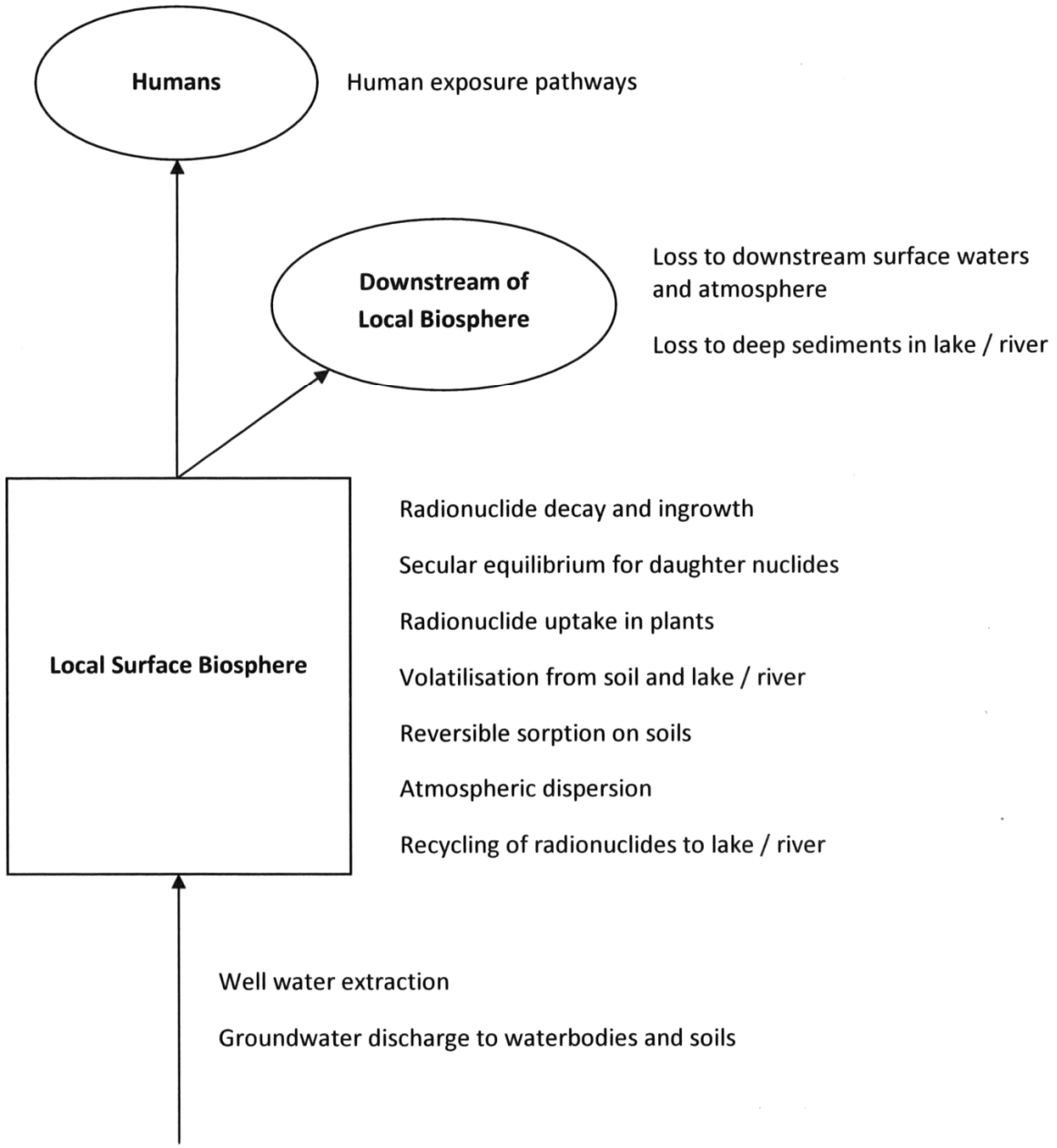

Figure 7-5: Conceptual Model for the Constant Biosphere

Following international practice, the site is assumed occupied by a group of people (i.e., the "critical group") that behaves in a plausible manner but with lifestyle characteristics that maximize their exposure to any radionuclides entering the biosphere. It is assumed that the members of the critical group spend all their lives in the local biosphere and obtain all their food, water, fuel and building materials from the local vicinity.

The characteristics of the critical group will change with climate; however, since a constant temperate climate is assumed, a self-sufficient farming family is selected as the critical group.

This group uses a well that intercepts the contaminant plume from the repository, and grows its own crops and raises animals. Their food includes plants grown in a garden, domesticated animals and fish. This lifestyle is more self-sufficient than current habits and will lead to higher estimates of impacts. Note that future safety assessments may consider additional lifestyles.

Plants growing near the repository can become contaminated directly by atmospheric deposition of radionuclides that reach the biosphere and become volatilized (e.g., I-129) or suspended due to aerosol formation (all nuclides). Plants can also become contaminated due to root absorption of groundwater discharge, irrigation with contaminated surface water (edible crops), and with radionuclides that are deposited to the soil from the atmosphere.

In this site, a deep groundwater well is assumed to intercept the radionuclide plume in the Guelph formation. Radionuclides released from the repository reach the local surface biosphere via the well. Radionuclides not intercepted by the well would be diluted to lower concentrations than in the well by the flow in the aquifer and carried to other locations not represented in the model domain. Section 7.5.3.1 shows that 93.7% of the contaminant plume is captured by the well, so that any dose associated with the remaining aquifer radionuclides would be considerably less than that associated with the well water.

The biosphere model:

- describes the movement of radionuclides through soil, plants and animals, and the atmosphere in the surface environment near the repository;
- calculates the concentrations of radionuclides in water and air in the local habitat of the critical group; and
- calculates radiological dose rates to an individual in the critical group caused by ingestion and inhalation of radionuclides and by external exposure to radiation from radionuclides in the environment (air immersion, water immersion, building materials and groundshine).

A schematic representation of the environmental transfer model is shown in Figure 7-6. The dose model uses the concentration of radionuclides in the various biosphere compartments (well, soil, plants, animals and air) to calculate the annual dose to a member of the critical group.

The internal exposure pathways considered are:

- soil-to-man;
- soil-to-plant-to-man;
- soil-to-plant-to-animal-to-man;
- soil-to-animal-to-man;

- air-to-man;
- air-to-plant-to-man;
- air-to-plant-to-animal-to-man;
- air-to-animal-to-man;

- water-to-man;
- water-to-plant-to-man;
- water-to-animal (including fish)-to-man; and
- water-to-plant-to-animal-to-man.

The external exposure pathways considered are:

- air immersion;
- water immersion (bathing or swimming if a suitable water body is nearby);
- groundshine (exposure to radiation from contaminated soil); and
- building materials (exposure to radiation from building materials).

These exposure pathways are similar to those considered in the guidelines used to calculate derived release limits for normal operation of a nuclear facility (CSA 2008).

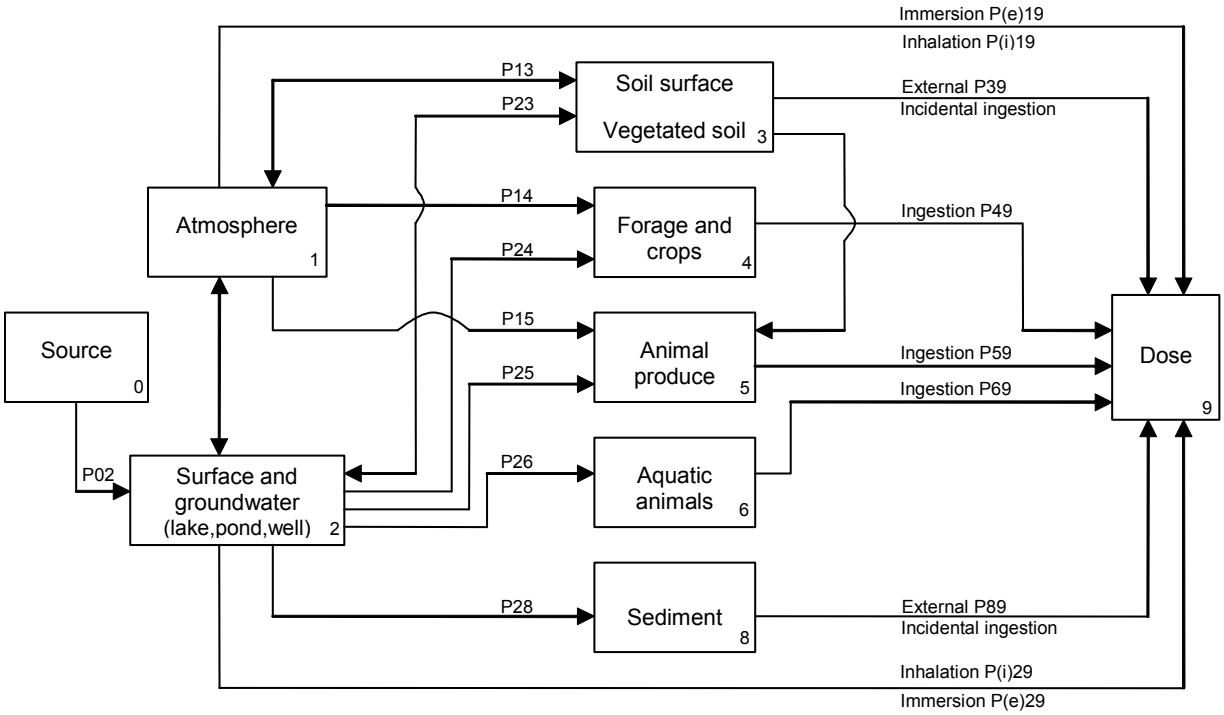

Notes: The nomenclature is from CSA (2008) and the Pij represent transfer parameters from compartment i to compartment j. The biosphere model includes all these environmental transfers and exposure pathways. The building material exposure pathway is not shown here since it is not included in the CSA (2008) dose model.

Figure 7-6: Environmental Transfer Model Showing Critical Group Exposure Pathways

7.4 Computer Codes

The conceptual model for contaminant transport is numerically represented in a suite of computer codes used in postclosure safety assessment modelling.

Figure 7-7 identifies the codes used and their interrelationship. Information from used fuel characteristics, engineering design and site characterization is used to develop site-specific input parameters.

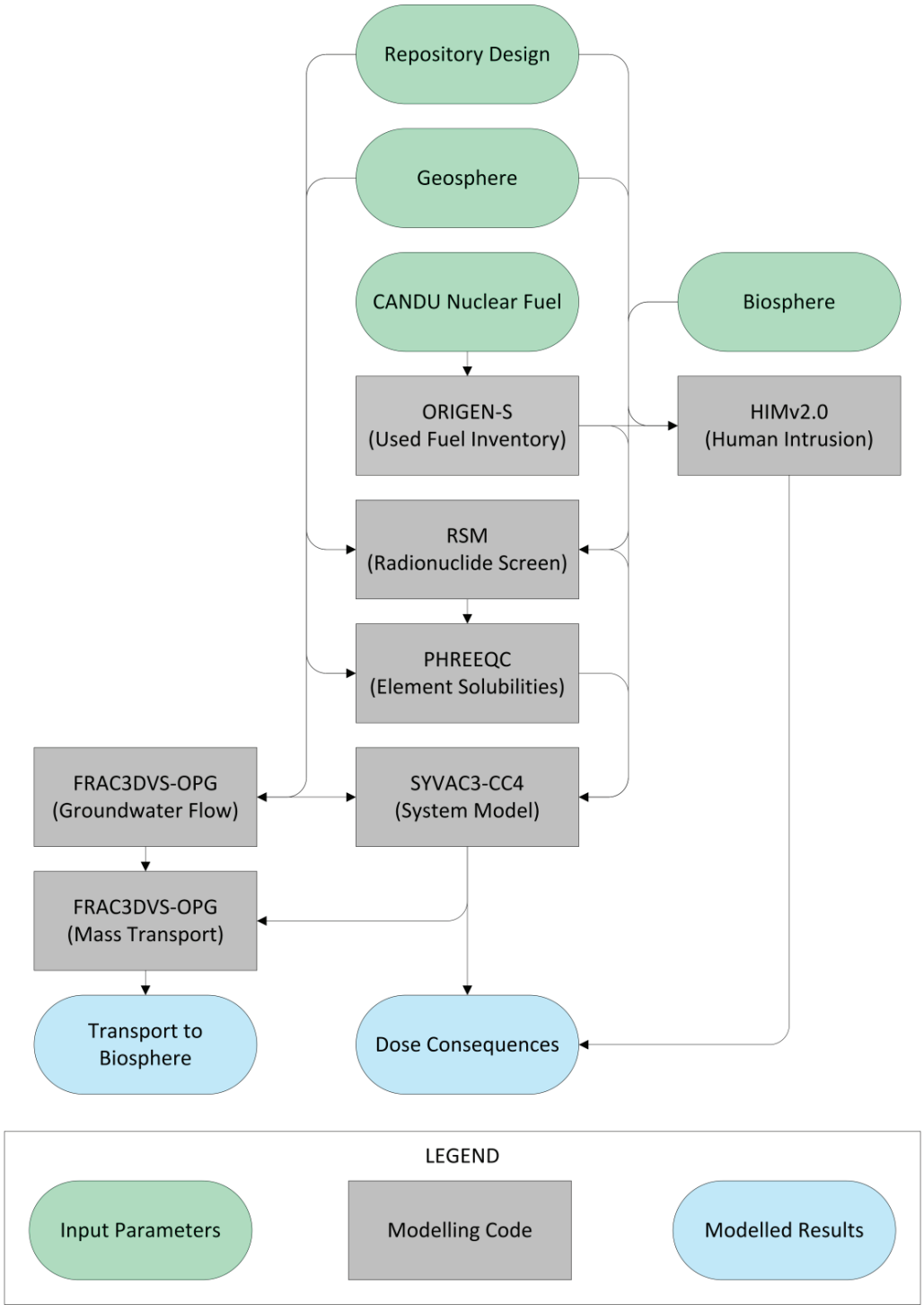

Figure 7-7: Main Computer Codes

ORIGEN-S is a CANDU-industry standard code used to calculate radionuclide inventories in the fuel and Zircaloy cladding at the time of placement, based on a defined reactor exposure scenario (Hermann and Westfall 1995, Tait et al. 1995).

ORIGEN-S was used to derive the used fuel inventories used in this study (see Chapter 3).

PHREEQC is a widely used and tested open source computer program developed by the United States Geological Survey (Parkhurst and Appelo 1999). PHREEQC is based on an ion-association aqueous model and is designed to perform a wide variety of low-temperature aqueous geochemical calculations.

In this assessment, PHREEQC Version 2.17 has been used for solubility and speciation calculations. The ThermoChimie v.7.b thermodynamic dataset was used, as described in Gobien et al. (2013).

RSM (Radionuclide Screening Model) is a project-specific simple model of groundwater transport of radionuclides from container to humans via a well. Through a conservative choice of input parameters, a large input set of radionuclides can be screened so as to objectively identify which are worth analyzing using more detailed models. RSM incorporates data for all radionuclides with half-lives longer than 0.1 years as well as radionuclides with half-lives longer than one day if they have a parent with a half-life longer than 0.1 years.

Table 7-6 provides more information on RSM.

SYVAC3-CC4 is the reference system model for the assessment of radionuclide release, transport, decay, biosphere transfer and dose assessment. It has been developed for a deep geological repository concept based on used fuel placed in durable containers, surrounded by engineered barrier material and located deep underground. The code can perform both deterministic and probabilistic calculations.

Table 7-7 provides more information on SYVAC3-CC4.

FRAC3DVS-OPG is the reference groundwater flow and transport code. This is a commercially available 3D finite-element / finite-difference code (Therrien et al. 2010). FRAC3DVS-OPG supports both equivalent porous medium and dual porosity representations of the geologic media.

Table 7-8 provides more information on FRAC3DVS-OPG.

HIMv2.0 is a project-specific code that assesses the consequences of the Inadvertent Human Intrusion Scenario. The model considers a scenario in which a used fuel container is unknowingly intersected by a drilled borehole, resulting in used fuel being brought directly to surface. Dose consequences are estimated for the drill crew and for a resident subsequently using the contaminated area.

Table 7-9 provides more information on HIMv2.0.

Table 7-6: RSM, Version RSM110

Parameter	Comments
Components:	
SYVAC3	Executive module, Version SV3.10.1
RSM	System model, Version RSM 1.10
Main Documents	*RSM Version 1.1 - Theory* (Goodwin et al. 2001) *RSM Version 1.1 Verification and Validation* (Garisto 2001)
Main Features	- Linear decay chains - Radionuclide release by instant release and by congruent dissolution - UO_2 dissolution calculated from user-supplied time-dependent data - Precipitation in container when user-supplied solubility limits exceeded - Durable containers, some fail with small defects - 1D buffer and backfill layer that surrounds the container and inhibits groundwater flow and radionuclide transport - Repository model based on one room containing failed container(s) - Linear sequence of 1D transport segments that connect the repository to a well. Transport segments are user-supplied; transport is solved considering diffusion, advection/dispersion and sorption - Dose impacts to a self-sufficient human household that uses well water, based on conservative model for drinking, immersion, inhalation and ground exposure. Effect of other ingestion pathways is included through a user-input multiplier - Ability to represent all input parameters with a probability density function (PDF) and to run Monte-Carlo type simulations - Time-independent material properties and biosphere characteristics - Database of all radionuclides with half-lives longer than 0.1 years as well as radionuclides with half-lives longer than one day if they have a parent with a half-life longer than 0.1 years

Table 7-7: SYVAC3-CC4, Version SCC4.09.1

Parameter	Comments
Components:	
SYVAC3	Executive module, Version SV3.12
CC4	System model, Version CC4.09.1
ML3	SYVAC3 math library, Version ML3.03
SLATEC	SLATEC Common Mathematical Library, Version 4.1
Main Documents	*SYVAC3-CC4 Theory Manual (NWMO 2012)* *SYVAC3-CC4 User Manual (Kitson et al. 2012)* *SYVAC3-CC4 Verification and Validation Summary (Garisto and Gobien 2013)*
Main Features	- Linear decay chains - Radionuclide release by instant release and by congruent dissolution - UO_2 dissolution rate calculated using radiation dose-rate based model - Precipitation in container when user-supplied solubility limits exceeded - Durable container, but some fail due to small defects - Cylindrical buffer and backfill layer that surrounds the container and inhibits groundwater flow and radionuclide transport - Multiple sector repository connected to the geosphere at sector-specific nodes chosen considering the local groundwater flow - Geosphere network of 1D transport segments that connect the repository to various surface discharge locations, including a well - Transport considers diffusion, advection / dispersion and sorption - Biosphere model that calculates field soil concentrations, well water concentrations, and uses a surface water body as a final collection point - Dose impacts to a self-sufficient human household that uses water body or well water, locally grown crops and food animals, local building materials and heating fuel - Dose impacts to generic non-human biota - Flow-based models in repository and geosphere, concentration-based models in biosphere - Generally time-independent material properties and characteristics for the biosphere and geosphere model. Transitions from one geosphere (or biosphere) state to another at specific times can be accommodated - Ability to represent all input parameters with a probability density function and to run Monte-Carlo type simulations

Table 7-8: FRAC3DVS-OPG, Version 1.3

Parameter	Comments
Components:	
FRAC3DVS-OPG	Main code, Version 1.3
Main Documents	*A Three-dimensional Numerical Model Describing Subsurface Flow and Solute Transport* (Therrien et al. 2010)
Main Features	- Linear decay chains - 3 D groundwater flow and solute transport in saturated and unsaturated media - Variable density (salinity) fluid - 1D hydromechanical coupling - Equivalent porous medium or dual-continuum model; fractures may be represented as discrete 2D elements - Finite-element and finite-difference numerical solutions - Mixed element types suitable for simulating flow and transport in fractures (2D rectangular or triangular elements) and pumping / injection wells, streams or tile drains (1D line elements) - External flow boundary conditions can include specified rainfall, hydraulic head and flux, infiltration and evapotranspiration, drains, wells, streams and seepage faces - External transport boundary conditions can include specified concentration and mass flux and the dissolution of immiscible substances - Options for adaptive time-stepping and sub-gridding

Table 7-9: HIMv2.0

Parameter	Comments
Components:	
AMBER	Executive Code, Version 5.5
HIMv2.0	Main Model Version
Main Documents	*Human Intrusion Model for the Fourth and Fifth Case Studies: HIMv2.0 (Medri 2012)*
Main Features	- Linear decay chains - Dose consequences by external, inhalation and ingestion pathways to drill crew and site resident - Surface contamination decreases with time due to radioactive decay and soil leaching - Time-independent material properties and biosphere characteristics - Includes data for potentially relevant radionuclides

7.5 Analysis Methods and Key Assumptions

This section describes the analysis approach and the manner in which the FRAC3DVS-OPG and SYVAC3-CC4 models are used in the analysis.

Data for selected parameters are also given to provide context. Gobien et al. (2013) should be consulted if more details are required.

7.5.1 Overall Approach

The general approach for conducting the postclosure safety assessment is as follows:

1. Conduct Radionuclide and Chemical Hazard Screening

Used nuclear fuel initially contains hundreds of radionuclides and chemically hazardous stable elements; however, most are short lived and / or present in very small amounts. Following placement in a deep geological repository, only a small subset poses a potential risk to humans and the environment. The RSM code is used to identify this subset for more detailed assessment.

The methods used for performing the screening analysis are described in Section 7.5.2.

2. Perform 3D Groundwater Flow and Radionuclide Transport Modelling

Detailed 3D steady-state hydrogeological modelling is performed with FRAC3DVS-OPG to determine the groundwater flow field near the repository.

Once the flow field is determined, detailed 3D diffusive and advective radionuclide transport calculations are performed to determine radionuclide transport for I-129, Cs-135, U-234 and U-238. These radionuclides are typically the most important in terms of potential radiological impact or in representing a range of low-sorption to high-sorption species. Radionuclide releases from the defective containers are provided from the SYVAC3-CC4 container release model and imposed as a source term on the FRAC3DVS-OPG mass transport calculation.

Dose consequences cannot be determined because the FRAC3DVS-OPG code does not have biosphere and dose models. Transport results are therefore expressed in units of Bq/a.

Due to the large size of the modelled environment, three different nested models are created. These are:

- Regional Model - described in Chapter 2, this model encompasses a large region with an east-west extent of 152 km, a north-south extent of 179 km, and extending deep into the Precambrian basement rock. This model was used to determine the boundary conditions for the Site-Scale Model, as described in Section 7.5.3.1.

  No repository features are incorporated at this scale of resolution (1 km by 1 km, horizontally).

- Site-Scale Model – the domain includes the repository and a section of the surrounding geosphere. The portion of the regional flow system into which groundwater flow from the repository travels and discharges is not included.

  The model is used to determine the most conservative source location (i.e., the container location with the most rapid contaminant transport to a conservatively located water-supply well). Reference Case and various sensitivity simulations are performed to determine radionuclide transport to the well. The model also supplies boundary conditions to the Repository-Scale Model.

  A simplified representation of the repository and the Engineered Barrier System (EBS) is included at this scale of resolution; however, individual containers are not modelled.

- Repository-Scale Model - the model domain is a small section of the repository surrounding the defective containers and the adjacent geosphere.

  Reference Case and various sensitivity simulations are performed to corroborate results of the Site-Scale Model and to provide a more complete understanding of repository component functions.

  The model incorporates a high level of detail and individual containers are represented at the source location.

Figure 7-8 illustrates the spatial relationships for the Site-Scale and Repository-Scale models.

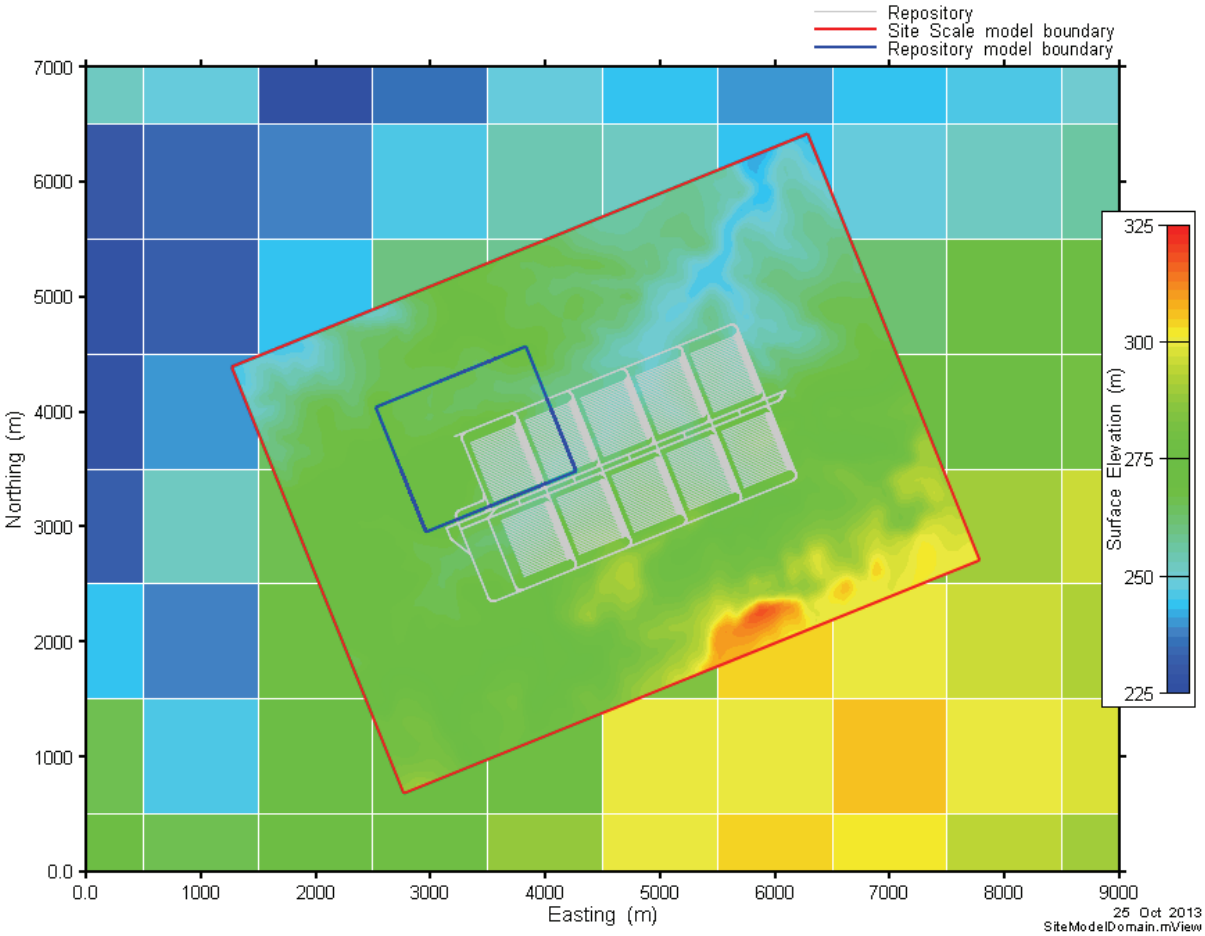

Figure 7-8: FRAC3DVS-OPG Site-Scale and Repository-Scale Model Domains

The nested models are also used to obtain a description of the groundwater flow field for use in subsequent SYVAC3-CC4 system modelling. To provide data for confirming that the resulting SYVAC3-CC4 system model is appropriate for use, radionuclide transport calculations (taking into account both diffusion and advection) for I-129, Cs-135, U-234 and U-238 are performed with FRAC3DVS-OPG. Results are generated for radionuclide transport out of a virtual volume around the placement room containing the defective containers and for transport to the biosphere.

The methods used in this phase of the assessment are described in Section 7.5.3.

3. Perform System Modelling

The 3D groundwater flow field generated with FRAC3DVS-OPG is used to guide development of the geosphere model in the SYVAC3-CC4 system model.

The SYVAC3-CC4 geosphere model is verified by comparing the radionuclide transport results with radionuclide transport results from FRAC3DVS-OPG. These comparisons are performed for I-129, Cs-135, U-234 and U-238, as these represent the key radionuclides for groundwater transport, as well as provide a test of the two models for species that cover a range of sorptions as well as a simple decay chain.

All other aspects of the system model - used fuel, container, near-field and biosphere are defined by the scenario and by input data.

The dose consequences for the Reference Case and for various deterministic sensitivity cases are determined for the full suite of radionuclides of interest.

The SYVAC3-CC4 system model is also used for the probabilistic safety assessment, assuming a fixed geosphere. The radionuclide inventory, release and transport properties are varied about the Reference Case values, as are the characteristics of the biosphere and dose receptor.

The methods used in this phase of the assessment are described in Section 7.5.4.

7.5.2 Radionuclide and Chemical Hazard Screening Model

This section describes how the radionuclide and chemical hazard screening is performed.

Section 7.5.1 shows how this fits into the overall assessment approach. Note that because the Inadvertent Human Intrusion Disruptive Scenario bypasses the geosphere barrier, the screening assessment described here does not apply and a separate case-specific screening assessment is required. This separate assessment is described in Section 7.9.1.

The screening uses the RSM model. RSM closely resembles the SYVAC3-CC4 system model used to perform the primary dose assessment; however, some simplifications are incorporated to ensure conservative results are obtained. The following discusses the RSM model in terms of its key features and whether they differ from those in the SYVAC3-CC4 model.

- Solubility limits, diffusion coefficients, sorption coefficients and decay constants are the same.
- The radionuclide source term is the same.
- The container release model is the same.
- The near field model (representing the engineered barriers) is represented by a simple one dimensional pathway consisting of a 0.63 m thick bentonite buffer. The bentonite properties are identical to those in the SYVAC3-CC4 model.
- The geosphere model is similar in that it is based on a one dimensional diffusion-dispersion-advection transport model; however, unlike the detailed geosphere model in SYVAC3-CC4, only a single fast transport pathway is represented. This pathway is composed of five zones

corresponding to the primary sedimentary layers between the repository and the Guelph aquifer. The incorporated layers are: Cobourg, Georgian Bay, Queenston, Manitoulin, and Cabot Head.

All failed containers share the same transport pathway.

The properties used to represent the five geosphere zones are shown in Table 7-10. These properties are selected to ensure a conservative representation of the transport time to the surface. The model assumes that the advective velocity in the geosphere is zero in all layers due to the extremely low permeability of the various rock types.

Table 7-10: Screening Model Geosphere Zone Properties

Geosphere Zone	Material Type	Length (m)	Diffusion Coefficient in Water (m^2/a)	Porosity (-)	Tortuosity (-)
1	Cobourg	25.4*	0.13	0.015	0.03
2	Georgian Bay	154.3	0.13	0.07	0.014
3	Queenston	77.6	0.13	0.073	0.02
4	Manitoulin	15.6	0.13	0.028	0.006
5	Cabot Head	15.8	0.13	0.116	0.03

Note: * the repository is located in approximately the middle of this layer

- The biosphere model is greatly simplified. Both codes use the same critical group based on a self-sufficient farming family living on the site; however, SYVAC3-CC4 incorporates the biosphere model in Figure 7-6 with explicit modelling of various pathways while RSM has a more limited set of exposure pathways. RSM calculates doses from water ingestion, groundshine, air immersion and air inhalation. The plant ingestion dose rate is estimated

  The following assumptions are also incorporated in the biosphere model to ensure conservative results:

  - The well demand is set to that corresponding to a single person, excluding irrigation. This ensures the minimum amount of dilution.
  - The surface soil is a small irrigated garden large enough to support only a single person. This maximizes the soil concentration.
  - Contaminant concentrations in any surface water present are set equal to those in the well. This maximizes the surface water concentrations.

Prior to running the model, a pre-screening is done. All radionuclides with half-lives longer than 0.1 years as well as radionuclides with half-lives longer than one day if they have a parent with a half-life longer than 0.1 years are included. This results in a total of 251 distinct radionuclides and 96 stable elements remaining in the used fuel and zirconium fuel sheath for further consideration.

The RSM model is then run for the suite of analysis cases shown in Table 7-11, with the cases selected to bound the cases described in Section 7.2 (i.e., the sensitivity cases included in the safety assessment). For each case listed in Table 7-11, the screening assessment conservatively assumes failure of all containers. All RSM cases are run for a 10 million year simulation time.

For the radiological dose assessment, the set of radionuclides that together contribute 0.1% or less of the total peak dose rate are screened out.

For the chemical hazard assessment, all stable chemically hazardous elements whose peak groundwater, surface water or soil concentration exceed 10% of their associated interim acceptance criterion are screened in.

Finally, the results are compared with previous Canadian and international case studies to verify that all important radionuclides and elements are included. Section 7.6 describes the results of the screening assessment.

Table 7-11: Cases Considered for the Radionuclide and Chemically Hazardous Element Screening Assessment

Case	Description
Base Case	The "All Containers Fail Scenario" with all parameter values set to their median values.
No Sorption	The "All Containers Fail Scenario" with sorption coefficients for the geosphere and engineered sealing materials set to zero and all other parameters maintained at their Base Case values.
High Solubility	The "All Containers Fail Scenario" with solubility limits for all species set to an arbitrarily high value of 2000 mol/m^3 and all other parameters maintained at their Base Case values.
High Instant Release Fraction	The "All Containers Fail Scenario" with instant release fractions for all elements set to 10% and all other parameters maintained at their Base Case values.
10x Diffusion Coefficient	The "All Containers Fail Scenario" with all diffusion coefficients in the engineered sealing materials and geosphere increased by a factor of 10 and all other parameters maintained at their Base Case values.

7.5.3 Detailed Flow and Transport Models

This section provides descriptions of the two nested models illustrated in Figure 7-8 and used in the FRAC3DVS-OPG groundwater and radionuclide transport calculations. Section 7.5.1 describes how this fits into the overall assessment approach.

All flow modelling is steady-state. This is consistent with the Reference Case assumption of constant climate. Small changes in climate may affect the shallow groundwater system, but would not affect the deep geosphere. The effects of large changes in climate associated with glacial cycles are discussed separately in Section 7.10.

The reference groundwater composition at repository depth is shown in Table 7-12. The flow modelling assumes a freshwater fluid, and the justification and methodology behind this assumption are discussed near the end of Section 7.5.3.1.

Table 7-12: Groundwater Composition for the Cobourg Formation (Repository Level)

Composition	SR-270 EQ	SR-270 NF
pH	6.3	8.1
Environment	Reducing	Reducing
Eh (mV)	-200	-535
Density (g/L)	1.192	1.192
Solutes (mg/L)		
Na	50,025	48,673
K	12,486	3,482
Ca	32,494	37,285
Mg	8,173	9,940
HCO_3	135	3
SO_4	1,784	1,813
Cl	168,058	168,744
Br	1,698	1,703
Sr	1,198	1,200
Li	5	5
F	1	1
I	3	3
B	80	80
Si	4	10
Fe	30	579
NO_3	10	10
PO_4	-	-
TDS (mg/l)	276,184	273,531

Notes: SR-270 EQ is equilibrated with minerals in the bentonite and SR-270 NF is equilibrated with both the carbon steel insert and bentonite.

TDS – Total Dissolved Solids

From Gobien et al. (2013)

Element solubilities are shown in Table 7-13. These have been calculated for the two groundwater compositions shown above at 25°C, with the higher of the resulting values selected. To account for higher temperatures and uncertainties associated with non-homogeneity in material composition, the solubility values shown in Table 7-13 are increased by a factor of 10 in the safety assessment calculations.

Elements not listed are assigned a solubility of 2000 mol/m^3 to ensure precipitation does not occur.

Table 7-13: Element Solubilities

Element	Value (mol/m^3)	GSD	Distribution Type
C	2.2	3.2	Lognormal
Cu	2.6×10^{-2}	3.2	Lognormal
Np	1.7×10^{-6}	3.2	Lognormal
Pa	3.2×10^{-5}	10	Lognormal
Ra	1.7×10^{-2}	3.2	Lognormal
Se	3.4×10^{-6}	3.2	Lognormal
Sn	9.1×10^{-5}	3.2	Lognormal
Tc	4.4×10^{-6}	3.2	Lognormal
Th	1.4×10^{-4}	3.2	Lognormal
U	4.5×10^{-6}	3.2	Lognormal
Zr	1.8×10^{-5}	3.2	Lognormal
Other	2000	-	Constant

Note: From Gobien et al. (2013)

Data for effective diffusion coefficients, sorption coefficients, and material porosities are shown in Table 7-14 through Table 7-16. These data are described in Gobien et al. (2013). Note that the effective diffusion coefficients are conservative, in some cases exceeding the estimated free-water diffusion coefficient (e.g., dense backfill blocks). Sorption coefficients are taken from data generated using high salinity water.

For creating input files for FRAC3DVS, tortuosity is calculated based on the effective diffusivity and porosity values reported in Table 7-14 and Table 7-16, according to the following formula:

$$\tau = \frac{D_e}{\varphi D_o} \qquad (7\text{-}2)$$

where τ is tortuosity;
D_e is effective diffusion coefficient (m^2/a, Table 7-14);
φ is porosity (Table 7-16); and
D_o is free water diffusion coefficient (m^2/a).

Table 7-14: Data for Effective Diffusion Coefficients, Reference Case Values

Effective Diffusion Coefficients (Vertical) (m^2/a)			
Material	**Neutral and Anionic Species**	**Cationic Species**	**$D_{e.H} : D_{e,V}$**
Drift	3.79×10^{-2}	1.14×10^{-1}	1
Unit G	2.71×10^{-5}	8.14×10^{-5}	2
Unit F	2.59×10^{-4}	7.76×10^{-4}	2
Unit E	2.97×10^{-4}	8.90×10^{-4}	2
Unit B and C	7.26×10^{-4}	2.18×10^{-3}	2
Unit A-2 Carbonate	7.57×10^{-5}	2.27×10^{-4}	2
Unit A-1 Upper Carbonate	4.29×10^{-4}	1.29×10^{-3}	1
Unit A-1 Carbonate	1.14×10^{-5}	3.41×10^{-5}	2
Unit A-1 Evaporite	1.89×10^{-6}	5.68×10^{-6}	2
Unit A0	1.89×10^{-6}	5.68×10^{-6}	2
Guelph	1.83×10^{-3}	5.49×10^{-3}	1
Fossil Hill	2.71×10^{-6}	8.14×10^{-6}	2
Cabot Head	1.96×10^{-4}	5.87×10^{-4}	2
Manitoulin	9.47×10^{-6}	2.84×10^{-5}	2
Queenston	6.31×10^{-5}	1.89×10^{-4}	2
Georgian Bay / Blue Mountain	5.18×10^{-5}	1.55×10^{-4}	2
Cobourg	2.34×10^{-5}	7.01×10^{-5}	2
Sherman Fall	1.39×10^{-5}	4.17×10^{-5}	2
Kirkfield	2.65×10^{-5}	7.95×10^{-5}	2
Cobokonk	1.70×10^{-5}	5.11×10^{-5}	2
GullRiver	1.64×10^{-5}	4.92×10^{-5}	2
Shadow Lake	8.20×10^{-5}	2.46×10^{-4}	2
Placement Room Bentonite (Homogenized Backfill)	1.28×10^{-2}	3.72×10^{-2}	1
Tunnel Seal Bentonite (Compacted Bentonite)	9.47×10^{-3}	1.58×10^{-2}	1
Shaft Bentonite/Sand	9.47×10^{-3}	1.58×10^{-2}	1
Tunnel Dense Backfill	6.31×10^{-2}	1.89×10^{-1}	1
Low Heat High Performance Concrete (LHHPC), degraded	3.94×10^{-3}	1.18×10^{-2}	1
Shaft Asphalt	3.16×10^{-6}	9.47×10^{-6}	1
Shaft Soil Backfill	7.89×10^{-3}	2.37×10^{-2}	1

Note: All elements are either neutral or anions, with the exception of Cs which is treated as a cation.
All material properties are defined for 25°C except for Placement Room Bentonite which is defined for 70°C

Table 7-15: Data for Sorption Coefficients (K_d), Reference Case Values

Sorption Coefficients (m^3/kg)				
Element	**Bentonite**	**Dense Backfill**	**Limestone**	**Shale**
Am	0.23	0.070	0.020	0.23
Cs	4.0×10^{-3}	1.2×10^{-3}	3.6×10^{-4}	0.060
Cu	7.0×10^{-3}	2.1×10^{-3}	2.0×10^{-4}	1.0×10^{-4}
Nb	0.10	0.030	0	0.050
Np	4.3	1.3	2.6	1.2
Pa	0.020	6.0×10^{-3}	0.014	0.014
Pb	1.0×10^{-3}	3.0×10^{-4}	0	0.030
Pu	0.50	0.15	0.020	0.20
Th	40	12	2.6	1.2
U	40	12	2.6	1.2
Zr	0.050	0.015	0	0.010
Other	0	0	0	0

Note: To be conservative, sorption coefficients for concrete and asphalt are assumed to be zero.
Data are from Gobien et al. (2013)

Table 7-16: Data for Material Porosity

Material	Porosity (-)
Drift	0.200
Unit G	0.172
Unit F	0.100
Unit E	0.100
Unit B and C	0.165
Unit A-2 Carbonate	0.120
Unit A-1 Upper Carbonate	0.070
Unit A-1 Carbonate	0.019
Unit A-1 Evaporite	0.007
Unit A0	0.032
Guelph	0.057
Fossil Hill	0.031
Cabot Head	0.116
Manitoulin	0.028
Queenston	0.073
Georgian Bay / Blue Mountain	0.070
Cobourg	0.015
Sherman Fall	0.016
Kirkfield	0.021
Cobokonk	0.009
GullRiver	0.022
Shadow Lake	0.097
Tunnel Seal Bentonite (Compacted Bentonite)	0.481
Placement Room Bentonite (Homogenized Backfill)	0.413
Shaft Bentonite/Sand	0.411
Tunnel Dense Backfill	0.194
Concrete (LHHPC), degraded	0.100
Shaft Asphalt	0.020
Shaft Soil Backfill	0.200

7.5.3.1 Site-Scale Model

The Site-Scale Model is used to investigate the mass flows to the well and surface environment for I-129, Cs-135, U-234 and U-238 released from failed containers in the repository. The source containers are placed in the location with the shortest transport time and the maximum I-129 mass transport to the well. The model supplies boundary conditions for use in the Repository-Scale Model, and examines sensitivity cases investigating the effect on transport of the EDZ hydraulic conductivity, geosphere hydraulic conductivity and overpressure in the Shadow Lake formation. Spatial and temporal convergence testing is also done with this model.

The model domain is specified as the repository footprint together with approximately 1200 m of surrounding geosphere that encompasses the repository influenced flow domain. A new coordinate system is established, with the new system rotated 158 degrees counter-clockwise, so that the X axis follows the middle of Access Drift 1. This allows natural finite-difference discretization of the generally orthogonal repository features.

Figure 7-9 shows the coordinate system and model boundaries.

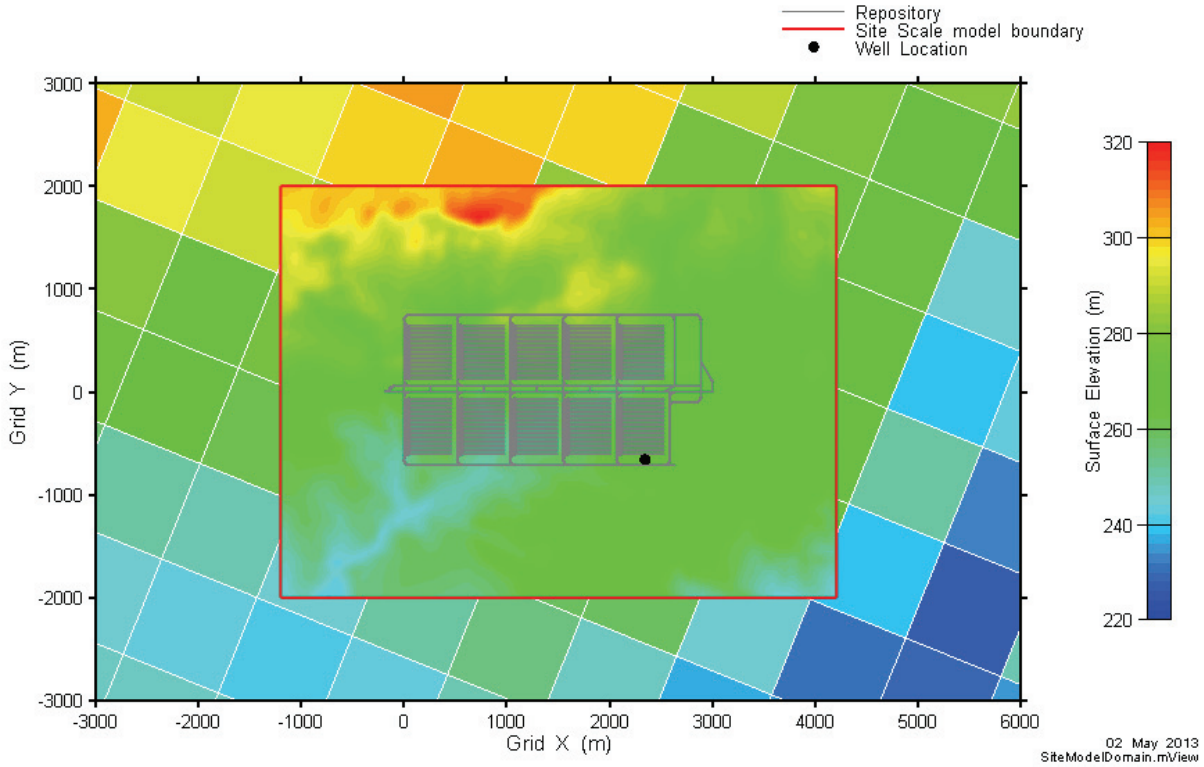

Figure 7-9: Site-Scale Model - Coordinate System and Domain Boundary

Domain Discretization

The repository is about 500 m below ground surface (mBGS). Since the surface elevation varies slightly across the repository, the horizontal depths are also defined in terms of an

absolute measure of metres above sea level (mASL). The floor of the hypothetical repository is located at an average elevation of -237 mASL.

Unlike the Regional Model (see Chapter 2), which is discretized with constant 1000 m by 1000 m square elements, the Site-Scale Model uses variable element sizes in X, Y, and Z directions to incorporate repository related features with good geometric fidelity. The maximum element area is 50 × 50 m in the corners of the grid. The smallest XY dimension is 1.25 × 1.5 m, and is used to incorporate the shaft excavation damaged zone and tunnel seal features. This results in grid layers containing 148,635 elements.

Vertical discretization is driven by the requirement to incorporate geosphere and repository features as well as shaft sealing materials. Eighty layers are incorporated, yielding a total of 11.7 million elements. Figure 7-10 presents elemental volumes. Individual element edges are not shown due to the density of the elements.

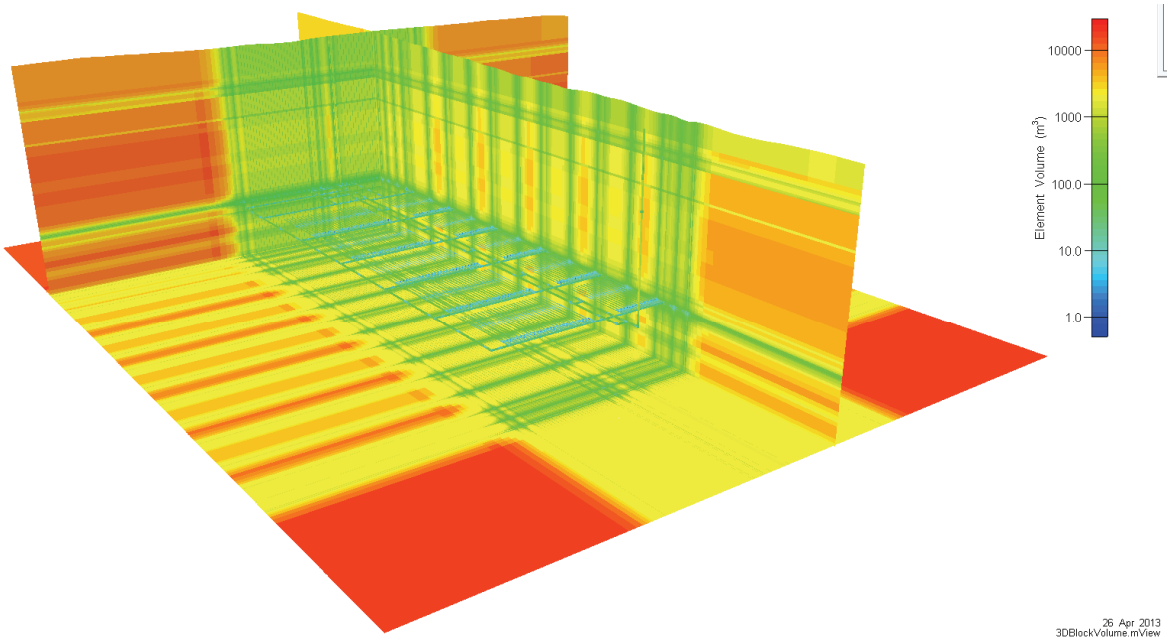

Figure 7-10: Site-Scale Model Element Volume

Hydraulic Conductivity Profile

The bulk rock properties are described as a layered system dipping towards the southwest. Hydraulic conductivity is generally lower in the deeper formations, as discussed in Chapter 2. Hydraulic conductivities and model discretization are shown in Table 7-17. Reference Case values are used in all simulations except for the sensitivity study that examines the effect of a factor of 10 increase in geosphere hydraulic conductivity.

Table 7-17: Geosphere Hydraulic Conductivity and Layering

Formation	Average Thickness (m)	Hydraulic Conductivity (m/s)*			Model Layers
		Reference Case (K_h)	Sensitivity Case	Anisotropy K_h:K_v	
Drift	40.64	1.0×10^{-7}	1.0×10^{-6}	2	5
Unit F	60.30	5.0×10^{-14}	5.0×10^{-13}	10	6 shared
Unit E		2.0×10^{-13}	2.0×10^{-12}	10	
Unit B and C		4.0×10^{-13}	4.0×10^{-12}	10	
Unit A-2 Carbonate	15.39	3.0×10^{-10}	3.0×10^{-9}	10	3
Unit A-1 Upper Carbonate	3.11	2.0×10^{-7}	2.0×10^{-6}	1	1
Unit A-1 Carbonate	22.12	9.0×10^{-12}	9.0×10^{-11}	10	4
Unit A-1 Evaporite	4.19	3.0×10^{-13}	3.0×10^{-12}	10	1
Guelph	71.57	3.0×10^{-8}	3.0×10^{-7}	1	5
Fossil Hill	6.86	5.0×10^{-12}	5.0×10^{-11}	10	1
Cabot Head	15.82	9.0×10^{-14}	9.0×10^{-13}	10	1
Manitoulin	15.53	9.0×10^{-14}	9.0×10^{-13}	10	1
Queenston	77.52	2.0×10^{-14}	2.0×10^{-13}	10	4
Georgian Bay and Blue Mountain	154.40	4.0×10^{-14}	4.0×10^{-13}	13	10
Cobourg	46.32	2.0×10^{-14}	2.0×10^{-13}	10	23
Sherman Fall	47.34	1.0×10^{-14}	1.0×10^{-13}	10	6
Kirkfield	39.53	8.0×10^{-15}	8.0×10^{-14}	10	3
Cobokonk	7.97	4.0×10^{-12}	4.0×10^{-11}	1000	1
Gull River	53.39	7.0×10^{-13}	7.0×10^{-12}	1000	4
Shadow Lake	7.58	1.0×10^{-9}	1.0×10^{-8}	1000	1

Notes: * Sensitivity Case examines the effect of a factor of 10 increase in geosphere hydraulic conductivity. Section 7.2.1 and Table 7-3 provide further explanation. Data are from Gobien et al. (2013).

Properties of the engineered barrier system are shown in Table 7-18. Within the repository, excavation damaged zone (EDZ) properties are derived from the properties of the Cobourg limestone host rock. All repository tunnels have an inner EDZ with hydraulic conductivity 1000 times higher than the host rock horizontal hydraulic conductivity, and porosity twice that of the host rock. Outer EDZ is assigned hydraulic conductivities 100 times greater than the host rock, while porosity is set equal to the host rock.

An inner and outer EDZ were defined for the shafts as well, with inner EDZ having hydraulic conductivity 100 times greater than the vertical hydraulic conductivity and outer EDZ conductivity increased by a factor of 10 relative to the host rock vertical conductivity. Inner EDZ porosity is doubled compared to the host rock.

All other EDZ parameters are set equal to those of the host rock.

There are minor simplifications in the implementation; in particular, the inner and outer EDZ is specified only on the tops and bottoms of the access tunnels and placement rooms. However, the EDZ hydraulic conductivity is increased to match the transmissivity of the reference EDZ cross section to account for the missing EDZs at the sides of tunnels. Similarly, porosity of the EDZ is corrected to achieve the same effective cross sectional area for flow, and thus match flow velocities along the EDZ given the same hydraulic gradient. The scaling factors used depend on the type of tunnel (i.e., access, perimeter or placement) but values are on the order of two.

More details on the definition of EDZ properties can be found in Gobien et al. (2013).

Table 7-18: Engineered Barrier Hydraulic Conductivity

Property Identifier	Description	Hydraulic Conductivity (m/s)		
		Reference Case	Shaft Seal Failure* (Base Case)	Shaft Seal Failure* (Extreme Case)
Tunnel Dense Backfill	Used to backfill repository tunnels	1.0×10^{-10}	1.0×10^{-10}	1.0×10^{-10}
Tunnel Seal Bentonite (Compacted Bentonite)	Used for room seals	8.2×10^{-13}	8.2×10^{-13}	8.2×10^{-13}
Placement Room Bentonite (Homogenized Backfill)	100% bentonite, homogenized mixture of gap fill and compacted pedestals in placement rooms	5.3×10^{-12}	5.3×10^{-12}	5.3×10^{-12}
Concrete (LHHPC), degraded	LHHPC concrete used for room closure and shaft bulkheads	1.0×10^{-10}	1.0×10^{-9} (degradation of all shaft-seal materials)	1.0×10^{-7} (further degradation of all shaft-seal materials to the equivalent of fine silt or sand)
Shaft Bentonite/Sand	Primary Shaft Seal material, 70:30 bentonite to sand	1.6×10^{-11}		
Shaft Soil Backfill	Well compacted soil backfill	1.0×10^{-8}		
Shaft Asphalt	Additional shaft sealing material	1.0×10^{-12}		

Note: * See Table 7-4 for a description of these cases. Data are from Gobien et al. (2013)

Figure 7-11 shows the vertical hydraulic conductivity profile on a cross-section through the Site-Scale Model. The figure shows properties of the repository along Access Drift 1, and two of the three shafts (Vent and Service shaft).

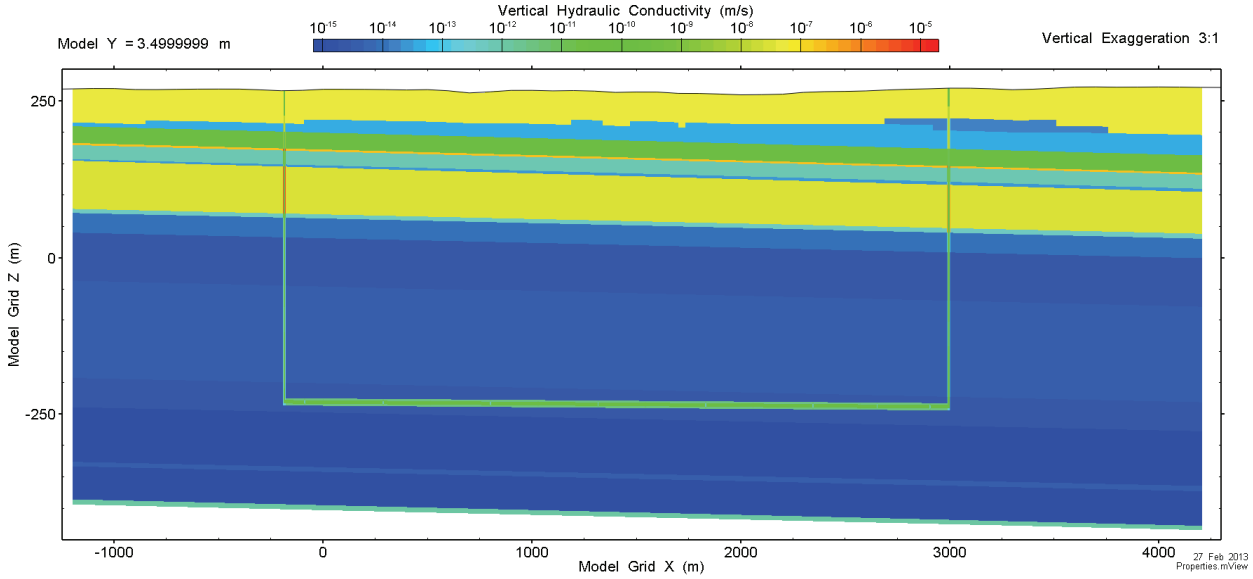

Figure 7-11: Site-Scale Model - Vertical Hydraulic Conductivity Profile

Transport properties include dispersivity, diffusivity, and sorption. Longitudinal dispersivity is set to 50 m for all materials, approximately 10% of the plume travel path length to discharge at the well, with transverse dispersivity specified as 5 m. Diffusivity and sorption values in the Site-Scale Model are shown in Table 7-14 and Table 7-15.

Figure 7-12 shows property assignments on a vertical cross-section through the entire domain while Figure 7-13 and Figure 7-14 illustrate property assignments on vertical cross-sections through a placement room seal and the main shaft. Figure 7-15 shows a plan section through part of the repository, showing a number of placement rooms, access tunnels, and associated seals, along with their material property assignments. The curved entrances to the rooms are simplified and represented as right-angle intersections.

Figure 7-16 shows a three-dimensional illustration of the property distribution, showing layered geology and the representation of the repository and shafts within the model.

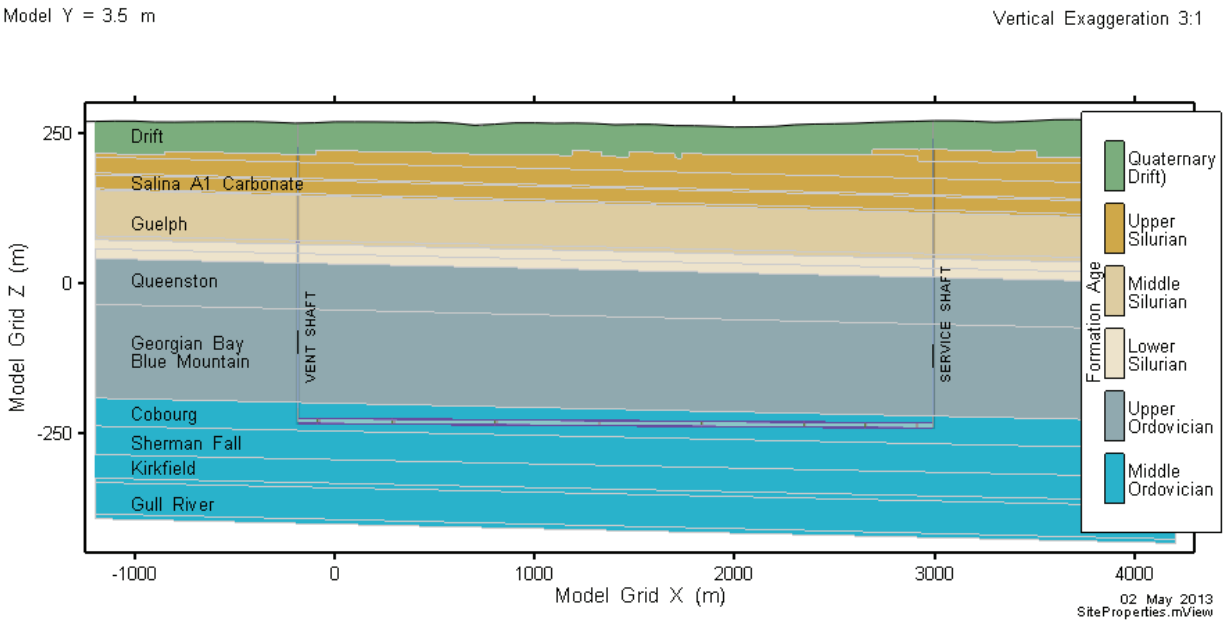

Figure 7-12: Site-Scale Model - Property Assignment on Vertical Cross-Section through Entire Model Domain

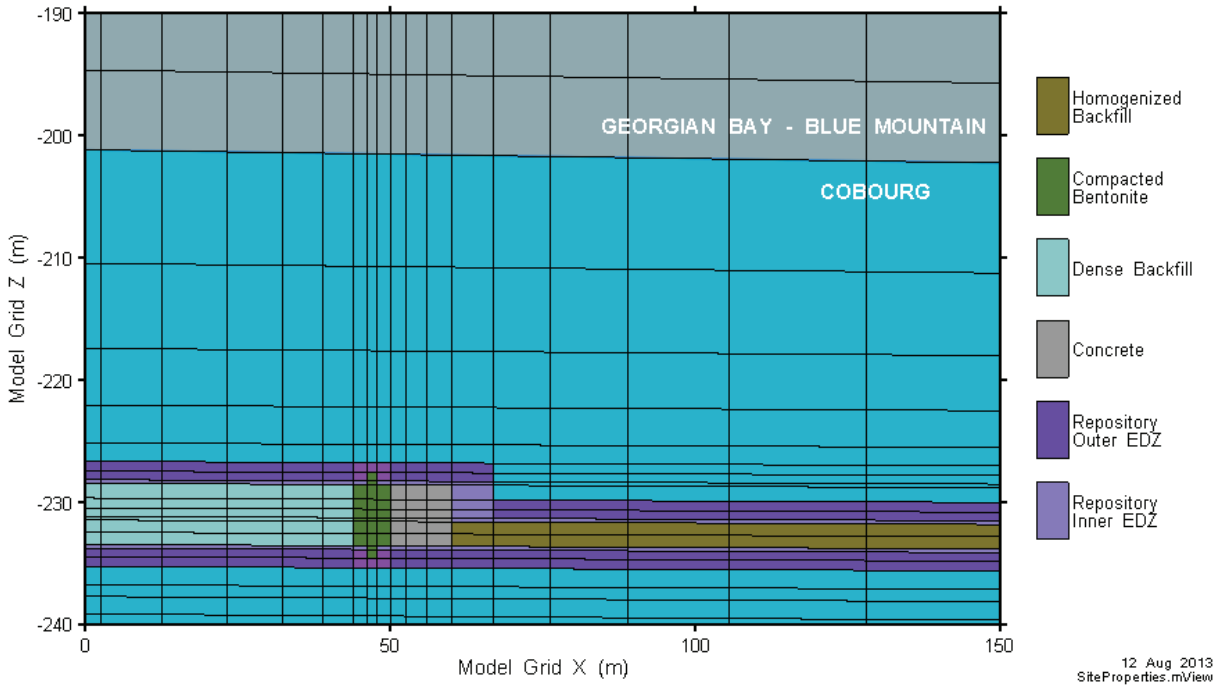

Note: 2:1 Vertical Exaggeration. The pink material around the seal is a combination of tunnel Seal Inner EDZ and outer EDZ

Figure 7-13: Site-Scale Model - Property Assignment on Vertical Cross-Section through Placement Room Seal

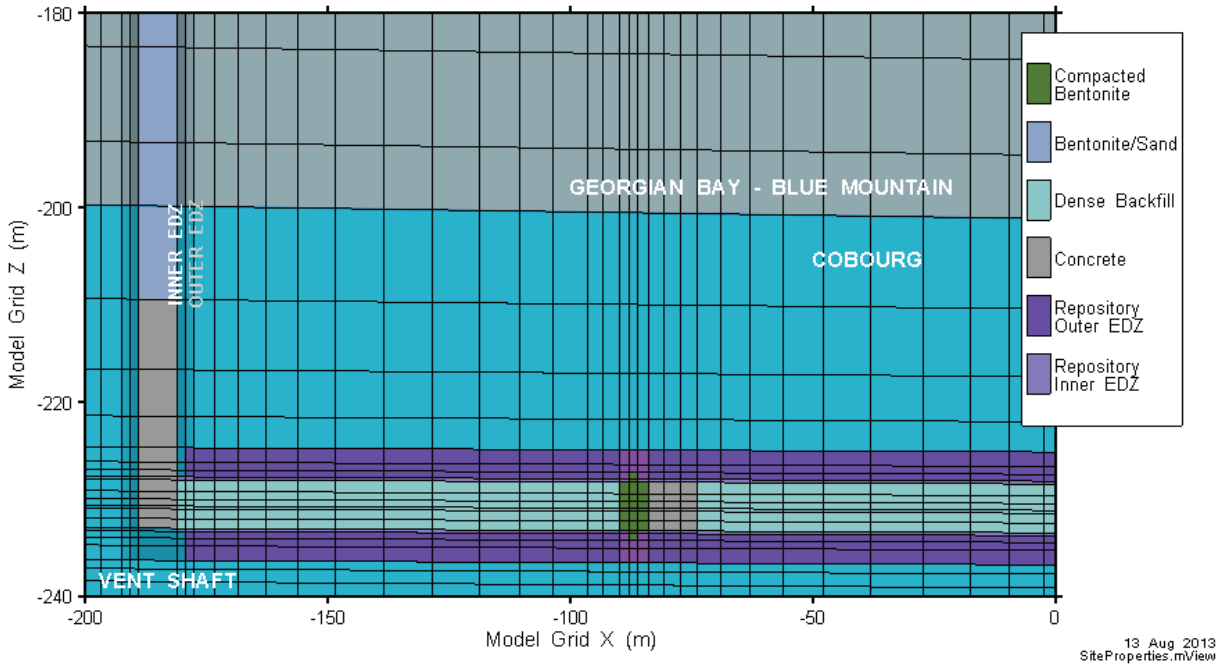

Note: 2:1 Vertical Exaggeration. The pink material around the seal is a combination of tunnel Seal Inner EDZ and outer EDZ

Figure 7-14: Site-Scale Model - Property Assignment on Vertical Cross-Section through Base of Vent Shaft

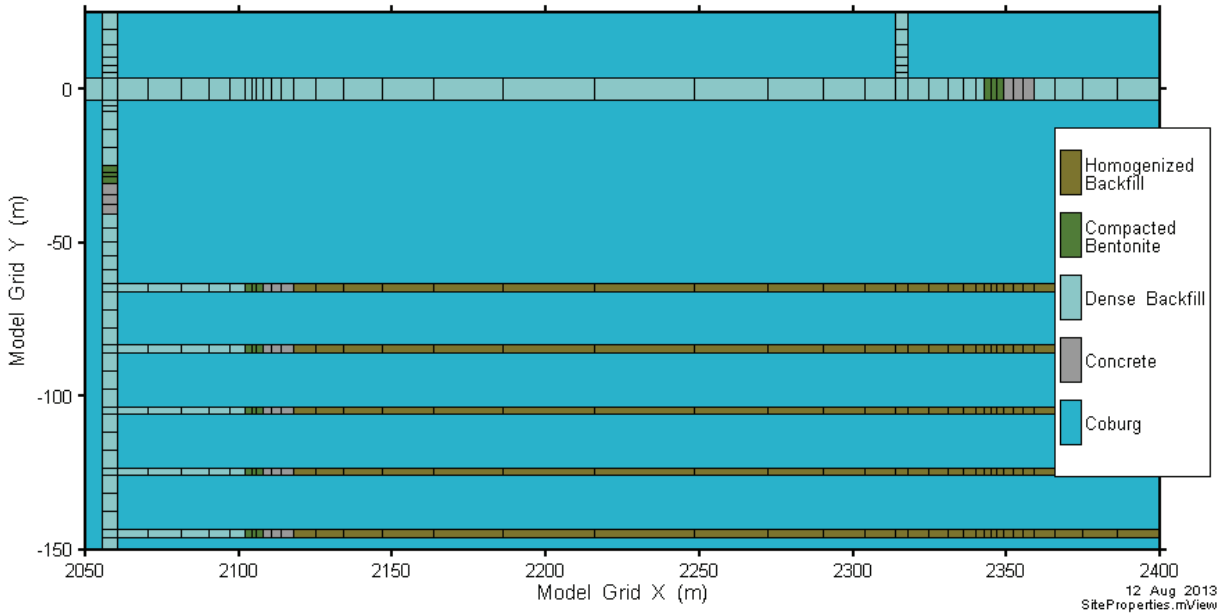

Figure 7-15: Site-Scale Model - Property Assignment on Plan View through Placement Rooms

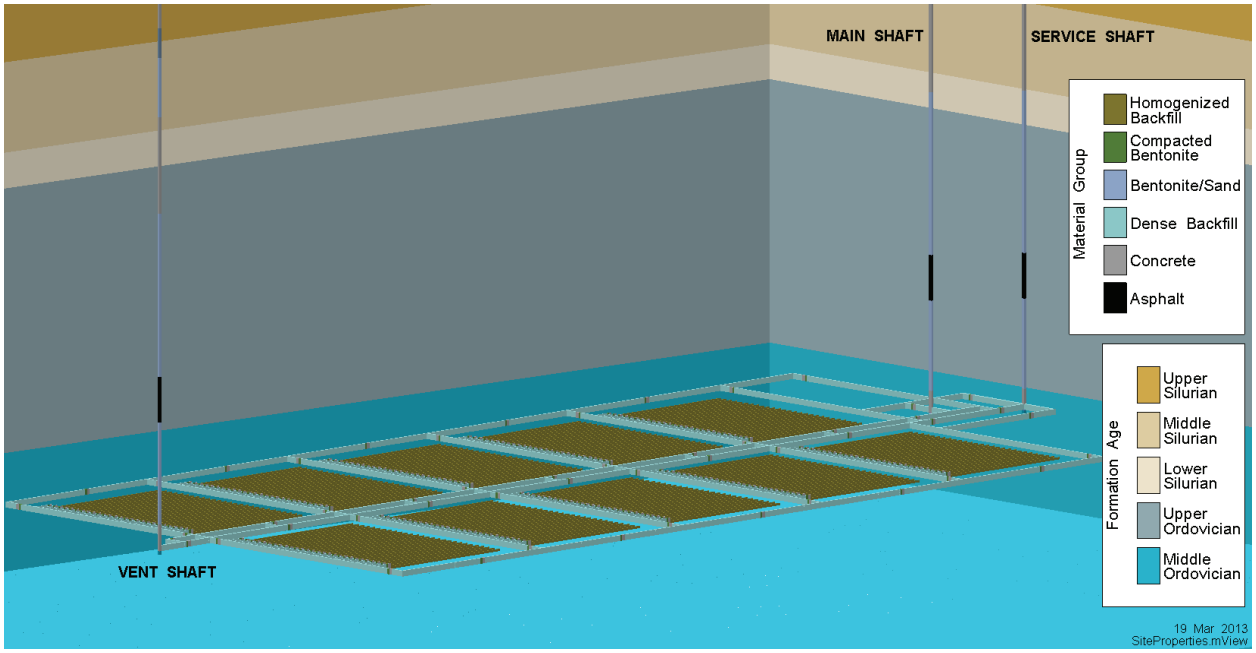

Figure 7-16: Site-Scale Model - Property Assignment in 3D View

Water Supply Well and Defective Containers

The water supply well is located based on results from simulations performed using the Reference Case hydraulic conductivities. The goal is to choose the most conservative location, largely based on the maximum rate of contaminant uptake at the well. At this hypothetical site, the very low hydraulic conductivities in the geosphere create a diffusion-dominated transport regime. In such a system, particle tracking does not provide useful information to locate the shortest transport pathway with the greatest mass transport rate. An alternative approach is to release a tracer from all locations across the repository footprint and examine the results to determine whether there are any variations in concentration at the base of the Guelph aquifer (i.e., the water supply aquifer for the well). The I-129 container release term was used as the tracer, and a release from all containers in the repository was simulated. The model was run without a pumping well.

Figure 7-17 shows the results of this simulation at ten million years. The repository floor is at an average elevation of approximately -237 mASL. The grey contours show the plume in the Fossil Hill formation, at an average depth of 55 mASL. This formation is directly below the Guelph formation, where the transport is still diffusion-dominated. The blue contours show the plume in the lowest layer of the Guelph (average elevation 66 mASL). Here, advection is the dominant transport process and the I-129 plume is swept down-gradient. Finally, the colours on the plot indicate the distance between the base of the Guelph and the top of the placement room outer EDZ, essentially the thickness of the diffusive barrier separating the repository from the Guelph aquifer. It is evident that where this barrier is thinnest, transport is fastest and the

concentrations in the plume, both in the Fossil Hill (diffusive) and Guelph (advective) portions of the plume, are highest.

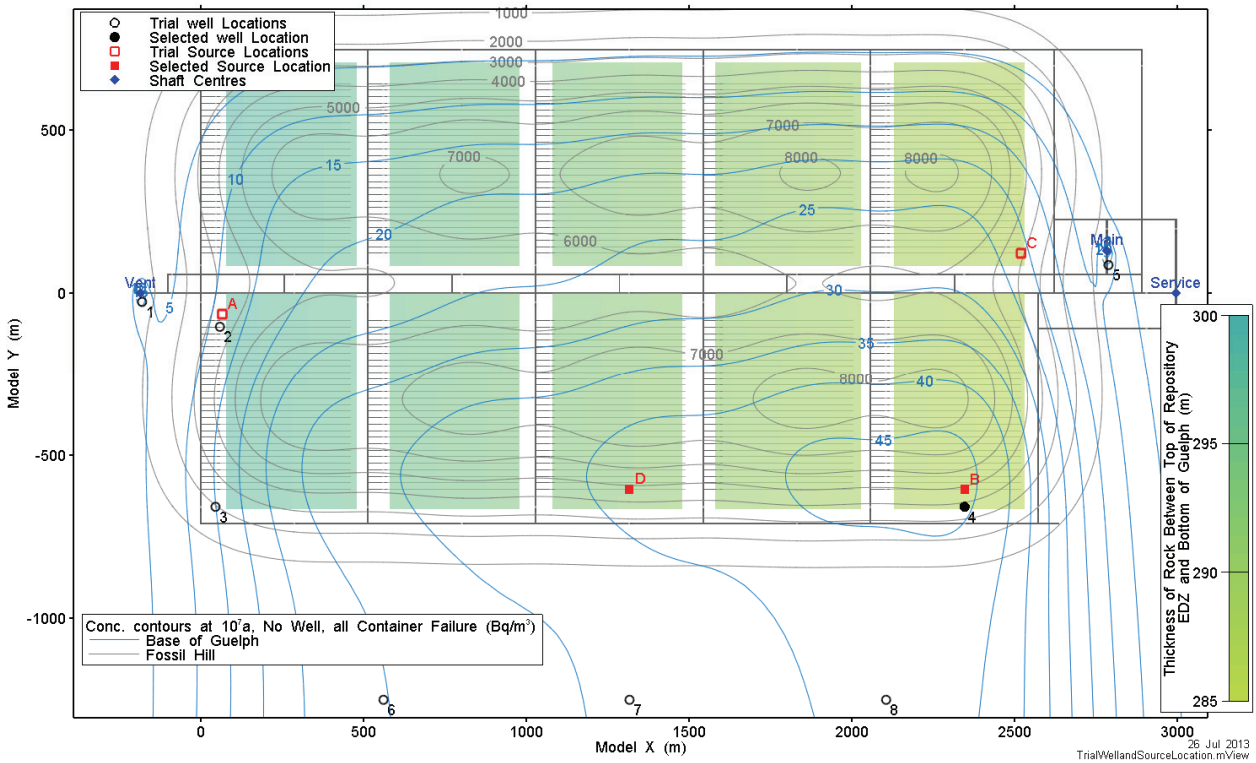

Figure 7-17: Site-Scale Model - Selecting Well Location

To discount the possibility that other factors, such as the more permeable shafts and EDZ, could outweigh the effect of the diffusive barrier thickness, a number of different well locations and source locations were also assessed. This was done in two stages. First, the model was run with releases from all containers with the well locations varied as shown in Table 7-19. Wells were placed in three downstream locations (Wells 6, 7, and 8 in Figure 7-17), and at the location of highest concentration at the base of the Guelph formation (Well 4 in Figure 7-17).

Table 7-19: Source and Well Locations, Release from All Containers

Well Location*	Description
4	Well near plume centre
6	Well downstream of repository footprint, closer to vent shaft side
7	Well downstream of repository footprint, closer to center
8	Well downstream of repository footprint, closer to main shaft side

Note: * For well locations refer to Figure 7-17

Maximum radionuclide concentration is relatively insensitive to the location of the well, as shown in Figure 7-18. Well 7 has a slightly higher maximum radionuclide transport rate, largely due to its higher plume capture rate.

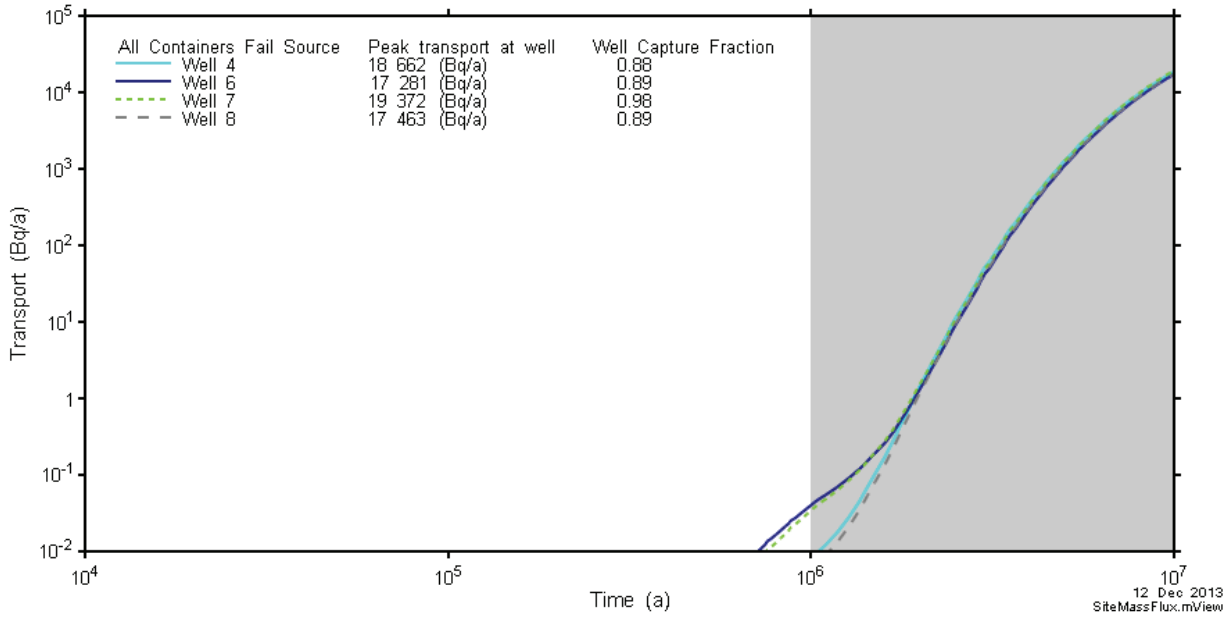

Figure 7-18: Site-Scale Model - Radionuclide Transport, Release from All Containers

To examine the possible influence of the shafts as a more rapid pathway for transport, the source term for three failed containers was used. The source release points and well locations were placed in various combinations in close proximity to the shafts in the location where the diffusive barrier is thinnest and in the location closest to Well 7, as shown in Figure 7-17 and described in Table 7-20.

Figure 7-19 shows that while there is relatively little variation in maximum transport rate, the combination of Source B and Well 4 yielded the maximum rate, while the second highest rate is for Source C and Well 5. This shows that the thickness of the diffusive barrier is the most important factor determining maximum contaminant transport to the well.

Table 7-20: Source and Well Locations, Release from Three Containers

Source Location*	Well Location*	Description
A	1	Source near the vent shaft, well directly adjacent to vent shaft.
A	2	Source near the vent shaft, well above the source.
A	3	Source near vent shaft, well downstream of source (in the Guelph).
B	4	Source near all container failure plume centre (see Figure 7-17), well above the source.
C	5	Source near the main shaft, well directly adjacent to the main shaft.
D	7	Source near centre of repository, well downstream of source.

Note: * For source and well locations refer to Figure 7-17

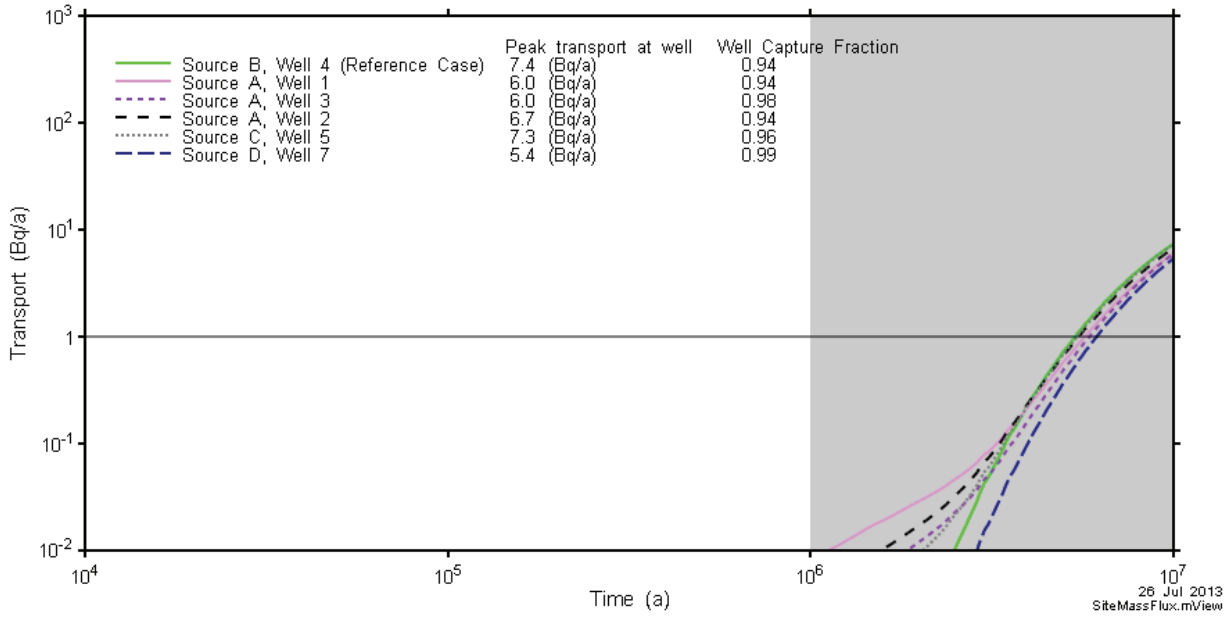

Figure 7-19: Site-Scale Model - Radionuclide Transport to Different Well Locations, Release from Three Containers

The relative homogeneity of the layered geology means that the rate of solute transport to the well is not very sensitive to the exact location of the source and well, although the two should be located relatively near each other on a horizontal projection to maximize well capture. Accordingly, the Reference Case water supply well was placed above the region where the diffusive barrier is thinnest, and the source term is placed in the centre of the nearest placement room (Source B and Well 4).

The well is represented as a 2D line element forming a segment, or edge, of a 3D element. Properties appropriate to a nominal 4” diameter well are assigned to the segment to specify the

hydraulic conductivity of the well. The lowest node on the segment is defined as the withdrawal node from which water is abstracted. The well location is shown on a cross sectional view in Figure 7-20.

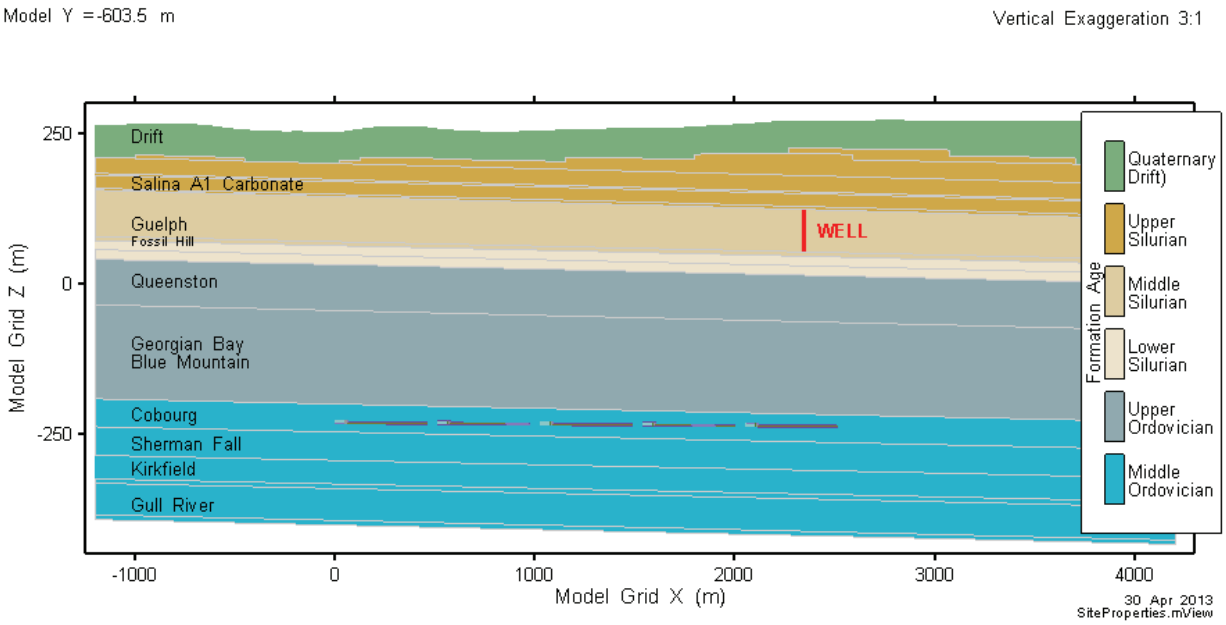

Figure 7-20: Site Scale Model – Well Location on Cross-Section

Hydraulic Head Boundary Conditions

Head boundary conditions for the Site-Scale Model were extracted from the head field calculated with the Regional Model described in Chapter 2. Boundary conditions remain unchanged for each well demand case, and are based on a flow field in which no pumping well is present. Head values for the Reference Case along the vertical model boundaries are shown in Figure 7-21.

Surface boundary conditions follow the surface topography and bottom boundary conditions (1500 mBGS) are set to zero flow; these are not illustrated in the figure.

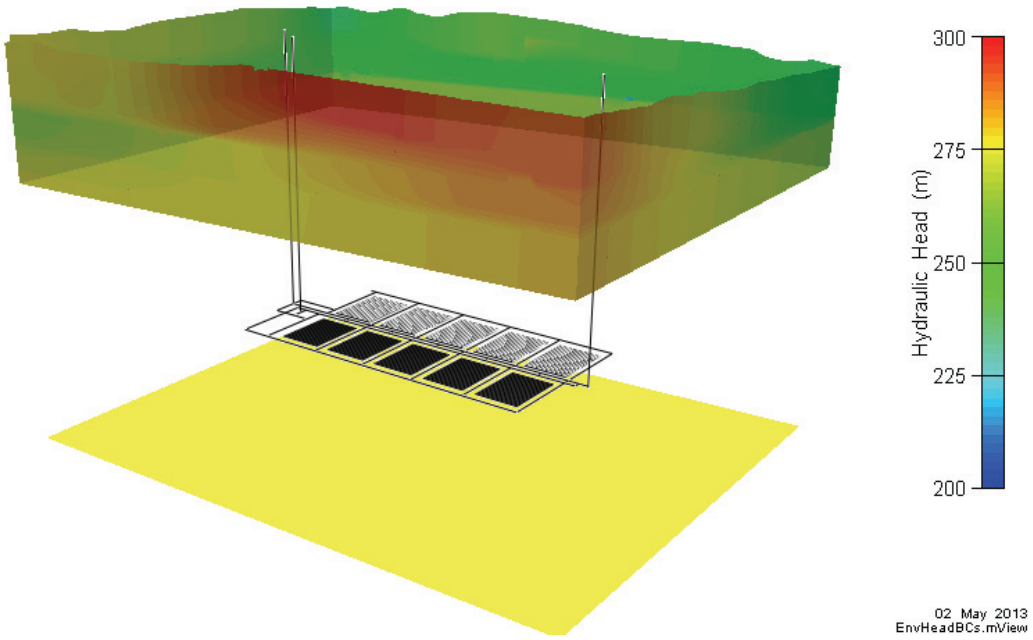

Note: Sides are no-flow boundaries

Figure 7-21: Site-Scale Model - Reference Case Head Boundaries, Sides and Bottom.

The hydraulic head was set by assuming constant head boundary conditions at the surface, with the water table following the surface topography. As the digital elevation model for the Site-Scale Model is more accurate than the coarser Regional Model, this leads to some differences between the heads in the two models.

For the vertical boundaries between the base of the unconsolidated drift and the base of the relatively permeable Guelph unit, constant head boundaries were set by interpolating heads directly from the Regional Model. In the permeable units (Guelph and above), the Regional Model predicts that the pore water is largely fresh within the Site-Scale Model domain, with a moderate increase in salinity down-dip in the Guelph. As a result, within the Site-Scale Model there is a good correspondence between flow directions and freshwater head in the Guelph without accounting for the slightly saline water in the deeper parts of the Guelph unit (see Figure 7-35 and Figure 7-36.

In the very low permeablility units below the Guelph, vertical boundaries were set as no-flow boundaries. This is a reasonable approximation of the Regional Scale Model, as within these units velocities are extremely low, and the flow direction is predominantly vertical.

Due to the low permeability of the Ordovician host rock and the resulting very low flow velocity (see Chapter 2, Figure 2-13), transport through these limestone and shale formations is

diffusion-dominated. For the lower boundary condition, the concept of environmental head was used to estimate a freshwater head that would provide a similar vertical driving force for flow in a steady-state freshwater model to the brine head derived from the density-driven Regional Model. A freshwater head of 275 m was found to approximate the brine head in the upper Precambrian predicted by the Regional Model at the one million year pseudo-equilibrium state. A scenario with a constant head boundary of 433 m was also run, and showed that due to the low permeability of the Ordovician host rock, the transport results are largely insensitive to the specified head at this boundary.

In summary, representative boundary conditions for the Site-Scale Model were achieved as follows:

- In the permeable (and largely fresh) units (Guelph and above), freshwater heads were extracted from the regional model and surface elevations are used to set constant head (Dirichlet) boundaries.
- In the units below the Guelph, no-flow (Neumann) boundaries were applied at the Site-Scale Model vertical boundaries, neglecting any horizontal flows across this boundary. This is reasonable given the very low permeability of these units and the predominantly vertical nature of the flow field.
- For the lower boundary, a constant head (Dirichlet) boundary was specified to approximate the regional model pseudo-equilibrium state and provide a similar vertical driving force.

7.5.3.2 Repository-Scale Model

This model encompasses a small section of the repository surrounding the source location and the adjacent geosphere. The model incorporates significant detail and individual containers are represented. The model is used to corroborate results of the Site-Scale Model, to provide radionuclide transport results for comparison with results of the SYVAC3-CC4 system model, and to provide a more complete understanding of repository component functions.

Radionuclide transport calculations are performed for I-129, Cs-135, U-234 and U-238. These radionuclides are typically the most important in terms of potential radiological impact or in representing a range of low-sorption to high-sorption species.

Domain Discretization and Property Assignment

The model is discretized over a domain of approximately 1410 m × 1170 m × 560 m in the X, Y, and Z directions, respectively. The domain incorporates a small number of placement rooms and a section of the perimeter access tunnel near the well. The model extends from the Shadow Lake formation to the top of the Guelph formation, and includes the water supply well. The model discretization is 239 nodes in the X direction, 702 nodes in the Y direction, and 105 node layers in the Z direction, for a total of 17.35 million elements.

The extent of the model is shown in Figure 7-22. Material properties are the same as those listed in Table 7-17 and Table 7-18.

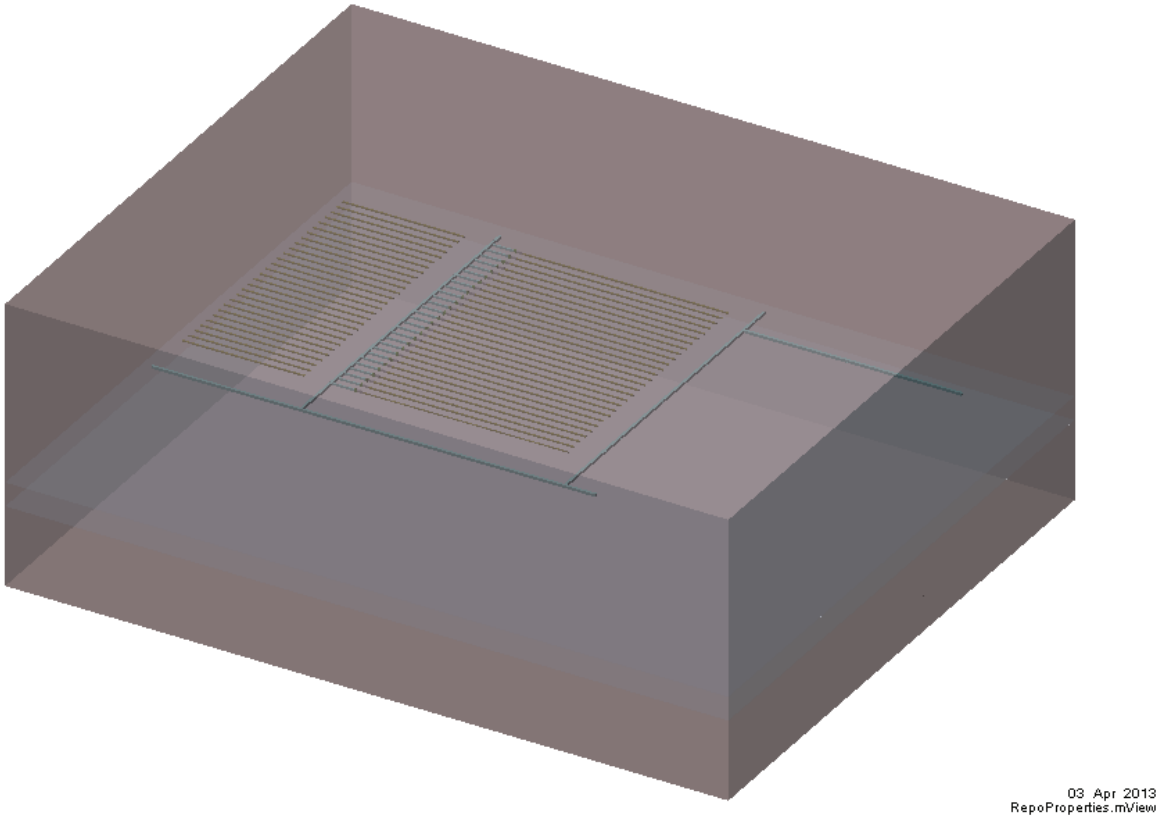

Figure 7-22: Repository-Scale Model - 3D Visualization of Domain Elements

The placement rooms and engineered barrier system are discretized at differing levels of detail. The room containing the radionuclide source is discretized at the highest level and contains representations of the containers in the room. The geometry includes a basic representation of the round room cross-section, and includes homogenized backfill surrounding the containers in the source room. All other placement rooms and access tunnels are square, as shown in Figure 7-23.

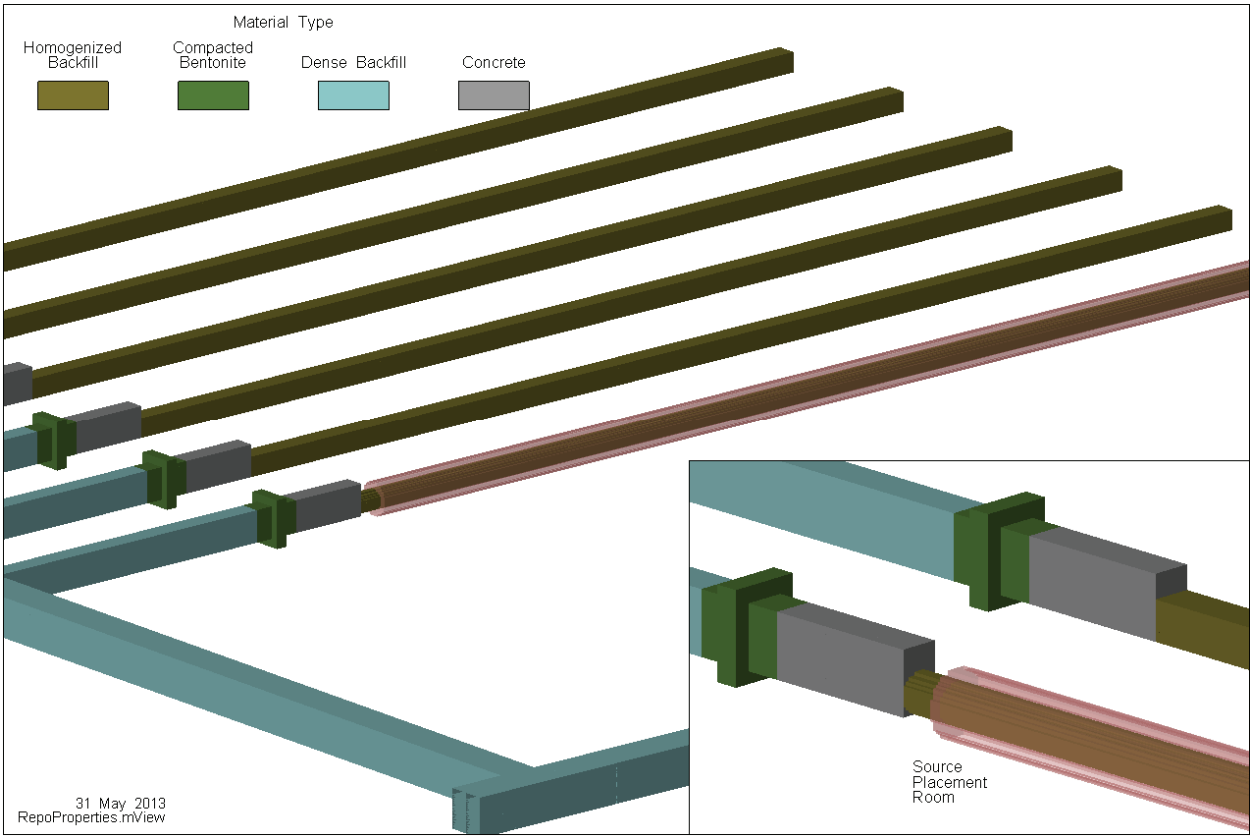

Figure 7-23: Repository-Scale Model - 3D View of Repository Room and Tunnel Seals

Figure 7-24 is a cross section through the model domain showing repository properties and geological setting at Y = 0 metres. The coordinate system is modified slightly from the Site-Scale Model, in that the X axis (Y = 0 m) is centred on the detailed placement room and the Y axis (X = 0 m) is shifted to the start of the placement room, as shown in Figure 7-25.

Figure 7-26 and Figure 7-27 show property assignments in vertical cross-sections along the placement room containing the containers with undetected defects (source room) and perpendicular through the room seal, respectively.

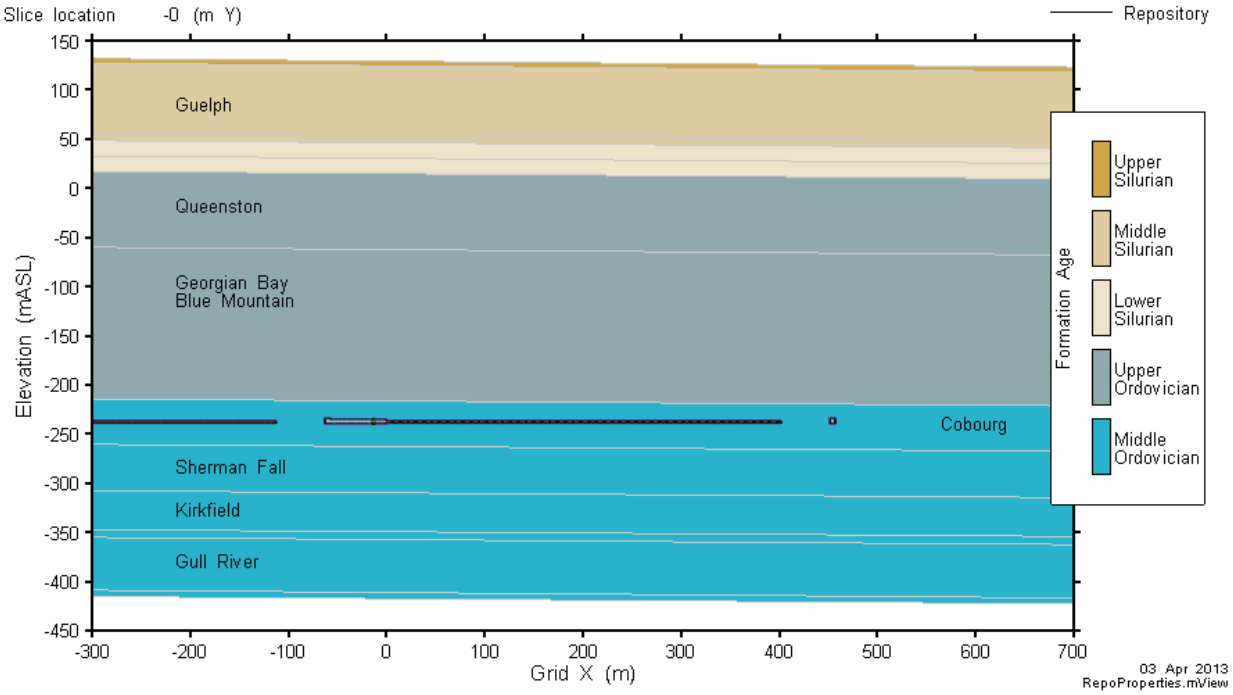

Figure 7-24: Repository-Scale Model - Section View of Repository and Geology

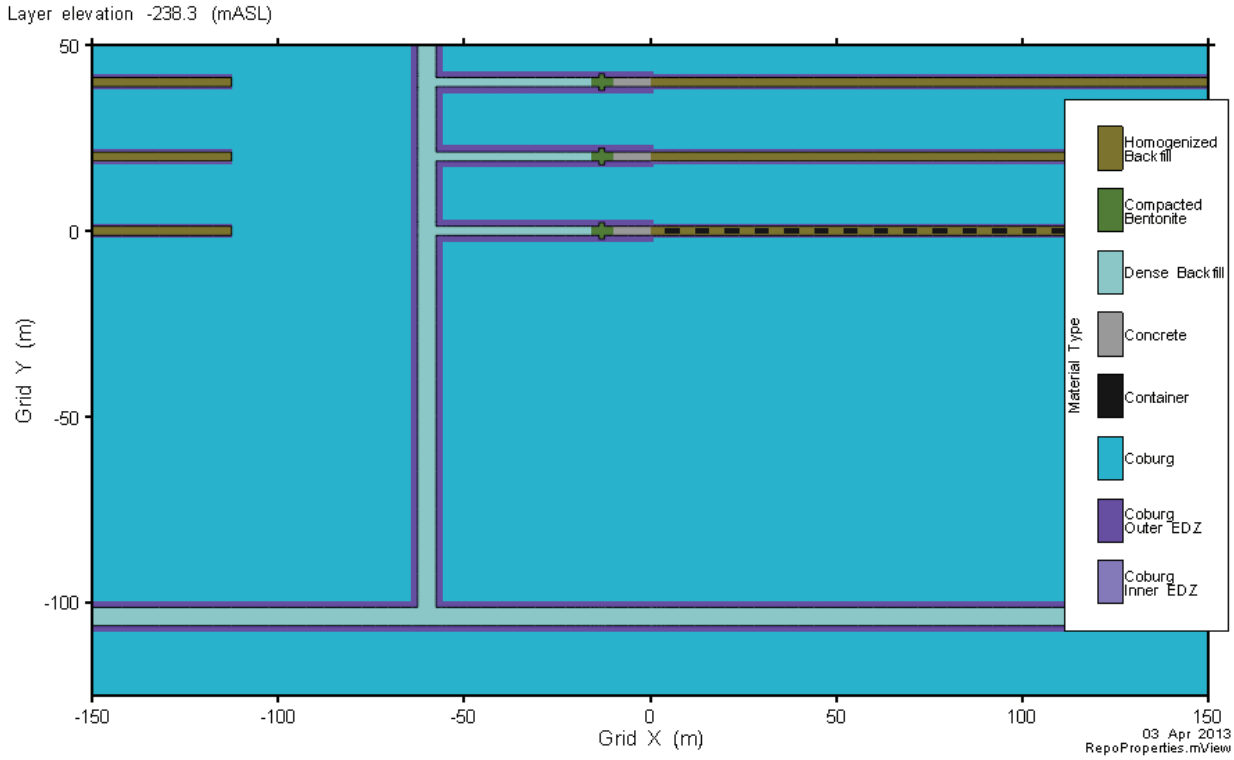

Figure 7-25: Repository-Scale Model - Plan View of Rooms and Tunnel

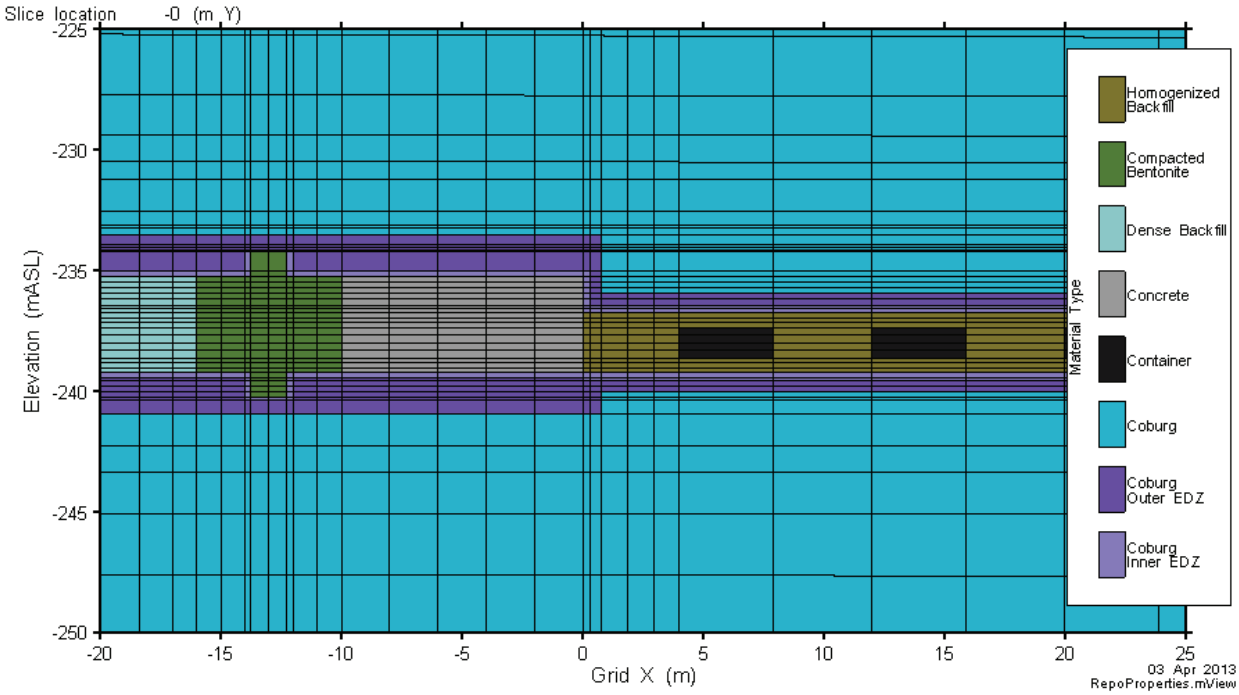

Figure 7-26: Repository-Scale Model - Vertical Slice along Placement Drift (Y = 0 m)

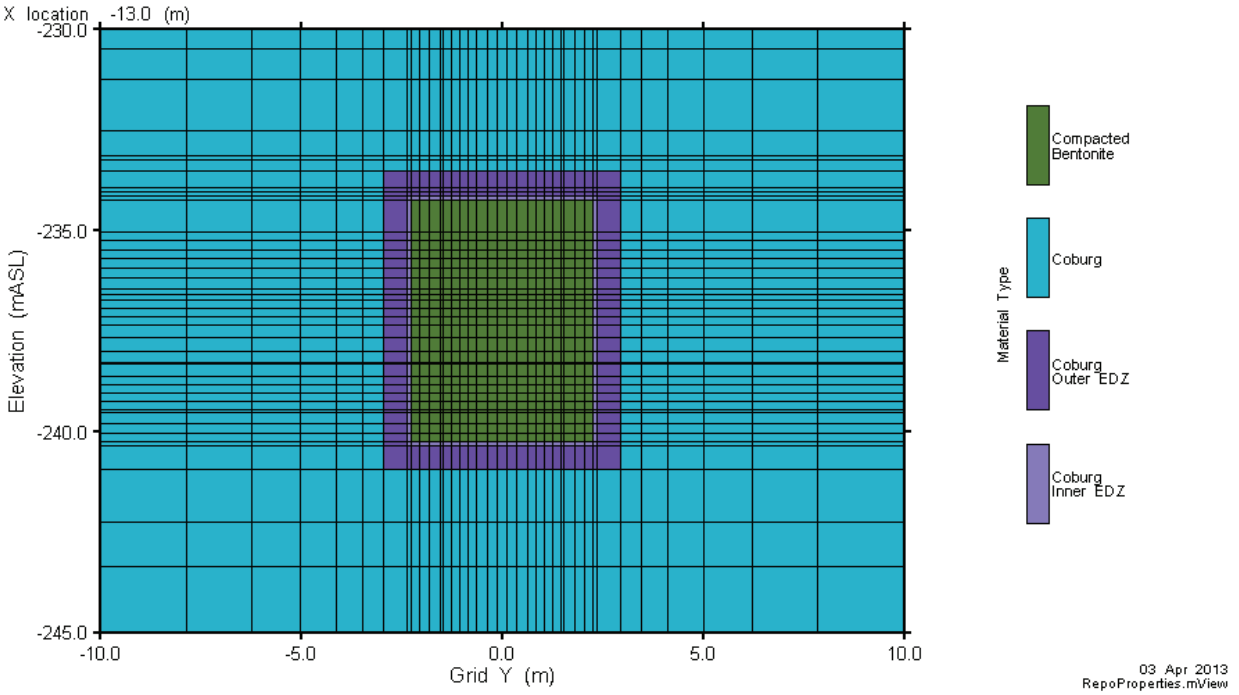

Figure 7-27: Repository-Scale Model - Vertical Slice through Placement Drift Room Seal (X = -13.0 m)

Figure 7-28 is a 3D cutaway showing the assignment of EBS and EDZ materials.

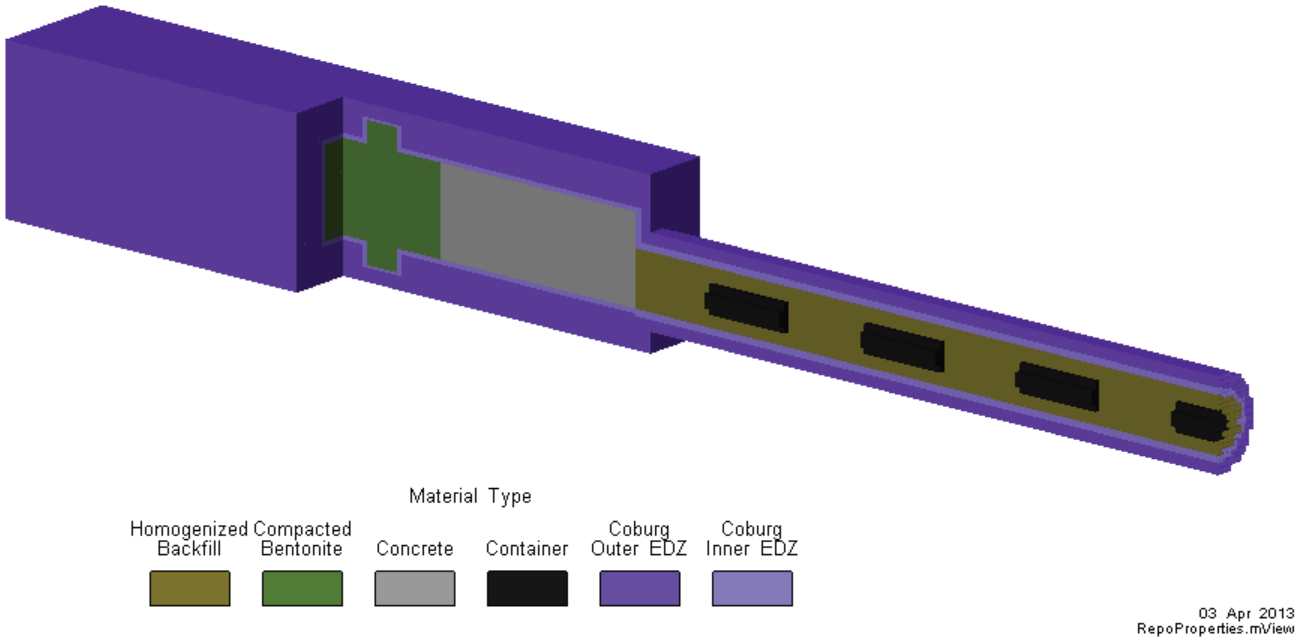

Figure 7-28: Repository-Scale Model - 3D View Showing Engineered Barrier System

Source term nodes are shown in Figure 7-29. Contaminants that escape the containers are applied over four nodes at the interface between the container[1] and the surrounding buffer material, at the container-lid weld to represent a small hole. Note that only one source node is visible in the figure.

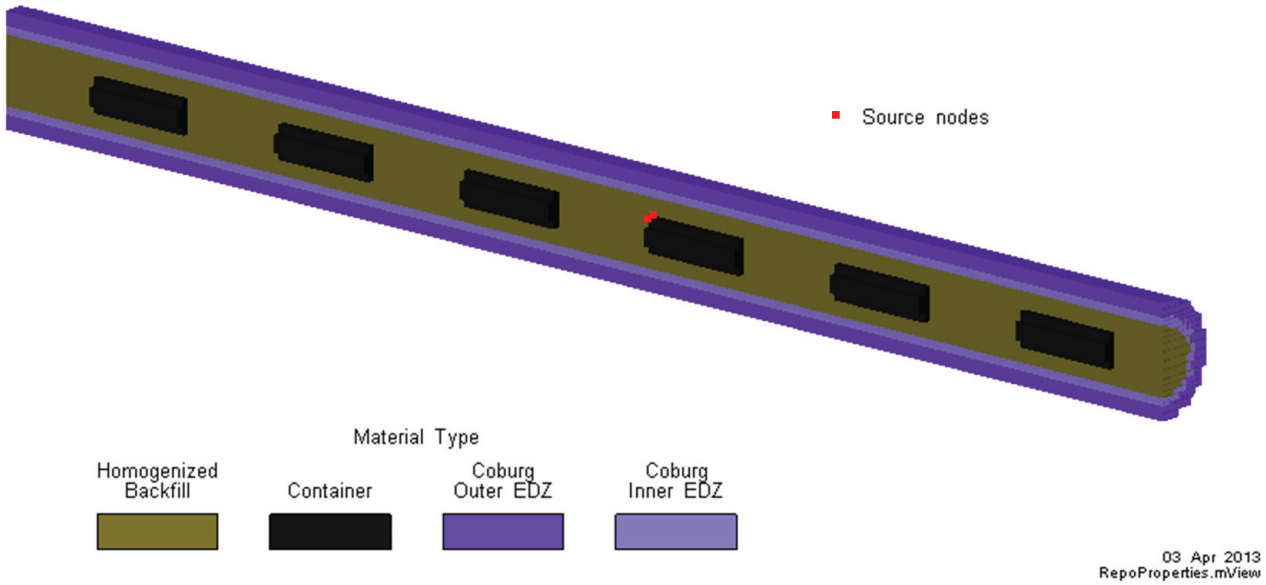

Figure 7-29: Repository-Scale Model - 3D View Showing Defective Container Source Nodes

[1] The Reference Case assumes three used fuel containers are placed in the repository with small undetected defects. Accordingly, mass transport simulations assume the release rate from the defective container is equivalent to the calculated release from three defective containers.

Hydraulic Head Boundary Conditions

Head boundary conditions are extracted from the Site-Scale Model and values are specified for all external model nodes.

Boundary conditions for the Reference Case are shown in Figure 7-30.

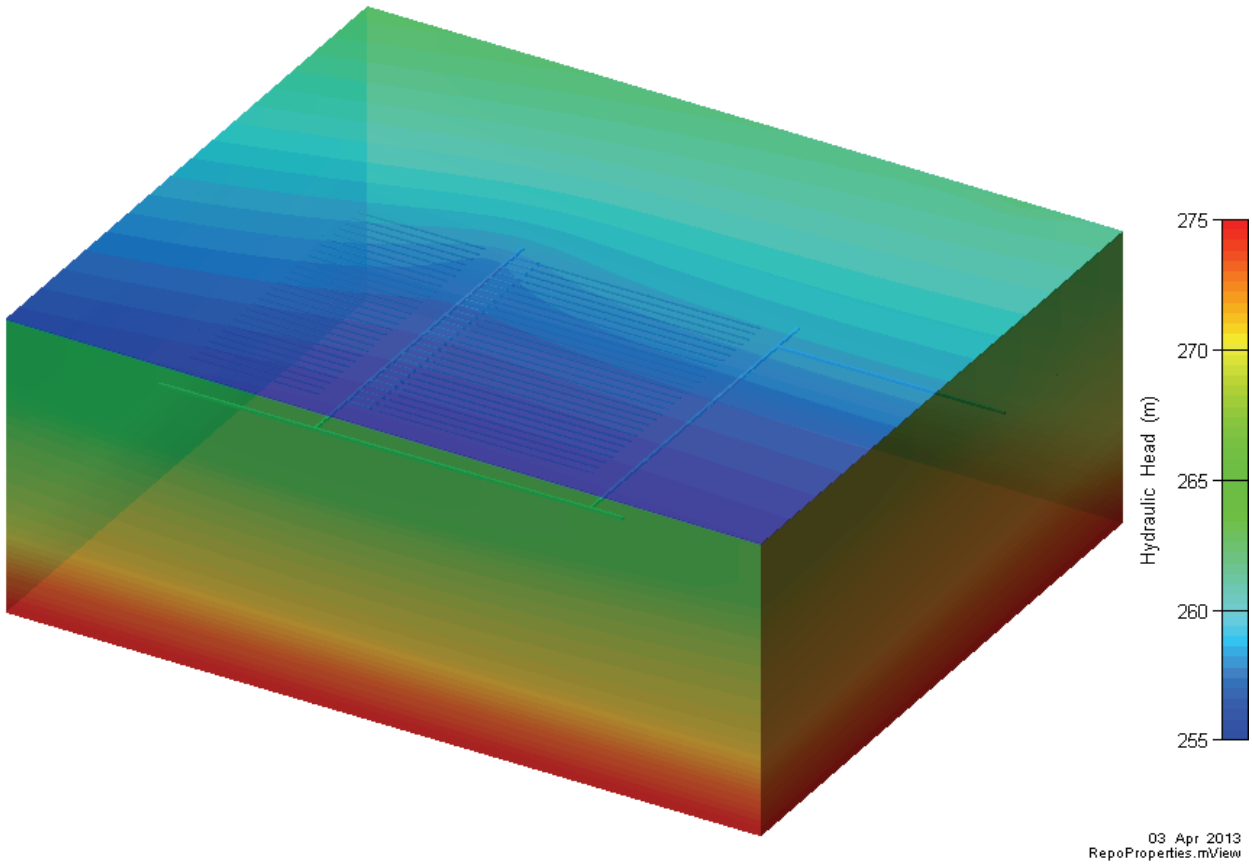

Figure 7-30: Repository-Scale Model - 3D View of Reference Case Head Boundary Conditions

7.5.3.3 Radionuclide Source Term

The FRAC3DVS-OPG code does not have a contaminant release model. Radionuclide release rates from the container[2] are therefore calculated with the SYVAC3-CC4 release model and imposed as a boundary condition at the source nodes, one of which is shown in Figure 7-29.

The radionuclide release rates used are shown in Figure 7-31. The same source term is used in both the Site-Scale and Repository-Scale Models.

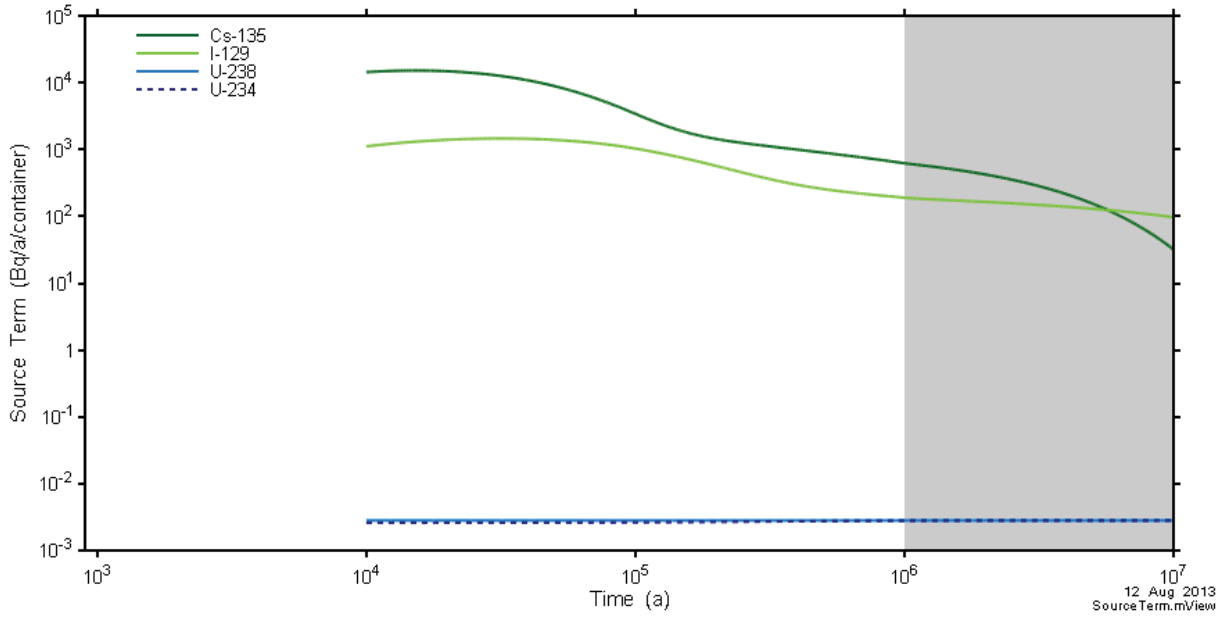

Figure 7-31: Radionuclide Release Rate per Container

7.5.4 System Model

The SYVAC3-CC4 system model combines an idealized geometric description of the repository and a simple geosphere transport model with more detailed representations of releases from the used fuel and radionuclide transport in the biosphere to compute the radiological consequences of releases to the environment.

The description provided here applies to the situation in which the climate, biosphere and geosphere are constant throughout the simulation. The groundwater flow field is also constant.

[2] The Reference Case assumes three used fuel containers are placed in the repository with small undetected defects. Accordingly, mass transport simulations assume the release rate from the defective container is equivalent to the calculated release from three defective containers.

7.5.4.1 Radionuclide Source Term

The reference waste form is a standard CANDU 37-element fuel bundle with a burnup of 220 MWh/kgU and an average fuel power during operation of 455 kW. Chapter 3 identifies the radionuclides of interest and their associated inventories.

Section 7.3.1 describes that radionuclides within the UO_2 fuel are released by two distinct mechanisms which operate on very different time scales. These mechanisms are referred to as "instant release" and "congruent dissolution".

Table 7-21 shows the instant release fractions for selected elements used in this study.

Table 7-21: Fuel Instant-release Fractions for Selected Elements

Radionuclide	Instant-Release Fraction (% of Inventory)
C	2.7
Cl	6
Cs, I, Po, Rn	4
Ra	2.5
Pd, Tc	1
Bi, Se	0.6
Ac, Am, Np, Pa, Pu, Sm, Th, U	0

Note: From Gobien et al. (2013)

Figure 7-32 presents fractional and cumulative information for congruent dissolution of the fuel.

The system model uses the instant release and congruent release together with solubility limits and information on the water volume inside the container to calculate radionuclide concentrations. Radionuclides thereafter escape the container and enter the surrounding low hydraulic conductivity buffer.

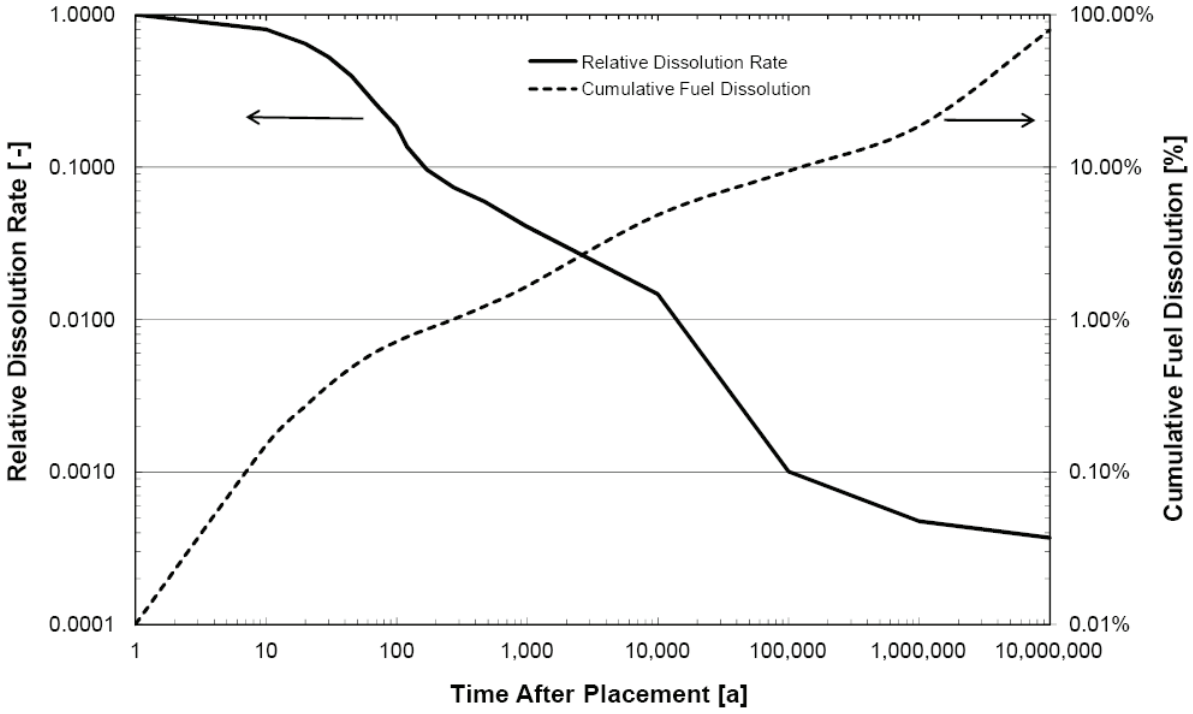

Notes: Relative Dissolution Rate is the ratio of the time-dependent fuel dissolution rate to the maximum fuel dissolution rate. The maximum dissolution rate is 3.12×10^{-3} [mol/m^2/a] where the area is the surface area of the fuel in contact with water. A contact area of 1570 m^2 per container is used in this study which assumes the fuel is highly fragmented. The maximum dissolution rate is therefore 4.9 mol/a.

Figure 7-32: Fuel Dissolution Rate

7.5.4.2 Repository Model

The repository model uses a series of concentric cylinders of varying thicknesses as shown in Figure 7-33 to approximate radionuclide transport through the buffer, backfill and excavation damaged zone. This simplification allows for the use of semi-analytical solutions which result in fast computation times suitable for use in probabilistic analyses.

Conceptually, the model represents one container within a placement room surrounded by concentric cylinders of buffer material, backfill material and EDZ. Because the conceptual repository in this study does not have placement room backfill, input data for the concentric

cylinders are specified such that only the buffer (63 cm thick) and placement room inner EDZ (30 cm thick) are represented. The outer EDZ is and its associated rock thickness is conservatively ignored. The length of the concentric cylinders is about 401 m, corresponding to the length of the placement room. A semi-infinite boundary condition that maintains continuity of concentration and continuity of flux is established at the outer boundary.

The radionuclide release from the defect is represented by a source that lies along the axis of the nested cylinder. The container is not physically represented.

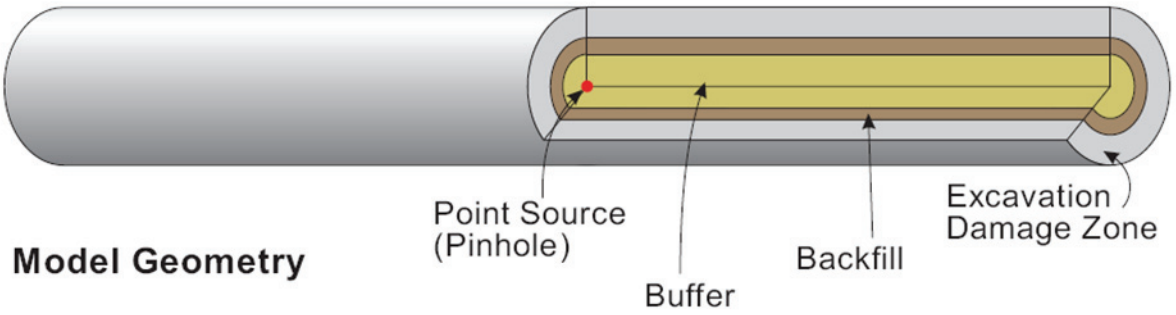

Note: the backfill thickness is 0 cm in the repository model used in this study.

Figure 7-33: SYVAC3-CC4 Repository Model

The repository model simulates the following processes:

- Container Failure – At a specified time some of the containers are assumed to fail. In the Normal Evolution Scenario failure occurs in the form of a small initial defect in the corrosion resistant copper shell allowing water to enter the container.

- Instant Release – A fraction of soluble fission products at the UO_2 fuel grain boundaries and cladding gap is instantaneously dissolved once the container is breeched and water comes into contact with the fuel. A fraction of the C-14 in the Zircaloy is also released instantaneously when water contacts the Zircaloy.

- Congruent Release – A slow long-term radionuclide release consistent with the long-term corrosion / dissolution of the ceramic fuel pellet and release of radionuclides trapped within the fuel matrix. Radionuclides are also released from the Zircaloy as it dissolves.

- Precipitation – The precipitation of elements whose concentration in the container exceeds the solubility of the element.

- Radioactive Decay and Ingrowth – Radioactive decay of radionuclides and progeny.

- Transport – The diffusive and advective transport of radionuclides through the engineered barrier system (including the defective container).

The failed container begins to fill with water as soon as the surrounding buffer is saturated. Buffer saturation is assumed to occur 10,000 years after the container is placed in the repository. The time for the container to fill with water is conservatively neglected so that a continuous water pathway between the container interior and the surrounding buffer is assumed to exist immediately at 10,000 years.

In the deterministic analyses, the three failed containers are conservatively assumed to be in the repository location with the shortest contaminant transport time to the well. In the probabilistic analysis, since each container has only two states (i.e., intact or failed), the failure rate is described by a binomial distribution with the probability of failure being approximately 1 in 5000 containers. The location, the time of failure, and the number of failed containers are random variables.

The radius of the container defect for the Reference Case of the Normal Evolution Scenario is 1 mm. An upper limit of 2 mm is applied in the probabilistic analysis since defects of this size and larger will be readily detectable during the container inspection process prior to placement.

7.5.4.3 Geosphere Model

The geosphere is represented as a network of 1D transport segments. Each 1D segment represents a path in which transport is primarily in one direction, with relatively uniform material properties. This network is defined to approximate the stratigraphy and the hydrological and geochemical features of the geosphere zones located between the repository and the surface biosphere. Transport in each segment is characterized using the 1D advection-diffusion equation, for which robust semi-analytical solutions are available.

The starting point for generation of the SYVAC3-CC4 geosphere network is a detailed steady-state groundwater flow field for the site computed using the FRAC3DVS-OPG code. However, because the hydraulic conductivity of the hypothetical geosphere is so low, radionuclide transport is effectively entirely diffusive and advective flow trajectories have not been used. Instead, a series of diffusive transport pathways have been independently defined and the geosphere model created through execution of the following steps:

- Sector Selection – The repository is divided into sectors. A sector is typically defined so that its properties are uniform. For example, it has the same waste form type and room length, and it connects to a portion of the groundwater flow field (when applicable) whose properties are approximately uniform for the entire sector. Different sectors typically have different properties, and often the properties of the surrounding geosphere are the delineating factor.

- Selection of Representative Pathways – A representative pathway for each sector is generally chosen to give the conservatively shortest travel time to the surface. In areas of low flow velocity, diffusion towards fractures (if present) may be the shortest travel path.

- Selection of Nodes along Pathways – Nodes are generally selected at material property boundaries so that the resulting segments have constant properties.

- Addition of Well and Near-surface Nodes – Additional nodes are required for the well - for example, upper and lower reference nodes define the range of positions for the well and drawdown nodes, which give a better representation of the drawdown cone in the vicinity of the well.

- Property Assignment – Data needed include the Cartesian coordinates of all the nodes, hydraulic heads and temperatures at the nodes, and hydraulic and chemical properties of the different geosphere zones.

- Well Model – The effects of the well drawdown on adjacent node heads is accounted for via an analytical well model within the aquifer, and by a site-specific well-effects model outside the aquifer.

Sector Selection

Since all containers contain the same used fuel waste form and the placement room design is common across the repository, the main distinction between the sectors is generally the influence of the surrounding groundwater flow field. However, for this study, with diffusion-dominated sedimentary rock, the key feature of the geosphere is the geologic layering. The pathways start in the placement rooms at the repository horizon and end at the Guelph formation. There is sufficient variation in the distance from the mid room vertical location and the top of the Cobourg layer over the 10 repository panels to warrant the use of five sectors to represent the repository. Panels A and B, C and D, E and F, G and H, and I and J, are numbered 1 through 5 respectively. Figure 4-14 shows the panel labelling scheme.

Table 7-22 shows the numbers of containers in each sector and their contributions to transport via the host rock and the shafts.

Table 7-22: Container Distribution by Repository Sector

Repository Sector	Number of Containers	Transport Fraction	
		Host Rock (%)	Shaft (%)
1	2555	100	$6.92\times10^{-5*}$
2	2556	100	0%
3	2556	100	0%
4	2556	100	0%
5	2555	100	$1.47\times10^{-4*}$

Note: *this is the ratio between the shaft footprint and the repository footprint. The Sector 1 value represents the area ratio for the ventilation shaft while the Sector 5 value represents the area ratio for the combined main and access shafts.

Selection of Representative Pathways

For each sector, a representative transport pathway is selected to approximate the transport segment leading to the surface discharge point(s). These pathways may converge and combine on the way to the surface, or conversely may diverge and lead to different discharge points, depending on conditions such as the well demand rate.

In this study, the representative pathways are straight lines directly up to the Guelph aquifer because the geosphere is diffusion-dominated. This results in five pathways leading away from the five sectors of the repository to the top of the Cobourg layer. From the top of the Cobourg layer, a single pathway is used through the next four layers to the bottom of the Guelph layer. The transport pathway to the Guelph layer is vertical and eventually discharges to the Well with a capture fraction of 93.7% (Section 7.5.3.1). In parallel to this single pathway, another vertical pathway representing the shaft is also included. Note that no credit is taken for contaminant transport into the deeper geosphere below the repository.

Although a Lake is not present in the biosphere, a small Lake discharge is included in the model since the code assumes there is an Aquatic Discharge somewhere. The Lake is sufficiently far down-aquifer of the well that no additional dose to the critical group occurs. In practice, doses to people exposed to these radionuclides would be less than those associated with the critical group due to the smaller radionuclide fraction entering the Lake and the much greater dilution.

Selection of Nodes along Pathways

Nodes are defined at material property boundaries and at some intermediate points. Pathways are merged where appropriate, and divergence nodes are located where the fraction of the flow is re-directed to a shaft.

Addition of Well, Overburden and Sediment, and Other Features

Four additional nodes are associated with the well. A well discharge node is located at the ground surface immediately above the well aquifer node. The fraction of the contaminant plume entering the Guelph layer captured by the well as a function of well demand is determined using the FRAC3DVS-OPG code, as discussed in Section 7.5.3.1.

For proper operation of the code, the Lake is assumed to have both a terrestrial discharge node and an aquatic discharge node. The aquatic and terrestrial discharges have an overburden and associated sediment / soil node for a total of 4 additional nodes.

With these additional 8 nodes, the complete network consists of 41 nodes. The network and its connectivity are shown schematically in Figure 7-34.

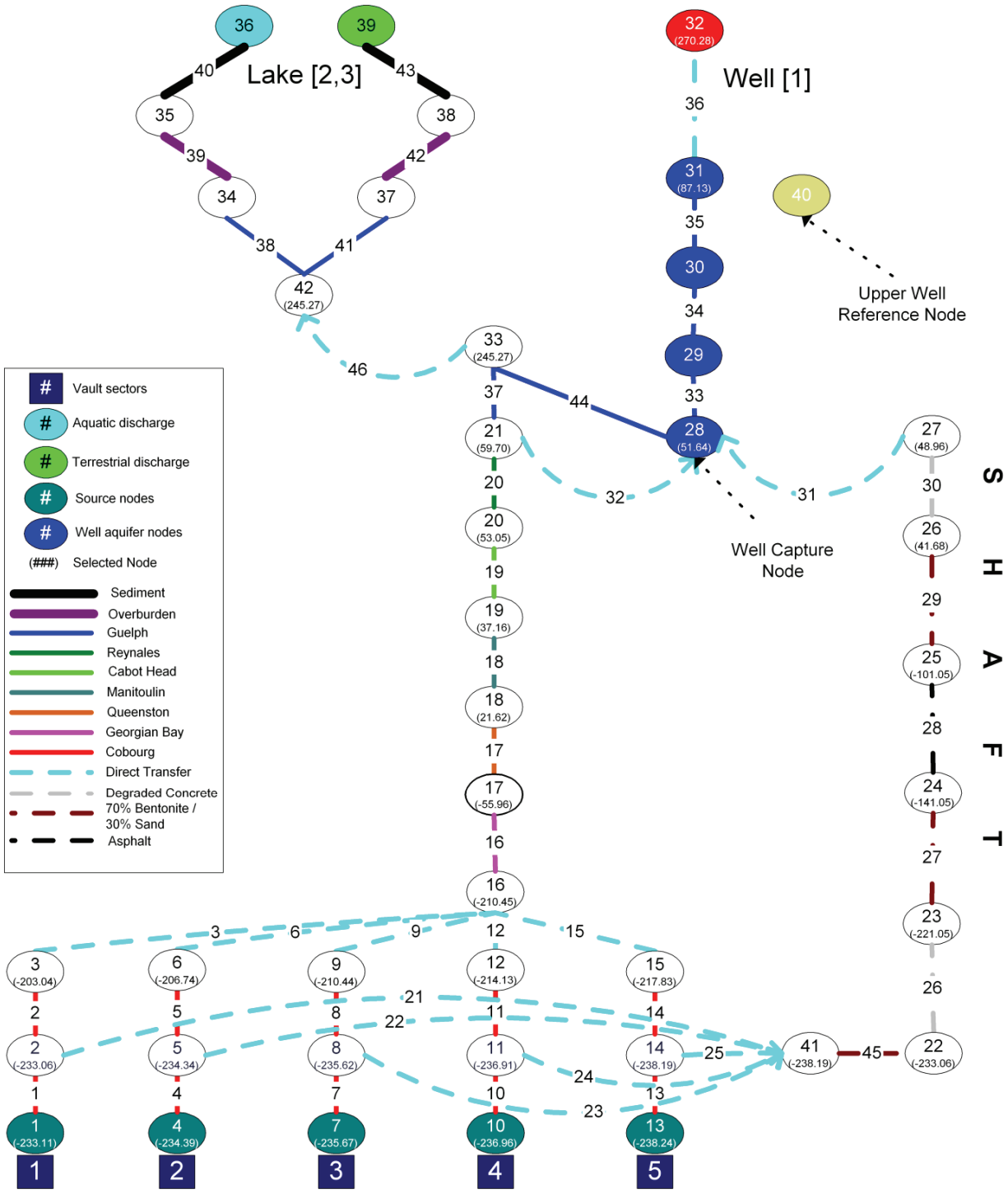

Notes: Only nodes (ellipses) with a particular function are colour coded. The line segments, representing the 1D transport pathways, are colour coded (see legend) to indicate the geosphere zone through which they pass.

Figure 7-34: SYVAC3-CC4 Transport Network Showing Connectivity

Well Model

The well must be located in a permeable zone capable of supplying significant water. This permeable zone is referred to as an “aquifer”. In the current study, the aquifer is located in the permeable, slightly sub-horizontal Guelph formation. This is a conservatively deep groundwater well, at 219 m.

SYVAC3-CC4 uses an analytical solution to provide the hydraulic head drawdown at the nodes and the capture envelope for the groundwater flowing in the aquifer. The analytical solution is based on a constant head boundary condition at the discharge end of a non-leaky aquifer (where “non-leaky” means there is little inflow from the surrounding rock). The well model allows the assessment of well demands other than the Reference Case value, which is useful in assessing alternative lifestyles or other critical groups, and in probabilistic calculations.

Property Assignment

Once the network is defined, physical and chemical properties are assigned to the various rock, overburden, and sediment nodes and segments.

Values for the hydraulic heads at each node location are obtained from the FRAC3DVS-OPG results. Values for transport parameters such as porosity and permeability and sorption are supplied for each network segment. The model accounts for both advective and diffusive transport processes.

Table 7-23 shows times corresponding to the transport peaks calculated using the SYVAC3-CC4 geosphere model for I-129 transport through the various rock layers at the reference well demand of 1,307 m^3/a. These results show that the transport through the shales is very slow, around 20 million years. This can be compared with Figure 7-41 that shows Mean Life Expectancies of a similar range.

Table 7-23: I-129 Transport from the Repository to Surface

Layer	Time of Maximum Release from Layer [a]	Time of 0.1% of Maximum Release from Layer [a]
Geosphere Pathway		
Cobourg	205,000	25,000
Georgian Bay	15,200,000	1,190,000
Queenston	18,500,000	2,290,000
Manitoulin	19,100,000	2,590,000
Cabot Head	19,600,000	2,780,000
Reynales/Fossil Hill	20,000,000	3,010,000
Shaft Pathway (0.015 % of release from Sector 5 only)		
Shaft Bentonite/Sand	685,000	72,000
Concrete (LHHPC)	691,000	74,000
Shaft Bentonite/Sand	1,400,000	118,000
Shaft Asphalt	2,810,000	264,000
Shaft Bentonite/Sand	5,600,000	410,000
Concrete (LHHPC)	5,900,000	418,000
Combined Geosphere and Shaft Pathway Flow into Well		
Well	20,000,000	2,423,000

7.5.4.4 Biosphere Model

The biosphere model represents a hypothetical but plausible Southern Ontario site.

The topography of the watershed area near the repository is relatively flat as shown in Figure 7-8. The local biosphere is assumed to have the characteristics of a temperate climate region of Southern Ontario and its properties are assumed constant during the simulation period. The normal present-day variation of climate and other biosphere parameters are included via the use of probabilistically sampled parameter values.

Key elements of the model are discussed below. A detailed description of the input data used in the model is available in Gobien et al. (2013).

Surface Water Submodel

Surface waters are not modelled in this study. As explained in Section 7.5.4.3, any radionuclides not directed to the well would remain in the Guelph aquifer, be diluted and travel to regions outside the boundary of the model.

Soil Submodel

The soil submodel calculates the concentration of contaminants in the surface (rooting or cultivated) soil layer. This layer is assumed to be well-mixed due to, for example, plowing in an agricultural field or bioturbation. Two soil models are considered, one for upland soil and one for shallow soil. The upland soil model describes a typical soil layer, with the water table a reasonable distance below the surface soil layer. In the shallow soil model, the water table extends into the surface soil layer on a regular and extended basis (as in the case of marsh or swamp land). The distinction between these two soil types is important in determining how readily contaminated groundwater can reach the surface. In the upland soil model, it must be transported by processes such as capillary action while in the shallow soil model groundwater is discharged directly into the surface soil.

Areas of surface soils have specific designations including use as a vegetable garden, a forage field, and a woodlot. Some of the parameters describing the transport pathways in the soil model are dependent on the type of field (i.e., irrigation rate).

The transport processes considered in the soil submodel are:

- Irrigation – contaminated water from the well (or surface water if present) is added to the soil.
- Groundwater Discharge – direct discharge from a contaminated groundwater water source below the surface soil (shallow soil only).
- Capillary Rise – upwelling of contaminated groundwater from the water table (upland soil only).
- Leaching – contaminants in surface soil migrate to deeper soil layers as water percolates through the soil layer.
- Runoff – precipitation runoff from the watershed area entering the water body.
- Root Uptake – uptake of contaminants by plants and trees.
- Suspension and Volatilization – loss from the soil to the atmosphere due to soil resuspension (wind erosion) and volatilization.
- Deposition – deposition of contaminants from the atmosphere onto surface soils.

Some of the physical characteristics of the soil at the hypothetical site are described in Table 7-24 (Gobien et al. 2013). These reflect the values in CSA (2008) where available.

Table 7-24: Soil Properties

Parameter	Reference Case Value	Comment
Soil types	Clay type	Distribution of soil types: 10% sand, 40% organic, 40% clay, and 10% loam. Soil properties (e.g., sorption coefficient) depend on soil type.
Active surface soil depth	0.2 m	This is the active or root zone layer for which radionuclide concentrations in the soil are determined.
Soil Depth to water table	1.5 m	Normal PDF, 1.5 m mean, 0.5 m standard deviation, and bounds of 0.01 to 2.5 m.
Minimum soil depth to water table for upland soil model	0.5 m	This is the minimum depth-to-water-table at which the upland soil model is used. For smaller depths, a shallow soil model is used that allows for flooding of the surface soil by contaminated groundwater.
Upland soil leach rate fraction	0.55	Fraction of net precipitation (precipitation + irrigation - evapotranspiration) that infiltrates into soil. The remainder runs off along the surface. Uniform PDF from 0.1 to 1.

Note: Data taken from Gobien et al. (2013).

Atmosphere Submodel

The atmosphere submodel calculates radionuclide concentrations in air due to the following transport processes:

- Suspension and Volatilization – contamination of the air from particulate or gaseous releases from surface water (if present) and soil.
- Dispersion – reduction in the concentration of contaminants in the air by having them disperse over a larger area.
- Fire – release of contamination into the air from fires assumed to occur on-site. This includes fuel fires used by the critical group as well as natural fires such as a forest fire.

A list of parameters important to the concentration of airborne contaminants is given in Table 7-25 (Gobien et al. 2013). When calculating the concentrations in the atmosphere, all contaminants are conservatively assumed to be located within a couple of metres above the land surface.

Table 7-25: Climate and Atmosphere Parameters

Parameter	Reference Case Value*	Comment
Annual total precipitation	0.84 m/a	Normal PDF, with a standard deviation of 0.15 m/a and bounds of 0.39 and 1.68 m/a.
Annual average runoff	0.19 m/a	This is the balance between total precipitation and evapotranspiration, and includes surface runoff as well as infiltration into the water table.
Average wind speed	2.36 m/s	Normal PDF with mean of 2.36 m/s (8.5 km/h), standard deviation of 0.64 m/s, and bounds of 0.44 and 6 m/s.
Dry deposition velocity	0.006 m/s	Constant
Atmospheric dust load	3.2×10^{-8} $kg_{drysoil}/m^3_{air}$	Lognormal PDF with geometric mean calculated from suspended particulate matter concentrations in Ont, NB, Que and Sask during years 1996 to 2002. Geometric standard deviation (GSD) of 1.7 with bounds of 7.0×10^{-9} and 7.5×10^{-8} $kg_{drysoil}/m^3$air.
Atmospheric aerosol load	2.9×10^{-10} m^3_{water}/m^3_{air}	Lognormal PDF with geometric mean of 2.9×10^{-10} m^3_{water}/m^3_{air}, and GSD of 1.41. Based on estimate for sea salt aerosol over oceans.
Washout Ratio	630 000	CSA (2008) washout ratio for deposition to plants for all elements other than noble gases and iodine. This value is conservative for iodine. CSA (2008) recommends 200 000 for elemental iodine and 8400 for organic iodine.

Note: Data taken from Gobien et al. (2013).

Dose Calculations

The dose model uses the concentrations of radionuclides in the various biosphere compartments to calculate the annual dose to a member of the critical group.

To ensure that dose rates are not underestimated, conservative assumptions are made concerning the characteristics of the critical group. Specifically, it is assumed that the members of the critical group spend all their lives in the local biosphere and obtain all their food, water, fuel and building materials from the local biosphere. The water source for the critical group is a well that intercepts the radionuclide plume. The food includes plants grown in a garden, domesticated animals and fish. All plant and animal biota used as food are subject to contamination from surface water, soil and air. This lifestyle is consistent with but more self-sufficient than current habits and leads to an overestimate of the impact. Because of these characteristics, the hypothetical member of the critical group is referred to as a Self-Sufficient Farmer. The Self-Sufficient Farmer has been found in previous studies to be a good indicator of risk for a range of plausible lifestyles (Garisto et al. 2005).

Some critical group lifestyle characteristics are shown in Table 7-26.

Table 7-26: Human Lifestyle Data

Parameter	Reference Case Value	Comment
People per household	3	Piece-wise uniform PDF from 1 to 12 people.
Domestic water demand per person	110 m^3/a	Lognormal PDF with geometric mean 110 m^3/a, geometric standard deviation of 2 and bounds of 40 and 240 m^3/a.
Total energy needs per person	18744 kJ/d	Fixed value, set conservatively high at 90th percentile value.
Man's air inhalation rate	8400 m^3/a	95th percentile
Man's water ingestion rate	840 L/a	90th percentile
Man's meat ingestion rate*	103 g/d	Median intake for male adult. Defined as lognormal PDF with geometric mean equal to median and geometric standard deviation equal to 1.65. For a total energy intake of 18744kJ/d, this intake is prorated to 249 g/d.
Man's milk ingestion rate*	283 g/d	Median intake for male adult. Defined as lognormal PDF with geometric mean equal to median and geometric standard deviation equal to 1.35. For a total energy intake of 18744kJ/d, this intake is prorated to 685 g/d.
Man's plant ingestion rate*	796 g/d	Median intake for male adult. Defined as lognormal PDF with geometric mean equal to median and geometric standard deviation equal to 1.65. For a total energy intake of 18744 kJ/d, this intake is prorated to 1928 g/d.
Man's poultry ingestion rate*	53 g/d	Median intake for male adult. Defined as lognormal PDF with geometric mean equal to median and geometric standard deviation equal to 1.65. For a total energy intake of 18744 kJ/d, this intake is prorated to 128 g/d.
Man's fish ingestion rate*	7.9 g/d	Median intake for male adult. Defined as lognormal PDF with geometric mean equal to median and geometric standard deviation equal to 4.48. For a total energy intake of 18744 kJ/d, this intake is prorated to 19 g/d.
Soil ingestion rate	0.12 kg/a	95th percentile of incidental soil ingestion rate.
Annual energy consumption per household	$1.2x10^5$ MJ/a	Normal PDF with mean of 1.2×10^5 MJ/a, standard deviation of 8×10^3 MJ/a and bounds of 10^5 MJ/ and 1.3×10^5 MJ/a.
Building occupancy factor	0.8	Fixed value
Building air infiltration rate	0.35 /hr	Fixed value, minimum recommendation for tightly-sealed house.

Notes: Data taken from Gobien et al. (2013). * Based on a total energy intake of about 7750 kJ/d.

7.6 Results of Radionuclide and Chemical Hazard Screening Analysis

This section presents the results of the RSM screening analysis performed to identify the potentially significant radionuclides and potentially significant chemically hazardous elements. The methodology used is described in Section 7.5.2.

Table 7-27 lists the radionuclides and hazardous elements that emerged from the screening assessment. Results are shown for each case simulated, with radionuclides listed in order of their dose contribution and hazardous elements listed in alphabetical order.

The results indicate the most important potentially significant radionuclides are I-129, Cs-135, Pd-107 and Cl-36. Actinides only appear in simulation cases with no sorption or no solubility limits. The parents and progeny of the screened in radionuclides are also included in the simulations to ensure that ingrowth is accounted for.

For the potentially significant chemically hazardous elements, the “No Sorption” case has the highest number of contributors (due to the conservative nature of this case) while elements associated with the other cases are Ag, Be, Cr, Hg, Mo and Sm. It should be noted that the amount of some the chemical elements of interest (e.g., Pb, Te and Ag) increase with time due to radioactive decay of parent nuclides. Consequently, these parent nuclides are also included in the simulations of the potentially chemically hazardous elements carried out with system model.

Table 7-27: Summary of Screened in Radionuclides and Chemically Hazardous Elements for Each Case Considered

Case	Radionuclide	Chemically Hazardous Element
Base Case*	I-129, Cs-135, Cl-36, Pd-107, Se-79, Sm-147	Ag, Be[1], Mo, Sm
No Sorption	Ra-225, Th-229, Th-230, Po-210, Pb-210, Ac-225, Th-234, Pa-231, Ra-228, Ra-226, Ac-227, Ra-223, Np-237, U-233, Pa-233, U-234, U-238, U-236, Ra-224, I-129, Th-232, Pu-242, Th-227, Th-228, Cs-135	Ag, Al, Ba, Be[1], Cd[2], Ce, Co, Cr[2], Eu, Hg, La, Mo, Nd, P, Pb, Pr, Se, Sm, Te, U, Y, Zr[2]
High Solubility	I-129, Cs-135, Ra-228, Cl-36, Pd-107, Ra-224, Se-79, Th-232, Tc-99, Th-228	Ag, Be[1], Cr[1], Mo, Sm
High Instant Release Fraction	I-129, Cs-135, Cl-36, Ra-228, Pd-107, Se-79, Ra-224, Tc-99, Sm-147	Ag, Be[1], Hg, Mo, Sm
10x Diffusion	Th-230, Po-210, Ra-226, Cl-36, I-129, Ra-228, Cs-135, Tc-99, Se-79, Th-234, Ra-224, Pb-210, Rn-222	Ag[2], Al, Be[1], Bi, Co, Cr[2], Hg, Mo, Ni, Sb[2], Se, Sm, U, V[2]

Notes:
*The Base Case corresponds to the All Containers Fail Scenario (see Table 7-11) with all parameter values set at their median values
[1] From Zircaloy only, [2] From Fuel and Zircaloy

Table 7-28 shows the set of potentially significant radionuclides and Table 7-29 shows the set of potentially significant chemically hazardous elements. Items in red are items identified directly in the screening (i.e., Table 7-27) while items in black are added to include in-growth contributions.

Table 7-28: List of Potentially Significant Radionuclides

Radionuclides	
Single Nuclides	I-129, Cl-36, Cs-135, Pd-107, Se-79, Sm-147, Tc-99
Chain	
Neptunium Series	Am-241 → Np-237 = Pa-233 → U-233 → Th-229 = Ra-225 = Ac-225
Uranium Series	Pu-242 → U-238 = Th-234 → U-234 → Th-230 → Ra-226 = Rn-222 = Pb-210 = Bi-210 = Po-210
Actinium Series	Pu-239 → U-235 = Th-231 → Pa-231 = Ac-227 = Th-227 = Ra-223
Thorium Series	Pu-240 → U-236 → Th-232 = Ra-228 = Th-228 = Ra-224

Note: '=' means the radionuclides are assumed to be in secular equilibrium with their parent

Table 7-29: List of Potentially Significant Chemically Hazardous Elements

Chemically Hazardous Elements	
Fuel	
Elements	Al, Cd, Ce, Co, Cr, Hg, La, Mo, Nd, Ni, P, Pr, Sb, Se, Sm, V, Y
Chain	
Neptunium Series	Am-241 → Np-237 = Pa-233 → U-233 → Th-229 = Ra-225 = Ac-225 → Bi-ST
Uranium Series	Pu-242 → U-238 = Th-234 → U-234 → Th-230 → Ra-226 = Rn-222 = Pb-210 = Bi-210 = Po-210 → Pb-ST
Actinium Series	Pu-239 → U-235 = Th-231 → Pa-231 = Ac-227 = Th-227 = Ra-223 → Pb-ST
Thorium Series	Pu-240 → U-236 → Th-232 = Ra-228 = Th-228 = Ra-224 → Pb-ST
Misc	Sn-126 → →Te Sr-90→ →Zr Cs-135→Ba Cs-137→Ba Pd 107 → Ag Sm-151 → Eu
Zircaloy	
Elements	Be, Cr, Cd, Sb, V
Chain	
Misc	Pd-107→Ag Sr-90→ →Zr

Note: '=' means the radionuclides are assumed to be in secular equilibrium with their parent

7.7 Results of Detailed 3D Groundwater Flow and Transport Analysis

This section presents results of the detailed FRAC3DVS-OPG groundwater flow and radionuclide transport analysis performed for the Reference Case of the Normal Evolution Scenario and for those sensitivity cases with the potential to affect the groundwater flow field. The sensitivity cases examined are:

- Geosphere hydraulic conductivities increased by a factor of 10 times the Reference Case values;
- Hydraulic conductivity of the EDZ increased by a factor of 10;
- Overpressure in the Shadow Lake formation (i.e., a constant head boundary at the bottom of model domain);
- 100 m of surface erosion;
- Increased spatial resolution (assessed by comparing Site-Scale and Repository-Scale results); and
- Increase and decrease in the number of time steps.

A further description of the cases is provided in Section 7.2.

A detailed description of the models used to generate the results is provided in Section 7.5.

Radionuclide transport is calculated for I-129, Cs-135, U-234 and U-238. These radionuclides are typically the most important in terms of potential radiological impact and / or represent a range of low-sorption to high-sorption species.

Figures in this section show advective[3] velocity vectors only in locations where velocities are greater than 10^{-4} m/a. Transport is diffusion-dominated at lower velocities.

7.7.1 Site-Scale Model

The Site-Scale Model domain includes the repository and a section of the surrounding geosphere that encompasses the repository influenced flow domain. The model is used to determine:

- the container location with the fastest contaminant transport to the well;
- Reference Case and sensitivity case radionuclide transport to the well and surface environment; and
- boundary conditions for the Repository-Scale Model.

A simplified representation of the repository and engineered barrier system is included at this scale of resolution; however, individual containers are not modelled.

[3] Advective velocity is the Darcy velocity divided by the material porosity.

The sensitivity simulations examine the effects of:

- geosphere hydraulic conductivities increased by a factor of 10;
- hydraulic conductivity of the EDZ increased by a factor of 10;
- overpressure in the Shadow Lake formation; and
- increased spatial resolution and increase / decrease in the number of time steps.

A discussion of the anticipated effects of 100 m erosion is included.

The Site-Scale model is also used in the assessment of the Shaft Seal Failure Disruptive Scenario.

7.7.1.1 Flow Results

7.7.1.1.1 Reference Case – No Well

Figure 7-35 and Figure 7-36 compare hydraulic head and Darcy velocity results in the Guelph aquifer with similar results from the Regional Model described in Chapter 2 to verify correct implementation of the boundary conditions. In these simulations the well demand was set to zero in the Site-Scale model to allow direct comparison.

The results show continuity of heads at the Site-Scale Model boundary and close correspondence within the model domain. Flow directions and velocities are also very similar between the two models. Minor differences are seen at the boundaries, largely due to the influence of the different surface Digital Elevation Models used to define the top surface hydraulic head boundary. These differences do not influence flow within the Guelph layer to a significant degree.

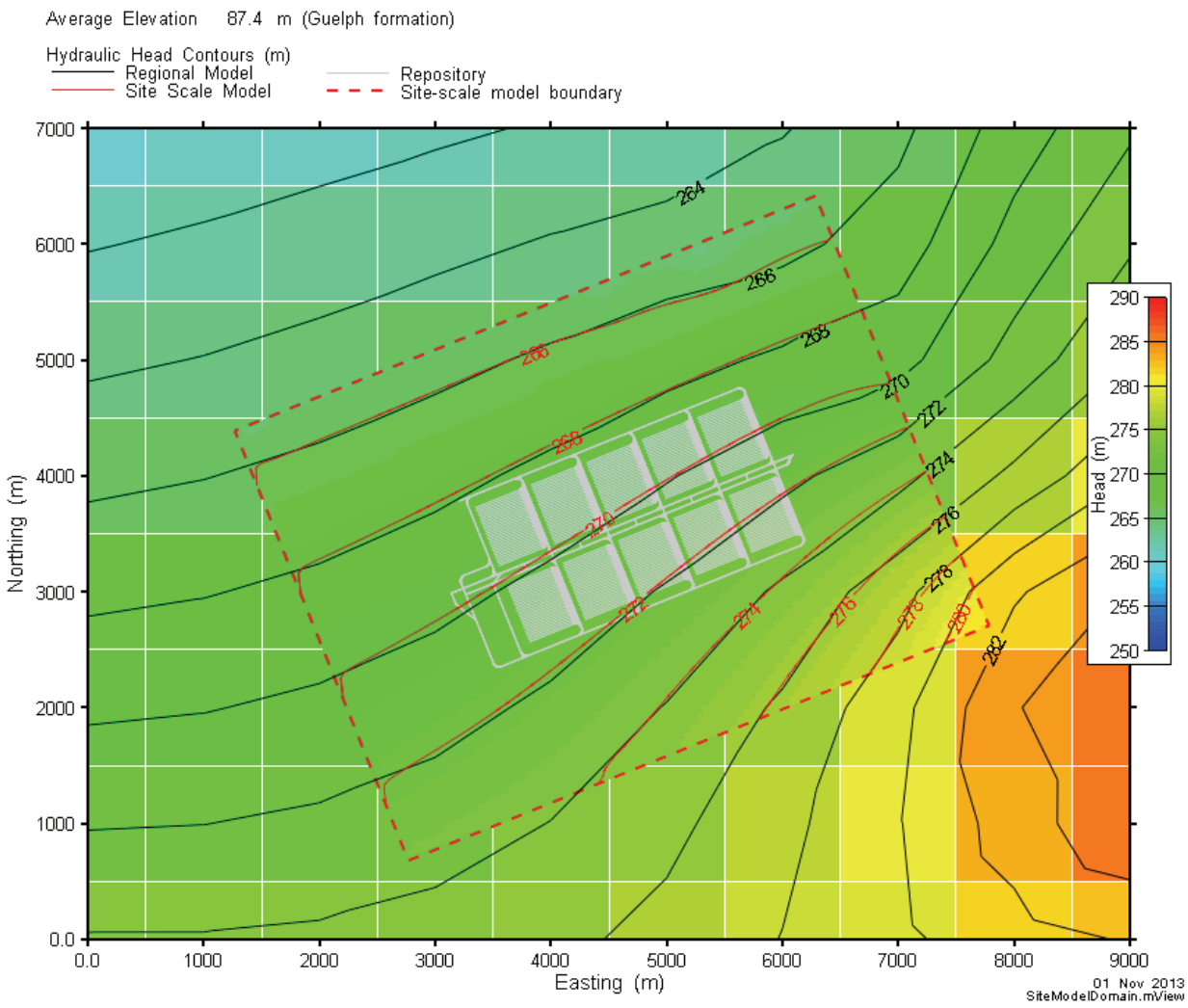

Figure 7-35: Site-Scale Model - Comparison of Hydraulic Heads with Regional Model at Guelph Formation Elevation (87 mASL)

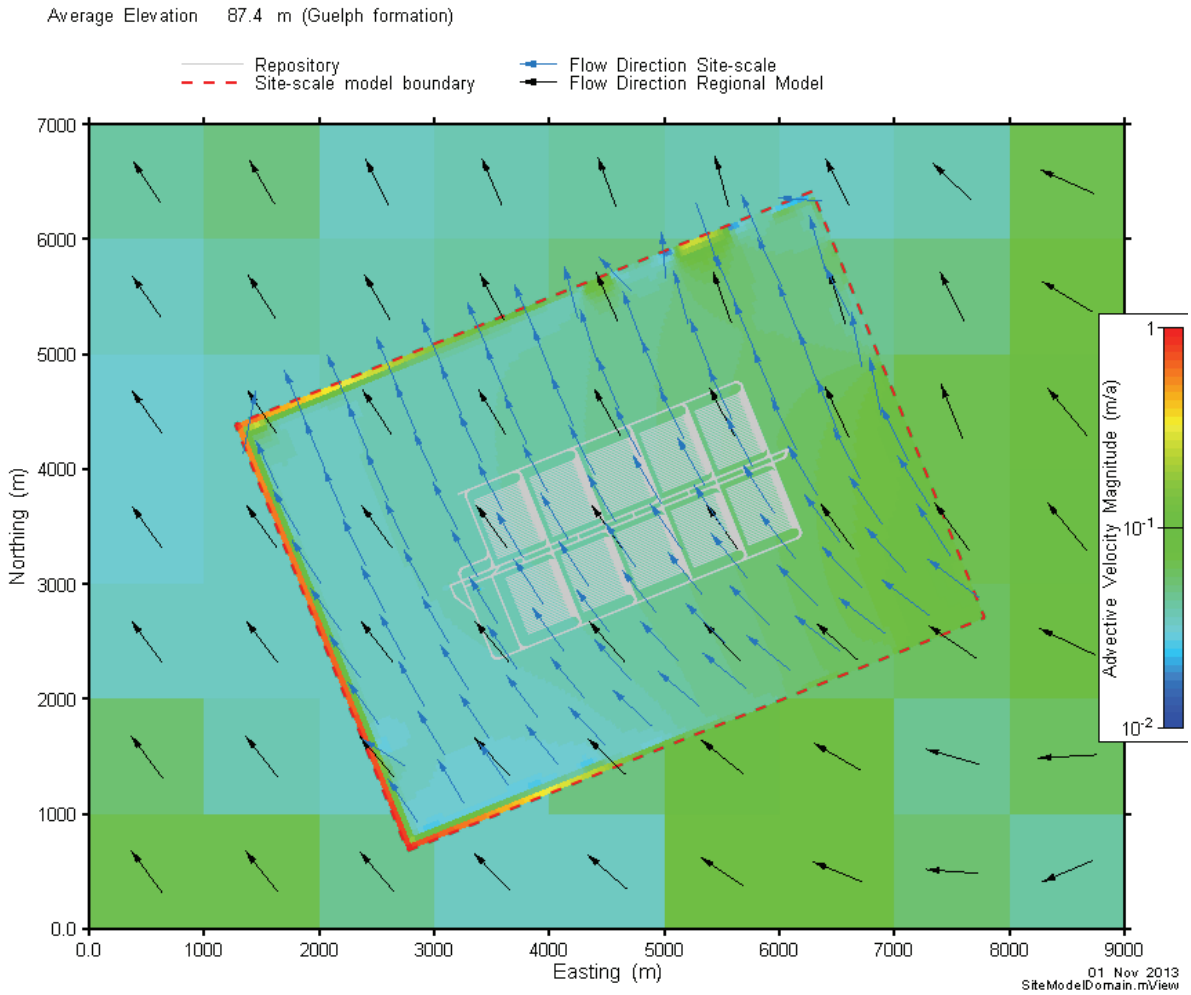

Note: minor differences occur due to the influence of a higher resolution Digital Elevation Model

Figure 7-36: Site-Scale Model - Comparison of Velocities in the Guelph Formation with Regional Model

Figure 7-37 shows a similar comparison of Darcy velocity magnitudes between the Regional and Site-Scale Models. The figure illustrates that repository features have no significant effect on the flow system (since the repository is not included in the Regional Model). The higher hydraulic conductivities of the repository EBS and EDZ cause higher velocity within the repository and shafts; however, even these velocities are very low – transport is clearly diffusion-dominant even in these features.

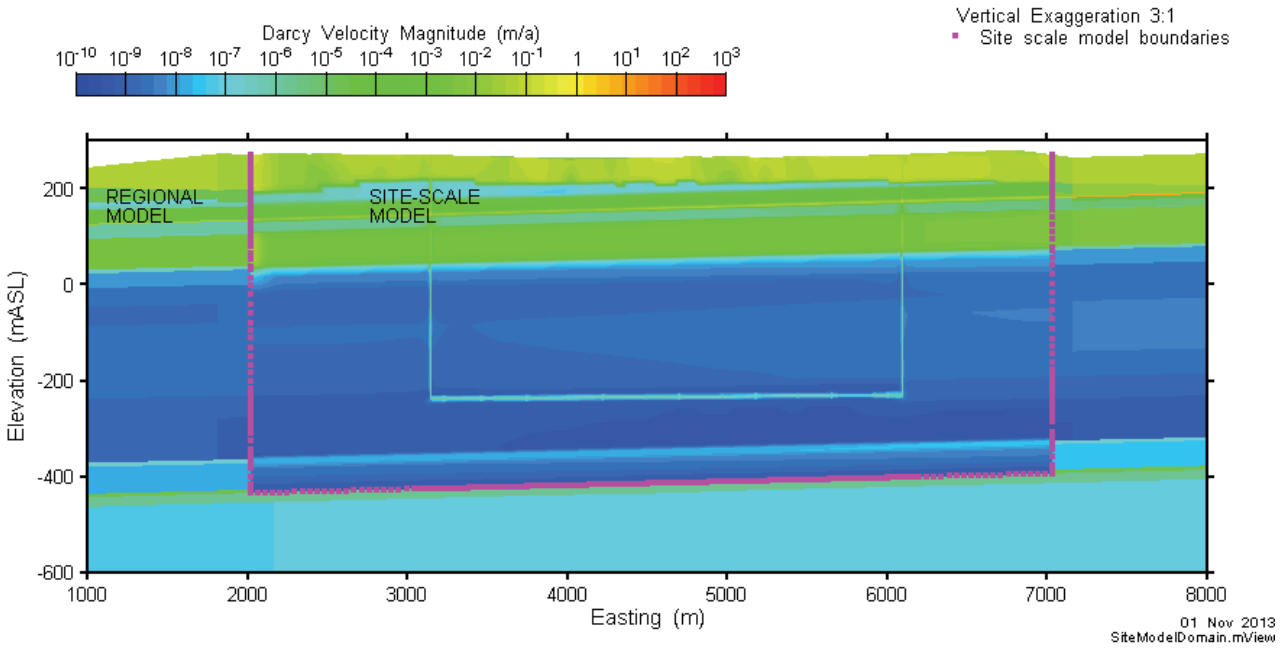

Figure 7-37: Site-Scale Model - Comparison of Velocities at a Vertical Cross-Section along Access Tunnel 1

Figure 7-38 shows the Mean Life Expectancy (MLE), taking both advective and diffusive processes into account. In this context, “Life Expectancy” is the time for a contaminant at any subsurface location to discharge to the biosphere. Since transport disperses the species through the geosphere, life expectancy is represented by a probability density function, obtained by solving for transport at each nodal upstream point. The Mean Life Expectancy represents the average time for a contaminant at any subsurface location to discharge to the biosphere.

In the Site-Scale model, MLEs are defined by the time taken for a contaminant to reach a model boundary and then exit the model. Contaminants can only exit through boundaries defined by fixed hydraulic heads, not through no-flow boundaries. Accordingly, MLEs for the Site-Scale model illustrate the time for contaminants to reach the surface or the sides of the model above the Guelph – the sides of the model below the Guelph are defined as no-flow.

The figure shows the majority of the repository is situated in rock in which the MLEs are 10^8 to 10^9 years. The relatively minor effect of the repository and shafts on the MLE is also evident.

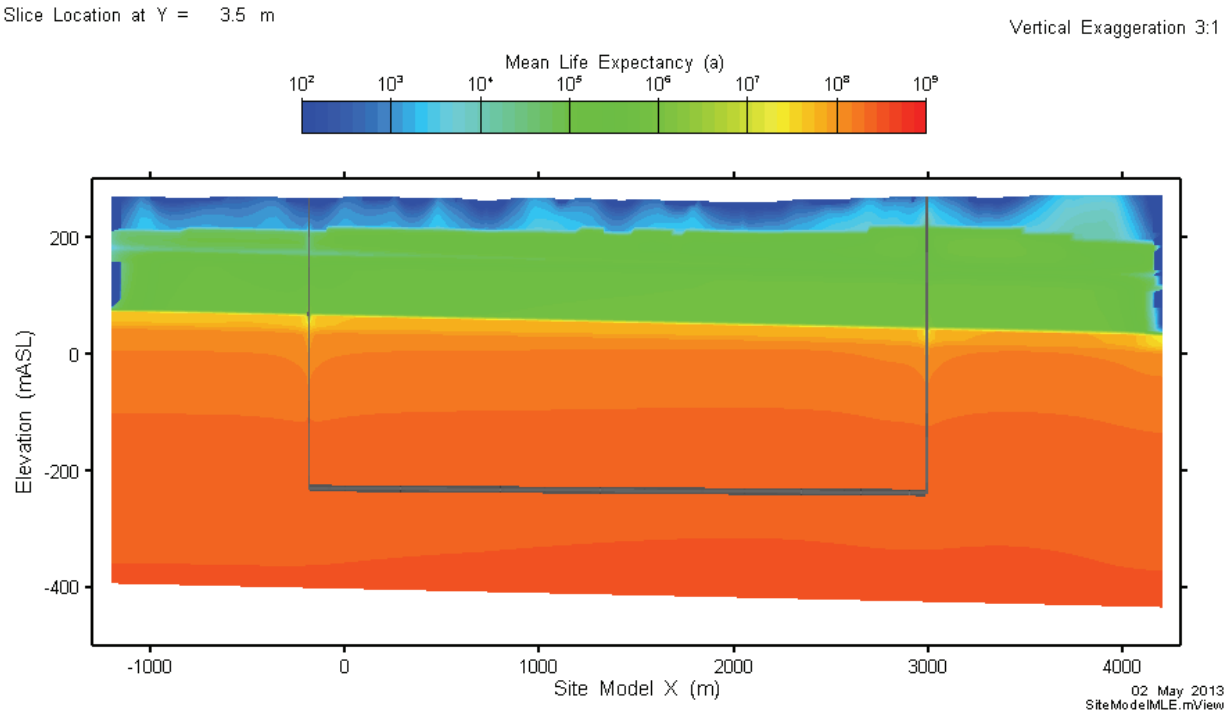

Note: The shafts and repository are shown to provide orientation.

Figure 7-38: Site-Scale Model - Mean Life Expectancy

7.7.1.1.2 Reference Case

Figure 7-39 and Figure 7-40 show the results of flow modelling on two cross sections (an XZ and a YZ section) and two plan sections at different elevations (repository depth and bottom of the Guelph aquifer) with well demand set to 1307 m^3/a.

Figure 7-39 displays the hydraulic head distribution. The cross sections were chosen to intersect the pumping well in the Guelph layer, and do not intersect the shafts. There is a small upward vertical hydraulic head gradient from the bottom of the model towards the Guelph and parts of the model surface. The two cross sections and the Guelph plan section clearly show the influence of the water supply well.

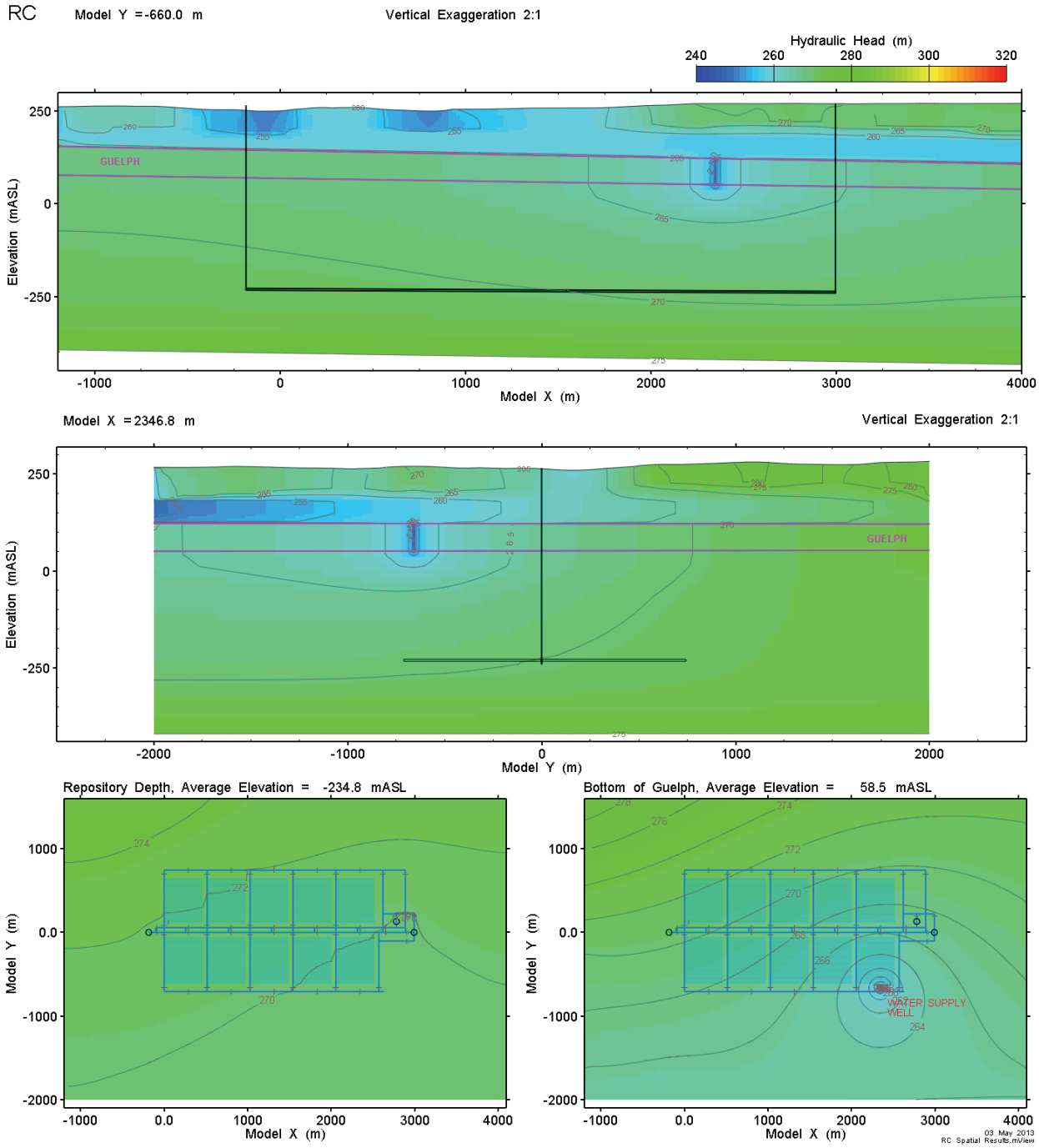

Note: The shafts and repository are shown to provide orientation.

Figure 7-39: Site-Scale Model - Reference Case Hydraulic Head Distribution

Figure 7-40 shows advective velocities on the same set of sections, with the exception of the XZ section which has been moved to show velocities along the main tunnel and in two shafts. It is clear that velocities in the deep system are extremely low. Even where shafts and tunnels are

present the velocity remains very low. Due to the low relief of the terrain and the higher conductivity of the Guelph unit there is very little hydraulic gradient between the shafts. Velocity arrows are only shown where velocity exceeds 10^{-4} m/a, below which the system is diffusion-dominated. Once again, the plan section through the Guelph shows the area influenced by the water supply well.

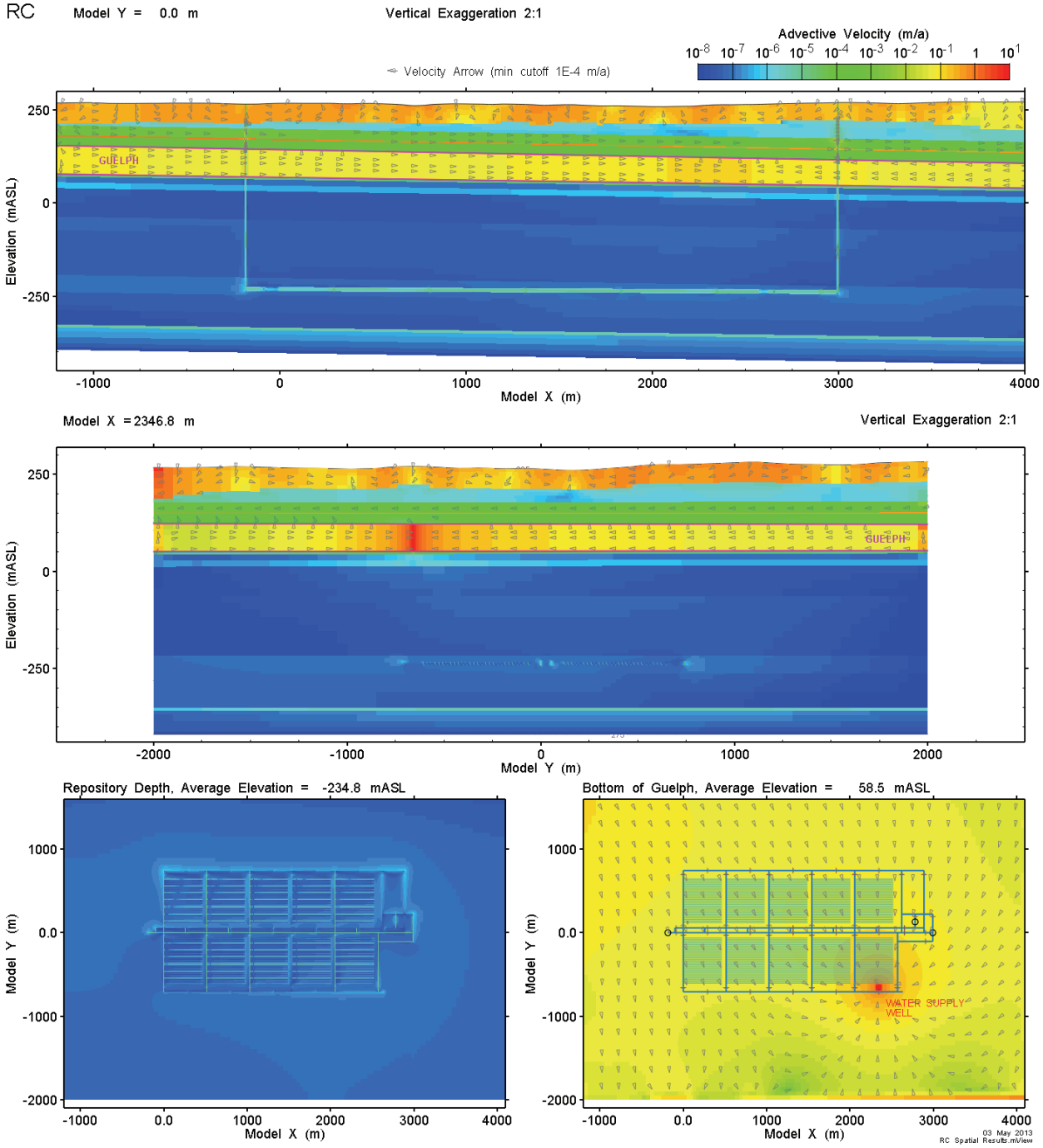

Figure 7-40: Site-Scale Model - Reference Case Advective Velocity Distribution

Figure 7-41 and Figure 7-42 show mean life expectancy on two cross sections. As was the case with no pumping well, mean life expectancy in the repository is very long.

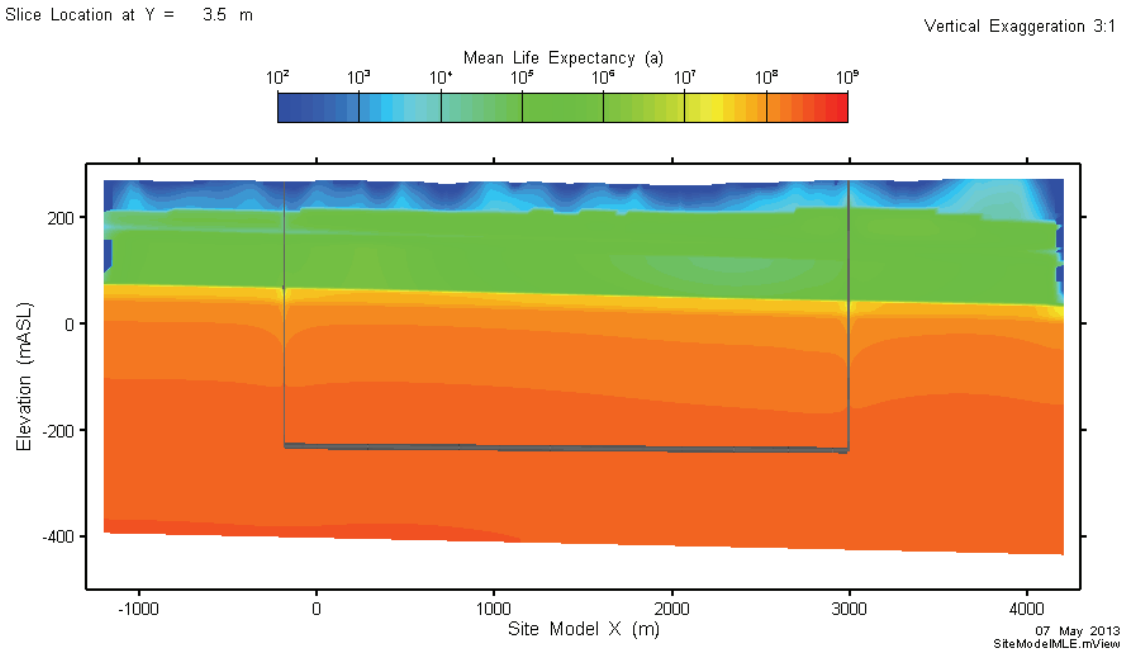

Note: The shafts and repository are shown to provide orientation.

Figure 7-41: Site-Scale Model - Mean Life Expectancy at Repository Centre

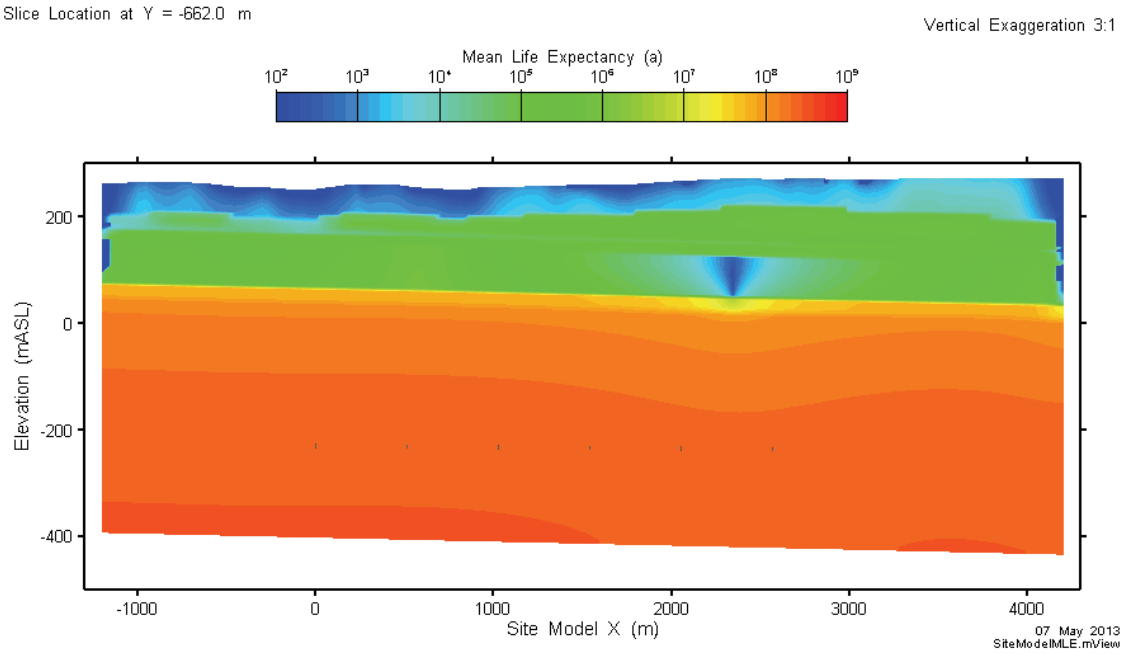

Figure 7-42: Site-Scale Model - Mean Life Expectancy at Water Supply Well

7.7.1.2 Radionuclide Transport Results

Radionuclide transport modelling has been performed for I-129, Cs-135, U-234 and U-238. The FRAC3DVS-OPG model calculates both advective and diffusive transport.

Radionuclide fluxes out of the defective containers, determined from the SYVAC-CC4 model, are applied as a boundary condition equally over two nodes located at the vertical midpoint of the placement room at the location of the three defective containers[4]. The defective containers are located approximately midway through the room closest to the water supply well, in the corner of the repository where the geological barrier is thinnest.

Figures are shown with shading at times greater than one million years to emphasize that results at these times are illustrative and included only to indicate model behaviour.

7.7.1.2.1 Location of the Well and Defective Containers

The choice of well location is based on earlier modelling (Section 7.5.3.1) in which seven different well locations were assessed in terms of the flux of contaminants captured by each well, while simulating a release from all containers in the repository. Some of the well locations were near the sealed shafts, while others were located downstream of the plume in the Guelph aquifer. This analysis found the maximum contaminant transport is to a well located slightly downstream (in the Guelph) of the repository sector for which the rock separating the Guelph from the repository (essentially, the diffusive barrier thickness) is thinnest.

7.7.1.2.2 Reference Case

Figure 7-43 and Figure 7-44 illustrate the time dependent behaviour of the I-129 plume on two cross sections (an XZ and a YZ section) and two plan sections at different elevations (repository depth and bottom of the Guelph aquifer). The contour plots are on a logarithmic scale. The outer concentration contour, 1 Bq/m^3, corresponds to an effective I-129 drinking water dose of about 0.1 μSv/a based on the Table 7-26 water consumption rate of 0.84 m^3/a per person.

The round shape of the plume indicates that transport is diffusion-dominated. Higher diffusivity, particularly in the dense backfill blocks does cause some preferential transport along tunnels in the repository, evident in the repository-depth plan sections.

[4] Although applied at two nodes, the source term represents a simultaneous failure of three containers.

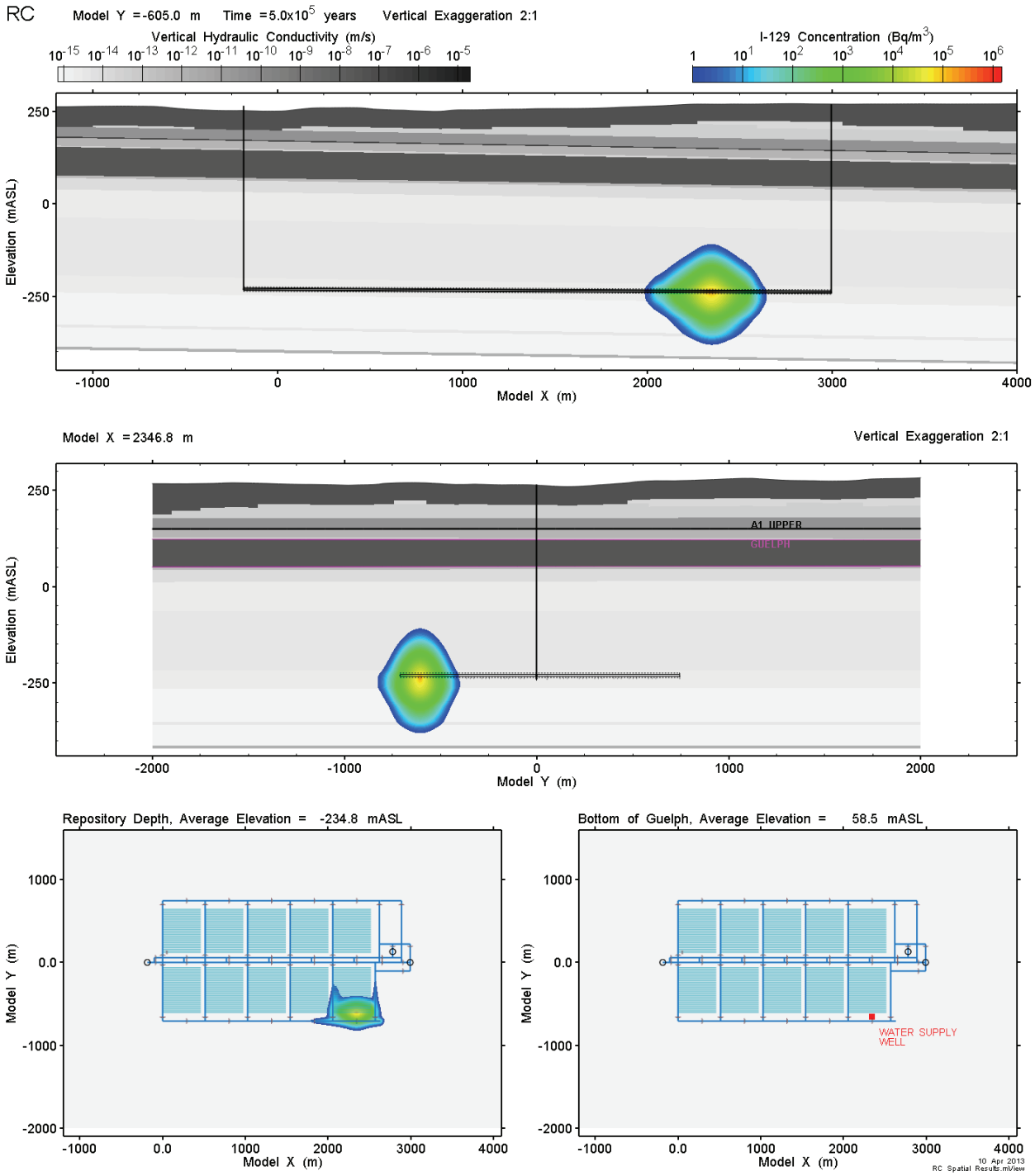

Note: The shafts and repository are shown to provide orientation.

Figure 7-43: Site-Scale Model - Reference Case I-129 Concentration at 500,000 Years

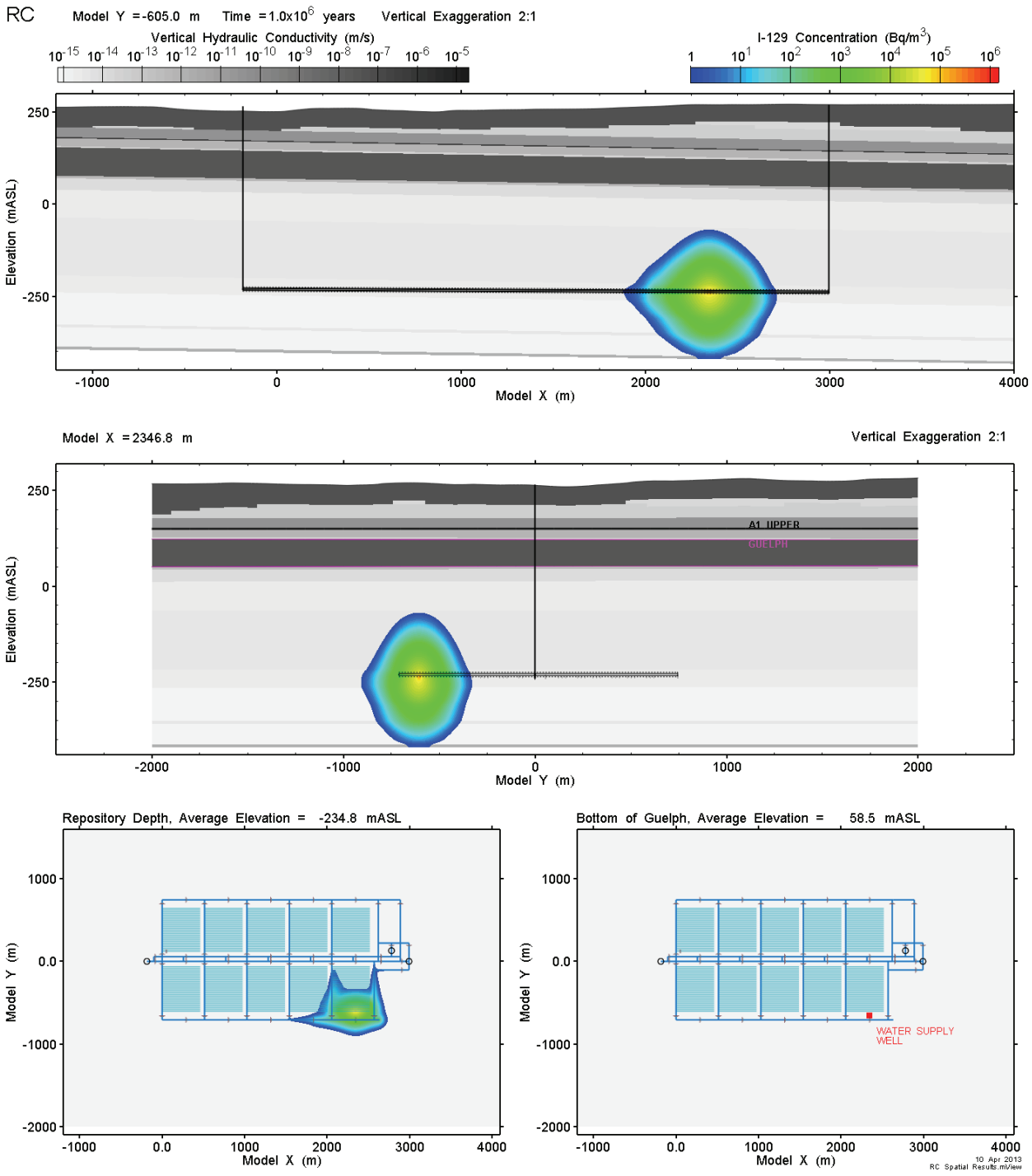

Note: The shafts and repository are shown to provide orientation.

Figure 7-44: Site-Scale Model - Reference Case I-129 Concentration at One Million Years

Figure 7-45 shows the Cs-135 concentration distribution on a vertical cross section at 1 million years. Compared to I-129, transport of Cs-135 is greatly reduced by sorption of cesium on rock and EBS materials. The asymmetrical shape of the plume is caused by much higher sorption coefficients in the Georgian Bay, Blue Mountain, and Queenston shale above the repository compared to those in the predominantly limestone Cobourg, Sherman Fall, and Kirkfield units (see Table 7-15).

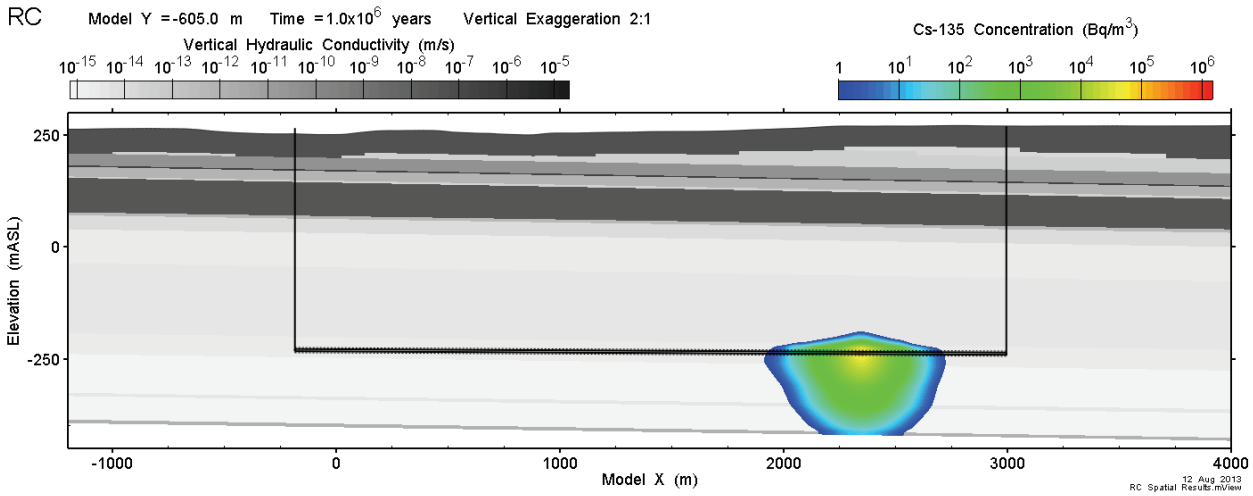

Note: The shafts and repository are shown to provide orientation.

Figure 7-45: Site-Scale Model - Reference Case Cs-135 Concentration at One Million Years

The U-234 and U-238 concentration distributions at 1 million years are not resolvable on the scales used in these figures. Sorption coefficients for uranium (see Table 7-15) are much higher than those for cesium, and this has a clear impact on the movement and concentration of uranium.

Figure 7-46 presents radionuclide transport rates to the well for all simulated nuclides. The results show that there is essentially no release to the well over the one million year baseline period.

Beyond that time, I-129 would start to be seen, while the sorbing species Cs-135, U-234, and U-238 do not reach the well in significant amounts due to retention and decay in the engineered barrier system and geosphere near the repository. The time of peak concentration for I-129 at the well is outside the 1 million year time frame of interest, and also outside the 10 million year period that is shown to illustrate model behaviour.

The maximum I-129 transport rate over the 10 million year period is 7.4 Bq/a.

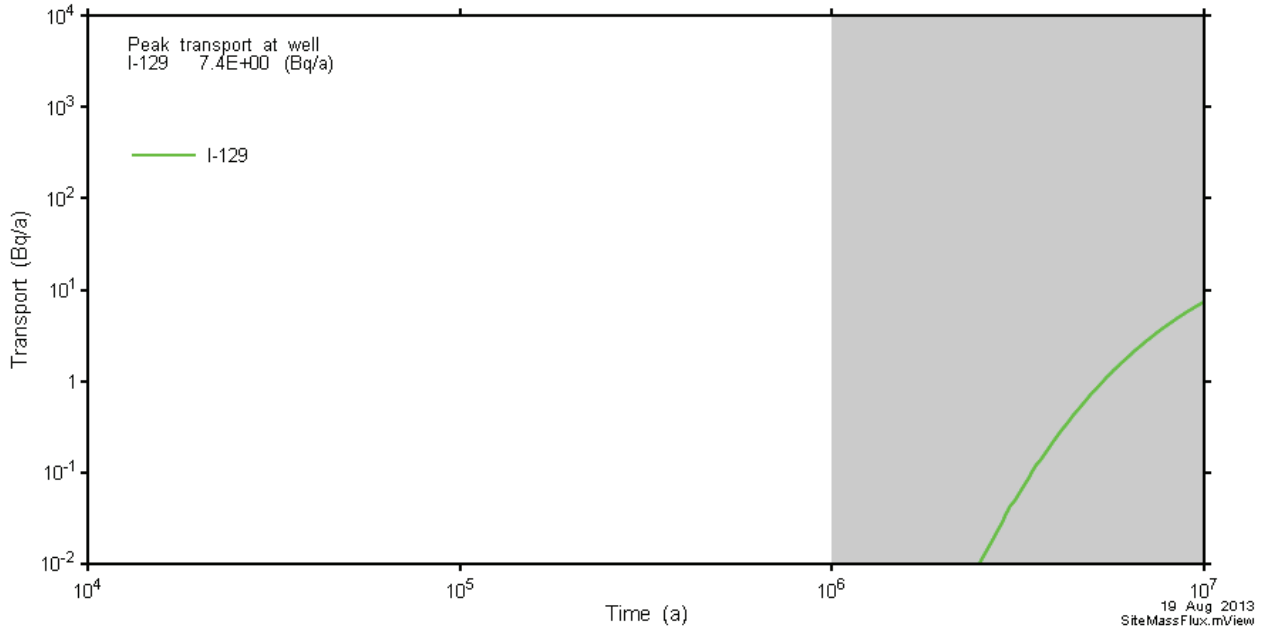

Note: Cs-135, U-234 and U-238 are off-scale low

Figure 7-46: Site-Scale Model - Reference Case Radionuclide Transport to Well

7.7.1.2.3 Sensitivity to a Factor of 10 Increase in Geosphere Hydraulic Conductivity

This section examines the effect of increasing geosphere hydraulic conductivities by a factor of 10. Table 7-17 shows the values used.

Figure 7-47 and Figure 7-48 show I-129 plume development over time is very similar to the Reference Case. The round shape of the plume indicates that transport is diffusion-dominated with no apparent effect of the upward vertical flow gradient on the shape of the plume. As before, higher diffusivity causes some preferential transport along tunnels in the repository, evident in the repository depth plan sections. Results for uranium and cesium are not shown, as they are also similar to the Reference Case results discussed in the previous section.

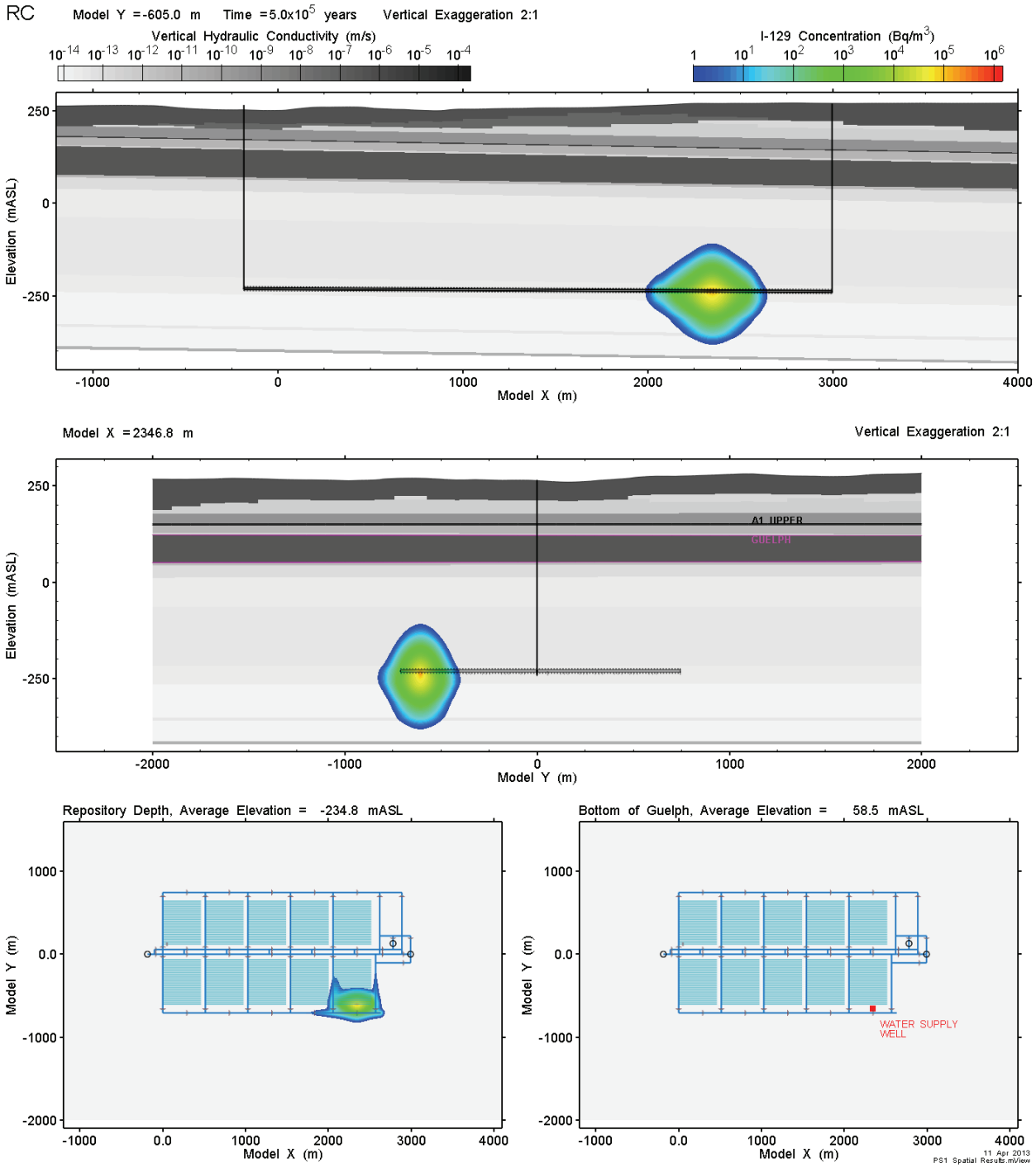

Figure 7-47: Site-Scale Model - Geosphere Hydraulic Conductivity Increased by a Factor of 10: I-129 Concentration at 500,000 Years

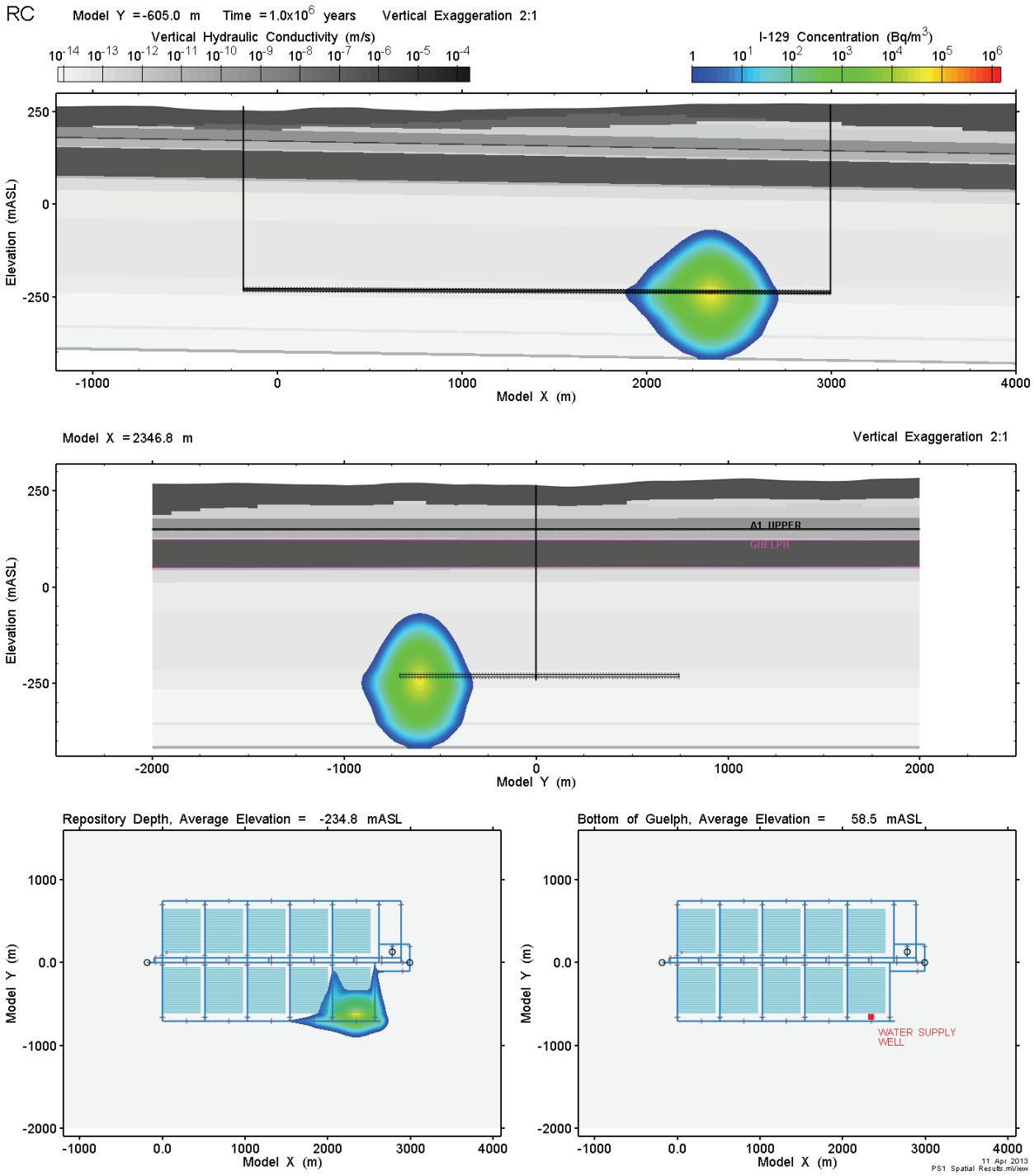

Figure 7-48: Site-Scale Model - Geosphere Hydraulic Conductivity Increased by a Factor of 10: I-129 Concentration at One Million Years

Figure 7-49 shows the radionuclide transport rates to the well for I-129 together with the Reference Case results.

The I-129 transport rate reaches a maximum value of 6.2 Bq/a at 10 million years. This is lower than the Reference Case value of 7.4 Bq/a due to the higher hydraulic conductivity of the Guelph unit. This higher conductivity reduces the capture zone of the well, allowing a larger proportion of the plume to bypass the well and cross the model boundary. The radionuclide arrival time is only very slightly earlier, again indicating that the transport of radionuclides from the repository remains diffusion-dominated.

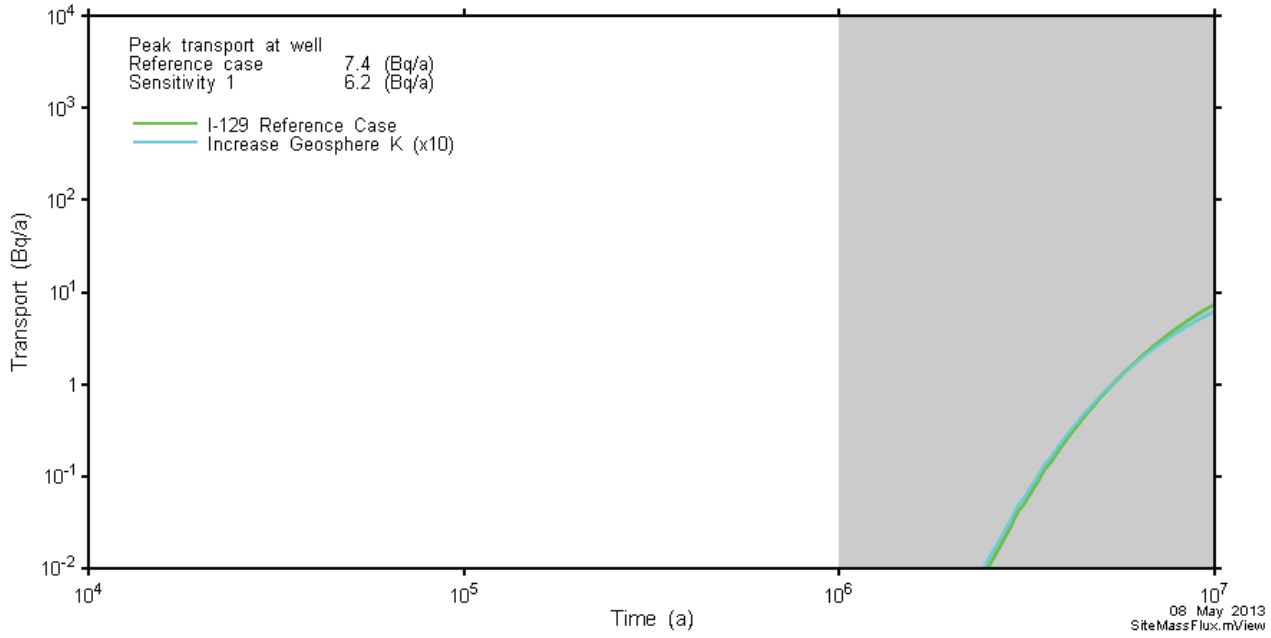

Figure 7-49: Site-Scale Model - Hydraulic Conductivity Increase by a Factor of 10: Radionuclide Transport to Well

7.7.1.2.4 Sensitivity to 100 m of Surface Erosion

This section examines the effect of 100 m of surface erosion caused by repeated glaciations occurring over the one million year period of interest.

FRAC3DVS-OPG simulations have not been performed for this case. With 100 m of erosion, the top of the Guelph formation would be about 40 m below grade (rather than 140 m below grade), but still capped with the very low permeability units of the Salina formation. Even if these units become more permeable due to their nearer surface exposure, the overall system would remain diffusion-dominant, with radioactivity reaching the Guelph on the same time-scale and proceeding from there to the well and biosphere with the same capture rate.

No significant changes to the rate of radionuclide release to the biosphere would therefore result.

7.7.1.2.5 Sensitivity to Spatial Resolution and Time Step Size

This section examines the effect of increasing the spatial resolution and decreasing the time step size on the Reference Case results.

Spatial Resolution

The potential impact of changing spatial resolution has been assessed by comparing results obtained from the Site-Scale Model and the Repository-Scale Model. The Repository-Scale Model has a more highly resolved grid, with a node density increase of more than 10 times.

Figure 7-50 shows a comparison of head contours between the two models. There is very good correspondence, indicating that the resolution of the Site-Scale Model is sufficient to adequately model the flow field.

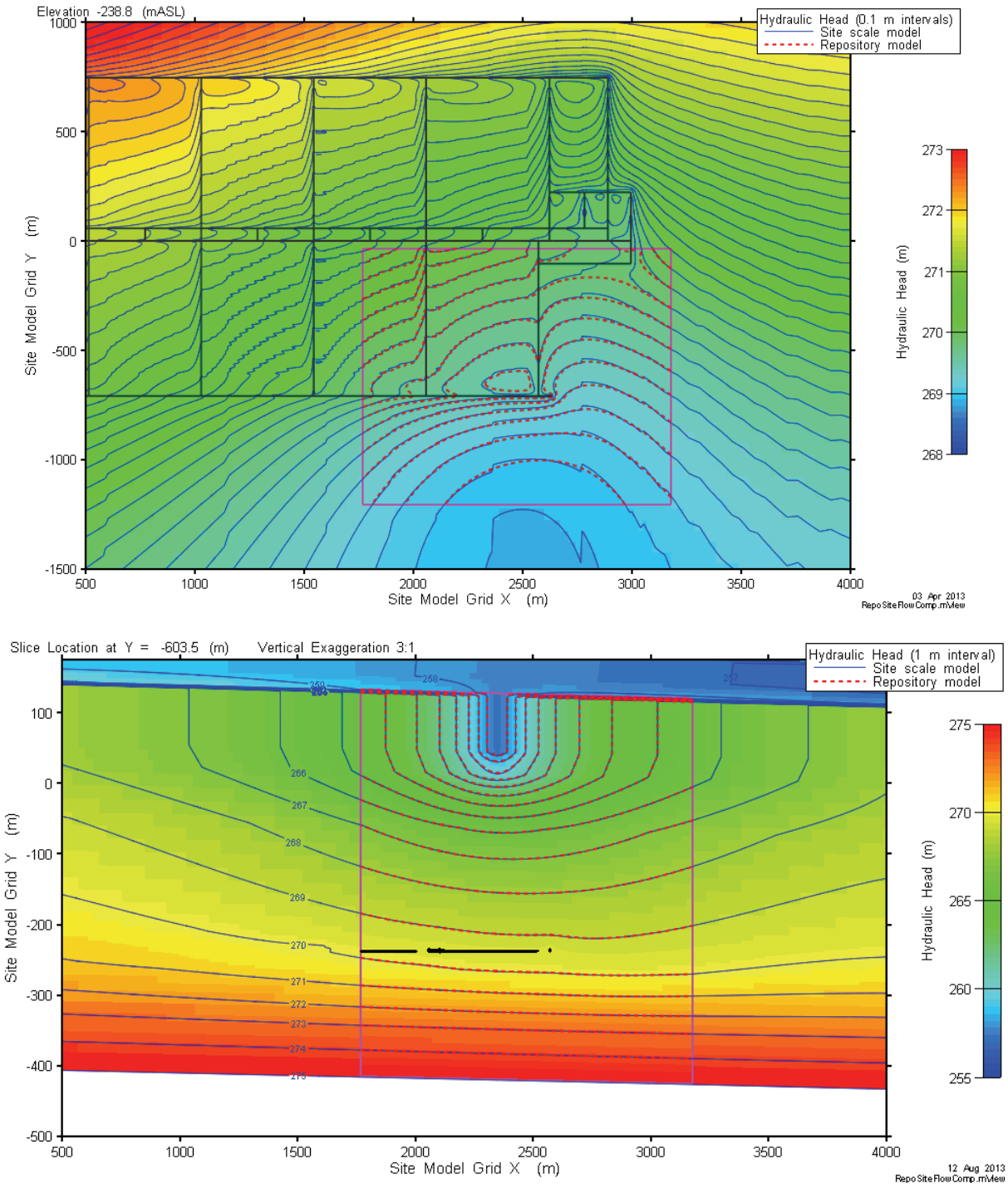

Figure 7-50: Site-Scale Model - Spatial Convergence Sensitivity Comparison of Head Contours

Figure 7-51 compares results for the I-129 plume at 1 million years. The figure shows only minor differences in concentration contours, with the largest variations occurring where differences in tunnel representation (especially the EDZ representation) have a minor influence on solute transport. The lower resolution grid slightly increases diffusive flux in the formations above the repository.

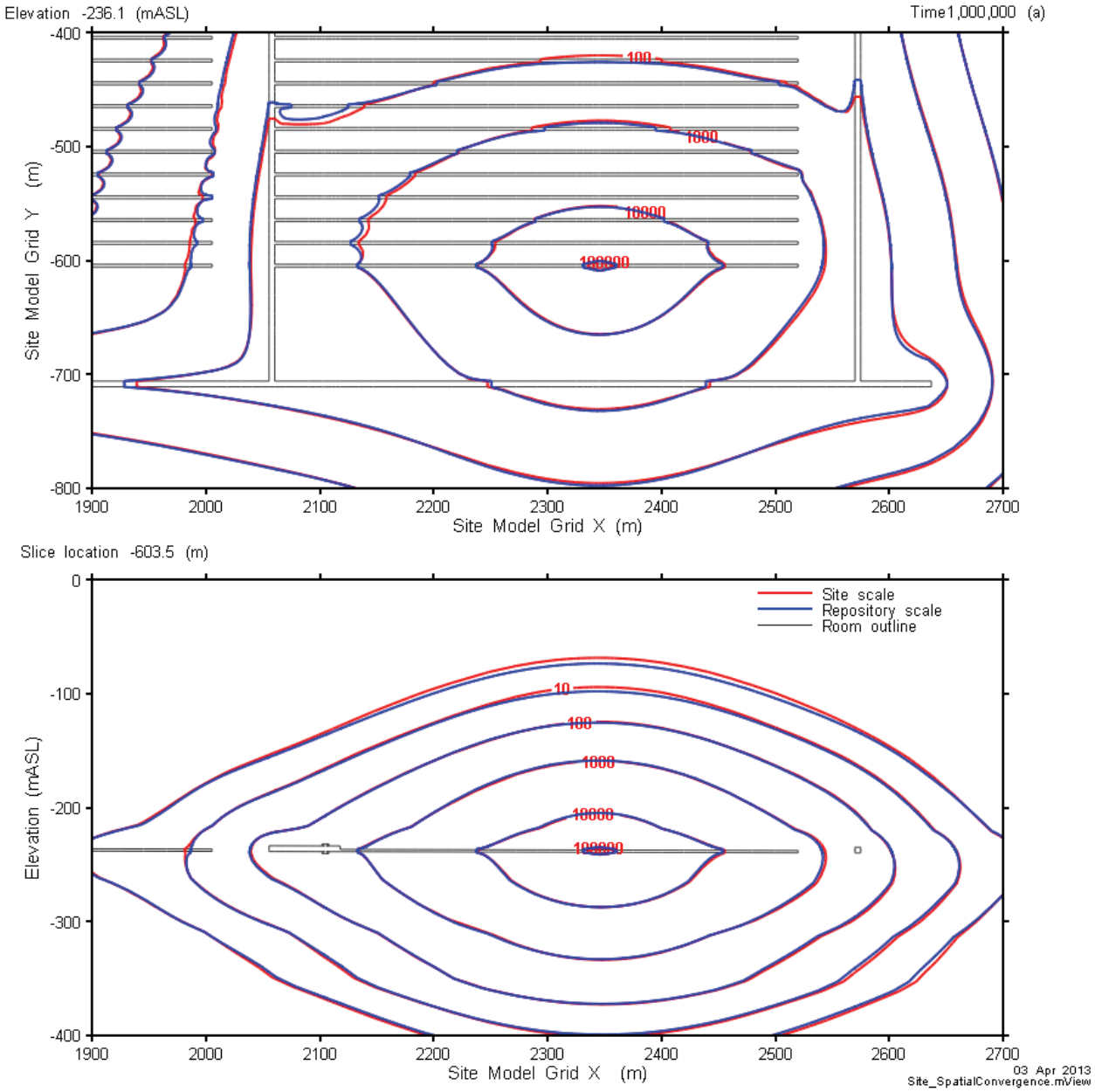

Figure 7-51: Site-Scale Model - Spatial Convergence Sensitivity I-129 Plume

Figure 7-52 compares results for I-129 transport across two planar surfaces (i.e., the top of the Cobourg and Georgian Bay formations) as well as transport to the well. Results compare very well, and the minor differences are not significant in the context of the postclosure safety assessment.

It is therefore concluded that the spatial discretization in the Site-Scale Model is appropriate.

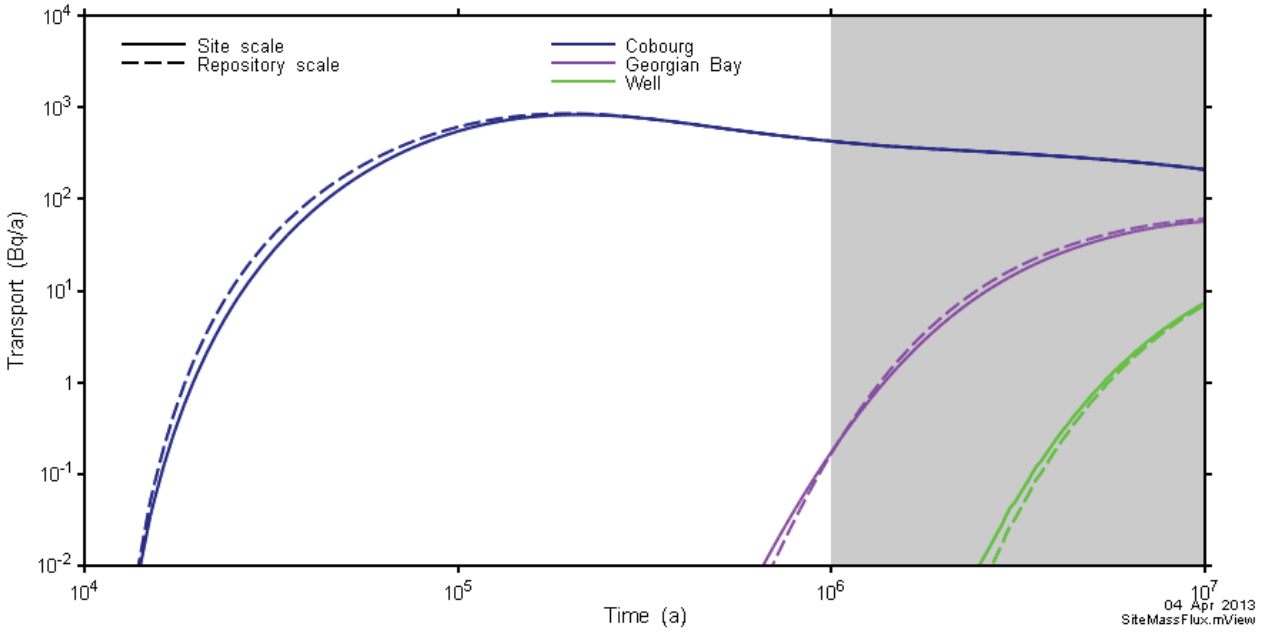

Figure 7-52: Site-Scale Model - Spatial Convergence Sensitivity, I-129 Transport

Temporal Resolution

To determine the effect of time step size, control parameters were modified in the Reference Case Site-Scale Model. These changes result in a factor of two decrease in the number of time steps in one simulation and a factor of three increase in another.

Figure 7-53 shows that these changes have essentially no effect on the I-129 transport rate to the well.

It is therefore concluded that the temporal discretization in the Site-Scale Model is appropriate.

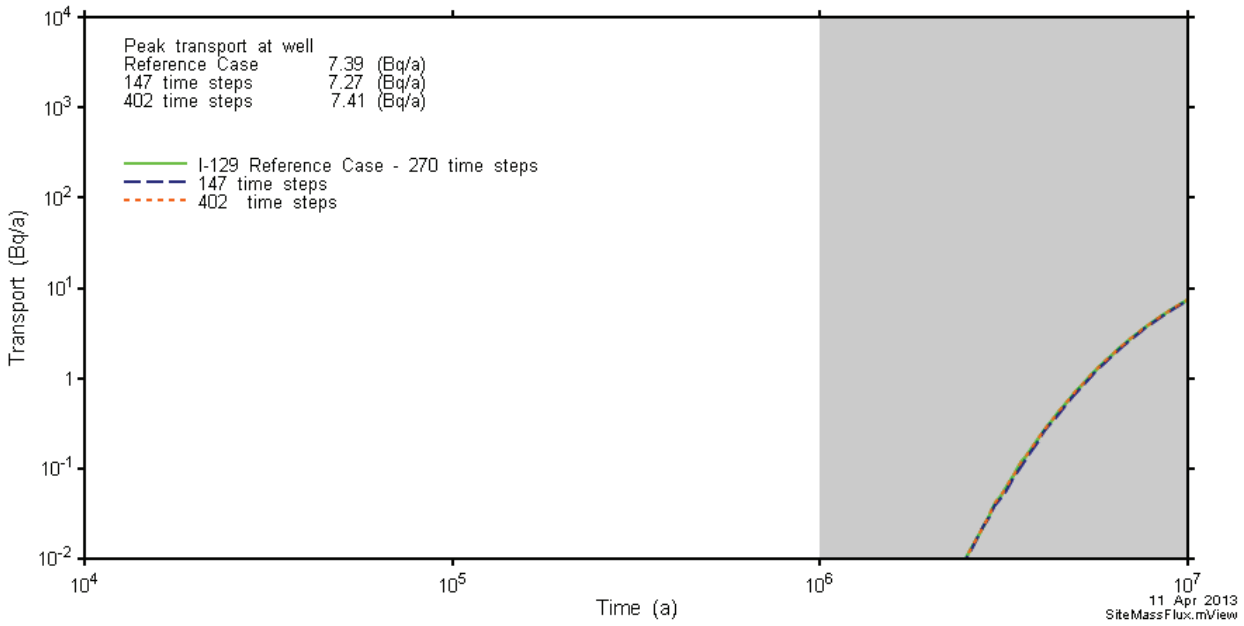

Figure 7-53: Site-Scale Model - Time Step Convergence Sensitivity: I-129 Transport to the Well

7.7.1.2.6 Other Sensitivity Cases

This section presents results for the sensitivity cases listed in Table 7-30.

Results for the Shaft Seal Failure Disruptive Scenario are also presented here for ease of comparison.

Table 7-30: Site-Scale Transport Sensitivity Cases

Sensitivity Case	Description
EDZ High	Reference Case EDZ permeabilities increased by a factor of 10.
Shaft Seal Failure*	The hydraulic conductivities of all shaft seal materials are set to $1x10^{-9}$ m/s and to 1.0×10^{-7} m/s in a subsequent simulation. Results are shown for the latter case. The locations of the defective container and the well are the same as in the Reference Case.
Overpressure in the Shadow Lake Formation	The constant head boundary at the base of the model domain is increased from 275 m to 433 m.

Note: * Disruptive Scenario

Figure 7-54 shows summary results for I-129 transport to the well for all cases. Included for comparison are results for the Reference Case.

The results show there is very little effect on either radionuclide arrival times at the well or on radionuclide transport rates. Increasing the EDZ (the “EDZ High” case) or the shaft permeability

(the “Shaft Seal Failure” case) results in no perceptible difference in transport. Increasing the constant pressure boundary at the base of the model domain from 275 m to 433 m (the “Increased Overpressure” case) increases the vertical hydraulic gradient by approximately a factor of 10. This leads to a slightly earlier plume arrival and slightly higher transport to the well.

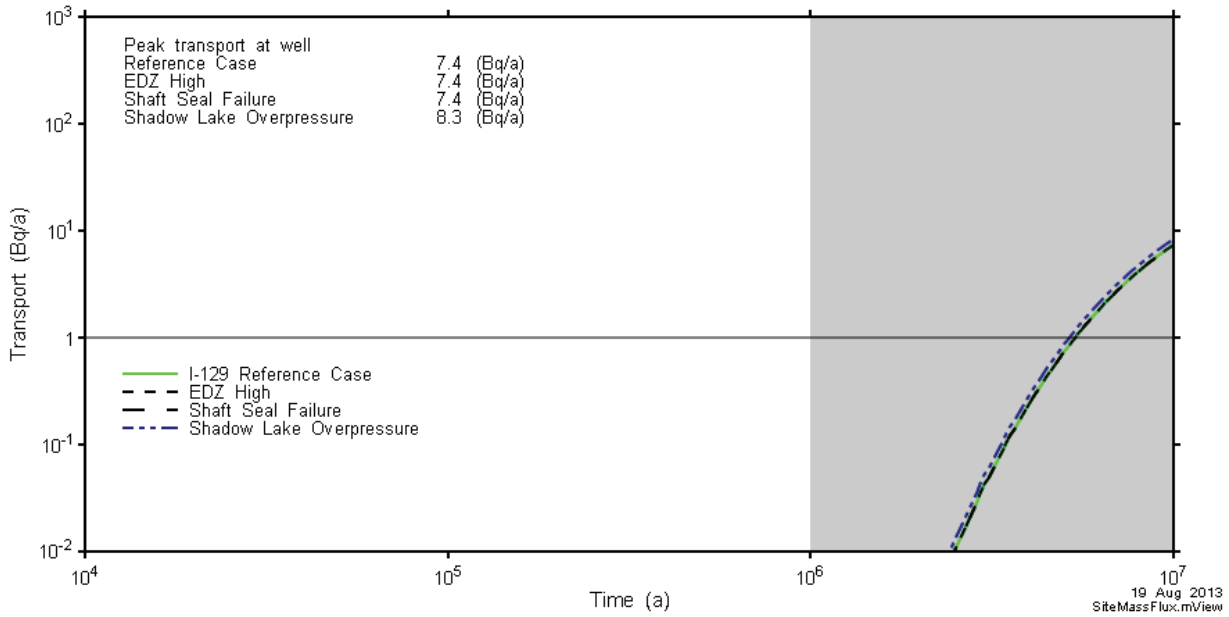

Figure 7-54: Site-Scale Model - I-129 Transport in Sensitivity Cases

7.7.1.2.7 Effect of Barriers on Radionuclide Transport

This section provides information on the effect of the various barriers on radionuclide transport for the Reference Case.

Figure 7-55 through Figure 7-57 show the transport rate for I-129 (a non-sorbing fission product), Cs-135 (an intermediate-sorbing fission product), and U-238 (a highly sorbing actinide). Each figure shows:

- The release rate from the defective containers. As noted in Section 7.5.3.3, the release rates are determined using the SYVAC3-CC4 release model and specified as input to the FRAC3DVS-OPG simulation. The release rates are the same as those shown in Figure 7-31.
- The release rate from the repository. This corresponds to transport through the pink-hued surface in Figure 7-61.
- The release rate through the top of the Cobourg and Georgian Bay formations.
- The release rate to the well and all surface locations.

The figures show the retarding effects of the various barriers on the transport of the different radionuclides.

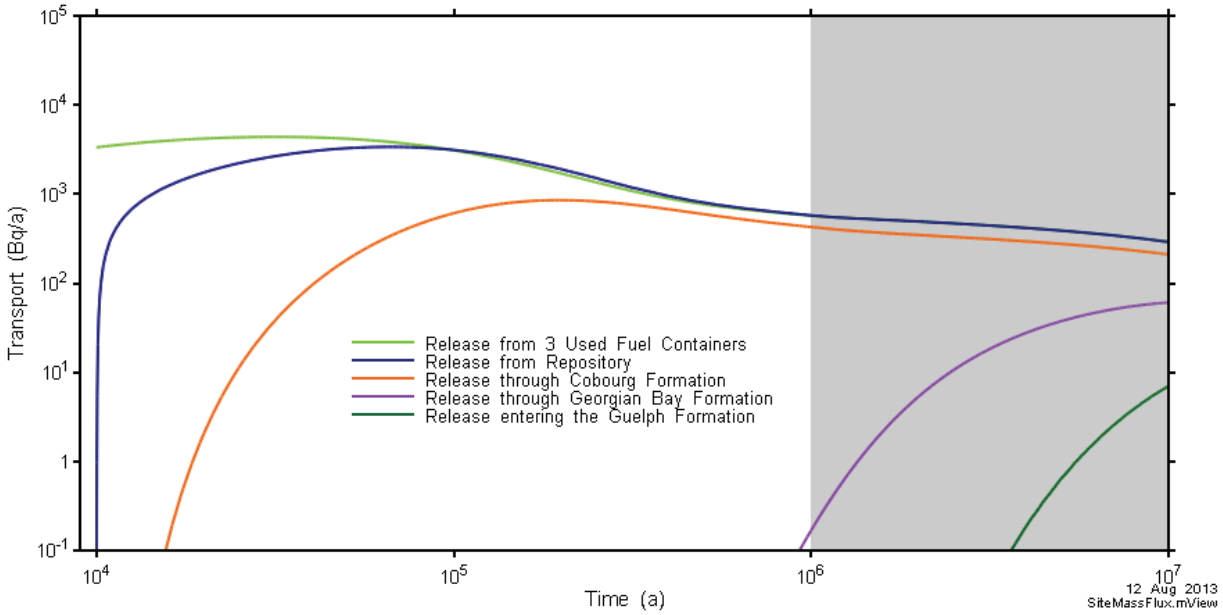

Figure 7-55: FRAC3DVS-OPG - I-129 Transport through Barriers and Selected Geosphere Formations

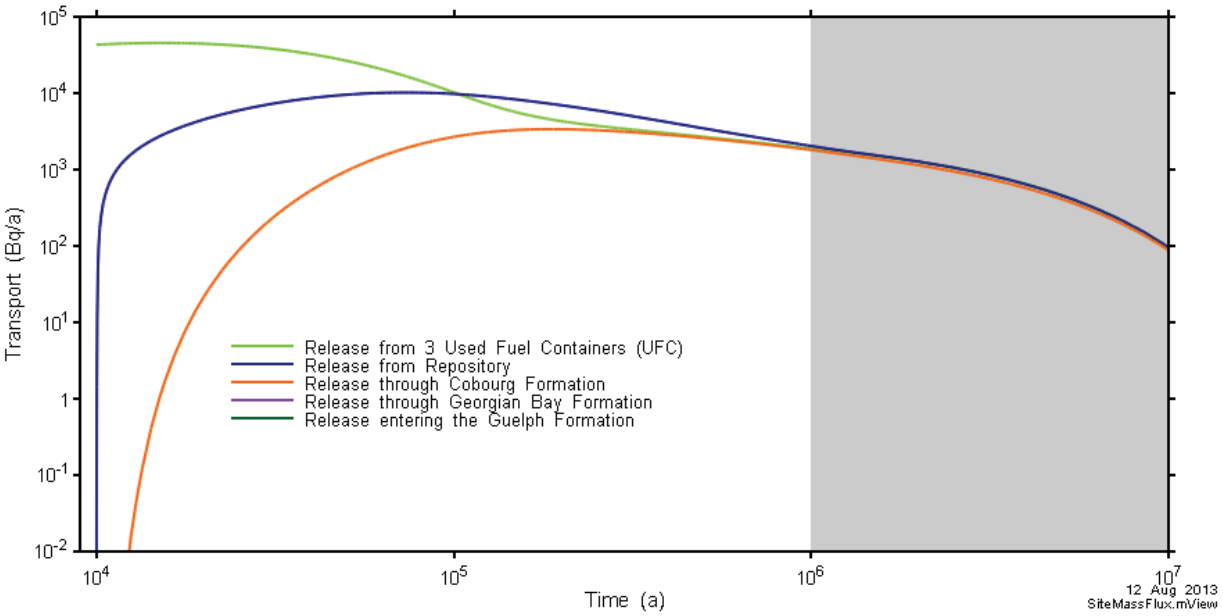

Note: Releases through the Georgian Bay formation and to the Geosphere are off-scale low

Figure 7-56: FRAC3DVS-OPG - Cs-135 Transport through Barriers and Selected Geosphere Formations

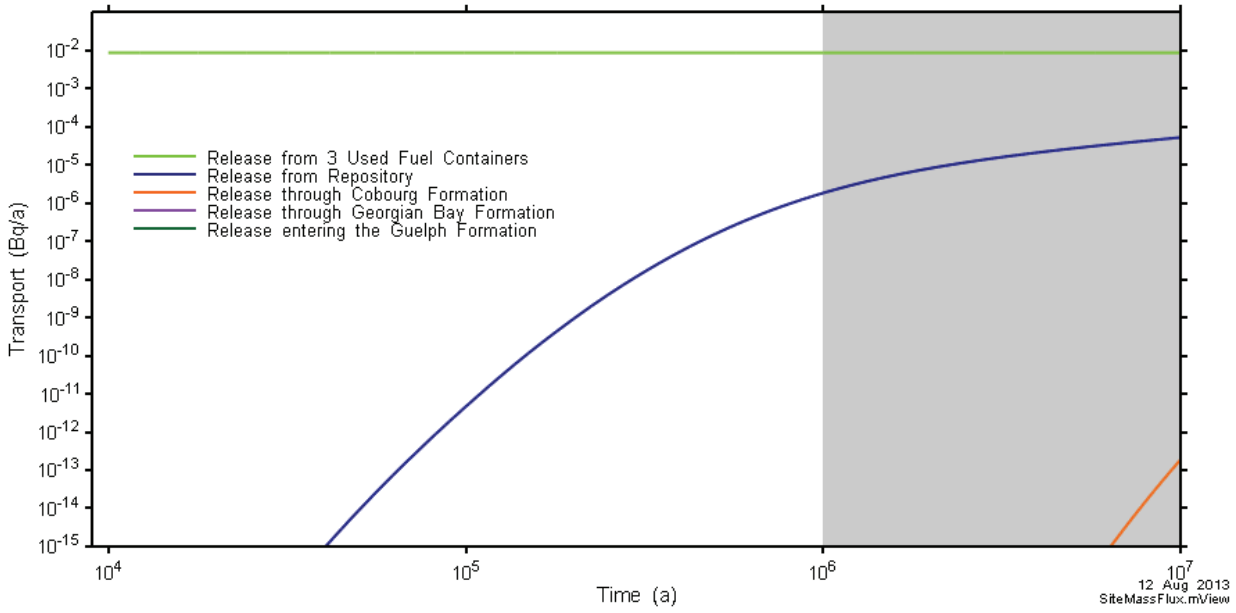

Note: Releases through the Georgian Bay formation and to the Geosphere are off-scale low

Figure 7-57: FRAC3DVS-OPG - U-238 Transport through Barriers and Selected Geosphere formations

In Figure 7-56, releases through the Georgian Bay formation and from the geosphere are off-scale low as a consequence of cesium sorption in Ordovician shales.

In Figure 7-57 releases of U-238 through the top of the Cobourg formation are very low due to sorption on bentonite and Cobourg limestone.

The figures also show that for non-sorbing or moderately sorbing species in a diffusion-dominated system, the bentonite surrounding the containers provides a relatively minor barrier to radionuclide transport. For such species, the geosphere (in this case the Ordovician shales) acts as the primary barrier isolating the radioactive waste from the environment.

7.7.2 Repository-Scale Model

The Repository-Scale Model represents a small section of the repository surrounding the defective containers and the adjacent geosphere. The model incorporates a high level of detail and individual containers are represented at the source location.

Reference Case simulations are performed to corroborate results of the Site-Scale Model and to provide a more complete understanding of repository component functions.

7.7.2.1 Flow Results

7.7.2.1.1 Reference Case

Figure 7-58 and Figure 7-59 show hydraulic head and advective velocities on a plan section through the placement room at the elevation of the repository tunnels. The isolation of the placement rooms and the low velocities throughout the repository are evident in the figures.

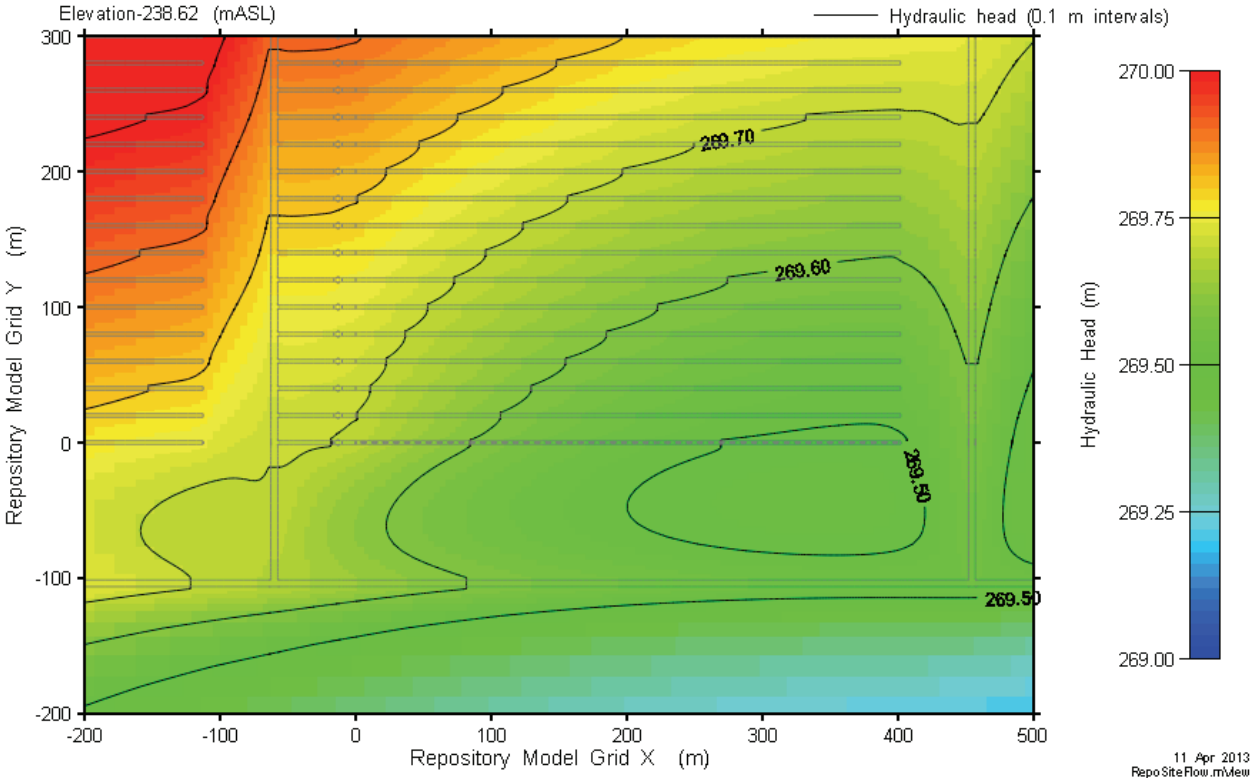

Figure 7-58: Repository-Scale Model - Head at Tunnel Elevation

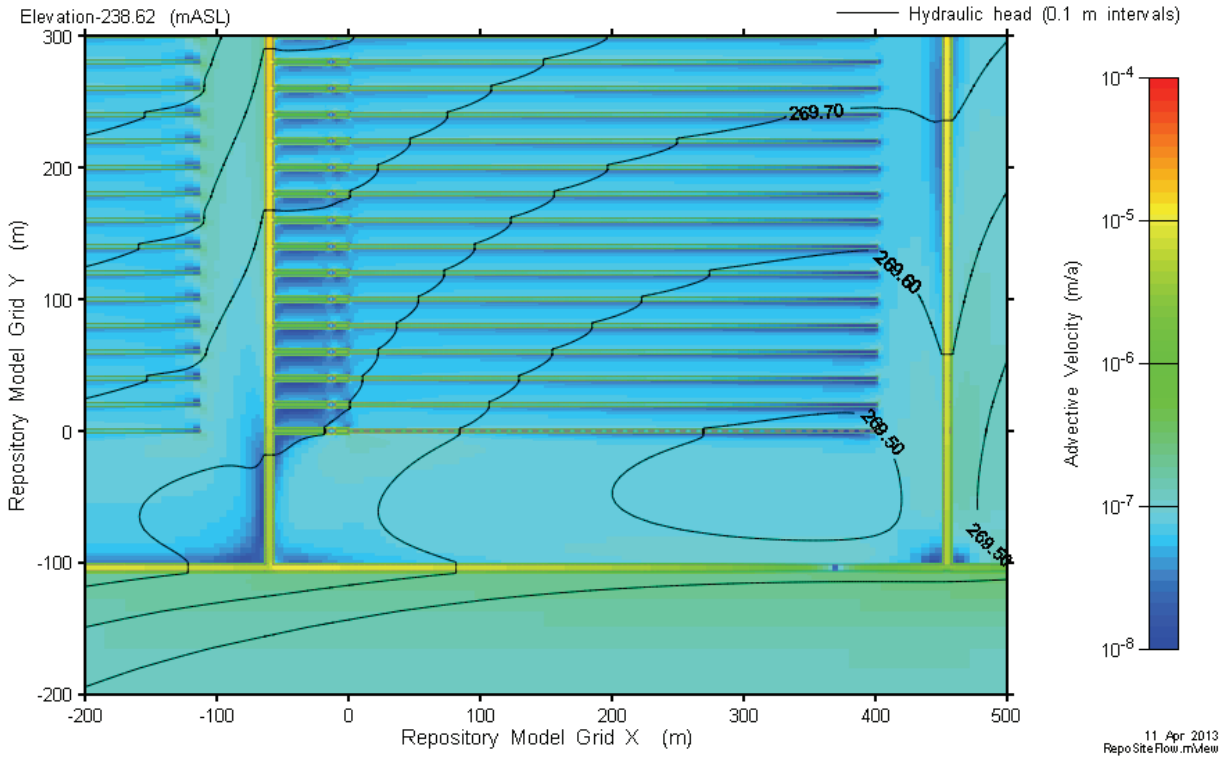

Figure 7-59: Repository-Scale Model - Advective Velocities at Tunnel Elevation

Figure 7-60 shows advective velocities in a 3D view through the EBS and EDZ materials. The highest velocities are in the inner EDZ and in the thin section of inner EDZ around the seal EDZ intercept. The maximum velocities in this plot are below 10^{-4} m/a. At such low velocities, diffusive transport will dominate over advective transport, as the Site-Scale Model results in the previous section indicate.

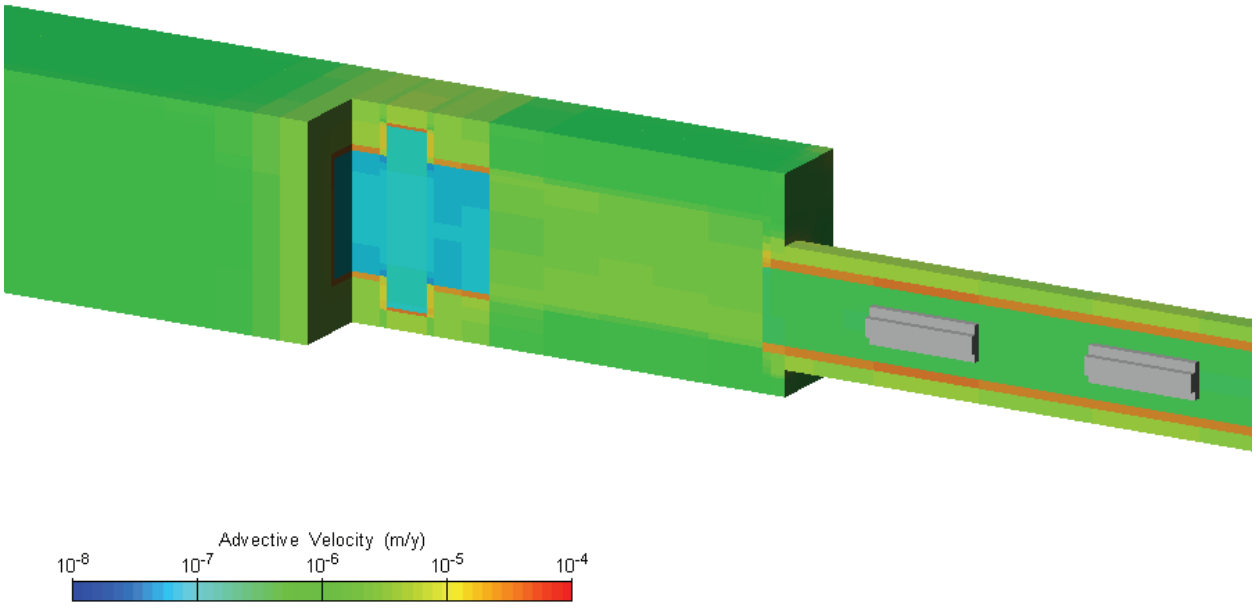

Figure 7-60: Repository-Scale Model - 3D View of Advective Velocity Magnitudes

7.7.2.2 Radionuclide Transport Results

Radionuclide transport modelling is performed for I-129, Cs-135, U-234 and U-238.

Although the source term is from three defective containers, the release is applied to a single container for modelling simplicity. The results are indistinguishable from adjacent container releases at significant distances from the source.

To provide data for later verification of the SYVAC3-CC4 model (Section 7.8.1), radionuclide transport from the used fuel container into the placement room and geosphere (i.e., out of the buffer) is computed over a volume surrounding the defective container as shown in Figure 7-61.

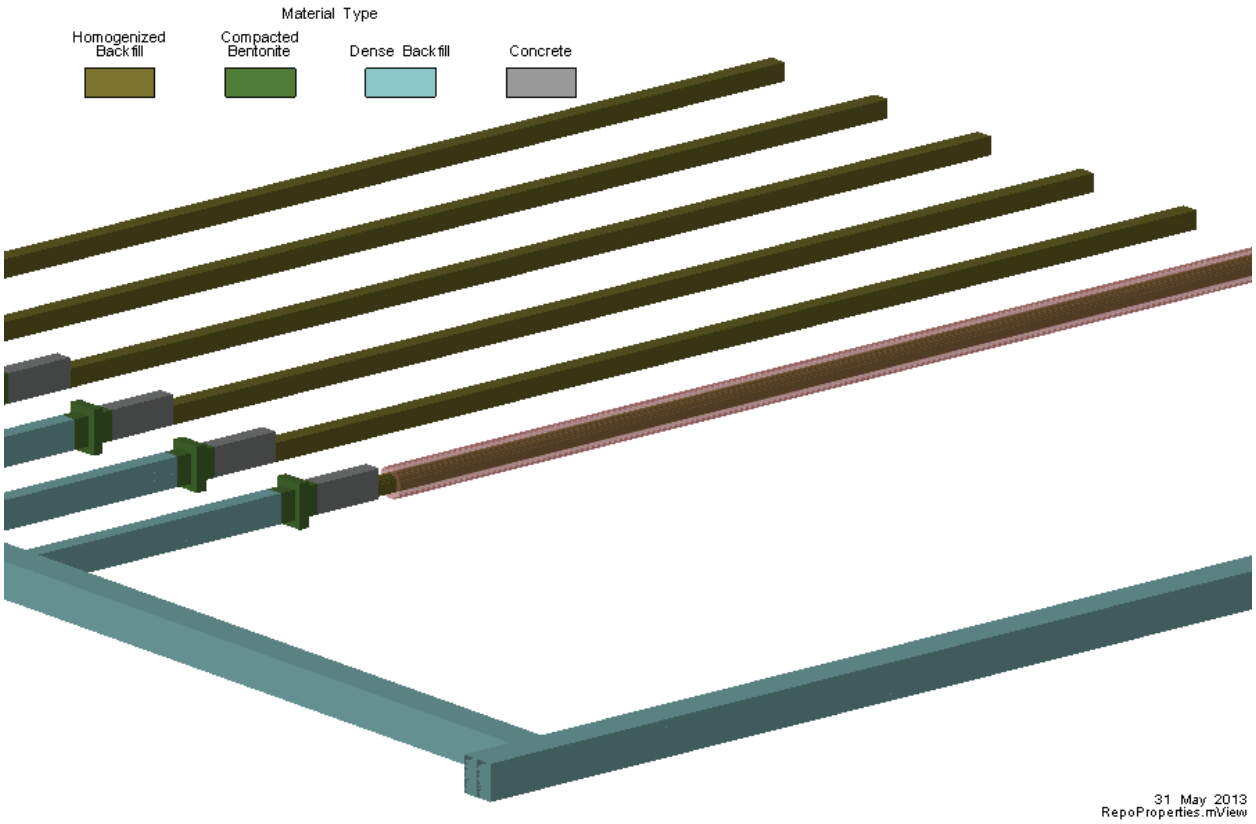

Notes: the pink-hued surface is set at the boundary between the EDZ and the intact rock surrounding the placement room. The surface extends the full length of the room to include all 50 containers.

Figure 7-61: Repository-Scale Model - Control Surface for Calculation of Radionuclide Releases from Repository

7.7.2.2.1 Reference Case

This section presents detailed results for I-129, U-238 and Cs-135. The three selected radionuclides are representative of the behaviours for non-sorbing, highly sorbing and intermediate-sorbing species.

Figure 7-62 through Figure 7-64 illustrate the time dependent behaviour of the I-129 plume along the repository level and on a vertical slice through the placement room. Contours of equivalent results from the Site-Scale Model are overlaid for comparison. The results show similar core concentration profiles with slightly lower I-129 concentrations at the plume margins, likely due to the more detailed discretization.

This comparison provides confidence in the Site-Scale results.

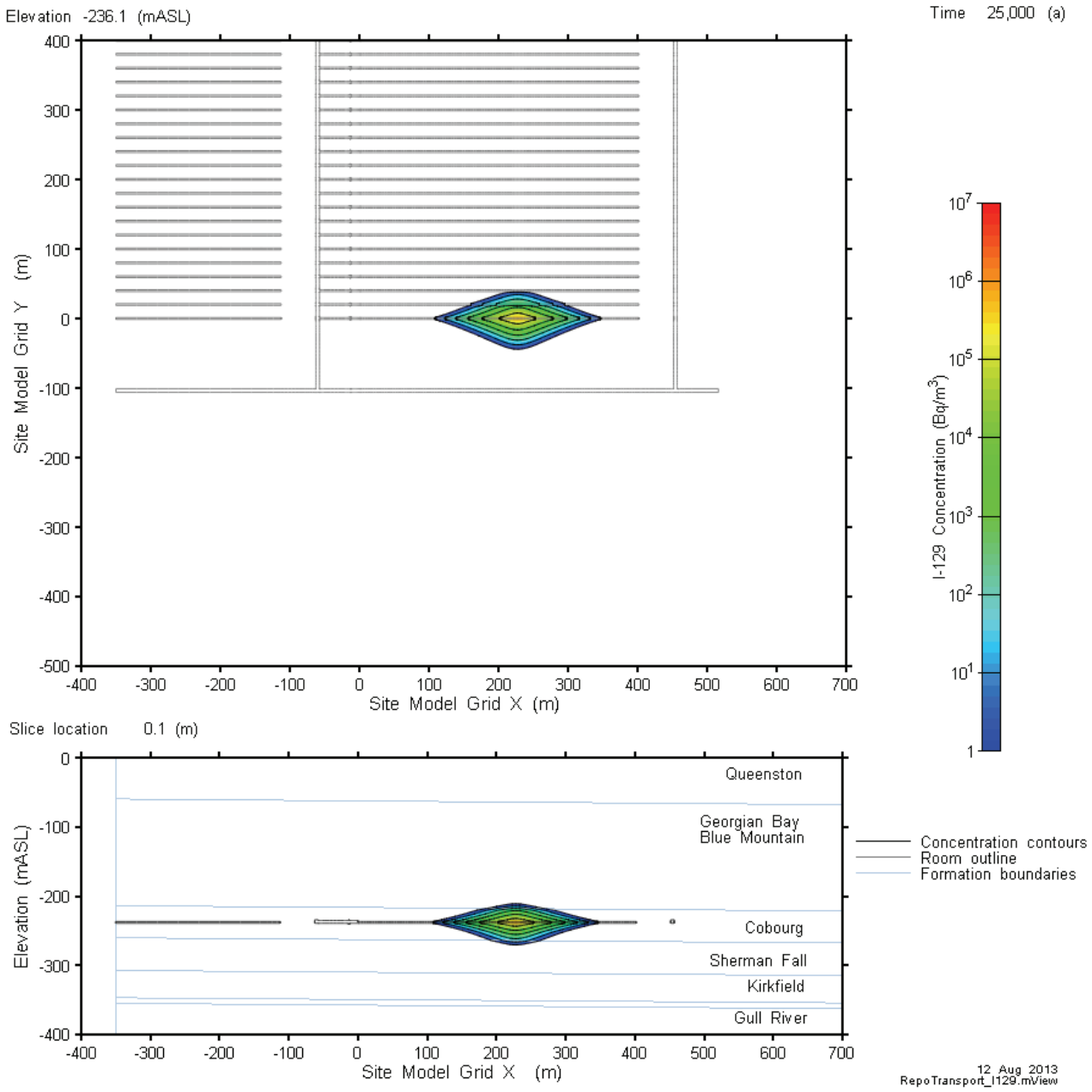

Figure 7-62: Repository-Scale Model - I-129 Concentrations at 25,000 Years

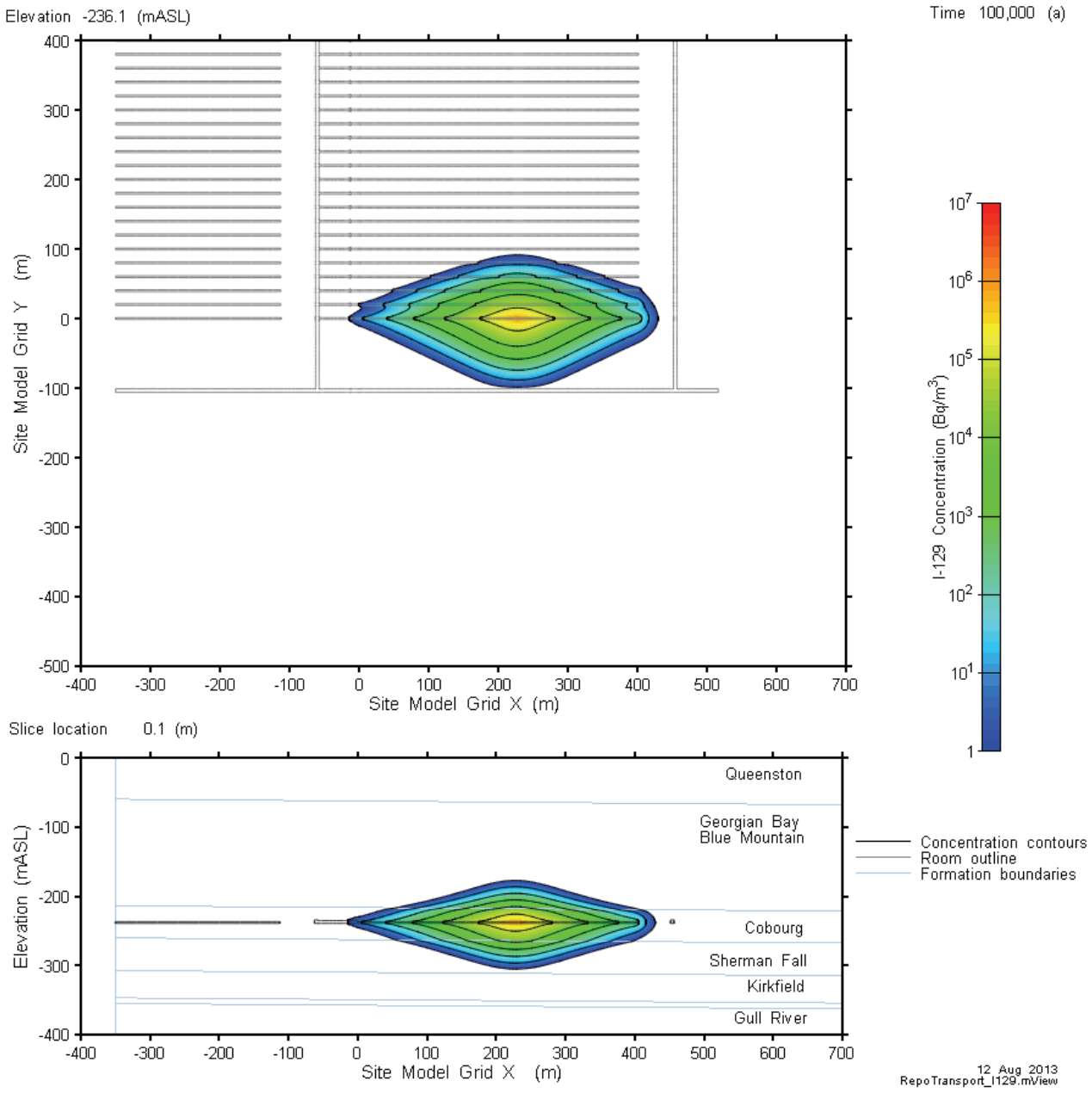

Figure 7-63: Repository-Scale Model - I-129 Concentrations at 100,000 Years

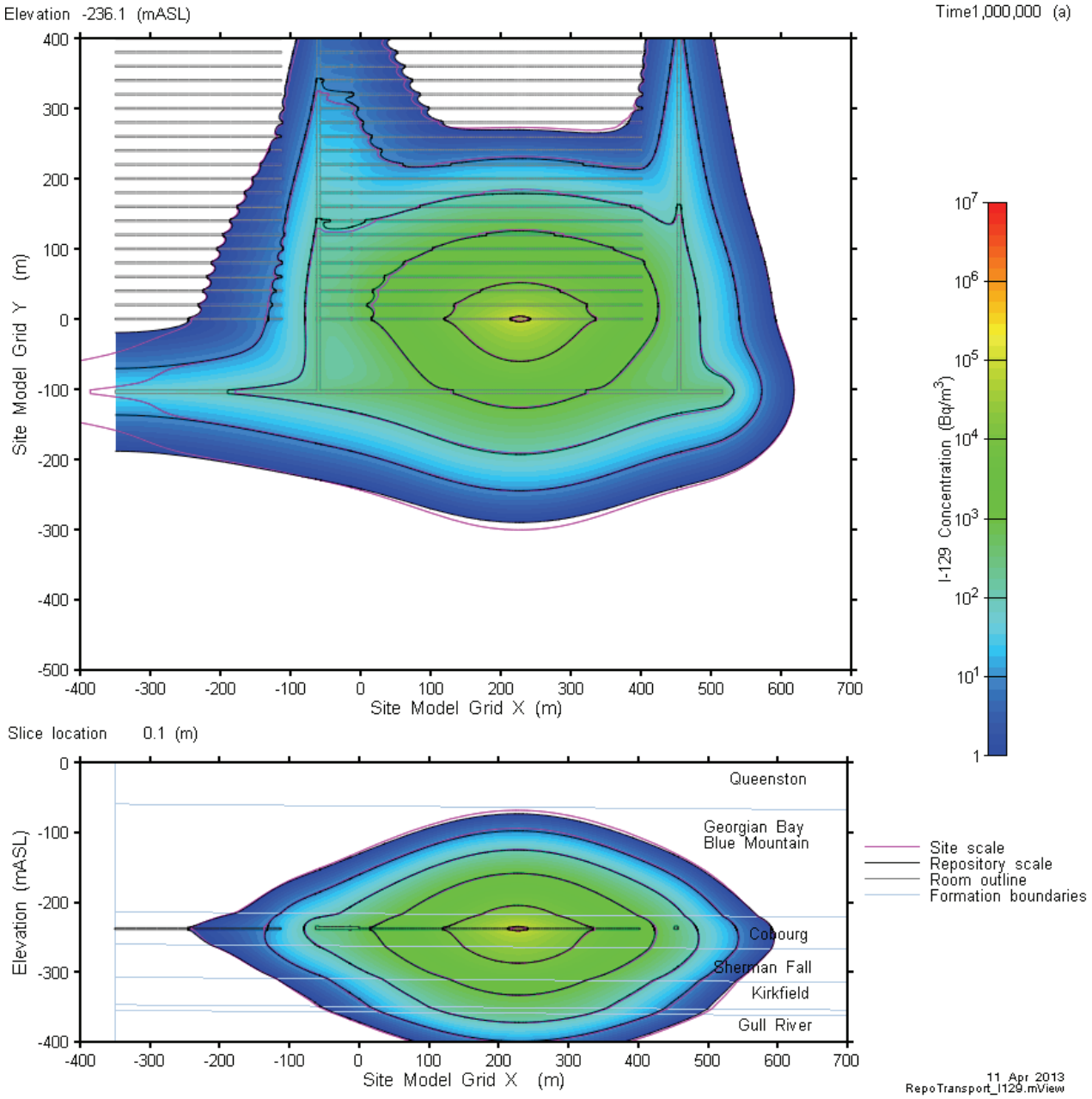

Figure 7-64: Repository-Scale Model - I-129 Concentrations at One Million Years

Unlike I-129, U-238 is strongly sorbed onto sealing materials and the host rock. Consequently, transport of U-238 is limited to a very small domain immediately surrounding the defective container. Figure 7-65 shows sectional views through the release plane and adjacent buffer at one million years.

The contour plots are on a logarithmic scale. The 0.001 Bq/m^3 concentration contour corresponds to an effective U-238 drinking water dose of about 0.00003 µSv/a based on the Table 7-26 water consumption rate of 0.84 m^3/a per person.

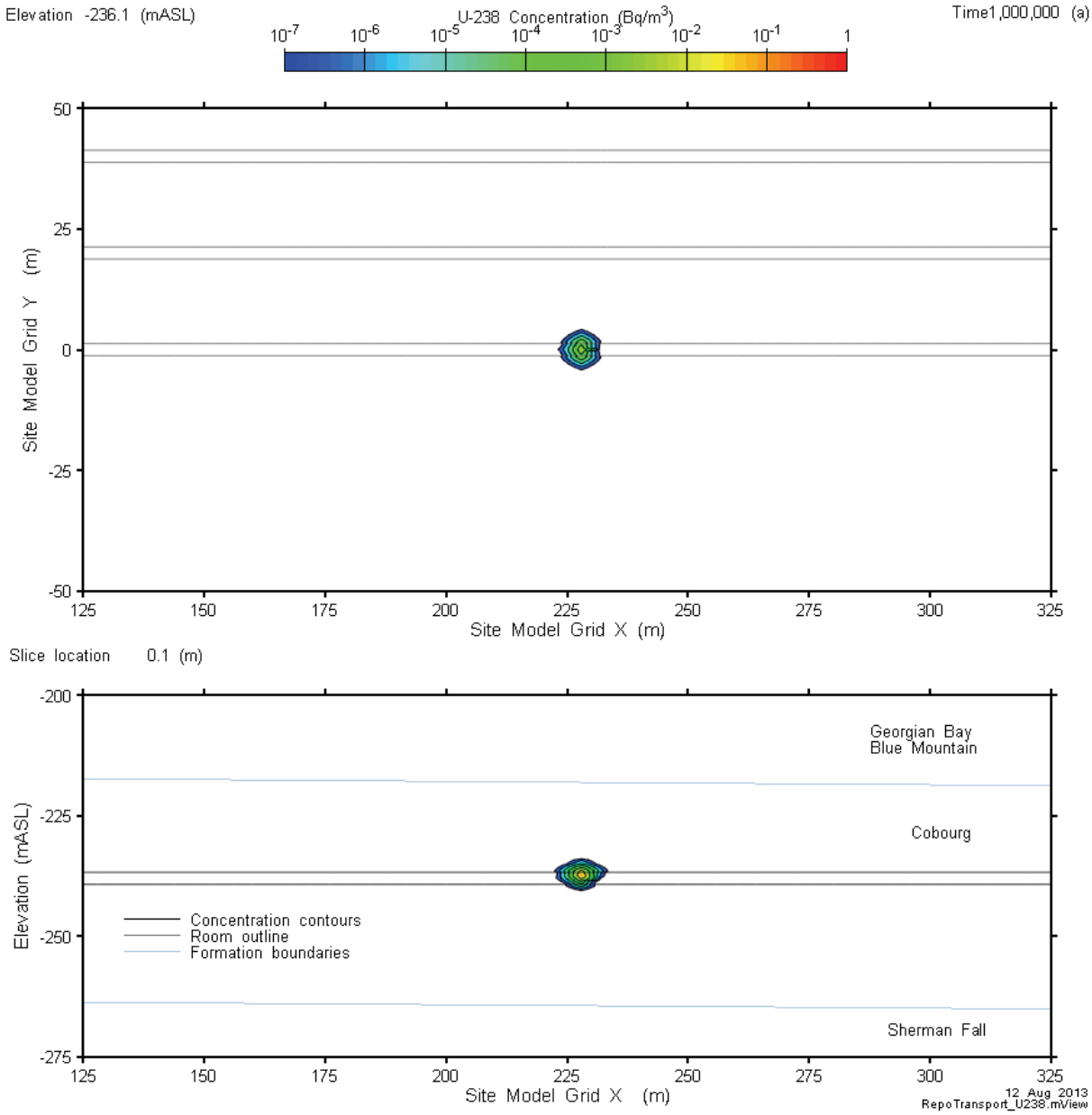

Figure 7-65: Repository-Scale Model - U-238 Concentration at One Million Years

Figure 7-66 and Figure 7-67 show the Cs-135 plume at 100,000 years and one million years. Cs-135 is less strongly sorbed than U-238 but is still subject to retardation. The results show transport is largely confined to the vicinity of the placement room and that the room seal is effective in limiting transport towards the access tunnels. As previously noted, the non-spherical

shape of the Cs-135 plume is due to the fact that cesium is sorbed more strongly by the geosphere layers above the repository than those below the repository.

The 100 Bq/m^3 contour line corresponds to a Cs-135 drinking water dose of about 0.02 µSv/a based on the Table 7-26 water consumption rate of 0.84 m^3/a per person.

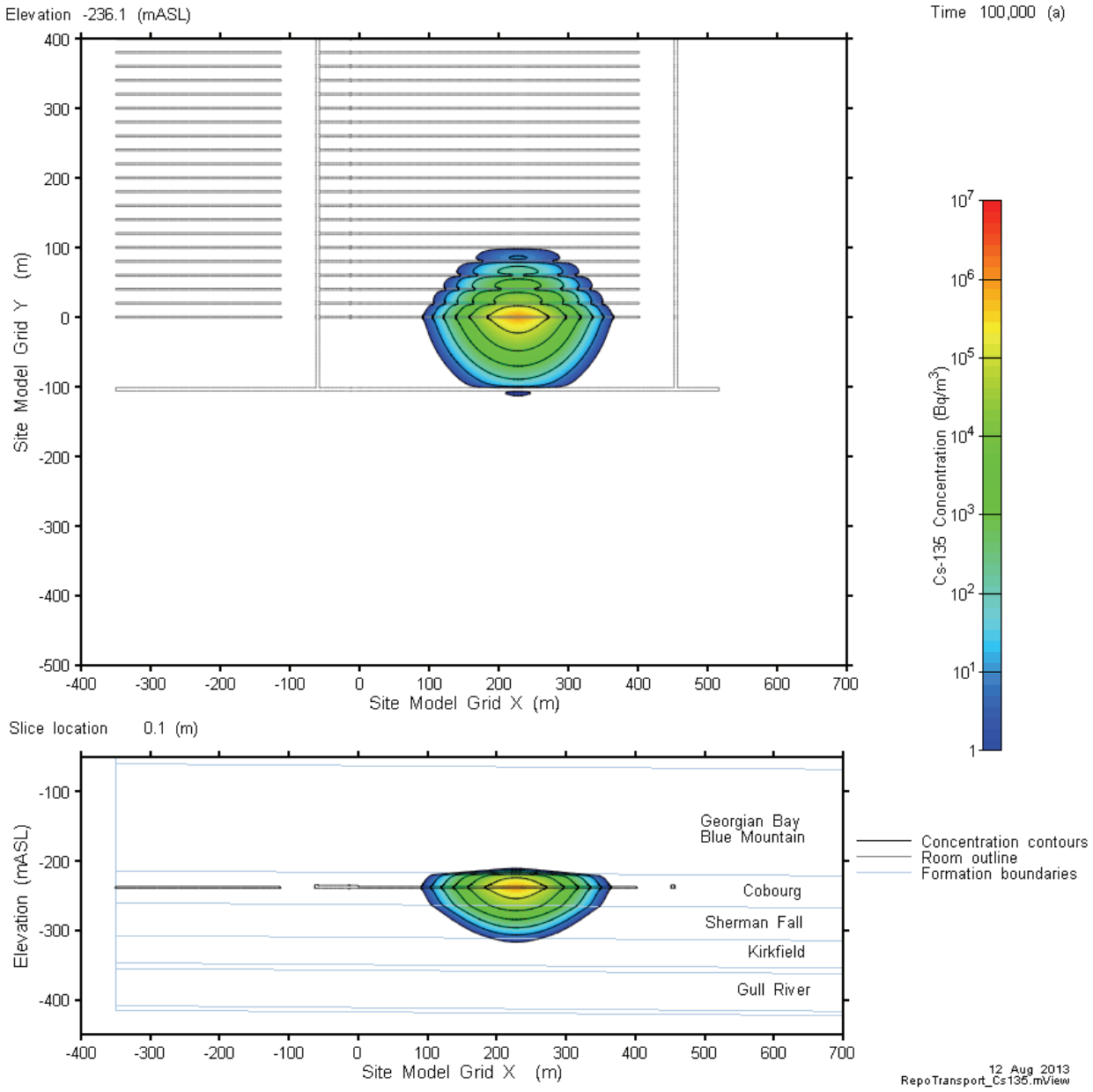

Figure 7-66: Repository-Scale Model - Cs-135 Concentrations at 100,000 Years

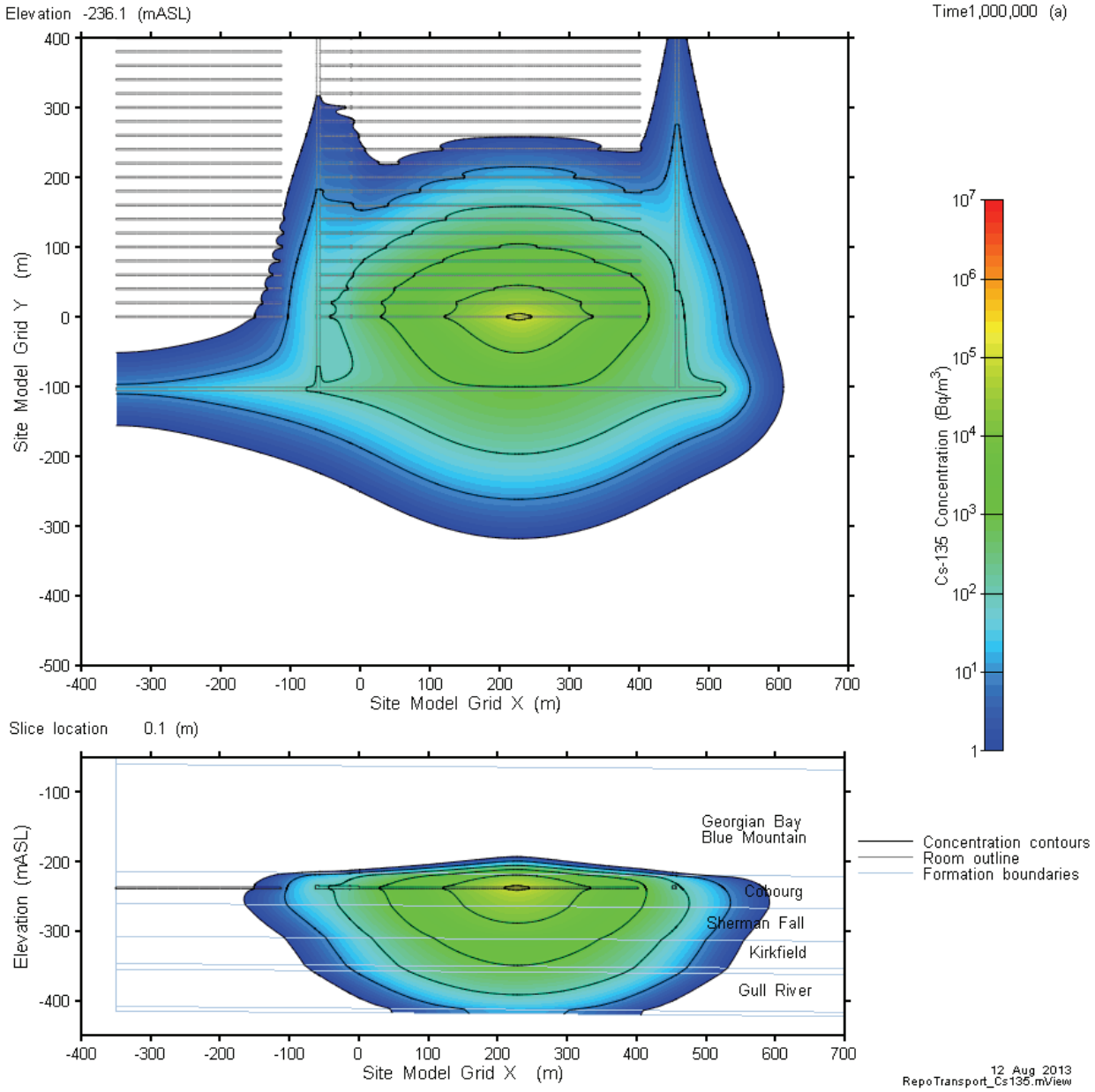

Figure 7-67: Repository-Scale Model - Cs-135 Concentrations at One Million Years

Figure 7-68 shows summary results for all radionuclides considered. This figure shows the transfer rates out of the boundary volume surrounding the placement room shown in Figure 7-61.

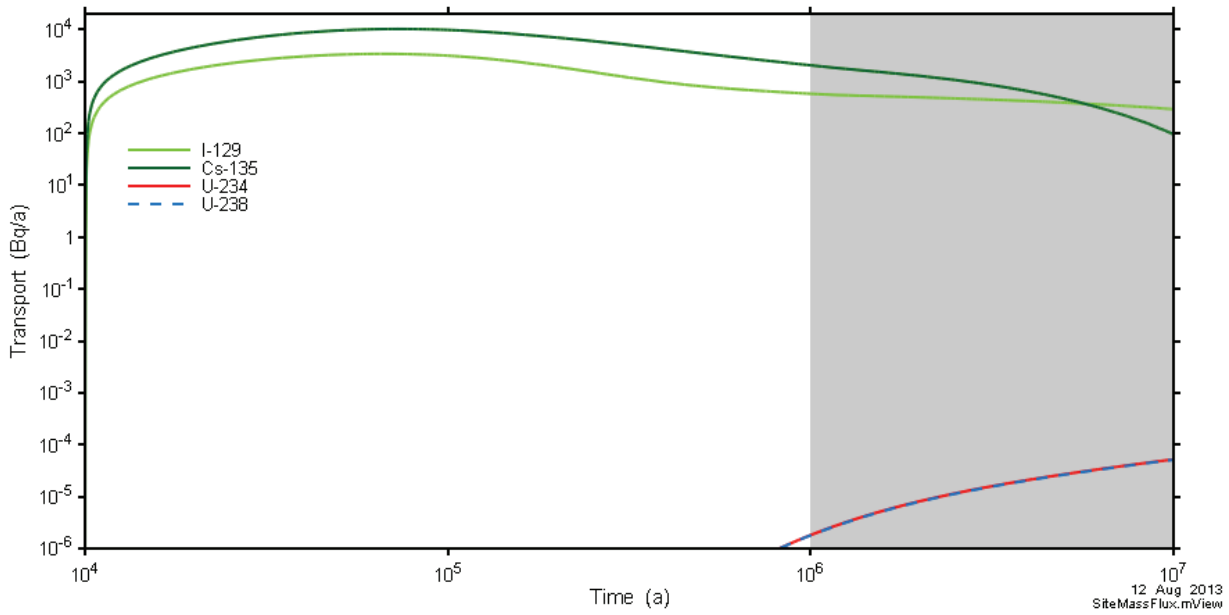

Figure 7-68: Repository-Scale Model - Transport Rates out of the Placement Room for I-129, Cs-135, U-234 and U-238

7.8 Results of System Modelling

The SYVAC3-CC4 system model combines an idealized geometric description of the repository and a simple geosphere transport model with representations of releases from the used fuel and container, and radionuclide transport in the biosphere to determine the radiological consequences of releases to the environment.

This section presents the results of deterministic and probabilistic analysis of the Reference Case and a set of related sensitivity cases.

The deterministic sensitivity cases are:

- Fuel dissolution rate increased by a factor of 10;
- Instant release fractions set to 0.10 for all radionuclides;
- Container defect area increased by a factor of 10;
- No solubility limits in the container;
- No sorption in the EBS;
- No sorption in the geosphere;
- Low sorption in the geosphere with coincident high solubility limits in the container; and
- Geosphere diffusivity increased by a factor of 10.

For ease of presentation, the sensitivity cases are separated into those that represent a degraded physical barrier and those that represent a degraded chemical barrier.

Probabilistic simulations examine the effect of simultaneous variation of all probabilistically defined parameters.

Deterministic and probabilistic simulations are also performed for complementary indicators.

A detailed description of these cases is provided in Section 7.2.1.

Figures in this section are shown with shading at times greater than one million years to emphasize that these results are illustrative and included only to indicate maximum impacts. Shading for dose rates below 10^{-9} Sv/a indicates these values are negligible and are included to indicate trends.

7.8.1 Transport Model Verification

To provide confidence in the SYVAC3-CC4 model, transport results for I-129, Cs-135, U-234 and U-238 are compared with similar results obtained from the detailed FRAC3DVS-OPG 3D simulations.

Near-Field Transport Comparison

Transport from the container to the geosphere for the Reference Case is shown in Figure 7-69 and Figure 7-70. For FRAC3DVS-OPG the transport is across the surface of the pink hued cylinder in Figure 7-61 while for SYVAC3-CC4 the transport is across the outer surface of the grey cylinder in Figure 7-33. In both cases, the surface represents the excavation damaged zone / rock boundary around a placement room.

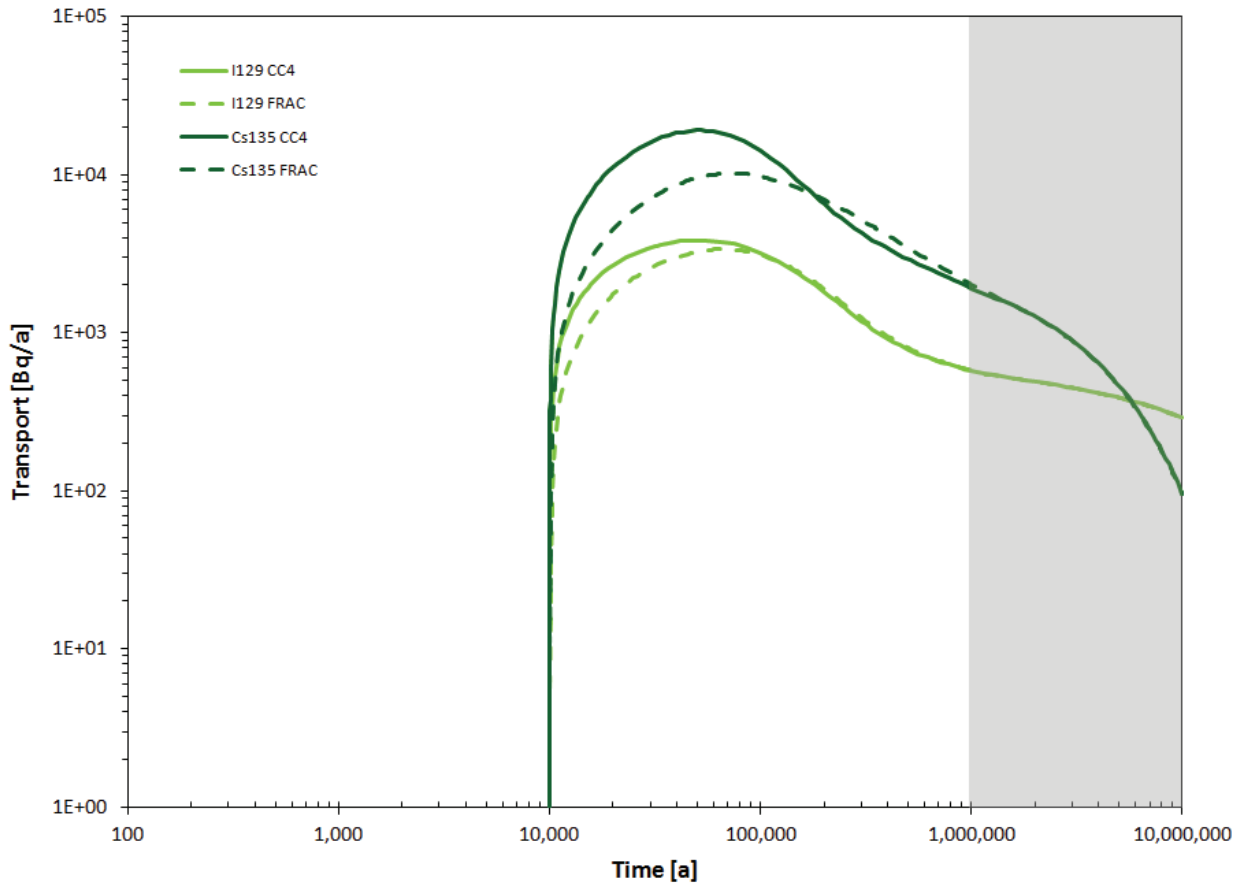

Figure 7-69: Comparison of SYVAC3-CC4 and FRAC3DVS-OPG Transport of I-129 and Cs-135 to the Geosphere

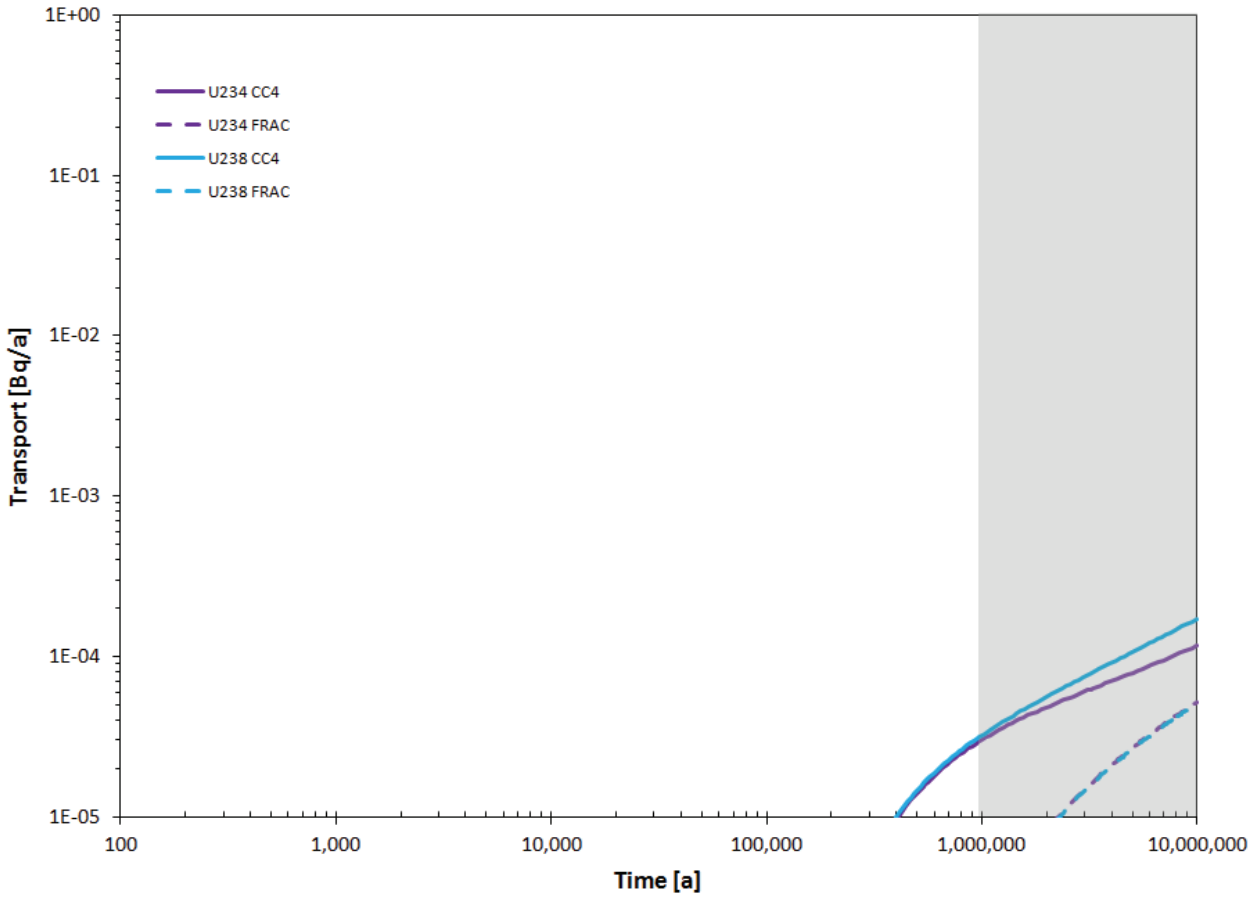

Note: FRAC3DVS-OPG-calculated transport of U-234 and U-238 overlap

Figure 7-70: Comparison of SYVAC3-CC4 and FRAC3DVS-OPG Transport of U-234 and U-238 to the Geosphere

Results for the maximum values and their associated time occurrences are shown in Table 7-31. The agreement is very close for the non-sorbing and weakly sorbing radionuclides I-129 and Cs-135. The peak rates for the strongly sorbing U-234 and U-238 are not reached during the simulation period in either model. The greater differences for sorbing radionuclides occur because the buffer in the SYVAC3-CC4 model (Figure 7-33) is represented as a cylinder whereas in reality it is an annulus. Even though the buffer thickness is maintained, the cylinder representation has less material volume and less sorbing surface area.

Table 7-31: Comparison of Maximum Transport Rates to the Geosphere

Nuclide	Highest Transport Rate in 10 million years (Bq/a)			Time of Highest Value (a)		
	SYVAC3-CC4	FRAC3DVS-OPG	Ratio[1]	SYVAC3-CC4	FRAC3DVS-OPG	Ratio[1]
I-129	3.86×10^{3}	3.38×10^{3}	1.14	4.98×10^{4}	6.75×10^{4}	0.74
Cs-135	1.91×10^{4}	1.02×10^{4}	1.87	5.26×10^{4}	7.27×10^{4}	0.72
U-234	1.16×10^{-4}	5.21×10^{-5}	2.23	1×10^{7}	1×10^{7}	1.0
U-238	1.72×10^{-4}	5.12×10^{-5}	3.35	1×10^{7}	1×10^{7}	1.0

Note: [1] Ratio is the SYVAC3-CC4 value divided by the FRAC3DVS-OPG value.

Geosphere Transport Comparison

The transport of I-129 and Cs-135 through the geosphere for the Reference Case is shown in Figure 7-71, with Table 7-32 summarizing the highest transport rates in the 10 million year time frame. The figure also compares the transport of I-129 at various sedimentary layers including the Cobourg and Georgian Bay formations.

For U-238 and U-234, the release rates are effectively zero in both models due to the highly sorbing nature of these radionuclides.

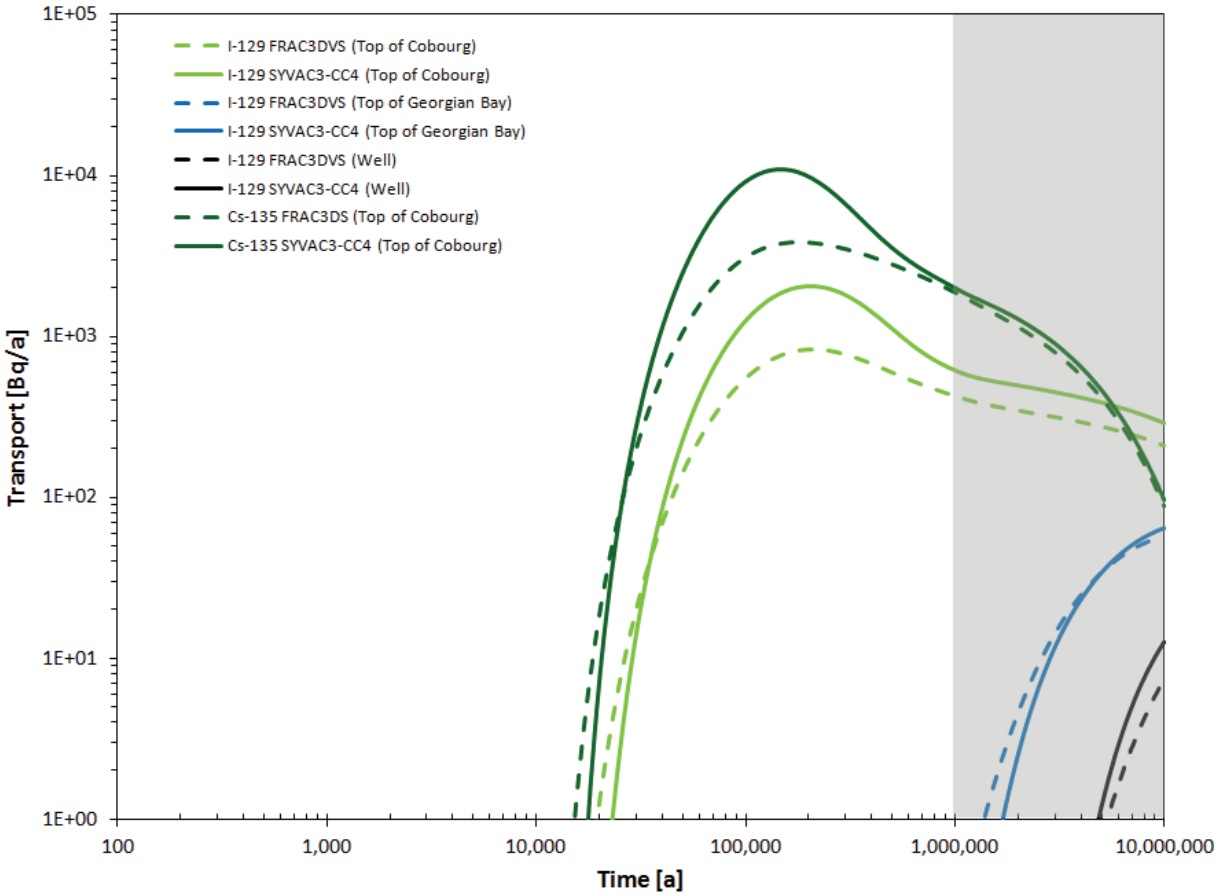

Note: Cs-135 transport through the top of the Georgian Bay layer and to the Well is off-scale low

Figure 7-71: Comparison of SYVAC3-CC4 and FRAC3DVS-OPG Transport of I-129 and Cs-135

Table 7-32: Comparison of Maximum Transport Rates to the Surface

Nuclide	Layer	Highest Transport Rate (Bq/a)			Time of Highest Transport (a)		
		SYVAC3-CC4	FRAC3DVS-OPG	Ratio[1]	SYVAC3-CC4	FRAC3DVS-OPG	Ratio[1]
I-129	Cobourg	2.06×10^{3}	8.29×10^{2}	2.48	2.05×10^{5}	2.10×10^{5}	0.98
	Georgian Bay	6.45×10^{1}	5.69×10^{1}	1.13	1×10^{7}	1×10^{7}	1.0
	Well	1.28×10^{1}	7.39×10^{0}	1.73	1×10^{7}	1×10^{7}	1.0
Cs-135	Cobourg	1.09×10^{4}	3.82×10^{3}	2.86	1.49×10^{5}	1.75×10^{5}	0.85

Note: [1] Ratio is the SYVAC3-CC4 value divided by the FRAC3DVS-OPG value.

The above comparisons indicate the SYVAC3-CC4 maximum transport rates are greater than those arising from the FRAC3DVS-OPG model while their associated time of occurrences are earlier. This implies that the SYVAC3-CC4 near-field and far-field models provide a conservative representation of radionuclide transport for key radionuclides as compared to FRAC3DVS-OPG.

7.8.2 Deterministic Analysis

Due to the very low hydraulic conductivity of the host rock and the dominance of diffusive transport, the dose rates arising in the one million year period of interest are below the 10^{-9} Sv/a threshold value for almost all cases. The peak dose rate is also not reached in this time frame.

To provide a basis for comparing cases, results are therefore quoted for a 10 million year period; however, even with this extension the peak dose rate for many cases is not reached.

To put the quoted results into context, results obtained for the sensitivity case with geosphere diffusivities increased by a factor of 10 can be used. These results, illustrated in Figure 7-77 in Section 7.8.2.2, indicate that a peak dose rate of 2.6×10^{-8} Sv/a is reached at 5.6×10^{6} years. This shows that the long-term doses are expected to remain extremely low, even in cases where the peak dose rate is not reached in the 10 million year simulation time.

7.8.2.1 Reference Case

Figure 7-72 shows the total dose rate for the Reference Case. This is the sum of the individual contributions from all radionuclides of potential interest and their progeny (Section 7.6).

The maximum dose rate is 2.0×10^{-9} Sv/a occurring at 1.0×10^{7} years. The peak dose rate is not reached within this simulation period. This dose rate maximum is well below the average natural background dose rate and the 3×10^{-4} Sv/a interim dose acceptance criterion established in Section 7.1 for the radiological protection of persons.

Figure 7-73 shows the individual contributions to the total dose rate from the most significant radionuclides. I-129 is the dominant dose rate contributor, followed to a much lesser extent by Pd-107 and Sm-147. This is because I-129 has a sizeable initial inventory, a non-zero instant release fraction, a very long half-life, is non-sorbing in the buffer, backfill and geosphere and

has a radiological impact on humans. The shape of the curve is defined by the release of radionuclides into the Guelph layer from both the shaft and the rock layers. The shaft releases are low and appear first. The rock layer releases are greater and appear later. When the two are summed together, this results in the shape of the curve shown in Figure 7-72.

Pd-107 and Sm-147 are not usually identified as dose contributors in used fuel repository assessments, but show here at very low levels as they are long-lived and, in the absence of data, have been assumed to have no sorption and no solubility limits. Other fission products and actinides either decay away, or are released very slowly as the fuel dissolves and are thereafter sorbed in the engineered barriers and geosphere.

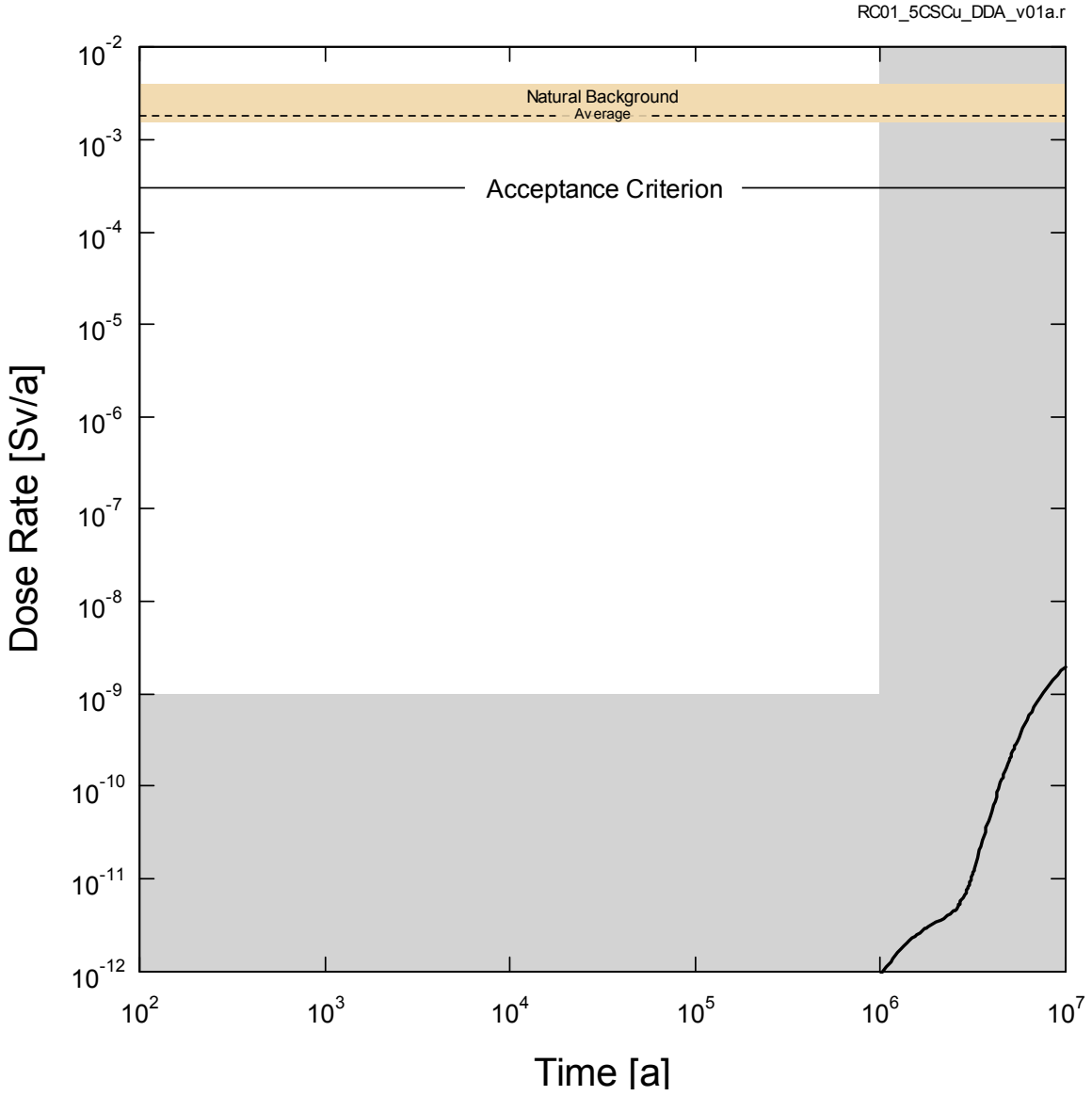

Figure 7-72: SYVAC3-CC4 - Reference Case Total Dose Rate

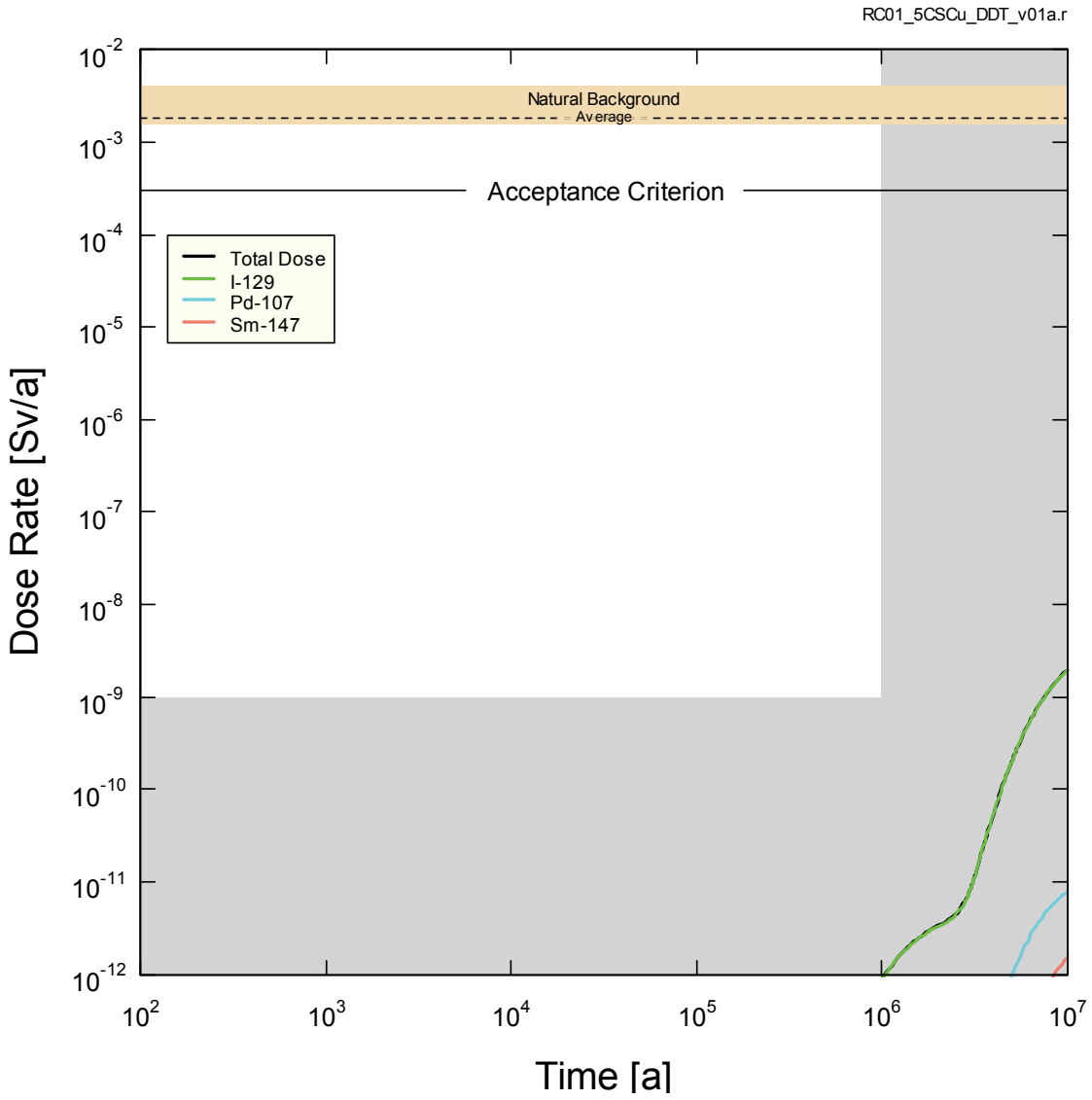

Figure 7-73: SYVAC3-CC4 - Reference Case Individual Radionuclide Dose Rates

Table 7-33 shows the dose pathways for each of the main dose contributors in Figure 7-73. These data are tabulated for times corresponding to the maximum individual radionuclide contributions.

Table 7-33: Radionuclide Dose Pathways for the Reference Case

Element	Internal Dose [Sv/a]	Primary Pathway(s)	%	External Dose [Sv/a]	Primary Pathway(s)	%
I-129	2.0×10^{-9}	Food Ingestion Water Ingestion	54 46	6.4×10^{-14}	Groundshine Water Immersion	86 13
Pd-107	7.9×10^{-12}	Food Ingestion Water Ingestion	90 8	0	None	0
Sm-147	1.6×10^{-12}	Food Ingestion Air Inhalation	57 34	0	None	0

7.8.2.2 Sensitivity to a Degraded Physical Barrier

The following sensitivity cases investigate the effect of a degraded physical barrier on the Reference Case results:

- Fuel dissolution rate increased by a factor of 10;
- Container defect area increased by a factor of 10;
- Instant release fractions set to 10% for all radionuclides; and
- Geosphere diffusivities increased by a factor of 10.

Figure 7-74 shows the individual contributions to the total dose rate from the most significant radionuclides for the sensitivity case with the fuel dissolution rate increased by a factor of 10. For this case, all fuel in the container dissolves within one million years whereas in the Reference Case only about 22% of the fuel dissolves in this time frame (see Figure 7-32).

As in the Reference Case, I-129, Pd-107 and Sm-147 are the most significant dose contributors. The maximum total dose rate occurs at 1.0×10^{7} years and reaches a value of 5.9×10^{-9} Sv/a or about 3 times that of the Reference Case. The maximum dose does not increase by a factor of 10 because the instant release fraction for I-129 also affects its dose rate and this parameter is independent of the fuel dissolution rate.

Actinide dose rates are zero because they are strongly sorbed in the buffer and geosphere and do not reach the biosphere during the simulation time.

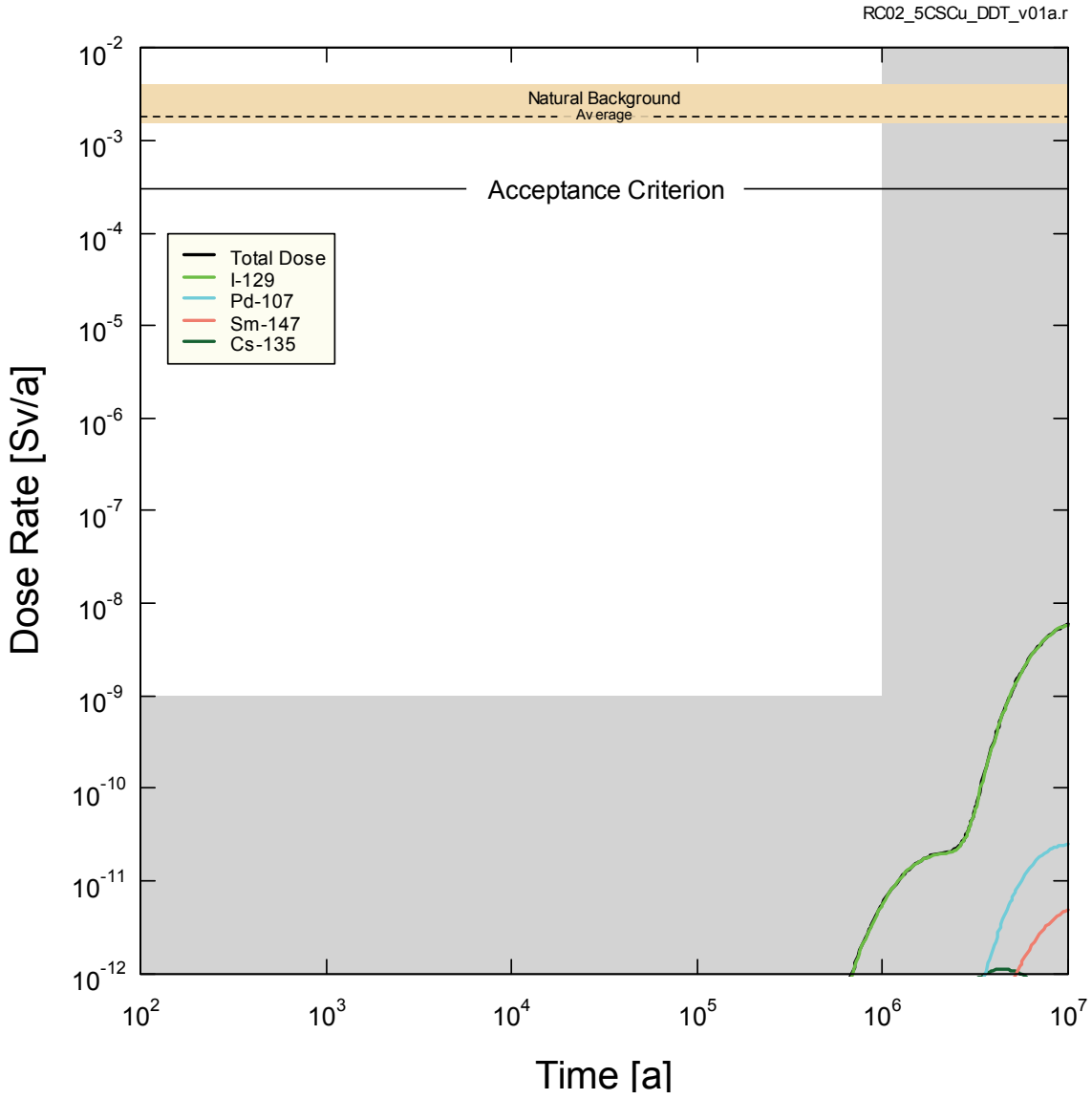

Figure 7-74: SYVAC3-CC4 - Sensitivity to a Factor of 10 Increase in Fuel Dissolution Rate

Figure 7-75 shows the individual contributions to the total dose rate from the most significant radionuclides for the sensitivity case with the defect area in the three defective containers increased by a factor of 10.

As in the Reference Case, I-129 is the main dose contributor. The maximum total dose rate occurs at 1.0×10^{7} years and reaches a value of 2.0×10^{-9} Sv/a or about the same as the Reference Case. The I-129 maximum dose rate is largely unaffected by the defect size because the release of I-129 is buffer-limited rather than defect size-limited.

The actinide dose rates are zero because they are strongly sorbed in the buffer and geosphere and do not reach the biosphere during the simulation time.

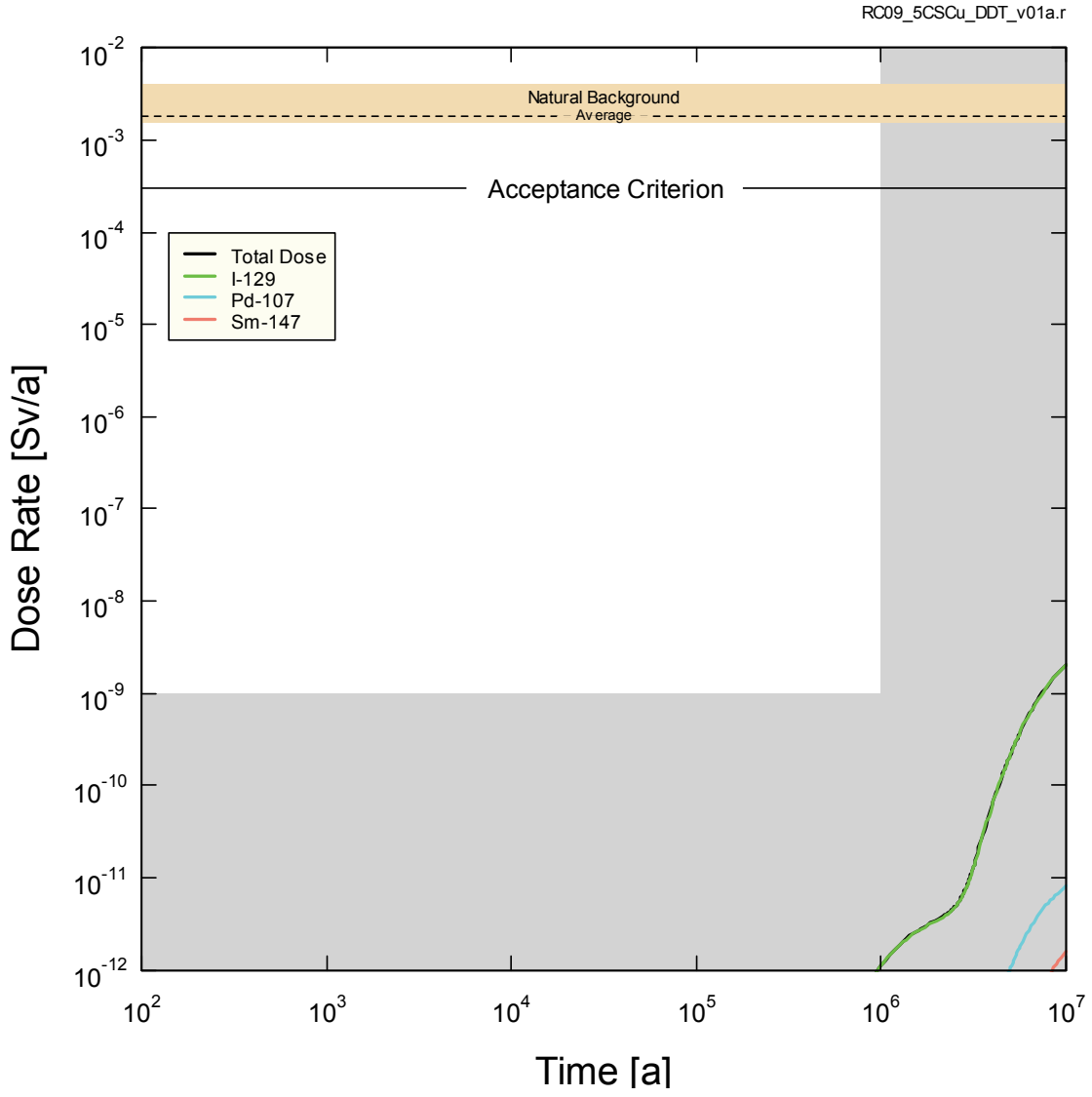

Figure 7-75: SYVAC3-CC4 - Sensitivity to a Factor of 10 Increase in Container Defect Area

Figure 7-76 shows the individual contributions to the total dose rate from the most significant radionuclides for the sensitivity case with the instant release fractions set to 10%.

As in the Reference Case, I-129 is the main dose contributor. The maximum total dose rate occurs at 1.0×10^{7} years and reaches a value of 2.2×10^{-9} Sv/a or about 1.1 times that of the Reference Case. The increase is smaller than the increase in instant release fraction because of spreading of the plume as it rises to the surface.

The actinide dose rates are zero because they are strongly sorbed in the buffer and geosphere and do not reach the biosphere during the simulation time.

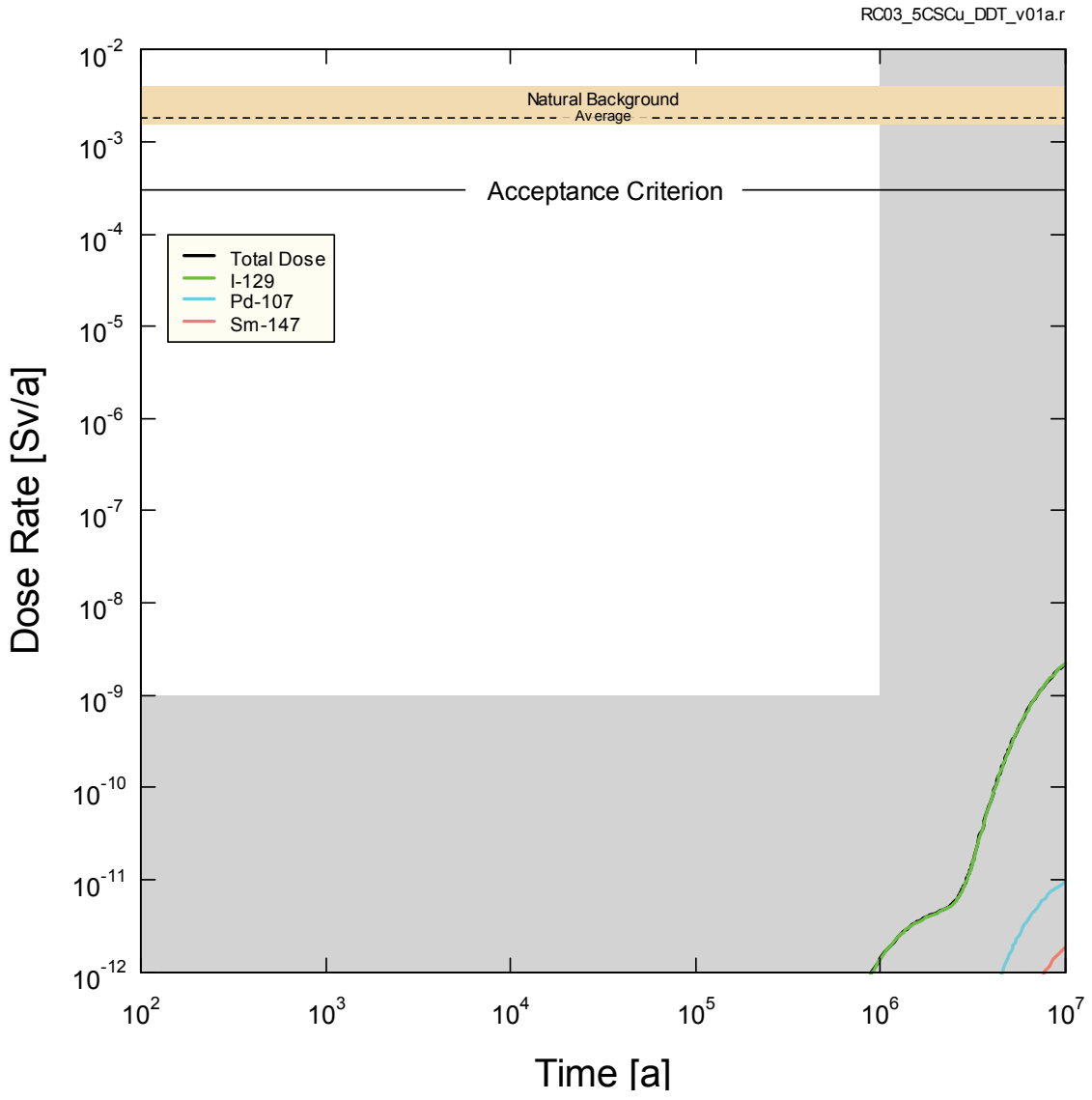

Figure 7-76: SYVAC3-CC4 - Sensitivity to All Instant Release Fractions Set to 10 Percent

Figure 7-77 shows the individual contributions to the total dose rate for the most significant radionuclides for the sensitivity case with geosphere diffusivity increased by a factor of 10.

As in the Reference Case, the highest dose contributor is I-129. Since the geosphere diffusivities are higher, I-129 reaches its peak dose rate within the 10 million year simulation time frame. The peak total dose rate occurs at 5.6×10^{6} years and reaches a value of 2.6×10^{-8} Sv/a. This is about 13-fold higher than for the Reference Case; however, as in the Reference Case, the peak total dose rate is still well below the average natural background dose rate and the 3×10^{-4} Sv/a interim dose acceptance criterion established in Section 7.1 for the radiological protection of persons.

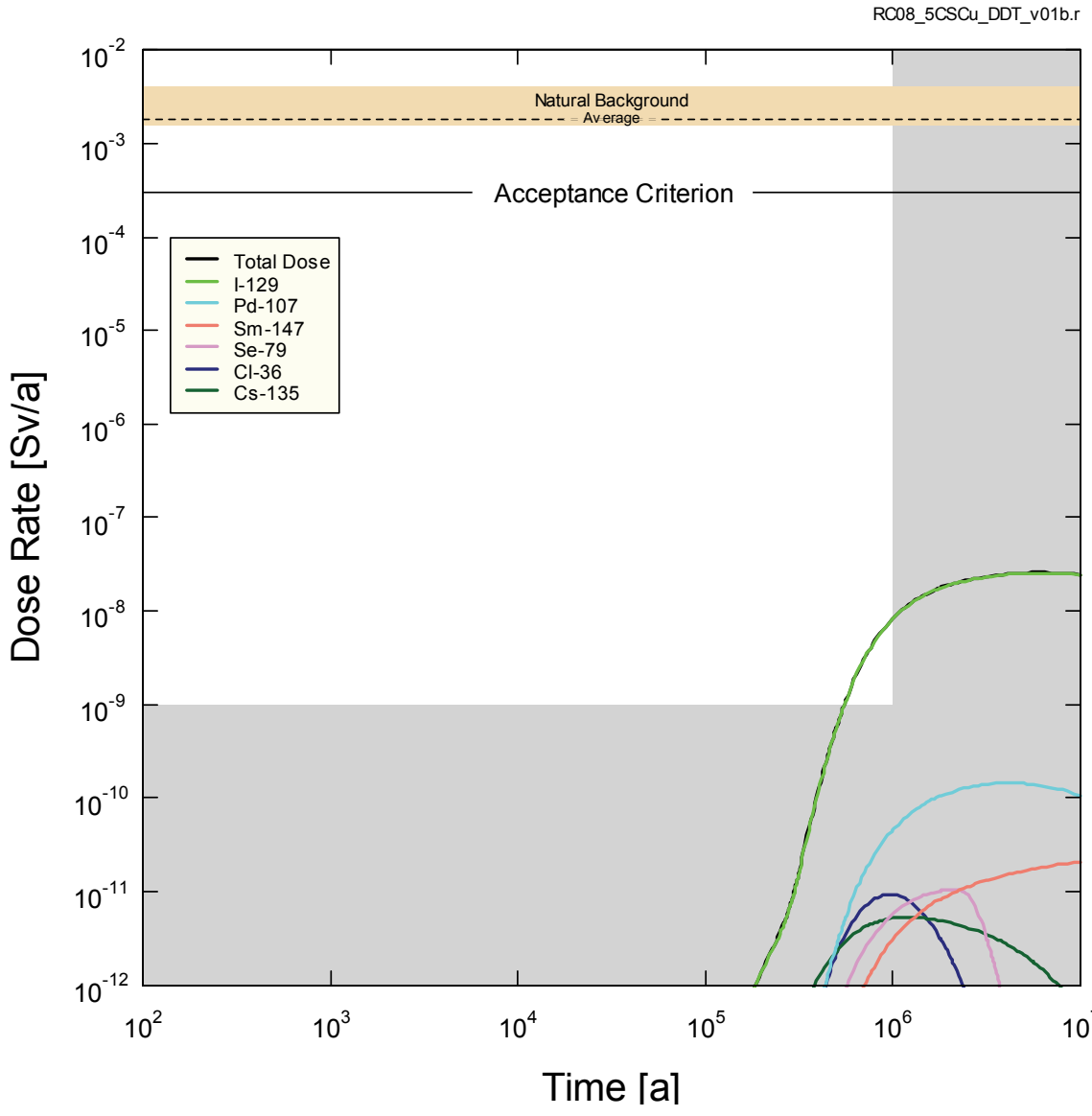

Figure 7-77: SYVAC3-CC4 - Sensitivity to a Factor of 10 Increase in Geosphere Diffusivity

Figure 7-78 summarizes the total dose rates for the Reference Case and all four degraded physical barrier cases. Table 7-34 provides results in numerical form. All results are many orders of magnitude below the interim dose acceptance criterion. The peak dose rate is not reached in the one million year period of interest except for the high geosphere diffusivity sensitivity case.

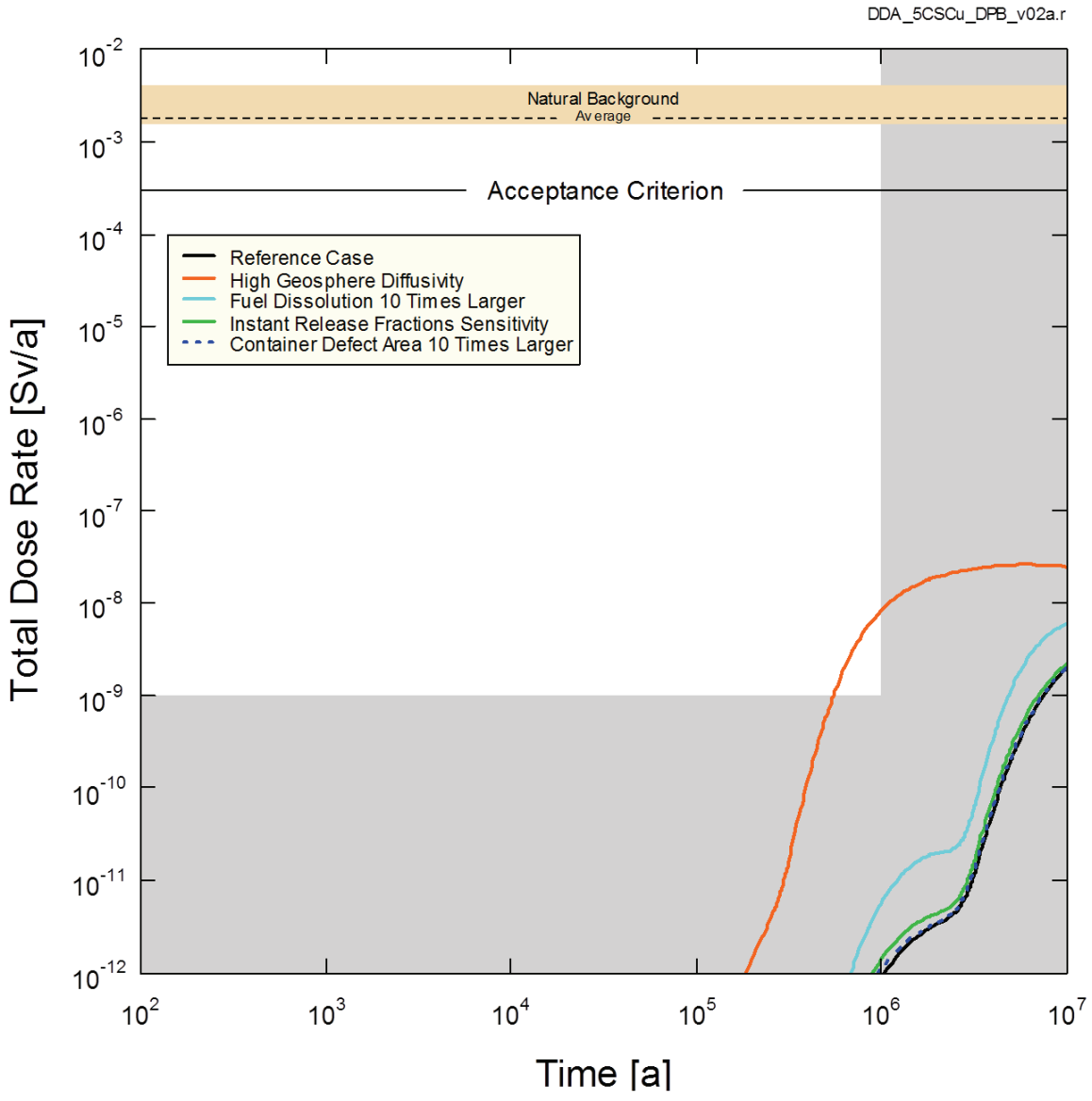

Figure 7-78: SYVAC3-CC4 - Result Summary for Defective Physical Barrier Sensitivity Cases

Table 7-34: Result Summary for Defective Physical Barrier Sensitivity Cases

Case	Maximum Dose Rate (Sv/a)	Ratio to Reference Case	Time of Maximum Dose Rate* (a)
Reference Case	***2.0×10^{-9}***	**-**	***1.0×10^{7}***
Fuel Dissolution Rate 10 times Higher	5.9×10^{-9}	3.0	1.0×10^{7}
Container Defect Area 10 times Higher	2.0×10^{-9}	1.0	1.0×10^{7}
Instant Release Fraction Sensitivity	2.2×10^{-9}	1.1	1.0×10^{7}
Geosphere Diffusivity Increased by a Factor of 10	2.6×10^{-8}	13	5.6×10^{6}

Note: * The peak dose rate will be greater than the maximum dose rate if the maximum is not obtained within the 10 million year simulation time.

7.8.2.3 Sensitivity to a Degraded Chemical Barrier

The following sensitivity cases investigate the effect of a degraded chemical barrier on the Reference Case results:

- No sorption in the geosphere;
- No solubility limits in the container;
- No sorption in the EBS; and
- Low sorption in the geosphere with coincident high solubility limits in the container.

Figure 7-79 shows the individual contributions to the total dose rate from the most significant radionuclides (i.e., those accounting for 99% of the total dose) for the sensitivity case with no sorption in the geosphere.

The maximum total dose rate occurs at 1×10^{7} years and reaches a value of 3.3×10^{-9} Sv/a or 1.7 times higher than the Reference Case.

The dominant dose contributors are Cs-135 and I-129; however, at longer times there are also contributions from U-238 and U-235 progeny. Since there is no sorption in the geosphere, the long-lived U-238 and U-235 are able to reach the surface biosphere, where they decay to form their progeny.

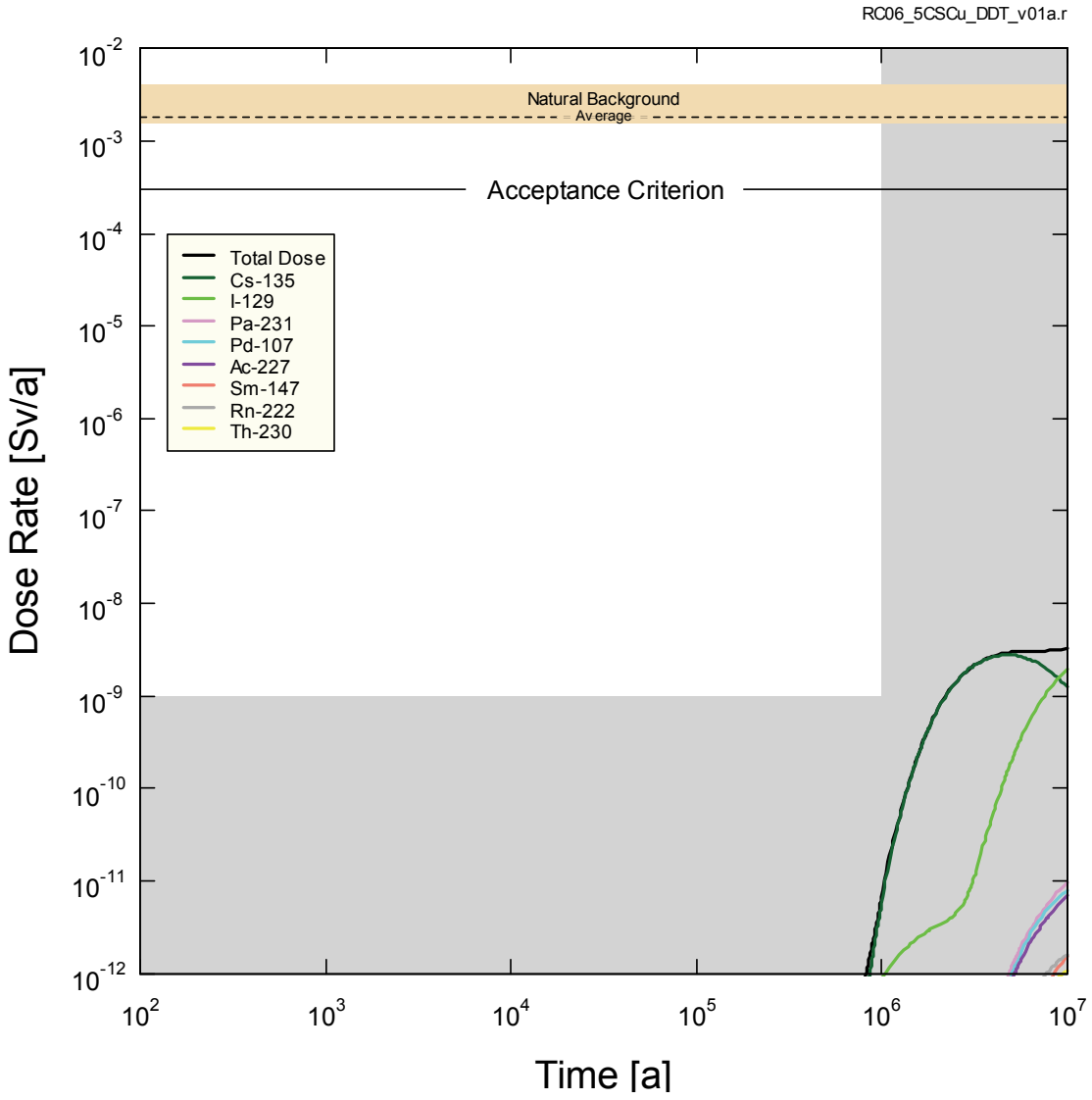

Figure 7-79: SYVAC3-CC4 - Sensitivity to No Sorption in the Geosphere

Figure 7-80 shows the individual contributions to the total dose rate for the most significant radionuclides for the sensitivity case with no radionuclide solubility limits.

As in the Reference Case, I-129 is the main dose contributor. The maximum total dose rate occurs at the same time as in the Reference Case and reaches the same value of 2.0×10^{-9} Sv/a. There is low sensitivity to solubility because I-129 is not solubility limited and because the actinides (which are solubility limited) continue to be strongly sorbed in the geosphere and do not reach the biosphere in the time period of interest.

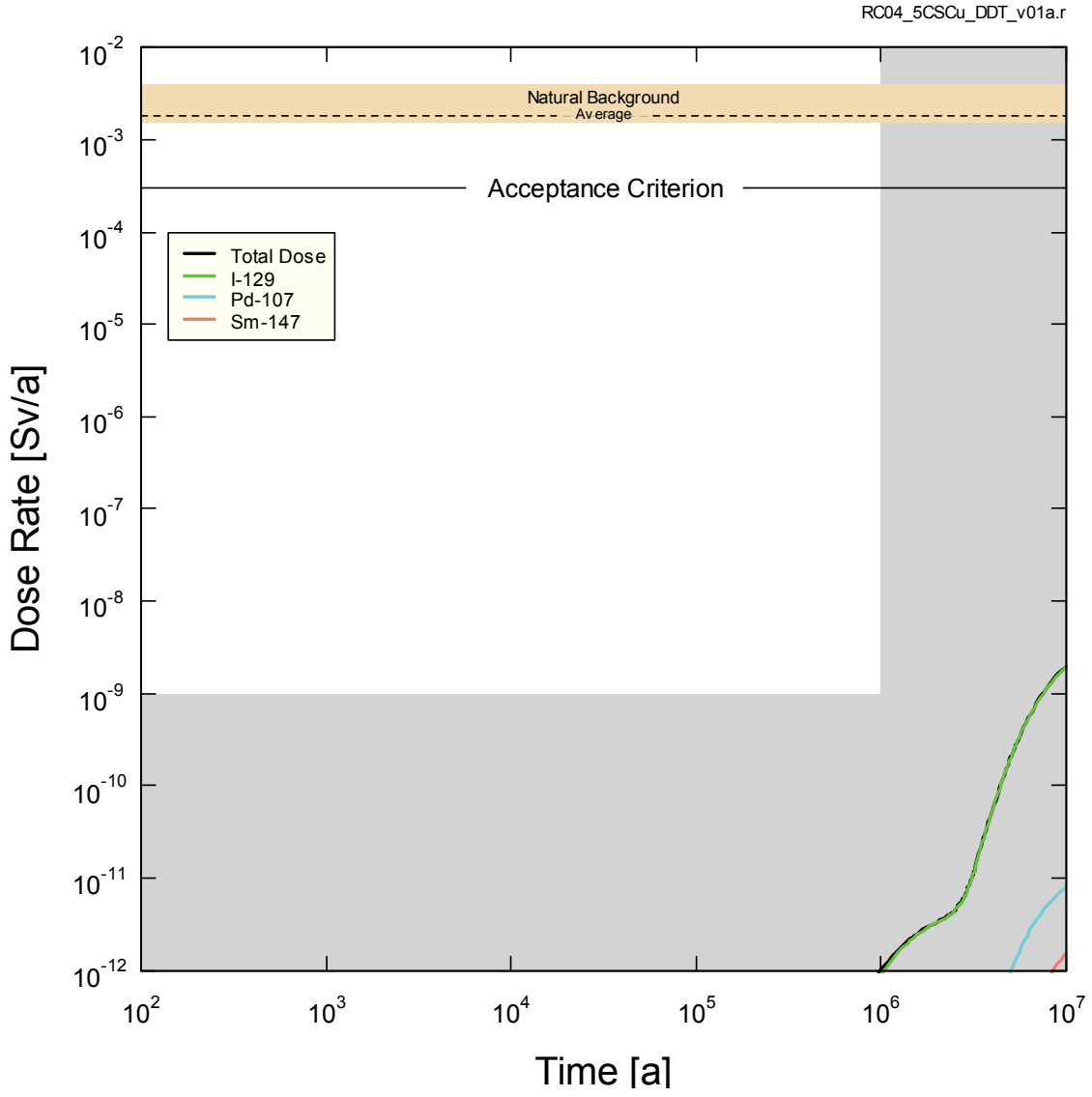

Figure 7-80: SYVAC3-CC4 - Sensitivity to No Solubility Limits

Figure 7-81 shows the individual contributions to the total dose rate for the most significant radionuclides for the sensitivity case with no sorption in the EBS.

The maximum total dose rate occurs at 1.0×10^{7} years and reaches a value of 6.7×10^{-9} Sv/a or about 3.4 times higher than the Reference Case. Unlike the Reference Case, the main dose contributor is Ac-227 followed by I-129 and several other actinides. Since there is no sorption in the near field (where they are normally sorbed), the long-lived U-238 and U-235 are able to migrate via the shafts to the surface biosphere, where they decay to form their progeny radionuclides.

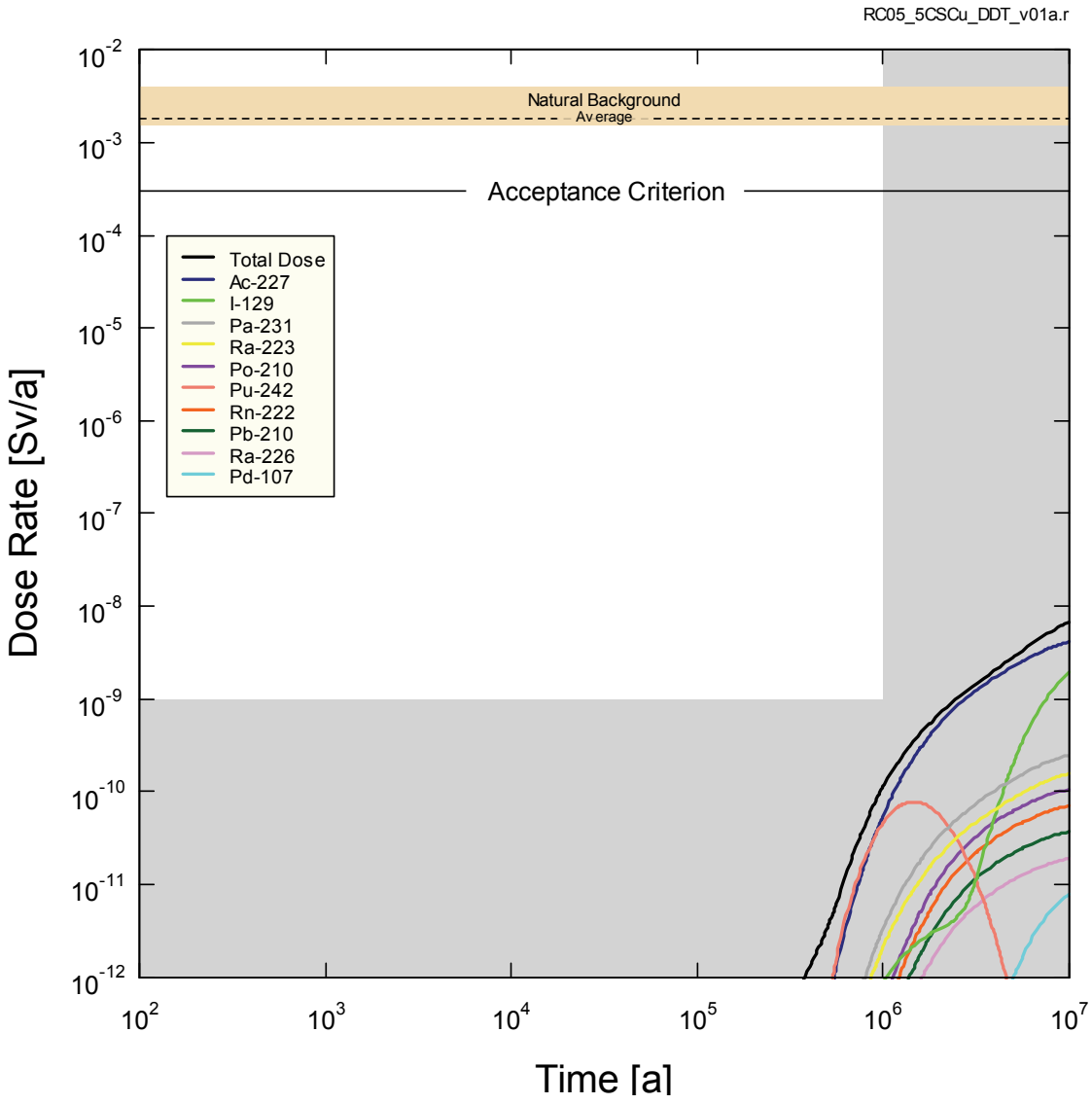

Figure 7-81: SYVAC3-CC4 - Sensitivity to No Sorption in the EBS

Figure 7-82 shows the individual contributions to the total dose rate for the most significant radionuclides for the sensitivity case with low sorption in the geosphere and coincident high radionuclide solubility limits (where "low" and "high" mean 1st percentile and 99th percentile, respectively, of their sampling ranges).

As in the Reference Case, the highest dose contributor is I-129. The maximum total dose rate occurs at the same time as in the Reference case ($1x10^7$ years) and reaches a value of 2.0×10^{-9} Sv/a or the same as in the Reference Case. Actinides (which are solubility limited) continue to be sorbed in the buffer and geosphere.

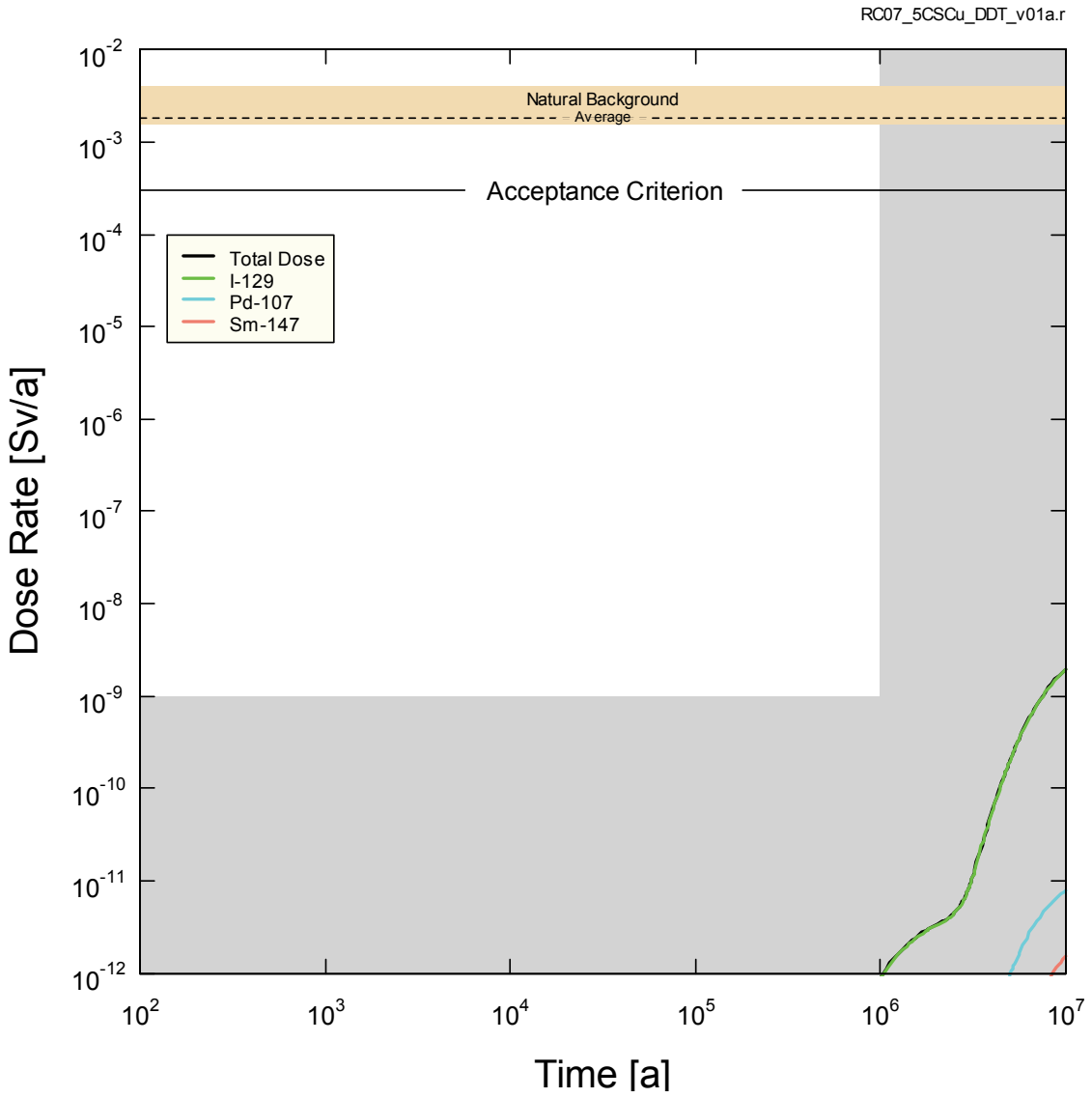

Figure 7-82: SYVAC3-CC4 - Sensitivity to Low Sorption in the Geosphere with Coincident High Solubility Limits

Figure 7-83 shows the total dose rates for the Reference Case and all four degraded chemical barrier cases. Table 7-35 provides the results in numerical form. All results are orders of magnitude below the interim dose acceptance criterion. The peak dose rate is not reached in the one million year period of interest.

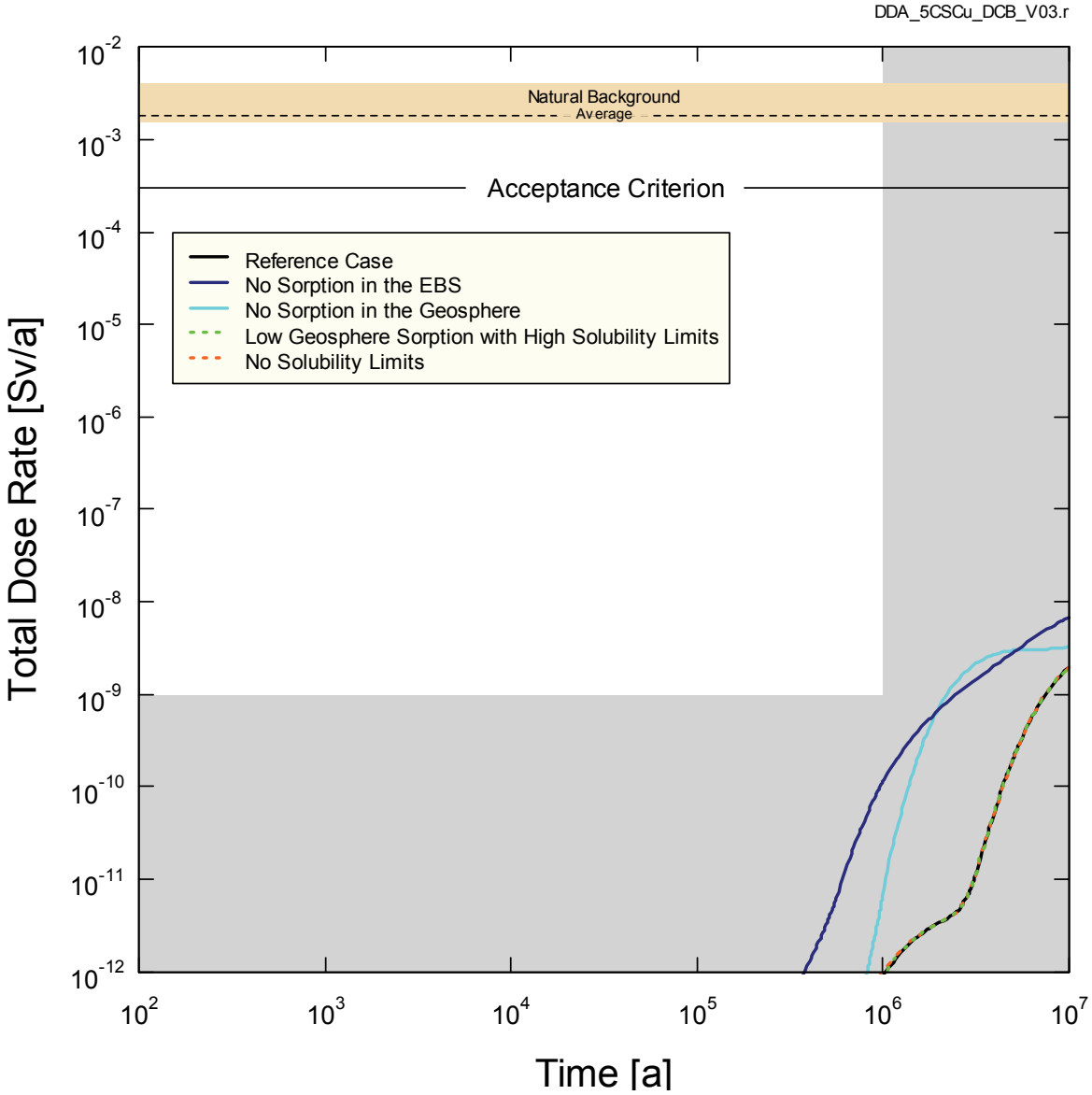

Figure 7-83: SYVAC3-CC4 - Summary for Defective Chemical Barrier Sensitivity Cases

Table 7-35: Result Summary for Defective Chemical Barrier Sensitivity Cases

Case	Maximum Dose Rate (Sv/a)	Ratio to Reference Case	Time of Maximum Dose Rate* (a)
Reference Case	$\boldsymbol{2.0x10^{-9}}$	**-**	$\boldsymbol{1.0x10^{7}}$
No Sorption in the Geosphere	$3.3x10^{-9}$	1.7	$1.0x10^{7}$
No Solubility Limits	$2.0x10^{-9}$	1.0	$1.0x10^{7}$
No Sorption in EBS	$6.7x10^{-9}$	3.4	$1.0x10^{7}$
Low Sorption in the Geosphere With Coincident High Radionuclide Solubility Limits	$2.0x10^{-9}$	1.0	$1.0x10^{7}$

Note: * The peak dose rate will be greater than the maximum dose rate if the maximum is not obtained within the 10 million year simulation time.

7.8.3 Probabilistic Analysis

In the previous sections, deterministic analyses are performed for a Reference Case and a series of sensitivity studies that examine the effect of degraded physical and chemical barriers.

Many of the modelling parameters are uncertain or have a natural degree of variability, and are therefore more generally characterized by a range or distribution of values. Simultaneous accounting of these uncertainties is achieved by using the SYVAC3-CC4 system model in probabilistic mode.

Probabilistic mode uses a Monte Carlo random sampling strategy that considers the full range of possible parameter values. The results presented here draw from 120,000 simulations in which parameter values are sampled randomly from their probability density functions. Each of these thousands of simulations produces a unique estimate of impact that is used to collectively generate a distribution that reflects the underlying uncertainty. An important caveat is that parameter values that could affect groundwater flow are not varied in these simulations. Groundwater flow effects are very limited in this geosphere because transport is diffusion dominant.

Geosphere diffusivities are varied according to a loguniform distribution with upper and lower bounds set to 10 and 0.1 times the median value.

A selection of biosphere parameters represented by probability distributions is provided in Table 7-24 through Table 7-26. A detailed description of the probability distributions for all parameters is provided in Gobien et al. (2013).

Number of Defective Containers

The number of defective containers is described by a binomial distribution that is characterized by the number of containers in the repository and the probability of a container with an initial penetrating defect escaping detection. Uncertainty in the container failure probability is

accounted for by expressing the failure probability per container as a lognormal probability density function with a geometric mean of 2×10^{-4}, a geometric standard deviation of 2, and bounds of 10^{-4} and 10^{-3}. The best-estimate failure probability is 2×10^{-4} per container. The locations of defective containers are randomly assigned within the repository in each simulation.

Figure 7-84 shows the as-sampled distribution of container failures.

From Monte Carlo sampling of the probability distribution, the most probable number of defective containers, or *mode* of the distribution, is 2 (i.e., the peak in the profile), while the average or *mean* value is 2.6. The maximum number in any one simulation is 12, and in 60% of the simulations there is at least one defective container in Sector 5. Defective containers in Sector 5 produce the highest dose rates to the critical group.

There are 9259 simulations (about 8% of the total) with zero defective containers.

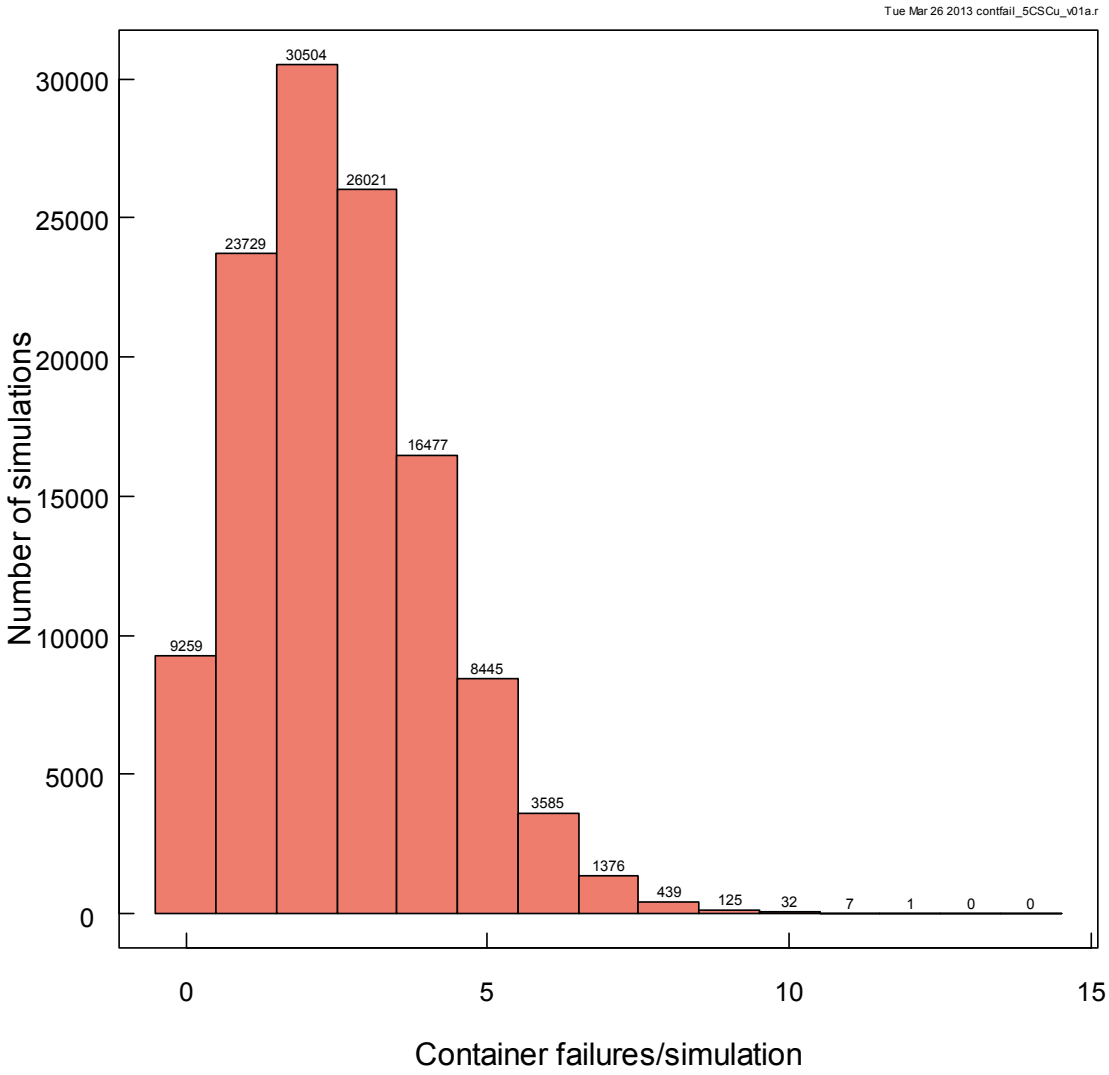

Figure 7-84: SYVAC3-CC4 - Distribution of Container Failures for 120,000 Simulations

Dose Rates

Figure 7-85 shows the distribution of the maximum total dose rate over a 10 million year simulation period to a member of the critical group for simulations with at least one defective container. The maximum total dose rate is the maximum, at any time during a simulation, of the sum of the individual dose rates for all radionuclides. The average dose rate, representing the arithmetic average of the maximum total dose rates over all simulations, is also shown.

The median maximum total dose rate is 1.5×10^{-9} Sv/a while the average maximum dose rate is 1.6×10^{-8} Sv/a. The average dose rate is greater than the median dose rate because of the asymmetrical shape of the distribution. These values can be compared against the maximum dose rate for the Reference Case of 2.0×10^{-9} Sv/a.

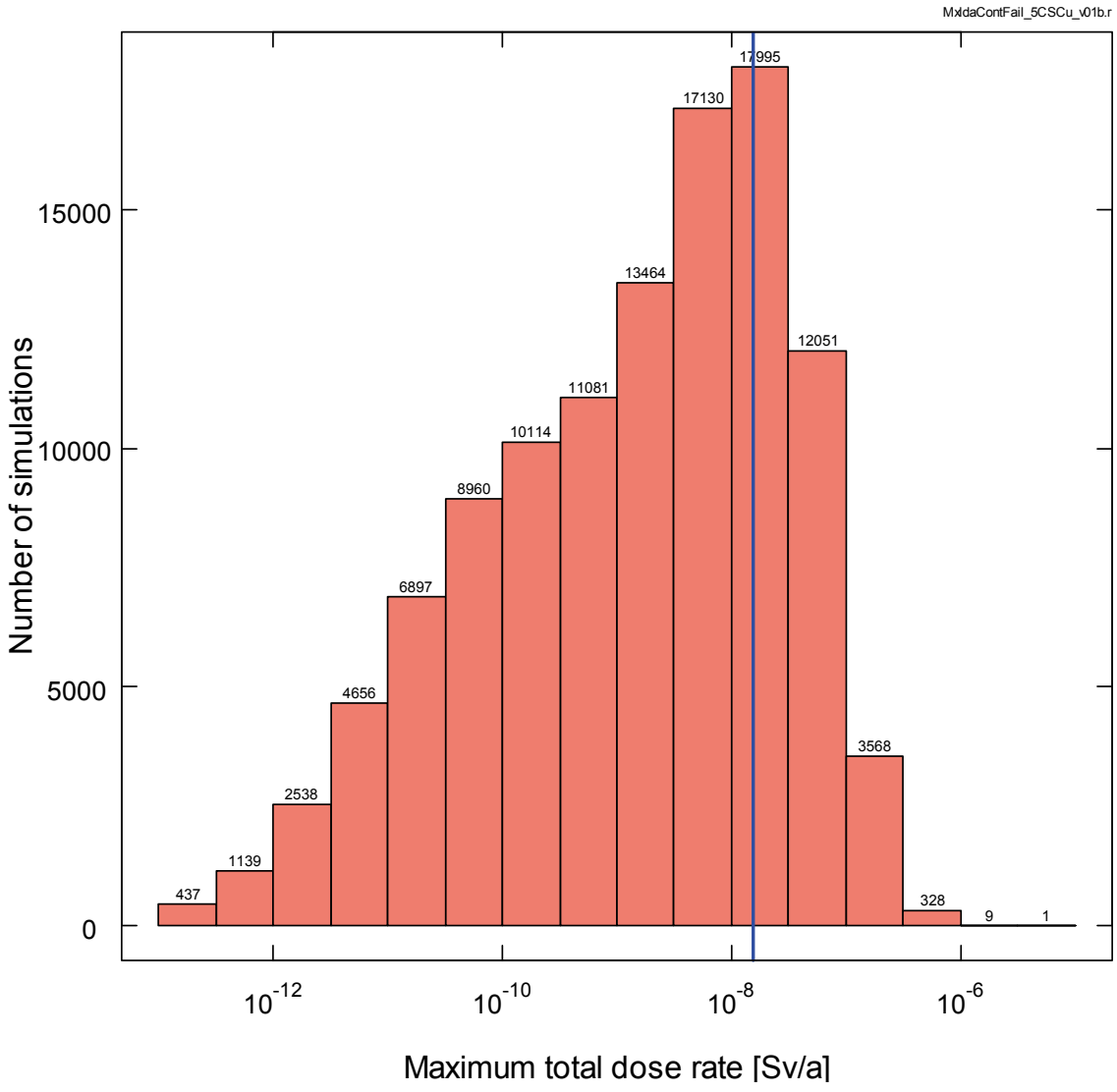

Note: the blue line represents the average value of 1.6×10^{-8} Sv/a

Figure 7-85: SYVAC3-CC4 - Distribution of the Maximum Dose Rate for Simulations with at Least One Defective Container

Statistical information concerning the distribution is summarized in Table 7-36. This table shows that the 95% confidence bound is symmetric around the average value. The median value and the average value differ by approximately a factor of 10, indicating that the average maximum dose is influenced by a number of higher-consequence simulations (i.e., the distribution of results is somewhat skewed). The simulations causing the results to be skewed have been reviewed and are discussed later in this section; however, none were found to result in dose rates very close to the interim dose acceptance criterion of 3.0×10^{-4} Sv/a.

Table 7-36: Statistical Information Concerning the Distribution of the Peak Dose Rate

Statistic	Value	Bootstrap 95% Confidence Bounds[1]	
		Lower Bound	Upper Bound
Average (Sv/a)	$1.55\text{x}10^{-8}$	$1.52\text{x}10^{-8}$	$1.57\text{x}10^{-8}$
95th Percentile (Sv/a)	$7.46\text{x}10^{-8}$	$7.35\text{x}10^{-8}$	$7.57\text{x}10^{-8}$
99th Percentile (Sv/a)	$1.82\text{x}10^{-7}$	$1.78\text{x}10^{-7}$	$1.88\text{x}10^{-7}$
Probability the peak dose rate exceeds $3.0\text{x}10^{-4}$ Sv/a [2]	0%	0%	0%
Median (Sv/a)	$1.52\text{x}10^{-9}$	$1.47\text{x}10^{-9}$	$1.57\text{x}10^{-9}$

Notes:

[1] Based on 10,000 replicates of the dataset obtained using the bootstrap methodology. The confidence intervals are calculated using the bootstrap method (with replacement). Since the distribution of peak dose rates is skewed, the bootstrap BC_a methodology described by DiCiccio and Efron (1996) is used.

[2] Interim dose acceptance criterion.

The average and median maximum dose rates for the individual radionuclides for all simulations are shown in Table 7-37. As in the Reference Case, I-129 is the dominant dose contributor.

Table 7-37: Average and Median Maximum Dose Rates for Individual Radionuclides

Radionuclide*	Average (Sv/a)	Median (Sv/a)
I-129	$1.50\text{x}10^{-8}$	$1.00\text{x}10^{-9}$
Pd-107	$4.49\text{x}10^{-10}$	$4.10\text{x}10^{-12}$
Sm-147	$8.68\text{x}10^{-11}$	$1.10\text{x}10^{-12}$
Cl-36	$4.10\text{x}10^{-11}$	-
Cs-135	$2.19\text{x}10^{-11}$	-
Se-79	$1.08\text{x}10^{-11}$	-
Tc-99	$6.93\text{x}10^{-13}$	-

Note: * A cutoff of 10^{-14} Sv/a is used.

Figure 7-86 shows the average dose rate as a function of time together with its 95% confidence intervals. The intervals are calculated using Chebychev's inequality (Guttman and Wilks 1965). Note that the Chebychev inequality gives upper bounds for the confidence intervals. The narrowness of the 95% confidence band indicates high statistical confidence.

The peak average dose occurs at 5.6×10^6 years.

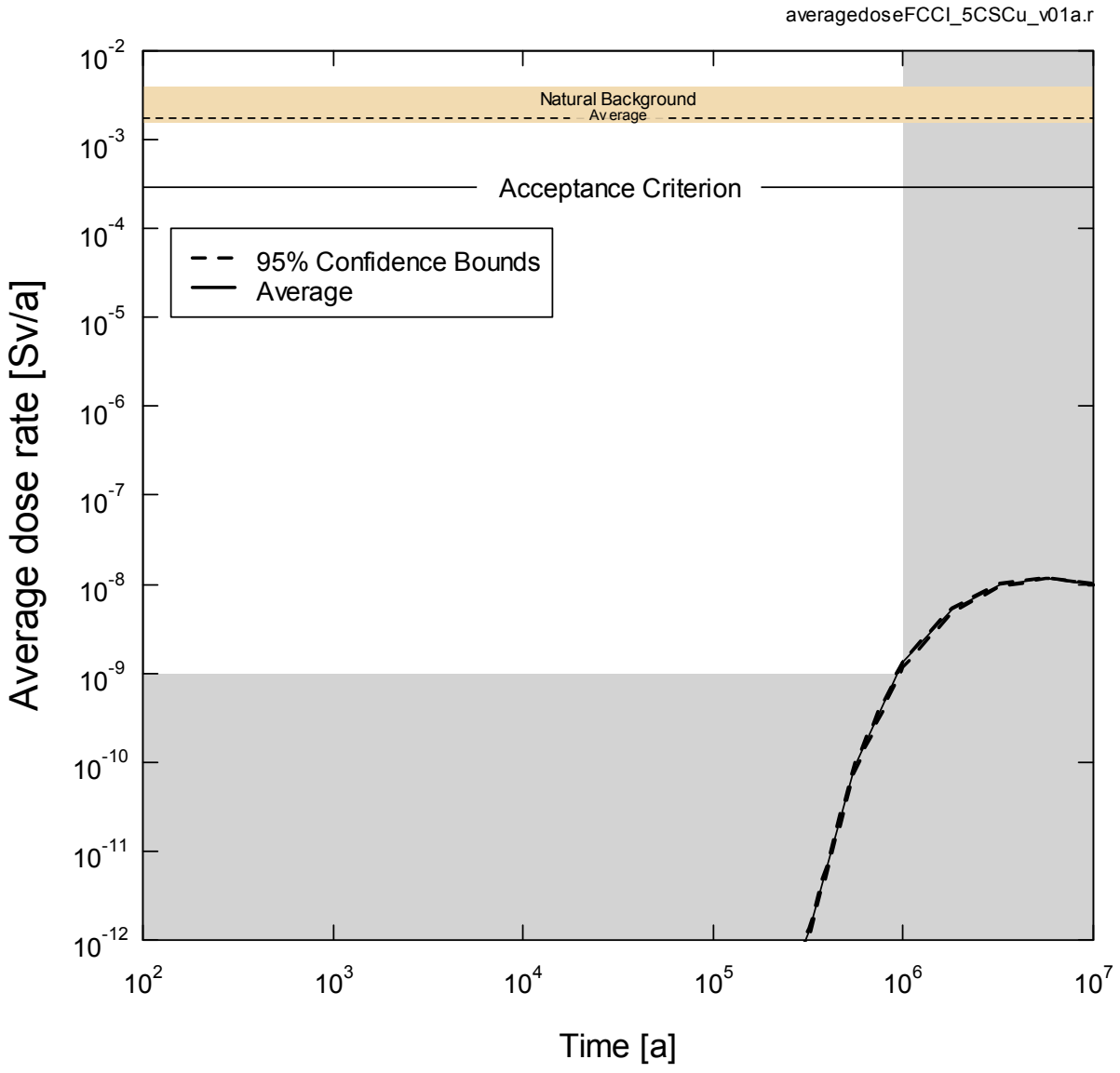

Figure 7-86: SYVAC3-CC4 - Average Dose Rate With 95% Confidence Bounds

Figure 7-87 shows the distribution of dose rates from all 120,000 simulations illustrating the 25, 50, 67, 90 and 99th percentile bands. These curves are all well below the interim dose

acceptance criterion of 3.0×10^{-4} Sv/a established in Section 7.1.1 for the radiological protection of persons.

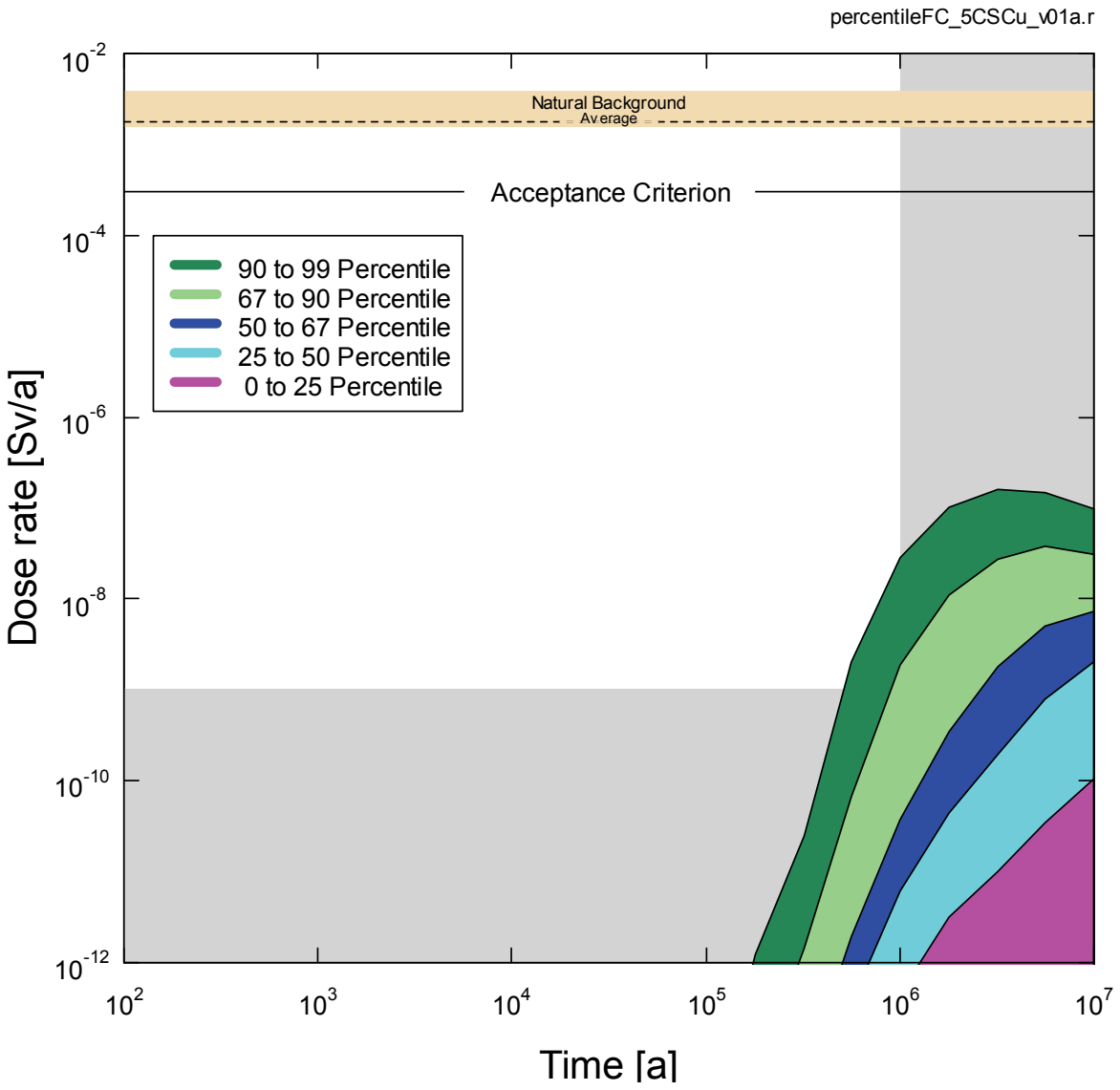

Figure 7-87: SYVAC3-CC4 - Dose Rate Percentile Bands

Maximum Value Simulations

Regulatory document G-320 (CNSC 2006) specifies that if the range of assessment results from probabilistic simulations indicates that acceptance criteria are exceeded, then it should be demonstrated that those results do not represent unreasonable risk to the environment or to the health and safety of persons, taking into account the conservatism built into the assessment and the likelihood of the circumstances leading to the results.

As per this guidance, all simulations were reviewed to identify runs that result in dose rates either very close to or above the interim dose acceptance criterion of 3.0×10^{-4} Sv/a. No such cases were identified.

7.9 Disruptive Scenarios

Disruptive Scenarios postulate the occurrence of unlikely events leading to possible penetration of barriers and abnormal loss of containment. Chapter 6 describes how the Disruptive Scenarios are identified and concludes that the following are relevant to the hypothetical site and conceptual repository design:

- Inadvertent Human Intrusion;
- Shaft Seal Failure;
- Abandoned Repository;
- Poorly Sealed Borehole;
- Undetected Fault;
- Severe Erosion;
- All Containers Fail; and
- Container Failure.

As noted in Section 7.2, a limited scope of work has been adopted in this study to reflect the level of effort required to meet the study objectives. The Abandoned Repository Scenario, the Poorly Sealed Borehole Scenario, the Undetected Fault Scenario, the Severe Erosion Scenario, the Container Failure Scenario and the variant case of the Human Intrusion Scenario in which the intrusion borehole is assumed to remain open are not within the scope of work.

Analysis results and dose consequences for the remaining Scenarios are discussed below.

7.9.1 Inadvertent Human Intrusion

The Inadvertent Human Intrusion Scenario considers the same evolution of the repository system as for the Normal Evolution Scenario with the only difference being the occurrence of human intrusion some time after institutional control of the site is no longer effective. In this scenario, an exploratory borehole is drilled through the geosphere and into the repository. The drill bit is assumed to intersect a used fuel container.

In an exploratory borehole, the investigators will most likely collect samples or conduct measurements at the repository level, which will readily identify any significant residual radioactivity (e.g., gamma logging is a standard borehole measurement). The investigators would then likely initiate appropriate precautions to prevent further exposure, including ensuring that any surface-released materials were appropriately disposed and that the borehole was sealed. Under normal drilling circumstances, there would be little impact.

Nevertheless, the Inadvertent Human Intrusion Scenario assumes:

- Interception of the repository is not recognized and therefore no safety restrictions are imposed; and
- The drill site is not managed according to current standards, and material from the borehole is released onto the surface.

As per Section 7.2.2, the scope of this study does not include the variant case in which the borehole is poorly sealed thereby resulting in a long-term pathway for contaminants to escape the repository. Such a case has been considered in SKB (2010a), and this work shows the consequences are orders of magnitude less than the SKB acute exposure dose rate for the human intrusion scenario. Although not calculated here, a similar conclusion is expected because there is little driving force to transport contaminated material up the (narrow) borehole, and any such release would be further diluted in the groundwater flowing in the upper geosphere aquifers.

7.9.1.1 Description

Figure 7-88 presents an event tree defining the possible outcomes associated with drilling in a repository location.

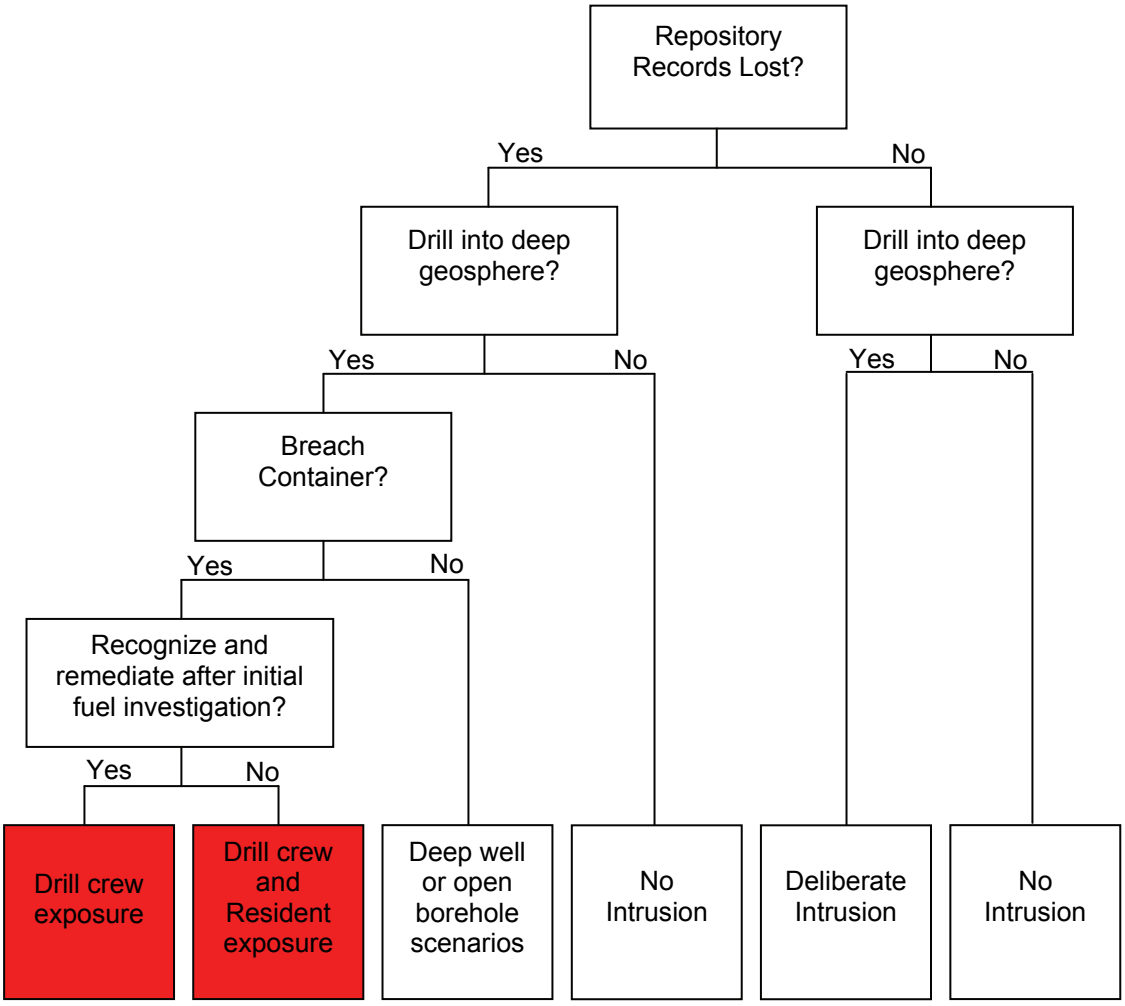

Figure 7-88: General Sequence of Events for Inadvertent Human Intrusion

Of interest to this discussion is the outcome in which:

- The repository records are lost;
- There is drilling into the deep geosphere; and
- The drilling breaches a used fuel container such that used fuel is inadvertently brought to the surface.

This then leads to potential exposure of the following two groups:

- The drill crew, exposed to contaminated drill slurry spread on the surface around the drill rig and to a core section containing used fuel; and
- A resident at the site, exposed by living nearby and growing food on soil contaminated by drill slurry[5].

To provide context, Table 7-38 presents a summary of the exposure groups considered in recent national and international inadvertent human intrusion safety assessments.

Table 7-38: Human Intrusion Pathways Considered in Recent Safety Assessments

Assessment	Scenario / Exposure Cases Considered
Gierszewski et al. 2004 (Canada)	Drill crew Core examination technician Construction worker on contaminated soil from drilling slurry Resident on contaminated soil from drilling slurry *
SKB 2011 (Sweden)	Drill crew * Resident on contaminated soil from slurry growing a garden or exposed from irrigation and drinking from well using open borehole into waste
JNC 2000 (Japan)	Excavation workers (exposed externally to core sample and internally by inhalation)
DOE 2008 (USA)	Reasonable Maximally Exposed Individual (Resident) exposed as a result of direct pathway to the groundwater created by the borehole.
Nagra 2002 (Switzerland)	Resident exposed as result of open borehole into waste creating pathway for waste to reach aquifer

Note: * Represents most limiting exposure case.

Intrusion Likelihood

Regulatory document G-320 (CNSC 2006) recognizes that inadvertent human intrusion events could result in dose rates that exceed the regulatory limit and it states that reasonable efforts

[5] Note that current drilling standards would not permit drill slurry to be left at the drill site, but is conservatively assumed here.

should be made to limit the probability of such high consequence scenarios. The following repository characteristics have been adopted to minimize the likelihood of this event:

- A deep location;
- Site selection based on an absence of groundwater resources at repository depth that could be used for drinking or agricultural purposes;
- Site selection based on an absence of economically exploitable natural resources; and
- The use of records and markers to preserve institutional memory to the extent practicable.

7.9.1.2 Model and Assumptions

Computer Code

The radiological consequences are determined using HIMv2.0 (Medri 2012), a human intrusion computer model developed using the AMBER v5.5 platform.

Screening calculations were initially done to identify the potentially radiologically significant radionuclides; consequently, 74 radionuclides are tracked in HIMv2.0. Short-lived radionuclides are included through the dose coefficients of their parents. Doses are obtained using inhalation, ingestion, groundshine and external dose coefficients.

A detailed description of the parameters and equations used in HIMv2.0 is available in Medri (2012).

Exposure Scenarios

The HIMv2.0 model determines the dose consequences to both exposure groups from the pathways illustrated in Figure 7-89. It models the acute dose to the drill crew at the time the material is brought to the surface and the annual chronic dose to residents who are assumed to live nearby and grow crops on the site after the intrusion has occurred.

In the Drill Crew exposure case, waste is brought to surface in the form of drill core and drill mud / slurry. Normal practice is for drill slurry to be contained at the site and ultimately be disposed of according to regulatory requirements. In this analysis, the drill slurry is conservatively assumed to be spilled around the drill rig without containment. The contaminated slurry would become mixed with surface material, as well as with subsequent drilled material. The waste is assumed to be uniformly mixed through a small near-surface volume of soil around the rig. The drill crew member handles the core sample containing used fuel for a short period of time, leading to an external exposure. This exposure is modelled using a point source approximation. The drill crew member is also exposed to the waste through groundshine, inhalation of contaminated dust and ingestion of contaminated soil from the mixed volume of near-surface material. The drill crew member is assumed not to wear a mask.

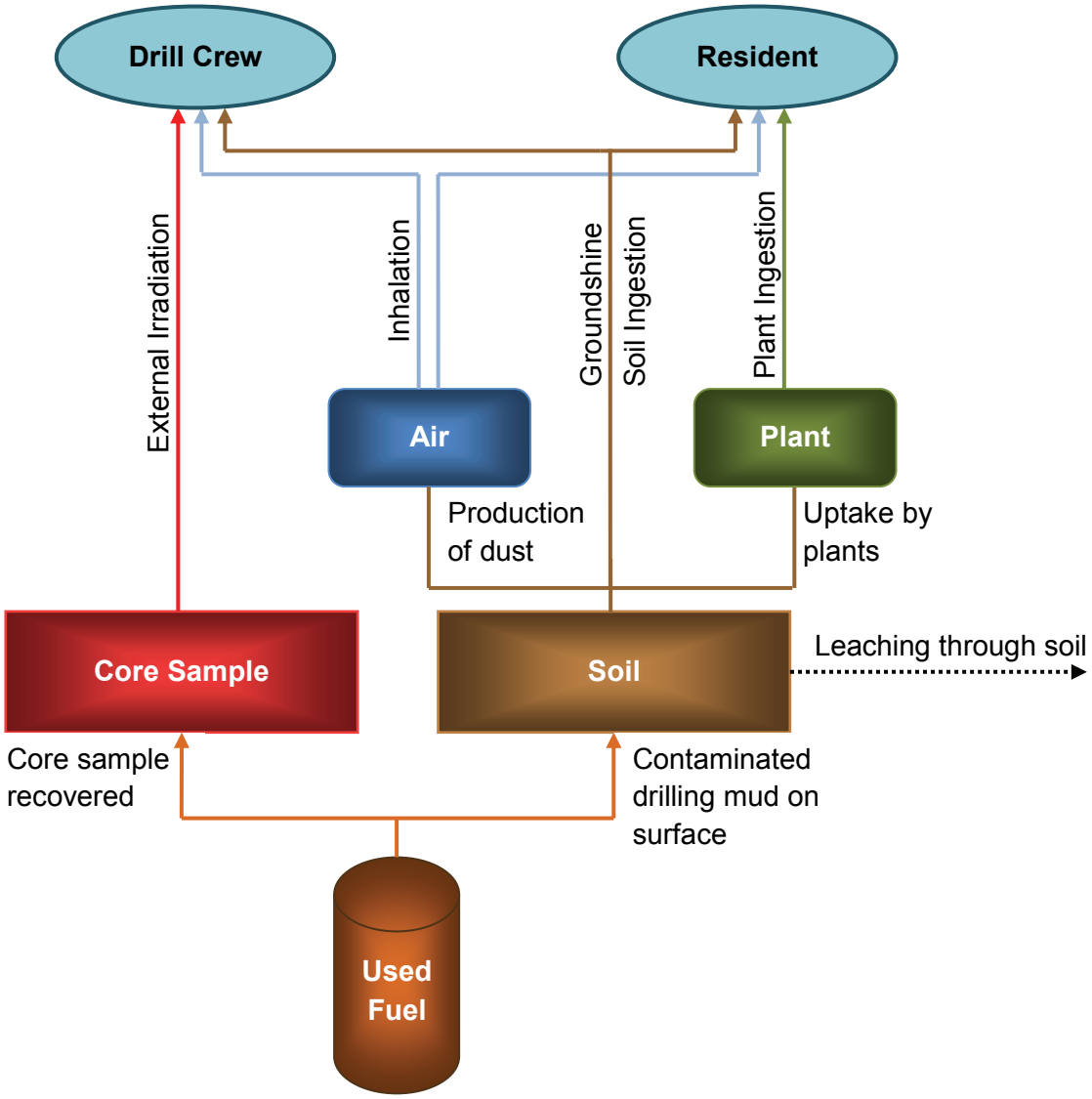

Figure 7-89: Inadvertent Human Intrusion - General Conceptual Model

In the Resident exposure case, the waste brought up with the drill slurry and deposited on the surface around the drill rig is assumed to remain in place without remediation. It remains on the surface, subject only to radioactive decay and leaching. Leaching is caused by precipitation that percolates downwards into the deeper soil. The resident lives around the contaminated site some time after the original intrusion, and grows some food on the contaminated soil. The resident is exposed to the contaminants through groundshine, dust inhalation and through ingestion of contaminated plants and soil. The area contaminated by drilling fluid would be small but have high contaminant concentrations, and therefore an allowance is made for the fraction of time that the resident is exposed to the contaminated site on an annual basis.

As a conservative estimate, the Resident case assumes that the exposure occurs in the first year after intrusion, before leaching has any significant effect on contaminant levels in the soil.

Key Assumptions and Parameters

Key assumptions are:

- Institutional control is maintained for a minimum of 300 years after closure, at which point intrusion becomes possible;
- Decay and ingrowth calculations start at the time of placement, at which point the used fuel is 30 years old;
- There is a minimum period of 70 years of extended monitoring and 25 years of decommissioning and closure following placement, which means the fuel is 425 years old (i.e., 30 + 70 + 25 +300) at the earliest time of intrusion. This is conservative in that the fuel will likely be older at a real site; and
- The drill intercepts a container in the repository and brings used fuel debris to the surface, either mixed with the drill slurry or as a section of intact drill core.

Table 7-39 lists parameters common to the intrusion cases and Table 7-40 lists the main exposure specific parameters used in HIMv2.0. Source references for these values can be found in Medri (2012).

Table 7-39: Common Parameters for Human Intrusion Scenario

Parameter	Value
Fraction of used fuel per container that is damaged by borehole	0.04
Mass of used fuel in a container (kg)	8650
Net infiltration rate of water through soil (m/a)	0.325
Human air inhalation rate (m^3/a)	8400
Soil type	Clay
Soil density (kg/m^3)	1400
Soil water content (m^3/m^3)	0.3
Instant release fractions (selected radionuclides)	Table 7-21

Table 7-40: Exposure Specific Parameters for Human Intrusion Scenario

Parameter	Drill Crew	Resident
Slurry area (m^2)	30	80
Activity duration	168 hrs (14 days, 12 hr shifts) 1 hr (core handling)	10% of the time (year-round)
Dust loading in air (kg_{soil}/m^3)	1.0×10^{-7}	3.2×10^{-8}
Plant ingestion (kg/a)	-	291
Soil ingestion	4.62×10^{-3} kg	0.12 kg/a
Contaminated food fraction (%)	-	10
Thickness of contaminated soil (m)	0.2	0.2
Fraction of U intercepted brought to surface as core	0.4	-
Fraction of U intercepted brought to surface as slurry	0.3	0.3

7.9.1.3 Results

Dose Impact

Figure 7-90 shows the acute dose to the Drill Crew and chronic annual dose to the Resident as a function of time after closure.

The exposure scenarios are stylized. They include all credible exposure pathways such that the overall dose estimate is credible, but not necessarily accurate.

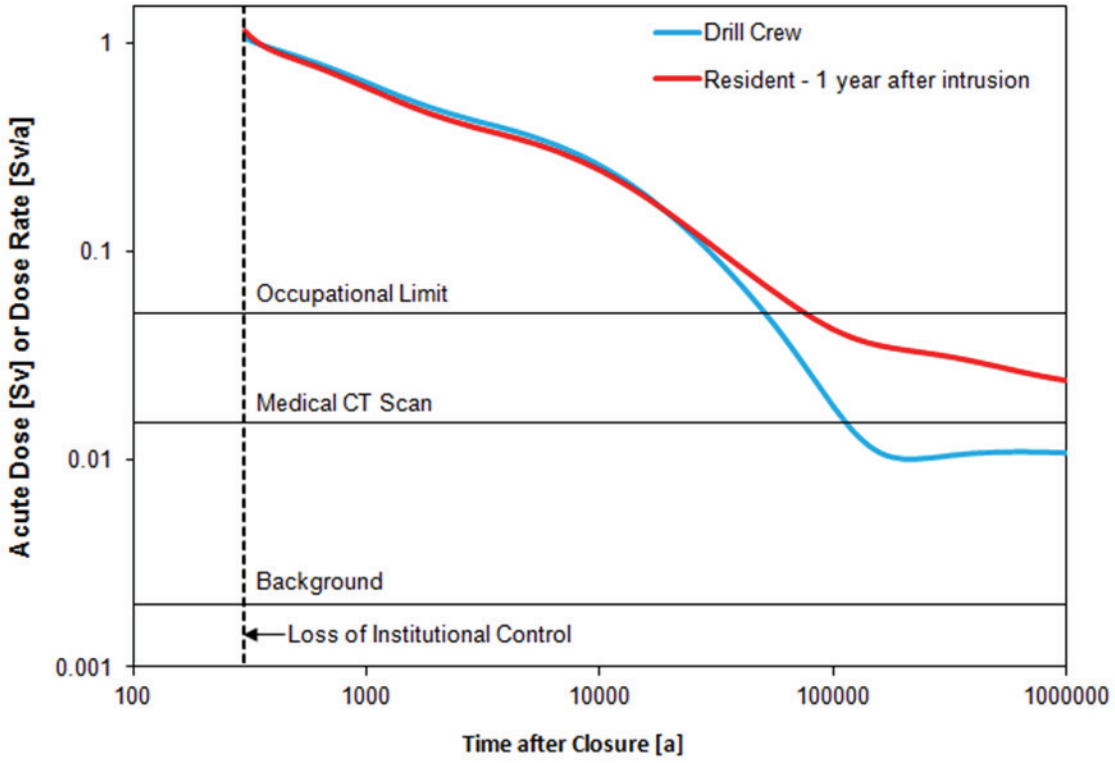

Note: The drill crew receives a one-time (acute) dose, while the resident receives a (chronic) dose rate

Figure 7-90: Inadvertent Human Intrusion - Exposure as a Function of Intrusion Time without Leaching

The results show:

- The maximum one-time dose to the Drill Crew is 1.06 Sv;
- The maximum annual chronic dose to the Resident in the first year after intrusion is 1.14 Sv;
- Doses decrease as a function of the assumed time of intrusion due to radioactive decay.

Figure 7-91 and Figure 7-92 show the breakdown of exposure pathways for the Drill Crew and the Resident.

The dose for both groups tends to be dominated by Am-241 for the first 300 to 1000 years, by Pu-240 and Pu-239 from 10^3 to 10^5 years, and by the U-238 decay chain radionuclides for longer times. This is in contrast to the Normal Evolution Scenario in which actinides are slow to dissolve, sorb strongly in the repository and geosphere, and generally do not reach the surface.

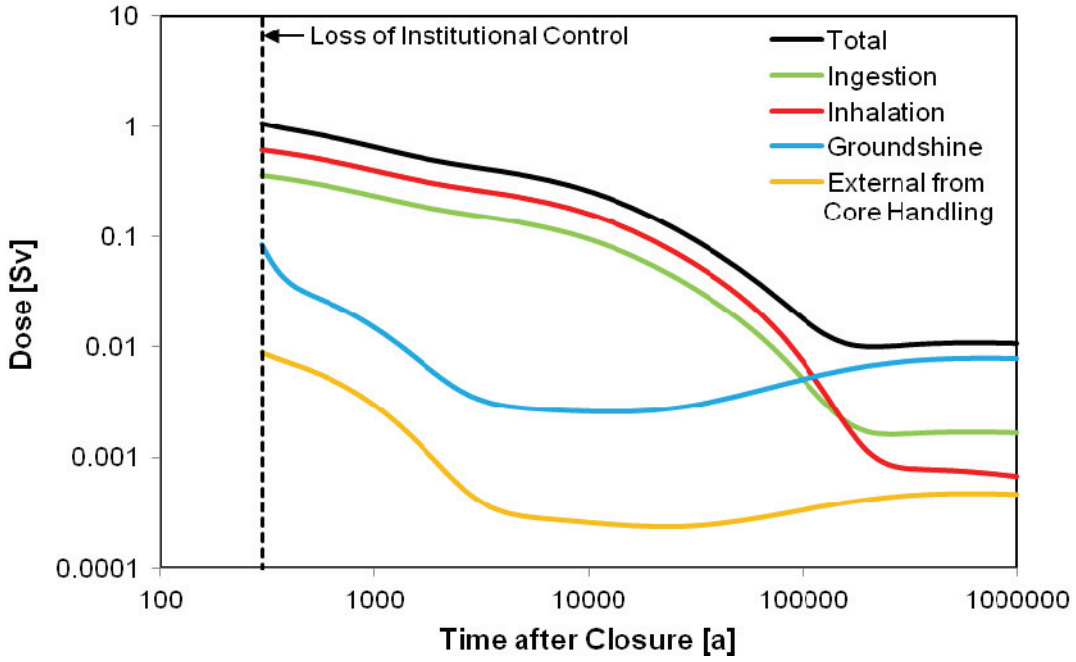

Note: Drill crew receives a one-time (acute) dose

Figure 7-91: Inadvertent Human Intrusion - Exposure Pathway Doses for Drill Crew

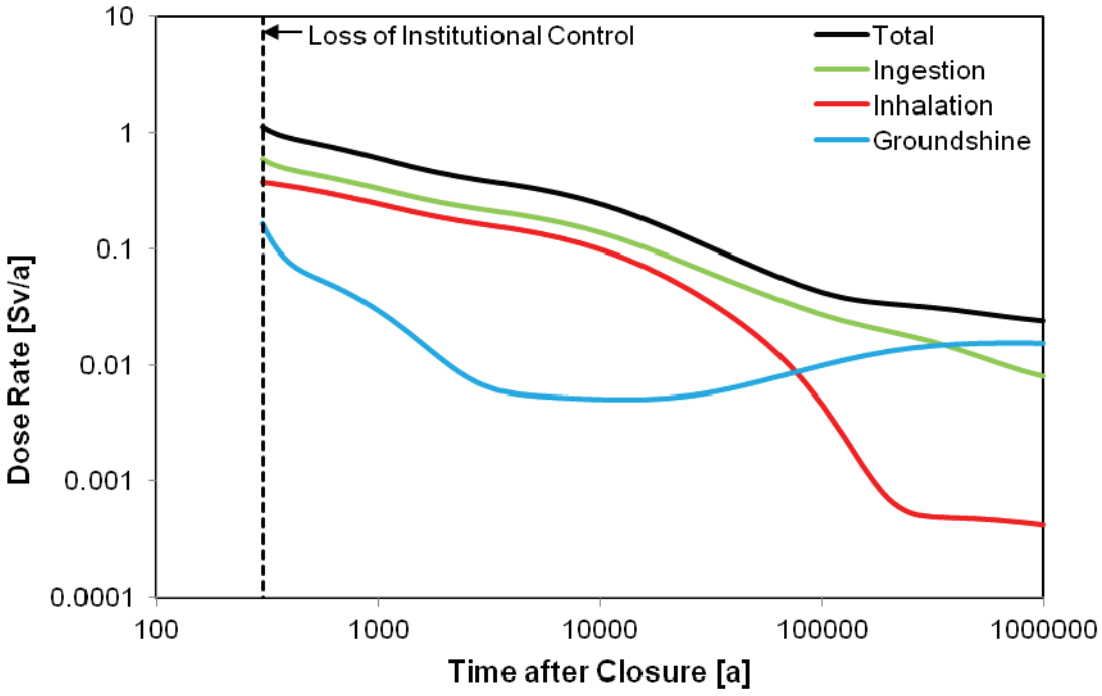

Note: Resident receives a chronic dose rate

Figure 7-92: Inadvertent Human Intrusion - Exposure Pathway Dose Rates for Resident

For the Resident, the exposure could potentially occur any time after the used fuel is deposited on the surface, assuming the site is not remediated in the interim. Figure 7-93 shows the dose to the Resident as a function of arrival time at the site, assuming the intrusion occurs at the earliest possible time after closure (i.e., 300 years). The results show that leaching can cause a substantial reduction in dose at later times.

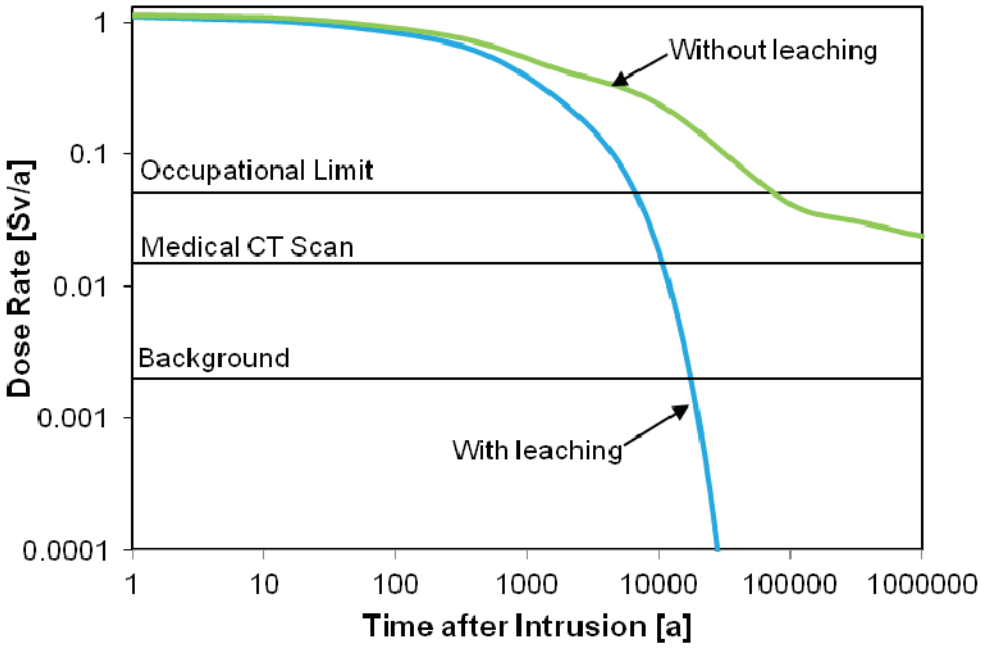

Figure 7-93: Dose Rate to Resident as a Function of Arrival Times Assuming Intrusion Occurs 300 Years after Closure

The results shown for the Resident dose in Figure 7-90 and Figure 7-92 conservatively assume all Rn-222 stays in the soil. In reality, because Rn-222 is a gas, much of it is likely to escape the soil and be dispersed in the atmosphere. Figure 7-94 shows the effect on the Resident dose of removing the groundshine contribution of Rn-222 and its short-lived daughters (i.e., Po-218, Pb-214, Bi-214 and Po-214) is significant at long times. The contribution from Pb-210 (a longer-lived daughter) is still included because Pb-210 formed underground would not quickly decay away when it reaches the surface.

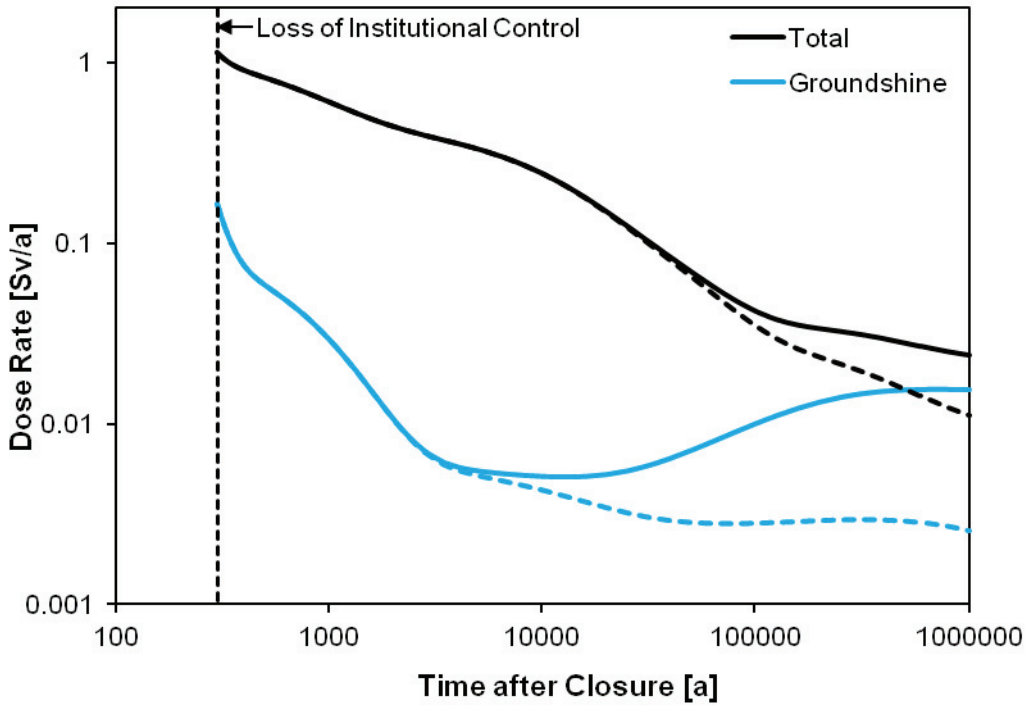

Note: Dotted lines show the dose rates without Rn-222 and its short-lived daughters

Figure 7-94: Effect of Rn-222 and Short-Lived Daughters in Groundshine Pathway on Resident Exposure

Annual Risk

To provide context for the dose rates, the annual risk to the most exposed individual can be estimated.

The annual risk to the Resident (R_R), which is the most exposed group, is determined via:

$$R_R = \Upsilon \cdot H \cdot P \qquad (7\text{-}3)$$

where: Υ is the probability coefficient for stochastic effects per Sv or 0.057 according to ICRP (2007);

H is the highest dose in the time period of concern; and

P is the intrusion frequency.

While the intrusion frequency could be estimated by assigning numerical values to each of the events in Figure 7-88, in practice these values are to a large extent non-quantifiable. Consequently, a more simplistic approach is adopted to illustrate the frequency with which an intrusion event may occur. This approach considers only the frequency of drilling.

Specifically, given that the area around the repository has no significant mineral resources, a deep drilling frequency to resurvey or update the geological information of about once every 100 years is estimated. Assuming this surveys an area of 10 km × 10 km, this is a drilling frequency of $10^{-10}/m^2a$. Since the repository consists of 275 rooms, with each room having a projected area of 1030 m^2, the frequency of inadvertent human intrusion into a room can be estimated as $2.8 \times 10^{-5}/a$. If only the container area is used, the intrusion frequency is estimated as $6.1 \times 10^{-6}/a$.

With Υ = 0.057/Sv, H = 1.14 Sv and P = $2.8 \times 10^{-5}/a$, the annual risk to the Resident from an inadvertent human intrusion event is $1.8 \times 10^{-6}/a$. This is below the risk target of $10^{-5}/a$ for disruptive scenarios identified in Section 7.1.1.

The intrusion probability does not take into account the beneficial effect of institutional memory. Institutional memory could decrease with time, but at earlier times when high doses are more likely, ongoing institutional memory would significantly reduce the intrusion probability (and the risk) of such an event.

The repository might also be detected through surface geophysical measurements, but not recognized as a used fuel facility. In this case exploration drilling would specifically aim for the repository and the intrusion probability could be higher than the above random drilling frequency. But since the drilling program would be specifically designed to explore the anomaly, it is also more likely that the repository would be recognized before or shortly after the repository level was reached and the consequences would therefore be less than those estimated above.

At long times, the cumulative probability of intrusion increases, but the consequences also decrease until eventually they are similar to those for inadvertent intrusion into a uranium ore body.

7.9.2 All Containers Fail

The long-lived used fuel containers are an important feature of the multi-barrier concept. The reference copper containers are anticipated to last for a period of time in excess of one million years, based on the copper corrosion barrier, sturdy mechanical design, and favourable site attributes. Nevertheless, the All Containers Fail Scenario considers the hypothetical case in which all the containers fail.

Since the containers are durable and there is no identified mechanism to fail all containers, the base case considers failure at 60,000 years. This corresponds, for example, to the earliest possible timeframe for an ice sheet to cover the site, and it is possible that some unanticipated effect of the ice sheet might cause failure.

The sensitivity to earlier failure times is examined in a sensitivity case in which all containers are assumed to fail at 10,000 years.

7.9.2.1 Model and Assumptions

The dose assessment is performed using the same SYVAC3-CC4 model described in Section 7.5.4. All model parameters are identical to those in the Reference Case of the Normal Evolution Scenario except that:

- All 12,778 containers fail simultaneously;
- The radionuclide release model takes no credit for the presence of the container. As such, the release of radionuclides from the slowly dissolving fuel to the near field is limited only by the buffer properties; and
- The potential presence of a few containers with small initial defects is not included. This modelling simplification does not affect the peak dose rate.

The behaviour of hydrogen gas generated through corrosion of the internal steel container is discussed in Chapter 8.

7.9.2.2 Results

<u>All Containers Fail at 60,000 Years</u>

Figure 7-95 shows the dose rate for the base case in which all containers fail at 60,000 years. Also included for comparison is the dose rate for the Reference Case. The maximum dose rate is 7.5×10^{-6} Sv/a, occurring at 1.0×10^{7} years. While the maximum is about 3750 times that of the Reference Case, it remains a factor of 133 below the interim dose acceptance criterion of 1×10^{-3} Sv/a.

Although not shown in the figure, the simulation has been extended to allow for calculation of an illustrative peak value. The result shows a value of 1.62×10^{-5} Sv/a is reached at 2.1×10^{7} years.

The discussion in Chapter 8 indicates that no adverse dose consequences are anticipated due to gas generation and migration.

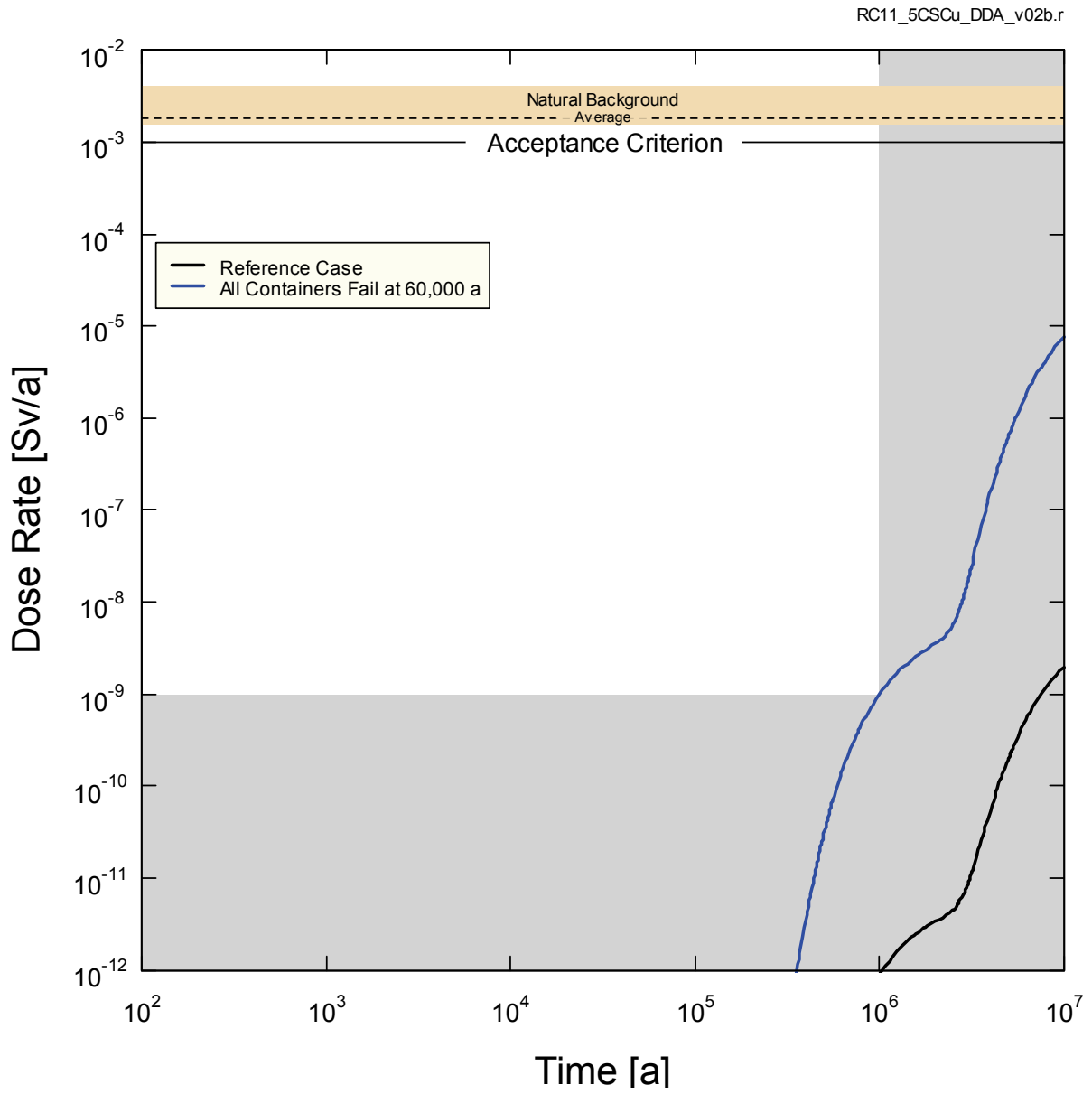

Figure 7-95: All Containers Fail at 60,000 Years - Dose Rate

Figure 7-96 shows the dose contributions from the most significant radionuclides. As in the Reference Case, I-129 is the dominant contributor.

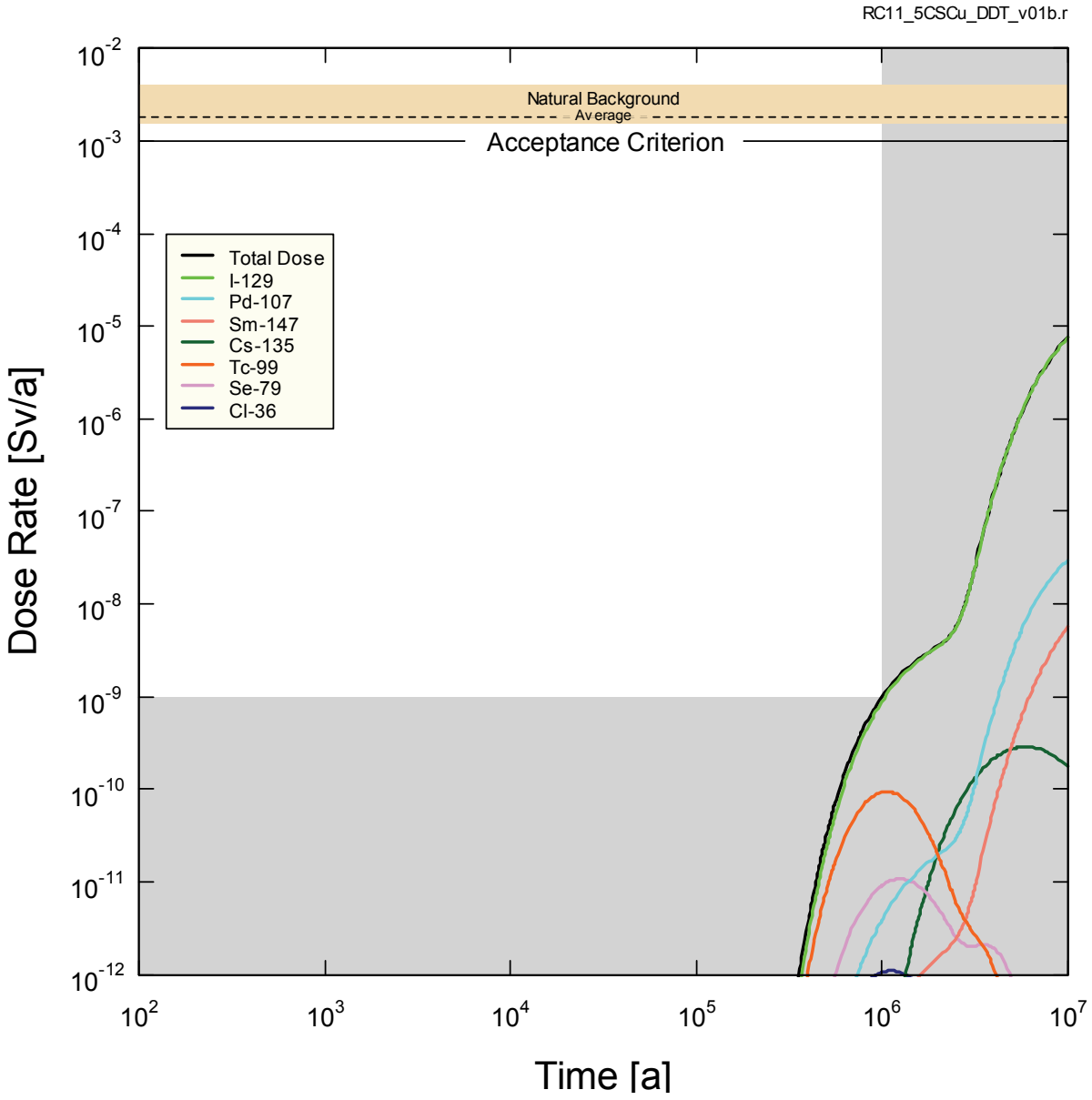

Figure 7-96: All Containers Fail at 60,000 Years – Contributing Radionuclides

All Containers Fail at 10,000 Years

Figure 7-97 compares the dose rate for the sensitivity case in which all containers fail at 10,000 years with results for the base case in which all containers fail at 60,000 years. The results are not substantially different, with a maximum dose rate of 8.4×10^{-6} Sv/a (or 1.1 times the base case value) occurring at 1.0×10^{7} years. The increase in dose rate occurs as a result of less time being available for radioactive decay.

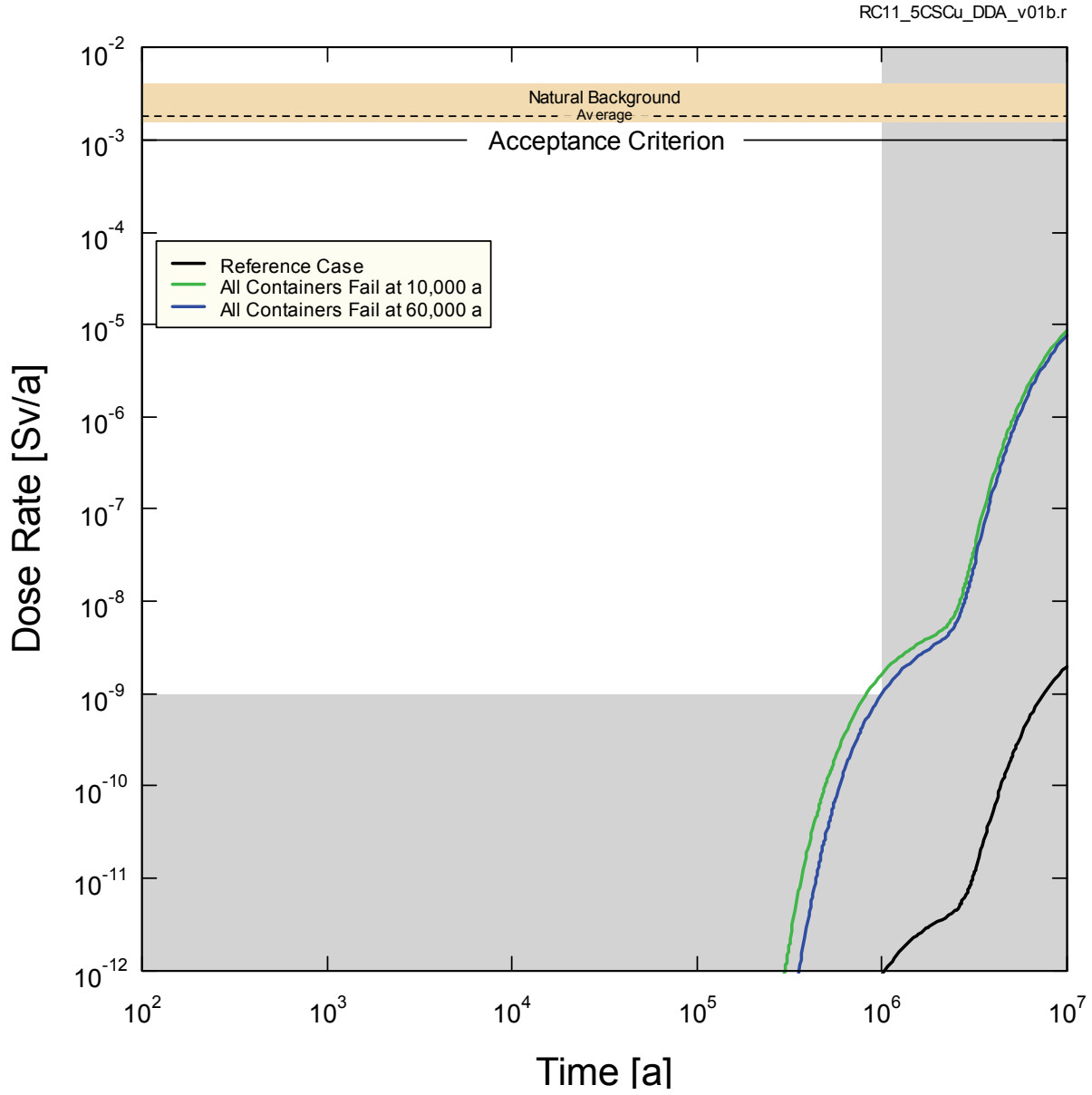

Figure 7-97: Sensitivity - All Containers Fail at 10,000 Years - Dose Rate

7.9.3 Shaft Seal Failure

The repository shafts represent a potentially important pathway for contaminant release and therefore the repository design includes specific measures to provide good shaft seals.

The Normal Evolution Scenario considers the likely behaviour of the shaft seals and the repository / shaft excavation damaged zones. The Shaft Seal Failure Scenario considers the same evolution of the repository system and the same exposure pathways as in the Reference Case of the Normal Evolution Scenario except that there is rapid and extensive degradation of

the shaft seals. For conservatism, it is assumed that this degradation occurs at the time of repository closure.

7.9.3.1 Model and Assumptions

Analysis of the Shaft Seal Failure Scenario is performed using the FRAC3DVS-OPG model described in Section 7.5.3. This model is used in lieu of the SYVAC3-CC4 system model because the groundwater flow field in the repository and near-field geosphere could be affected by degradation of the shaft seals.

All model parameters are the same as in the Reference Case, except that the hydraulic conductivities of all shaft seal materials are set to high values. Two simulations have been performed:

- Base Case: the hydraulic conductivities are set to 1.0×10^{-9} m/s; and
- Extreme Case: the hydraulic conductivities are set to 1.0×10^{-7} m/s.

The locations of the defective containers and the well have not been changed. This implies that the analysis may not result in the most conservative consequence and therefore the results should be considered illustrative only. For a real candidate site, these locations would be varied to ensure the most conservative locations are selected.

7.9.3.2 Results

The results for I-129 transport to the well are reported together with other FRAC3DVS-OPG sensitivity studies in Figure 7-54 in Section 7.7.1.2.6. Only the Extreme Case results are shown.

The results show no perceptible difference from the Reference Case. This is due to a combination of the distance to the shaft, the direction of groundwater flow, the low hydraulic conductivity of the host rock and the effectiveness of the other intact seals.

7.10 The Anticipated Effects of Glaciation on the Normal Evolution Scenario

During past glacial cycles, much of Canada has been covered by kilometre-thick ice sheets. The main factors that initiated these cycles (i.e., solar insolation variation due to Earth orbital dynamics and the location and size of the continents) are still present. Current levels of greenhouse gases in the atmosphere may delay the onset of the next glaciation (Berger and Loutre 2002); however, glacial cycles are expected to reassert themselves in the long run.

The scenario identification discussion in Chapter 6 identifies glaciation as an important external factor influencing the behaviour of the Normal Evolution Scenario. Because the dose assessment is performed for a constant temperate climate, the presence of glacial cycles represents a perturbation that has not been accounted for. The purpose of this section is to discuss the likely effects of glaciation on the calculated dose rates.

The discussion is partially based on results of the regional glaciation modelling study described in Chapter 2. Highlights of this are summarized below.

7.10.1 Regional Glaciation Modelling Summary

To explore the possible effects of glaciation, a representative future glacial cycle was generated using the University of Toronto Glacial System Model (GSM) (Peltier 2011). Of the eight ensembles of paleoclimate simulations for the last 120,000 years, nn9930 (warm-based) and nn9921 (cold-based) were selected for further modelling. Scenario nn9921 has more frequent glacial cycles, and longer glacial and permafrost presence than does nn9930. Three outputs (ice-sheet thickness, lake depth and permafrost depth) are applied as the transient boundary conditions in the regional paleohydrogeologic modelling studies.

A set of eleven sub-regional scale simulations has been defined to explore the potential effects of glaciation on the hypothetical study site. Of these, one simulation is for a reference scenario using actual parameter values while the remaining simulations are sensitivity cases using perturbed parameter values. The sensitivity cases examine the significance of surface hydraulic boundary conditions and the characterization of hydro-mechanical coupling. Due to the relative large size of the grid, repository features are not incorporated.

Results indicate that the glacial loading process tends to generate downward groundwater flow while the unloading process tends to induce an upward hydraulic gradient. The sensitivity analyses show that the change in hydraulic gradient is strongly associated with the hydro-mechanical coupling process. Even though vertical groundwater velocities increase during glacial periods, Peclet number results (Figure 2-29 to Figure 2-32) show that molecular diffusion remains the dominant mechanism for contaminant transport at the repository level throughout the entire 120,000 year glacial cycle.

Tracer simulations, representing the recharge of fresh water, show that boundary conditions have a substantial influence on the vertical tracer concentration profiles in the shallow and intermediate system (Figure 2-24). The simulations also show that tracer penetration is greatly retarded by the low permeability Cabot Head, Manitoulin and Queenston layers, so that oxygenated glacial meltwater does not percolate through the bottom of the Queenston formation (~320 mBGS) in any of the eleven cases examined.

The absence of meltwater penetration is also indirectly supported by the simulated TDS concentration results shown in Figure 2-36. TDS concentration increases sharply in the low permeability Manitoulin and Queenston formations and then remains at a high level (> 200 g/L) below the Queenston layer. Field data collected at the Bruce site (i.e., a site with similar characteristics to the hypothetical study site) (NWMO 2011) show similar trends. It is therefore expected that the deep groundwater regime would not be diluted by fresh recharge during a glacial cycle.

Permafrost forms prior to advance of the ice sheet. Due to its extremely low permeability, permafrost is viewed as beneficial in terms of contaminant transport, because it tends to inhibit the downward penetration of fresh recharge and the upward migration of contaminants. As shown in Figure 2-2 and Figure 2-3, the cold-based scenario nn9921 has a longer permafrost presence and a slightly greater permafrost extent in comparison to the warm-based scenario nn9930. The vertical permafrost extent in both scenarios does not reach a depth of 70 mBGS, which is more than 400 m above the proposed repository level (500 mBGS).

7.10.2 Applicability to the Dose Assessment

Section 7.2.1 notes that a constant temperate climate is assumed in the Normal Evolution Scenario. This section discusses the anticipated effects of glaciation on dose calculations performed using this assumption. Consideration is given to the effects of glaciation on the integrity of the used fuel containers, on contaminant transport and on human behaviour.

Integrity of the Used Fuel Containers:

As the ice sheet moves over the repository site, vertical stress will increase and the groundwater pressure will rise due to the hydro-mechanical coupling effect. If a unity loading coefficient is assumed, the water pressure at repository level could increase by about 27 MPa for a 3 km thick ice sheet. Chapter 4 describes that the used fuel containers are designed to withstand this additional load.

The Chapter 2 glaciation studies summarized above in Section 7.10.1 indicate that oxygenated fresh water does not percolate through the low permeability formations to the repository level. Dissolved oxygen is also likely to be consumed by organics and other reducing materials within the shallow groundwater regime. Conditions at repository level are therefore expected to remain anaerobic and reducing such that no change in the copper corrosion rate would occur.

The glaciation studies also show that the maximum vertical extent of permafrost does not reach to a depth greater than 70 mBGS. This implies that the temperature at the repository level (500 mBGS) will likely remain above 0°C so freeze-thaw induced failures are also not a concern.

It is therefore concluded that container integrity is not adversely affected during a glacial cycle.

Contaminant Transport:

The advancing and retreating ice sheets both erode and deposit rock and till, and glacial erosion could progressively remove a fraction of the rock overlying the repository. The Normal Evolution Scenario, defined in Section 7.2.1, assumes a small amount (tens of metres) of surface erosion occurs in the first one million years, with 100 metres (Hallet 2011) adopted as a sensitivity case.

With 100 m of erosion, the top of the Guelph formation would be about 40 m below grade rather than 140 m below grade, but still capped with very low permeability units of the Salina formation. Even if these units become more permeable due to their nearer surface exposure, the overall system enclosing the repository would remain diffusion-dominant because hundreds of metres of low permeability rock would still be present above the repository. Contaminants would still reach the Guelph formation on the same time-scale and proceed from there to the well and biosphere with the same capture rate as in the Reference Case simulation. Erosion is therefore not expected to adversely affect contaminant release in the one million year time period of interest.

The Chapter 2 glaciation studies also indicate that molecular diffusion remains the dominant transport mechanism at repository level throughout the entire 120,000 year glacial cycle. The rate of contaminant migration to the shallow groundwater system is therefore not expected to be

significantly adversely affected by the loading / unloading effects of glaciation on the deep groundwater system.

Tracer and TDS simulation results support this expectation. The vertical tracer profile shows that no freshwater recharge reaches the bottom of the Queenston formation at 120,000 years and that the TDS concentration remains high (> 200 g/L) at depths greater than 250 mBGS. The presence of high salinity brine at the Bruce site further indicates that there has been essentially no interaction with freshwater recharge during the last several glacial cycles.

It is therefore concluded that contaminant transport rates are not expected to be significantly different during a glacial cycle.

Human Behaviour:

Biosphere changes associated with glaciation will have a significant effect on human behaviour. The future climate would range between a temperate state, a permafrost state and an ice sheet state, with various intermediate states and possibly proglacial lakes forming at a variety of locations. Farming would not be possible for lengthy periods.

The adoption of different critical groups and different dose pathways to account for human behaviour during the changing climate states would result in dose predictions different from those presented here. However, given that the contaminant transport rates are largely unaffected by glaciation, doses to people and non-human biota are expected to remain very low.

Garisto et al. (2010) illustrates how the effect of different climate states could be modelled. Although this analysis is performed for a repository constructed in the crystalline rock of the Canadian Shield, the analysis methods and techniques are transferrable to a sedimentary rock environment.

Summary:

Because container integrity is not challenged and because the contaminant transport rate is expected to remain extremely low, the assumption of a constant temperate climate in the dose assessment for this study is deemed reasonable. While detailed transient modelling of contaminant transport could result in changes to the dose predictions, the consequences of these changes are expected to be relatively minor given the large margins available to the interim dose acceptance criteria.

Note that for a real site, an in-depth site-specific analysis of erosion and contaminant transport would be conducted. Garisto et al. (2010) provides an example of how this could be done.

7.11 Other Considerations

This section presents results for complementary indicators for radiological assessment, results for the radiological protection of the environment, and results for the protection of persons and the environment from hazardous substances.

The effects of gas generation and migration are described in Chapter 8.

7.11.1 Complementary Indicators for the Radiological Assessment

An “indicator” is a characteristic or consequence of a repository which can be used to indicate the overall safety or performance of the system. The most widely used indicator is the peak radiological dose rate, which is calculated from the characteristics of the waste and repository, the properties of the geosphere and biosphere, and the characteristics of the critical group.

The relevance of the calculated dose rates as indicators of potential exposure tends to decrease with time, in part because of uncertainties in the models used to calculate them. In particular, assumptions concerning the biosphere (e.g., climate), human lifestyles (i.e., critical group characteristics) and water flows in the near-surface environment become increasingly uncertain. The purpose of complementary long-term indicators is to supplement the dose rate indicator using system characteristics that are much less sensitive to such assumptions.

The types of complementary indicators considered here address:

- Radionuclide concentrations in the biosphere; and
- Radionuclide transport to the biosphere.

Indicators of the first type avoid assumptions about biosphere pathways but make assumptions about flow rates in surface water bodies (i.e., dilution rates). Indicators of the second type avoid assumptions about surface water flows. Concentration type indicators are more useful on medium timeframes (about 10^4 to 10^5 years), while transport type indicators are more useful for very long timeframes (> 10^5 years) when there is more uncertainty about surface conditions.

The specific complementary indicators considered were selected based on the recommendations of the SPIN project (Becker et al. 2002). The indicators are:

- Radiotoxicity concentration in a water body, for medium time scales; and
- Radiotoxicity transport from the geosphere, for longer time scales.

Radiotoxicity concentration (in Sv/m^3) is the sum over all radionuclides of the activity concentrations in the water body (in Bq/m^3) multiplied by the corresponding radionuclide ingestion dose coefficient. Radiotoxicity transport from the geosphere (in Sv/a) is similarly defined.

Although these complementary indicators are expressed in units of Sv/m^3 or Sv/a, they do not represent a dose; rather, they are radiotoxicity-weighted concentration or transport indicators.

7.11.1.1 Reference Indicator Values

To make use of indicators, reference values are required for comparison purposes.

<u>Radiotoxicity Concentration in a Water Body:</u>

A reference value for the radiotoxicity concentration in a water body has been derived using information on present-day natural background radionuclide concentrations in Canadian surface waters. Table 7-41 shows these concentrations for a variety of radionuclides. Data

representative of Canadian surface waters are taken from Sheppard and Sanipelli (2011a) while Southern Ontario data are taken from a subset of samples in Sheppard and Sanipelli (2011b).

Table 7-41: Background Concentration of Radionuclides in Surface Waters

Surface Water Concentration [Bq/L]					Ingestion DCF [Sv/Bq]	Radiotoxicity [Sv/m^3]
Radionuclide	Canadian		Southern Ontario			
H-3	3.2×10^{0}		3.7×10^{0}		1.8×10^{-11}	5.8×10^{-8}
Cl-36	5.1×10^{-6}		2.0×10^{-6}		9.3×10^{-10}	4.7×10^{-12}
K-40	3.3×10^{-2}		3.4×10^{-2}	a	6.2×10^{-9}	2.0×10^{-7}
Rb-87	2.6×10^{-4}		1.1×10^{-3}	b	1.5×10^{-9}	3.9×10^{-10}
I-129	1.0×10^{-7}		8.7×10^{-8}		1.1×10^{-7}	1.1×10^{-11}
Bi-210	6.4×10^{-3}	c	2.0×10^{-2}	c	1.3×10^{-9}	8.3×10^{-9}
Pb-210	6.4×10^{-3}		2.0×10^{-2}		6.9×10^{-7}	4.4×10^{-6}
Po-210	7.1×10^{-3}		2.0×10^{-2}	c	1.2×10^{-6}	8.5×10^{-6}
Rn-222	2.7×10^{-3}	d	5.8×10^{-3}	d	2.5×10^{-10}	6.8×10^{-10}
Ra-223	2.0×10^{-7}	f	4.8×10^{-7}	f	1.0×10^{-7}	2.0×10^{-11}
Ra-224	7.8×10^{-3}	h	6.3×10^{-3}	h	7.1×10^{-8}	5.6×10^{-7}
Ra-226	2.7×10^{-3}		5.8×10^{-3}		2.8×10^{-7}	7.6×10^{-7}
Ac-227	2.0×10^{-7}	f	4.8×10^{-7}	f	1.1×10^{-6}	2.2×10^{-10}
Th-227	2.0×10^{-7}	f	4.8×10^{-7}	f	8.8×10^{-9}	1.8×10^{-12}
Ra-228	2.9×10^{-4}		3.1×10^{-4}	g	6.9×10^{-7}	2.0×10^{-7}
Th-228	9.6×10^{-4}		3.1×10^{-4}	g	7.2×10^{-8}	6.9×10^{-8}
Th-230	1.9×10^{-3}		5.1×10^{-3}	e	2.1×10^{-7}	4.0×10^{-7}
Pa-231	2.0×10^{-7}	f	4.8×10^{-7}	f	7.1×10^{-7}	1.4×10^{-10}
Th-231	1.5×10^{-7}		4.8×10^{-7}	f	3.4×10^{-10}	5.1×10^{-14}
Th-232	3.9×10^{-4}		3.1×10^{-4}		2.3×10^{-7}	9.0×10^{-8}
Th-234	3.3×10^{-3}	e	5.1×10^{-3}	e	3.4×10^{-9}	1.1×10^{-8}
U-234	7.3×10^{-3}		5.1×10^{-3}	e	4.9×10^{-8}	3.6×10^{-7}
U-235	9.3×10^{-5}		2.4×10^{-4}		4.7×10^{-8}	4.4×10^{-9}
U-238	3.3×10^{-3}		5.1×10^{-3}		4.5×10^{-8}	1.5×10^{-7}
					Total	1.6×10^{-5}

Notes:

(-) Indicates no data for that species
(a) Estimated using stable K concentration
(b) Estimated using stable Rb concentration
(c) Assumed to be in secular equilibrium with Pb-210
(d) Assumed to be in secular equilibrium with Ra-226
(e) Assumed to be in secular equilibrium with U-238
(f) Values are 500 times lower than for U-235 in water, as recommended by Amiro (1992, 1993)
(g) Assumed to be in secular equilibrium with Th-232
(h) Values are 20 times higher than for Th-232 in water, as recommended by Amiro (1992, 1993)

Sheppard and Sanipelli (2011a) suggest that the background concentration of radioactive species in surface water remains fairly homogeneous across Canada. Data extracted specifically for Southern Ontario appears to verify this with most radionuclide concentrations within a factor of two of the Canadian values. The largest difference is for Rb-87, with the Canadian value 4.5 times lower than the Southern Ontario value. However, given the limited number of samples for the Southern Ontario data and the error associated with measuring concentrations around the detection limit, it is likely that the variations between the Canadian values and the Southern Ontario values are within the variability of the measurements. Consequently, Canadian surface water data have been selected as representative of the surface waters applicable to this hypothetical site.

Radiotoxicity concentration is determined by multiplying the surface water concentrations by the appropriate ingestion dose conversion factor (Gobien and Garisto 2012). The results are shown in the rightmost column of Table 7-41, with the total value of 1.6×10^{-5} Sv/m^3 indicated at the bottom. For comparison, use of data specific to Southern Ontario only results in a higher radiotoxicity concentration of 4.2×10^{-5} Sv/m^3. Thus, the selected reference value is conservative when used as a comparative baseline.

Dose impacts associated with these natural background levels are not likely of concern so it follows that any dose impacts from the repository that are small in comparison are also not likely of concern.

Radiotoxicity Transport from the Geosphere:

Natural transport processes carry small amounts of natural radioactivity from within the geosphere to the biosphere. The most important process for the sedimentary rock site in the hypothetical geosphere is erosion. Surface erosion rates are primarily due to wind and surface water runoff; however, the likely source of significant long-term erosion is glaciation. Surface soil erosion rates can vary significantly (0.5-1.5 kg dw/m^2/a, CSA 2008) depending on the soil type, corresponding to about 0.0005 m/a (assuming a soil density of 2000 kg/m^3); however, soil is also naturally replenished. A realistic but conservative estimate of glacial erosion of 100 m over 1 million years is given in Hallet (2011), which implies an average erosion rate of 0.0001 m/a.

The natural radioactivity transport from the geosphere is estimated using the elemental composition of surface soils and shallow rocks. The primary source of Canadian surface rock concentrations is Sheppard and Sanipelli (2011a); however, Southern Ontario data from Sheppard and Sanipelli (2011b) and elemental data from shallow rock layers from rock cores drilled in the Michigan basin (Wigston and Jackson 2010a, 2010b; Jackson and Murphy 2011) have also been used.

Table 7-42 shows the natural concentration of the various radionuclides from Canadian sites, Southern Ontario sites and borehole data from the upper 100 m of the Michigan Basin. These data show limited variability for most species. Similar to the surface water data discussed above, the relatively small number of samples for Southern Ontario and the borehole data suggest that differences between the datasets may be within the natural variability of the measurements. Consequently, the more robust Canada wide dataset from Sheppard and Sanipelli (2011a) is selected as representative of the natural concentrations applicable to this hypothetical site.

The resulting radiotoxicity is shown in the rightmost column of Table 7-42 and is determined by multiplying the Canadian data in by the ingestion dose conversion factor. The total radiotoxicity is 1.2×10^{-4} Sv/kg.

Table 7-42: Background Concentration of Radionuclides in Surface Soils and Rocks

Soil/Rock Concentration [Bq/kg]							Radiotoxicity [Sv/kg]
Radionuclide	Canadian		Southern Ontario		Borehole		
H-3	0.04		-		-		7.2×10^{-13}
Cl-36	2.0×10^{-4}		-		-		1.9×10^{-13}
K-40	430		-		118	a	2.7×10^{-6}
Rb-87	25		-		17	b	3.8×10^{-8}
I-129	1.40×10^{-4}		3.4×10^{-4}		-		1.5×10^{-11}
Bi-210	49	c	77	c	16	e	6.4×10^{-8}
Pb-210	49		77		16	e	3.4×10^{-5}
Po-210	40		77	c	16	e	4.8×10^{-5}
Rn-222	29	d	30	d	16	e	7.2×10^{-9}
Ra-223	1	f	3.7	f	0.73	f	1.0×10^{-7}
Ra-224	22	g	16	g	8.3	g	1.6×10^{-6}
Ra-226	29		30		16	e	8.1×10^{-6}
Ac-227	1	f	0.83	f	0.73	f	1.1×10^{-6}
Th-227	1	f	0.83	f	0.73	f	8.8×10^{-9}
Ra-228	22	g	147		8.3	g	1.5×10^{-5}
Th-228	22	g	20		8.3	g	1.6×10^{-6}
Th-230	19		17	e	16	e	4.0×10^{-6}
Pa-231	1	f	0.83	f	0.73	f	7.1×10^{-7}
Th-231	1	f	0.83	f	0.73	f	3.4×10^{-10}
Th-232	22		16		8.3		5.1×10^{-6}
Th-234	23	e	17	e	16	e	7.8×10^{-8}
U-234	21		17	e	16	e	1.0×10^{-6}
U-235	1		0.83		0.73		4.7×10^{-8}
U-238	23		17		16		1.0×10^{-6}
					Total		1.2×10^{-4}

Notes:

(-) Indicates no data for that species
(a) Estimated using stable K concentration
(b) Estimated using stable Rb concentration
(c) Assumed to be in secular equilibrium with Pb-210
(d) Assumed to be in secular equilibrium with Ra-226
(e) Assumed to be in secular equilibrium with U-238
(f) Assumed to be in secular equilibrium with U-235
(g) Assumed to be in secular equilibrium with Th-232

Repeating the calculation using Southern Ontario data and borehole data results in total radiotoxicity values of 2.7×10^{-4} Sv/kg and 5×10^{-5} Sv/kg, respectively.

For the assumed erosion rate of 0.0001 m/a, the radiotoxicity transport over the 6 km^2 repository footprint is 200 Sv/a (assuming an average rock density of 2750 kg/m^3). For comparison, the resulting radiotoxicity transport computed using the Southern Ontario data and the borehole data are 400 Sv/a and 80 Sv/a respectively.

Reference Values:

Table 7-43 summarizes the reference values for the dose rate indicator and the complementary long-term indicators developed for use in this study. The reference values proposed in the EC SPIN project (Becker et al. 2002) are also shown for comparison.

Table 7-43: Reference Values for Indicators

Indicator	Reference Value	
	Current Study	SPIN
Dose rate (Sv/a)	3×10^{-4}	1×10^{-4} to 3×10^{-4}
Radiotoxicity concentration in surface water (Sv/m^3)	1.6×10^{-5}	2×10^{-5}
Radiotoxicity transport from the geosphere (Sv/a)	200	60

7.11.1.2 Results for Complementary Indicators

The portion of the hypothetical geosphere described in Chapter 2 that is modelled with the FRAC3DVS-OPG code in Section 7.5.3 does not contain any surface water bodies that receive contaminants within the modelled domain. The 'radiotoxicity concentration in a waterbody' indicator has therefore not been calculated. For a real site, water bodies would likely be nearby and this indicator would be assessed.

The radionuclide transport to the biosphere for the individual radionuclides is used to calculate the radiotoxicity transport indicator.

Figure 7-98 shows the radiotoxicity transport indicator for the Reference Case together with the dose rate indicator. The indicators have the same general shape because they both depend on radionuclide transport to the biosphere. The figure shows very large margins to the associated criteria for both indictors.

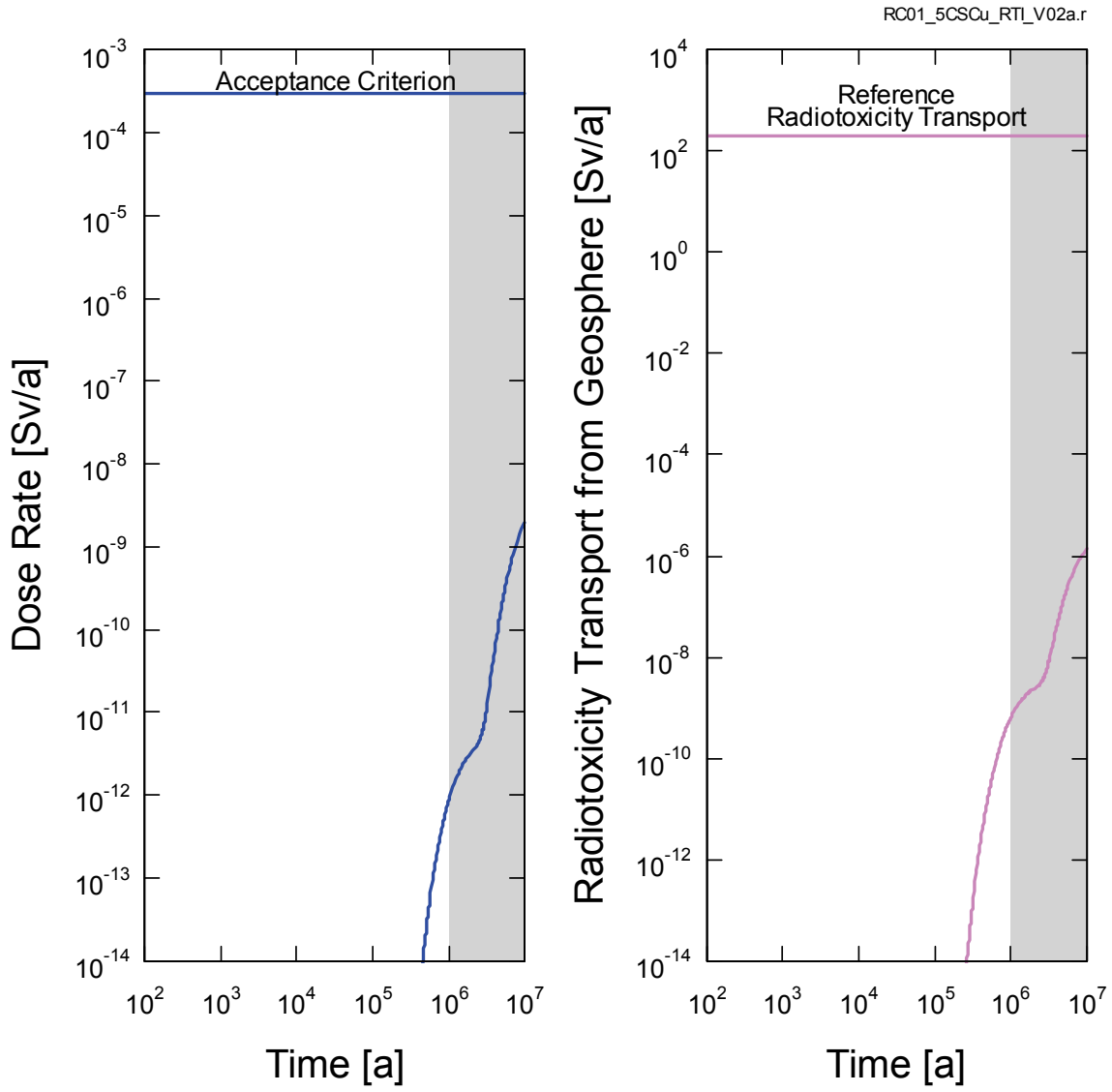

Figure 7-98: SYVAC3-CC4 – Reference Case Results for Complementary Indicators

Figure 7-99 shows the calculated distribution of the radiotoxicity transport indicator over the 120,000 probabilistic simulations. The average radiotoxicity transport to the biosphere is 5.8×10^{-6} Sv/a and the maximum transport to the biosphere is 1.8×10^{-4} Sv/a. These are orders of magnitude below the indicator reference value of 200 Sv/a.

Since the indicator is well below the acceptance / reference value, additional confidence is provided that at long times (i.e., when the dose rate is more uncertain) the impacts of the repository are likely to be very small.

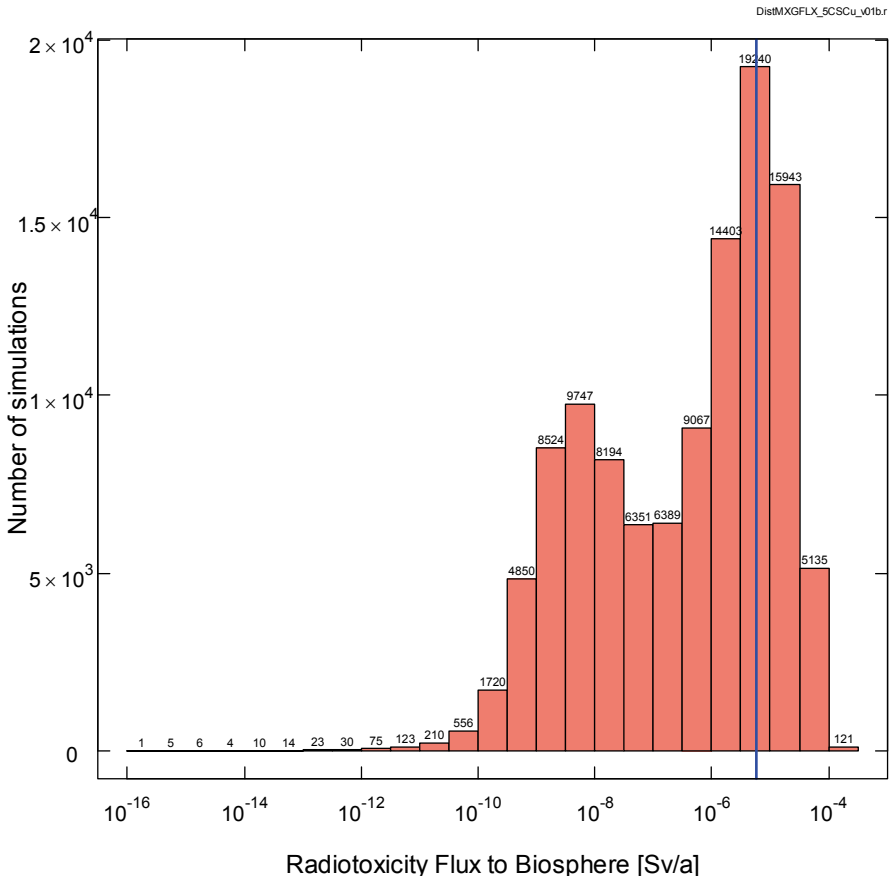

Note: The vertical blue line indicates the average value.

Figure 7-99: SYVAC3-CC4 – Radiotoxicity Transport Complementary Indicator

7.11.2 Radiological Protection of the Environment

The results presented in Section 7.7 through Section 7.9 address the potential radiological impact on persons. This section addresses the potential radiological impact on the environment.

The approach taken is to compare results obtained for the Reference Case of the Normal Evolution Scenario and its associated High Geosphere Diffusivity sensitivity case, and the All Containers Fail Disruptive Scenario against the interim acceptance criteria established in Section 7.1.3 for the radiological protection of the environment. The High Geosphere Diffusivity sensitivity case is selected because its dose rate is considerably higher than that of the Reference Case. Similarly, the All Containers Fail at 10,000 years is a relatively high dose rate Disruptive Scenario.

Table 7-44 shows this comparison for the Reference Case for the set of potentially significant radionuclides identified in the screening analysis (Section 7.6) for which interim acceptance criteria are available (Section 7.1.3). Similar to the dose results presented in Section 7.8.2, these are the maximum values reached over a 10 million year time period.

Because there is no lake or river in the system models used for the safety assessment calculations, sediment values are generated using sorption coefficients taken from Gobien et al. (2013) and contaminant concentrations in the well. The resulting values are expected to be very conservative for the situation in which a lake or river is present because of the much greater dilution that would be available.

The comparison shows very large margins to the interim acceptance criteria. It is therefore concluded that the radiological effects on the environment associated with the Reference Case of the Normal Evolution Scenario are negligible.

Table 7-44: Comparison of Reference Case Concentrations with Interim Acceptance Criteria for the Radiological Protection of the Environment

Radionuclide	Media					
	Water* [Bq/L]			Soil [Bq/kg]		
	Calculated	Criteria	Ratio	Calculated	Criteria	Ratio
Cl-36	3.8×10^{-10}	2.8	1.4×10^{-10}	1.4×10^{-10}	3.8×10^{-1}	3.7×10^{-10}
I-129	9.8×10^{-6}	3.2	3.0×10^{-6}	1.1×10^{-4}	2.4×10^{3}	4.7×10^{-8}
Cs-135	4.2×10^{-9}	2.1×10^{-3}	2.0×10^{-6}	8.8×10^{-6}	8.5	1.0×10^{-6}
Tc-99	4.7×10^{-11}	8.0×10^{-1}	5.9×10^{-11}	7.9×10^{-11}	4.3×10^{1}	1.8×10^{-12}
Ra-226	0	5.9×10^{-4}	0	0	2.5×10^{2}	0
Np-237	0	5.8×10^{-2}	0	0	5.0×10^{1}	0
U-238	0	2.3×10^{-3}	0	0	4.2×10^{1}	0
Pb-210	0	4.3	0	0	3.7×10^{3}	0
Po-210	0	7.0×10^{-3}	0	0	3.0×10^{1}	0

Radionuclide	Sediment** [Bq/kg]		
	Calculated	Criteria	Ratio
Cl-36	8.3×10^{-4}	4.1×10^{4}	2.0×10^{-8}
I-129	7.4×10^{-1}	1.2×10^{6}	6.2×10^{-7}
Cs-135	1.1×10^{-3}	3.5×10^{5}	3.2×10^{-9}
Tc-99	7.1×10^{-8}	3.0×10^{6}	2.4×10^{-14}
Ra-226	0	9.3×10^{2}	0
Np-237	0	1.1×10^{3}	0
U-238	0	1.1×10^{4}	0
Pb-210	0	6.3×10^{3}	0
Po-210	0	5.6×10^{3}	0

Notes: *Well water: **Generated from well water concentrations

Table 7-45 shows this comparison for the High Geosphere Diffusivity sensitivity case of the Normal Evolution Scenario.

The comparison shows large margins to the interim acceptance criteria. It is therefore concluded that the radiological effects on the environment associated with this sensitivity case of the Normal Evolution Scenario are negligible.

Table 7-45: Comparison of High Geosphere Diffusivity Sensitivity Case Concentrations with Interim Acceptance Criteria for the Radiological Protection of the Environment

Radionuclide	Media					
	Water* [Bq/L]			Soil [Bq/kg]		
	Calculated	Criteria	Ratio	Calculated	Criteria	Ratio
Cl-36	3.4×10^{-6}	2.8	1.2×10^{-6}	1.2×10^{-6}	3.8×10^{-1}	3.3×10^{-6}
I-129	1.3×10^{-4}	3.2	4.0×10^{-5}	1.5×10^{-3}	2.4×10^{3}	6.1×10^{-7}
Cs-135	8.4×10^{-8}	2.1×10^{-3}	4.0×10^{-5}	1.8×10^{-4}	8.5	2.1×10^{-5}
Tc-99	4.4×10^{-7}	8.0×10^{-1}	5.6×10^{-7}	7.4×10^{-7}	4.3×10^{1}	1.7×10^{-8}
Ra-226	1.0×10^{-18}	5.9×10^{-4}	1.7×10^{-15}	5.6×10^{-17}	2.5×10^{2}	2.2×10^{-19}
Np-237	0	5.8×10^{-2}	0	0	5.0×10^{1}	0
U-238	0	2.3×10^{-3}	0	0	4.2×10^{1}	0
Pb-210	1.0×10^{-18}	4.3	2.4×10^{-19}	8.8×10^{-17}	3.7×10^{3}	2.4×10^{-20}
Po-210	1.0×10^{-18}	7.0×10^{-3}	1.5×10^{-16}	8.9×10^{-17}	3.0×10^{1}	3.0×10^{-18}

Radionuclide	Sediment** [Bq/kg]		
	Calculated	Criteria	Ratio
Cl-36	7.4	4.1×10^{4}	1.8×10^{-4}
I-129	9.6	1.2×10^{6}	8.0×10^{-6}
Cs-135	2.3×10^{-2}	3.5×10^{5}	6.5×10^{-8}
Tc-99	6.7×10^{-4}	3.0×10^{6}	2.2×10^{-10}
Ra-226	4.8×10^{-14}	9.3×10^{2}	5.2×10^{-17}
Np-237	0	1.1×10^{3}	0
U-238	0	1.1×10^{4}	0
Pb-210	2.3×10^{-11}	6.3×10^{3}	3.6×10^{-15}
Po-210	7.5×10^{-12}	5.6×10^{3}	1.3×10^{-15}

Notes: *Well water: **Generated from well water concentrations

Table 7-46 shows this comparison for the All Containers Fail Disruptive Scenario.

The comparison shows reduced margins as compared to the Normal Evolution Scenario, as would be expected due to the significantly greater source term.

Given the low values, it is concluded that the All Containers Fail Scenario will not result in an exceedance of the interim acceptance criteria.

Table 7-46: Comparison of All Containers Fail at 10,000 years Disruptive Scenario Concentrations with Interim Acceptance Criteria for the Radiological Protection of the Environment

Radionuclide	Media					
	Water* [Bq/L]			Soil [Bq/kg]		
	Calculated	Criteria	Ratio	Calculated	Criteria	Ratio
Cl-36	5.8×10^{-7}	2.8	2.0×10^{-7}	2.1×10^{-7}	3.8×10^{-1}	5.6×10^{-7}
I-129	4.2×10^{-2}	3.2	1.3×10^{-2}	4.8×10^{-1}	2.4×10^{3}	2.0×10^{-4}
Cs-135	5.2×10^{-6}	2.1×10^{-3}	2.5×10^{-3}	1.1×10^{-2}	8.5	1.3×10^{-3}
Tc-99	8.4×10^{-5}	8.0×10^{-1}	1.0×10^{-4}	1.4×10^{-4}	4.3×10^{1}	3.3×10^{-6}
Ra-226	0	5.9×10^{-4}	0	0	2.5×10^{2}	0
Np-237	0	5.8×10^{-2}	0	0	5.0×10^{1}	0
U-238	0	2.3×10^{-3}	0	0	4.2×10^{1}	0
Pb-210	0	4.3	0	0	3.7×10^{3}	0
Po-210	0	7.0×10^{-3}	0	0	3.0×10^{1}	0

Radionuclide	Sediment** [Bq/kg]		
	Calculated	Criteria	Ratio
Cl-36	1.3	4.1×10^{4}	3.1×10^{-5}
I-129	3.2×10^{3}	1.2×10^{6}	2.6×10^{-3}
Cs-135	1.4	3.5×10^{5}	4.0×10^{-6}
Tc-99	1.3×10^{-1}	3.0×10^{6}	4.2×10^{-8}
Ra-226	0	9.3×10^{2}	0
Np-237	0	1.1×10^{3}	0
U-238	0	1.1×10^{4}	0
Pb-210	0	6.3×10^{3}	0
Po-210	0	5.6×10^{3}	0

Notes: *Well water: **Generated from well water concentrations

7.11.3 Protection of Persons and the Environment from Hazardous Substances

This section considers the potential non-radiological effects of contaminants arising from the used fuel bundles and from the container on the health and safety of persons and the environment.

The approach compares results obtained for the Reference Case of the Normal Evolution Scenario, its associated High Geosphere Diffusivity sensitivity case and the All Containers Fail Disruptive Scenario against the interim acceptance criteria shown in Table 7-1. The High Geosphere Diffusivity sensitivity case is selected because its dose rate is considerably higher than that of the Reference Case. Similarly, the All Containers Fail at 10,000 years is a high dose rate Disruptive Scenario.

Table 7-1 shows different acceptance criteria for background groundwater and potable groundwater. For the purpose of this assessment, groundwater concentrations are taken to be those in the well of the SYVAC3-CC4 model. These concentrations are compared against the background groundwater values and if an exceedance occurs, the exceeding concentration is then compared against the potable groundwater value with a supporting justification provided.

Because there is no lake or river in the nearby biosphere, well water concentrations are used as a proxy for surface water concentrations, with the well water concentrations reduced by a factor of 10 to account for anticipated dilution (MoE 2011b). Sediment values are similarly generated using well water concentrations reduced by a factor of 10 and then multiplied by sorption coefficients taken from Gobien et al. (2013).

The ratio determined by dividing an element concentration by its acceptance criterion is called the ‘Concentration Quotient’. Concentration Quotients less than 1.0 indicate the interim acceptance criterion is not exceeded.

7.11.3.1 Contaminants from the Used Fuel Bundles

Table 7-47 shows the Concentration Quotients computed for the Reference Case.

All concentration quotients are well below 1.0, indicating that wide margins are available to the interim acceptance criteria.

Table 7-47: SYVAC3-CC4 - Concentration Quotients for the Reference Case

Element	Groundwater	Surface Water*	Soil	Sediment*
Ag	1.1×10^{-5}	3.4×10^{-6}	1.4×10^{-6}	8.0×10^{-5}
Al	-	2.6×10^{-7}	6.4×10^{-7}	-
Ba	3.6×10^{-7}	5.5×10^{-6}	6.5×10^{-7}	-
Be	4.4×10^{-12}	2.0×10^{-14}	1.3×10^{-12}	-
Bi	-	5.5×10^{-9}	2.9×10^{-7}	-
Cd	4.1×10^{-9}	1.2×10^{-8}	1.4×10^{-9}	1.4×10^{-8}
Ce	-	1.2×10^{-7}	1.2×10^{-5}	1.1×10^{-6}
Co	1.9×10^{-7}	8.0×10^{-8}	2.4×10^{-8}	1.9×10^{-6}
Cr	1.8×10^{-7}	2.0×10^{-7}	8.7×10^{-6}	2.3×10^{-7}
Cs	-	2.1×10^{-14}	-	-
Cu	5.7×10^{-8}	5.7×10^{-9}	8.7×10^{-10}	1.8×10^{-7}
Eu	-	1.2×10^{-8}	1.8×10^{-8}	1.1×10^{-8}
Hg	5.8×10^{-7}	1.4×10^{-6}	3.6×10^{-8}	1.9×10^{-6}
La	-	1.3×10^{-7}	2.8×10^{-7}	1.7×10^{-7}
Mo	1.6×10^{-6}	9.2×10^{-8}	1.9×10^{-6}	-
Nd	-	2.4×10^{-6}	1.3×10^{-6}	4.7×10^{-7}
Ni	1.7×10^{-7}	9.6×10^{-9}	5.1×10^{-8}	4.5×10^{-6}
P	-	6.0×10^{-8}	-	-
Pb	1.9×10^{-8}	3.6×10^{-9}	5.2×10^{-10}	1.9×10^{-6}
Pd	-	5.1×10^{-10}	-	-
Pr	-	1.3×10^{-7}	1.6×10^{-7}	7.5×10^{-8}
Sb	9.6×10^{-8}	7.2×10^{-10}	4.1×10^{-8}	7.2×10^{-7}
Se	7.1×10^{-10}	3.6×10^{-10}	1.3×10^{-10}	-
Sm	-	7.7×10^{-8}	1.9×10^{-6}	-
Sr	-	0	0	-
Te	-	2.7×10^{-8}	1.9×10^{-8}	-
U	0	0	0	-
V	2.0×10^{-7}	1.3×10^{-8}	1.9×10^{-8}	-
Y	-	7.2×10^{-8}	1.1×10^{-7}	2.4×10^{-7}
Zr	-	5.3×10^{-29}	8.5×10^{-29}	-

Note: * Values are estimated using the well concentration as described in Section 7.11.3.

The Concentration Quotients for the High Geosphere Diffusivity sensitivity case are shown in Table 7-48. In this sensitivity case, the concentrations of all species have increased and the concentrations of many of the chemical elements have peaked in the 10 million year simulation time.

All Concentration Quotients are well below 1.0, indicating that wide margins are available to the interim acceptance criteria.

Table 7-48: SYVAC3-CC4 - Concentration Quotients for the High Geosphere Diffusivity Sensitivity Case

Element	Groundwater	Surface Water*	Soil	Sediment*
Ag	1.5×10^{-4}	4.5×10^{-5}	1.9×10^{-5}	1.1×10^{-3}
Al	-	3.2×10^{-6}	7.8×10^{-6}	-
Ba	9.9×10^{-7}	1.5×10^{-5}	1.8×10^{-6}	-
Be	7.9×10^{-10}	3.6×10^{-12}	2.4×10^{-10}	-
Bi	-	1.2×10^{-7}	6.1×10^{-6}	-
Cd	6.5×10^{-9}	1.9×10^{-8}	2.1×10^{-9}	2.2×10^{-8}
Ce	-	1.6×10^{-6}	1.6×10^{-4}	1.5×10^{-5}
Co	2.6×10^{-6}	1.1×10^{-6}	3.3×10^{-7}	2.5×10^{-5}
Cr	2.4×10^{-6}	2.7×10^{-6}	1.2×10^{-4}	3.1×10^{-6}
Cs	-	4.4×10^{-13}	-	-
Cu	1.9×10^{-6}	1.9×10^{-7}	2.9×10^{-8}	6.0×10^{-6}
Eu	-	1.6×10^{-7}	2.5×10^{-7}	1.5×10^{-7}
Hg	7.1×10^{-6}	1.8×10^{-5}	4.4×10^{-7}	2.3×10^{-5}
La	-	1.8×10^{-6}	3.8×10^{-6}	2.3×10^{-6}
Mo	2.1×10^{-5}	1.2×10^{-6}	2.6×10^{-5}	-
Nd	-	3.2×10^{-5}	1.7×10^{-5}	6.4×10^{-6}
Ni	2.3×10^{-6}	1.3×10^{-7}	7.0×10^{-7}	6.1×10^{-5}
P	-	8.0×10^{-7}	-	-
Pb	1.2×10^{-7}	2.4×10^{-8}	3.4×10^{-9}	1.2×10^{-5}
Pd	-	9.4×10^{-9}	-	-
Pr	-	1.8×10^{-6}	2.1×10^{-6}	1.0×10^{-6}
Sb	1.3×10^{-6}	9.7×10^{-9}	5.5×10^{-7}	9.7×10^{-6}
Se	1.3×10^{-7}	6.3×10^{-8}	2.4×10^{-8}	-
Sm	-	1.0×10^{-6}	2.6×10^{-5}	-
Sr	-	0	0	-
Te	-	3.7×10^{-7}	2.5×10^{-7}	-
U	0	0	0	-
V	2.7×10^{-6}	1.8×10^{-7}	2.6×10^{-7}	-
Y	-	9.9×10^{-7}	1.5×10^{-6}	3.2×10^{-6}
Zr	-	8.5×10^{-11}	1.4×10^{-10}	-

Note: * Values are estimated using the well concentration as described in Section 7.11.3.

Table 7-49 shows the Concentration Quotients for the All Containers Fail Disruptive Scenario.

The quotients are higher than in the Normal Evolution Scenario, as expected due to the significantly greater source term. Nevertheless, all Concentration Quotients remain below 1.0.

Table 7-49: SYVAC3-CC4 - Concentration Quotients for the All Containers Fail Case

Element	Groundwater	Surface Water*	Soil	Sediment*
Ag	4.8×10^{-2}	1.4×10^{-2}	6.1×10^{-3}	3.4×10^{-1}
Al	-	1.1×10^{-3}	2.7×10^{-3}	-
Ba	1.6×10^{-3}	2.4×10^{-2}	2.8×10^{-3}	-
Be	4.5×10^{-4}	2.0×10^{-6}	1.4×10^{-4}	-
Bi	-	2.3×10^{-5}	1.2×10^{-3}	-
Cd	5.2×10^{-6}	1.5×10^{-5}	1.7×10^{-6}	1.7×10^{-5}
Ce	-	5.1×10^{-4}	4.9×10^{-2}	4.8×10^{-3}
Co	8.0×10^{-4}	3.4×10^{-4}	1.0×10^{-4}	7.9×10^{-3}
Cr	1.0×10^{-3}	1.1×10^{-3}	5.0×10^{-2}	1.3×10^{-3}
Cs	-	2.7×10^{-11}	-	-
Cu	2.4×10^{-4}	2.4×10^{-5}	3.6×10^{-6}	7.5×10^{-4}
Eu	-	5.1×10^{-5}	7.9×10^{-5}	4.7×10^{-5}
Hg	2.5×10^{-3}	6.1×10^{-3}	1.5×10^{-4}	7.9×10^{-3}
La	-	5.6×10^{-4}	1.2×10^{-3}	7.0×10^{-4}
Mo	6.8×10^{-3}	3.9×10^{-4}	8.3×10^{-3}	-
Nd	-	1.0×10^{-2}	5.4×10^{-3}	2.0×10^{-3}
Ni	7.3×10^{-4}	4.1×10^{-5}	2.2×10^{-4}	1.9×10^{-2}
P	-	2.5×10^{-4}	-	-
Pb	2.6×10^{-5}	5.0×10^{-6}	7.3×10^{-7}	2.6×10^{-3}
Pd	-	2.2×10^{-6}	-	-
Pr	-	5.6×10^{-4}	6.7×10^{-4}	3.2×10^{-4}
Sb	4.3×10^{-4}	3.2×10^{-6}	1.8×10^{-4}	3.2×10^{-3}
Se	1.1×10^{-3}	5.6×10^{-4}	2.1×10^{-4}	-
Sm	-	3.3×10^{-4}	8.2×10^{-3}	-
Sr	-	0	0	-
Te	-	1.2×10^{-4}	7.9×10^{-5}	-
U	0	0	0	-
V	8.8×10^{-4}	5.7×10^{-5}	8.5×10^{-5}	-
Y	-	3.1×10^{-4}	4.6×10^{-4}	1.0×10^{-3}
Zr	-	8.6×10^{-22}	1.4×10^{-21}	-

Note: * Values are estimated using the well concentration as described in Section 7.11.3.

7.11.3.2 Copper Container Chemical Hazard Assessment

Chemical elements of potential concern could also be released from the copper containers and the engineered sealing materials. While the hazard from the sealing materials is expected to be very low because the components tend to be natural clay materials, an assessment is performed to determine the hazard associated with the copper containers.

The rate of release of contaminants from the copper metal depends on the copper corrosion or dissolution rate. Although reducing conditions are expected after closure, a small amount of copper corrosion can still occur as discussed in Chapter 5. As corrosion occurs, copper and any associated impurities are released into the buffer porewater.

In this assessment, a solubility-limited dissolution model is used to determine the rate of corrosion of the copper shell. In this model, the corrosion rate is controlled by the rate at which copper diffuses away from the container / buffer interface. FRAC3DVS-OPG is used to model the transport of copper to the biosphere and to calculate copper concentrations.

The transport of copper away from the container is simulated by applying a constant concentration boundary condition of 2.6×10^{-1} mol/m^3 at every grid node intersecting containers in the repository. This concentration corresponds to the copper solubility limit shown in Table 7-13 increased by a factor of 10 to account for uncertainties in the temperature and chemical conditions near the container. This results in a continuous input of copper into the model over the course of the 10 million year simulation.

Figure 7-100 shows the transport of copper to the surface as a function of time both with and without sorption.

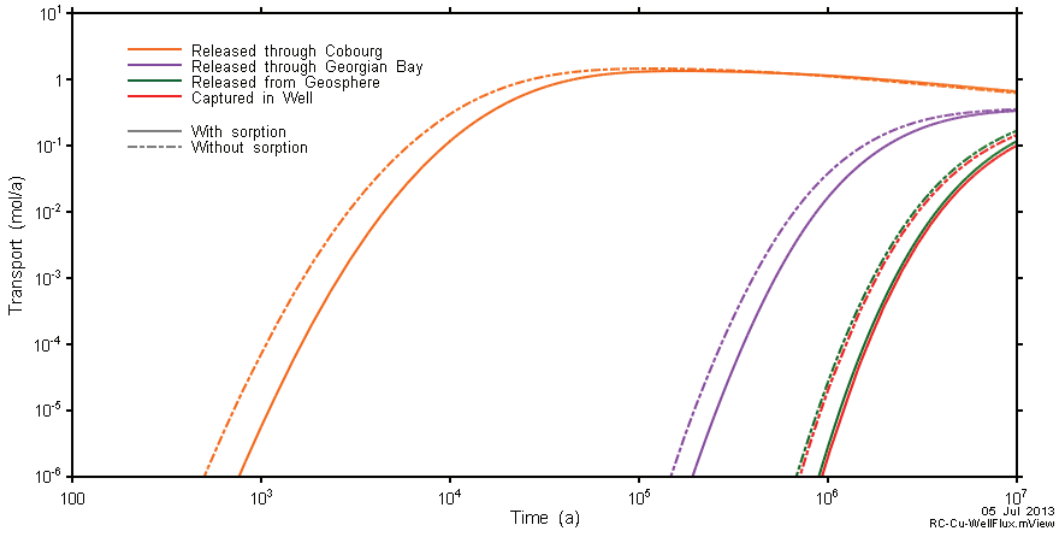

Figure 7-100: FRAC3DVS-OPG - Copper Transport to the Surface both With and Without Sorption

To determine the Concentration Quotient, the maximum total copper transport to the surface (i.e., 0.10 mol/a with sorption and 0.14 mol/a without sorption) is assumed to enter the well, with the well pumping at the reference rate of 1307 m^3/a. The resulting well water concentration (with sorption) is 7.65×10^{-5} mol/m^3 or 4.9 µg/L which is essentially equal to the background groundwater acceptance criterion of 5 µg/L (see Table 7-1). Because the well is the source of drinking water, a less conservative but appropriate comparison can also be made against the potable groundwater acceptance criterion of 69 µg/L (also see Table 7-1). For this comparison, the Concentration Quotient is 0.07 indicating a wide margin to the acceptance criterion.

Surface water concentrations are estimated by reducing the well water concentrations by a factor of 10 (see Section 7.11.3). The resulting maximum Concentration Quotient is about 0.1 which indicates the surface water concentration is well below the acceptance criterion.

To estimate the maximum soil and sediment concentrations, the well concentration of 7.65×10^{-5} mol/m^3 is reduced by a factor of 10 to generate a proxy for surface water (see Section 7.11.3) and this proxy is then conservatively multiplied by the respective soil and sediment sorption coefficients. For copper, the sediment K_d is 0.37 m^3/kg and the soil K_d is 0.03 m^3/kg resulting in maximum copper concentrations of 0.18 µg/g and 1.5×10^{-2} µg/g in sediment and soil, respectively. This results in Concentration Quotients of 2.4×10^{-4} for soil and 1.1×10^{-2} for sediment.

Chemical element impurities are present in the copper at the levels shown in Table 7-50 (SKB 2010b and SKB 1998). These impurities are also released as the copper corrodes. The calculation of copper impurity concentrations assumes the impurities are transported with the copper. Element specific K_d values in the buffer and geosphere for the impurities may produce some variation in the transport time and consequently the copper transport without sorption is used as a surrogate for impurity transport.

The well water and surface water Concentration Quotients for the impurity elements are shown in Table 7-50. Since these quotients are all well below 1.0, it is concluded that these elements would not pose a health and safety hazard to persons or to the environment.

Table 7-50: SYVAC3-CC4 - Concentration Maximum Impurity Levels in Copper and Estimated Impurity Element Concentration Quotients for Well Water

Element	Maximum Impurity Level (ppm)	Impurity Level [mol/mol Cu]	Estimated Maximum Element Conc in Well Water [mol/m^3]	Back-ground Ground-water Criteria [µg/L]	Surface Water Criteria [µg/L]	Groundwater Concentration Quotient	Surface Water Concentration Quotient
Cu	-	-	7.65×10^{-5}	5	5	9.72×10^{-1}	9.72×10^{-2}
Ag	25	1.47×10^{-5}	1.13×10^{-9}	0.3	1.2	4.05×10^{-4}	1.01×10^{-5}
As*	5	4.24×10^{-6}	3.24×10^{-10}	13	5	1.87×10^{-6}	4.86×10^{-7}
Bi	1	3.04×10^{-7}	2.33×10^{-11}	-	150	-	3.24×10^{-9}
Cd	1	5.65×10^{-7}	4.33×10^{-11}	0.5	0.017	9.72×10^{-6}	2.86×10^{-5}
Co	20	2.16×10^{-5}	1.65×10^{-9}	3.8	0.9	2.56×10^{-5}	1.08×10^{-5}
Cr	15	1.83×10^{-5}	1.40×10^{-9}	11	1	6.63×10^{-6}	7.29×10^{-6}
Fe*	10	1.14×10^{-5}	8.71×10^{-10}	-	300	-	1.62×10^{-8}
Hg	1	3.17×10^{-7}	2.42×10^{-11}	0.1	0.004	4.86×10^{-5}	1.22×10^{-4}
Mn*	0.5	5.78×10^{-7}	4.42×10^{-11}	-	200	-	1.22×10^{-9}
Ni	10	1.08×10^{-5}	8.28×10^{-10}	14	25	3.47×10^{-6}	1.94×10^{-7}
O*	5	1.99×10^{-5}	1.52×10^{-9}	-	-	-	-
P**	100	2.05×10^{-4}	1.57×10^{-8}	-	4	-	1.22×10^{-5}
Pb	5	1.53×10^{-6}	1.17×10^{-10}	1.9	1	1.28×10^{-5}	2.43×10^{-6}
S*	15	2.97×10^{-5}	2.27×10^{-9}	-	670	-	1.09×10^{-8}
Sb	4	2.09×10^{-6}	1.60×10^{-10}	1.5	20	1.30×10^{-5}	9.72×10^{-8}
Se	3	2.41×10^{-6}	1.85×10^{-10}	5	1	2.92×10^{-6}	1.46×10^{-6}
Si*	20	4.53×10^{-5}	3.46×10^{-9}	-	3200	-	3.04×10^{-9}
Sn*	2	1.07×10^{-6}	8.19×10^{-11}	-	73	-	1.33×10^{-8}
Te	2	9.96×10^{-7}	7.62×10^{-11}	-	20	-	4.86×10^{-8}
Zn*	1	9.72×10^{-7}	7.44×10^{-11}	160	20	3.04×10^{-8}	2.43×10^{-8}

Note: '-' indicates that there are no defined criteria for that element in the given medium.

*Element not included in Table 7-1. Detailed information on the individual source documents is available in Gobien et al. (2013).

** Impurity level for P is from SKB (2010b) others remain unchanged from SKB (1998).

7.11.3.3 Complementary Indicators

Natural processes carry small amounts of naturally occurring chemical elements from within the geosphere to the surface. Reference values for natural chemical element fluxes to the biosphere can be obtained using the elemental composition of Michigan Basin Sedimentary formations and the erosion rate of this formation over long time periods.

Soil erosion in the Michigan Basin can be due to a number of factors including the soil characteristics, rainfall frequency, rainfall intensity, topography, and land management practices. CSA (2008) recommends a soil erosion rate of 1.5 kg dw/m^2/a for clay soils. Erosion of the bedrock via glaciation is another potential concern for sedimentary formations and is expected to be the dominant form of erosion over the lifetime of the repository. Hallet (2011) recommends a conservative realistic glacial erosion rate of 100 m over 1 million years or 0.0001 m/a. Assuming the erosion rate is constant over a repository footprint area of 6 km^2 and using an average sedimentary rock density of 2750 kg/m^3, an erosion rate of about 1.65×10^6 kg/a can be determined. This rate is somewhat lower than the surface soil erosion rate for plowed soils of 9.0×10^6 kg/a estimated using the surface soil erosion rate from CSA (2008); however, the use of a lower erosion rate for calculating reference values for natural chemical element fluxes is conservative.

Table 7-51 lists the concentrations of the chemical elements of potential concern in Michigan Basin sedimentary rock. Using these values and the selected erosion rate, the natural chemical element transport rates from the geosphere to the biosphere can be calculated and compared with the transport rates associated with the All Containers Fail Disruptive Scenario. This comparison is shown in Table 7-51.

The results indicate that even under the conservative assumptions of the All Containers Fail Disruptive Scenario, transport to the biosphere is considerably less than the corresponding transport arising from natural erosion processes. This adds confidence to the conclusion that the potential chemical hazard from the repository is likely not significant even for the All Containers Fail Disruptive Scenario.

Table 7-51: Erosion Fluxes out of the Geosphere

Element	Michigan Basin Surface Bedrock* (g/Mg)	Michigan Basin Erosion Flux (mol/a)	All Containers Fail Flux to Surface** (mol/a)	Ratio of All Containers Fail Flux to Erosion Flux
Ag	4.67×10^{-2}	7.14×10^{-1}	1.73×10^{-4}	2.42×10^{-4}
Al	1.08×10^{4}	6.62×10^{5}	2.66×10^{-3}	4.02×10^{-9}
Ba	6.80×10^{1}	8.18×10^{2}	9.00×10^{-3}	1.10×10^{-5}
Be	2.50×10^{-1}	4.58×10^{1}	3.28×10^{-5}	7.16×10^{-7}
Bi	9.00×10^{-2}	7.11×10^{-1}	2.17×10^{-4}	3.05×10^{-4}
Cd	6.83×10^{-2}	1.00×10^{0}	3.02×10^{-8}	3.01×10^{-8}
Ce	9.13×10^{0}	1.08×10^{2}	1.04×10^{-3}	9.68×10^{-6}
Co	2.33×10^{0}	6.53×10^{1}	6.78×10^{-5}	1.04×10^{-6}
Cr	1.15×10^{1}	3.64×10^{2}	2.84×10^{-4}	7.80×10^{-7}
Cu	4.08×10^{0}	1.06×10^{2}	2.46×10^{-5}	2.32×10^{-7}
Eu	1.63×10^{-1}	1.76×10^{0}	4.41×10^{-5}	2.50×10^{-5}
La	4.41×10^{0}	5.23×10^{1}	5.37×10^{-4}	1.03×10^{-5}
Mo	1.13×10^{0}	1.95×10^{1}	2.12×10^{-3}	1.09×10^{-4}
Nd	4.13×10^{0}	4.72×10^{1}	1.65×10^{-3}	3.50×10^{-5}
Ni	9.33×10^{0}	2.62×10^{2}	2.28×10^{-4}	8.70×10^{-7}
P	8.22×10^{1}	4.38×10^{3}	4.29×10^{-4}	9.79×10^{-8}
Pb	2.55×10^{0}	2.03×10^{1}	3.17×10^{-7}	1.56×10^{-8}
Pr	1.10×10^{0}	1.28×10^{1}	4.76×10^{-4}	3.72×10^{-5}
Sm	7.65×10^{-1}	8.39×10^{0}	2.32×10^{-4}	2.77×10^{-5}
U	1.27×10^{0}	8.80×10^{0}	0.00×10^{0}	0.00×10^{0}
V	1.34×10^{1}	4.32×10^{2}	8.80×10^{-5}	2.04×10^{-7}
Y	2.82×10^{0}	5.24×10^{1}	2.90×10^{-4}	5.54×10^{-6}
Zr	1.26×10^{1}	2.28×10^{2}	4.95×10^{-22}	2.17×10^{-24}

Note: *: Data are average values for shallow rock layers in Wigston and Jackson (2010a, b) and Jackson and Murphy (2011).

**: 'Surface' is taken to be transport to the well. As discussed in Section 7.5.3.1, the well captures 93.7% of all contaminants entering the Guelph formation.

7.12 Summary and Conclusions

This section summarizes the postclosure safety assessment for liquid-borne contaminant transport.

Due to the very low hydraulic conductivity of the host rock and the dominance of diffusive transport, the dose rates arising in the one million year time period of interest are several orders of magnitude below the applicable interim acceptance criteria for all cases. Since the peak dose rate is not reached in this timeframe, results are quoted for a 10 million year period; however, even with this extension the peak dose rate is not reached for nearly all cases.

To put the quoted results into context, results obtained for the sensitivity case with geosphere diffusivities increased by a factor of 10 can be used. These results, illustrated in Figure 7-77 in Section 7.8.2.2, indicate that a peak dose rate of 2.6×10^{-8} Sv/a is reached at 5.6×10^{6} years. This shows that the long-term doses are expected to remain extremely low, even in cases where the peak rate is not reached in the 10 million year simulation time.

7.12.1 Scope Overview

The Normal Evolution Scenario represents the normal (or expected) evolution of the site and facility. Disruptive Scenarios consider the effects of unlikely events that lead to possible penetration of barriers and abnormal degradation and loss of containment.

Section 7.2 discusses the detailed scope of the assessment. Both Normal Evolution and Disruptive Scenarios are considered.

The containers are robust and there would be multiple inspection steps to ensure they are fabricated and placed correctly. However, given the large number of containers, it is possible that some containers could be placed with undetected defects. In particular, based on a simple estimate of the likelihood of failure in the copper shell welding and inspection process (i.e., 1/5000, Maak et al. 2001), statistically there could be three containers with undetected defects placed in the repository. For the assessment of the Normal Evolution Scenario, it is assumed that three containers with undetected defects are present at the time of repository closure.

Recognizing that the geosphere characteristics at a candidate site and the design of the repository may be different from the reference conditions assumed in this study, a number of sensitivity cases are also examined to illustrate the function of various engineered and natural barriers. Both deterministic and probabilistic simulations are conducted.

In the deterministic simulations, parameter variations are performed about a Reference Case of the Normal Evolution Scenario, where the Reference Case has the following attributes:

- Geosphere properties as per Chapter 2;
- Used fuel inventories as per Chapter 3;
- Repository design as per Chapter 4;
- Three containers each with an undetected defect placed in the repository at the location with the shortest groundwater transport time to the well;
- Defect radius = 1 mm, no evolution of the defect size with time;
- No other container failures occur;

- Groundwater fills the defective containers 10,000 years after the containers are placed in the repository (Gobien et al. 2013);
- Constant temperate climate and steady-state groundwater flow;
- Self-sufficient farming family growing crops and raising livestock on the surface above the repository;
- Drinking and irrigation water for the family obtained from a 219 m deep well that penetrates the entire thickness of the Guelph formation, and located along the main pathway for contaminants released from the defective containers;
- The well is pumping at a rate of 1307 m^3/a. This is sufficient for drinking water and irrigation of household crops;
- A small amount (tens of metres) of surface erosion occurs in the first one million years[6]; and
- Input parameters that are represented by probability distributions are set to either the most probable value (when there is one) or to the median value otherwise.

The deterministic sensitivity cases are:

- Fuel dissolution rate increased by a factor of 10;
- Instant release fractions set to 0.10 for all radionuclides;
- Container defect area increased by a factor of 10;
- No solubility limits in the container;
- No sorption in the EBS;
- Geosphere hydraulic conductivity increased by a factor of 10;
- Geosphere diffusivities increased by a factor of 10;
- No sorption in the geosphere;
- 100 m erosion occurring in the first one million years;
- Overpressure in the Shadow Lake formation;
- Hydraulic conductivity of the excavation damaged zone increased by a factor of 10; and
- Low sorption in the geosphere with coincident high solubility limits in the container.

For the probabilistic simulations, random sampling is used to simultaneously vary all input parameters for which probability distribution functions are available, including contaminant release, transport, and biosphere parameters. However, parameter values that could affect groundwater flow are not varied in these simulations.

These deterministic and probabilistic cases are described in detail in Table 7-3.

Results are generated for one complementary indicator of radiological safety.

Results are generated to address the radiological protection of the environment, and the protection of persons and the environment from hazardous substances. A complementary indicator of safety for hazardous substances is also evaluated.

[6] This is neglected in the analysis simulations due to its anticipated negligible effect.

The Disruptive Scenarios examined are:

- Inadvertent Human Intrusion;
- All Containers Fail at 60,000 Years (with a sensitivity case that has the failure occurring at 10,000 years); and
- Shaft Seal Failure.

These scenarios are described in detail in Table 7-4. All Disruptive Scenarios are analysed with deterministic methods only.

Some additional sensitivity cases were simulated in the course of the analysis as issues emerged that challenged the integrity of the simulations. These cases are listed below and further described in Table 7-5:

- Increased spatial resolution to confirm model convergence; and
- Increased temporal resolution to confirm model convergence.

Neither of the modelling choices had any material effect on the results and they are therefore not discussed further.

7.12.2 Results for the Normal Evolution Scenario

Reference Case

Section 7.8.2.1 reports the maximum dose rate for the Reference Case of the Normal Evolution Scenario is 2.0×10^{-9} Sv/a, occurring at 1.0×10^{7} years[7]. This is orders of magnitude below the average Canadian background dose rate of 1.8×10^{-3} Sv/a and is a factor of 150,000 times less than the 3×10^{-4} Sv/a interim dose acceptance criterion established in Section 7.1.1 for the radiological protection of persons.

The analysis shows that I-129 is the dominant contributor to dose rate. This is because I-129 has a sizeable initial inventory, a non-zero instant release fraction, a very long half-life, is non-sorbing in the buffer, backfill and geosphere and has a radiological impact on humans. All other fission products and actinides either decay away, or are released very slowly as the fuel dissolves and are thereafter sorbed in the engineered barriers and geosphere.

Section 7.10 discusses the effects of glaciation, and argues that only relatively minor effects are anticipated.

Section 7.11.1 discusses two complementary indicators that can be determined using radionuclide releases from the Reference Case. These indicators (i.e., radiotoxicity concentration in a water body and radiotoxicity transport from the geosphere) supplement the dose rate indicator using system characteristics that are much less sensitive to assumptions regarding the biosphere and human behaviour. Due to the absence of a lake or river in the nearby hypothetical biosphere model, results are reported only for the radiotoxicity transport

[7] The time of peak total dose is outside the 1 million year time frame of interest, and also outside the 10 million year period shown to illustrate model behaviour.

indicator. The discussion shows that this indicator is well below its reference value, thereby providing additional confidence that at long times the impact of the repository is likely to be very small.

Section 7.11.2 presents results addressing the radiological protection of the environment (i.e., on non-human biota). The discussion concludes that these effects are negligible for the Normal Evolution Scenario.

Section 7.11.3 discusses the protection of persons and the environment from hazardous substances. Such non-radiological hazards could arise due to release of copper and other potentially hazardous elements from the containers and used fuel. The discussion concludes that all contaminant concentrations are below their associated acceptance criteria.

Sensitivity Cases

Section 7.7.1.2 and Section 7.8.2 present radionuclide transport results for the deterministic sensitivity cases examining the effects of degraded physical barriers, degraded chemical barriers, and the geosphere sensitivity cases.

These results are summarized in Table 7-52 and discussed below. The table shows the maximum impacts (expressed in Bq/a I-129 or in Sv/a), the time of the maximum impact, the effect of the parameter variation on the Reference Case result and the factor by which the result is below the interim dose acceptance criterion for the radiological protection of persons. Results are shown in Bq/a I-129 for FRAC3DVS-OPG simulations because this model does not include representations of the biosphere and critical group. Inferences on dose impacts can be made from the I-129 transport results by comparison to cases for which both I-129 transport (in Bq/a) and dose rates (in Sv/a) are calculated.

Table 7-52: Result Summary

Case	Maximum Impact*		CC4 Result for Time of Maximum Impact (a)	Ratio to Reference Case+	Factor to Dose Limit
	I-129 (Bq/a)	Dose (Sv/a)			
Reference Case of the Normal Evolution Scenario	**7.4**	**2.0×10^{-9}**	**10,000,000**	**-**	**150,000**
Geosphere Sensitivity Cases					
Geosphere Conductivity 10 times Higher	6.2	-	10,000,000	0.8	180,000
EDZ Conductivity 10 times Higher	7.4	-	10,000,000	1.0	150,000
100 m Erosion in One Million Years**	7.4	2.0×10^{-9}	10,000,000	1.0	150,000
Shadow Lake Overpressure	8.3	-	10,000,000	1.1	134,000
Degraded Physical Barrier Sensitivity Cases					
Fuel Dissolution Rate 10 times Higher	-	5.9×10^{-9}	10,000,000	3.0	51,000
Container Defect Area 10 times Higher	-	2.0×10^{-9}	10,000,000	1.0	150,000
Instant Release Fraction set to 10%	-	2.2×10^{-9}	10,000,000	1.1	136,000
Geosphere Diffusivity 10 times Higher	-	2.6×10^{-8}	5,600,000	13	12,000
Degraded Chemical Barrier Sensitivity Cases					
No Sorption in the Geosphere	-	3.3×10^{-9}	10,000,000	1.7	91,000
No Solubility Limits	-	2.0×10^{-9}	10,000,000	1.0	150,000
No Sorption in the EBS	-	6.7×10^{-9}	10,000,000	3.4	45,000
Low Sorption in the Geosphere With Coincident High Solubility Limits	-	2.0×10^{-9}	10,000,000	1.0	150,000
Probabilistic Simulations					
All parameters varied: average dose	-	1.6×10^{-8}	5,600,000	8	19,000
All parameters varied: maximum dose rate, 95th percentile	-	7.5×10^{-8}	5,600,000	37	4,000
Disruptive Scenarios					
All Containers Fail at 60,000 Years	-	7.5×10^{-6}	10,000,000	N/A	133
All Containers Fail at 10,000 Years	-	8.4×10^{-6}	10,000,000	N/A	119
Shaft Seals Failure	7.4	-	10,000,000	N/A	500,000

Notes:

* Maximum impacts are determined from simulations performed with either the FRAC3DVS-OPG code or the SYVAC3-CC4 code. The FRAC3DVS-OPG model does not include biosphere and dose models and therefore results are presented for I-129 transport to the surface. This is a reasonable surrogate for dose because SYVAC3-CC4 simulations show that I-129 is the dominant dose contributor.

** A qualitative argument is used to show there is no significant effect on the Reference Case Results

+ N/A: not applicable

Geosphere Sensitivity Cases

These cases examine the individual effects of increasing the hydraulic conductivity of the host rock, increasing the hydraulic conductivity of the EDZ regions within the repository, 100 m of erosion occurring over one million years, and a 158 m overpressure in the Shadow Lake formation.

Table 7-52 shows that none of these cases have a material effect on the results.

Degraded Physical Barrier Sensitivity Cases

These cases examine the individual effects of increasing the fuel dissolution rate, increasing the container defect area, increasing the instant release fractions and increasing the geosphere diffusivity by a factor of 10. Key features to note are:

- Increasing the fuel dissolution rate by a factor of 10 increases the calculated dose rate by a factor of 3.0 compared to the Reference Case. Even with this increase, the dose consequence remains a factor of 51,000 times below the interim dose acceptance criterion;
- Increasing the geosphere diffusivity by a factor of 10 increases the maximum dose rate by a factor of 13. Even with this increase, the maximum dose rate for the high geosphere diffusivity case remains a factor of almost 12,000 times below the interim dose rate acceptance criterion.
- The other sensitivity cases have no material effect on the results.

Degraded Chemical Barrier Sensitivity Cases

These cases examine the individual effects of not crediting sorption in the geosphere, not crediting solubility limits, not crediting sorption in the EBS, and the combined effect of crediting low sorption in the geosphere with coincident high solubility limits.

Compared to the Reference Case, there is a 1.7 times increase in dose rate for the case with no sorption in the geosphere and a 3.4 times increase for the case with no sorption in the engineered barrier system.

The other cases show no material difference.

Probabilistic Cases

Table 7-52 also presents summary results for the probabilistic case. In this case 120,000 simulations are performed in which all parameters represented by probability distributions are simultaneously varied. The 95th percentile of the maximum dose rate is 7.5×10^{-8} Sv/a or 37 times that of the Reference Case. This is 4000 times less than the interim dose rate acceptance criterion.

7.12.3 Results for the Disruptive Scenarios

Table 7-52 also presents summary results for two Disruptive Scenarios. These scenarios examine the consequences of all containers failing and the effects of degraded shaft seals. Key features to note are:

- Failure of all containers at 60,000 years results in a maximum dose rate of 7.5×10^{-6} Sv/a while failure of all containers at 10,000 years results in a maximum dose rate of 8.4×10^{-6} Sv/a, indicating a slight sensitivity to the assumed failure time. These results are factors of 133 and 119 times below the interim dose rate acceptance criterion.
- The Shaft Seal Failure Scenario has no effect on the dose consequence. This is likely because the three failed containers are located some distance away from the degraded shaft seal (i.e., the failed container location was selected to maximize radionuclide transport to the well and not to the degraded shaft seal).

Section 7.9.1 presents a stylized analysis for the Inadvertent Human Intrusion Scenario. This scenario is not included in Table 7-52 because it is a special case, as recognized in CNSC Regulatory Guide G-320 (CNSC 2006). The assumed intrusion bypasses all barriers, and therefore the associated dose consequence exceeds the regulatory limit. The results show potential doses to the Drill Crew of about 1.06 Sv and to a site Resident of about 1.14 Sv/a conservatively assuming early intrusion, leaving contaminated material on the site, and a future resident living on the contaminated material. The risk of inadvertent human intrusion is minimized by placing the used fuel deep underground in a location with no viable mineral resources and no potable groundwater resources, and by the use of markers and institutional controls. The likelihood of this event occurring cannot be accurately determined; however, based on simple estimates of deep drilling rates, it is roughly estimated as 3×10^{-5} per annum, which implies a risk to the Resident of 2×10^{-6} per annum. This is less than the reference risk criterion 10^{-5} per annum.

7.12.4 Conclusion

The safety assessment shows, for the Normal Evolution Scenario and associated sensitivity cases, as well as for selected Disruptive Scenarios (excluding Inadvertent Human Intrusion), that all radiological and non-radiological interim acceptance criteria are met for liquid-borne contaminants during the postclosure period.

For the Inadvertent Human Intrusion Disruptive Scenario, Regulatory document G-320 (CNSC 2006) recognizes that this event could result in dose rates that exceed the regulatory limit and it states that reasonable efforts should be made to limit the probability of occurrence. The following repository characteristics have been adopted to minimize the likelihood of this event:

- A deep location;
- Site selection based on an absence of groundwater resources at repository depth that could be used for drinking or agricultural purposes;
- Site selection based on an absence of economically exploitable natural resources; and
- The use of records and markers to preserve institutional memory to the extent practicable.

7.13 References for Chapter 7

Amiro, B.D. 1992. Baseline concentrations of nuclear fuel waste nuclides in the environment. Atomic Energy of Canada Limited, AECL10454, COG 91231. Pinawa, Canada.

Amiro, B.D. 1993. Protection of the environment from nuclear fuel waste radionuclides: a framework using environmental increments. Science of the Total Environment 128: 157-89.

Becker, D.-A., D. Buhmann, R. Storck, J. Alonso, J.-L. Cormenzana, M. Hugi, F. van Gemert, P. O'Sullivan, A. Laciok, J. Marivoet, X. Sillen, H. Nordman, T. Vieno and M. Niemeyer. 2002. Testing of Safety and Performance Indicators (SPIN). European Commission Report FIKW-CT2000-00081. European Commission, Brussels, Belgium.

Berger, A. and M.F. Loutre. 2002. An exceptionally long interglacial ahead? Science 297, 1287-1288.

Brown, J.E., B. Alfonso, R. Avila, N.A. Beresford, D. Copplestone, G. Pröhl and A. Ulanovsky. 2008. The ERICA Tool. J. Environ. Radioactivity 99: 1371-1383.

CCME. 2002. Canadian Sediment Guidelines for the Protection of Aquatic Life, Summary Tables. Canadian Council of the Environment 2002 update. Accessed through website of the Canadian Environmental Quality Guidelines: http://st-ts.ccme.ca/

CCME. 2007a. Canadian Soil Quality Guidelines for the Protection of Environmental and Human Health, Summary Tables. Canadian Council of Environment 2007 update. Access through website of the Canadian Environmental Quality Guidelines: http://st-ts.ccme.ca/

CCME. 2007b. Canadian Water Quality Guidelines for the Protection of Agricultural Water Uses, Summary Tables. Canadian Council of Environment 2007 update. Accessed through website of the Canadian Environmental Quality Guidelines: http://st-ts.ccme.ca/

CCME. 2007c. Canadian Water Quality Guidelines for the Protection of Aquatic Life, Summary Tables. Canadian Council of Environment 2007 update. Accessed through website of the Canadian Environmental Quality Guidelines: http://st-ts.ccme.ca/

CNSC. 2006. Regulatory Guide G-320: Assessing the Long Term Safety of Radioactive Waste Management. Canadian Nuclear Safety Commission. Ottawa, Canada.

CNSC. 2011. Setting Radiation Requirements on the Basis of Sound Science: The Role of Epidemiology. Canadian Nuclear Safety Commission, INFO-0812. Ottawa, Canada.

CSA. 2008. Guidelines for Calculating Derived Release Limits for Radioactive Material in Airborne and Liquid Effluents for Normal Operation of Nuclear Facilities. Canadian Standards Association. N288.1-08. Toronto, Canada.

Curti E. and P. Wersin. 2002. Assessment of Porewater Chemistry in the Bentonite Backfill for the Swiss SF/HLW Repository. Nagra Technical Report 02-09. Wettingen, Switzerland.

DiCiccio, T.J. and B. Efron. 1996. Bootstrap Confidence Intervals. Statistical Science Volume 11(3), 189-228.

DOE. 2008. Final Supplemental Environmental Impact Statement for a Geologic Repository for the Disposal of Spent Nuclear Fuel and High-Level Radioactive Waste at Yucca Mountain. US Department of Energy Report DOE/EIS-0250F-S1. Nevada, USA.

EC/HC. 2003. Priority Substances List Assessment Report: Releases of Radionuclides from Nuclear Facilities (Impact on Non-Human Biota). Environment and Health Canada. Canadian Environmental Protection Act. Ottawa, Canada.

Ferry, C., J.-P. Piron, A, Poulesquen, and C. Poinssot. 2008. Radionuclides Release from the Spent Fuel under Disposal Conditions: Re-evaluation of the Instant Release Fraction. Material Research Society Symposium Proceedings 1107, 447-454.

Garisto, F. 1989. The Energy Spectrum of α-particles Emitted from Used CANDU Fuel, Annals of Nuclear Energy 16. 33-38.

Garisto, F. 2001. Radionuclide Screening Model (RSM) Version 1.1 Verification and Validation. Ontario Power Generation Report 06819-REP-01300-10029-R00. Toronto, Canada.

Garisto, F. and M. Gobien. 2013. SYVAC3-CC4 Verification and Validation Summary. Nuclear Waste Management Organization Report NWMO TR-2013-14. Toronto, Canada.

Garisto, F., T. Kempe, P. Gierszewski, K. Wei, C. Kitson, T. Melnyk, L. Wojciechowski, J. Avis and N. Calder. 2005. Horizontal Borehole Concept Case Study: Chemical Toxicity Risk. Ontario Power Generation Report 06819-REP-01200-10149-R00. Toronto, Canada.

Garisto, N.C., F. Cooper and S.L. Fernandes. 2008. No-effect Concentrations for Screening Assessment of Radiological Impacts on Non-human Biota. Nuclear Waste Management Organization Report NWMO TR-2008-02. Toronto, Canada.

Garisto, F., J. Avis., T. Chshyolkova, P. Gierszewski, M. Gobien, C. Kitson, T. Melnyk, J. Miller, R. Walsh and L. Wojciechowski. 2010. Glaciation Scenario: Safety Assessment for a Used Fuel Geological Repository. Nuclear Waste Management Organization Report NWMO TR-2010-10. Toronto, Canada.

Gierszewski, P., J. Avis, N. Calder, A. D'Andrea, F. Garisto, C. Kitson, T. Melnyk, K. Wei and L. Wojciechowski. 2004. Third Case Study - Postclosure Safety Assessment. Ontario Power Generation Report 06819-REP-01200-10109-R00. Toronto, Canada.

Gobien, M and F. Garisto. 2012. Data for Radionuclide and Chemical Element Screening. Nuclear Waste Management Organization Report NWMO TR-2012-11. Toronto, Canada.

Goodwin, B.W., P. Gierszewski and F. Garisto. 2001. Radionuclide Screening Model (RSM) Version 1.1 - Theory. Ontario Power Generation Report 06819-REP-01200-10045-R00. Toronto, Canada.

Grambow, B., J. Bruno, L. Duro, J. Merino, A. Tamayo, C. Martin, G. Pepin, S. Schumacher, O. Smidt, C. Ferry, C. Jegou, J. Quiñones, E. Iglesias, N. Rodriguez Villagra, J. M. Nieto, A. Martínez-Esparza, A. Loida, V. Metz, B. Kienzler, G. Bracke (GRS), D. Pellegrini, G. Mathieu, V. Wasselin-Trupin, C. Serres, D. Wegen, M. Jonsson, L. Johnson, K. Lemmens, J. Liu, K. Spahiu, E. Ekeroth, I. Casas, J. de Pablo, C. Watson, P. Robinson, and D. Hodgkinson. 2010. MICADO Model Uncertainty for the Mechanism of Dissolution of Spent Fuel in Nuclear Waste Repository. European Commission Report EUR 24597 EN. Brussels, Belgium.

Grasty, R.L. and J.R. LaMarre. 2004. The Annual Effective Dose from Natural Sources of Ionising Radiation in Canada. Radiation Protection Dosimetry 108, No 3, 215-226.

Guo, R. 2010. Coupled Thermal-Mechanical Modelling of a Deep Geological Repository using the Horizontal Tunnel Placement Method in Sedimentary Rock using CODE_BRIGHT. Nuclear Waste Management Organization Report NWMO TR-2010-22. Toronto, Canada.

Guttman, I. and S.S. Wilks. 1965. Introductory Engineering Statistics. John Wiley & Sons. New York, USA.

Hallet, B. 2011. Glacial Erosion Assessment, NWMO Report DGR-TR-2011-18, Toronto, Canada.

Hermann, O.W. and R.M. Westfall. 1995. ORIGEN-S - SCALE System Module to Calculate Fuel Depletion, Actinide Transmutation, Fission Product Buildup and Decay, and Associated Radiation Source Terms. In: SCALE: A Modular Code System for Performing Standardized Computer Analyses for Licensing Evaluations. Oak-Ridge National Laboratory NUREG/CR-0200, Rev.4 (ORNL/NUREG/CSD-2/R4) Volume II, Part I. Oak-Ridge, USA.

IAEA. 2006. Safety Requirements: Geological Disposal of Radioactive Waste. International Atomic Energy Agency Safety Requirements WS-R-4. Vienna, Austria.

ICRP. 1995. Age-dependent Doses to the Members of the Public from Intake of Radionuclides - Part 5 Compilation of Ingestion and Inhalation Coefficients. International Commission on Radiological Protection Publication 72, Annals of the ICRP 26(1). Vienna, Austria.

ICRP. 2007. The 2007 Recommendations of the International Commission on Radiological Protection. International Commission on Radiological Protection Publication 103, Annals of the ICRP (W2-4). Vienna, Austria.

ICRP. 2013. Radiological Protection in Geological Disposal of Long-lived Solid Radioactive Waste. International Commission on Radiological Protection Publication 122, Annals of the ICRP 42(3). Vienna, Austria.

Jackson R. and S. Murphy. 2011. Mineralogy and Lithogeochemical Analysis of DGR-5 and DGR-6 Core. Intera Engineering Technical Report TR-09-06. Ottawa, Canada.

JNC. 2000. H12: Project to Establish the Scientific and Technical Basis for HLW in Japan. Japan Nuclear Cycle Development Institute JNC TN1410 2000-004. Tokai, Japan.

King, F. and M. Kolar. 2006. Simulation of the Consumption of Oxygen in Long-term in situ Experiments and in the Third Case Study Repository using the Copper Corrosion Model CCM-UC.1.1. Ontario Power Generation Report 06819-REP-01300-10084-R00, Toronto, Canada.

Kitson C.I., T.W. Melnyk, L.C. Wojciechowski, T. Chshyolkova. 2012. SYVAC3-CC4 User Manual, Version SCC409. Nuclear Waste Management Organization Report NWMO TR-2012-21. Toronto, Canada.

Maak, P., P. Gierszewski and M. Saiedfar. 2001. Early Failure Probability of Used-Fuel Containers in a Deep Geologic Repository. Ontario Power Generation Report 06819-REP-01300-10022-R00, Toronto, Canada.

Medri, C. 2012. Human Intrusion Model for the Fourth and Fifth Case Studies: HIMv2.0. Nuclear Waste Management Organization Report NWMO TR-2012-04. Toronto, Canada.

MoE. 2011a. Soil, Groundwater and Sediment Standards for Use under Part XV.1 of the Environmental Protection Act. Ontario Ministry of the Environment. Toronto, Canada.

MoE. 2011b. Rationale for the Development of Soil and Groundwater Standards for Use at Contaminated Sites in Ontario. Ontario Ministry of the Environment. Toronto, Canada.

MoEE. 1994. Water Management Policies Guidelines Provincial Water Quality Objectives of the Ministry of Environment and Energy. Toronto, Canada.

Muurinen, A. and J. Lehikoinen. 1999. Porewater chemistry in compacted bentonite. Engineering Geology 54, 207-214.

Nagra. 2002. Project Opalinus Clay: Safety Report, Demonstration of the Disposal Feasibility for Spent Fuel, Vitrified HLW and Long-lived ILW. Nagra Technical Report 02-05. Wettingen, Switzerland.

NRC. 2006. Health Risks from Exposure to Low Levels of Ionizing Radiation: BEIR VII Phase 2. Committee on the Biological Effects of Ionizing Radiations (BEIR). The National Academies Press, Washington, DC, USA.

NWMO. 2011. Geosynthesis. Nuclear Waste Management Organization Report NWMO DGR-TR-2011-11 R000. Toronto, Canada.

NWMO. 2012. SYVAC3-CC4 Theory, Version SCC409. Nuclear Waste Management Organization Report NWMO TR-2012-22. Toronto, Canada

Oregon Department of Environmental Quality (ODEQ). 2001. Guidance for Ecological Risk Assessments, Levels I, II, III and IV:P Level II Screening Level Values. Portland, USA

Parkhurst, D.L. and C.A.J. Appelo. 1999. User's Guide to PHREEQC (Version 2) – A Computer Program for Speciation, Batch-Reaction, One-Dimensional Transport, and Inverse Geochemical Calculations. U.S Department of the Interior and U.S. Geological Survey Water-Resources Investigations Report 99-4259. Denver, USA.

Peltier, W.R. 2011. Long-term Climate Change. Nuclear Waste Management Organization Technical Report DGR-TR-2011-14. Toronto, Canada.

Sheppard, S.C. and B. Sanipelli. 2011a. Review of Environmental Radioactivity in Canada Nuclear Waste Management Organization report NWMO-TR-2011-17. Toronto, Canada.

Sheppard, S.C. and B. Sanipelli. 2011b. Environmental radioactivity in Canada - Measurements. Nuclear Waste Management Organization report NWMO-TR-2011-16. Toronto, Canada.

Shoesmith, D. 2008. The Role of Dissolved Hydrogen on the Corrosion/Dissoluton of Spent Nuclear Fuel. Nuclear Waste Management Organization Report NWMO TR-2008-19. Toronto, Canada.

SKB. 1998. Design Premises for Canister for Spent Nuclear Fuel. Swedish Nuclear and Waste Management Company Technical Report TR-98-08. Stockholm, Sweden

SKB. 2004. Interim Main Report of the Safety Assessment SR-Can. Swedish Nuclear Fuel and Waste Management Report SKB TR-04-11. Stockholm, Sweden.

SKB. 2010a. Handling of future human actions in the safety assessment SR-Site. Swedish Nuclear and Waste Management Company Technical Report TR-10-53. Stockholm, Sweden.

SKB. 2010b. Design, Production and Initial State of the Canister. Swedish Nuclear and Waste Management Company Technical Report TR-10-14. Stockholm, Sweden

SKB. 2011. Long-term Safety for the Final Repository for Spent Nuclear Fuel at Forsmark, Main Report of the SR-Site Project. Swedish Nuclear Fuel and Waste Management Company Report SKB TR-11-01. Stockholm, Sweden.

Tait, J.C., I.C. Gauld and A.H. Kerr. 1995. Validation of the ORIGEN-S Code for Predicting Radionuclide Inventories in Used CANDU Fuel. Journal of Nuclear Materials 223, 109-121.

Therrien, R., R. G. McLaren, E. A. Sudicky, S.M. Panday and V. Guvanasen. 2010 FRAC3DVS-OPG: A Three-Dimensional Numerical Model Describing Subsurface Flow and Solute Transport. User's Guide, Groundwater Simulations Group, University of Waterloo. Waterloo, Canada.

Vilks, P. 2011. Sorption of Selected Radionuclides on Sedimentary Rocks in Saline Conditions – Literature Review. Nuclear Waste Management Organization Report NWMO TR-2011-12. Toronto, Ontario.

Wigston, A., and R. Jackson 2010a. Mineralogy and Geochemistry of DGR-3 Core. Intera Engineering Technical Report TR-08-22. Ottawa, Canada.

Wigston, A., and R, Jackson. 2010b. Mineralogy and Geochemistry of DGR-4 Core. Intera Engineering Technical Report TR-08-23. Ottawa, Canada.

THIS PAGE HAS BEEN LEFT BLANK INTENTIONALLY

8. POSTCLOSURE SAFETY ASSESSMENT – GAS GENERATION AND TRANSPORT

This chapter, together with Chapter 7, presents an illustrative postclosure safety assessment for a used fuel repository located in the sedimentary rock of the Michigan Basin. The focus of this chapter is on gas generation and transport of volatile radionuclides. Chapter 7 addresses waterborne contaminant transport.

Exposure of the steel components of an engineered barrier system (EBS) to groundwater will result in the generation of gas due to corrosion processes. Microbial processes, if present, may also generate (or consume) gas. The fate of this gas, as it migrates through the repository, the excavation damaged zone (EDZ) and the surrounding host rock can affect both the internal repository pressure and the transport of gaseous radionuclides.

The assessment is arranged as follows:

- Section 8.1 – Interim Acceptance Criteria: presents the acceptance criteria against which the results of the gas generation and transport analysis are measured.
- Section 8.2 – Scope: describes the analysis case and the rationale for its selection.
- Section 8.3 – Conceptual Model: discusses the conceptualization of gas generation and migration.
- Section 8.4 – Computer Code: introduces T2GGM, the main computer code used.
- Section 8.5 – Analysis Methods and Key Assumptions: the computer code representations are described in detail.
- Section 8.6 – Results of Gas Generation and Transport Analysis: discusses simulations of gas generation and transport on the scale of an individual placement room and on the scale of the repository.
- Section 8.7 – Dose Consequences: postulates gas transport of volatile radionuclides to the biosphere and hypothetical dose consequences to a member of the critical group.
- Section 8.8 – Summary and Conclusions.

8.1 Interim Acceptance Criteria

For radiological consequences, the interim acceptance criteria are identical to those adopted for the waterborne contaminant transport assessment described in Chapter 7.

For pressure, the target acceptance criterion is that pressure in the intact host rock surrounding the repository should remain below 80% of lithostatic pressure (i.e., below 9.9 MPa).

Note that preliminary geophysical analysis indicates that lithostatic pressure must be exceeded before fracturing of the host rock can occur. If this latter criterion is met, the possibility that gas pressure build-up will lead to fracturing can be excluded.

8.2 Scope

This chapter considers the variant case of the All Containers Fail Disruptive Scenario in which all containers are assumed to fail at 10,000 years (see Chapter 6). This case assumes that an undefined event or process causes the copper cladding on all used fuel containers to fail, thereby exposing the entire carbon steel container surface area to anoxic, deep groundwater that has entered the repository following closure. This initiates carbon steel corrosion, gas generation and gas migration.

This is the bounding scenario, in that it has the largest potential for gas production and radiological impact from gas-borne radionuclides.

Additional gas sources, such as those arising from corrosion of rock bolts, degradation of trace organic materials in the backfill, and radiolysis of water are neglected on the basis that the amount of gas produced by such processes is much less than the amount of gas produced due to corrosion of all containers.

8.3 Conceptual Model

The generation and migration of gas is a coupled process, in which gas generation is dependent on the availability and transport of groundwater near the container. Gas can migrate through the repository by:

- Dilational flow, where gas pressure exceeds the local confining stress and physically displaces material, with gas moving through the resultant open pathway. Pathways are typically small scale and are localized. They will generally propagate until sufficient pathway volume has been opened to reduce the pressure. Dilational flow paths are typically unstable and will close once the pressure is reduced below the confining stress.

- Conventional two-phase flow, where gas pressure is sufficient to partially or completely displace water from the pore space of a material, allowing gas to travel through the connected porosity.

- Dissolving in groundwater, where dissolved gas can travel with groundwater flow or diffuse through groundwater.

The following sections describe the conceptual model for gas generation and transport applied in the analysis.

8.3.1 Gas Generation

In low-permeability sedimentary rock, saturation of the repository may take thousands of years. This leads to the definition of the following four phases in the evolution of the corrosion environment (see Chapter 5):

Phase 1: This is an early aerobic period that occurs prior to the onset of aqueous corrosion, immediately following closure of the repository. In this phase, saturation of the materials surrounding the container has not yet occurred, no liquid water is available for corrosion, and the material immediately adjacent to the container remains unsaturated due to high

temperatures. Oxygen is initially present in the unsaturated pore space. If relative humidity is also low, corrosion is limited to slow air oxidation.

Phase 2: This is an unsaturated aerobic phase that occurs following the condensation of liquid water on the steel surface. Steel corrosion is higher under these conditions.

Phase 3: This corresponds to an unsaturated anaerobic phase that occurs following the consumption of oxygen but prior to full saturation of the materials surrounding the container. Corrosion during this period is supported by the cathodic reduction of water accompanied by the evolution of hydrogen.

Phase 4: This is a saturated anaerobic phase that is entered once the materials surrounding the container have become fully saturated by groundwater. As with Phase 3, corrosion during Phase 4 is supported by the cathodic reduction of water accompanied by the evolution of hydrogen.

These four phases do not necessarily occur sequentially. Phases 1 and 2 both occur under aerobic conditions and the degree to which the Phase 1 and Phase 2 corrosion processes are active depends on the relative humidity. The Phase 3 and 4 corrosion processes proceed under anaerobic conditions after Phase 1 and Phase 2 and may occur concurrently. The Phase 3 process also depends on relative humidity.

There are a number of processes, such as methanogenesis, through which the quantity of gas in the repository may be reduced as discussed in Suckling et al. (2012). The gas modelling presented in this chapter takes no credit for these pressure mitigation processes.

Parameter values used in the corrosion calculations are discussed in Gobien et al. (2013).

8.3.2 Gas Migration and Transport

In this assessment, conventional two-phase flow and groundwater dissolution processes are considered sufficient for estimating gas migration through the repository. Whereas dilational flow describes transport through EBS materials that are near-fully saturated, in this system gas generation and migration are expected to desaturate different components of the EBS to varying degrees. This approach is consistent with other programs in which numerical modelling of gas migration has focussed primarily on conventional two-phase flow (Senger et al. 2011, Yu and Weetjens 2009, Marschall et al. 2005).

Two-phase flow gas migration modelling is based on the van Genuchten model for water retention (van Genuchten 1980, Mualem 1976). This model describes the relationship between the water content of a porous matrix and the suction, or capillary pressure. Capillary pressure is the difference in pressure across the interface between two immiscible fluids, and is defined here as the difference in pressure between the gas phase (non-wetting phase) and the water phase (wetting phase). The pressure difference is a function of the pore throat radius, with capillary pressure increasing as the wetting fluid is displaced into smaller and smaller pores. The model parameters have been fitted to the measured behavior of bentonites and also low permeability limestone and shale rocks.

The van Genuchten equations for capillary pressure as a function of liquid saturation are as follows.

$$P_c = -\frac{1}{\alpha}\left[S_{ec}^{-1/m} - 1\right]^{1/n} \tag{8-1}$$

$$S_{ec} = \frac{S_l - S_{lrc}}{1 - S_{lrc}} \tag{8-2}$$

where:

- P_c is the capillary pressure, Pa;
- α is a van Genuchten fitting parameter, Pa^{-1}. The inverse of α is analogous to the air entry pressure, but is often larger than the actual air entry pressure;
- S_{ec} is the effective saturation for the capillary pressure relationship (volume ratio);
- S_l is the liquid saturation (volume ratio);
- S_{lrc} is the residual liquid saturation for capillary pressure (volume ratio), the liquid saturation below which liquid does not flow, and capillary pressure is confined;
- m is a van Genuchten fitting parameter (unitless); and
- n is a van Genuchten fitting parameter (unitless).

Relative permeability of gas and liquid is described using the Luckner form of the van Genuchten-Mualem equations, as follows:

$$k_{rl} = S_{ek}^{1/2}\left[1 - (1 - S_{ek}^{1/m})^m\right]^2 \tag{8-3}$$

$$k_{rg} = (1 - S_{ek})^{1/3}\left[1 - S_{ek}^{1/m}\right]^{2m} \tag{8-4}$$

$$S_{ek} = \frac{S_l - S_{lr}}{1 - S_{lr} - S_{gr}} \tag{8-5}$$

where:

- k_{rl} is the liquid phase relative permeability (ratio);
- k_{rg} is the gas phase relative permeability (ratio);
- S_{ek} is the effective saturation for the relative permeability relationship (volume ratio);
- S_{lr} is the residual liquid saturation (volume ratio), the liquid saturation below which liquid does not flow; and
- S_{gr} is the residual gas saturation (volume ratio), the gas saturation below which gas does not flow.

Table 8-1 shows the two-phase flow properties used for each material.

Table 8-1: Two-Phase Flow Properties

Material	1/α(MPa)	n	m	S_{lrc}	S_{lr}	S_{gr}
Unit B and C	0.31	4.22	0.35	0.54	0.55	0.00
Unit A-2 Carbonate	0.76	3.06	0.50	0.00	0.00	0.00
Unit A-1 Upper Carbonate	0.04	4.89	0.15	0.24	0.25	0.00
Unit A-1 Carbonate	38.9	2.41	0.99	0.00	0.00	0.00
Unit A-1 Evaporite	2.06	2.28	0.99	0.00	0.01	0.10
Unit A0	2.06	2.28	0.99	0.00	0.01	0.10
Guelph	0.04	4.89	0.15	0.24	0.25	0.00
Fossil Hill	27.9	6.11	0.68	0.02	0.03	0.00
Cabot Head	14.6	6.82	0.24	0.00	0.00	0.05
Manitoulin	40.8	3.65	1.31	0.10	0.11	0.05
Queenston	35.6	4.45	1.13	0.08	0.09	0.06
Georgian Bay/Blue Mountain	30.1	3.82	1.10	0.16	0.17	0.04
Cobourg	61.7	3.13	1.69	0.05	0.06	0.03
Sherman Fall	28.2	2.33	1.00	0.16	0.17	0.11
Kirkfield	173	2.17	7.22	0.00	0.00	0.15
Cobokonk	66.2	1.82	1.73	0.00	0.00	0.03
Gull River	40.0	4.06	0.78	0.20	0.21	0.11
Shadow Lake	0.23	1.20	0.58	0.03	0.04	0.00
Cambrian	0.23	1.20	0.58	0.03	0.04	0.00
Upper Precambrian	0.23	1.20	0.58	0.03	0.04	0.00
Precambrian	0.23	1.20	0.58	0.03	0.04	0.00
Fossil Hill EDZ	5.57	6.11	0.68	0.02	0.03	0.00
Cabot Head EDZ	2.90	6.82	0.24	0.00	0.00	0.05
Manitoulin EDZ	8.16	3.65	1.31	0.10	0.11	0.05
Queenston EDZ	7.12	4.45	1.13	0.08	0.09	0.06
Georgian Bay EDZ	6.02	3.82	1.10	0.16	0.17	0.04
Cobourg EDZ	1.23	3.13	1.69	0.05	0.06	0.03
Repository Inner EDZ	2.47	3.13	1.69	0.05	0.06	0.03
Repository Outer EDZ	6.17	3.13	1.69	0.05	0.06	0.03
Placement Room Bentonite (Homogenized Bentonite)	20.6	1.06	0.61	0.03	0.40	0.00
Tunnel Seal Bentonite (HCB Seal)	34.6	1.36	0.67	0.03	0.40	0.00
Tunnel Dense Backfill	10.0	1.80	0.40	0.10	0.10	0.01
Concrete (LHHPC), degraded	1.00	2.00	0.50	0.20	0.20	0.10
Shaft Asphalt	-	-	-	-	0.00	0.00
Shaft Bentonite/Sand	10.0	1.80	0.40	0.01	0.01	0.01

Note: Data taken from Gobien et al. (2013)

The two-phase flow relationship between gas and liquid is based on a capillary pressure function and a relative permeability function. Figure 8-1 to Figure 8-3 show these functions for Placement Room Bentonite, Repository Inner EDZ, and the intact host rock of the Cobourg formation. These curves are formulated using the two-phase flow parameters associated with these materials.

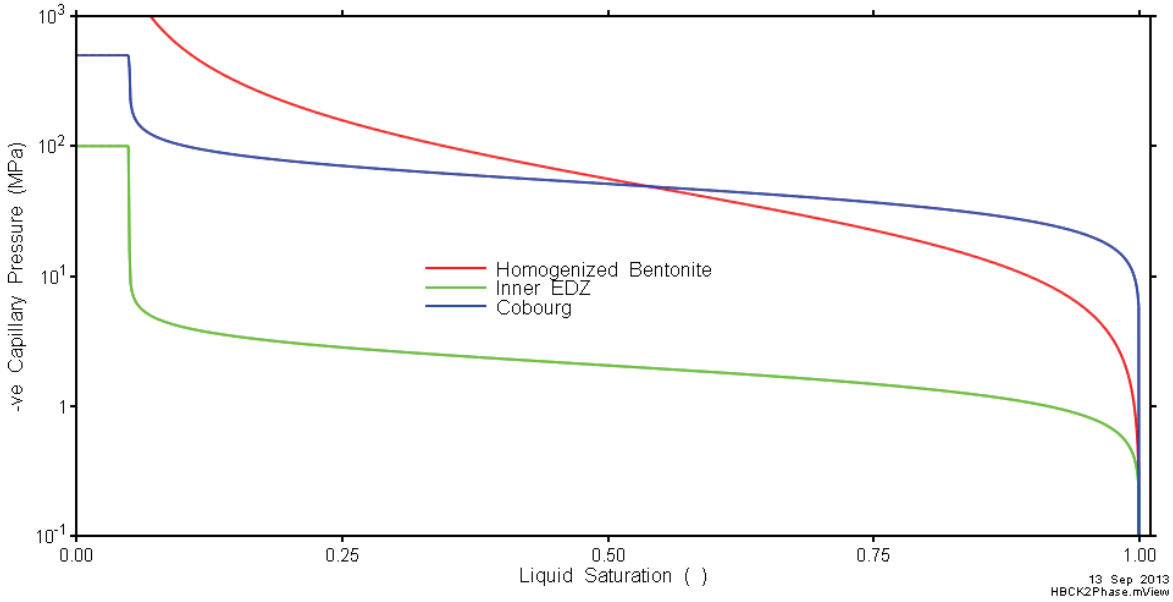

Figure 8-1: Capillary Pressure Curves for Placement Room Bentonite (Homogenized Bentonite), Repository Inner EDZ, and the Cobourg Formation

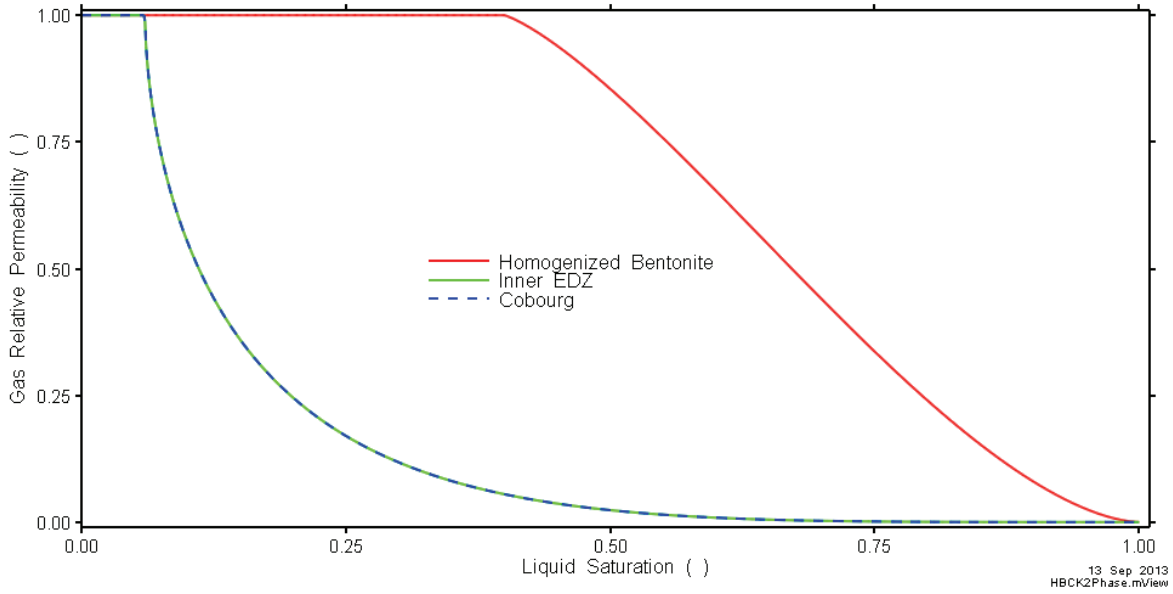

Figure 8-2: Relative Gas Permeability Curves for Placement Room Bentonite (Homogenized Bentonite), Repository Inner EDZ, and the Cobourg Formation

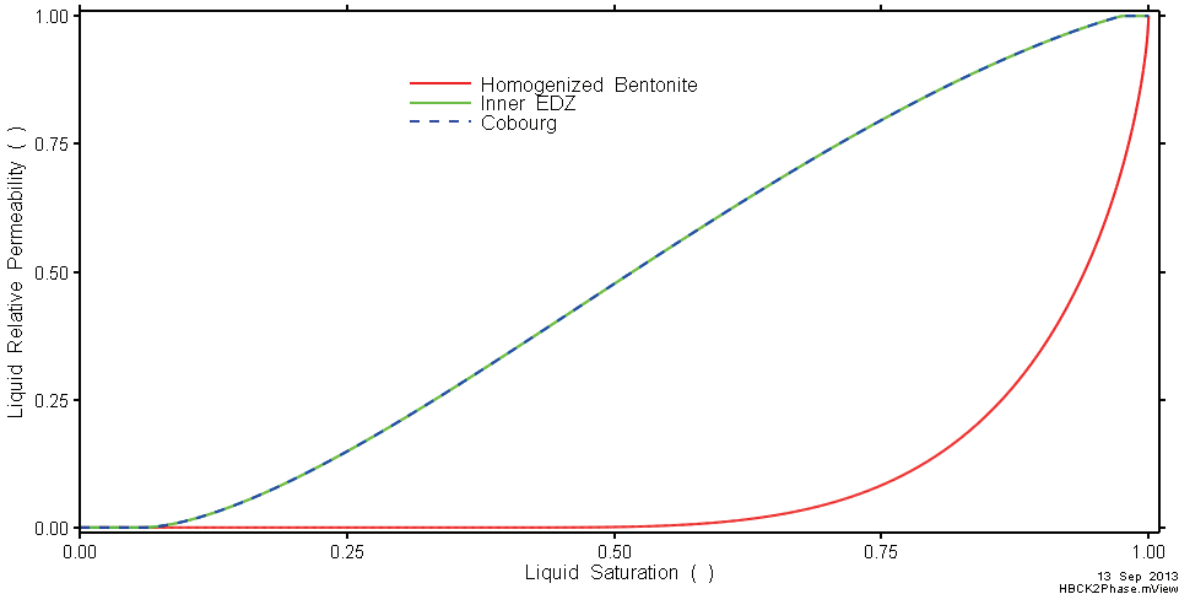

Figure 8-3: Relative Liquid Permeability Curves for Placement Room Bentonite (Homogenized Bentonite), Repository Inner EDZ, and the Cobourg Formation

Dissolution of gas in water is described by Henry's law, where the concentration of dissolved gas is proportional to the partial pressure of the gas. Salinity reduces the Henry's law coefficient, and a value of 4×10^{-11} mol fraction/Pa is used for hydrogen in this study (Quintessa and Geofirma 2011).

8.4 Computer Code

The conceptual model is numerically represented in the T2GGM computer code (Suckling et al. 2012).

Figure 8-4 identifies the interrelationship with repository parameters. Information from engineering design and site characterization is used to develop a site-specific system description.

T2GGM assesses the coupled behaviour between gas generation, temperature and the movement of gas and water. It is composed of two coupled models: the Gas Generation Model (GGM) used to describe the generation of gas due to corrosion of steel components, and the TOUGH2 model (Pruess et al. 1999) used to describe gas and water transport from the repository and within the geosphere. Key outputs are estimates of the repository pressure, repository saturation, and gas flow rates within the geosphere and repository system.

T2GGM has recently been used for gas modelling in support of the postclosure safety assessment for the Low and Intermediate Level Waste DGR proposed by Ontario Power Generation (Geofirma and Quintessa, 2011). T2GGM was used to calculate the generation and build-up of gas in the repository, the exchange of gas and groundwater between the repository and the surrounding rock, and between the rock and the surface environment.

The two coupled models are described below.

Table 8-2 provides more information on T2GGM.

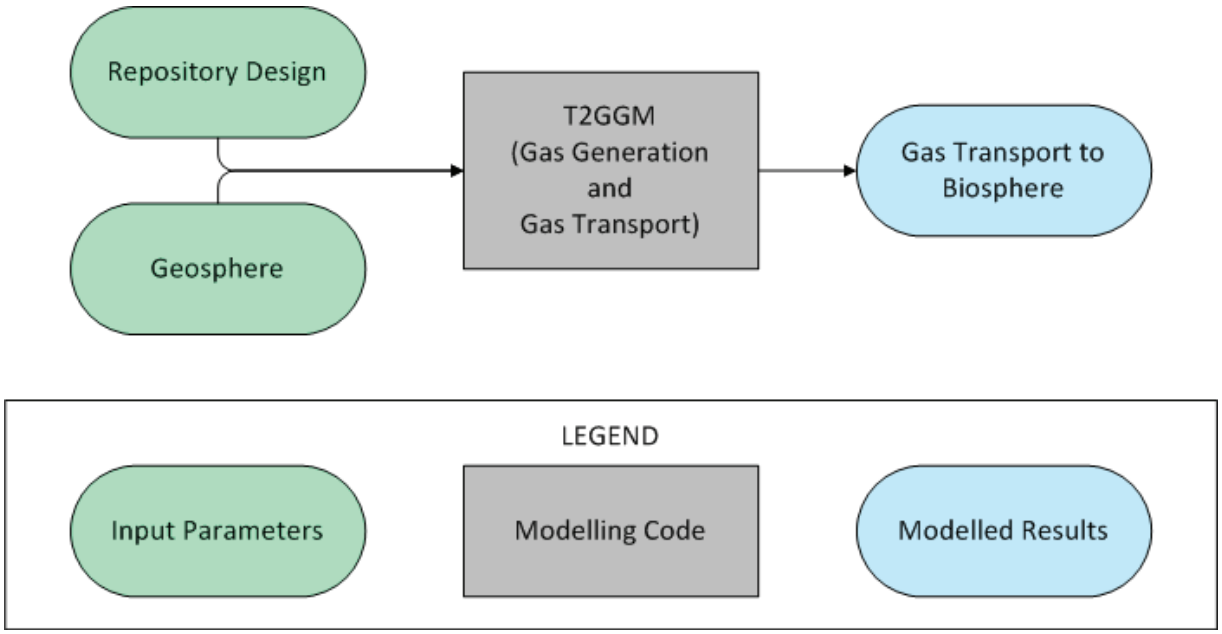

Figure 8-4: Main Computer Code

TOUGH2:

The TOUGH2 gas transport model is a widely used code for two-phase flow and gas transport in geological media, including for deep geological repositories (e.g., Talandier et al. 2006, Nagra 2008, FORGE 2010, Bate et al. 2012).

TOUGH2 is a multi-phase flow and heat transport program for fluid mixtures. T2GGM Version 3.1 includes TOUGH2 Version 2.0 with the EOS3 V1.01 equation-of-state module (ideal gas – air and water) (Pruess et al. 1999). The EOS3 module defines two-phase flow of water and air, or single-phase flow of water or air. Thermophysical properties of water are represented by steam-table equations, while the air is treated as an ideal gas. Dissolution of air in water is modelled with Henry's law. For T2GGM Version 3.1, an option is provided to represent the gas phase by an alternative gas, such as H_2.

GGM:

GGM is a gas generation model developed for NWMO (Suckling et al. 2012). It is implemented as a FORTRAN module that is used by TOUGH2 to incorporate gas generation due to corrosion and degradation processes. GGM includes a kinetic description of the various microbial and corrosion processes that lead to the generation and consumption of various gases. GGM can also be used to assess the effect of different gas-mitigation methods and other processes that can lead to the consumption of gas in the repository.

The GGM gas generation model is consistent with general literature and with approaches adopted in other waste management organizations for similar models.

Table 8-2: T2GGM, V3.1

Parameter	Comments
Components:	
TOUGH2	Core Code Version 2.0
EOS3	TOUGH2 Equation of State Module 3 Version 1.01
GGM	Gas Generation Component of T2GGM Version 3.1
Main Documents	T2GGM Version 3.1: Gas Generation and Transport Code (Suckling et al. 2012) TOUGH2 User Guide (Pruess et al. 1999)
Main Features:	- Temperature-dependent corrosion product and hydrogen gas generation from corrosion of steel and other alloys under aerobic and anaerobic conditions in the presence of a bentonite buffer - CO_2-enhanced corrosion of carbon steel and passive alloys - CO_2 and CH_4 gas generation from degradation of organic materials under aerobic and anaerobic conditions - H_2 gas reactions, including methanogenesis with CO_2 - Limitation of both microbial and corrosion reactions by the availability of water - Carbon, iron and water are mass balanced within repository reactions - Exchange of gas and water between the repository and the surrounding geosphere - Calculation of the generation and build-up of gas in each repository volume - Two-phase flow of water and gas within the geosphere with gas dissolution according to Henry's law - Heat flow coupled to two-phase flow of water and gas - 1D hydro-mechanical model to assess the effects of a uniformly applied glacial stress - Time-variable permeability, allowing the permeability properties of certain materials, such as engineered materials or EDZ, to evolve or degrade with time - Time-variable Dirichlet boundary conditions - The ability to stop and restart the simulations

8.5 Analysis Methods and Key Assumptions

Gas generation and transport are investigated using models at two different scales of resolution: Room-Scale and Repository-Scale.

The Room-Scale Model considers hydrogen gas generation from corrosion processes and two-phase flow with a simplified EBS geometry. It also considers thermal effects on groundwater flow and gas flow associated with heat transfer from the used fuel containers. The model domain extends to include a single full placement room and associated cross-cut drift.

Gas behaviour within each placement room is assumed sufficiently similar for Room-Scale results to be representative of gas behaviour in all placement rooms. Gas transport results are scaled to represent entire panels, each compromising either 27 or 28 placement rooms, with the scaled results used as input to the Repository-Scale Model. Gas transport data are provided to the Repository-Scale Model at locations where the cross-cut drifts intersect the main access tunnel. A constant pressure is specified at the cross-cut drift external boundary.

The Repository-Scale Model considers the transport of gas and water, without thermal effects, along the main drifts and shaft of the repository, using results from the Room-Scale Model to estimate the amount of gas reaching the drifts.

8.5.1 Overall Approach

During setup, the model is initially run for a sufficient period of time to allow the pre-construction conditions to equilibrate. Thereafter, simulations are conducted in three consecutive segments to account for the evolution of repository conditions. These are:

1. Preclosure – the engineered facilities are open to atmospheric pressure and are fully saturated with gas[1] for the operational period prior to closure. This is assumed to be seven years for placement rooms and 60 years for the main drift. Desaturation of the neighbouring rock is modelled and used to initialize the postclosure period.

2. Postclosure / pre-failure – the EBS is placed with specified gas saturations[2] at atmospheric pressure within the room and cross-cut drift (Room-Scale Model) or main drift and shaft (Repository-Scale Model) as the system is sealed. The system repressurizes and resaturates for 10,000 years with no gas generation taking place.

3. Post-failure – the steel container is exposed to the surrounding EBS and gas generation commences. Gas generation processes and rates are calculated as described in Section 8.3.1.

---

[1] Although the actual gas present in the pre-closure period is air, hydrogen is used in the simulations for consistency with the post-failure stage.

[2] Gas saturation is the volumetric fraction of a material's porosity that is filled with free-phase gas. Similarly, liquid saturation is the fraction of porosity filled with liquid. Within a pore's volume, the sum of the gas and liquid saturations is unity.

Pressure, gas saturation and dissolved gas content are continuous within the geosphere from one segment to the next.

The Room-Scale and Repository-Scale models are separate models and manual iteration is performed to ensure consistency between the model pressures at the interface location. A fully integrated model would allow time-dependent calculation of the interface pressure.

8.5.2 Detailed Transport Models

This section describes the Room-Scale and Repository-Scale Models.

Both models use the geosphere and repository material properties described in Chapter 2 and Chapter 4. Thermal processes are considered in the Room-Scale Model while the Repository-Scale Model is isothermal.

Within the host rock and the various engineered sealing materials, interactions between gas and liquid are modelled using the van Genuchten equations for water retention described in Section 8.3.2.

8.5.2.1 Room-Scale Model

The Room-Scale Model uses a simplified EBS geometry. The model domain consists of a full placement room and associated cross-cut drift. Gas generation, thermal effects and two-phase flow are simulated, with gas flow rates in the cross-cut drift calculated for input to the Repository-Scale Model.

The domain includes all 50 containers, the concrete and bentonite seals, and the access drift connecting it to the cross-cut drift. Horizontal symmetry is assumed and only one-half of the cross-section is modelled, including 10 m of host rock horizontally adjacent to the room. The plan section domain of 514.4 m × 10 m represents the full length of the single room located in the middle of the repository including one-half the intact rock separating the room from adjacent repository panels. The vertical extent of the model is from 1000 metres below the repository to the top of the Salina Unit B and C formations.

The 50 containers in the room are grouped into 10 combined containers where each combined container has the corrosion and heat generating characteristics of 5 individual containers. The combined containers have the length and volume of 5 individual containers so that the amount of bentonite is the same as in the actual system. Figure 8-5 illustrates the model.

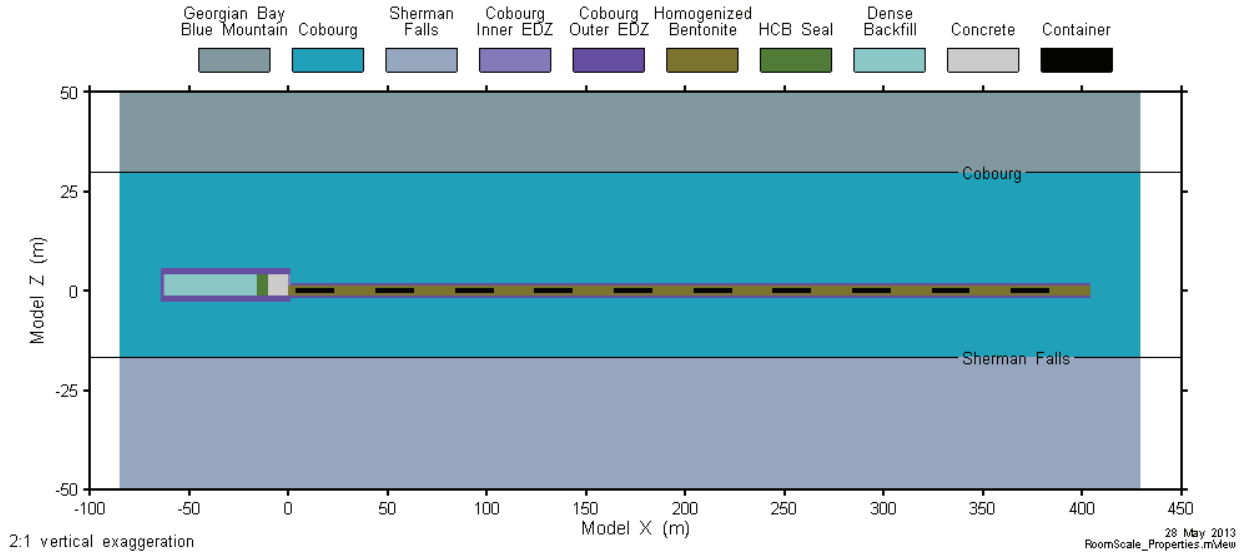

Figure 8-5: Room-Scale Model – Illustration

Figure 8-6 shows the drift end of the room. The drift is rectangular. Although the room is designed as circular with a radius of 1.25 m, it is implemented in the model as a square with equivalent cross-sectional area (i.e., 2.2 m width and height).

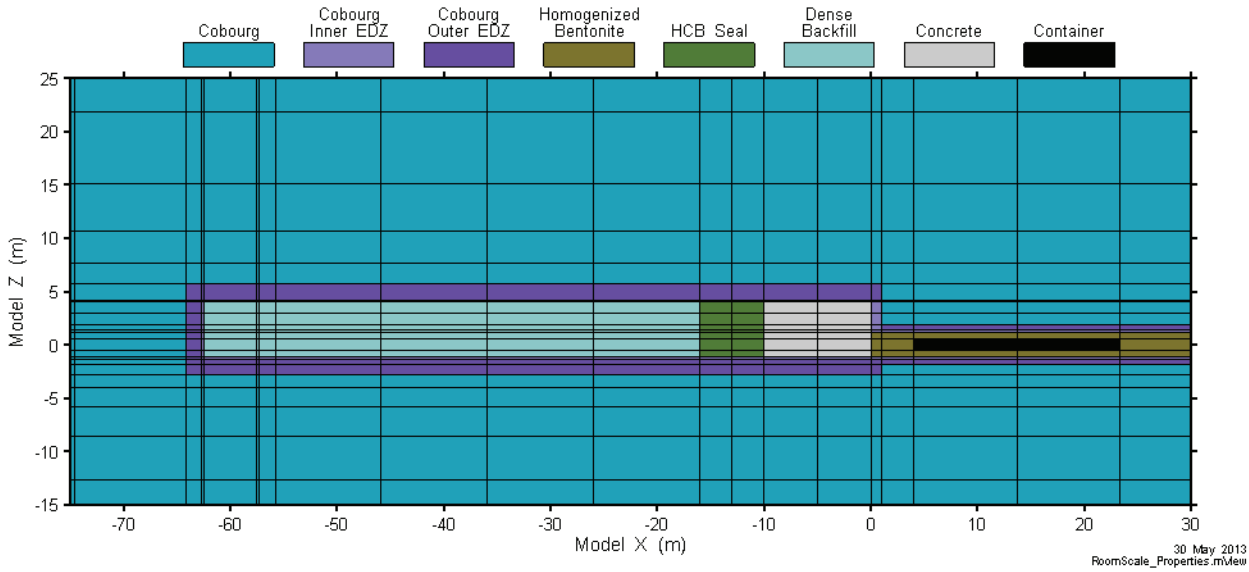

Figure 8-6: Room-Scale Model – Drift End of Room

Cross-sections through the first container and through the seal portion of the room entry drift are shown in Figure 8-7.

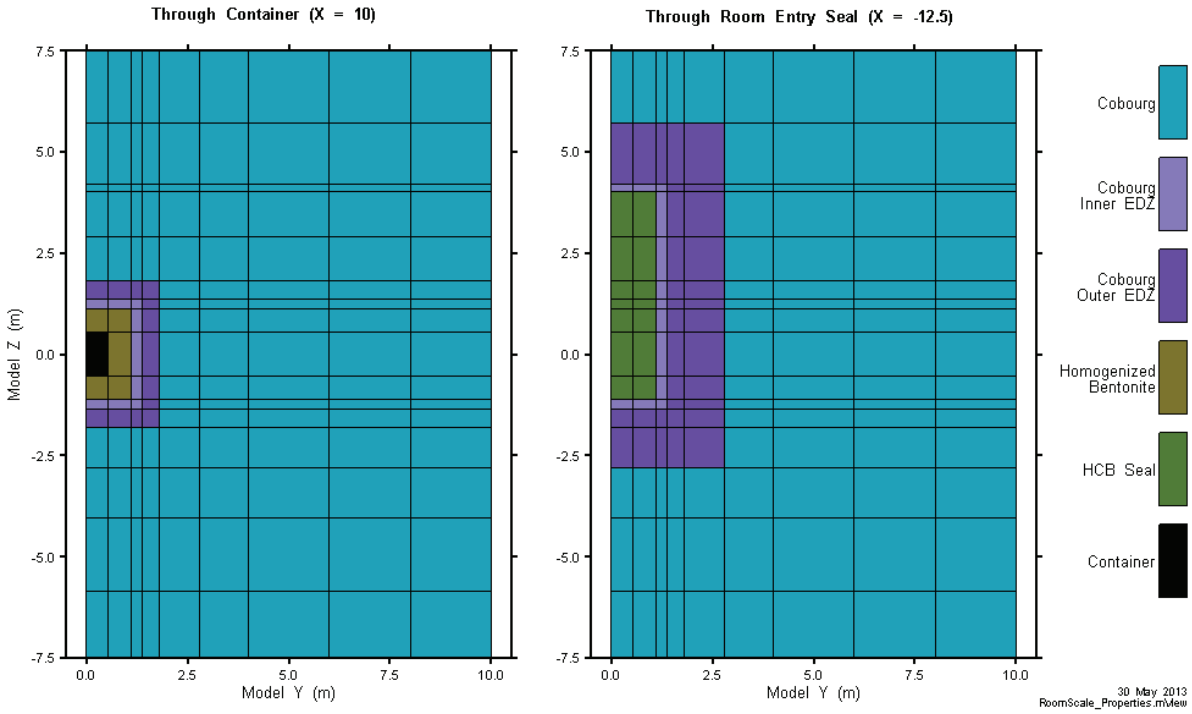

Figure 8-7: Room-Scale Model – Cross-Sections showing Container and Seal

Figure 8-8 is a plan section showing the container, room seal and cross-cut drift discretization. Some elements of the room dimensions and property assignments have been modified from the design specification to simplify the discretization. Specifically:

- The room entry drift is straight, rather than curved.
- The room entry drift width is 2.2 m (consistent with the simplified placement room) rather than 2 m, as specified in the design.
- The seal design is simplified in the model as it does not intersect the inner EDZ[3].
- The pedestal and surrounding bentonite pellets are combined into a single material with blended material properties.

These simplifications are not expected to materially affect model results.

The discretization contains 63 layers and 12,622 nodes.

[3] An additional smaller EDZ is associated with excavation of the seals and is assigned the same hydraulic conductivity as the EDZ surrounding all excavated spaces (see Section 7.3.2).

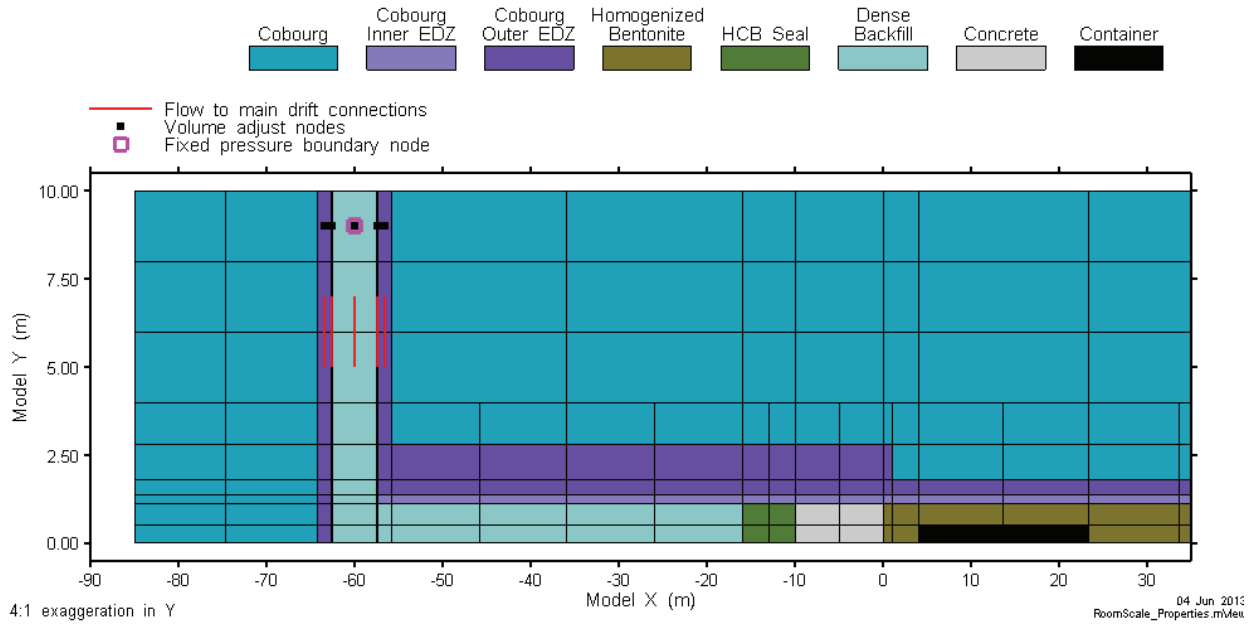

Figure 8-8: Room-Scale Model – Plan Section Cutting Middle of Placement Room

Boundary and Initial Conditions:

Pressure boundary conditions at the top and bottom of the model (i.e., the Salina Units B and C formations and 1000 m below the repository, respectively) are set to simulate a system at hydrostatic equilibrium. Initial pressures for all intact rock nodes are set to freshwater hydrostatic[4].

Highly compacted bentonite and dense backfill used in room seals and tunnels are assigned liquid saturations of 65% and 80% respectively. The bentonite around the containers was homogenized and initialized at 11% liquid saturation, representing the volumetrically averaged initial saturations of the pellet backfill (6%) and compacted block pedestal material (65%).

Thermal boundary conditions are defined according to Guo (2008). A temperature of 5°C was specified at the top of the model (ground surface). A temperature at the bottom of the model (1000 m below the repository) was defined based on a thermal gradient of 0.016°C/m through the sedimentary sequence, and a gradient of 0.012°C/m through the lower granite due to its higher thermal conductivity.

[4] Variations in fluid density will have negligible impact on the simulations, where pressures and flows are largely driven by processes occurring within the placement room. T2GGM has the ability to scale water density to simulate saline water; however, this feature was not used.

The thermal source term for heat released as a result of radioactive decay has been adopted from Guo (2008). Only heat generated by radioactive decay is considered. Although aerobic corrosion of steel is exothermic, the total heat generated would be negligible compared to the decay heat. Anaerobic corrosion of steel is endothermic. The watt-per-container values from Guo (2008) were multiplied by 50 to account for the 50 containers in the room, and then divided by two to reflect the half-room geometry. The resulting thermal source term was uniformly distributed among each of the two nodes in each of the ten combined containers.

Because the Room-Scale and Repository-Scale Models are each run independently, a fixed-pressure boundary node (see Figure 8-8) with pressure set to 6.8 MPa is used to couple the Room-Scale Model to the Repository-Scale Model. The 6.8 MPa value was determined by manual iteration of the two models. The node is defined to remain at 100% liquid saturation - this allows gas to exit the model, but does not allow gas to enter the model from the boundary.

Temperature at the boundary node is set to 14°C, determined by preliminary runs to be the long-term average temperature after 100,000 years. The fixed-temperature value is an approximation to simplify implementation. This affects the temperature in the drift, but has only a very small effect on the average temperature in the placement room.

GGM Implementation:

Preliminary scoping simulations indicated that the thermal state and resaturation profile did not vary significantly over the length of the room. Consequently, a single GGM compartment is used to simulate corrosion-generated gas from all containers in the room. The compartment consists of all homogenized bentonite nodes that are directly connected to a container node, as shown in Figure 8-9. The source term mass and surface areas are specified consistent with 50 half containers.

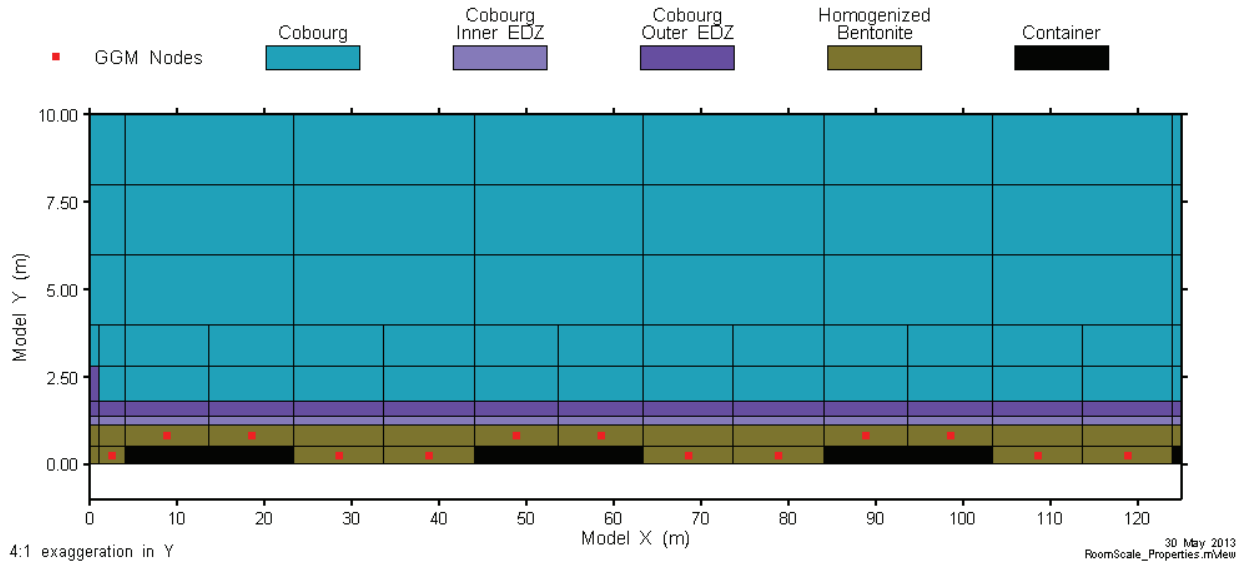

Figure 8-9: Room-Scale Model – Plan View Showing GGM Nodes

8.5.2.2 Repository-Scale Model

The Repository-Scale Model considers the transport of gas and water, without thermal effects, along the main drifts and shaft of the repository, using results from the Room-Scale Model to represent the amount of gas reaching the drifts. The model does not simulate any placement rooms.

The model domain consists of a single drift connecting the main and ventilation shafts. Horizontal symmetry is assumed; half the shafts are modelled. The model extends vertically from the bottom of the Coboconk formation up to the top of the Fossil Hill formation.

Figure 8-10 shows the model XY discretization, through the middle of the drift. Figure 8-11 shows an XZ slice through the middle of the drift intersecting one of the shafts. Figure 8-12 shows the shaft discretization in plan view. The outer EDZ is not represented.

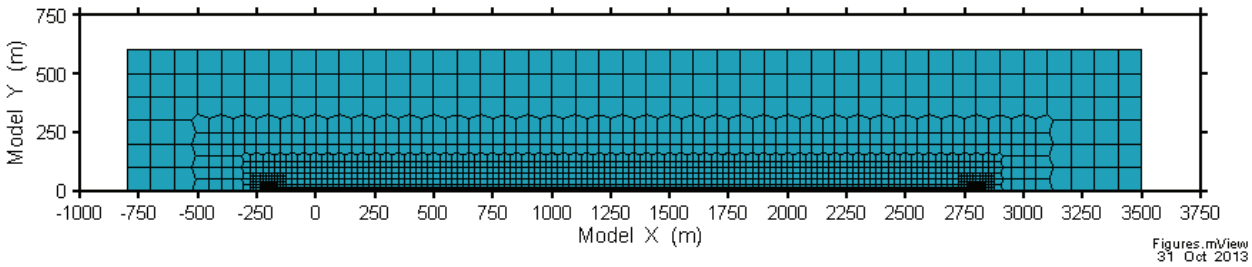

Figure 8-10: Repository-Scale Model – Plan View through the Main Drift

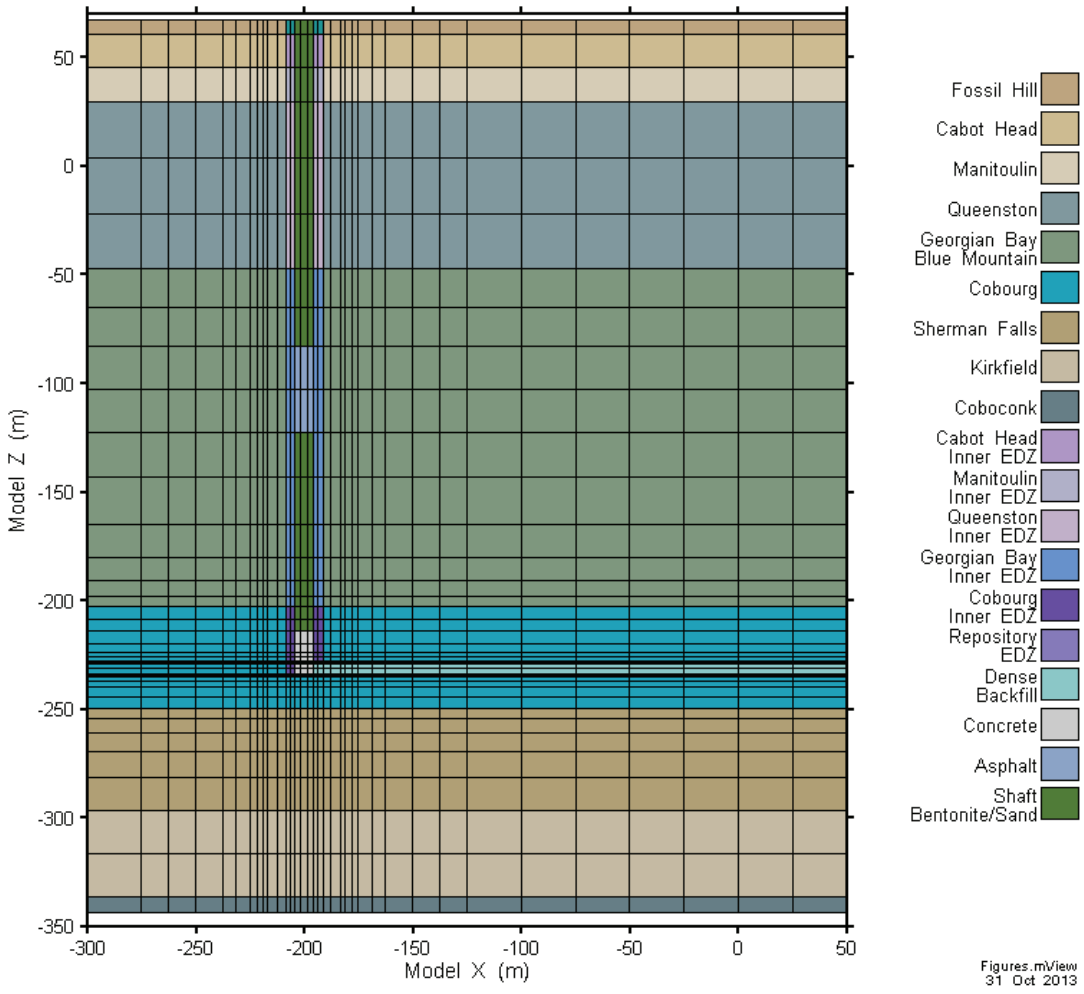

Figure 8-11: Repository-Scale Model – Drift and Shaft Discretization

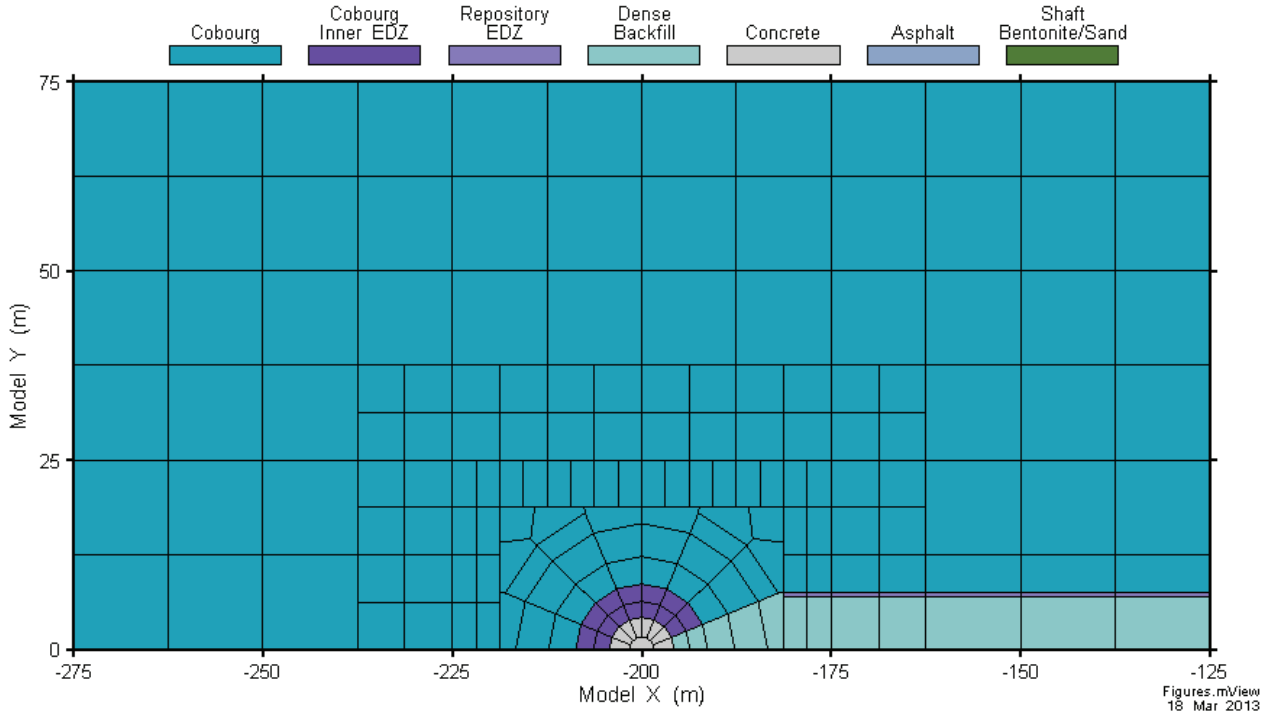

Figure 8-12: Repository-Scale Model – Plan View of Main Shaft Discretization

Boundary and Initial Conditions:

Pressure boundary conditions in the top and bottom layers of the model are calculated hydrostatic pressures based on a single point pressure obtained from the FRAC3DVS-OPG Site-Scale Model described in Chapter 7. This single point is located in the XY plane mid-way along the drift host rock, at the top of the Fossil Hill formation. The remaining sides of the model are no-flow boundaries.

Initially, the geosphere is assumed to be fully water-saturated. EBS materials have 80% saturation in the dense backfill and shaft seal at the start of the postclosure phase.

Gas is injected into the model at five locations, corresponding to intersections of the main access tunnel and the cross-cut drifts (Figure 8-13). The gas source term is calculated from results of the Room-Scale Model, multiplying the gas flow exiting a single room (i.e., from the end of the cross-cut drift segment, see Figure 8-8) by the average number of rooms in each panel[5]. This source term ignores the migration and accumulation of gas in the cross-cut drifts

[5] Half of the repository panels comprise 27 placement rooms while the other half comprise 28, providing an average of 27.5 placement rooms per panel. Multiplication factors are applied as required to account for the half-scale representation to ensure correct gas flows are used.

so that all gas leaving the Room-Scale Model is assumed to immediately reach the main access tunnel.

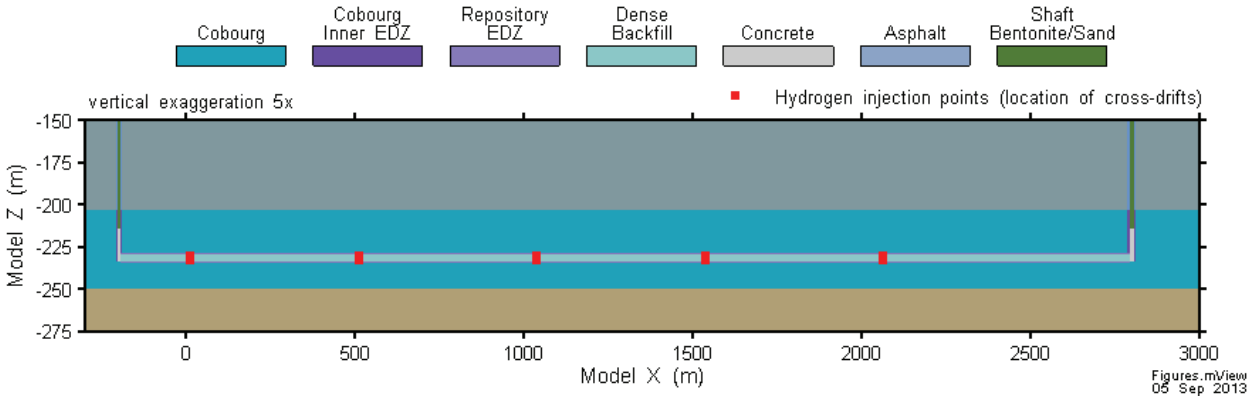

Figure 8-13: Repository-Scale Model – Gas Injection Locations

8.6 Results of Gas Generation and Transport Modelling

8.6.1 Room-Scale Model

Results from the Room-Scale Model simulation are shown in Figure 8-14 to Figure 8-20.

Figure 8-14 shows corrosion results in terms of container mass remaining (per container) and corrosion rates by process. The right hand axis shows the container mass remaining in terms of container wall thickness. The initial period of Phase 4 corrosion is caused by the high average liquid saturation (93%) within the EBS at the time of assumed failure. Phase 4 corrosion continues until the average gas saturation reaches 10%, after which only Phase 3 corrosion occurs. The corrosion rate decreases as temperature declines. Gas saturations near the container are relatively constant and remain high enough (greater than 10%) so that the criterion for resumption of Phase 4 corrosion is not reached until approximately 85,000 years. The container mass is exhausted by 440,000 years.

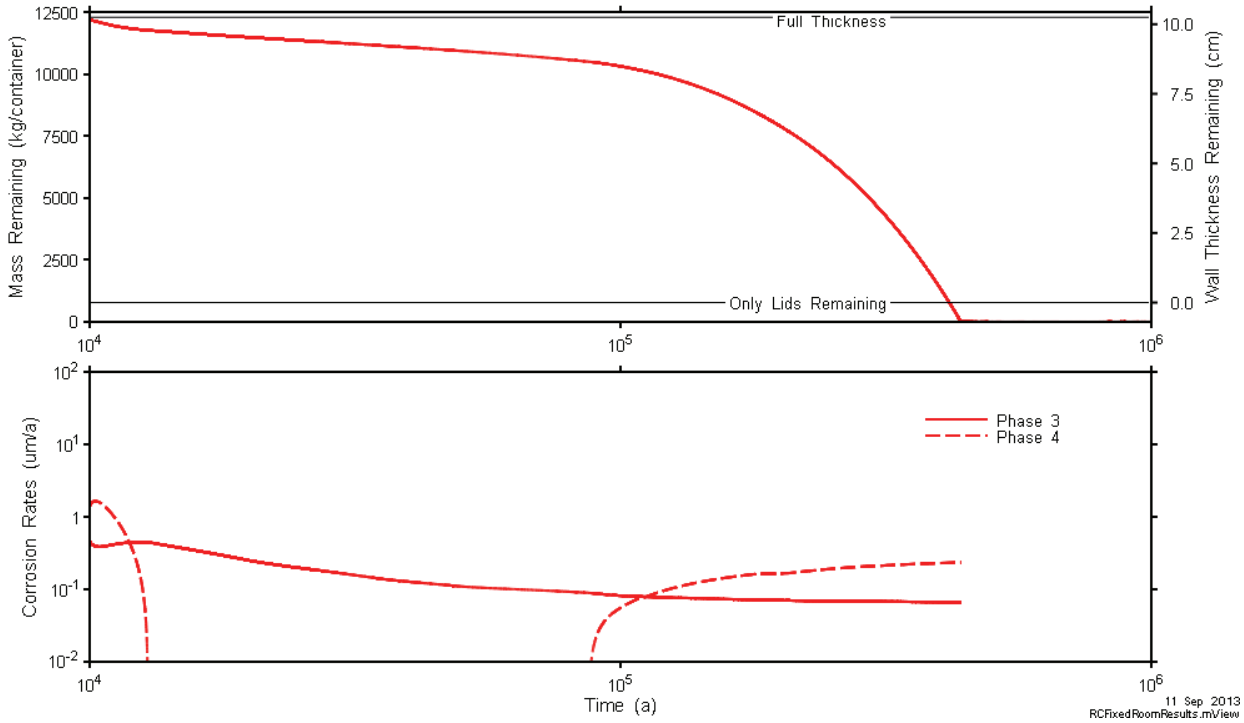

Note: the line labelled "Only Lids Remaining" indicates when the walls of the used fuel container have corroded. The lids are thicker than the walls.

Figure 8-14: Room Scale Model – Steel Consumption and Corrosion Processes

Figure 8-15 to Figure 8-18 show thermal profiles and gas saturation results for the following locations:

- Container – all nodes corresponding to the combined containers. These nodes have essentially no gas or liquid transport, but serve as thermal sources only.
- EBS – all engineered barrier system material (homogenized bentonite) for the nodes within the placement room beyond the concrete seal (i.e., Model X > 0).
- Inner EDZ – the inner EDZ of the placement room beyond the concrete seal.
- Intact rock – the closest intact rock nodes to the placement room beyond the concrete seal (i.e., nodes adjacent to the outer EDZ nodes).
- Intact rock 10 m – intact rock at the model boundary at Y =10 m.
- Cross-cut drift – the EBS material in the cross-cut drift.

The thin, lighter-coloured lines represent individual nodal values while the thicker, darker-coloured lines are the average of all nodes. For the intact rock and cross-cut drift, results are shown only for those nodes at the same elevation as the centre of the container (i.e., Model Z = 0.0).

Figure 8-15 and Figure 8-16 shows results for the first 10,000 years, or for the period of time prior to the assumed container failures. Figure 8-15 shows that the peak thermal pulse does not propagate to the drift, although drift temperatures have risen to near 50°C prior to the time of container failure. The placement room EBS and cross-cut drifts resaturate throughout the period and are approximately 90% saturated by 10,000 years. The inner EDZ does not start to resaturate until near the end of this time period, due in part to the high suction potential of the compacted bentonite within the placement room.

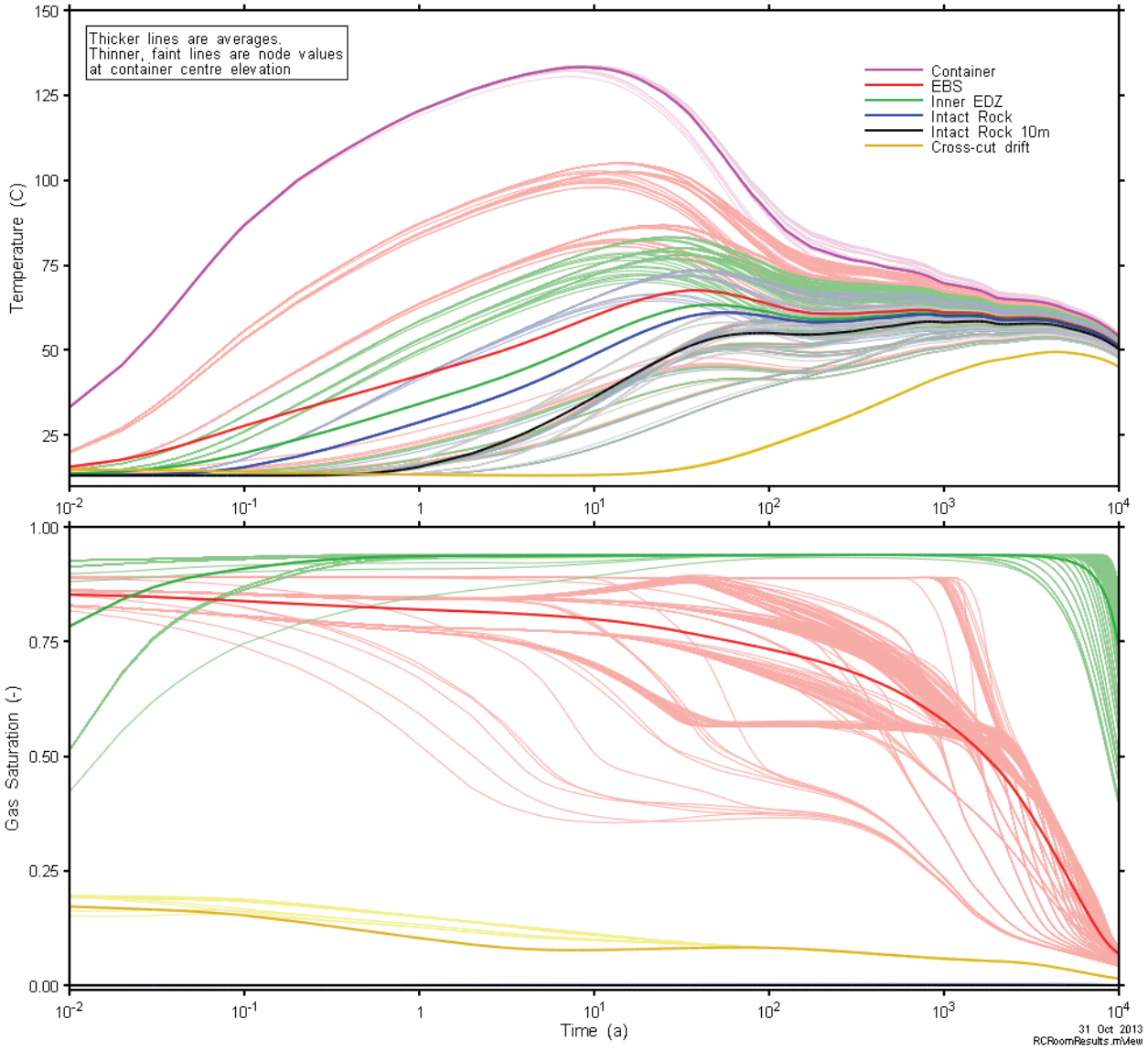

Figure 8-15: Room Scale Model – Conditions Prior to Container Failure

Figure 8-16 presents the gas, liquid and pore pressures[6] for the various locations. The figure shows that room and EBS pressures remain close to atmospheric (i.e., the pressure present when the repository is closed). Pressures in the intact rock at 10 m are initially hydrostatic but decrease in the 10 to 100 year period as fluid drains from the formation into the room during the resaturation process. The negative liquid and pore pressures represent suction pressures as calculated from the capillary pressure relationship.

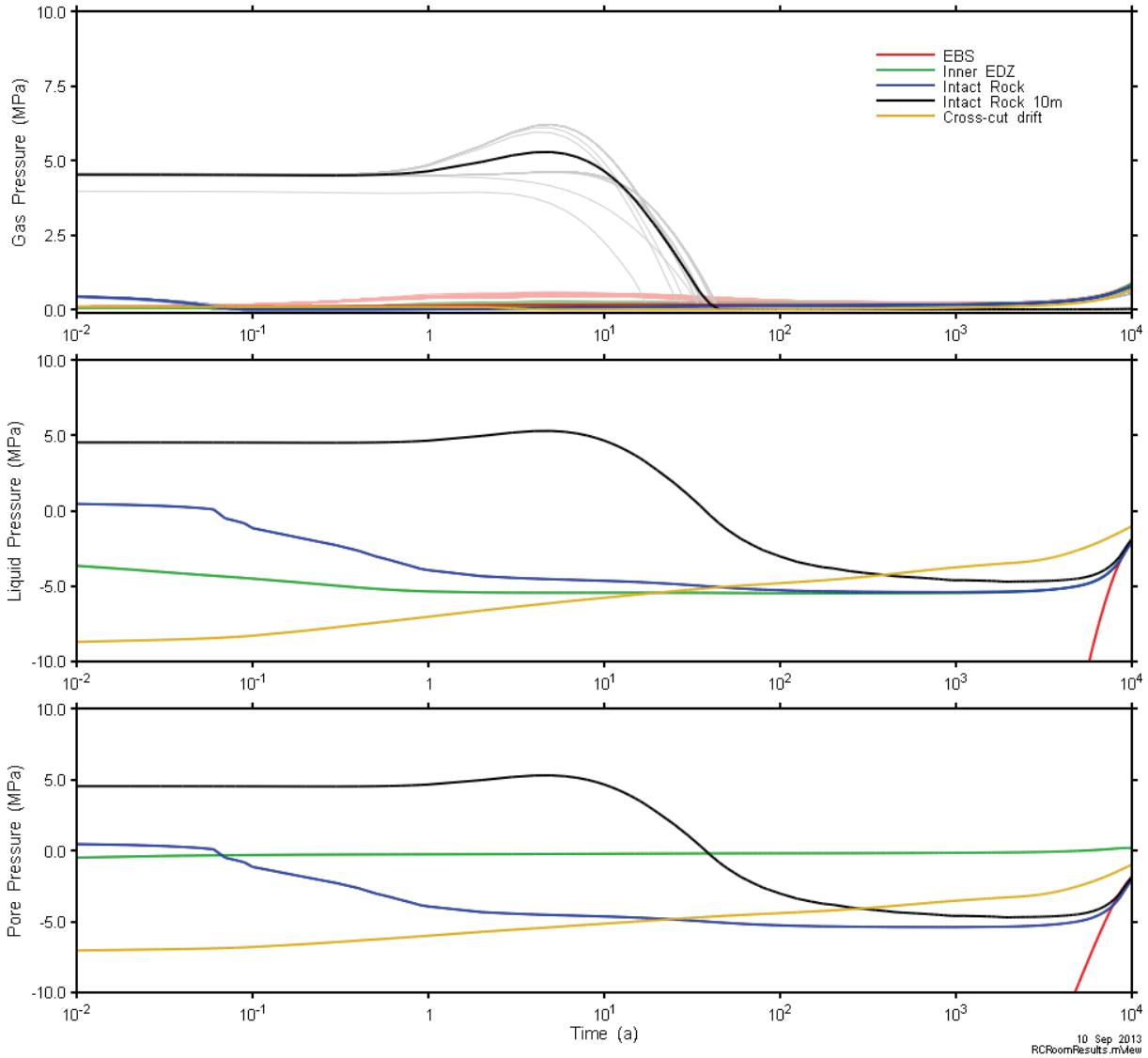

Figure 8-16: Room Scale Model – Nodal and Average Pressures Prior to Container Failure

[6] Pore pressure is calculated as the saturation-weighted average of gas and liquid pressures. The fluid volumetric saturations are used as a proxy for fluid surface areas on the contact surface. The resultant fluid pressure on the contact surface can be taken as a weighted average of the pressures in each of the two fluid phases (water and gas).

Figure 8-17 and Figure 8-18 show results for the period of time after the assumed container failures. Figure 8-17 shows that the thermal profile is uniform across the room, EDZ and intact rock, and that temperature declines to a near-steady state by 100,000 years. Gas saturations in the Inner EDZ reach 94% as generated gas moves from the EBS to the EDZ and porewater flows from the EDZ to the EBS due to the capillary pressure gradient. Gas saturations within the EBS and cross-cut drift increase slowly over the simulation with maximum gas saturations in the EBS reaching approximately 15%. Gas saturations in the intact rock at 10 m are essentially zero. The change in slope occurring at 440,000 years correlates with the time at which corrosion ceases because the entire mass of the container has corroded (Figure 8-14).

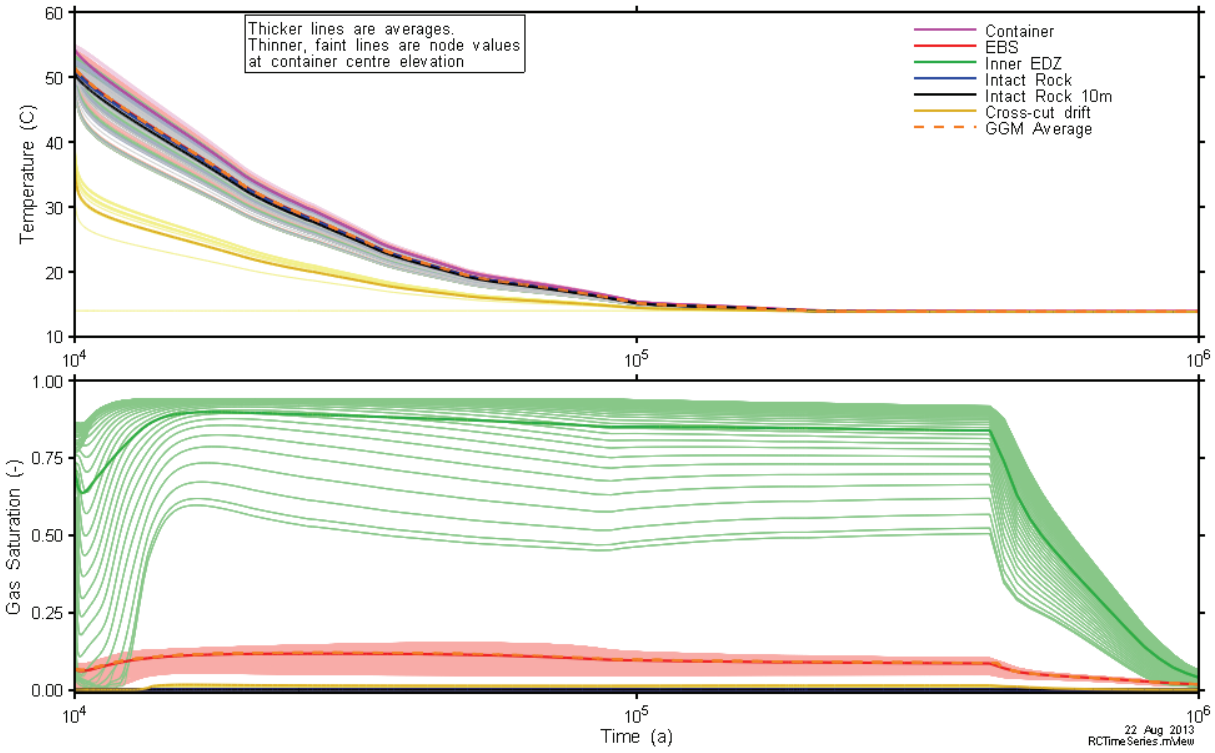

Figure 8-17: Room Scale Model – Conditions after Container Failure

Figure 8-18 presents the gas, liquid and pore pressures for the various locations. Pore pressures, shown in the bottom figure, represent the pressure experienced in the identified component. The results show that pore pressure in the intact rock (blue and black lines) remains well below 80% of lithostatic pressure (i.e., 9.9 MPa) throughout the simulation. Pressure in the cross-cut drift (yellow line) is constant because this is the imposed boundary condition, as discussed in Section 8.5.2.1. The change in slope occurring at 440,000 years correlates with the time at which corrosion ceases because the entire mass of the container has corroded (Figure 8-14).

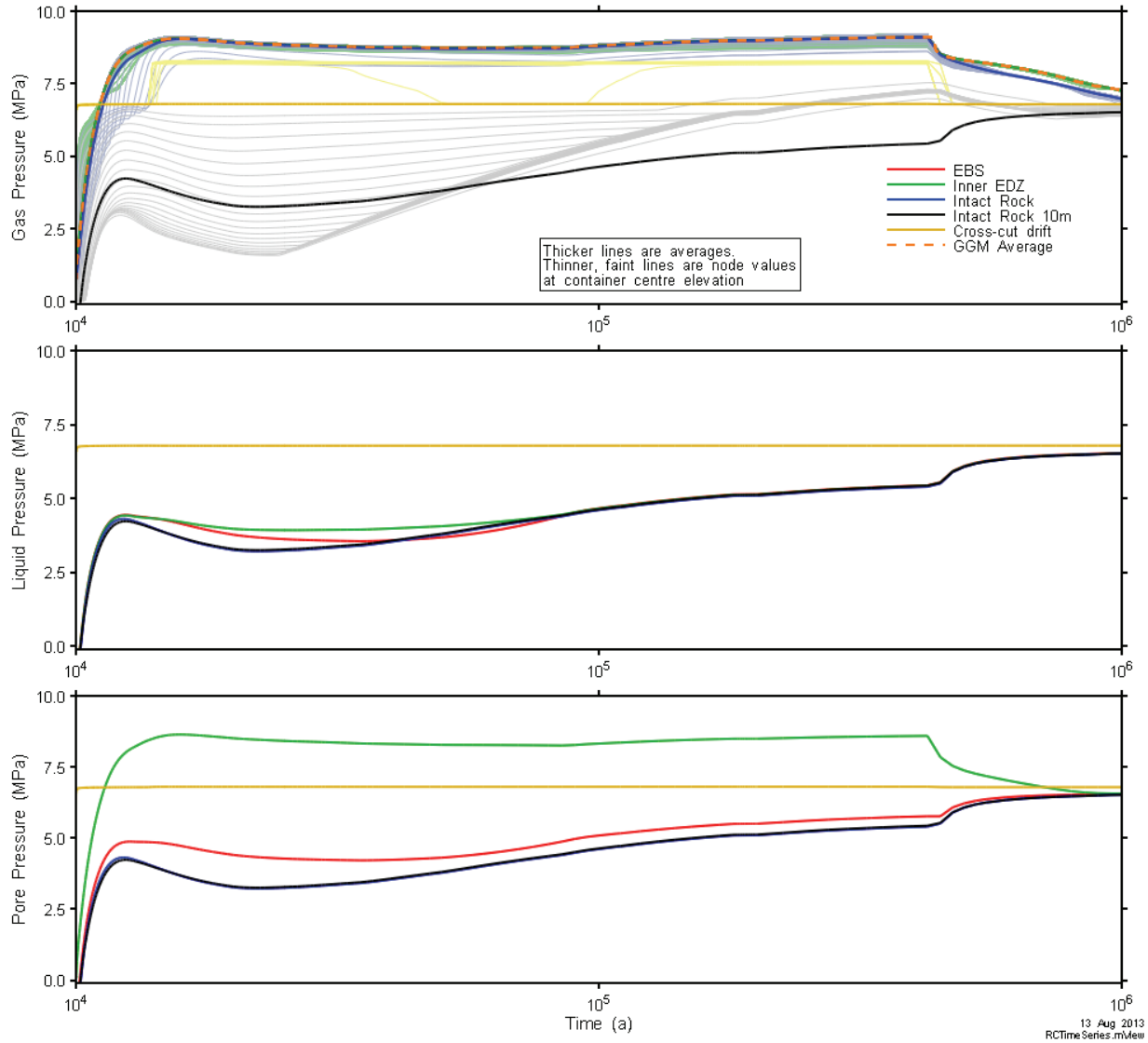

Figure 8-18: Room Scale Model – Nodal and Average Pressures after Container Failure

Figure 8-19 presents information on the gas distribution. The upper figure shows absolute distribution, while the lower figure presents the ratio by location of gas retained within the model. In general, nearly all generated gas leaves the room model through the cross-cut drift boundary. Of the gas retained, the placement room EBS contains the bulk of the generated gas, with the EDZ also containing a significant component for the first half of the simulation. The difference between the dashed line and the topmost solid line indicates the amount of gas that has exited the model domain and entered the Repository-Scale Model.

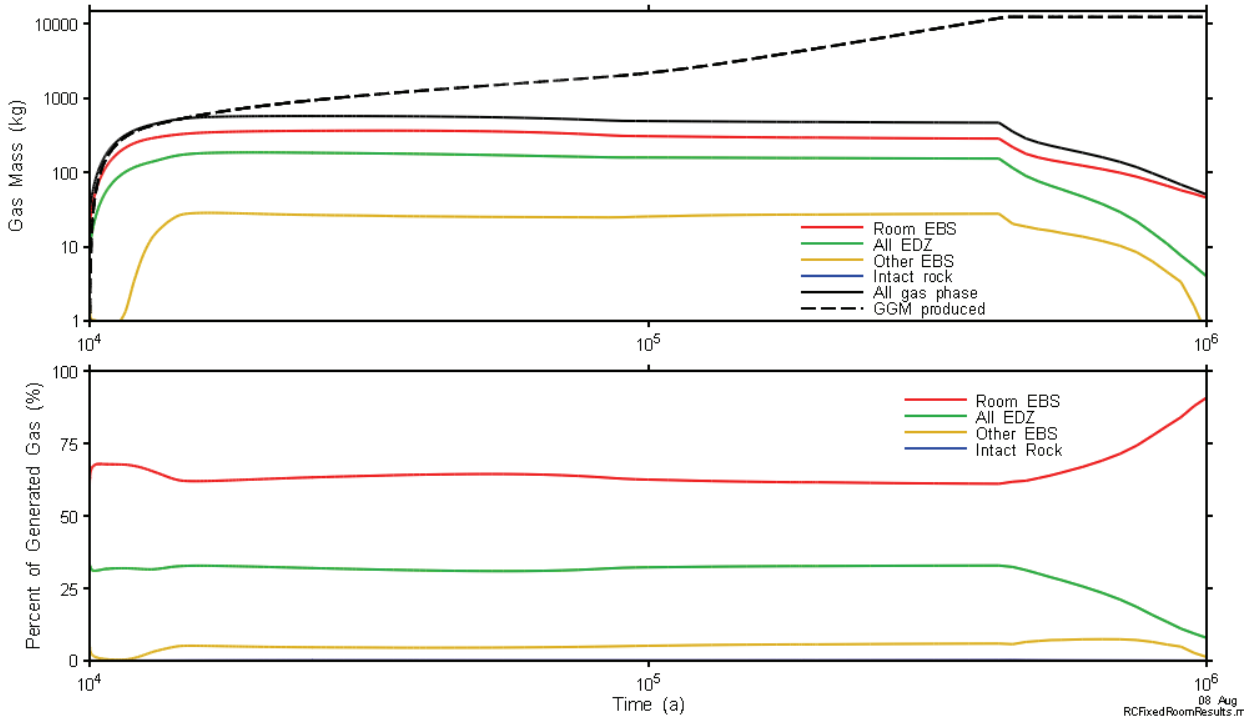

Figure 8-19: Room Scale Model – Gas Distribution

Figure 8-20 shows the gas generation rate within the placement room (red line) and the gas flow rate out of the placement room through the drift (blue line). The gas generation rate is computed using the GGM module and input at the locations shown in Figure 8-13. The flow rate out of the model corresponds to that at the flow location (red lines) in Figure 8-8.

The placement room buffers the initial pulse of gas until approximately 16,000 years, at which time gas begins to flow out of the model. The onset of Phase 4 corrosion (see Figure 8-14) is responsible for the change in slope that occurs just prior to 100,000 years. The Phase 4 period conservatively assumes that there is sufficient carbonate available to allow the reaction to proceed unabated (otherwise corrosion and gas generation would continue but at a slower rate). Gas flow ceases at 440,000 years when container mass is exhausted.

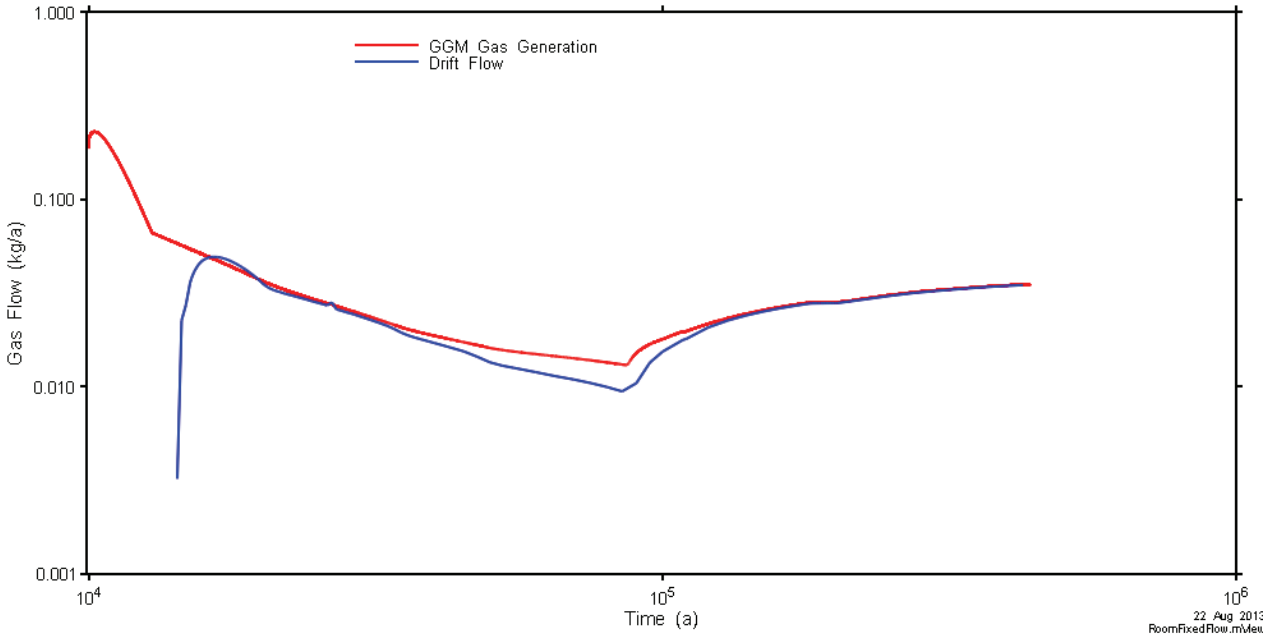

Figure 8-20: Room Scale Model – Gas Flow Rates

8.6.2 Repository-Scale Model

Results from the Repository-Scale Model are shown in Figure 8-21 to Figure 8-24.

Figure 8-21 shows the total amount of free-phase hydrogen gas within the Repository-Scale Model. Hydrogen gas is found mostly within the engineered sealing materials in the repository tunnels and shafts; however, significant amounts are also within the excavation damaged zone. Very little is in the host rock. The onset of Phase 4 corrosion (see Figure 8-14) is responsible for the change in slope that occurs just prior to 100,000 years.

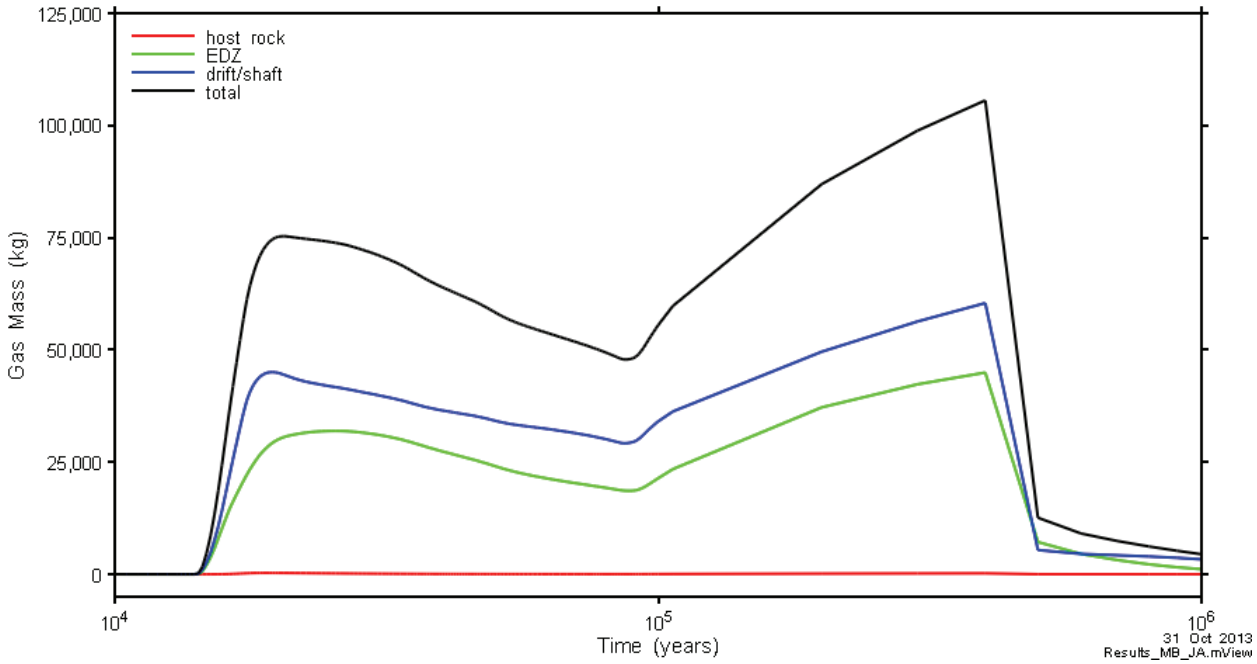

Figure 8-21: Repository-Scale Model – Distribution of Free-Phase Gas

Flow results shown in Figure 8-22 and Figure 8-23 illustrate the amount of hydrogen, in both a gas phase and as dissolved gas, leaving the top of the model. The grey line in Figure 8-22 represents the total rate at which gas enters the model from the placement rooms while the black line represents the total rate at which gas leaves the model via the shafts and, to a much lesser degree, the rock. The other colours indicate the exit pathways used by the gas. Because the Guelph formation has a much lower gas entry pressure than does the concrete seal and the bentonite / sand seal above the concrete, the rising hydrogen gas will exit the shafts and enter the Guelph formation.

Comparison of Figure 8-22 and Figure 8-23 shows that hydrogen is moving primarily in gaseous form, with dissolved hydrogen accounting for approximately 0.01% of hydrogen transport.

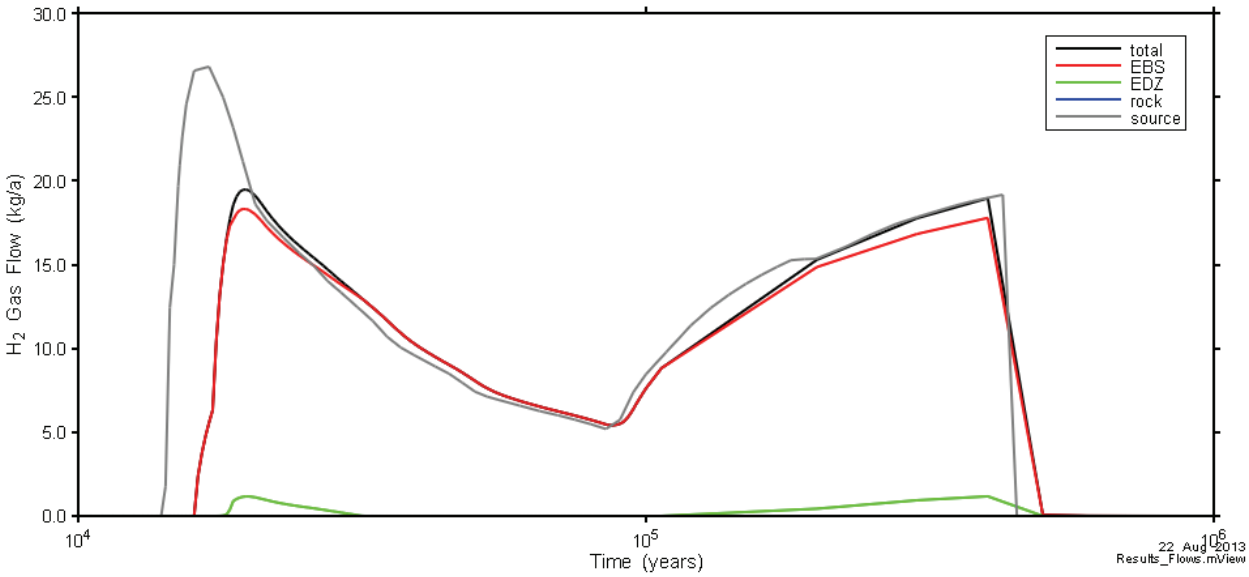

Figure 8-22: Repository-Scale Model – Gas flow Out of the Top of the Model

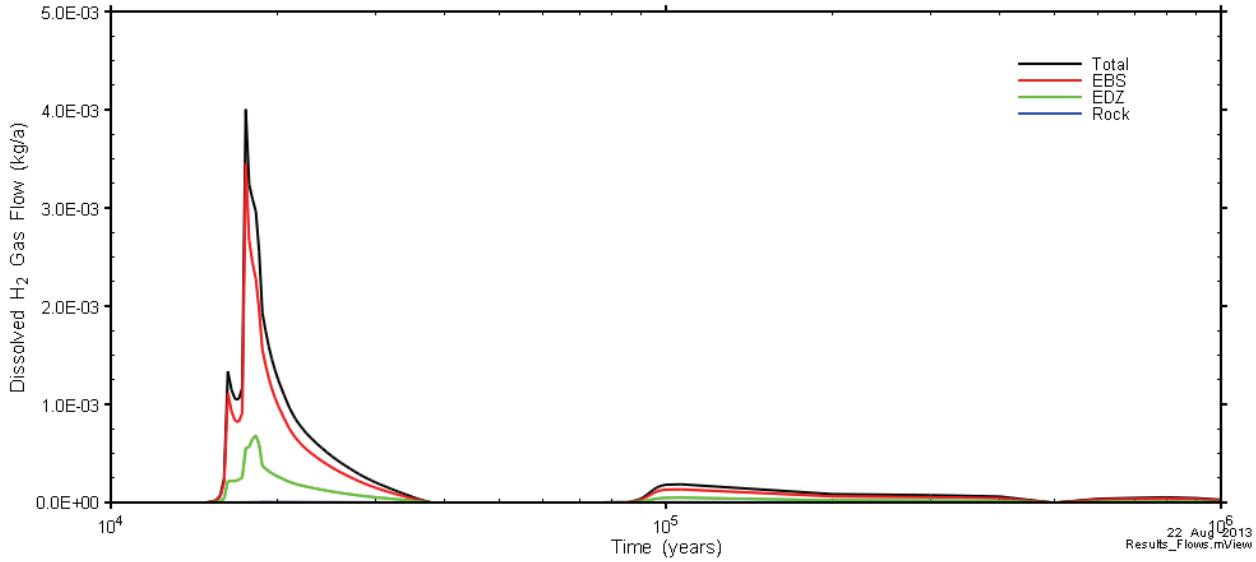

Figure 8-23: Repository-Scale Model – Dissolved Gas Flow Out of the Top of the Model

Model calculations indicate that pore pressures within the intact rock do not exceed 80% of lithostatic pressure over the 1 million year simulation period. As shown in Figure 8-24, pore pressure within the host rock neighbouring the repository reaches a maximum of 9.6 MPa at

15,700 years. As discussed in Section 8.1, this indicates the gas pressure is insufficient to fracture the rock.

While accounting for model / data uncertainties could result in higher pressures, the conservatism associated with the All Containers Fail at 10,000 Years analysis case provides confidence that the possibility of rock damage can be excluded. This will be further explored in future studies as modelling techniques improve and the knowledge base for gas generation and migration behaviour grows.

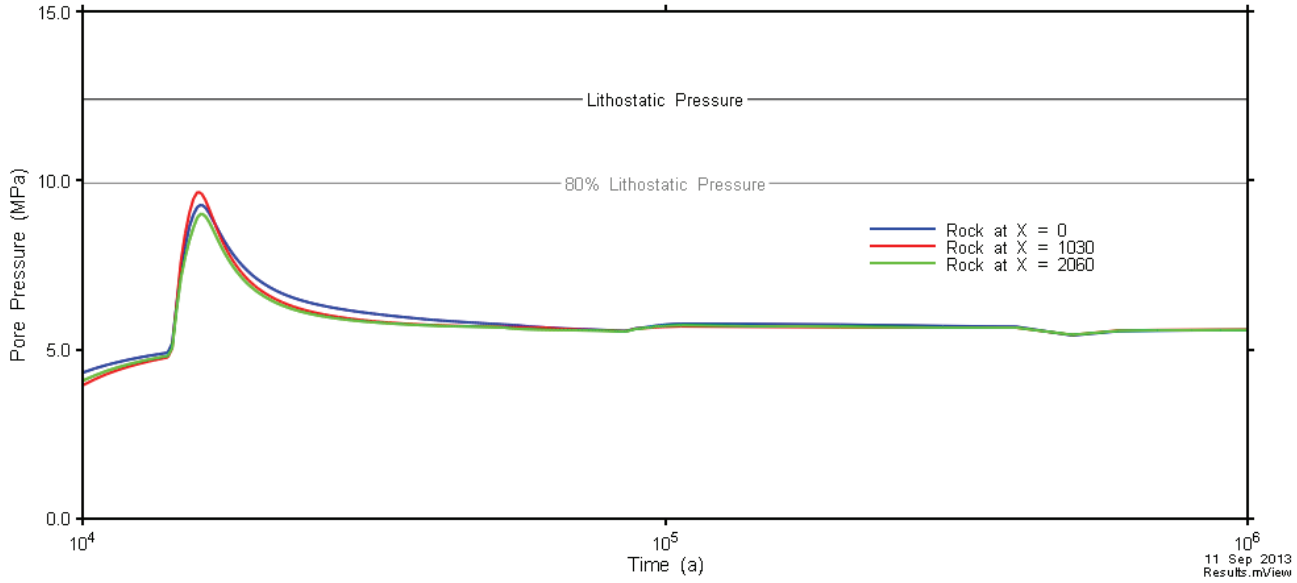

Figure 8-24: Repository-Scale Model – Pore Pressure

8.7 Dose Consequences

Of the radionuclide species present within the used fuel, very few are volatile or semi-volatile under repository conditions. Of these, only C-14, Cl-36, Se-79, and I-129 have half-lives sufficiently long to be of potential concern (Quintessa and Geofirma 2011, Gobien et al. 2013).

Table 8-3 shows the source term for each radionuclide together with their inhalation dose coefficients and Henry's law constants. The products of these three values are also shown to allow a comparison of the relative hazard. Because the product for C-14 is about four orders of magnitude greater than the others, only C-14 is considered further in the dose calculations.

Table 8-3: Comparison of Volatile, Long-lived Radionuclides

Nuclide	Half-Life (a)	Source*, 10,000 years (Bq/kgU)	Inhalation Dose Coefficient (Sv/Bq)	Henry's Law Constant (C_{gas}/C_{aq})	Product (Sv/kgU)
C-14	5700	4.7×10^{5}	6.2×10^{-12}	10^{2}	2.9×10^{-4}
Cl-36	301,000	1.8×10^{4}	7.3×10^{-9}	10^{-6}	1.3×10^{-10}
Se-79	295,000	1.9×10^{4}	6.8×10^{-9}	10^{-4}	1.2×10^{-8}
I-129	15,700,000	2.1×10^{4}	3.6×10^{-8}	10^{-4}	7.5×10^{-8}

Notes:

*The source term includes instant release from the fuel, instant release from the Zircaloy and congruent release from the fuel for the period of time between the assumed container failure (i.e., 10,000 years) and the time of maximum release to the Guelph aquifer (i.e., 18,000 years – Figure 8-25).

Data are taken or derived from Gobien et al. (2013), excepting the C-14 dose coefficient (Eckerman et al. 2012). The C-14 value is for CO_2.

The Repository-Scale Model results presented in Figure 8-21 and Figure 8-22 provide data needed to estimate the rate at which C-14 activity leaves the repository. Figure 8-21 shows the total amount of hydrogen gas in the repository while Figure 8-22 shows the rate at which hydrogen moves up the shafts.

As noted in Section 8.6.2, because the Guelph formation has a much lower air-entry pressure than the concrete seal and the bentonite / sand seal above the concrete, the rising hydrogen gas will exit the shafts and enter the more permeable Guelph formation. Once in the Guelph formation, the gas will most likely disperse and dilute laterally underground so there is no significant vertical flux upwards and no dose consequence to the critical group. Figure 8-25 shows the rate at which C-14 activity would enter the Guelph formation, taking into account radioactive decay of C-14.

A bounding estimate of the dose consequence can be conservatively obtained by assuming the gas is not dispersed in the Guelph formation and the critical group is exposed. This is done by assuming that all C-14 exits the repository via a single shaft, and that all C-14 in the shaft remains in the shaft until it reaches the surface. After reaching the surface, the C-14 then enters a house that is built directly on top of the shaft, exposing the occupants to an inhalation hazard. Under these assumptions, the rate information in Figure 8-25 also represents the rate at which C-14 activity enters the house. The maximum value is 320 kBq/hr.

The peak inhalation dose rate to the occupant is determined using data in Gobien et al. (2013). For a house volume of 228 m^3, an air exchange rate equivalent to a volume fractional turnover rate of 0.35 per hour (i.e., 7×10^{5} m^3/a), a dweller inhalation rate of 8400 m^3/a, an occupancy factor of 0.8, and an adult inhalation dose coefficient for C-14 (as CO_2) of 6.2×10^{-12} Sv/Bq (Eckerman et al. 2012), the peak dose rate is 0.17 mSv/a occurring at 18,000 years. Even with the extreme conservatism of assuming simultaneous failure of all containers at 10,000 years, this remains a factor of six below the interim Disruptive Event acceptance criterion of 1 mSv/a.

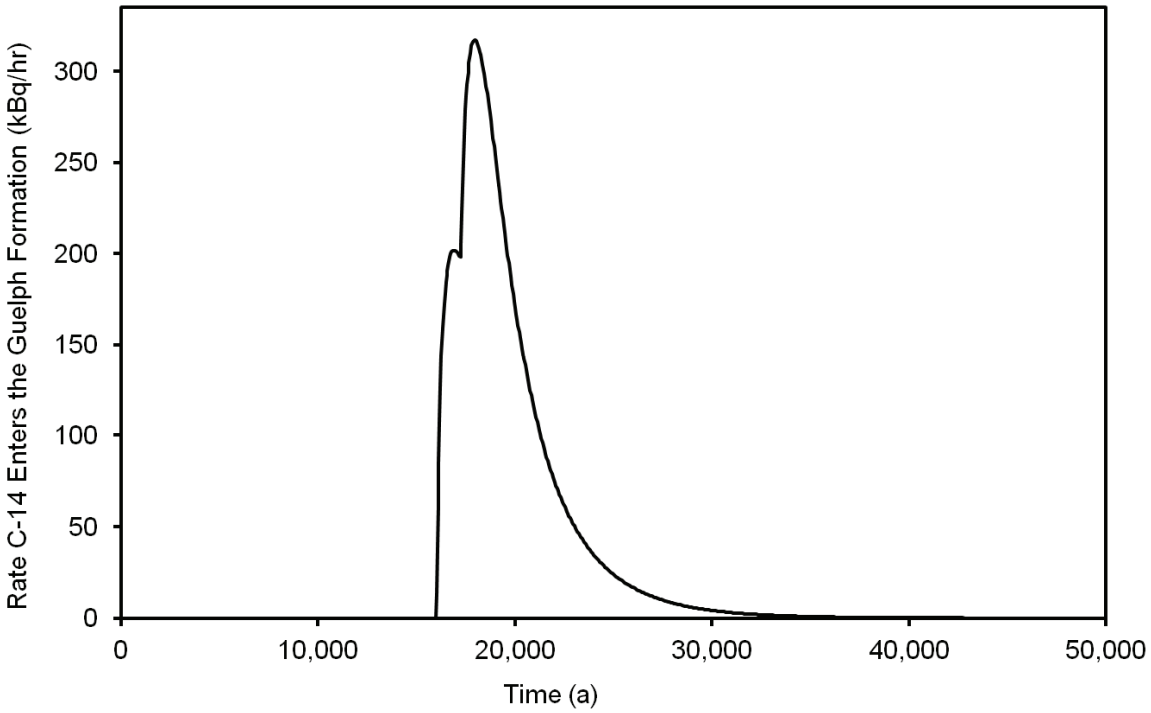

Figure 8-25: Rate at Which C-14 Enters the Guelph Formation

8.8 Summary and Conclusions

Exposure of the steel components of an engineered barrier system (EBS) to groundwater will result in the generation of gas due to corrosion processes. This gas can affect both the internal repository pressure and the transport of gaseous radionuclides.

Under the Normal Evolution Scenario, gas is not important because the rate of generation from the three defective containers is small, and because the primary gas-borne radionuclide (C-14) essentially decays away on a 60,000 year time frame (i.e., the half-life of C-14 is 5700 years).

A conservative assessment of the consequences of gas generation is determined by considering the variant case of the All Containers Fail Disruptive Scenario in which the container failures are all assumed to occur at 10,000 years. In this case, the steel in all containers is exposed and starts to corrode. Results indicate that gas is generated faster than it can leave through the rock, and it accumulates within the repository EBS and EDZ. The gas pressure builds sufficiently to allow gas to escape through the room seals and into the tunnels, where the pressure builds again and gas eventually escapes through the shaft seals.

Model calculations determine that pore pressure within the intact rock does not exceed 80% of lithostatic pressure over the 1 million year simulation period. Pressure within the host rock neighbouring the repository reaches a maximum of 9.6 MPa after 15,700 years.

Based on a set of extremely conservative assumptions, gas-borne dose consequences reach a peak dose rate of 0.17 mSv/a, which is a factor of six below the 1 mSv/a acceptance criterion for disruptive events. The peak occurs at 18,000 years. For a more realistic case of failure of copper containers over longer times, the dose rates would be lower. For example, if the copper containers all fail on time scales associated with the next glaciation or later, the associated dose rates would be well below 1 μSv/a due to decay of C-14.

8.9 References for Chapter 8

Bate, F., D. Roberts, A. R. Hoch, and C.P. Jackson. 2012. Gas migration calculations on the vault scale. Serco Assurance report SA/ENV-0924 Issue 3.1. Oxfordshire, UK (available at http://www.nda.gov.uk/documents/biblio/upload/Gas-Migration-calculations-on-the-vault-scale-report_I3_1.pdf).

Eckerman, K., J. Harrison, H.G. Menzel and C.H. Clement. 2012. ICRP Publication 119: Compendium of Dose Coefficients based on ICRP Publication 60. Annals of the ICRP, 41, 1-130.

FORGE. 2010. FORGE Milestone M15: Summary of Gas Generation and Migration. Current State-of-the-Art. Euratom 7th Framework Project, FORGE 2010. Deliverable D1.2-R.

Geofirma and Quintessa. 2011. Postclosure Safety Assessment: Gas Modelling. Geofirma Engineering Ltd. and Quintessa Ltd. report for the Nuclear Waste Management Organization NWMO DGR-TR-2011-31. Toronto, Canada.

Gobien, M., F. Garisto and E. Kremer. 2013. Fifth Case Study: Reference Data and Codes. Nuclear Waste Management Organization Technical Report NWMO TR-2013-05.

Guo, R. 2008. Sensitivity Analyses to Investigate the Influence of the Container Spacing and Tunnel Spacing on the Thermal Response in a Deep Geological Repository. Nuclear Waste Management Organization Report TR-2008-24.

Marschall, P., S. Horseman and T. Gimmi. 2005. Characterisation of gas transport properties of the Opalinus Clay, a potential host rock formation for radioactive waste disposal. Oil & gas science and technology, 60(1), 121-139.

Mualem, Y. 1976. A New Model for Predicting the Hydraulic Conductivity of Unsaturated Porous Media, Water Resour. Res., Vol. 12, No. 3, pp. 513 – 522, 1976.

Nagra. 2008. Effects of post-disposal gas generation in a repository for low- and intermediate-level waste sited in the Opalinus Clay of Northern Switzerland. Nagra Technical Report 08-07. Wettingen, Switzerland.

Pruess, K., C. Oldenburg and G. Moridis. 1999. TOUGH2 User's Guide, Version 2.0. Lawrence Berkeley National Laboratory LBNL-43134. Berkeley, USA.

Quintessa and Geofirma. 2011. Postclosure Safety Assessment: Data. Quintessa Ltd. and Geofirma Engineering Ltd. Report for the Nuclear Waste Management Organization. NWMO DGR TR-2011-32.

Senger, R., J. Ewing, , K. Zhang, J. Avis, P. Marschall and I. Gaus. 2011. Modeling approaches for investigating gas migration from a deep low/intermediate level waste repository (Switzerland). Transport in porous media, 90(1), 113-133.

Suckling, P., J. Avis, N. Calder, P. Humphreys, F. King and R. Walsh. 2012. T2GGM Version 3.1: Gas Generation and Transport Code. Quintessa Ltd. and Geofirma Engineering Ltd. Report for the Nuclear Waste Management Organization NWMO TR-2012-23. Toronto, Canada.

Talandier, J., G. Mayer and J. Croisé. 2006. Simulations of the Hydrogen Migration out of Intermediate-Level Radioactive Waste Disposal Drifts using TOUGH2. Proceedings, TOUGH Symposium 2006, Lawrence Berkeley National Laboratory. Berkeley, USA.

Van Genuchten, M. T. 1980. A Closed-Form Equation for Predicting the Hydraulic Conductivity of Unsaturated Soils. Soil Science Society of America Journal, 44(5), 892-898.

Yu, L. And E. Weetjens. 2009. Summary of gas generation and migration: current state-of-the-art. Extern. Rep. Belg. Nucl. Res. Cent. ER-106. Eur. Comm. FP7 FORGE. Fate Repos. Gases.

THIS PAGE HAS BEEN LEFT BLANK INTENTIONALLY

9. TREATMENT OF UNCERTAINTIES

All analysis calculations have an associated uncertainty. CNSC Regulatory Guide G-320 (CNSC 2006) expects that uncertainty will be taken into account.

9.1 Approach

Many organizations use the following three broad categories[1] to structure the analysis of uncertainties in postclosure safety assessments (e.g., Marivoet et al. 2008):

- **Scenario Uncertainty**: Arises from uncertainty in the evolution of the repository system and human behaviour over the time scales of interest.
- **Model Uncertainty**: Associated with uncertainty in the conceptual, mathematical and computer models used to simulate the behaviour of the repository system (e.g., due to approximations used to represent the system).
- **Data Uncertainty**: Arises from uncertainty in the data and parameters used as input in the modelling (e.g., due to incomplete site-specific data or due to parameter estimation errors from interpretation of test results).

The following briefly discusses the approach adopted for uncertainties in this pre-project review.

Scenario Uncertainty

Uncertainty in the future evolution of the site is addressed by assessing a range of scenarios that describe the potential evolution of the system. The scenario identification process, described in Chapter 6, ensures that key uncertainties are identified and scenarios are defined to explore their consequences.

The scenarios defined include the Normal Evolution Scenario (which describes the expected evolution of the repository) and a series of Disruptive Event Scenarios that postulate the occurrence of unlikely events leading to possible penetration of barriers and abnormal loss of containment.

To estimate potential future impacts, a stylized representation[2] of the biosphere and human receptors is used to allow illustrative estimates to be made. A stylized representation is adopted because it is unrealistic to predict human habits and behaviour over the time scale of relevance to the repository system, because major changes to the surface and near-surface environment are likely to occur as a result of natural changes such as ice sheet advance / retreat or as a result of future human actions, and because societal and technological changes are inherently unpredictable over such timescales.

---

[1] The boundaries between these categories can overlap. Depending upon how models are formulated, an uncertainty may be classed as a model or a data uncertainty.

[2] A stylized representation of the biosphere, and human habits and behaviour is a representation that has been simplified to reduce the natural complexity to a level consistent with the objectives of the analysis using assumptions that are intended to be plausible and internally consistent but that will tend to err on the side of conservatism.

In the stylized representation, it is assumed that future humans are generally similar to present day humans, and will adopt behaviors that would be consistent with current or past human practice. People are assumed to live on the repository site in the future in a manner that maximizes their potential dose from exposure to releases from the repository.

Since assumptions concerning the biosphere (e.g., climate), human lifestyles (e.g., critical group characteristics) and water flows in the near-surface environment become increasingly uncertain with time, two complementary long-term indicators are also used to supplement the dose rate indicator using system characteristics that are much less sensitive to such assumptions.

Model Uncertainty

Conceptual and mathematical model uncertainties are identified in the model development process. Key uncertainties are addressed by using alternative conceptual representations of the system. This is facilitated by the availability of a range of computer codes (e.g., FRAC3DVS-OPG and SYVAC3-CC4) that are capable of representing different conceptualizations and mathematical descriptions of the system.

Some conceptual and mathematical model uncertainties are amenable to representation with parameter values, and these are investigated using the methods applied to data uncertainties. For example, uncertainties in the representation of sorption are treated by considering bounding cases in which the sorption values are set to zero.

Data Uncertainty

Data uncertainties are identified in Gobien et al. (2013). These are accounted for through:

- Deterministic Calculations – alternative sets of parameter values, each providing a self-consistent representation of the system. Results are compared to the Reference Case and the differences explored. A limitation of this approach is that there is often no systematic or complete coverage of the uncertainty space in parameter values.

  Sensitivity cases in this pre-project review (identified in Section 7.2.1) explore the effect of variations in key parameters affecting the performance of various physical and chemical barriers.

- Probabilistic Calculations – parameters are assigned probability distribution functions that describe their inherent uncertainty. The model is evaluated a large number of times, with each case using input values randomly selected from the distribution functions. The model output is a distribution of results. The strength of the probabilistic approach lies in its ability to be comprehensive in exploring the space of the phenomena considered, and their associated model parameters. Its weakness is the need to make use of simplified models.

Conservatisms

Throughout the assessment process, it is necessary to make various assumptions relating to scenarios, models or data. Assumptions are often categorized as 'realistic'[3] or 'conservative'[4], although care needs to be taken when using such terms. The key is to ensure that each major assumption used in the assessment is considered and documented, and that the potential implications are understood.

While it may appear sensible to adopt a conservative approach to ensure that potential impacts are not under-estimated, care is needed because the net effect of many conservative assumptions can be an unrealistic estimate of impacts. Thus, the postclosure safety assessment adopts scientifically informed, physically realistic assumptions for processes and data that are understood and can be justified on the basis of the results of research and / or site investigation. Where there are high levels of uncertainty, conservative assumptions are adopted to allow the impacts of uncertainties to be bounded.

In particular, the following conservative assumptions are incorporated in the Normal Evolution Scenario:

- The defective containers fill with water in the first 10,000 years;
- No credit is taken for the presence of the fuel sheath in maintaining fuel integrity and in preventing contact of the fuel matrix with water that may enter the container;
- No credit is taken for the effect of H_2 (produced by corrosion of the defective container) on the dissolution rate of the UO_2 fuel;
- No credit is taken for the effect of iron oxides (produced by corrosion of the defective container) providing a high surface area for adsorption of some of the radionuclides released from the fuel;
- No credit is taken for the likely filling of the defect with bentonite and / or corrosion products which could significantly increase the transport resistance of the defect;
- The defective containers are positioned in the repository location with the shortest contaminant travel time to the surface;
- Adoption of a 219 m deep well penetrating to the bottom of the Guelph layer located in the position with the shortest transport time to the surface;
- Positioning the well so that it maximizes the capture of radionuclides released from the defective containers; and
- Defining conservative properties of the critical group (e.g., use of 90th percentile food ingestion rates; obtaining all food, fuel, water and building material locally; and all drinking and irrigation water taken from the well).

---

[3] Realism is defined as "the representation of an element of the system (scenario, model or data), made in light of the current state of system knowledge and associated uncertainties, such that the safety assessment incorporates all that is known about the element under consideration and leads to an estimate of the expected performance of the system attributable to that element" (IAEA 2006).

[4] Conservatism is defined as "the conscious decision, made in light of the current state of system knowledge and associated uncertainties, to represent an element of the system (scenario, model or data) such that it provides an under-estimate of system performance attributable to that element and thereby an over-estimate of the associated radiological impact (i.e., dose or risk)" (IAEA 2006).

9.2 Key Uncertainties

The postclosure safety assessment summarized in Section 7.12 and Section 8.8, indicates that the deep geological repository in geologic settings similar to the assumed site could tolerate large changes in the properties of key chemical and physical barriers without challenging the interim dose acceptance criteria.

The key uncertainties in terms of their importance to modify potential impacts are:

- **Chemical Reactions**: Under the highly saline conditions of the deep geosphere, several aspects of the chemistry in the repository are uncertain due to the limited database. These include the sorption of contaminants on seal materials and host rocks, as well as mineral precipitation / dissolution reactions. These uncertainties have been addressed in the pre-project review through the adoption of conservative values, the analysis of various sensitivity cases, and the identification of appropriate disruptive scenarios such as the Container Failure Scenario.

- **Gas Pressure and Repository Saturation**: The presence of robust copper containers ensures gas generated from potential corrosion of the steel inner containers is not a significant issue for the Normal Evolution Scenario. However, gas behaviour becomes increasingly important when large number of containers are assumed to fail, such as in the All Containers Fail Disruptive Scenario. This report includes a detailed study of the expected gas evolution for this event.

- **Glaciation Effects**: Although geological evidence at a real site is expected to indicate the deep geosphere has not been affected by past glaciation events and that the deep groundwater system has remained stagnant, glaciation will have a major effect on the surface and near-surface environment that is not entirely predictable. Glaciation is not likely to occur before 60,000 to 100,000 years, at which point the remaining hazard will be long-lived radionuclides and potentially hazardous chemical elements.

- **Fracture Characterization**: For a real site, there will be some uncertainty in the nearby fracture network. However, in principle a sedimentary rock site may have features that provide high confidence that there are no significant fractures nearby. These uncertainties can be reduced through site selection and repository location and depth, and any residual uncertainties can be handled through the adoption of conservative assumptions and / or Disruptive Scenarios (such as the Undetected Fault Scenario) within the postclosure analysis.

9.3 References for Chapter 9

CNSC. 2006. Regulatory Guide G-320: Assessing the Long Term Safety of Radioactive Waste Management. Canadian Nuclear Safety Commission. Ottawa, Canada.

Gobien, M., F. Garisto, E. Kremer and C. Medri. 2013. Fifth Case Study: Reference Data and Codes. Nuclear Waste Management Organization Report NWMO TR-2013-05. Toronto, Canada.

IAEA. 2006. Safety Requirements: Geological Disposal of Radioactive Waste. International Atomic Energy Agency Safety Requirements WS-R-4. Vienna, Austria.

Marivoet, J., T. Beuth, J. Alonso and D.-A. Becker. 2008. Safety Functions, Definition and Assessment of Scenarios, Uncertainty Management and Uncertainty Analysis, Safety Indicators and Performance/Function Indicators. PAMINA Deliverable D-No. 1.1.1, European Commission. Brussels, Belgium.

THIS PAGE HAS BEEN LEFT BLANK INTENTIONALLY

10. NATURAL ANALOGUES

Natural analogues are natural features (materials or processes) that are similar to those expected in some part of a deep geological repository. Natural analogues can include both natural and man-made materials provided the processes that affect them are natural. They provide understanding or demonstration of how a repository may behave over time scales ranging to many millions of years. Analogues exist for most features of the repository system, including the used fuel, engineered and natural containment systems, and key processes such as transport of contaminants.

The use of natural analogues in supporting key assumptions in safety assessment and adding credibility to its findings is recommended in IAEA (1999) and in Regulatory Guide G-320 (CNSC 2006). G-320 states: "*Natural analogue information should be used to build confidence that the system will perform as predicted by demonstrating that natural processes will limit the long-term release of contaminants to the biosphere to levels well below target criteria.*"

The natural analogues presented here can assist in understanding many of the underlying principles relevant to the long-term isolation and containment of used nuclear fuel.

10.1 Analogues for Used Nuclear Fuel

10.1.1 Natural Uranium Deposits

Natural uranium is relatively abundant. Like all other elements, it is cycled through biological and geological systems and tends to concentrate in some locations by natural processes. Uranium will slowly dissolve under oxidizing conditions and precipitate under reducing conditions. Most uranium ore bodies form by this process. Once formed, until local conditions change, a uranium deposit will remain in place. Uranium ore bodies that are being mined today were formed hundreds of millions of years ago.

Used fuel consists predominantly of uranium dioxide, with about 2% of the total being fission and activation products resulting from the nuclear reactions occurring in the fuel during power production. These are mostly incorporated within the solid matrix of the used fuel. Natural uranium minerals are comparable in that they consist of uranium dioxide along with uranium decay products.

One gram of natural uranium, as it is extracted from the earth in equilibrium with its progeny contains a little less than 2×10^5 Bq of radioactivity. In comparison, after discharge from a reactor and 30 years of cooling, used fuel has an inventory of 2.7×10^9 Bq per gram of uranium, principally in the form of fission and activation products (Tait et al. 2000), and is considerably more radioactive than the original uranium ore. Due to the rapid decay of most of the fission product isotopes present in used fuel, radioactivity decreases to 2.3×10^7 Bq per gram after 1000 years while after approximately one million years, radioactivity decreases to a level similar to that in natural uranium.

The Cigar Lake uranium deposit found in Northern Saskatchewan (Figure 10-1) provides a Canadian example of an analogue for geological placement of used nuclear fuel. The Cigar Lake deposit is under development as a uranium mine and has been well studied as a natural analogue (Cramer and Smellie 1994, Miller et al. 2000).

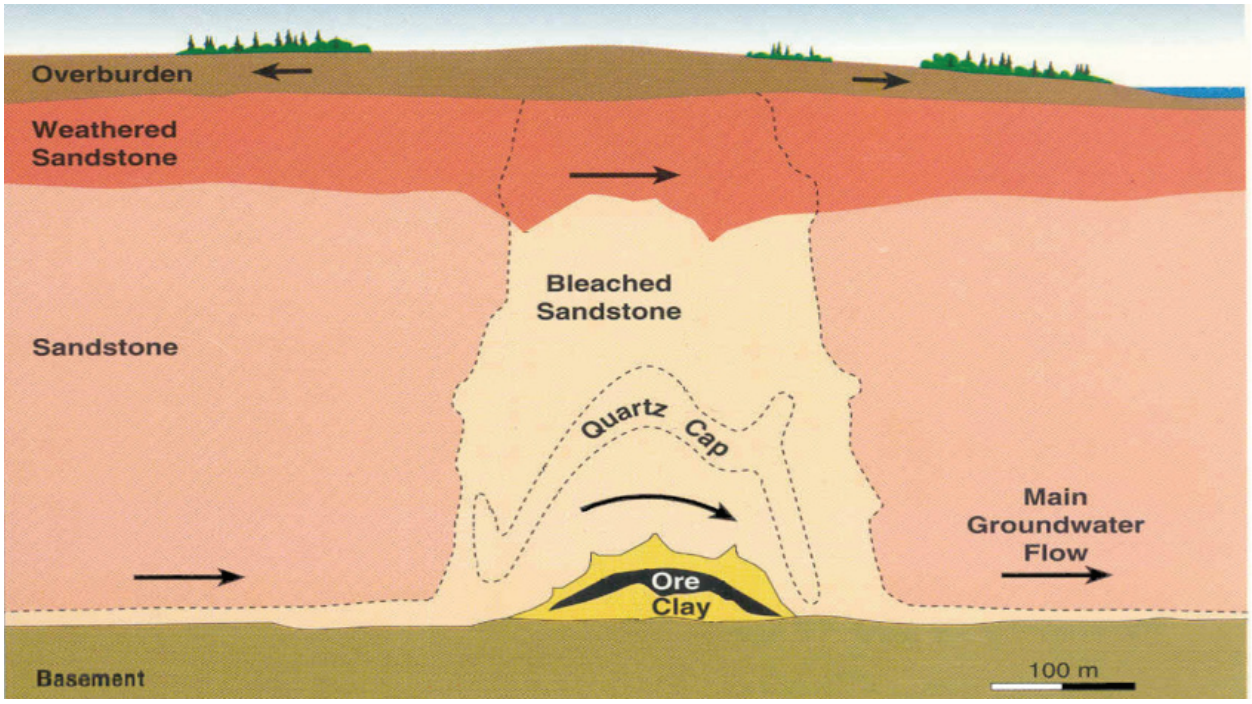

Figure 10-1: Cigar Lake Ore Deposit

The Cigar Lake uranium deposit is located about 430 m below surface, similar in depth to the repository considered in this pre-project review (i.e., 500 metres underground). The ore body formed about 1.3 billion years ago. It is similar in general composition to used fuel, and the ore is surrounded by a clay envelope somewhat similar to the clay buffer specified in the repository design. It can be considered analogous to a “worst case” simulation, as it lacks any specially designed used fuel containers and the host rock above the ore body is highly fractured sandstone.

Based on the Cigar Lake natural analogue study (Cramer and Smellie 1994), it was concluded that:

- uranium dioxide will remain stable over 100 million year time scales under the chemically-reducing conditions found adjacent to the Cigar Lake ore body, with very little uranium migrating from the deposit;
- the natural clay surrounding the ore has provided an effective long-term seal, preventing migration of radionuclides from the deposit (see Section 10.2.2);
- dissolved organic matter in groundwater migrating past the ore has not played a significant role in mobilizing radionuclides from the deposit; and
- natural hydrologic barriers and appropriate geochemical conditions found at the site are effective in preventing significant radionuclide migration from the deposit.

Insufficient radionuclide migration has occurred to produce any detectible concentration anomalies in the soil, surface water and lake sediments and waters overlying the ore body. Environmental and geological exploration in the area has shown no surface expression of the ore body, and it had to be discovered by geophysical techniques. Indeed, on a map of surface radioactivity in Canada, the area of the Saskatchewan deposits generally shows up as having below-average surface radioactivity (McKee and Lush 2004).

Reducing conditions are expected in the repository due to buffering by the rock and engineered sealing materials; however, radiolysis of groundwater may produce oxidizing conditions locally. Redox conditions are critical because the geochemical behaviour of many elements strongly depends on their redox state. The long-term performance of the repository is therefore strongly dependent on the redox conditions assumed.

In some parts of the world, uranium found in permeable rocks is mined by “in-situ” mining methods. Some of the ore bodies mined in this manner are called roll-front ore bodies, as they are continuously migrating or rolling through the permeable host rock. The front of the ore body is in a reduced state, while the rear of the ore body is in a more oxidized state as a consequence of oxidizing groundwaters that are slowly driving the ore body through the rock formation. This creates a condition at the rear of the ore body in which the uranium becomes soluble and migrates to the front of the ore body where it again precipitates.

A well-studied example of a roll-front uranium deposit is the Osamu Utsumi mine in Brazil (Hofmann 1999). Measuring reducing materials such as iron or organic carbon provides an indication of how uranium and other radionuclides in used fuel will be immobilized in the repository. Hoffman reported that migration of uranium, along with palladium and selenium, was strongly inhibited at a redox front, causing immobilization. Results indicated that reducing conditions inhibit transport of these elements under most natural low-temperature conditions.

Roll-front uranium deposits illustrate how migration of used fuel through locally oxidizing conditions in the container (assuming groundwater infiltration of used fuel containers and subsequent radiolysis) would be effectively suppressed by the reducing conditions of the placement rooms and repository host rock.

10.1.2 Natural Fissioned Uranium

Nuclear fission occurred naturally on Earth over two billion years ago. In Gabon, Africa, there are 15 deposits of uranium ore that have acted as natural nuclear reactors (Miller et al. 2000), sometimes referred to as the Oklo fossil reactors (Figure 10-2). The remnants of natural uranium fission provide the closest natural analogue for used nuclear fuel over long time periods in a geologic environment.

The quantity of U-235 present in natural uranium ore bodies today is low at 0.7%. However, approximately two billion years ago, when the Oklo ore bodies formed, the fraction of U-235 present in natural uranium was much greater, comprising just over 5%. The Oklo reactors operated at low power over about one million years. Results of material sampling infers that approximately 6 to 12 tonnes of U-235 underwent fission, producing plutonium and generating temperatures in the natural reactors of up to 600°C.

Oklo reactor studies provide data regarding the stability of uranium dioxide in the presence of other fission products and the transport of radionuclides within the surrounding shale and sandstone formations. These studies indicate that more than 90% of the uranium “fuel” present in the reactors 2 billion years ago has remained in place, including transuranic elements, most of the fission products and their decay products. The plutonium generated has moved less than 3 metres over two billion years. This is in the absence of the engineered barriers incorporated into a geological repository. The surrounding rock has proved to be a well-sealed vault.

The stability of the Oklo used fuel has lasted through two billion years of continental drift and groundwater movement. This is additionally impressive considering the present day near-surface location of these natural reactors.

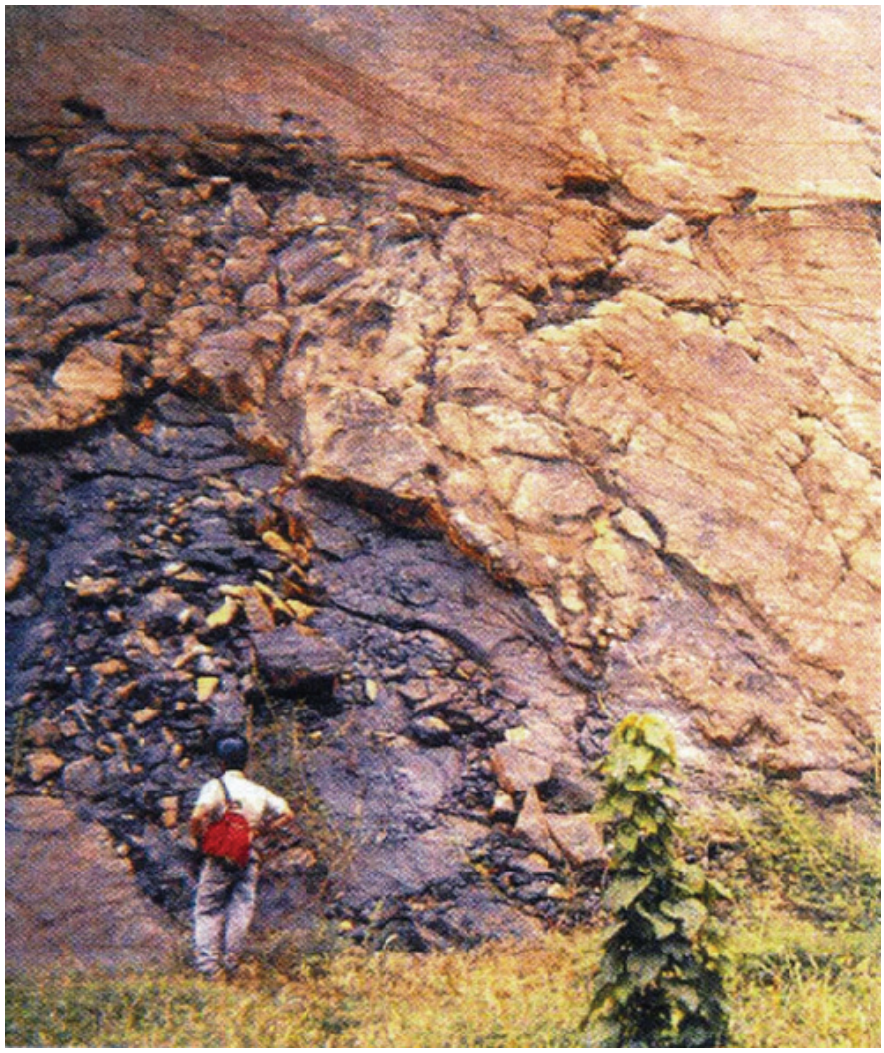

Notes: In Oklo, Gabon, the remains of an ancient natural nuclear reactor indicate the resulting plutonium has moved less than 3 metres over two billion years. From Miller et al. (2000).

Figure 10-2: Naturally Occurring Fission Reactor

The Oklo fossil reactors provide a snapshot in time of the condition of a natural used fuel repository two billion years after decommissioning. Information is obtained through indirect evidence such as the quantity and location of fission products and their decay products, and the actinides that can still be found in association with these natural reactors. This evidence indicates that careful selection of the host rock formation for a used fuel deep geological repository can render many fission products and actinides largely immobile.

10.1.3 Fractured Uranium Deposits

The Tono uranium ore body, located near Tokyo, has been the subject of analogue studies relating to transport of uranium (Miller et al. 2000). The ore body lies within a sedimentary formation containing significant quantities of carbonaceous material and pyrite, making it a highly reducing environment; as such, it provides an opportunity to evaluate radionuclide migration through sedimentary rocks under reducing conditions. The ore body is approximately 3.4 km long; however, the area is tectonically active and between 5 and 10 million years ago, the ore body was split by a fault. This displaced a portion of the ore body 30 m upward. Despite this large fault, many other nearby faults, and the occurrence of frequent tremors, Yoshida (1994) found that no significant uranium transport occurred from the ore body to the adjacent environment. The rock provided substantial opportunity for matrix diffusion and very large surface area for sorption of radionuclides. Consequently, no substantial remobilisation of the uranium has occurred, despite the faulting history of the area.

The preferred location for a used fuel repository will be tectonically inactive, providing even greater physical stability and security than seen at this site.

10.2 Analogues for Barriers

The repository design uses multiple barriers, including materials such as iron, copper, clays, concrete and asphalt to inhibit or prevent movement of radioactive elements and other materials from the facility into the surrounding environment.

10.2.1 Metals

In the current study, used fuel bundles are placed into large, durable containers designed to hold 360 fuel bundles each. For the reference container design, the inner vessel is made from 100 mm-thick carbon steel which provides the mechanical strength to withstand the pressures of the overlying rock and future glacial loading. The outermost layer of the container is corrosion-resistant copper, 25 mm thick, of which a few mm is required for corrosion resistance over one million years.

The used fuel container prevents water from contacting the used fuel bundles, thereby preventing radionuclides in the fuel from escaping into the underground environment. The used fuel container is engineered to remain intact for at least 100,000 years, and is expected to last much longer, keeping the used fuel completely isolated from the surroundings.

10.2.1.1 Copper

Copper is one of the relatively few metals that naturally occurs in its metallic state. Solid pieces of native copper have been found containing more than 99% copper. The largest known

deposit of metallic copper is in the Keweenaw Peninsula of Michigan (Crissman and Jacobs 1982), where large pieces of almost pure copper were either mined or found in glacial outwash. Data from these natural analogues provide copper corrosion rates for both reducing and oxidizing environments, which are useful in assessing the longevity of the used fuel containers.

Copper "plates" found in the mudstones from South Devon in England (Figure 10-3) provide a natural analogue for the corrosion of used fuel containers placed in a clay backfill. These copper plates were formed 200 million years ago (lower Jurassic period) and show little corrosion since that time, due in part to the protection of the clay-rich mudstone (Milodowski et al. 2000).

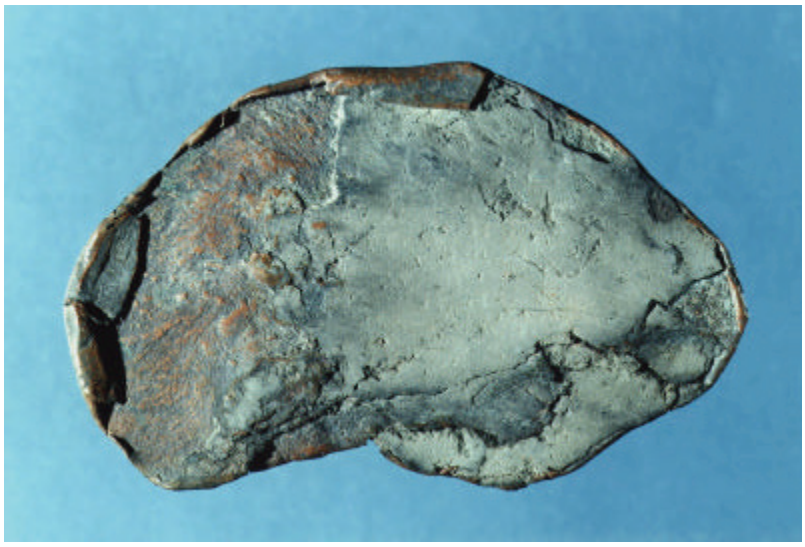

Note: From Milodowski et al. (2000).

Figure 10-3: Copper Analogues

10.2.1.2 Iron

Recorded use of iron dates to Egypt in 1900 BCE (Miller et al. 2000). Johnson and Francis (1980) studied the corrosion of artifacts under a wide range of environmental conditions and reported annual corrosion ranging from 0.1 to 10 microns.

The large amounts of iron (carbon steel) in the used fuel containers may buffer redox conditions in the repository, preventing oxidizing conditions near the used fuel. The Inchtuthil Roman nails found in Scotland provide an interesting analogue for this. At a Roman fortress that was abandoned in 87 CE (Angus et al. 1962; Pitts and St. Joseph 1985), over 1 million nails were buried in a 5-m deep pit under 3 m of earth. When the nails were unearthed in the 1950s, the nails on the outside of the mass were found to have corroded and formed a solid crust of iron oxides (rust) around the remaining mass of nails. The outside layer of nails formed a sacrificial redox sink, consuming oxygen before it could penetrate to the interior of the mass of nails. The physical expansion of the rust also served to self-seal the remaining nails from intruding

groundwater and water vapour. As a result, the nails inside the rusty barrier experienced minimal-to-no corrosion over nearly 2,000 years.

In Greenland, on Disko Island, magmatic conditions within a crystalline rock formation (basalt) promoted deposition of native iron over a period of volcanism spanning from about 63 to 30 million years ago. An estimated 10 million tons of iron were deposited. Mass transport limitations (low diffusivity of reactants combined with high redox capacity) favoured preservation of the native iron. Native iron has survived millions of years in the rock matrix (Hellmuth 1991).

The natural redox buffering capacity of the bentonite and rock surrounding the Cigar Lake ore body is due mainly to ferrous compounds in the mafic mineral phases (Smellie and Karlsson 1996). These reducing conditions have suppressed transport of uranium and other oxidising species, playing a major role in preserving the stability of the ore. The outer clay in contact with groundwater migrating past the ore body is a light reddish colour, indicating that the iron in the clay has oxidized. Deeper within the clay, the reddish colour disappears, suggesting that oxygen has been precluded and reducing conditions maintained (Miller et al. 2000). The result is a very stable ore body.

10.2.2 Clays

The primary sealing material within the engineered containment systems is the swelling clay component of bentonite, usually referred to as smectite or, more specifically, montmorillonite. Bentonite (Figure 10-4) is a group of naturally occurring clays. Bentonite swells when exposed to water, minimizing water seepage and making an excellent sealing material when physically confined. It also has a high chemical sorption capacity, able to bind many elements to its crystalline surfaces, which greatly slows the migration of radionuclides. Bentonite is also very stable, typically formed millions to hundreds of millions of years ago. Clay materials can act as a very robust physical and chemical barrier, as illustrated in the discussion above of Cigar Lake where naturally formed clays acted as a protective barrier for geological time periods. Laine and Karttunen (2010) recently produced a wide-ranging review of natural analogues for bentonite.

Each used fuel container is surrounded by compacted bentonite clay and all excavated spaces are filled with mixtures of clay, sand, and crushed rock. As the closed and sealed repository is slowly infiltrated by groundwater, the bentonite will swell and fill any remaining void spaces. Radionuclides will only be able to move through the bentonite by diffusion, greatly restricting their migration. In addition, the clay's high adsorption capacity for many elements will significantly inhibit their movement.

Note: Figure from EUBA (2011)

Figure 10-4: Bentonite Clay

The Dunarobba Forest in Italy (Figure 10-5) provides a natural analogue of the effectiveness of clays in minimizing groundwater movement (Benvegnú et al. 1988; Ambrosetti et al. 1992). The sequoia-like Dunarobba trees were buried in clay for 1.5 million years. The clay minimized the flow of water to the trees and prevented oxygen from reaching the wood. This maintained reducing conditions around the wood, protecting the wood from bacterial or fungal decay or chemical oxidation. As a result, the trees did not decay. They also did not fossilize - they are still made of wood.

Similar analogues have been found in the Canadian Arctic on Axel Heiberg Island (Greenwood and Basinger 1994) and at the Strathcona Fiord on Ellesmere Island (Francis 1988), where shale deposits over 40 million years old were found to contain preserved specimens of redwood, walnut, elm, birch and alder; also, gingko and katsura, now native to eastern Asia. The shale, which is consolidated clay, provided an effective barrier to oxygen and preserved the wood such that the wood grain and bark are preserved without chemical alteration – the cellular structure and most of its molecular structure remain intact.

Note: Retrieved Aug 1 2013 from http://it.wikipedia.org/wiki/File:Dunarobba.jpg.

Figure 10-5: 1.5 Ma Sequoia-like Tree Stumps at Dunarobba, Italy

Sensitivity to Temperature

Thermal alteration of bentonite has been studied, with a focus on higher temperatures that are of relevance to the near field. These studies indicate little reaction or degradation of bentonite physical properties below 150°C (Wersin et al. 2007). This compares well with repository temperatures (see Section 5.2.4), where the temperature at the surface of the container is predicted to peak at less than 120°C within 10 years of closure, then steadily decrease to 90°C after 100 years and ultimately return to ambient temperature by approximately 100,000 years.

The bentonite beds at Kinnekulle in Southern Sweden were exposed to temperature of 140-160°C over a period of about 1000 years as a result of a basaltic intrusion (Pusch et al. 1998). The measured swelling pressures are still substantial and hydraulic conductivities are reasonably low. Wersin et al. (2007) reviewed natural analogue data on thermally-exposed bentonite to assess its stability, concluding that even for an extended heating period with resulting cementation and illitization, the hydraulic properties of the bentonite remain favourable.

Laine and Karttunen (2010) report on the Ishirini bentonite body in Libya. Some of the bentonite formations were crosscut by basaltic intrusions about 20.2 million years ago, causing local thermal alteration near the intrusions. Kolařiková and Hanus (2008) found that the minimum

temperature experienced by the bentonite during the intrusions was probably higher than 190°C. The impact of raised temperatures, however, appears minimal: while some local cementation occurred, the majority of the bentonite remains unaltered.

Sensitivity to Salinity:

Under postclosure conditions, high salinity of the groundwater is expected to affect the swelling properties of the bentonite; however, it is not expected to alter the mineral stability of the bentonite.

Alexander and Milodowski (2013) observe that the Perapedhi bentonites studied under the Cyprus Natural Analogue Project likely remained in a marine, saline environment until the formation of Cyprus and the initiation of fresh groundwater circulation.

Figure 10-6 compares the swelling pressure of the Cyprus bentonite with a range of industrial bentonites (plus one other natural bentonite from Avonlea), indicating that exposure of the Perapedhi bentonite to marine saline conditions for nearly 90 million years had no significant impact on its swelling capacity.

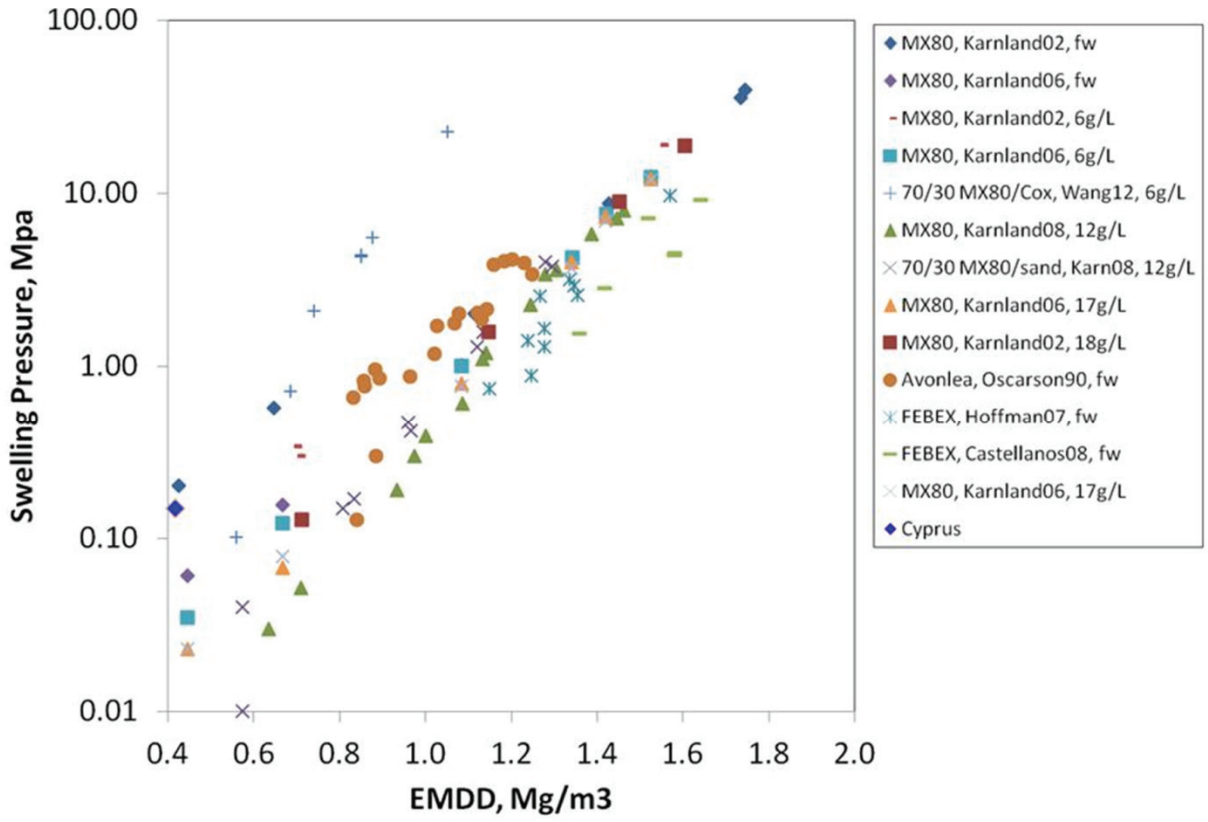

Note: The legend indicates that saturation waters range in salinity from fresh water (fw) to 18 g/L of dissolved salt.

Figure 10-6: Swelling Pressures of Various Bentonites across a Range of Equivalent Montmorillonite Dry Densities (EMDD)

Sensitivity to Alkalinity

Bentonite, particularly the swelling clay component (smectite), is unstable under high pH conditions. In the repository, concrete may produce alkaline conditions locally, affecting adjacent bentonite. However, as the low-heat high-performance concrete leachates will have a lower pH (10 - 11) than Ordinary Portland Cement, it is expected that any reaction with the bentonite will be local. Furthermore, the concrete plugs are placed at a distance from the bentonite buffer around the containers.

Significant degradation of smectite under alkaline groundwater has been observed in conditions with large amounts of alkaline groundwater; however, in natural analogue systems with limited groundwater flow, the reaction is limited. For example, although the International Philippines Natural Analogue Project is at an early stage (Fujii et al. 2010), results to date show that reaction with alkaline water (pH ~11) in the bentonite is restricted to the contact interface, with the width of the reaction zone a maximum of 5 cm. In another example, at the Cyprus Natural Analogue Project (Alexander and Milodowski, 2013), the groundwater ($10 < pH < 11$) appears to have been circulating under the bentonite for approximately 100,000 years. In this time, less than 1% of the smectite in the bentonite has reacted, indicating very slow reaction times. The authors note that sufficient swelling pressure remains in the reacted bentonite to minimize further reaction due to pore throat reduction (see also Wilson et al. 2011).

10.2.3 Concrete

Low-heat, high-performance concrete may be used to close container placement rooms. The concrete bulkheads will counteract the swelling pressure of the bentonite components and maintain the tunnel backfill materials in their intended position. Concrete bulkheads could also be used to provide structural support and confinement to the column of shaft sealing materials. Low-heat high-performance concrete is designed to minimize effects on the adjacent clay (Dixon et al. 2001).

Analogue studies of natural cements suggest that, within stable systems, the material is durable, with the oldest reported cements at Maqarin in north Jordan being some 2 million years old (Alexander 1992). Milodowski et al. (1989) also reported the presence of unreacted natural cements from the Scawt Hill and Carneal Plug sites in Northern Ireland. These cements were produced during the thermal metamorphism of the host limestone and are estimated to be some 58 million years old. In both examples, the natural cements are effectively impermeable and remain unchanged until accessed by groundwaters (through tectonic damage, for example). If damaged, the tendency is for these systems to reseal, either with secondary calcium silicate hydrate phases (Linklater 1998) or carbonates (Clark et al. 1994).

Of the natural analogue studies reported to date on cements, it is important to note that the natural cements examined are more akin to Ordinary Portland Cement, not low-heat high-performance cement (Gray and Shenton 1998). Low-heat high-performance cement is essentially the same as the pozzolanic cements developed by the Romans in the 3rd century BCE, or perhaps in Tiryns and Mycenae a millennium earlier (Middleton 1888). Recent studies of Roman cements exposed to marine salinities for about 2000 years tend to suggest little degradation of the cement (Oleson et al. 2004, Vola et al. 2011).

10.2.4 Asphalt

Bitumens are meltable substances distilled from fossil fuels while asphalts are solid bitumens containing various mineral materials[1]. The shaft seal design concept includes a layer of asphalt, providing a redundant low-permeability seal. The reference asphalt is the same as proposed for use in the Waste Isolation Pilot Plant (WIPP 2009).

Natural asphalts and bitumens have been used as glue or mastic for water-proofing for many thousands of years. In almost all cases where archaeological artifacts have been found coated in asphalt, they have been well preserved when mechanical disruption of the bitumen has not occurred: one example is provided by Babylonian buildings from 1300 BCE, where asphalt was used to coat floors and as a building material in river banks and piers (Hellmuth 1989); another comes from remains within the caves of Lascaux in France, approximately 15,000 years old (NAGRA 1988).

Natural asphalts are found in a number of geological environments and in all climatic zones. Examples include the asphalt lakes of Trinidad and Guanoco, Venezuela, impregnated sandstones and limestones in Athabasca (Canada), Utah (USA), Val de Travers (Switzerland), and Hannover (Germany), and hydrothermal veins in Derbyshire (England).

The Athabasca oil sands located in the McMurray Formation in Athabasca are the largest known reservoir of crude bitumen in the world. The host formation is of early Cretaceous age and composed of numerous lenses of unconsolidated oil-bearing sand. Isotopic studies show the oil deposits to be about 112 million years old (Selby and Creaser 2005). The study by Longstaffe (1993) indicates that the bitumen has remained stable for over 10 million years.

The bitumen deposits in sandstone rocks in the Uinta Basin in Utah are believed to be from the late Cretaceous to Eocene period, 70 to 30 million years ago (Schamel 2009), formed under basin waters that were likely comparable to marine salinity. This natural analogue provides another example of the long-term stability of bitumen under likely saline conditions.

Also within the Uinta Basin in Utah, extensive veins of another natural asphalt called gilsonite were formed by hydrothermal fluids during the Eocene period, 56 to 34 million years ago, and have subsequently remained little altered for several tens of millions of years (Boden and Tripp 2012).

Drake et al. (2006) report natural asphalt (asphaltite) in open and closed fractures at the Forsmark site in Sweden. This asphalt was exposed to brines (45 g/L at present) for at least several million years, suggesting very long-term stability of asphalt under saline conditions.

10.3 Analogue for Geosphere

The site itself is an important analogue for the future behaviour of the geosphere. In particular, geoscientific evidence of the past history of the site provides a direct analogue for future behaviour. This will be gathered for a real site as part of the site characterization, and

[1] Local preference may reverse this terminology (e.g., United Kingdom vs. United States); similarly, common usage may not align with preferred geological terminology.

presented in the geosynthesis. While this is not available for this hypothetical site, the Michigan Basin in general has low seismicity and no volcanism, with evidence that oxygen does not penetrate to any great depth during glaciation.

10.4 Natural Analogue Summary

Performance of repositories cannot be verified by experiment for time scales relevant to their long-term safety. Natural analogues provide qualitative and quantitative illustrations of long-term behaviour, providing support for key model assumptions and for the identification of processes that need to be represented and those that can be excluded. The natural analogues identified here provide additional understanding of the materials and processes that influence the behaviour of radionuclides in a deep geological repository. They provide confidence in the long-term performance of the repository.

10.5 References for Chapter 10

Alexander, W.R. (ed). 1992. A natural analogue study of cement-buffered, hyperalkaline groundwaters and their interaction with a sedimentary host rock - I: Source-term description and geochemical code database validation. NAGRA Technical Report Series NTB 91-10. NAGRA, Wettingen, Switzerland.

Alexander, W.R. and A.E. Milodowski (eds). 2013. Cyprus Natural Analogue Project (CNAP) Phase IV Final Report. Posiva Working Report. Posiva, Eurajoki, Finland.

Ambrosetti, P., G. Basilici, S. Gentili, E. Biondi, Z. Cerquaglia and O. Girotti. 1992. La Foresta Fossile di Dunarobba. Ediart, Todi, Italy.

Angus, N.S., G.T. Brown and H.F. Cleere. 1962. The Iron Nails from the Roman Legionary Fortress at Inchtuthil, Perthshire. Journal of Iron and Steel Institute 200, 956-968.

Benvegnú, F., A. Brondi and C. Polizzano. 1988. Natural Analogues and Evidence of Long-term Isolation Capacity of Clays Occurring in Italy: Contribution to the Demonstration of Geological Disposal Reliability of Long-lived Wastes in Clay. CEC Nuclear Science and Technology Report EUR 11896. Luxembourg.

Boden, T. and B.T. Tripp. 2012. Gilsonite veins of the Uinta Basin, Utah. Utah Geological Survey, Special Study 141. Utah Dept. of Natural Resources, Salt Lake City, USA.

Clark, I.D., R. Dayal and H.N. Khoury. 1994. The Maqarin (Jordan) natural analogue for 14C attenuation in cementitious barriers. Waste Management 14, 467-477.

CNSC. 2006. Regulatory Guide G-320: Assessing the Long Term Safety of Radioactive Waste Management. Canadian Nuclear Safety Commission. Ottawa, Canada.

Cramer, J.J. and J.A.T. Smellie. 1994. Final Report for the AECL/SKB Cigar Lake Analog Study. Atomic Energy of Canada Limited Report AECL-10851, COG-93-00147, SKB-TR-94-00004. Pinawa, Canada.

Crissman, D. and G Jacobs. 1982. Native Copper Deposits of the Portage Lake Volcanics, Michigan: Their Implications with Respect to Canister Stability for Nuclear Waste

Isolation in Columbia River Basalts beneath the Hanford Site, Washington. Rockwell Hanford Operations Technical Report RHO-BW-ST- 26P. Hanford, USA.

Dixon, D.A., N.A. Chandler and P.M. Thompson. 2001. The selection of sealing system components in AECL's 1994 Environmental Impact Statement. Ontario Power Generation Report 06819-REP-01200-10074-R00. Toronto, Canada.

Drake, H., B. Sandström and E-L. Tullborg. 2006. Mineralogy and geochemistry of rocks and fracture fillings from Forsmark and Oskarshamn: Compilation of data for SR-Can. SKB R-06-109. SKB, Stockholm, Sweden.

EUBA. 2011. Fact Sheet on Bentonite. The European Association of the Bentonite Producers (EUBA: Member of IMA-Europe). Brussels, Belgium.

Francis, J.E. 1988. A 50 million-year old fossil forest from Strathcona Fiord, Ellesmere Island, Arctic Canada: evidence for a warm polar climate. Arctic. 41 314-318.

Fujii, N., C.A. Arcilla, M. Yamakawa, C. Pascua, K. Namiki, T. Sato, N. Shikazono and W.R. Alexander. 2010. Natural analogue studies of bentonite reaction under hyperalkaline conditions: overview of ongoing work at the Zambales Ophiolite, Philippines. Proc. ICEM 2010 Conference, ASME, Washington, USA.

Gray, M.N. and B.S. Shenton. 1998. For better concrete, take out some of the cement. In Proc. 6th ACI/CANMET Symposium on the Durability of Concrete, Bangkok, Thailand.

Greenwood, D.R. and J.F. Basinger. 1994. The paleoecology of high latitude Eocene swamp forests from Axel Heiberg Island, Canadian High Arctic. Review of Palaeobotany and Palynology. 81 83-97.

Heikola, T., S. Kumpulainen, U. Vuorinen, L. Kiviranta and P. Korkeakoski. 2013. Influence of alkaline (pH 8.3-12.0) and saline solutions on chemical, mineralogical and physical properties of two different bentonites. Clay Minerals. 48 (2) 309-329.

Hellmuth, K-H. 1989. Natural analogues of bitumen and bitumenized waste. Finnish Centre for Radiation and Nuclear Safety, STUK-B-VALO 58, Helsinki, Finland.

Hellmuth, K-H. 1991. The existence of native iron – Implications for nuclear waste management. Helsinki, Finland: Finnish Centre for Radiation and Nuclear Safety. Report STUK-B-VALO 68.

Hofmann, B.A. 1999. Geochemistry of Natural Redox Fronts – A Review. NAGRA Technical Report NTB 99-05. Wettingen, Switzerland.

IAEA. 1999. Use of Natural Analogues to Support Radionuclide Transport Models for Deep Geological Repositories for Long Lived Radioactive Wastes. International Atomic Energy Agency TECDOC-1109. Vienna, Austria.

Johnson, A.B. and B. Francis. 1980. Durability of Metals from Archaeological Objects Metal Meteorites and Native Metals. Battelle Pacific Northwest Laboratory PNL-3198. Hanford, USA.

Kolaříková, I. and R. Hanus. 2008. Geochemistry and mineralogy of bentonites from Ishirini (Libya). Chemie der Erde-Geochemistry. 68 (1) 61-68.

Laine, H. and P. Karttunen. 2010. Long-Term Stability of Bentonite: A Literature Review. Posiva Working Report WR 2010-53, Posiva, Eurajoki, Finland.

Linklater, C.M. (ed). 1998. A natural analogue study of cement buffered, hyperalkaline groundwaters and their interaction with a repository host rock II. Nirex Science Report, S-98-003, NDA-RWMD, Harwell, UK.

Longstaffe, F. 1993. Meteoric Water and Sandstone Diagenesis in the Western Canada Sedimentary Basis, in SG36: Diagenesis and Basin Hydrodynamics. American Association of Professional Geologists AAPG Special Volume. Tulsa, USA.

McKee, P. and D. Lush. 2004. Natural and Anthropogenic Analogues - Insights for Management of Spent Fuel. Nuclear Waste Management Organization Report APM-REF-06110-24105. Toronto, Canada.

Middleton, J.H. 1888. On the chief methods of construction used in ancient Rome. Archaeologie LI, 41 – 60.

Miller, W., R. Alexander, N. Chapman, I McKinley and J. Smellie. 2000. Geologic Disposal of Radioactive Wastes & Natural Analogues Volume 2. Elsevier/ Pergamon Press. Oxford, UK.

Milodowski, A.E., P.H.A. Nancarrow and B. Spiro. 1989. A mineralogical and stable isotope study of natural analogues of Ordinary Portland Cement (OPC) and CaO–SiO2–H2O (CSH) compounds. United Kingdom Nirex Safety Studies Report, NSS/R240, NDA, Moor Row, UK.

Milodowski, A.E., M.T. Styles and V.L. Hards. 2000. A Natural Analogue for Copper Waste Canisters: The Copper-uranium Mineralised Concretions in the Permian Mudrocks of South Devon, United Kingdom. Swedish Nuclear Fuel and Waste Management Company Report SKB TR-02-09. Stockholm, Sweden.

NAGRA. 1988. Solidification of Swiss Radioactive Waste with Bitumen. National Cooperative for the Disposal of Radioactive Waste (NAGRA). NTB 85-28. Baden, Switzerland (in German).

Oleson, J.P., C. Brandon, S.M. Cramer, R. Cucitore, E. Gotti and R.L. Hohlfelder. 2004. The ROMACONS Project: a Contribution to the Historical and Engineering Analysis of Hydraulic Concrete in Roman Maritime Structures. Intern. J. Nautical Archaeol., 33.2, 199–229. doi: 10.1111/j.1095-9270.2004.00020.x

Pitts, L. and A. St. Joseph. 1985. Inchtuthil Roman Legionary Fortress Excavation 1952-1965. Society for the Promotion of Roman Studies. Britannia Monographs Series 6. London, England.

Pusch, R., H. Takase and S. Benbow. 1998. Chemical processes causing cementation in heat-affected smectite – the Kinnekulle bentonite. SKB Technical Report TR-98-25, Stockholm, Sweden.

Schamel, S. 2009. Strategies for in situ recovery of Utah's heavy oil and bitumen resources. Utah Geological Survey, Open File Report 551. Salt Lake City, USA.

Selby D. and R.A. Creaser. 2005. Direct Radiometric Dating of Hydrocarbon Deposits Using Rhenium-Osmium Isotopes. Science 308, 1293-1295.

Smellie, J.A.T. and F. Karlsson. 1996. A reappraisal of some Cigar Lake issues of importance to performance assessment. SKB Technical Report TR 96-08, SKB, Stockholm, Sweden.

Tait, J.C., H. Roman and C.A. Morrison. 2000. Characteristics and Radionuclide Inventories of Used Fuel from OPG Nuclear Generating Stations Volumes 1 and 2. Ontario Power Generation Report 06819-REP-01200-10029-R00. Toronto, Canada.

Vola, G., E. Gotti, C. Brandon, J.P. Oleson and R.L. Hohlfelder. 2011. Chemical, mineralogical and petrographic characterization of Roman ancient hydraulic concretes cores from Santa Liberata, Italy, and Caesarea Palestinae, Israel. Periodico di Mineralogia 80, 317–338.

Wersin, P., L.H. Johnson and I.G. McKinley. 2007. Performance of the bentonite barrier at temperatures beyond 100°C: A critical review. Physics and Chemistry of the Earth 32 780-788.

Wilson, J., D. Savage, A. Bond, S. Watson, R. Pusch and D. Bennett (2011). Bentonite: a review of key properties, processes and issues for consideration in the UK context. Quintessa Report QRS-1378ZG-1.1 for the NDA-RWMD, Quintessa, Henley - on - Thames, UK.

WIPP. 2009. Waste isolation pilot plant hazardous waste facility permit renewal application September 2009: Appendix I2, Appendix A, Material specification shaft sealing system compliance submittal design report. Waste Isolation Pilot Plant, U.S. Department of Energy, Carlsbad, USA.

Yoshida, H. 1994. Relation between U-series nuclide migration and microstructural properties of sedimentary rocks. Applied Geochemistry, 9 (5), 479-490.

11. QUALITY ASSURANCE

11.1 Introduction

This chapter describes how project activities important to safety in the APM Used Fuel Repository Conceptual Design and Postclosure Safety in Sedimentary Rock were conducted under an appropriate quality assurance framework.

11.2 Used Fuel Repository Conceptual Design and Postclosure Safety

11.2.1 APM Safety Case Project Quality Plan

The APM Safety Case Project Quality Plan (PQP) APM-PLAN-00120-0002-R002 (NWMO 2012a) was prepared by the NWMO Director, Quality Assurance and approved by the Project Manager for use during the preparation of the Used Fuel Repository Conceptual Design and Postclosure Safety in Sedimentary Rock. This APM Safety Case PQP meets the requirements of both CSA N286-12 and ISO 9001:2008.

The quality program applies to all organizational units with responsibilities for the preparation of the Used Fuel Repository Conceptual Design and Postclosure Safety in Sedimentary Rock project. The following processes implement the program:

- A managed system consisting of governing documents that prescribe controls and responsibilities to ensure activities are carried out in a quality assured, effective manner by qualified personnel;
- Individual accountability for implementing and adhering to the managed system elements;
- A specific APM Safety Case Project Execution Plan indentifying project scope, work breakdown, responsibilities and controls, and
- Evaluation and enhancement of the program elements through continuous improvement processes.

Selected vendors and suppliers are required to be qualified to appropriate quality assurance standards defined by the NWMO. Each of these vendors and suppliers selected is required to submit a detailed quality assurance and inspection plan, consistent with the APM Safety Case PQP, for review and subsequent approval.

The quality program includes provisions for systematic planned audits and assessments designed to provide a comprehensive, critical and independent evaluation of project activities. These audits and assessments cover the overall quality program, sub-tier programs, and interfaces between programs. The audits and assessments monitor compliance with governing procedures, standards and technical requirements, and confirm that quality program requirements are being effectively implemented. Audit and assessment results are documented, reported to and evaluated by a level of management having sufficient breadth of responsibility to assure actions are taken to address the findings.

Additional oversight of activities is provided through regular project monitoring and reporting, self-assessment and the non-conformance and corrective action program. In particular, the corrective action program assures that non-conformance conditions are identified, documented, reported, evaluated and corrected in a timely manner.

The APM Safety Case PQP is supported by NWMO governance that establishes expectations for engineering and design, safety assessment, procurement, occupational health and safety, environmental protection, product and services approval, document control and record keeping.

The following are key elements of the APM Safety Case PQP:

- Project specific quality objectives are established.
- Each person working on the project is responsible for achieving and maintaining quality and management is responsible for providing adequate resources and evaluating the quality of the work.
- APM project work is performed in accordance with applicable NWMO governing documents and established processes and procedures.
- Specific requirements for design, safety assessment and technical studies involving computer modeling are described.
- All work is conducted by qualified individuals.
- When work within the scope of the APM project is performed by another organization, the consultant/contractor performs work in compliance with ISO 9001:2008 or CSA N286-12 as appropriate and in compliance with an approved work specific quality plan and APM project-specific governing documents. When a consultant/contractor provides a specialized technical service, and their quality management system is not based on a recognized system, their quality management system may be accepted if it meets internal quality objectives and requirements.
- APM work is verified via verification processes and procedures. Furthermore for work conducted by contractors, project quality plans are approved and include appropriate verification procedures for deliverables including verification process documentation.
- Experience from related industries is obtained through planned activities including information exchanges with other nuclear waste management organizations, participation in technical conferences, contracting with organizations and obtaining independent expert review and input.
- NWMO APM project personnel have access to observe and verify consultants/contractors' quality processes and examine quality assurance documentation.
- Documents considered to be quality assurance records as per APM-LIST-08133-0001, Quality Assurance Documents (NWMO 2011), are transmitted into NWMO records.
- Targeted periodic assessments of work are performed on the APM project. Work performed by NWMO project personnel is assessed for compliance with the APM PQP and applicable procedures. Work performed by consultants/contractors and their subcontractors are assessed to confirm that it is being performed in compliance with their work specific quality plans.

11.2.2 Examples of Peer Review and Quality Assurance

Experienced contractors worked with NWMO to carry out the illustrative postclosure safety assessments for the APM project under approved project specific quality plans. The contractors committed to provide high quality work through effective application of a quality system that fostered best practice and included processes for continual improvement. Safety assessments were conducted consistent with NWMO's governance, NWMO-PROC-EN-0003 Safety Assessment Procedure (NWMO 2012b). For this illustrative safety case formally accepted data clearance forms were used between the geosciences, engineering and safety assessment

teams. Software and reference datasets were procured, developed and maintained consistent with NWMO's governance, NWMO-PROC-EN-0002 Technical Computer Software Procedure (NWMO 2010). The confidence in the software models used for this illustrative safety assessment is reinforced by the consistency in terms of nuclide transport observed between the models as described in Section 7.8.

NWMO and independent peer review of key results and conclusions in the illustrative postclosure safety assessment was planned by the NWMO and completed. The comments and suggested improvements provided by the independent reviewers have been addressed and incorporated as appropriate into the illustrative safety assessment prior to submission to the regulator.

11.2.3 Future Safety Case Quality Assurance

Once an actual repository site is selected, on-site work will commence to characterize the site in terms of its geophysical and environmental properties. Simultaneously, the conceptual design will progress towards the detailed design required for licensing and ultimately container manufacture and facilities construction. The project quality assurance plan will necessarily expand in scope to ensure that the site characterization, detailed design, associated preclosure and postclosure safety assessment and environmental assessment are prepared under a comprehensive and robust quality assurance regime. At an appropriate time in the future, specific quality assurance plans will be prepared and implemented for the manufacturing and qualification of containers and the construction and commissioning of the used fuel transfer facility and the repository.

11.3 References for Chapter 11

CSA N286-12. Management System Requirements for Nuclear Facilities. Canadian Standards Association. Canada.

ISO 9001:2008. Quality Management Systems Requirements. International Organization for Standardization.

NWMO. 2010. Technical Computer Software Procedure. Nuclear Waste Management Organization Procedure NWMO-PROC-EN-0002. Toronto, Canada.

NWMO. 2011. APM Deep Geological Repository Project Quality Assurance Documents. Nuclear Waste Management Organization List APM-LIST-08133-0001. Toronto, Canada.

NWMO. 2012a. APM Safety Case Project Quality Plan. Nuclear Waste Management Organization Plan APM-PLAN-00120-0002-R002. Toronto, Canada.

NWMO. 2012b. Safety Assessment Procedure. Nuclear Waste Management Organization Procedure NWMO-PROC-EN-0003. Toronto, Canada.

THIS PAGE HAS BEEN LEFT BLANK INTENTIONALLY

12. SUMMARY AND CONCLUSIONS

12.1 Purpose of the Pre-Project Report

As stated in Chapter 1, this report presents an illustrative case study of a postclosure safety assessment methodology applied to examine the long-term safety of a reference multi-barrier deep geological repository design for Canada's used nuclear fuel within a hypothetical sedimentary rock setting. The purpose of this case study is to present a postclosure safety assessment methodology to illustrate how CNSC expectations, documented in CNSC Guide G-320 (CNSC 2006), subsequently referred to as G-320, are satisfied. Table 1-4 provides links between G-320 and sections of this report.

It should be recognized that this report is not intended to provide a full deep geological repository safety case as described in G-320. Aspects of G-320 that are relevant to this case study are extracted from this guidance document and included in grey 'text' boxes throughout this chapter. This text is intended to be complementary to this summary and to highlight how key aspects of G-320 have been addressed by the postclosure safety assessment methodology. In this regard, the work presented has focused on describing the appropriate selection and application of assessment strategies.

Developing a long-term safety case, G-320 Section 5.0:

Demonstrating long term safety consists of providing reasonable assurance that waste management will be conducted in a manner that protects human health and the environment. This is achieved through the development of a safety case, which includes a safety assessment complemented by various additional arguments...

It is noteworthy that in the context of a postclosure deep geological repository safety case, this illustrative case study does not include a Geosynthesis. The purpose of a Geosynthesis is to provide an understanding of the geosphere proposed to enclose the repository and its evolution as it relates to establishing confidence in a repository safety case. In the absence of a specific site, a hypothetical sedimentary site was established using geologic information consistent with a location in southern Ontario.

Licensing considerations, G-320 Section 4.3:

It is up to the applicant to determine an appropriate methodology for achieving the long term safety of radioactive waste based on their specific circumstances; however, applicants are encouraged to consult with CNSC staff throughout the pre-licensing period on the acceptability of their chosen methodology.

This summary chapter is intended to highlight the means by which a safety assessment methodology has been applied to evaluate the long-term safety and associated uncertainty surrounding the performance of a repository for nuclear used fuel in a sedimentary setting. The strategy adopted is based, in part, on a defence-in-depth approach consistent with current best

international practice. The results of the safety assessment provide useful insight into the performance of the multi-barrier repository design and specific features of the design that could most influence long-term performance.

The request for a CNSC review of this repository design and illustrative safety assessment is consistent with the G-320 licensing considerations on determining methodology.

12.2 Repository System

System description, G-320 Section 7.3:

It is recognized that the system description may be less complete and rigorous early in the licensing lifecycle, and that the information used in long term assessments of safety for the purpose of design optimization or to support an environmental assessment or a licence application may therefore need to use some default or generic data. As licensing progresses through the facility's lifecycle, as-built information and operational data are acquired, and the site characteristics become better understood. It is expected that assessments of long term safety that are made later in the licensing lifecycle will be based on updated and refined models and data, with less reliance on default, generic, or assumed information, resulting in more reliable model results.

Section 4 of G-320 identifies several methods for long-term waste management, including surface facilities, near-surface facilities and deep geological facilities. As previous mentioned, this report describes the currently envisioned deep geological multiple barrier repository design for the long-term safe management of used nuclear fuel in a sedimentary rock setting. This design and waste management approach is commensurate with the waste's radiological, chemical, and biological hazard to the health and safety of persons and the environment.

The deep geological repository system is described in Chapters 2 through 5 of this report where:

- Chapter 2 describes the hypothetical geosphere setting;
- Chapter 3 describes the characteristics of the used nuclear fuel;
- Chapter 4 describes the repository design concept; and
- Chapter 5 describes how key components of the system will interact with each other and with the environment in the long term.

The key points from these chapters are summarized in this section along with parameters identified in the safety assessment as being influential to repository performance.

12.2.1 Geologic Description of the Hypothetical Site

Information related to the geologic characteristics of the site for the purpose of this illustrative safety assessment is presented in Chapters 1 and 2. Site-specific characterization activities at a candidate site would be designed to gather information on a broad range of geologic characteristics that would be used to develop a Descriptive Geosphere Site Model and support a repository safety case. For the purpose of this illustrative case study several key attributes

have been assumed for the hypothetical site as listed in Chapter 1 (Section 1.6.3.1). Such attributes that would be verified through site-specific investigation include:

- The repository is located in an area of low seismic hazard;
- The repository location is not associated with potable groundwater resources;
- The repository location is not associated with economically viable natural resources;
- The groundwater system at repository depth is reducing;
- No large-scale transmissive fractures are in close proximity to the repository site;
- The host rock formation can withstand transient thermal and mechanical stresses; and
- The rate of site uplift and erosion are sufficiently small not to influence repository safety.

Specific site characteristics for the case study are described in Chapter 2. In particular, this chapter describes a conceptual geosphere model for the site assessed. The properties assigned to the various bedrock formations within the sedimentary sequence has been informed by work conducted in Southern Ontario. Information presented in Chapter 2 describes the long-term behaviour of the groundwater system as relevant to developing an understanding of postclosure repository safety. In addition to a reference case geosphere, alternative conceptual models are described with the purpose of illustrating a range of possible characteristics and groundwater system behaviours. The uncertainty associated with these alternative models is explored through sensitivity, bounding and 'what-if' simulations performed as part of the safety assessment.

12.2.2 Used Fuel

The characteristics of the used fuel are described in Chapter 3. The durability of used fuel and distribution of radionuclides within the fuel are identified as characteristics of the multi-barrier system. These characteristics contribute to the low dissolution rate of the fuel and hence the low release rate of radionuclides from the fuel matrix.

12.2.3 Design Concept

Licensing considerations, G-320 Section 4.3:

The design of a nuclear facility should be optimized to exceed all applicable requirements. In particular, a radioactive waste management facility should more than meet the regulatory limits, remaining below those limits by a margin that provides assurance of safety for the long term.

The repository design concept is presented in Chapter 4. As part of the multi-barrier system, two engineered barriers are included in this concept: a copper-shell container and a clay-based sealing system. Appendix A summarizes a comparison of this engineered barrier system design to internationally proposed repository concepts. A notable difference in this case study with those presented in Appendix A is the copper-shell container design as opposed to a steel-only design. The container and clay-based sealing system designs will be further refined and optimized in advance of a future licence application. This approach is consistent with G-320, which identifies that the repository should more than meet the regulatory limits and remain below those limits by a margin that provides assurance of safety in the long term.

Waste management system, G-320 Section 4.1:

Waste management system for long term storage and disposal of waste refer to the combination of natural and engineered barriers and operational procedures that contribute to safely managing the waste. Long term assessment of these systems can provide information that can be used when making decisions concerning:

1. *Selection of an appropriate site;*
2. *Site characterization;*
3. *Selection of suitable design options during planning;*
4. *Optimization of selected design(s), including minimization of operational and post-operational impacts; and*
5. *Development of construction, operation, and decommissioning strategies and plans.*

Key assumptions in this case study include:

- The repository was positioned arbitrarily at a depth of 500 m. In an actual siting process, the repository location and layout geometry would be designed to improve passive safety based on site-specific host rock conditions.
- A long-lived container with a 25 mm copper corrosion barrier. Research indicates that 1.3 mm would be sufficient for corrosion protection for 1 million years under reducing conditions. The assumed thicker copper-shelled containers provide a much greater margin of safety and facilitate container manufacturing and handling.
- Highly compacted low permeability bentonite surrounds the containers.
- Low permeability clay-based repository sealing systems.

The influence of these design features on repository performance is explored through the safety assessment summarized in Section 7.12. For example, sensitivity and complementary bounding analyses are used to illustrate the effects of an increased fuel dissolution rate, increased container failure rate, increased bedrock hydraulic conductivity, increased geosphere diffusivities and decreased sorption.

Chapter 5 describes the repository system, and how key components of the system will interact with each other and the environment in the long-term, consistent with the G-320 guidance.

The long-term safety assessment presented in this report provides information that can be used to support and inform future decision making as described in G-320.

12.3 Safety Assessment

A structured approach is used to conduct the postclosure safety assessment where two classes of scenarios are assessed, consistent with Sections 5 and 7 of G-320. More specifically, the expectation to demonstrate the understanding of the system through a well structured, transparent, and traceable methodology is described in this report.

Performing long term assessments, G-320 Section 7.0:

The CNSC expects the applicant to use a structured approach to assess the long term performance of a waste management system. Although long term assessments are done with different levels of detail and rigor for different purposes, the overall methodology for performing them should include the following elements:

1. *Selection of appropriate methodology;*
2. *Assessment context;*
3. *System description;*
4. *Timeframes;*
5. *Assessment scenarios; and*
6. *Development of assessment models.*

The approach uses a systematic scenario identification process that acknowledges the timeframes of interest and that identifies features, events, and processes, which could have an impact on the repository's safety features, as described in Chapter 6. The different assessment strategies, including key assumptions and rationale, are described and complementary indicators are presented in Chapter 7, and summarized in this section.

The **Normal Evolution Scenario** is based on a reasoned extrapolation of the hypothetical site and repository features, events and processes. It accounts for the expected degradation of the site and repository over time, and addresses the effects of anticipated events. The computer models and key assumptions are discussed in Chapter 7, which includes a description of analyses of impact for a Reference Case and a range of variant cases in which the effects of changes in postulated physical and chemical conditions are examined.

Disruptive Event Scenarios examine the occurrence of unlikely events leading to the circumvention of barriers and loss of containment. Chapters 7 and 8 present the methods, assumptions and results associated with the analysis of disruptive events.

Criteria for protection of persons and the environment, G-320 Section 6.2:

The regulatory requirements for protection of persons and the environment from both radiological and non-radiological hazards of radioactive wastes lead to four distinguishable sets of acceptance criteria for a long term assessment:

1. *Radiological protection of persons;*
2. *Protection of persons from hazardous substances;*
3. *Radiological protection of the environment; and*
4. *Protection of the environment from hazardous substances.*

The results from the Normal Evolution and Disruptive Events Scenarios are compared against interim acceptance criteria consistent with the guidance of G-320. The interim acceptance criteria selected for comparison were proposed to the CNSC for the purpose of this pre-project report in the following categories:

- Radiological protection of persons;
- Protection of persons from hazardous substances;
- Radiological protection of the environment; and
- Protection of the environment from hazardous substances.

The interim acceptance criteria are described in Section 7.1 for this case study.

12.3.1 Assessment Strategies

Use of different assessment strategies, G-320 Section 5.2:

The strategy used to demonstrate long term safety may include a number of approaches, including, without being limited to:

1. *Scoping assessments to illustrate the factors that are important to long term safety;*
2. *Bounding assessments to show the limits of potential impact;*
3. *Calculations that give a realistic best estimate of the performance of the waste management system, or conservative calculations that intentionally over-estimate potential impact; and*
4. *Deterministic or probabilistic calculations, appropriate for the purpose of the assessment, to reflect data uncertainty.*

Any combination of these or other appropriate assessment strategies can be used in a complementary manner to increase confidence in the demonstration of long term safety.

Key activities that are included in the approach to assess long-term safety are described in Sections 7.5 and 8.5. These include:

- Performing a screening exercise to identify potentially significant dose contributing radionuclides so that subsequent assessments can focus on these radionuclides.
- Conducting 3-dimensional hydrogeological modelling of the groundwater system(s) hosting the repository.
- Performing deterministic and probabilistic calculations of radionuclide transport from fuel to surface. This includes analysis of both normal and disruptive scenarios accompanied by sensitivity cases and bounding assessments.
- Estimating dose consequences for a critical group assumed to be farming on the surface biosphere directly above the repository.
- Investigating gas generation and transport at two different scales of resolution (room-scale and repository-scale) to determine impact on dose consequence.

12.3.2 Modelling Tools and Computer Codes

As discussed in Sections 7.3, 7.4 and 8.3, appropriate modelling tools and computer codes are applied to assess key aspects of the repository's components and specific scenarios, consistent with the expectations in Section 7.6 of G-320.

The main computer models used to assess water-borne contaminant transport are FRAC3DVS-OPG v1.3 and SYVAC3-CC4 v4.09. These codes and their reference datasets are maintained under a NWMO software quality assurance system. They are the current generation of codes that have been in use for Canadian repository assessments for many years, with FRAC3DVS being a commercially available code.

Developing and using assessment models, G-320 Section 7.6:

An assessment model should be consistent with the site description, waste properties, and receptor characteristics, and with the quality and quantity of data available to characterize the site, waste, exposure pathways, and receptors. A systematic process should be used to ensure that the set of data used for developing the assessment model is accurate and representative. Complex models should not be developed if there is not sufficient data to support them. The use of generic or default data in place of site-specific data in developing the conceptual and computer models may be acceptable when there is no site-specific data available, such as in early stages of development; however, with the acquisition of as-built information and operational data, and increased understanding of site characteristics throughout the facility lifecycle, site-specific data should be used.

Confidence in assessment models:

Confidence in the assessment model can be enhanced through a number of activities, including (without being limited to):

1. *Performing independent predictions using entirely different assessment strategies and computing tools;*
2. *Demonstrating consistency between the results of the long term assessment model and complementary scoping and bounding assessments;*
3. *Applying the assessment model to an analog of the waste management system;*
4. *Performing model comparison studies of benchmark problems;*
5. *Scientific peer review by publication in open literature; and*
6. *Widespread use by the scientific and technical community.*

The codes are used in a complementary manner, with FRAC3DVS-OPG providing detailed 3-dimensional flow and mass transport results for a limited number of cases, and SYVAC3-CC4 extending the results to a broader range of nuclides and sensitivity cases. The simplified SYVAC-CC4 model for this case study is derived with help from the detailed FRAC3DVS-OPG transport results for I-129. This model was then verified by comparing the I-129 mass flow results from the two models at various locations in the geosphere, including the Cobourg and Georgian Bay formations. Further similar comparisons were performed for other specific

radionuclides that represented a range of decay and transport parameters (i.e., Cs-135, U-234 and U-238).

To explore uncertainties arising from data variability, SYVAC3-CC4 is used to conduct a probabilistic safety assessment of the entire repository system. Over 100,000 simulations are performed in which hundreds of input variables are simultaneously varied according to defined parameter distributions.

The main computer code used to assess gas-borne transport is T2GGM. It assesses the coupled behaviour between gas generation, temperature and the movement of gas and water. It is composed of two coupled models: the Gas Generation Model (GGM) used to describe the generation of gas due to corrosion of steel components, and the TOUGH2 model used to describe gas and water transport from the repository and within the geosphere, as described in Section 8.3.

12.3.2.1 Key Assumptions and Conservatisms in Modelling

Conservative over-estimates, G-320 Section 5.2.2:

A *conservative approach should be used when developing computer codes and models, and assumptions and simplifications of processes to make them more amenable for inclusion in computer models should not result in under-estimation of the potential risks or impacts*.

Chapter 7 describes the key attributes for the Reference Case of the normal evolution scenario. The illustrative assessment presented in this report uses different strategies consistent with expectations in G-320. The assessment of the Reference Case includes the following conservatisms as described in Chapter 9:

- The defective containers fill with water 10,000 years after the containers are placed in the repository;
- No credit is taken for the presence of the fuel sheath in maintaining fuel integrity and in preventing contact of the fuel matrix with water that may enter the container;
- No credit is taken for the effect of hydrogen gas (H_2) (produced by corrosion of the defective container) on the dissolution rate of the uranium oxide fuel (UO_2) fuel;
- No credit is taken for the effect of iron oxides (produced by corrosion of the defective container) in providing a high surface area for adsorption of some of the radionuclides released from the fuel;
- No credit is taken for the likely filling of the defect with bentonite and/or corrosion products which could significantly increase the transport resistance of the defect;
- Positioning the 3 defective containers in a repository location associated with the shortest travel time to the surface;
- A very deep well (219 m) is included in the assessment. It is positioned at the bottom of the Guelph formation layer, at about the deepest point where potable water may occur. This is

a position that would maximize dose consequence (i.e., it penetrates the entire thickness of the Guelph Formation and is located along the main pathway for contaminants released from the defective containers); and

- Conservative properties for the critical group (e.g., use of 90th percentile food ingestion rates; obtaining all food, fuel, water and building material locally; and all drinking and irrigation water taken from the well, etc.).

Since this Reference Case assumes a constant temperate climate, Section 7.10 also discusses the anticipated effects of glaciation on the assessment.

Analyzing uncertainties, G-320 Section 8.2:

A formal uncertainty analysis of the predictions should be performed to identify the sources of uncertainty. This analysis should distinguish between uncertainties arising from:

1. *Input data;*
2. *Scenario assumptions;*
3. *The mathematics of the assessment model; and*
4. *The conceptual models.*

These conservatisms are further described as part of the approach to assess uncertainties in Chapter 9. The division of uncertainties into scenario, model and data uncertainties is consistent with the guidance of G-320.

12.3.3 Normal Evolution Scenario

Normal evolution scenario, G-320 Section 7.5.1:

A normal evolution scenario should be based on reasonable extrapolation of present day site features and receptor lifestyles. It should include expected evolution of the site and degradation of the waste disposal system (gradual or total loss of barrier function) as it ages.

Depending on site-specific conditions and the timeframe for the assessment, a normal evolution scenario may need to include extreme conditions such as climate shifts or the onset of glaciations.

The Normal Evolution Scenario is based on a reasoned extrapolation of the site and repository, consistent with the expectations in Section 7.5 of G-320. The containers are designed to be durable over very long times, and will be fabricated and placed under careful quality control.

For the Reference Case, the primary dose contributor from the defective containers is determined to be I-129. This is because a fraction of the I-129 is instantly released from the gap and grain boundary inventory in the fuel when water first contacts the fuel. Also, it is long-lived and unretarded in the sub-surface environment. Other radionuclides, in particular

actinides, are only released as the fuel slowly dissolves and are then subsequently sorbed by the enclosing barrier systems.

Figure 12-1 illustrates how radionuclides from the assumed defective containers are expected to be transported through the system's barriers over time. Two timeframes (i.e., 15,000 years and 1 million years) are used to illustrate the changes in activity for the following three types of radionuclides:

- I-129 is non-sorbing in the buffer, backfill and geosphere and is therefore expected to eventually be released to the surface biosphere, with a predicted peak contribution to dose occurring at around 10 million years.

- Cs-135 is an intermediate sorbing fission product that is delayed by the buffer and backfill and hence it's released to the surface biosphere is delayed.

- U-238 is strongly sorbing to the buffer and backfill and is never expected to be released to the surface biosphere.

The calculated peak total dose for this case is determined to be about 0.000002 mSv per year (2 nSv/a) and occurs at the modelling cut-off time of 10 million years. As shown in Figure 7-73, I-129 is responsible for the dose consequence. The dose applies to a person living in the surface biosphere directly above the repository. It is about 150,000 times less than the dose constraint of 0.3 mSv per year, and is a small fraction of the average natural background dose (more than one million times lower). The peak dose occurs after 10 million years and is captured in the sensitivity analysis of increasing the rock diffusivity by a factor of 10, as described in Section 12.3.3.1.

The radiological impact on non-human biota is discussed in Section 7.11.2 and the assessment concludes that the effects are negligible for the Normal Evolution Scenario.

Chapter 7 also addresses the protection of persons and the environment from hazardous substances such as copper and other elements released from the used fuel and the containers. Section 7.11.3 concludes that all contaminant concentrations are below their associated acceptance criteria.

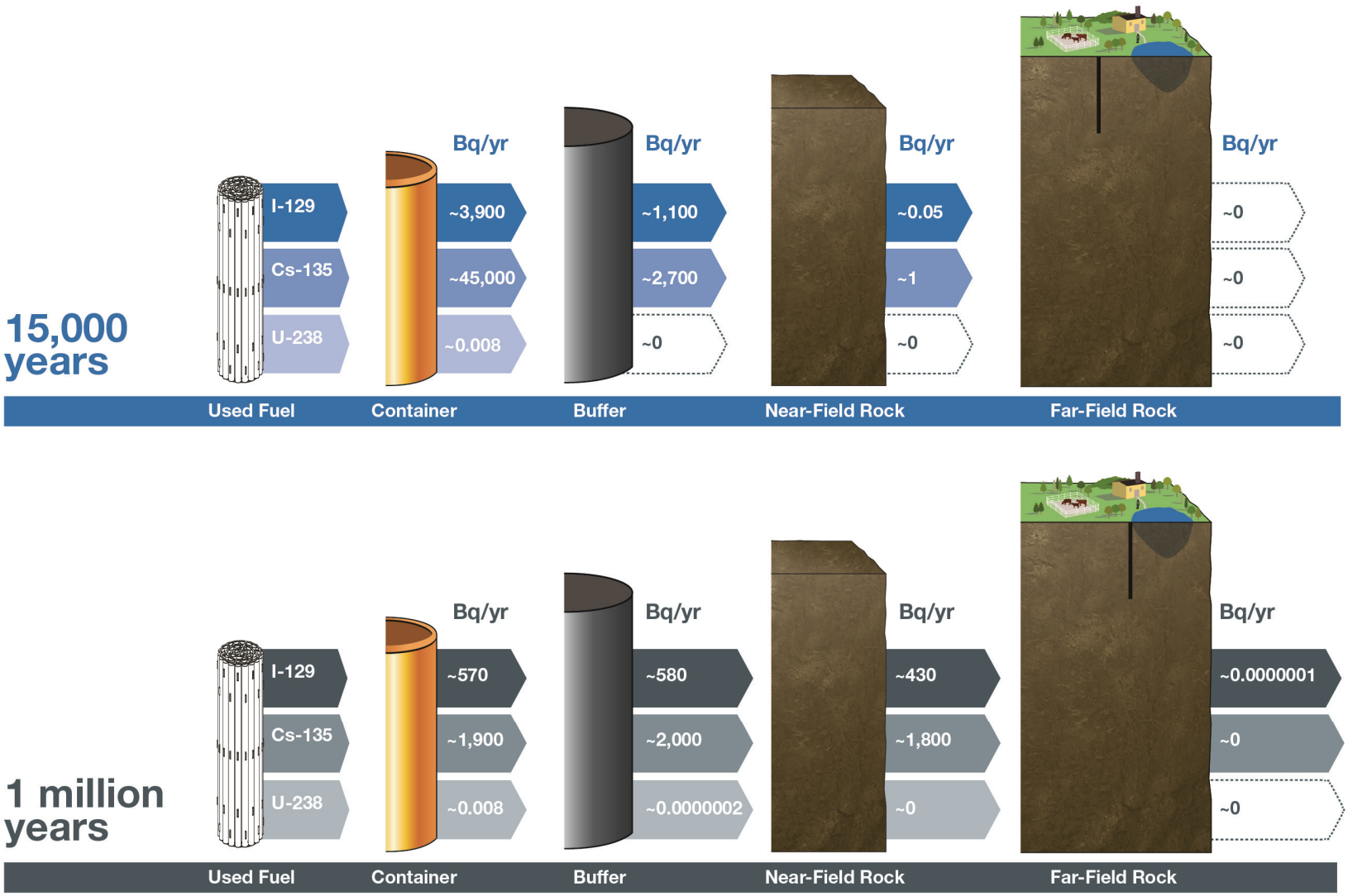

Figure 12-1: Illustration of Radionuclide Transport in the Repository System

12.3.3.1 Results from Sensitivity Analyses and Bounding Assessments

Deterministic calculations, G-320 Section 5.2.3:

The mathematical approach to analyzing the scenarios in the safety case is guided by the purpose of the long term assessment. A deterministic model uses single-valued input data to calculate a single-valued result that will be compared to an acceptance criterion. Variations in input data values are taken into account in these calculations. To account for data variability, individual deterministic calculations must be done using different values of input parameters.

This is the approach used for performing sensitivity analyses (determining the response of model predictions to variations in input data) and importance analyses (calculating the range of predicted values that corresponds to the range of input values) of deterministic models.

To account for the variation in the key input data values used in the Reference Case, a number of sensitivity analyses are completed for key parameters as described in Section 7.2. Some parameters are also pushed beyond their reasonable range of variations by setting their values to zero or by removing limits and running a set of bounding assessments, where a specific parameter is completely ignored. The identified parameters, the variation in their values and the rationale for selecting these cases are summarized in Chapter 7, Table 7-3.

The impacts are determined from simulations performed with either the FRAC3DVS-OPG or the SYVAC3-CC4 codes. The FRAC3DVS-OPG code does not have a biosphere model and therefore its results are presented in terms of I-129 transport to the surface. This provides a reasonable estimate of potential impacts by comparison with the I-129 transport to surface for the Normal Evolution Scenario, since SYVAC3-CC4 simulations show that I-129 dominates the dose consequence.

A summary of the cases, a comparison against the interim acceptance criterion and the key findings are presented in Table 12-1. This comparison of assessment results with interim acceptance criteria is consistent with the guidance in Section 8 of G-320.

The sensitivity analyses show that the impact on dose is small when key parameters are varied. The sensitivity analysis showing the largest effect on the calculated impacts is when the rock diffusivity is increased by a factor of 10. In this case, the peak dose is 13 times greater than in the Reference Case and occurs at 5.6 million years. This remains 12,000 times below the interim dose acceptance criterion. Increasing the dissolution rate of used fuel is also observed to have an impact. The dose consequence when the fuel dissolution rate is increased by a factor of 10 is 3 times greater than in the Reference Case. This remains approximately 51,000 times below the interim dose acceptance criterion with the maximum dose during the simulation occurring at the same time as in the Reference Case, i.e., at the modelling cut-off time of 10 million years.

Some sensitivity analyses are found to have a negligible impact on dose in this case study. When the hydraulic conductivity of the rock mass enclosing the repository is increased by a

factor of 10, the maximum dose consequence relative to the Reference Case is slightly lower. When a 158 m overpressure is used in the Shadow Lake Formation, which is located below the repository at a depth of approximately 675 m, the maximum dose consequence is 1.1 times greater than the Reference Case. Similarly, when the fuel's instant release fraction is increased, the maximum dose consequence is 1.1 times greater than the Reference Case. In all cases, the maximum dose occurs at the same time as the Reference Case, i.e., at the modelling cut-off time of 10 million years.

Some sensitivity analyses are found to have no impact on dose in this case study and these include: increasing the hydraulic conductivity value of the excavation damaged zone, increasing the container defect area, and reducing sorption in the geosphere at the same time as increasing solubility limits.

As noted above, a set of bounding assessments are included to explore the effects of varying some parameters beyond the reasonable range of variations.

The bounding assessments with an effect on dose are for the sensitivity cases where sorption is ignored. When sorption in the near field is ignored, the dose consequence is assessed to be 3.4 times greater than in the Reference Case. This remains approximately 45,000 times below the interim dose acceptance criterion, with the maximum dose occurring at the same time as the Reference Case, i.e., at the modelling cut-off time of 10 million years. When sorption in the geosphere is ignored, the dose consequence is assessed to be 1.7 times greater than in the Reference Case. This remains approximately 91,000 times below the interim dose acceptance criterion, with the maximum dose occurring at the same time at the Reference Case.

There is no impact on dose when radionuclide solubility limits are ignored.

12.3.3.2 Results from the Probabilistic Analysis

Probabilistic calculations, G-320 Section 5.2.3:

Probabilistic models can explicitly account for uncertainty arising from variability in the data used in assessment predictions. Such models may also be structured to take account of different scenarios (as long as they are not mutually exclusive) or uncertainty within scenarios. Probabilistic models typically perform repeated deterministic calculations based on input values sampled from parameter distributions, with the set of results expressed as a frequency distribution of calculated consequences. Frequency multiplied by consequence is interpreted as the overall potential risk of harm from the waste management system.

The results from the probabilistic cases are presented in Chapter 7, consistent with the expectations of G-320 in Section 5.2 on the use of different assessment strategies, where all parameters represented by probability distributions are simultaneously varied. In this case study, relevant parameters for contaminant release and mass transport (in the repository, geosphere and biosphere) were varied whereas the parameters associated with groundwater flow were not.

The probabilistic analysis uses a Monte Carlo random sampling strategy that considers the full range of possible parameter values. A total of 120,000 simulations are performed and examined to identify an average and 95th percentile peak dose rates. The results are summarized in Table 12-1. The average dose for all simulations is 8 times greater than the Reference Case, as shown in Figure 7-85. Whereas, the 95th percentile dose consequence is assessed to be 37 times greater than in the Reference Case. This remains 4,000 times below the interim dose acceptance criterion. The results also show that there are no simulations that exceed the interim dose acceptance criterion.

Table 12-1: Summary and Key Findings from Sensitivity Analyses, Bounding Assessments and Probabilistic Analysis

Case	Description	Key Findings
Reference Case	Reference Case parameters	• Peak dose occurs after 10 million years • Maximum dose occurs at 10 Ma and is 150,000 times lower than normal evolution dose acceptance criterion of 0.3 mSv per year
Degraded Physical Barrier Sensitivity Cases		
Fuel dissolution rate	Fuel dissolution rate increased by a factor of 10	Impact of variation is minimal • Maximum dose rate occurs at the same time • Dose consequence is 3 x Reference Case
Container defect area	Container defect area increased by a factor of 10	No impact • Maximum dose rate occurs at the same time • Dose consequence is equal to Reference Case
Fuel instant release fraction	Instant release fraction increased to 10%	Impact of variation is negligible • Maximum dose rate occurs at the same time • Dose consequence is 1.1 x Reference Case
Geosphere Sensitivity Cases		
Rock Mass Hydraulic Conductivity	Hydraulic conductivity increased by approximately a factor of 10	Impact of variation is negligible • Maximum dose rate occurs at the same time • Dose consequence is 0.8 x Reference Case
Conductivity of excavation damaged zone	Hydraulic conductivity value increased by a factor of 10	No impact • Maximum dose rate occurs at the same time • Dose consequence is equal to Reference Case
Rock diffusivity	Diffusivity increased by a factor of 10	Impact of variation is noticeable • Peak dose rate occurs at 5.6 million years • Dose consequence is 13 x Reference Case

Case	Description	Key Findings
Shadow Lake overpressure	158 m overpressure in the Shadow Lake Formation	Impact of variation is negligible • Maximum dose rate occurs at the same time • Dose consequence is 1.1 x Reference Case
Degraded Chemical Barrier Sensitivity Case		
Coincident sorption and radionuclide solubility limits	Low sorption in the geosphere with coincident high solubility limits	No impact • Maximum dose rate occurs at the same time • Dose consequence is equal to Reference Case
Bounding Assessments		
Sorption in the geosphere	Sorption in the geosphere is ignored	Impact of variation is negligible • Maximum dose rate occurs at the same time • Dose consequence is 1.7 x Reference Case
Radionuclide solubility limits	Radionuclide solubility limits are ignored	No impact • Maximum dose rate occurs at the same time • Dose consequence is equal to Reference Case
Sorption in the near field	Sorption in the near field is ignored	Impact of variation is minimal • Maximum dose rate occurs at the same time • Dose consequence is 3.4 x Reference Case
Probabilistic Simulations		
All parameters varied	Average dose	• Dose rate occurs at 5.6 million years • Dose rate is 19,000 times lower than normal evolution dose acceptance criterion of 0.3 mSv per year
All parameters varied	Maximum dose rate, 95th percentile	• Dose rate occurs at 5.6 million years • Dose rate is 4,000 times lower than normal evolution dose acceptance criterion of 0.3 mSv per year

12.3.3.3 Results from Complementary Indicators

Complementary indicators of safety, G-320 Section 5.4:

Several other safety indicators, such as those that reflect containment barrier effectiveness of site-specific characteristics that can be directly related to contaminant release and transport phenomena, can also be presented to illustrate the long term performance of a waste management system. Some examples of additional parameters include:

1. *Container corrosion rates;*
2. *Waste dissolution rates;*
3. *Groundwater age and travel time;*
4. *Fluxes of contaminants from a waste management facility;*
5. *Concentrations of contaminants in specific environmental media (for example, concentration of radium in groundwater); or*
6. *Changes in toxicity of the waste.*

Complementary indicators other than dose to an assumed human group are described in Section 7.11.1. Two indicators considered in this study are:

- Radiotoxicity concentration in a water body, for medium time scales; and
- Radiotoxicity transport from the geosphere, for longer time scales.

Due to the absence of a lake or river in the nearby hypothetical biosphere model, results are reported only for the radiotoxicity transport indicator. Chapter 7 shows that this indicator is well below its reference value, thereby providing additional confidence that at long times the impact of the repository is likely to be very small.

12.3.4 Disruptive Events Scenarios

Disruptive event scenarios, including human intrusion, G-320 Section 7.5.2

Disruptive event scenarios postulate the occurrence of unlikely events leading to possible penetration of barriers and abnormal loss of containment.

Disruptive scenarios are assessed where barriers are assumed to fail due to unlikely failure mechanisms, as described in Section 6.2 of this report and consistent with Section 7.5 of G-320.

Chapter 6 also includes a review of the scenarios considered in assessments of deep repositories in other countries. The results, summarized in Table 6-5 of this report, show that most assessments have identified a limited number of additional scenarios that consider the degradation / failure of engineered and natural barriers by external processes (e.g., earthquakes, climate change) and human actions (e.g., drilling, poor quality control). Although there are some scenarios identified that are not considered in the current study, these

are either not relevant to a sedimentary rock site or were identified as relevant but not analyzed in this case study.

The scenarios considered in this study and key findings are summarized in Table 12-2.

The impacts are determined from simulations performed with either the FRAC3DVS-OPG or SYVAC3-CC4 codes. The FRAC3DVS-OPG code does not have a biosphere model and therefore its results are presented in terms of I-129 transport to the surface. This provides a reasonable estimate of potential impacts by comparison with the I-129 transport to surface for the normal evolution scenario, since SYVAC3-CC4 simulations show that I-129 dominates the dose consequence.

Table 12-2: Summary of Key Findings from Disruptive Events

Scenario	Key Findings
All Containers Fail at 60,000 Years	• Maximum dose rate occurs at 10 million years • Dose consequence is 130 times below the disruptive events dose acceptance criterion of 1 mSv per year
All Containers Fail at 10,000 Years	• Maximum dose rate occurs at 10 million years • Dose consequence is 120 times below the disruptive events dose acceptance criterion of 1 mSv per year
Shaft Seal Failure	• Maximum dose rate occurs at 10 million years • Dose consequence is 500,000 times below the disruptive events dose acceptance criterion of 1 mSv per year

The results from the All Container Failure Scenarios, identified in Table 12-2, indicate that the containers are an important part of the multiple barriers in sedimentary rock, but also that there is sufficient redundancy in the system that safety is not compromised even in the unexpected event of simultaneous failure of all the containers at 10,000 years or later. The maximum impact is roughly proportional to the number of failed containers (a little less, as radionuclides released from some containers take a long time to reach the well location). However the maximum results are not highly sensitive to the time of container failure beyond 10,000 years. This occurs since the container failure time in both cases is longer than the short-lived fission product decay time, meaning that fuel dissolution rates are not influenced by these short-lived fission products. The remaining actinides and most of the remaining long-lived fission products are retained and delayed in the other engineered and natural barriers so that the maximum dose rate does not substantially change between these two cases.

Chapter 8 further examines the variant case of the All Containers Fail at 10,000 years Scenario in a bounding assessment that considers the largest potential for gas production (from the corrosion of steel within the copper container) and determines the radiological impact from gas-borne radionuclides. The model shows that gas generated within the repository could travel upward to the Guelph Formation.

Model calculations determine that pore pressure within the intact rock does not exceed 80% of lithostatic pressure over the one million year simulation period.

Gas-borne dose consequences are further assessed in Chapter 8 using a set of extremely conservative assumptions to bound the potential dose consequences. A peak dose rate of 0.17 mSv per year is obtained when all the Carbon-14 is assumed to discharge into a house above the repository. This remains a factor of six below the 1 mSv per year acceptance criterion. The peak occurs at 18,000 years. For a more realistic case of failure of copper containers over longer times, the dose rates would be substantially lower. For example, if the copper fails on time scales associated with the next glaciation or later, the corresponding dose rates would be well below 0.001 mSv per year due to decay of Carbon-14.

The Shaft Seal Failure Scenario shows negligible effect on the predicted dose consequence in this study due to the distance between the three defective containers and the shafts. The location of the defective containers relative to shaft will be further assessed in a future safety case.

Disruptive event scenarios, including human intrusion, G-320 Section 7.5.2

Scenarios assessing the risk from inadvertent intrusion should be case-specific, based on the type of waste and the design of the facility, and should consider both the probability of intrusion and its associated consequences. Surface and near-surface facilities (e.g., tailings sites) are more likely to experience intrusion than deep geological facilities.

Scenarios concerning inadvertent human intrusion into a waste facility could predict doses that are greater than the regulatory limit. Such results should be interpreted in light of the degree of uncertainty associated with the assessment, the conservatism in the dose limit, and the likelihood of the intrusion. Both the likelihood and the risk from the intrusion should therefore be reported.

As described in Chapter 7, Section 7.9.1 presents a stylized analysis for the Inadvertent Human Intrusion Scenario. This scenario is a special case, as recognized in Section 7.5.2 of G-320, since it bypasses all the barriers put in place, and therefore the associated dose consequence could exceed the regulatory limit.

The results from the human intrusion assessment show a potential maximum acute dose to the drill crew of about 1,100 mSv, and a potential chronic dose to a site resident (i.e., someone farming on the site) of about 1,100 mSv per year, assuming early intrusion and improper management of the drill site.

The likelihood of inadvertent human intrusion is addressed in the siting of a deep geological repository; in part through placing the used fuel deep underground in a geologic setting with low mineral resource potential, poor prospects for potable groundwater resources, and by the use of institutional controls.

The likelihood of this event occurring is roughly estimated as $3x10^{-5}$ per year, which implies a risk of serious health effects of $2x10^{-6}$ per year. This is less than the annual risk criterion of $1x10^{-5}$ per year.

12.4 Future Work

The conceptual design and illustrative postclosure assessment presented in this report for a hypothetical site represent a single case study in sedimentary rock. Other design concepts and other site conditions have been explored in other Canadian and international case studies. Most recently, the NWMO completed a similar study for a used fuel repository in crystalline rock (NWMO 2012).

Since this report is prepared for a hypothetical site and thus is not a full safety case, a number of aspects are not covered in detail. These are noted in Chapter 1. Also, the postclosure safety assessment illustrated the method and approach, but did not assess all scenarios or aspects of relevance for a full safety case (see Section 7.2.4).

There is ongoing work at NWMO to improve our understanding of key processes and uncertainties in both crystalline and sedimentary rock settings. These are described in the NWMO RD&D report (Villagran et al. 2011).

12.5 Conclusion

The purpose of the NWMO request for a review of this pre-project report is to obtain CNSC feedback on meeting general overall expectations of CNSC Guide G-320, Assessing the Long Term Safety of Radioactive Waste Management. The current case study work, done at a very early stage in the APM Project, supports the continuing development of a deep geological repository for used fuel in sedimentary rock. The illustrative postclosure safety assessment methodology is included for review.

12.6 References for Chapter 12

CNSC. 2006. Regulatory Guide G-320: Assessing the Long Term Safety of Radioactive Waste Management, Canadian Nuclear Safety Commission, Ottawa, Canada.

NWMO. 2012. Used Fuel Repository Conceptual Design and Postclosure Safety Assessment in Crystalline Rock, Pre-Project Report. Nuclear Waste Management Organization NWMO TR-2012-16. Toronto, Canada.

Villagran, J., M. Ben Belfadhel, K. Birch, J. Freire-Canosa, M. Garamszeghy, F. Garisto, P. Gierszewski, M. Gobien, S. Hirschorn, N. Hunt, A. Khan, E. Kremer, G. Kwong, T. Lam, P. Maak, J. McKelvie, C. Medri, A. Murchison, S. Russell, M. Sanchez-Rico Castejon, U. Stahmer, E. Sykes, A. Urrutia-Bustos, A. Vorauer, T. Wanne and T. Yang. 2011. RD&D Program 2011 – NWMO's Program for Research, Development and Demonstration for Long-Term Management of Used Nuclear Fuel. Nuclear Waste Management Organization Report NWMO TR-2011-01. Toronto, Canada.

THIS PAGE HAS BEEN LEFT BLANK INTENTIONALLY

13. SPECIAL TERMS

13.1 Units

a	annum
Bq	becquerel
^{o}C	degree Celsius
cm	centimetre
d	day
dm	decimetre
g	gram
Gy	gray
GPa	gigapascal
h	hour
K	Kelvin
kg	kilogram
kgU	kilogram of Uranium
kJ	kilojoule
km	kilometre
kW	kilowatt
L	litre
m	metre
Ma	million years
mASL	metres above sea level
mBGS	metres below ground surface
mg	milligram
Mg	megagram
MJ	megajoule
mL	millilitre
mm	millimetre
mol	mole
MPa	megapascal
mSv	millisievert
mV	millivolt

mW	milliwatt
MW	megawatt
n	neutron (associated with neutron fluence)
nm	nanometre
nSv	nanosievert
Pa	pascal
ppm	parts per million
s	second
Sv	sievert
W	watt
wt%	mass percentage
µg	microgram
µm	micrometre
µSv	microsieverts

13.2 Abbreviations and Acronyms

1D	One Dimensional
2D	Two Dimensional
3D	Three Dimensional
ADS	Adsorbed
AECL	Atomic Energy of Canada
ALARA	As Low as Reasonably Achievable
APM	Adaptive Phased Management
AQ or (aq)	Aqueous
BCE	Before Common Era
BSB	Bentonite-Sand Buffer
CANDU	CANada Deuterium Uranium
CANLUB	Thin graphite coating between the fuel pellet and the fuel sheath
CC4	Canadian Concept Generation 4
CC	Constant Climate
CCME	Canadian Council of the Environment
CCM-UC	Copper Corrosion Model for Uniform Corrosion

CE	Common Era
CEAA	Canadian Environmental Assessment Act
CFU	Colony Forming Units
CNSC	Canadian Nuclear Safety Commission
CRT	Container Retrieval Test
C-S-H	In the C-S-H term, the “C” stands for Ca, “S” for Si, and “H” for H_2O. The hyphens indicate that no specific solid phases or proportions are implied.
CSA	Canadian Standards Association
C Steel	Carbon Steel
DBF	Dense Backfill
DDW	Dry Density Weight
DEM	Digital Elevation Model
DFN	Discrete Fracture Network
DGR	Deep Geological Repository
DGSM	Descriptive Geosphere Site Model
EA	Environmental Assessment
EBS	Engineered Barrier System
EBW	Electron-Beam Welding
EC	Environment Canada
E_{CORR}	Corrosion Potential
EDZ	Excavation Damage Zone
Eh	Oxidation Potential
EIS	Environmental Impact Statement
EMDD	Effective Montmorillonite Dry Density
ENEVs	Estimated No Effect Values
EPM	Equivalent Porous Media
ERICA	Environmental Risks from Ionising Contaminants Assessment
FEPs	Features, Events and Processes
FP	Fission Product
FSW	Friction-Stir Welding
GGM	Gas Generation Model
GLFA	Glycol-Lipid Fatty Acid
GM	Geometric Mean

GSD	Geometric Standard Deviation
GSM	Glacial Systems Model
HC	Health Canada
HCB	Highly-Compacted Bentonite
HEPA	High-Efficiency Particulate Air
HIM	Human Intrusion Model
HM	Hydromechanical
IAEA	International Atomic Energy Agency
ICRP	International Commission on Radiological Protection
ID	Inner Diameter
Imp	Impurity
ISO	International Organization for Standardization
LBF	Light Backfill
LGM	Last Glacial Maximum
LHHPC	Low-Heat, High-Performance Concrete
MIC	Microbiologically Influenced Corrosion
MLE	Mean Life Expectancy
NDT	Non-Destructive Testing
NEA	Nuclear Energy Agency
NLFA	Neutral-Lipid Fatty Acid
NOAA	National Oceanic and Atmospheric Administration
NTS	National Topographic System
NWMO	Nuclear Waste Management Organization
OD	Outer Diameter
OFP	Oxygen-Free Phosphorus-doped
O/M	Oxygen/Metal
OPG	Ontario Power Generation
PDF	Probability Density Function
PLFA	Phospho-Lipid Fatty Acid
PPT	Precipitate
PQP	Project Quality Plan
PWR	Pressurized Water Reactor
RH	Relative Humidity

RSM	Radionuclide Screening Model
SCC	Stress Corrosion Cracking
SKB	Swedish Nuclear Fuel and Waste Management Company (Svensk Kärnbränslehantering AB)
SRTM	Shuttle Radar Topography Mission
SSM	Swedish Radiation Safety Authority
STP	Standard Temperature and Pressure
SYVAC3	System Variable Analysis Code
TDS	Total Dissolved Solids
TDZ	Thermal Damage Zone
THM	Thermal-hydraulic-mechanical
TWI	The Welding Institute
UFC	Used Fuel Container
UFPP	Used Fuel Packaging Plant
UFTP	Used Fuel Transportation Package
UofT GSM	University of Toronto Glacial Systems Model
URL	Underground Research Lab
WRA	Whiteshell Research Area

THIS PAGE HAS BEEN LEFT BLANK INTENTIONALLY

APPENDIX A – DESIGN OPTIMIZATION

A.1. Introduction

This report presents an illustrative postclosure safety assessment for a deep geologic repository for used nuclear fuel in a Canadian sedimentary rock geosphere.

Previous Canadian case studies have focussed on crystalline rock settings. The present study is the first detailed postclosure safety assessment of a Canadian repository in sedimentary rock. These results together with other NWMO studies will help support an optimized design that caters specifically to the features of Canadian sedimentary rock environments. Such features include the absence of water conducting features, high groundwater salinity and an extremely low rock hydraulic conductivity limiting water, gas and radionuclide transport.

Information to guide potential design optimization studies is also available from international experience in sedimentary rocks.

A.2. International Sedimentary Rock Concepts

Several countries are considering disposal of used fuel or high level waste in sedimentary rock formations. Some, such as Japan and the UK, are considering both crystalline and sedimentary rock sites. Presently, Switzerland, France and Belgium are well advanced in terms of sedimentary rock design concepts, and have operating underground research facilities. The repository design features considered by Switzerland, France and Belgium are described further below.

A.2.1 Switzerland (Nagra)

Switzerland is presently in a repository siting process. Nagra is proposing to dispose of spent fuel, high level waste and long-lived intermediate level waste in a repository in an Opalinus Clay rock formation (Figure A-1) in Switzerland. The safety concept, described in Nagra (2002), uses a multiple-barrier system to isolate radionuclides from the environment. The components of the system are:

- a stable, durable waste form;
- long-lived containers;
- low-permeability backfill (bentonite clay); and
- low-permeability self-sealing host rock.

The reference sedimentary host rock formation is Opalinus Clay. This rock has a high clay content with low hydraulic conductivity. It will self-seal in the presence of water.

In the reference design concept (Nagra 2012), placement tunnels are aligned in parallel and accessible by a ramp. The tunnel walls are stabilized with rock bolts and steel mesh, with the possibility that a cement-based liner will also be used. Used fuel containers are to be placed horizontally in tunnels, on bentonite blocks with the remaining space backfilled with bentonite pellets.

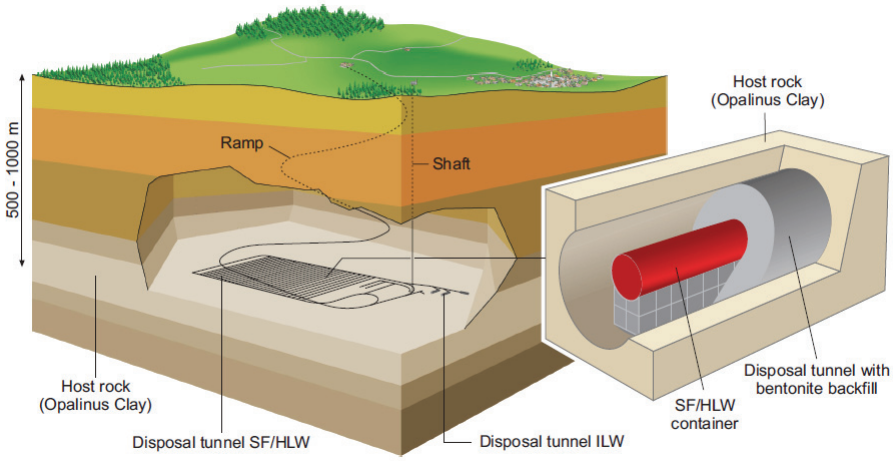

Note: From Nagra (2009).

Figure A-1: The Swiss Repository Concept in Opalinus Clay

The reference spent fuel containers are cast iron containers about 5 m long and 1.05 m diameter, with a 0.14 m wall thickness (Nagra 2012). The minimum required container lifetime is 1000 years; however, their design life is 10,000 years (Nagra 2012). Hydrogen gas produced from the corrosion of iron is assumed to disperse along the repository access structures through gas-permeable seals and also into the surrounding Opalinus Clay, in part through the porosity and in part through dilation-and-resealing in this high clay-content material (Nagra 2009).

Nagra is also considering a copper container with a steel insert as an alternative container concept (Nagra 2009, 2012).

A.2.2 France (Andra)

The French program is presently preparing a repository license application. Andra is proposing to dispose of spent fuel, vitrified high-level waste and long-lived intermediate-level waste in a deep geologic repository in a Callovo-Oxfordian clay formation. Like other organizations, Andra implements a multiple-barrier safety approach.

The main used fuel waste form (C waste) is in vitrified glass as a result of reprocessing. The reference C waste containers are made from P235 non-alloyed steel, about 1.6 m long × 0.6 m diameter, and 0.055 m thick. The container is expected to last at least 4,000 years (Andra 2005). The containers are placed horizontally in steel-lined tunnels within the clay. France will also have unreprocessed spent fuel (CU wastes). The reference CU waste containers for UO_2 fuel are 5.99 m long × 1.25 m diameter, and 0.110 m thick unalloyed steel. These are designed to be leak tight for 10,000 years. Figure A-2 shows the C waste container and placement concept, and Figure A-3 shows the CU waste container and placement concept (Quintessa 2007).

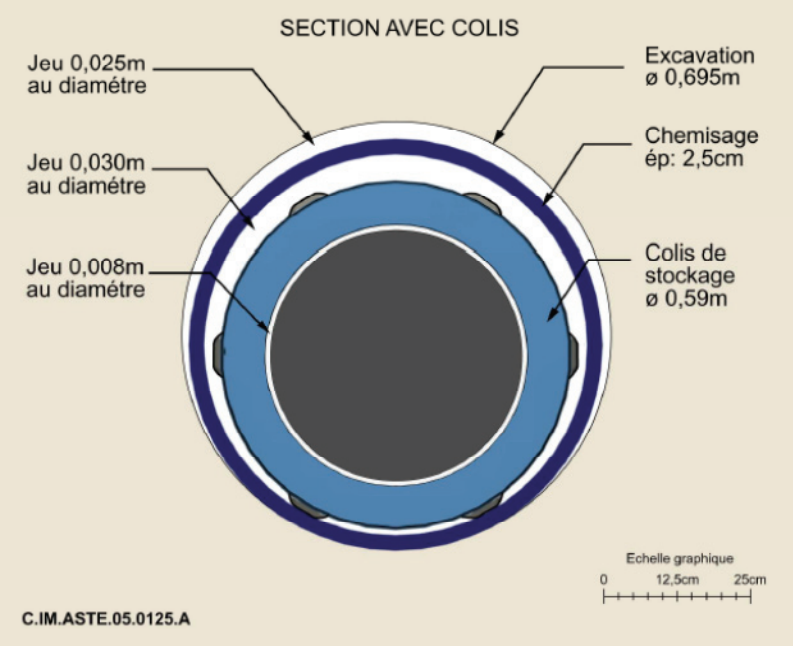

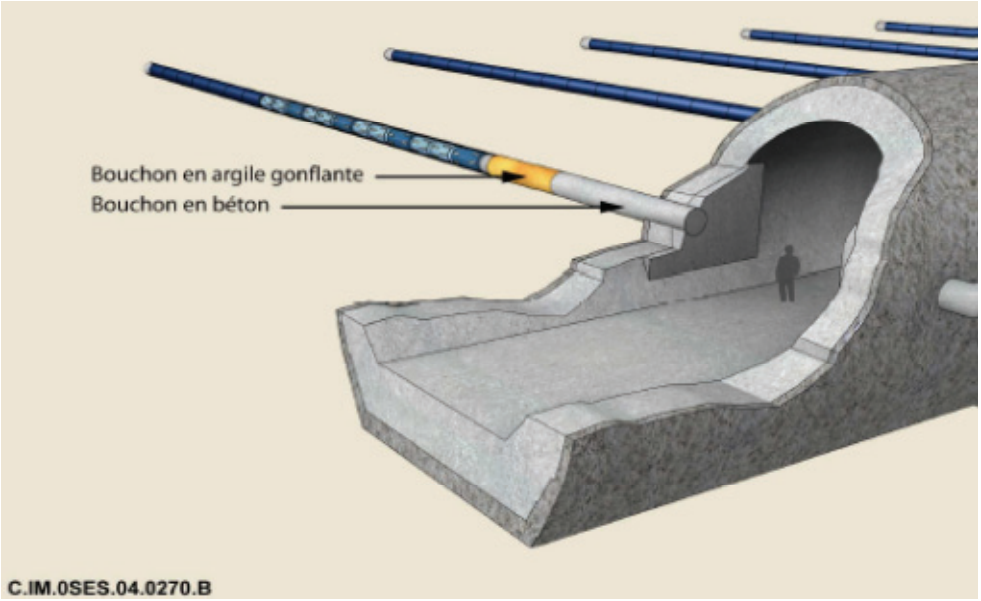

Note: From Andra (2005).

Figure A-2: The French Repository Concept for Vitrified HLW in Callovo-Oxfordian Clay

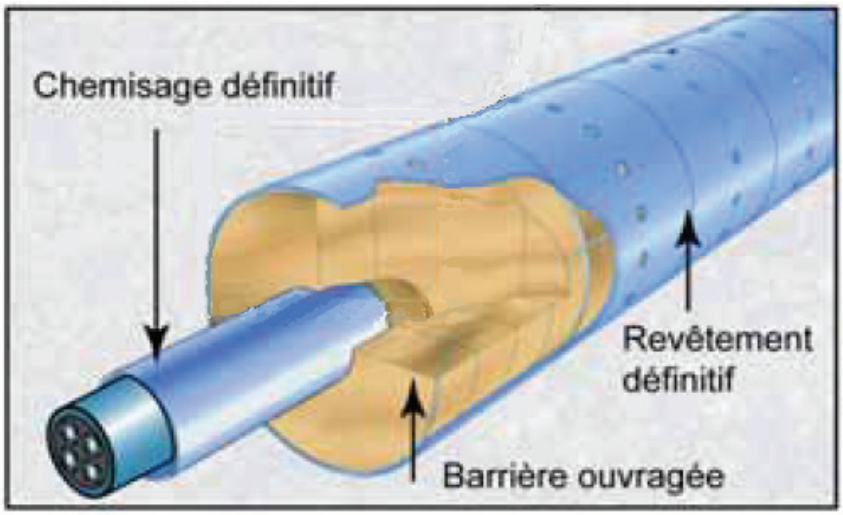

Note: From Andra (2005).

Figure A-3: The French Repository Concept for Spent Fuel in Callovo-Oxfordian Clay

A.2.3 Belgium (ONDRAF/NIRAS)

In Belgium there is no identified repository site. However, the potential host formations studied by ONDRAF/NIRAS for a geological repository are currently limited to poorly indurated argillaceous formations, with the Boom Clay as a reference host formation and Ypresion clays as an alternative. Geological conditions in the Boom Clay are being investigated at the underground research laboratory at SCK·CEN in Mol.

The repository concept also relies on multiple barriers. The reference design concept is referred to as the "supercontainer" (Yu and Weetjens 2009). The container stores both vitrified waste canisters and spent fuel assemblies (Figure A-4).

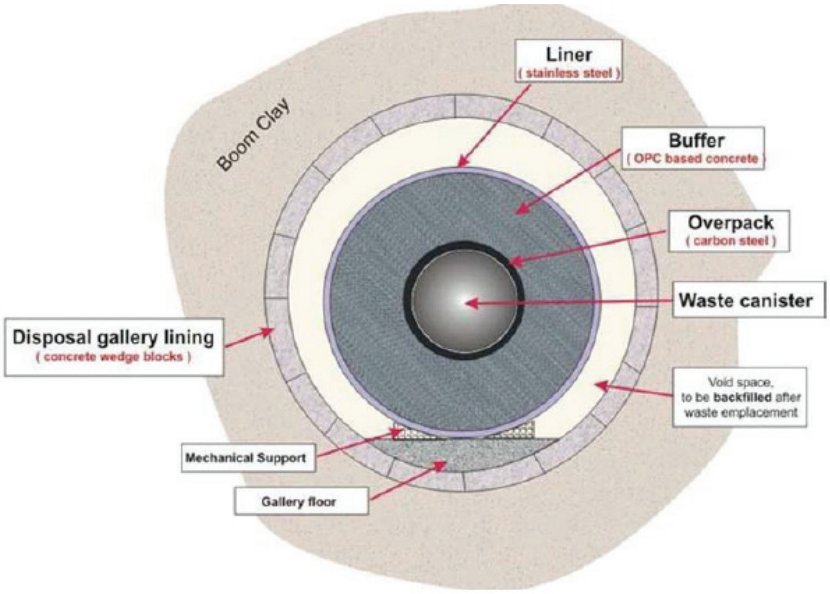

Note: From Mallants and Jacques (2004)

Figure A-4: Cross Section View of the Belgian Supercontainer Concept for HLW

The supercontainer design consists of a carbon steel overpack surrounded by a Portland cement-based concrete buffer and a stainless steel outer liner. Concrete has been chosen for the buffer because, under the high-pH conditions due to the surrounding concrete, the carbon steel overpack will undergo uniform and slow corrosion. This supercontainer has a minimum lifetime covering at least until the end of the thermal phase.

In the long term, hydrogen gas will be produced from steel corrosion. Experiments suggest the gas is released via preferential pathways opened in the Boom Clay. Since this is a soft clay, these pathways can be created at relatively low pressures, and they will close up and disappear after the gas passes (Yu and Weetjens 2009). The Boom Clay self-seals, with the clay returning to its original low-transport properties.

A.3. Key Differences

The above discussion indicates that the overall conceptual approach for sedimentary rock in other countries is the same as that adopted in Canada, that is, deep disposal in a multiple-barrier repository.

Although all of these cases involve low-permeability sedimentary rock, there are important differences in the rock properties. In particular, these European clay formations are softer than the shales and limestones under consideration in Canada. Furthermore, the Canadian sedimentary rock groundwaters are more saline.

Another difference is the container design. All containers rely on steel for structural support. However, the conceptual design considered in this study has a copper outer shell for corrosion resistance, whereas the other sedimentary rock countries are primarily considering steel-only

containers. The very low permeability and lack of fractures in sedimentary rocks supports their container design basis.

The use of steel-only containers has potential benefits. The main advantages cited are: well-understood and generally uniform corrosion under repository conditions; well-understood and readily available engineering material, leading to ease of manufacture, welding, and cost-effectiveness; and the ability of the thick steel overpack to provide a radiation shield (Quintessa 2007). The main disadvantage is that the predicted lifetime of steel containers is less than that predicted for copper shell containers. Generation of hydrogen gas may require accommodation within the design of the repository, depending on the rate of generation.

International experience indicates that robust safety cases that exceed regulatory requirements can be developed for steel-only containers. Work is underway to assess whether this is possible in relevant Canadian sedimentary rock formations. Other design optimizations are also under study, including use of copper coatings, alternative container size and alternative container placement methods.

A.4. References for Appendix A

Andra. 2005. Safety Evaluation of a Geological Repository. Agence Nationale Pour La Gestion. Dossier 2005 Argile. Paris, France.

Mallants, D. and Jacques, D., 2004. Performance assessment for deep disposal of low and intermediate level short-lived radioactive waste in Boom Clay, SCK•CEN-R-3793. Mol, Belgium

Nagra. 2002. Project Opalinus Clay, Safety Report. Nagra Technical Report 02-05. Nagra Wettingen, Switzerland.

Nagra. 2009. A Review of Materials and Corrosion Issues Regarding Canisters for Disposal of Spent Fuel and High-Level Waste in Opalinus Clay. National Cooperative for the Disposal of Radioactive Waste Technical Report 09-02. Wettingen, Switzerland.

Nagra. 2012. Canister Design Concepts for Disposal of Spent Fuel and High Level Waste. Nagra Technical Report TR-12-06. Wettingen, Switzerland.

Quintessa. 2007. International Precedents for HLW/SF Iron Canister Concepts; Review and Consideration of Applicability in the UK Context. Quintessa Limited report for Nirex. QRS-1376A-1 v2.0. Henley-on-Thames, UK.

Yu, L. and E. Weetjens. 2009. Summary of Gas Generation and Migration. SCK-CEN External Report SCK-CEN-ER-106. Mol, Belgium.